THE GEOMORPHOLOGICAL BEHAVIOUR OF A SNOW-FED, SEMI-ARID GULLY SYSTEM IN WESTERN COLORADO

Thesis submitted in accordance with the
requirements of the
Council for National Academic Awards
for the degree of Doctor of Philosophy

Research conducted in the
Department of Geography
Polytechnic of North London

PATRICIA HAZEL FAULKNER

October, 1984

ABSTRACT

THE GEOMORPHOLOGICAL BEHAVIOUR OF A SNOW-FED, SEMI-ARID GULLY SYSTEM IN WESTERN COLORADO

Hazel Faulkner

Western Colorado experiences a winter snowfall maximum and considerable snowmelt flooding in spring, followed by a summer characterised by short, high-intensity storms. An examination of local records and terrain characteristics suggests that not only are these two processes temporally distinct, but also that the environmental controls on runoff generation for each vary, so that each process affects different parts of the landscape.

A gully system lying within a small (0.4 km^2) sub-catchment of the Alkali Creek basin was surveyed in 1962, 1975, and 1980. Because the watershed materials are erodible and sensitive to all watershed runoff events, it is hypothesised that the distinctive downstream erosion pattern described by the surveys may be explained in terms of the sediment transfer capabilities of the two asymmetrical 'hydrological process intensity domains' routed into the channel phase.

Frequency-weighted runoff models for melt and overland flow are consequently developed and tested against field discharge data. Linking these simulations to sediment rating curves allows event sediment yields for watershed sites to be estimated. The procedure shows snowmelt to be overwhelmingly effective in transporting sediment out of the basin, but that in the headwaters summer storm erosion is locally more important. A complex annual sequence of entrainment, lodging and flushing emerges which can be compared with other areas. Spatially differencing these yield data as an index of site scour and fill suggests that main channel erosion is considerable during snowmelt, and tributary junctions emerge as the most active watershed sites by a factor of at least 10.

The peak power of simulated flows and the scour and fill indices work well in predicting contemporary form but less well against form change, nevertheless the methodology is generally supported by these results. Threshold behaviour is considered, and although it is argued that the sort of lodged sediments normally prone to trenching will not survive the snowmelt flushing on the main channel, there are possibilities for network integration through fans on 'summer-sensitive' parts of the watershed. These possibilities and the large negative sediment yield budget indicate a state of chronic transience, an observation supported by evidence from an adjacent watershed.

D E C L A R A T I O N

Whilst registered as a candidate for the degree of Doctor of Philosophy, the author has not been a registered candidate for another award of the C.N.A.A. or of a University during the research programme.

ACKNOWLEDGEMENTS

I am indebted to the U.S.D.A. Forest Service for the opportunity to use maps and other records relating to the Alkali Creek Soil and Water project, and particularly to Dr. B. Heede at the Research Station in Tempe, Arizona for introduction to the field area in 1975, and to Mr. J. Mangan at the Field Station in Rifle, Colorado for accommodation and valuable field assistance in 1981. Bernie Shafer at the U.S.D.A. Soil Conservation Service office at Diamond Hill, Denver Colorado was exceptionally generous with both advice and assistance in obtaining snowcourse data for McClure Pass, and the S.C.S. office in Glenwood Springs loaned the snow sampler and gave advice on its use in 1981. The U.S.G.S. supplied the air photographs and the West Divide Creek river records. I would also like to thank Mr. J. Martin, Glenwood Springs Police Department for the loan of the jeep despite some hairy moments and several parking tickets.

I am grateful to the Inner London Education Authority and the Polytechnic of North London for their generous grant towards field expenses, and Mr. T. Roberts for his recommendation. Appreciation for their support goes to the staff of the P.N.L. Geography Department, especially Dr. R.H. Bryant who supervised the project logistics and supplied considerable encouragement, and Dr. J.M. Lindsay for careful proof-reading. The fine state of the final draft is due to the high standards of Catherine Fisher who typed it, Robin Skinner who produced the photographs, and Prontoprint, Holloway Road, who rashly allowed the author a free rein with their copiers.

Professor S. Schumm, Professor W. Striffler, and Dr. M. Harvey of the Watershed Science Department at Colorado State University; and Professor J. Thornes of the Geography Department at Bedford College, University of London gave valuable advice at critical stages of production for which I am indebted. Finally the project would have suffered considerably without the encouragement and sound critical judgement of my supervisor, Dr. A.M. Harvey, Geography Department, University of Liverpool, to whom I offer my especial thanks.

CONTENTS

LIST OF FIGURES

LIST OF TABLES

LIST OF PHOTOGRAPHS

LIST OF APPENDICES

7 FIELD SNOWMELT DISCHARGES

A. (i) Spatial data : April 7th
April 19th, 1981

(ii) Temporal data : April 5th, 1981
April 18th, 1981

B. Derivation of indices to relate peak to mean daily flow

C. Peak diurnal flows listed with simulated peak and mean flows at field sties, including suspended sediment concentrations

(i) Spatial data

(ii) Temporal data

8 DATAFILES FOR ROUTE.PAS

A. Small discontinuous gully (Test file)
Continuous network

B. Large discontinuous tributary

9 INFILTRATION SURVEY

10 FIELD OVERLAND FLOW DISCHARGES, including a comparison with run 6 of ROUTE.PAS for equivalent sites, and suspended sediment data

11 PROGRAMMES WRITTEN FOR SPECIFIC PURPOSES

A. ROUTE.PAS
SEEP.PAS
YIELD.PAS (1) and (2)
SEDIF.PAS (1) and (2)

B. The Barnes Roughness table

12 REGRESSION STATISTICS for various regression tests included in the text

13 CALCULATIONS INVOLVED IN THE CONSTRUCTION OF AN ANNUAL SURFACE WASH INDEX AT WATERSHED SITES

14 DATAFILES AND OUTPUT FROM SEDIF.PAS AND YIELD.PAS

A. T-ratios

B. Input files for Sedif1.pas
Input files for Sedif2.pas

Chapter 1

INTRODUCTION

"It is the interaction between the total snow suite and the total rainfall suite which represents the principal challenge".

'The Geomorphology of snow' C.E. Thorn, 1978

Although a number of geomorphological models are available for the study of surface wash erosion in semi-arid areas, (Kirkby, 1978; Kirkby and Morgan, 1980) the semi-arid alpine environment of western North America experiences a winter snowfall maximum, and despite the high sediment discharge associated with snowmelt (Heede, 1977), the geomorphology of snowmelt is relatively unresearched (Thorn, 1978).

It is not clear why this is the case. It may be that snowmelt fieldwork is often difficult, slow or impossible, or that two methods of runoff so complicate the pattern of channel processes that most sensible academics avoid the problem, or it may be that the extensive attention given to surface wash processes in Colorado by Schumm (1956a, 1961, 1973, 1977, 1980), Schumm and Hadley (1957), has led to a misapprehension that melt processes in these environments must be largely cosmetic.

Whatever the reason, the author arrived in Colorado in 1975 armed with this misperception of the relative roles of these processes to undertake a geomorphological assessment of check dam efficacy in a rapidly eroding, heavily trenched gully network in the Alkali Creek Soil and Water Project study area in conjunction with the USDA Forest Service. Subsequent discussion and fieldwork, and an examination of the local recording raingauge records, and photographs made available from the Rifle and Glenwood Springs Forest Service Offices, and later snow accumulation data from the S.C.S. Offices in Glenwood Springs and Denver led to the unavoidable conclusion that the geomorphology of the gully system could not be considered without recognising the duality of the processes contributing to channel flows.

The work which follows emerges from this preliminary visit in 1975, and goes some way towards taking up the challenge laid down by Thorn (1978) in the introductory quotation, by exploring the relative roles

of melt and summer storm erosion in a small watershed context. To state this formally, this thesis aims to simulate the contemporary hydrological processes operating within a small, snow-fed semi-arid gully network in western Colorado, and, in conjunction with sediment relationships, examines the extent to which the simulations may be used to explain the contemporary pattern of channel excavation and short-term change.

The following section reviews some of the current literature relating to gullies and arroyos, and shows how many contemporary geomorphological concepts rely on evidence from such terrain. Following from this, the final sections introduce the idea that a dual domain approach to runoff generation in melt regimes might allow a revision of some of these ideas in relation to landforms in western Colorado, and outlines the methodology to be adopted in subsequent Chapters.

(I) THE STUDY OF ARROYOS AND GULLIES

Graf (1983) distinguishes between gullies and arroyos. Whereas an arroyo is "... a trench with a roughly rectangular cross-section excavated in valley-bottom alluvium with a major stream channel in the floor of the trench", a gully has a "... V or U-shaped cross-section ..." containing a "... minor channel in the bottom". Although these differences may appear to distinguish the features merely on the basis of topographic position, different initiation mechanisms may be involved. Horton (1945) explained how a regional system of dendritic gullies which terminate upstream in a line of rills a uniform distance from the divide can be considered a 'normal' climatic response to a low vegetation cover and high rates of overland flow on unprotected surfaces during the high-intensity short-duration storms which characterise semi-arid regions. By contrast, arroyo trenches are usually accredited to some sudden change in the hydrological regime which affects the power pattern and the sediment transfers in a previous untrenched valley floor. The overcoming of some local resistance threshold (Schumm, 1973, 1980) has been thought most likely to occur at key gradient or bed resistance sites (Graf, 1979a) during 'superfloods' (Schick, 1974; Harvey 1984a), although Cooke and Reeves (1976) show that in general hydroclimatic triggers are but one cause

and suggest that other environmental modifications (such as grazing and other land-use changes) may also be important.

The search for external explanations for arroyo initiation changed when Schumm (1973, 1977) showed that suitable sites for trenching may develop on valley beds by means of the progressive deposition of sediment which is known to occur in semi-arid areas particularly below tributary junctions (Thornes, 1977; Graf, 1982), or on lower course axial channels during periods of alluviation. There may therefore be no need to invoke external causes for the threshold behaviour characteristic of arroyo initiation, since the landscape operates in a manner which produces sites sensitive to such catastrophic shifts as a normal part of its operation (Brunsden and Thornes, 1979).

Sudden trenching means that arroyos tend to terminate upstream in a headcut (Brush and Wolman, 1960) rather than in the shoestring rill associated with cross-grading during sheetwash (Horton, 1945; Loepold, Wolman and Miller, 1964), and Leopold (1978) has shown that bed and bank erosion in the arroyo trench continues until an equilibrium condition prevails amongst water and sediment discharge, and channel configuration (Graf, 1983). Andrews (1982) associates this with a trend towards a stable width-to-depth ratio. Where arroyo gradient, which is less than that of the slope or valley into which it is incised approaches that of the pre-existing surface once again, the feature becomes discontinuous and terminates in a 'sink' such as a small alluvial fan (Leopold, 1978).

Bergstrom (1980) and Schumm (1977) have consequently identified a three-zone classification of semi-arid gully and arroyo systems; the first Production zone accords with the continuous net described above, the second is a predominantly Depositional zone below these headwaters in which cycles of scour and fill (Schumm and Hadley, 1957) occur in the context of a positive sediment budget, and a third zone where the deposition in zone 2 has oversteepened the channel downstream increasing the propensity for trenching, is a zone of re-Erosion (the P-D-E sequence). Consequently arroyos may go through quite long-term cycles of erosional and depositional activity as part of their intrinsic operation, and during the erosional phases in zone 3 in particular, the implication is that trenching may extend by headcut

migration back up-net to reintegrate and reactivate the continuous net in the headwaters (Heede, 1967). Schumm (1977) describes such behaviour as 'episodic', and once again may not need an external trigger.

As a result of these processes, which have been noted in a variety of gullied environments, a complex suite of abandoned fan terraces may remain at lower elevations in the landscape (Schick, 1974) whose nature, extent, and persistence depends not only on the order of occurrence of the frequent and infrequent watershed events, but also on the varying position of the point of alluviation in that particular network configuration during each event, and the varying pattern of bed resistances resulting from the operation of each sequential event. Thornes (1983) points out that "... too often perceived climatic changes based on comparative analysis of sediments and morphology in different catchments are actually differences in hydrologic response due to the inherent spatial variability within catchments".

Despite the distinction made above between the regionally characteristic continuous network and the valley-bottom arroyo, dendritic networks which start with a small headcut at points of hillslope inflexion in semi-arid areas can be found (Heede, 1974, 1977) which downslope may or may not be continuous. These are apparently caused by exceeding local resistance at points where the rate of slope change is maximum, i.e. on convex slope elements, and take the form of headcuts. Other locating influences, such as pipes, may have an additional role. Thornes (1980) sees gully initiation as a 'perturbation', and explains "... the cause of the initial perturbation may be random, as for example the trampling of vegetation by cattle, the survival of a rill through consecutive seasons, the collapse of a subsurface hollow, or the cutting of a forest for road construction". These types of gullies which terminate upstream in a headcut are more akin to arroyos in their causation, progressive erosion, and morphological relationships than the continuous regional nets described earlier, which are commonly found in the absence of vegetation and on fine-grained materials conducive to surface slaking and sealing.

Because of the different terms adopted in the literature for these three types of feature, the term 'gully' is used from here onwards to apply to all three types, although the differing nature of these features is assumed at various stages in the text.

(A) Geomorphological concepts in semi-arid areas

Because adjustments in gullied landscapes in semi-arid areas "... occur with unbelievably rapidity in the normal geologic sense" (Campbell and Honsaker, 1982) these environments have traditionally attracted considerable attention. It is perhaps not surprising, therefore, that the current conceptual basis of geomorphology as outlined by Brunsden and Thornes (1979) owes much to work in such environments.

For instance, their first landscape proposition that 'characteristic forms' might result from the operation of single process sets was implicit in the early work of Horton (1945), whose morphometric studies detailed the topological uniformity of the type of continuous network described in the last section as resulting from cross-grading during surface wash. These ideas were later developed by Schumm (1956b). Characteristic slope forms from the operation of wash were more recently modelled by Kirkby (1971) using a basically Hortonian view of wash, and the regularity of alluvial fan forms has been described by Hack (1975) and Bull (1977).

More recently there has been a movement away from the recognition and description of 'characteristic' forms, and Brunsden and Thornes (1979) imply that the regular nets described by Horton (1945) may be only regionally characteristic in 'domains' of operation within which the controls on surface wash processes remain relatively uniform. Where vegetation is sufficiently dense, for example, surface wash is inhibited (Langbein and Schumm, 1958), so that the attainment of characteristic forms may be ultimately constrained by the environmental control factors which affect vegetation response and thus surface wash intensity (Kirkby, 1978). Since these control parameters (potential evapotranspiration and rainfall) vary considerably with aspect, it can be deduced that the spatial intensity of wash, and therefore of characteristic forms, will vary with aspect even at a small scale.

The idea of spatial process intensity domains is complemented by the Wolman and Miller (1960) view that the work done by a process depends not only on the magnitude of the applied force at a place, but also on the frequency of its application, giving rise to the idea that if processes are relatively uniform spatially within their 'domains', then it is possible to recognise a particular frequency at which most of the geomorphologically effective work is done (the 'dominant' event) and additionally that the characteristic landform suite is 'in equilibrium' with this dominant event (Leopold and Maddock, 1953).

However there are some difficulties with this simple perception in semi-arid areas (Wolman and Gerson, 1978; Richards, 1982) because here the importance of the extreme events depends on their recurrence interval in comparison to the relaxation time necessary for restoration of a previous morphological state, which in turn depends on both the frequency of the smaller events and the sensitivity of the watershed materials and morphology to them. Brunsden and Thornes (1979) argue that abrupt discontinuities and a lack of smooth equilibrium forms is characteristic of landforms poorly adjusted to frequent events, and Harvey (1984a) argues that for an area he studied in S.E. Spain, the lower frequency, more persistent processes are inefficient so that the artifacts of 'superfloods' dominate the landform suite. Whereas the presence of downstream fan terraces flanking valley-bottom arroyos described in the last section (Schick, 1974) might support this 'extreme-event-sensitive' view of landscapes in semi-arid areas, the regularity of continuous gully nets as described by Horton (1945) argues against this view. One explanation for this apparent dichotomy may be that since all events in the continuous net are erosive, then the whole spectrum of events have an effect which is similar in direction and kind here, so that the idea of the 'dominant' discharge relating to this regularity holds. Further downstream, however, the lower frequency events become depositional, in contrast to the continuing erosive pattern of the extreme events here, so that there is a distinction between the direction and effect of persistent compared to extreme events, leading to a more 'oscillatory' landform response. The more disjointed nature of downstream landforms (headcuts, terraces) might be regarded as the morphological expression of such oscillations. We conclude that even in this small watershed context there is spatial variation in the definition of the 'dominant' or 'morphologically significant' event.

In a second landscape proposition, Brunsden and Thornes (1979) argue that sites of threshold excedence (the headcuts mentioned in the last section) may become the most important locations for morphological change, so that 'transient' rather than 'equilibrium' behaviour may dominate change in semi-arid areas. This view rests to a certain extent on the work of Schumm (1973, 1977) who distinguished between those major threshold exceeding episodes which require an external trigger, and those which occur as a 'normal' part of watershed operation ('extrinsic' and 'intrinsic' thresholds, although these names mislead in that the adjectives should refer to the trigger rather than the threshold itself). Brunsden and Thornes (1979) explain that in fact "... thresholds occur as transitions between the conditions necessary for different process domains or as structural instabilities in a system". In semi-arid areas the most common threshold-exceeding event is the formation of headcuts which may initiate trench-head gullies and arroyos. Graf (1979a) defines the threshold involved here in terms of bed resistance, and others have suggested that the sites most prone to this behaviour are the tail ends of persistently accumulating sediment wedges under the operation of normal watershed processes. Schumm (1977) sees the critical threshold in terms of channel gradient.

All geomorphic processes involve the overcoming of resistance thresholds before change can occur (Thornes, 1981) and current support for threshold ideas (Coates and Vitek, 1980; Rhodes and Williams, 1979) might almost imply that every small landform change must be seen in these terms. Whether or not the exceeding of a threshold is perceived as part of the progressive operation of a consistently evolving system, or as the main determinant of its operation depends, however, on whether the system response is reversible, such as is the case with the scour and fill cycle described by Schumm and Hadley (1957), or irreversible, as for instance in the case of arroyo trenching; this distinction itself is, however, scale dependent, (Campbell and Honsaker, 1982). If the relaxation time necessary for the checking of the 'positive feedback' characterising the initial stages of headcut or arroyo trenching is longer than the observation period, then the change will always appear to be irreversible, catastrophic and a dominant part of the geomorphic behaviour. In these situations the system is 'transient' and undergoing 'episodic' change. In the long-term, however, the position is rather different:

As long as the extreme event is infrequent and the intervening smaller events effective in restoration "... the knowledge that ultimately such changes must be checked is not at issue". (Brunsden and Thornes, 1979), and at this scale the trenching episode may appear as merely a minor 'cut and fill' perturbation around a wider-scale pattern of progressive denudation. The nature of this progression is complex, as suggested in the third proposition of Brunsden and Thornes (1979), who suggest that the character of the change may be linear, ubiquitous, or diffuse. If, however, the recurrence interval for major threshold-exceeding events is shorter than the watershed relaxation time, then a state of chronic transience is indicated and the nature of the long-term trend is completely unpredictable.

The fourth landscape proposition concerns landscape sensitivity, expressed as the ratio between the amount of energy required for change in comparison with the energy of the prevailing processes. It is this characteristic of the watershed which determines its response to the more prevalent watershed events and may be the most significant criteria determining the persistence of the extreme-event landforms. Brunsden and Thornes (1979) suggest that mobile, fast-responding systems react and relax quickly, and so exhibit primarily transient forms all the time, whereas intransigent, slow-responding, possibly over-adjusted forms such as plateaux, (which may or may not be composed of resistant material) are insensitive, passive, and change but slowly. A variety of elements of differing sensitivities may coexist within a small spatial area. The useful perception of the landscape as a range of sensitivities allows spatial variations in gully size and morphology to be at least partly accredited to lithology.

The conclusions which can be drawn from these observations which are pertinent to the current investigation of a gullied landscape are as follows ;

(1) Process intensity has an important spatial as well as temporal expression, the examination of which might lead to the identification of patterns of domain dominance for events of differing recurrence intervals even within the small scale of a single watershed.

(2) Because the spatial controls on wash, and therefore the intensity of wash in its spatial domain limits the process by aspect, and also because the direction of operation of frequent and infrequent events need (it is argued here) to be the same for non-threshold, simple characteristic forms to develop as a response to a single 'dominant' event, then the 'characteristic' forms described by Horton (1945) probably only exist in headwater nets, and even then their spatial extent is limited by those domain controls.

(3) The threshold-exceeding events that are significant at the scale of a small watershed are arroyo and fan-head trenching, the former being more commonly located on the tail end of alluviated sections where the persistent deposition during more common watershed events allows sites suitable for trenching to develop. Such sites are found more on the lower than upper parts of watersheds.

(4) Depending on the relationship between the extreme and the persistent events, such behaviour may dominate geomorphic evolution, in that for example fan trenching may lead to the reintegration of previously dissociated, discontinuous parts of the watershed.

(5) Because most mobile, rapidly eroding gully systems are probably chronically transient, concepts such as 'equilibrium' are inappropriate.

(6) Since landscape elements vary in sensitivity and may be partly overadjusted, landscape response may ultimately depend on the spatial variations in material and morphological resistance to change.

(B) Relationship to snow-fed, semi-arid gully landscapes.

Most of the semi-arid literature assumes that surface wash, caused by overland flow after flash floods, is the main formative process involved in gully development, and so many of the above arguments focus on the behaviour and power of the extreme versus persistent watershed events. Although these considerations go some way towards explaining the landforms described earlier, nevertheless there is little allowance made in this overview for the possibility that the persistent processes are those diurnal flows which characterise the decay of a considerable snowpack.

The possibility that melt flows modify the sensitivity and spatial and temporal response of gully systems is partly suggested by observations in the western slope of Colorado in 1975 which provide the backdrop to the present study, and also by the work of Heede (1974, 1977). Both investigations showed that the region contains both continuous and discontinuous examples of gullies of both the fingertip and trench-head type, although the phenomena are more spatially intermittent than spatially uniform, depending on lithology (Chapter 2). The thin vegetation cover suitable for the development of a Hortonian net is more common on south-facing slopes, restricting the initiation of these gully types to such sites, although in some locations such gully development can be linked to overgrazing in the 1930s (Heede, 1977). Field observations in 1975 suggested that the second type of gully network, which terminate upstream in a trench-head, appear to favour points of topographic convexity implying that piping may be an additional focussing factor. Although both gully types coexist, and both do seem to favour south-facing positions, the distinction between them is blurred sometimes by the subsequent modifications which can be made by piping to gully banks.

Below these generating ties, the downstream extension of the channel below the headwater net is usually in the form of a long, arroyo-type, axial channel which may run through quite well-vegetated lower slopes for some distance, and then suddenly terminate in an alluvial fan in quite wooded areas. In other situations, these long, well-trenched axial channels are continuous well beyond the headwater source areas, maintaining a well-defined course to the major rivers of the region. This general picture is modified by the observation that adjacent watersheds in the same topographic position and on similar lithologies may demonstrate striking differences in the degree of erosion, although the tendency for aspect influence is there, whatever the level of erosion attained.

These environmental characteristics are difficult to explain in terms of an overland flow model alone, and it is consequently argued here that the character and forms of the gullied landscapes of the western slope might be better explained in terms of a dual runoff model, rather than in terms of overland flow erosion alone as is the emphasis in most of the literature reviewed so far. The conceptual basis of this approach is explored below.

(II) DUAL PROCESS LANDSCAPES; CONCEPTS AND METHODS

Although the primary interest in this study is the explanation of the current pattern of gully excavation and patterns of gully size change over a 13-yr observational period, the position is taken here that to investigate the causal channel processes of erosion and deposition, the nature of the hydrological system, and the spatial and temporal patterns of flow production from watershed precipitation events consequently experienced by the channels are of primary importance.

These systems are here described by two <u>hydrological process intensity domains</u>, using the idea of a'domain' as suggested in section (A), but using the hydrological process rather than the geomorphic process as the basis for the domain definition. The emphasis on spatial domain intensity has had little attention previously, yet is implicit in the work of Harvey (1984b), and there is explicit recognition of these ideas in the work of Thornes (1979), Brunsden and Thornes, (1979); and Kirkby (1980a). The emphasis on spatial variability in both water and sediment transfer is recognised by Bello (1978), who suggests that "... there is immense spatial variation even within areas less than 10 km^2 in the operation and effectiveness of the work of water in the landscape", suggesting also that "... without details of the nature of ... cascades, lag times and retention mechanisms, catchment budgets may ignore many processes which are significant in landform evolution and fail to recognise those crucial localities within drainage basins where the bulk of the geomorphic work is done". These views are shared here; and for methodology, the opinion of Thornes (1980) points the way "... The hydrograph characteristics are determined in part by the network configuration, and magnitude and frequency of flows in the gully-channel system determine the character of erosion and deposition".

(A) Process intensity domains

The domains as envisaged by Thornes and Brunsden (1979) were viewed by them as essentially domains of geomorphic intensity. From this perspective the channel boundaries of the gully network constitute the physical limits of a 'channel process domain' within which erosion and deposition may be viewed as dominant. Nevertheless, it is argued here that the intensity and frequency of channel processes in snowfed

semi-arid landscapes are best understood as a response to the separate behaviour of two hydrological process intensity domains operating across the whole watershed, which are distinct in that different controls are involved both in the generation of the flows, and in the timing and methods of translation of water and sediment from slope to channel.

These two processes are those of snowmelt runoff following the collapse of a considerable snowpack in the spring, and that of overland flow following intense, short-duration storms in the summer months. In this approach, each hydrological process is conceptualised as occupying both a spatial intensity domain limited to a part only of the watershed, and a temporal intensity domain limited in both cases to a part only of the annual climatic record. This perception of two interacting process intensity domains which have both a spatial and a temporal expression usefully allows the relative importance of the two causes of erosion and depositional change to be examined, and results in the description of a unique pattern of channel sediment entrainment, transport and deposition which can be compared with monitored rates of channel change.

For each of the two processes, the intensity pattern of the spatial domain at any particular point in time reflects not only the environmental factors controlling flow generation on the hillslope (such as slope angle, aspect, soil type and vegetation) but also the network topology. A distinction can be made between the hillslope process intensity domain which sees the generation phase of the process, and where environmental controls are of primary importance, and the channel process intensity domain in which network position in the watershed cascade controls channel flow intensity, being the combined result of the routed contributions from hillslope generation at that site. The channel intensity domains for melt and for overland flow, which are of primary interest in this investigation, are thus network based and hierarchical, and characterised (except where flow becomes spatially discontinuous) by a high level of spatial autodependence. The hillslope spatial domain can be mapped on the basis of environmental controls and then the generated flow routed through the network from contributary source positions to produce the channel spatial intensity domain pattern. This method is used here to calibrate the channel process intensity domains for both processes, and fieldwork was designed to calibrate the models produced.

For each process, the intensity pattern of the temporal domain at any point in the network reflects the temporal pattern of inputs into the cascade as well as position in that cascade. The temporal process intensity domain at a site will have a high level of temporal autodependence when inputs are sufficiently continuous to maintain continued channel flow, but the temporal record is often treated as a long-term frequency distribution of independent events of varying magnitudes and frequencies, as discussed earlier (Wolman and Miller, 1960). This long-term record is capable of interpretation in terms of frequency of force applied, although amount of sediment mobilised (Kirkby, 1978; Richards, 1982) might substitute for 'force' as a measure of process importance.

Calibration of these temporal process intensity domains is undertaken in this study using recording raingauge records and snow accumulation data from local stations, allowing the spatial process intensity domains to be frequency weighted. Because during each of these processes, field-monitored sediment rating relationships allow discharge to be linked to sediment discharge, the weighted simulations of the channel process intensity domains can eventually be viewed as patterns of spatial sediment yield for each process, so that a complete watershed picture of the relative dominance of the two processes in terms of channel sediment behaviour may be obtained from both a spatial and a temporal position. In later sections, the spatial rate of sediment change with distance for each process is interpreted as an index of scour and fill during these events, finally providing a link between these models and morphology.

(B) Interactions

During periods when the two temporal process intensity domains superimpose in time at a site, and more importantly in zones where two spatial process intensity domains overlap, it is hypothesised that a reinforced, damped, or oscillatory response in terms of morphology is indicated. The nature of the morphological response depends on the sensitivity of the pre-existing morphology and of the local materials to the low intensity events, so that such interactions are difficult to model in any detailed way. Nevertheless by taking a dual domain approach it should be possible to identify those sites of reinforced response where as Bello (1978) puts it "... the bulk of the geomorphic

work is done", and those of oscillatory response, where threshold behaviour is indicated. Such interactions and possibilities for reinforced and threshold behaviour resulting from dual domain operation are considered in a final section.

(C) Morphological relationships

For purpose of examining the relationships which might exist between these weighted simulations and the patterns of overall morphology of the gully as mapped in 1962, 1975 and 1980, a 'functionalist' method is adopted (Chorley, 1978a), in which the strength of the process models are tested by means of their statistical correlation with these morphological parameters. Although the 'realist' approach of direct modelling these links is at the front of much recent research effort (Smith and Bretherton, 1972; Kirkby, 1971) the level of detail involved, and the problems of calibrating these models for the variety found in the real world, and also the multiplicity of ways in which channels respond at the detailed level eventually ruled out such an approach in this study. It is felt that the meso-scale questions which are being addressed here justify an approach in which the picture is painted with a broader brush. Chorley (1978a) has said "... Geomorphology can only make a unique contribution to the earth sciences if, in the study of process, physical truth is sufficiently coarsened in both space and time as to accord with the scale at which it is profitable to study geomorphologically-viable landform objects". In the sections which follow, the detailed methodologies and strategies adopted are described at relevant places in the text, and at each stage the methods adopted are considered with this coarser scale of resolution in mind.

After an initial consideration of the spatial and temporal expressions of these domains in a small sub-catchment of the Alkali Creek study area (using both watershed maps and raingauge records) in Chapter 2, Chapter 3 simulates the spatial intensity domain on slopes and in the channel for snowmelt, and Chapter 4 does the same for overland flow. In these latter two Chapters, fieldwork designed to calibrate and test the models is included. In Chapter 5, watershed materials are considered in terms of their sensitivity to the simulated flows, and here the calibrated sediment rating curves are presented, which are then used to translate the weighted channel simulations into sediment

yield values for each site during each simulated event. The two processes are then compared in 'importance' at a variety of watershed positions.

Using these models to describe patterns of scour and fill allows these spatial yield differences and the stream power of simulated flows to be compared as tools of morphological explanation in Chapter 6. At this stage the questions of landscape sensitivity and change, outlined in Section A, are readdressed in the context of the snow-fed semi-arid landscapes of the western slope of Colorado.

CHAPTER 2

THE STUDY AREA

In this Chapter, the Upper Alkali Creek study area, which lies in semi-arid, snow-fed Western Colorado, is presented as an appropriate environment within which the concepts outlined in Chapter 1 may be examined. First, the suitability of the geological setting, and the erosive nature of the Wasatch Formation in Western Colorado are described. Secondly, local precipitation, snowmelt, and discharge data are examined, and two temporal process intensity domains (those of snowmelt, and of overland flow following summer storms) are identified within the local climatic record. Thirdly, the Alkali Creek study area is described, from which discussion the spatial expression of these two process intensity domains is inferred. Following from this, the gully morphology is examined. Since sequential data is available, long-term patterns of erosion and deposition in the network emerge from which functional zonations can be hypothesised. These zonations can be compared to those described in other snowfed, semi-arid areas by Schumm (1977), and Bergstrom, (1980). It is suggested that at Alkali Creek these patterns result from interaction of the two process intensity domains already described.

The final section outlines the objectives of the work which follows in the remaining Chapters in terms of the conceptual and environmental picture presented so far.

(I) WESTERN COLORADO

(A) The geological setting

The part of Alkali Creek chosen as a study area (Figure 1) is a small (0.4 km^2) sub-catchment of the U.S. Forest Service 'Alkali Creek Soil and Water Project' basin in Western Colorado. Alkali Creek flows into West Divide Creek, a large (167.7 km^2) gauged river whch in turn joins the Colorado River 20 km north of the study area, near Silt.

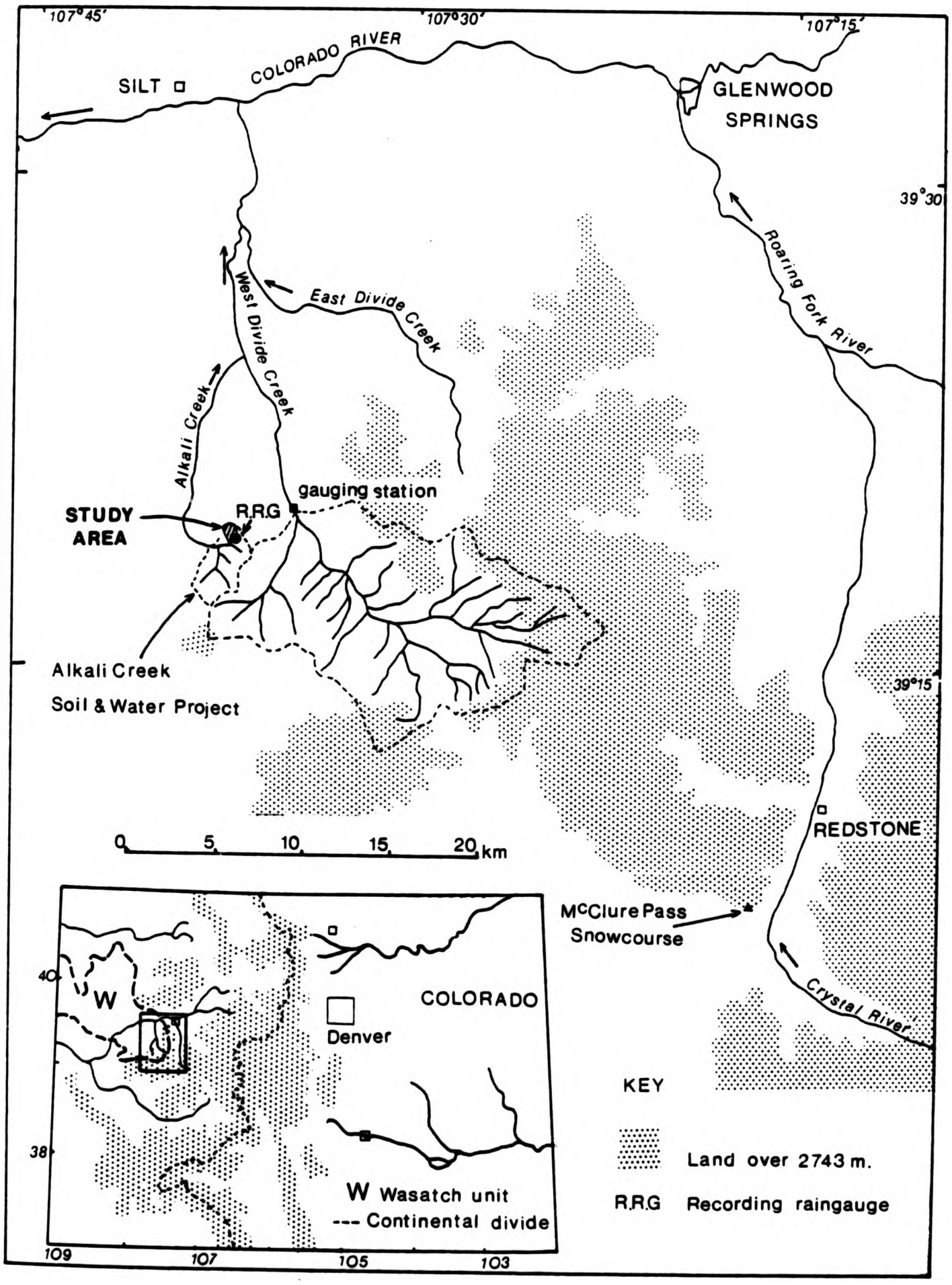

Figure 1: The Study Area

The combined headwaters of the East and West Divide Creek (including Alkali Creek) drain almost 300 km^2, forming part of the variable relief plateau generally referred to as the western slope (see inset, Figure 1). The area is high, rising at the top of West Divide Creek to 3085 metres. In the study area, elevations range from 2372 to 2560 metres a.s.l.

Much of the bedrock forming the Western Slope is of Pre-Cambrian age, with Middle Tertiary volcanics, mostly of basalt lenses and sheets, with some cinder cones. In the study area, however, these rocks are absent due to the faulting and overthrusting associated with the Laramide orogeny which threw up the Grand Hogback north of Silt, and placed older rocks west of Glenwood Springs. Later erosion of these eastern rocks in the Eocene and Palaeocene periods resulted in a sedimentary basin, now 1650 metres deep in the Piceance area (Tweto, 1973). In the study area the main unit of this sequence exposed is the Wasatch formation (Figure 1), which consists of shales and claystones, interbedded with volcanic material derived from the erosion of the eastern rocks.

In exposures of the Wasatch seen on the lower slopes in West Divide Creek, the unit consists here of arkosic sandstones and some conglomerates with clasts of the pre-existing Pre-Cambrian, and andesitic and dacitic volcanic rocks; a type described by Gaskill and Godwin (1966). At Alkali Creek, however, the unit appears to consist of claystones and shales (Photo 1) as described by Donnell in 1969 and mentioned by Tweto (1973) as more typical of the northern Piceance basin. Interbedded with these sodic clayshales are horizontally bedded lenses of arkosic sandstones which appear locally well-indurated. Recently, erosion has been accelerated by the White River uplift which began in the Wasatch period and may still be continuing. "... The uplift .... was probably also a source of sediment", (Tweto, 1973).

In the Quaternary period, glaciation was not extensive; in the Henry mountains further west, land over 3050 metres was above the snowline, and on the western slope in general only limited glacial deposits in cirques have been noted (Kottlowski et al, 1965), although Hunt (1956) noted three Pre-Wisconsin tills on the Colorado plateau north-west of Battlement Mesa. Hack (1942) has identified

Photo 1 : An exposure of the pink and buff claystones and shales of the Wasatch unit in the study area

Photo 1 : An exposure of the pink and buff claystones and shales of the Wasatch unit in the study area

three separate stages of alluviation, dating from this stage up to 1880, separated by periods of arroyo trenching, which appear to be more dominant in the landscape locally than glacial remnants. In the Alkali Creek area, the lower channel course cuts through an alluvial fill which is presumed to date from this period, although it has been suggested that this fill may be partly soliflucted material from earlier in the Quaternary.(1)

The swelling sodic clays of the Wasatch, which form the bulk of the headwaters and slope areas within the study area, produce poor soils under the present climate, prone to slaking and surface wash where vegetation is thin or removed. The resulting high rates of erosion mean that whereas in highly resistant landscapes it can be difficult to separate inherited from currently produced landforms, in highly sensitive low-resistance clayshales like these at Alkali Creek, only a short geomorphic record is retained. As a result, the investigation of form-process interrelations can be conducted without the confusion of landforms inherited from different climatic periods. This has proved to be an advantage in the current investigation.

(B) The climatic setting

Collbran (1889 m), is about 24 km south-west of the study area, and is the nearest weather bureau station. The average January temperature at the weather station is -5.6°C, whilst the July average is 20.4°C, however, a maximum of 38.3°C has been recorded. Mean annual precipitation on the Western Slope generally ranges from 203 mm to 813 mm per annum,(2) the study area receiving an average of 471.8 mm p.a. (1961-1972).(3) This low

---

(1) PERS. COMM., Ron Taskey, Univ. of California Soil Science Department.

(2) National Atlas of the U.S.A., 1970. U.S. Dept. of the Interior, Geological Survey, Washington, D.C.

(3) Recording rain gauge charts made available from the U.S.D.A. Forest Service, Rifle Ranger Station, Rifle, Colorado

total falls partly in the winter months as snow which accumulates slowly, to form a snowpack which persists until spring. Isothermal conditions occur in the snowpack in the early spring causing a sudden, dramatic snowmelt flood lasting five to six weeks. In the summer months, by contrast, high intensity, short-duration storms caused by convective cloudburst activity are common and these events produce overland flow on unprotected surfaces from which runoff and erosion are severe.

These two precipitation types have a distinct temporal expression, and this is reflected in the annual hydrographs of regional rivers. On Figure 2, monthly precipitation totals in centimetres derived from the automatic recording raingauge (R.R.G.), which was installed in the study area between 1967 and 1972, have been plotted in histogram form on a time-base. On the same base, the hydrograph from the larger, adjacent watershed of West Divide Creek[(4)] has been superimposed, in mean daily cumecs (where 1 cumec = $1m^3/sec.$) Because of the great range in these values, a log scale on the vertical axis is used. The precipitation trace from the automatic R.R.G. records allowed further analysis to be conducted on the summer storm behaviour. For each storm event the date, total precipitation, and duration could be easily read directly from the trace, from which intensity (total/duration) could be calculated. Plotting these data as bar graphs and triangles respectively on the same time base allows links with peaks on the West Divide Creek hydrograph to be inferred. (Data are in Appendix 1).

Also on this same Figure, an estimate of the accumulation of the snowpack and its depletion at Alkali Creek has been added. The Soil Conservation Service (S.C.S.) in Denver suggested that the monthly precipitation values should be accumulated, making no allowance for drifting and sublimation, between October and March, to give an estimate for the snow water equivalent (S.W.E.) in the accumulating pack. Since notes written on the rain gauge charts give an

---

(4) U.S. Geological Survey, Water Resources Data for Colorado, Vol.2, 1967-72

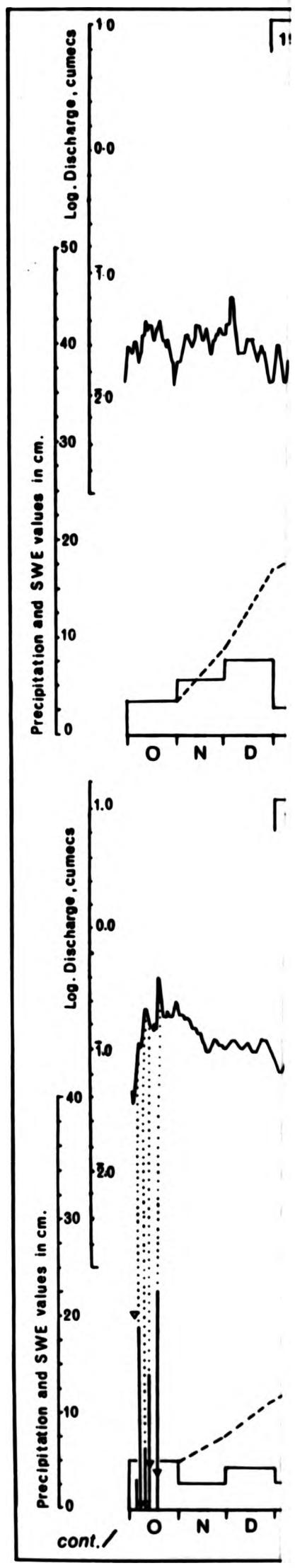

Figure 2: Climatological and Hydrological Characteristics of the Study Region 1967-1972

Figure 2: Climatological and Hydrological Characteristics of the Study Region 1967-1972

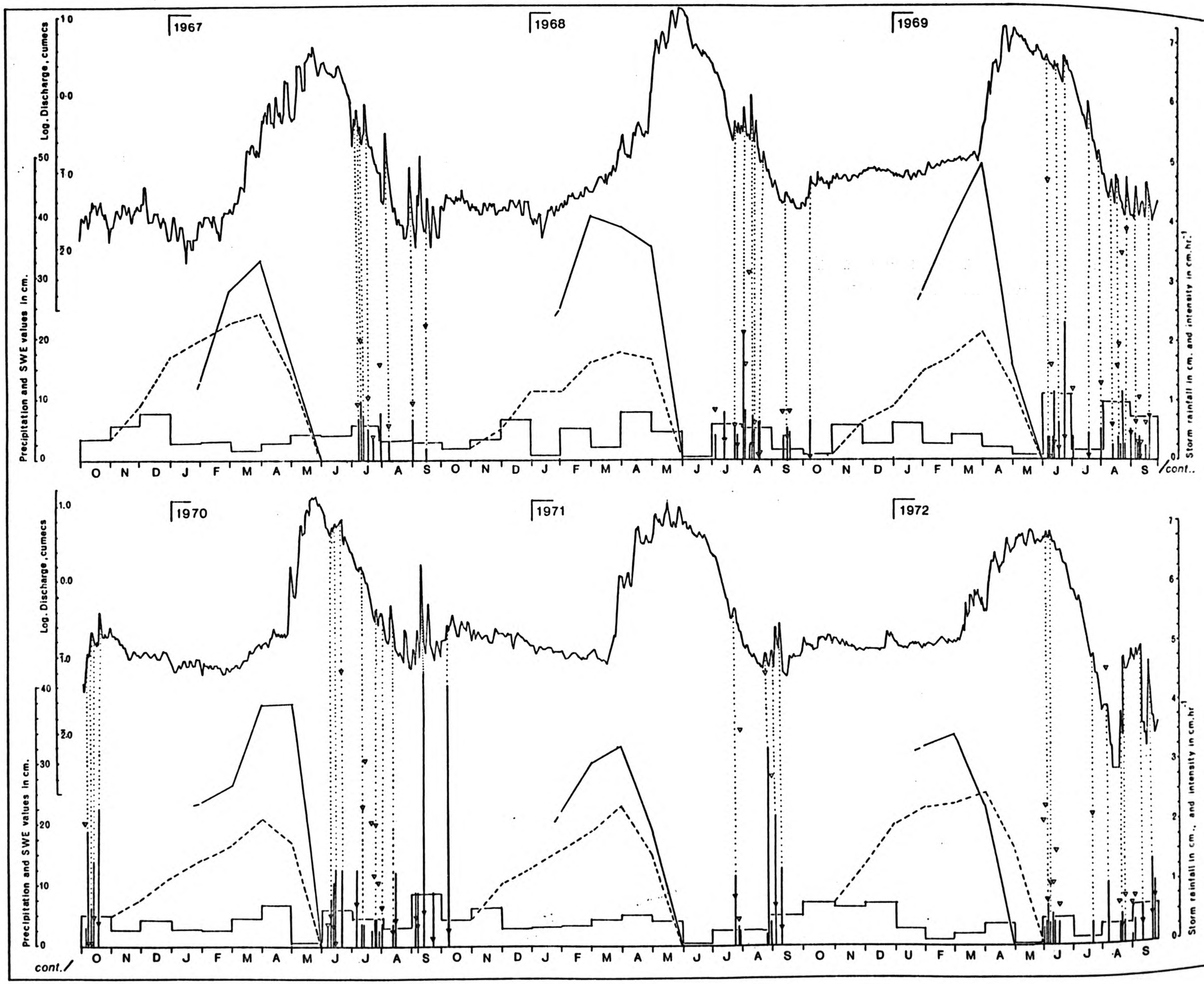

KEY

West Divide Creek Hydrograph;
Mean daily flows
(USGS data)

McClure Pass Site
Snow Water Equivalent
Feb 1 - June 1
(SCS data)

Alkali Creek Site
Snow Water Equivalent
(RRG estimate)

Alkali Creek
Monthly Precipitation
(RRG)

Alkali Creek
Summer Storms.
← Intensity;
← Inferred links;
← Total rain for event.
(RRG)

indication of melt commencement and end, the pack was assumed from these clues to have an eight-week melt, from March 31st to May 30th. Assuming the melt to be a linear process, the S.W.E. value for the end of April was therefore estimated for each year in the following way:-

$$\text{S.W.E. April 30th} = \left[\frac{\text{S.W.E. March 31st}}{2}\right] + \text{snowfall for April}$$

These estimates have been plotted on Figure 2.

As a comparison, the S.W.E. values for the nearest S.C.S. snowcourse, at McClure Pass (Figure 1) were obtained.(5) This is an accurate site, being doubly calibrated with a snow pillow which measures snow water content directly. Although higher than the study area at 2652 metres, it is on a south-facing site and is comparable to Alkali in other respects. Only data for January to April is available for the McClure Pass site, but a visual examination of the pattern of these data and the Alkali Creek estimate reveals some parallelism between the two. From this comparison, the estimation procedure appears at least partly justified. (All the data used in the construction of Figure 2 have been included as Appendix 1).

The hydrograph trace from West Divide Creek can be regarded as the resultant of two distinct flow contributions. The first, and most significant, contribution is clearly from snowmelt. As the water equivalent values in the snowpack at McClure pass and at Alkali Creek fall, so the discharge rises in West Divide Creek, showing a uniform trend paralleling the collapse of the regional snowpack. These snowmelt flows reach a peak in early June each year, which ranges from 5 cumecs in 1967 to over 11 cumecs in 1970. From the peak value, recession occurs occasionally in two phases (for example, in 1969 and 1971), but in other years following a simple inverse logarithmic trend (for example, in 1970 and 1972). The differences in recession rate may be due to variable radiation receipts during the melt period. West Divide Creek maintains a low baseflow

---

(5) Records held at U.S.D.A. Soil Conservation Service, Diamond Hill, Denver, Colo. (Water Years 1967-72 used).

component right into July, which is possibly groundwater recession (from a snowmelt recharge), gradually depleted during the summer months. However, such flow is unlikely to contribute to flow at Alkali Creek, partly because of the highly impermeable surface, short steep slopes, and shorter melt in the study area.

The second major flow contribution to the West Divide Creek hydrograph comes from summer storms. Although not all the events recorded at Alkali Creek produce a corresponding peak on the West Divide Creek hydrograph (possibly because of downstream transmission loss, or narrow storm tracts), nevertheless there is sufficient connection for the source of these peaks to be convincingly linked to summer storm activity - as for instance the events recorded at Alkali and West Divide Creek in mid-September 1970 and those in late August and early September, 1971. The rest of the year shows very little or no flow. Since in the late autumn and winter months the snowpack is accumulating, the small discharges recorded must be linked to deep baseflow recession in the lower parts of the watershed, and at such times there is unlikely to be any flow at all in the channels of the study area.

(i) Temporal Process intensity domains in Western Colorado

This examination of part of the climatic record of the Western Slope leads to the conclusion that there exists here evidence of two distinct temporal hydrological process intensity domains; those of snowmelt and of overland flow following summer storms. The relative importance of these processes varies during the year, with the snowmelt domain lasting from late March to early July and dominating the flow record, particularly in late May and early June. Summer storms are randomly variable within their temporal domain by contrast, this lasting from early June to late September. The two domains superimpose their flows at the West Divide Creek site from early June to mid or late July.

These observations concerning the relative dominance and extent of temporal superimposition of the two domains are specific to the size, elevation and relative relief of the contributing area above the gauging station. Because West Divide Creek drains a much larger area than Alkali Creek, and encompasses a much broader range of

elevation zones, it is not surprising that the temporal expression of snowmelt dominates the annual flow pattern in this way. On a watershed of this size, too, the effect of summer storms will be damped, due to downstream transmission losses in the headwaters where flow is generated, resulting in a far less significant overland flow contribution when recorded downstream. On a smaller site like the Alkali Creek study area, the relative domain dominance may shift in favour of the summer events, and because of the smaller relative relief and the lower elevation of the basin mouth, the melt flows will be somewhat earlier, and briefer.

To illustrate some of these points in a purely hypothetical manner reference can be made to Figure 3. Since Graf (1982) has suggested that stream power of watershed flows is a useful index of geomorphic behaviour, and since it is the product of discharge and gradient of the stream channel bed, then this summed value for melt and storm flows could behave downstream as shown on Figure 3a. The pattern for overland flow, it is suggested, would reach a peak value as headwaters join, and lose power partly by transmission loss and partly due to down-valley gradient reduction thereafter. By contrast, snowmelt dominates the summed pattern of stream power downstream because the frequency weighting of melt flows renders these clearly dominant. Consequently the summed melt power pattern increases away from the headwaters despite gradient reductions, declining only as lower elevations cease to provide snow to downstream sites. The approximate positions of Alkali Creek and West Divide Creek have been indicated, showing that overland flow erosion may be proportionately more significant in upstream positions, such as the study area.

Apart from spatial effects such as these, the extent of temporal superimposition of the domains will shift too, in this case with elevation and with relative relief (Figure 3b). Elevation controls the time of the onset of melt at the basin mouth, and relative relief controls the time-distribution of melt, since differing elevation zones melt out at differing times. Relative relief is thus inversely related to peakedness of the snowmelt hydrograph (Thomson and Striffler, 1980). The effect this would have on the Alkali Creek snowmelt pattern is suggested on Figure 3b. These

elevation zones, it is not surprising that the temporal expression of snowmelt dominates the annual flow pattern in this way. On a watershed of this size, too, the effect of summer storms will be damped, due to downstream transmission losses in the headwaters where flow is generated, resulting in a far less significant overland flow contribution when recorded downstream. On a smaller site like the Alkali Creek study area, the relative domain dominance may shift in favour of the summer events, and because of the smaller relative relief and the lower elevation of the basin mouth, the melt flows will be somewhat earlier, and briefer.

To illustrate some of these points in a purely hypothetical manner reference can be made to Figure 3. Since Graf (1982) has suggested that stream power of watershed flows is a useful index of geomorphic behaviour, and since it is the product of discharge and gradient of the stream channel bed, then this summed value for melt and storm flows could behave downstream as shown on Figure 3a. The pattern for overland flow, it is suggested, would reach a peak value as headwaters join, and lose power partly by transmission loss and partly due to down-valley gradient reduction thereafter. By contrast, snowmelt dominates the summed pattern of stream power downstream because the frequency weighting of melt flows renders these clearly dominant. Consequently the summed melt power pattern increases away from the headwaters despite gradient reductions, declining only as lower elevations cease to provide snow to downstream sites. The approximate positions of Alkali Creek and West Divide Creek have been indicated, showing that overland flow erosion may be proportionately more significant in upstream positions, such as the study area.

Apart from spatial effects such as these, the extent of temporal superimposition of the domains will shift too, in this case with elevation and with relative relief (Figure 3b). Elevation controls the time of the onset of melt at the basin mouth, and relative relief controls the time-distribution of melt, since differing elevation zones melt out at differing times. Relative relief is thus inversely related to peakedness of the snowmelt hydrograph (Thomson and Striffler, 1980). The effect this would have on the Alkali Creek snowmelt pattern is suggested on Figure 3b. These

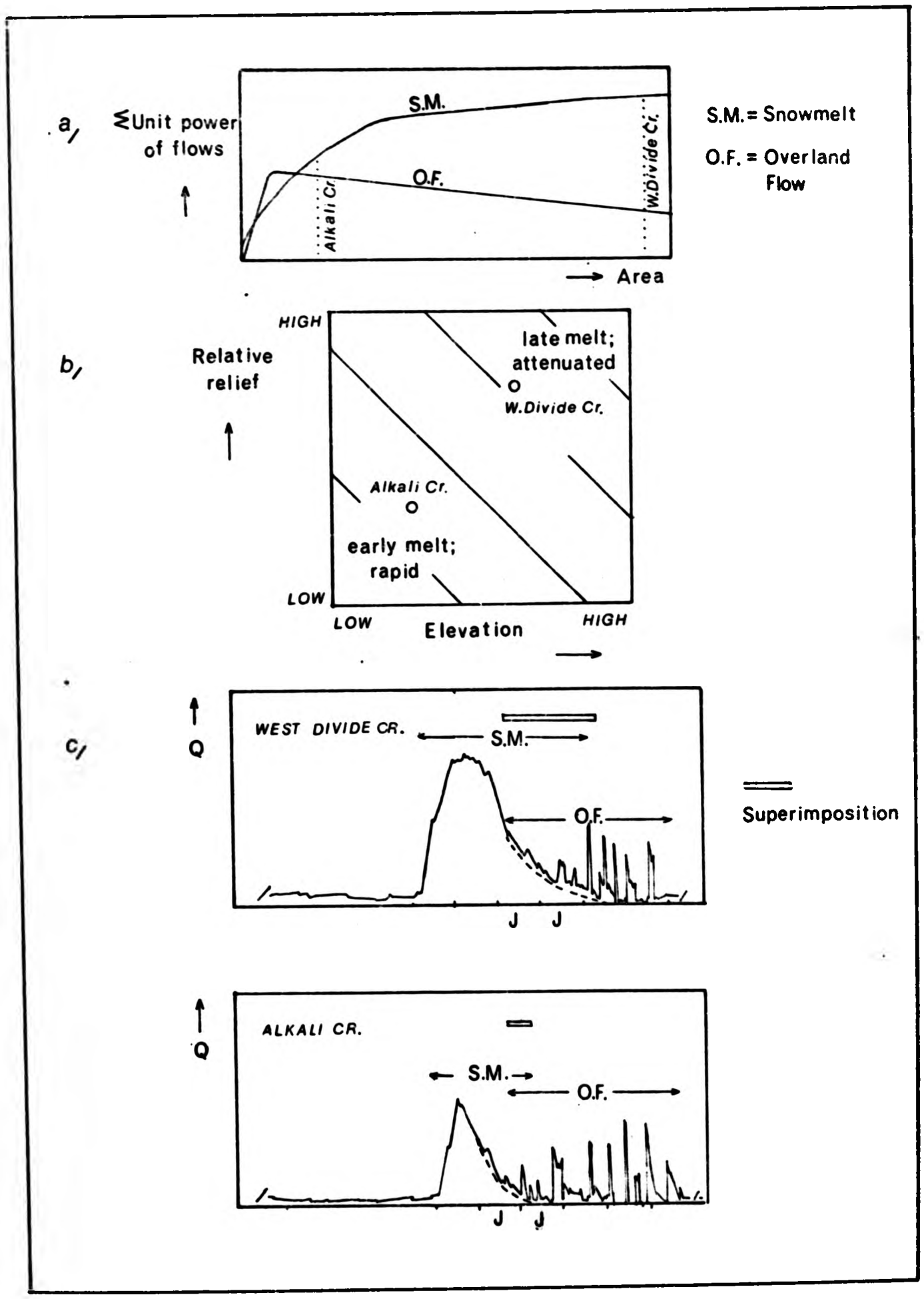

Figure 3: Hypothetical relationships between
(a) Stream power and increasing area downstream
(b) Elevation and relief, and the effect this has on peak timing; and
(c) The resulting effects on local hydrographs

conjectures have been summarised in terms of their likely effect on the Alkali Creek hydrograph (Figure 3c); in this illustration a hypothetical Alkali Creek annual hydrograph is contrasted with an idealised annual hydrograph for West Divide Creek, showing the differing extent of flow dominance, and the reduction in superimposition.

In terms of a 'dual process' model, Alkali Creek represents an ideal location for a detailed examination of the effects of spatial domain overlap in particular, partly because the two domains are initially inferred to be more equal in terms of their morphological impact here, and also because they are less superimposed temporally, being more separate within the temporal record.

(II) ALKALI CREEK : TOPOGRAPHY, SOILS AND VEGETATION

The United States Forest Service has been involved in experimental work in the Alkali Creek Soil and Water Project since 1952. Because of this, the small subcatchment of the area used for this investigation had an extensive pre-existing data-base by 1975. These data consist not only of the rain gauge data already discussed, which were collected in the study area between 1961 and 1972, but also a soil survey conducted in 1957 by Fox and Nishimura, and a channel slope and excavation survey carried out by Heede in 1962 prior to check-dam emplacement on the main channel in the lower part of the watershed. Good aerial photography, both vertical and oblique is also available, from which a detailed map has been produced by the U.S. Forest Service, with contours at 3.05 metre intervals[6]. This map provides the base for Figure 4 (back folder), which shows the general topographic characteristics of the area.

The small, pear-shaped basin has a relative relief of 188 metres and is drained by a trenched channel and a network of small headwater gullies. Adjacent to the main channel are two discontinuous

---

(6) These data were made available to the present investigation by the U.S. Forest Service Experiment Station in Tempe, Arizona. Photogrammetry was undertaken by Air Photo Serveys, Inc., Grand Junction.

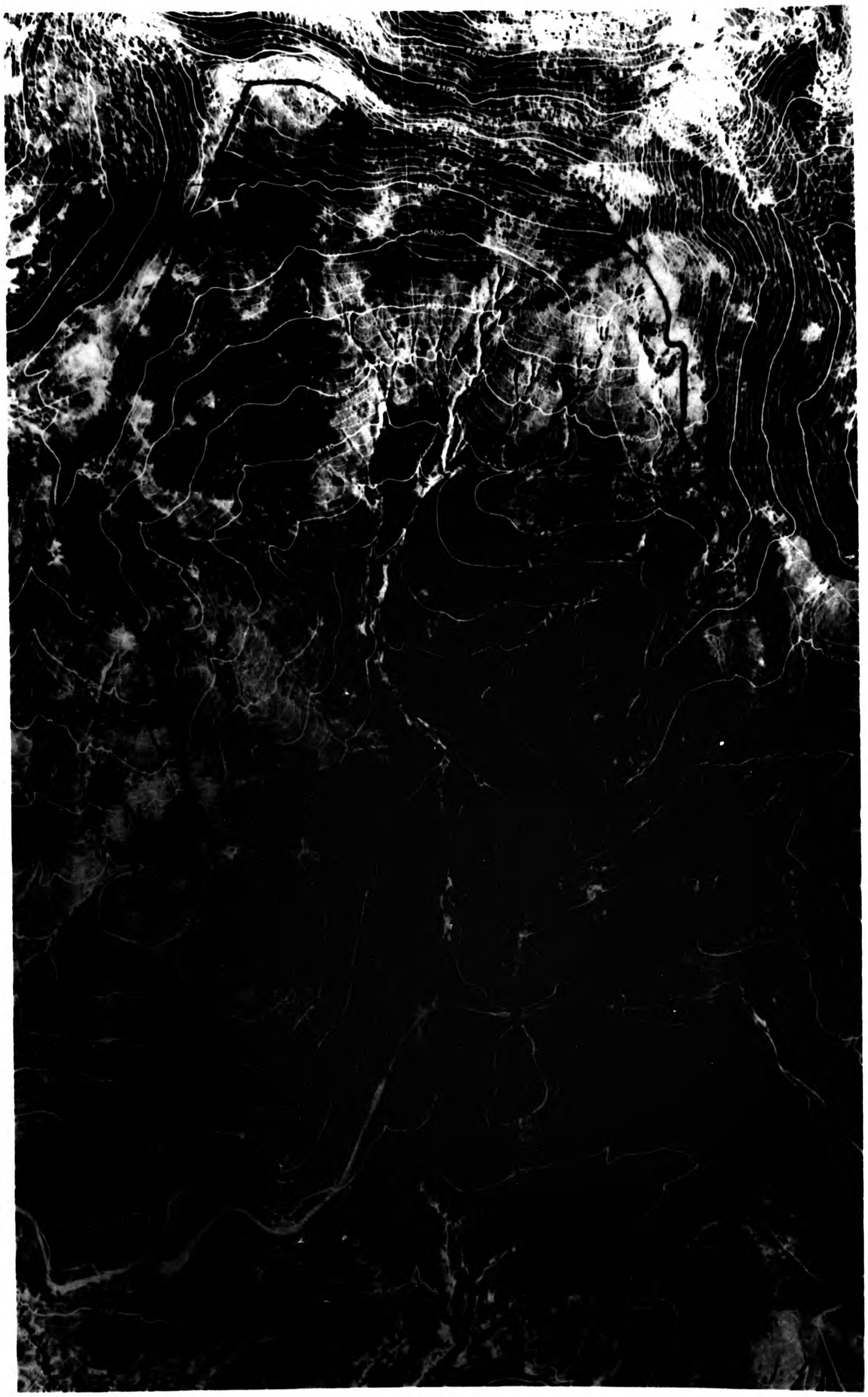

0 50 100 m.

Photo 2 : Contoured Aerial Photograph of the Study Area

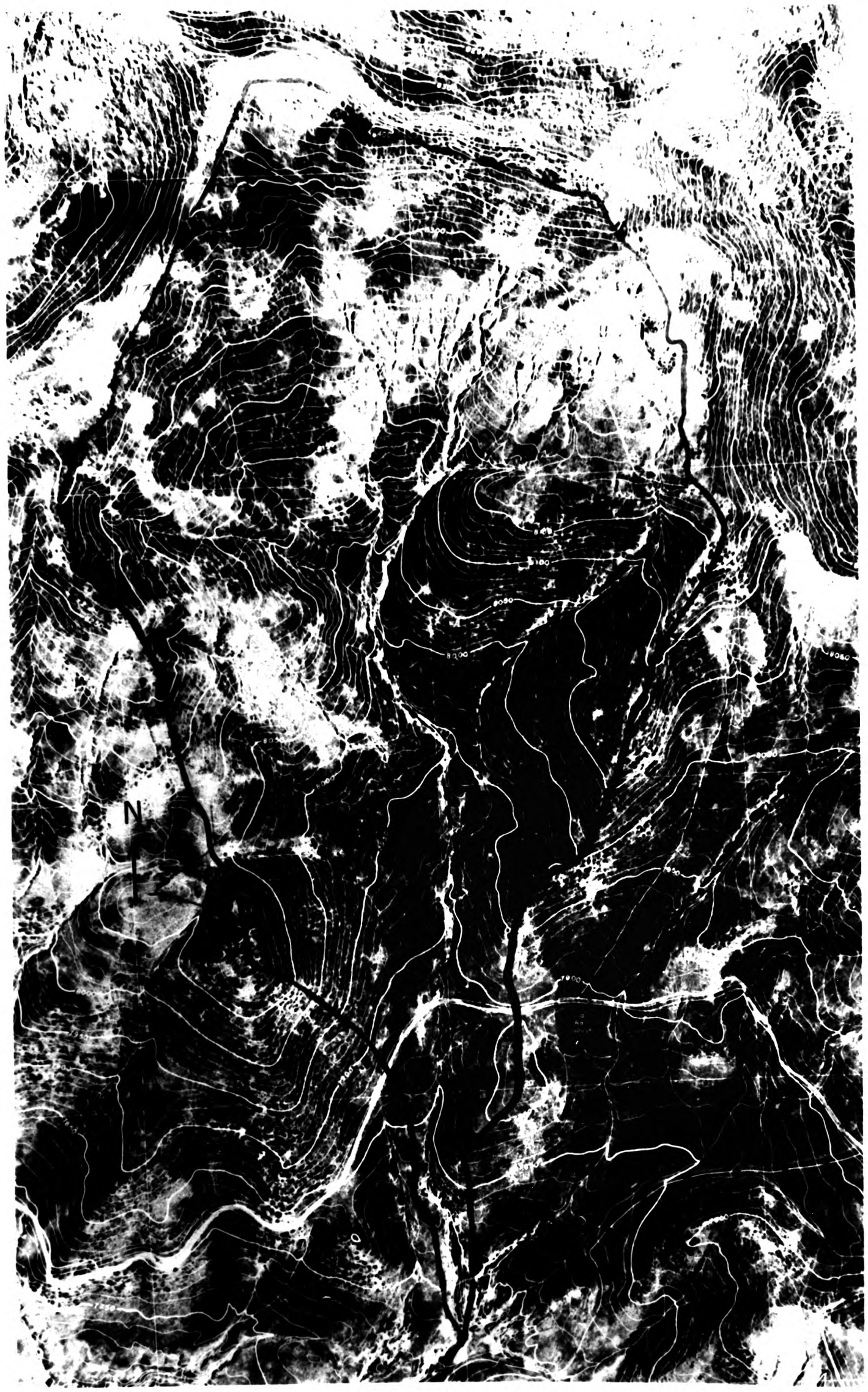

Photo 7 : Contoured Aerial Photograph of the Study Area


N

gullies, one in the upper western slopes, and another larger system on the eastern bank of the main channel. Both terminate in smallalluvial fans. The main channel, the headwaters and the two discontinuous gullies which flank it are, however, quite extensively trenched, and throughout the channel course the banks are bare, and precipitous in places. The aerial photograph (Photo 2) and the general views on Photos 3 and 4 show these characteristics, and Photo 5 illustrates the vertical nature of the gully banks at the main point of headwater tributary junction ('X').

(A) Slope Forms

Slopes in the study area are generally steep throughout. Channel gradients vary from 0.01 m/m to 0.03 m/m on the valley alluvium immediately adjacent to channels, rising to values of 0.08 to 0.25 m/m in the headwater areas. The headwaters have side slopes in the range 16^{o} to 32^{o}, and gully banks are mostly over 36^{o}.

An examination of the contour spacing on Figure 4 (back folder) reveals a series of minor topographic undulations across the headwater areas. These are formed by exposed lenses of the Wasatch sandstone, and have been mapped across the watershed as far as possible on Figure 5. Five separate exposed ledges were found in the study area with another possibly inferred from the topography. These ledges produce a stepped slope profile in the upper part of the catchment, where structure is not masked by vegetation. In general slopes appear increasingly detached from the channel at their base with increasing distance down channel, having in the lower course quite a pronounced basal concavity.

(B) Soils

The parent materials for soil development are the Tertiary sandstone and shales of the Wasatch formation. The sandstone varies from fine to coarse-grained and, in places, is strongly calcareous. In general, however, the soils of the area are predominantly formed from fine-textured, loose, unconsolidated shales with an admixture of sand from beds of sandstone. These highly erodible shales, combined with the climatic pattern already described, means that these soils are of a generally poor quality, with loam surfaces and heavy plastic subsoils (Fox and Nishimura, 1957).

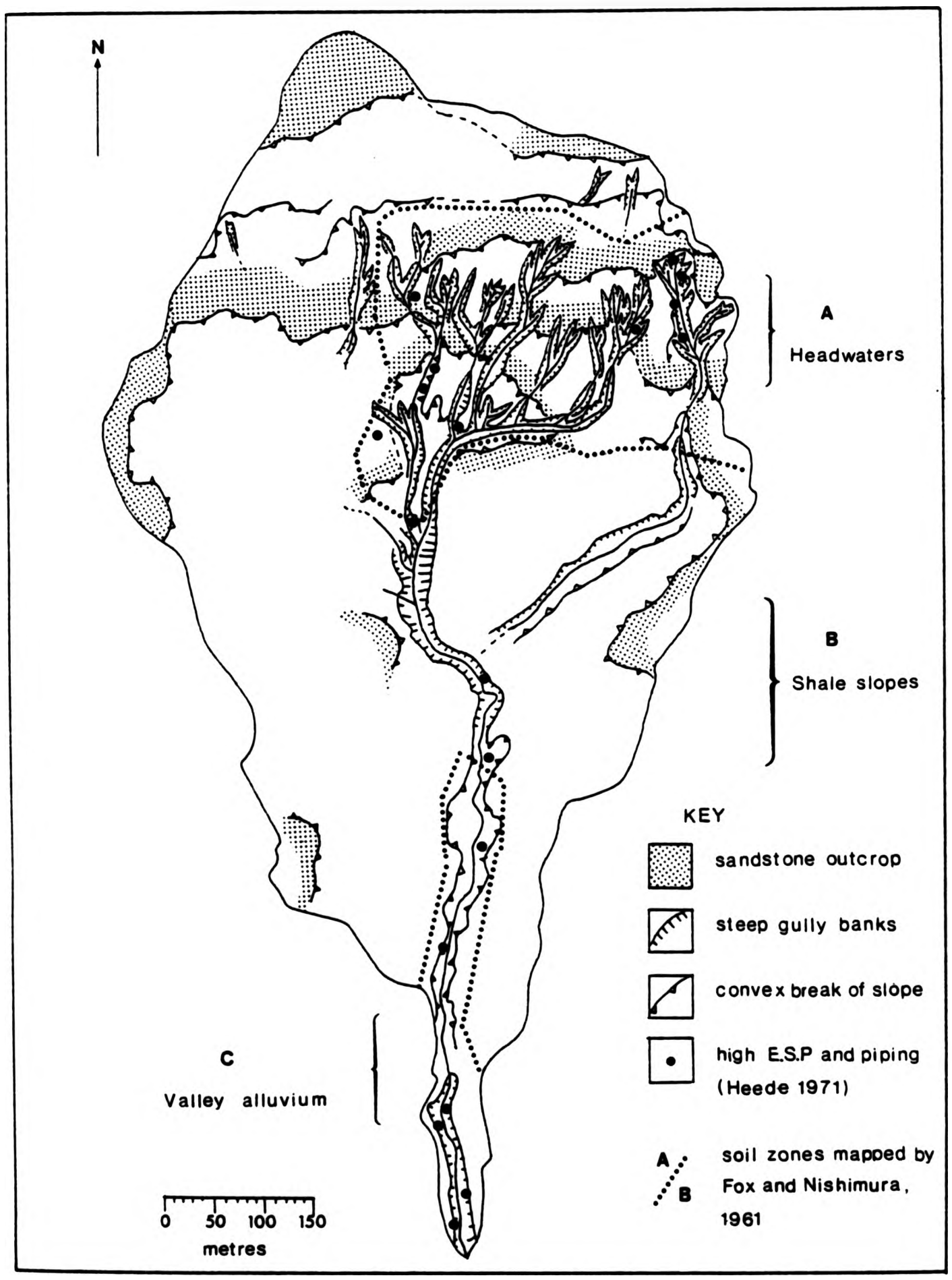

Figure 5: Aspects of the topography, geology, and soils of Alkali Creek

Photo 3 : An oblique view of the study area

Photo 4 : General view down the basin taken from point 'A'

Photo 3 : An oblique view of the study area

Photo 4 : General view down the basin taken from point 'A'

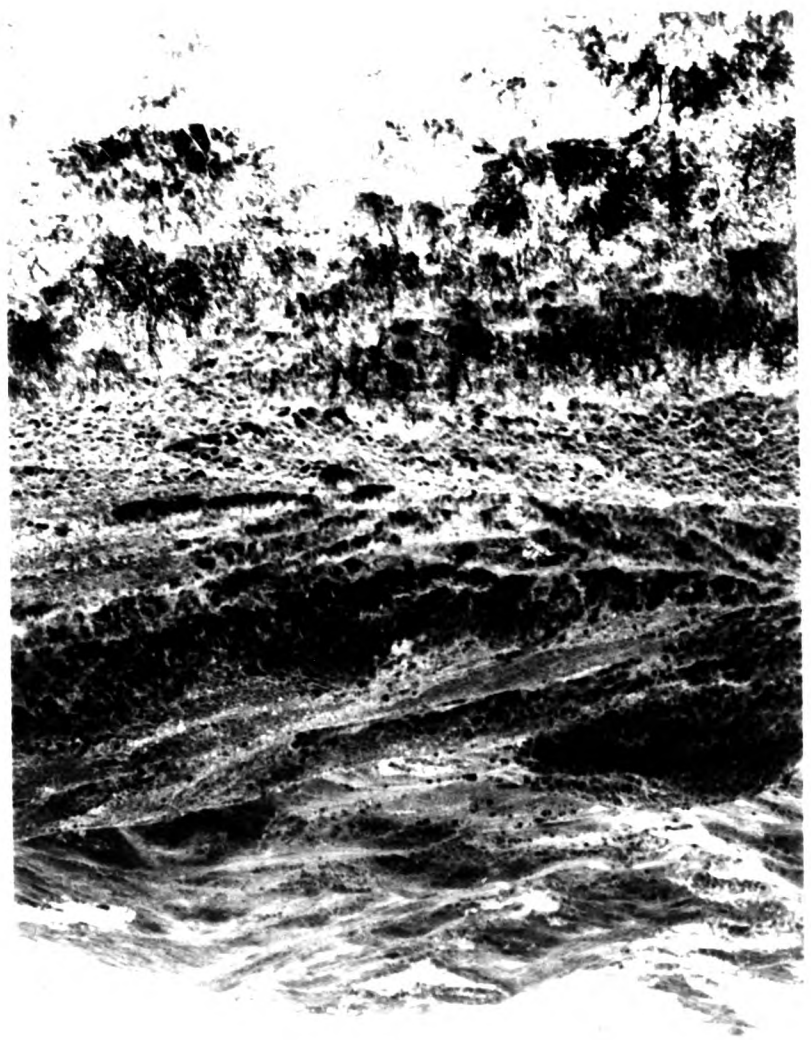

Photo 4 : General view down the basin
taken from point 'A'

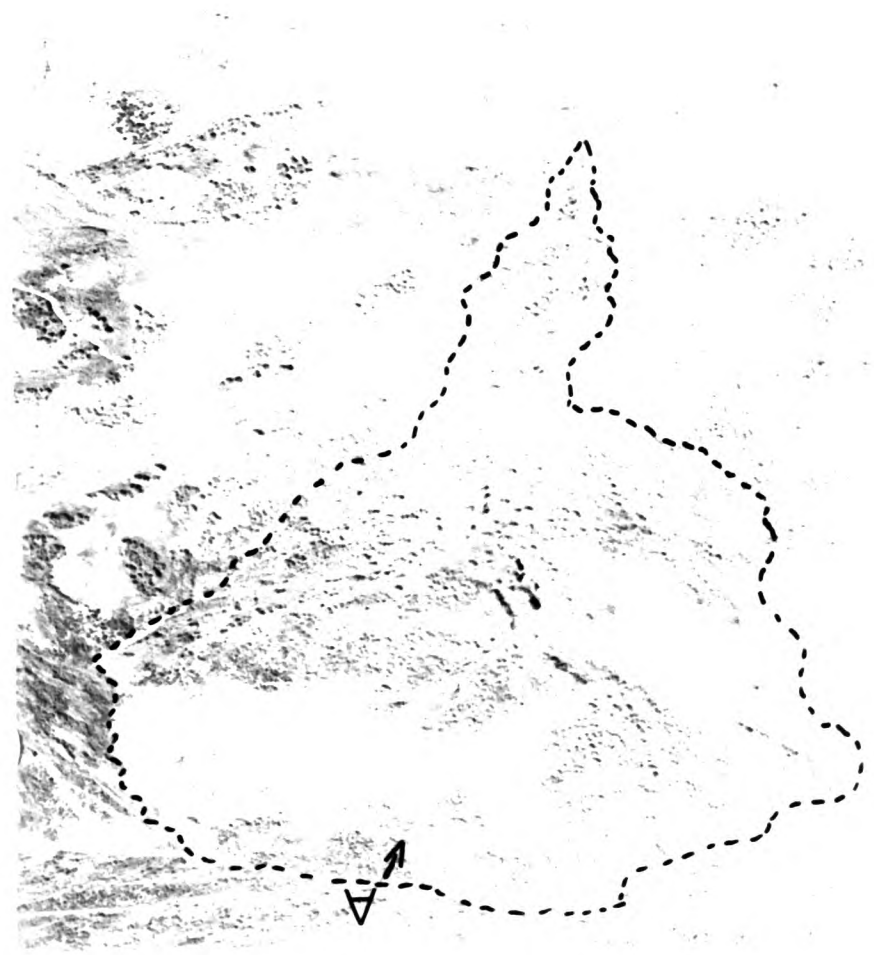

Photo 5 : An oblique view of the study area

(a)

(b)

Photos 5(a) and (b): The vertical nature of the gully banks around 'X', showing a 'popout' failure as it appeared in (a) 1975 and (b) 1980

(a)

(b)

Photos 5(a) and (b): The vertical nature of the gully banks around 'X', showing a 'popout' failure as it appeared in (a) 1975 and (b) 1980

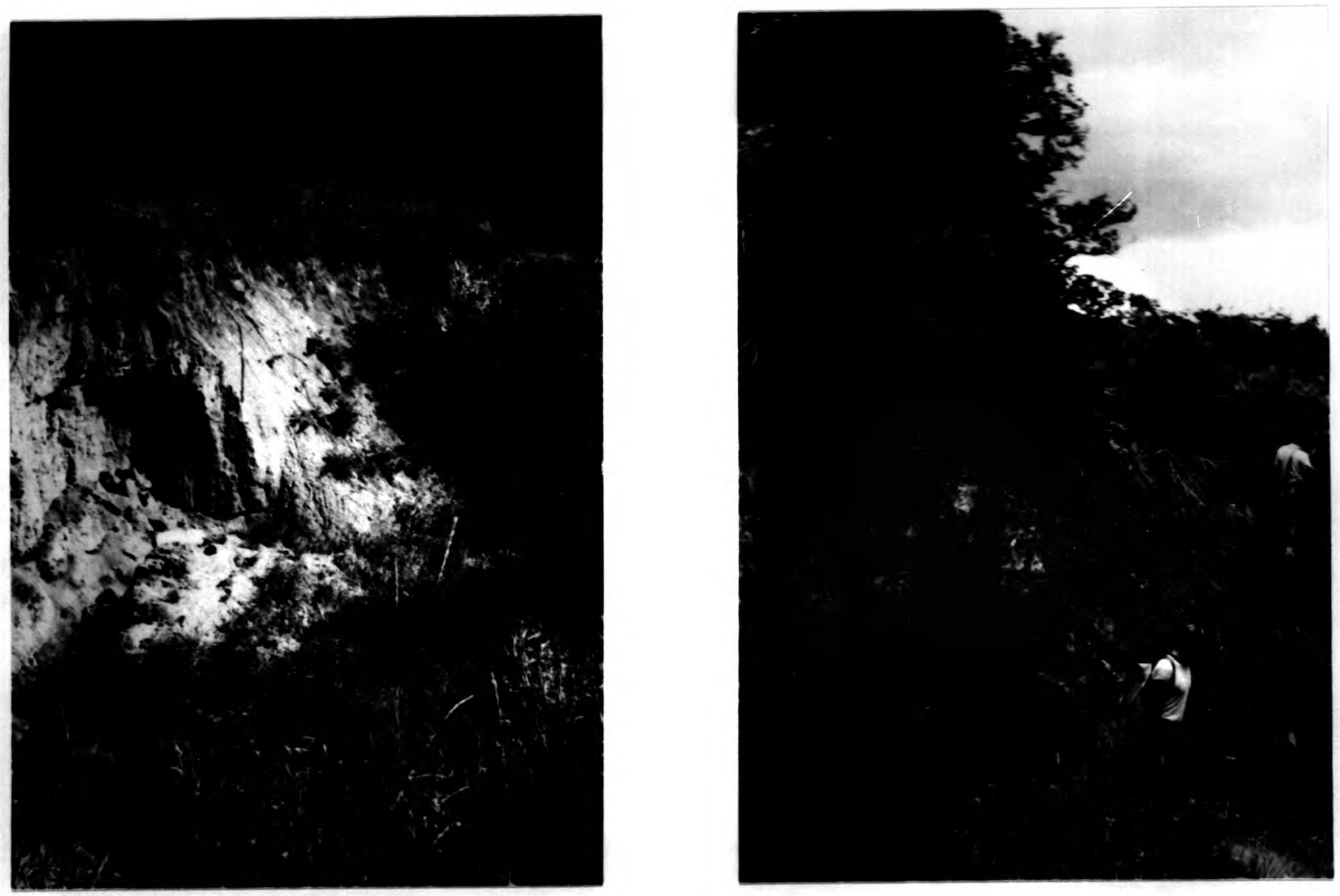

(a) (b)

Photos 5(a) and (b): The vertical nature of the gully banks around 'X', showing a 'popout' failure as it appeared in (a) 1975 and (b) 1980

The lime content of the parent materials is variable, ranging from noncalcareous to strongly calcareous. In many places the sandstone member of the formation is lime-cemented and weathers to calcareous soil parent material, but in other places iron is the principal cementing agent. It is expected that the soils contain sufficient amounts of all of the essential elements for plant growth except nitrogen, although the soils may be somewhat deficient in phosphates for some plants (Fox and Nishimura, 1957).

It is possible to recognise three main soil variations in the study area (Figure 5). These occupy (i) the badland area in the headwaters; (ii) the shale slope areas; and (iii) the zone of main channel alluvium.

(i) The badland area

The headwater areas are vegetation-free in most locations; and most of the soils are Solonetz. This soil type has been defined by Kelley (1951) as a clay-rich, alkali-sodic or saline-alkali soil in which the relocation of colloids by leaching produces a dense subsoil horizon prone to swelling. They have a columnar structure, the columns being generally 3 to 5 cm in diameter and 10 to 15 cm deep in the study area (Photos 6 and 7). Subsurface accumulation of soluble salts by leaching generally causes dispersion of the clays, and if a suitable hydraulic gradient and outfall site are available, this leads to piping. In the study area, high exchangeable sodium percentages (E.S.P.s) were noted by Heede in 1971, and he found that values of E.S.P. over 12 rendered local soils liable to dispersion, flocculation, and piping (Appendix 2).

In the badland area of the headwaters, many of the Solonetz columns were seen to be degenerate and thus less saline, with pH values 7.2 to 7.3 being more common than on actively piped sites, which had pH values over 8.0. On degeneration, the soil columns collapse into an almost 'inverted eggbox' appearance (Photo 8). This effect appears to be most closely associated with sites where clay shales are isolated from adjacent rocks of the same type by the sandstone lenses, which form minor structural ledges across this part of the watershed.

Photo 6 : Surface slaking and hexagonal cracking on the surface of the badland Solonetz (note the obvious depth of cracks)

Photo 7 : Many surface cracks accord with the subsurface columnar structure, implying infiltration and piping to be related to the location of these features

Photo 6 : Surface slaking and hexagonal cracking on the surface of the badland Solonetz (note the obvious depth of cracks)

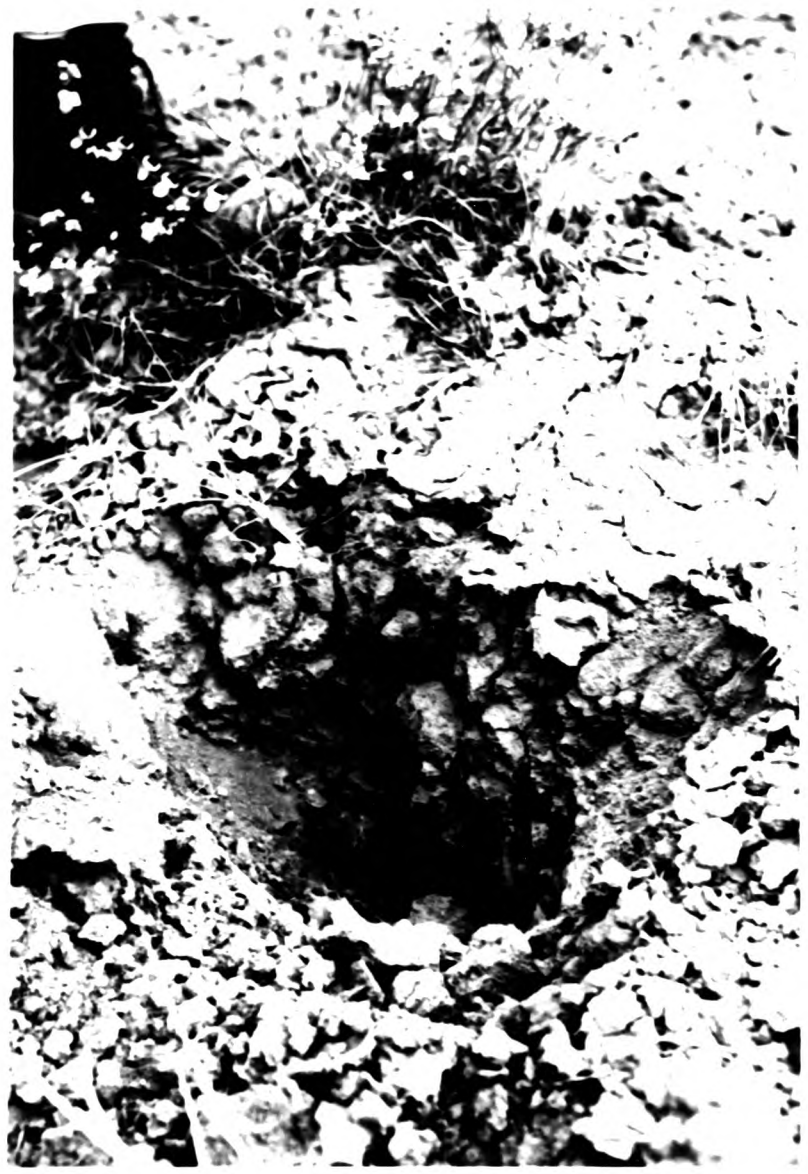

Photo 7 : Many surface cracks accord with the subsurface columnar structure, implying infiltration and piping to be related to the location of these features

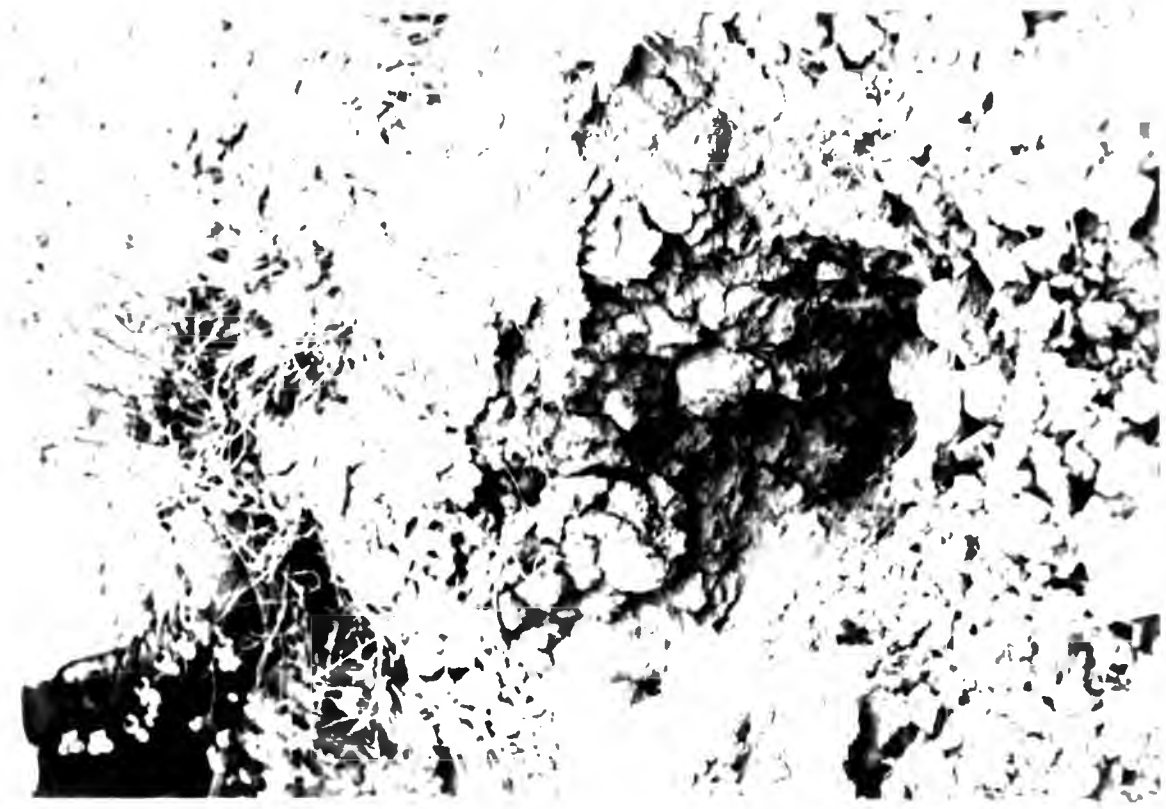

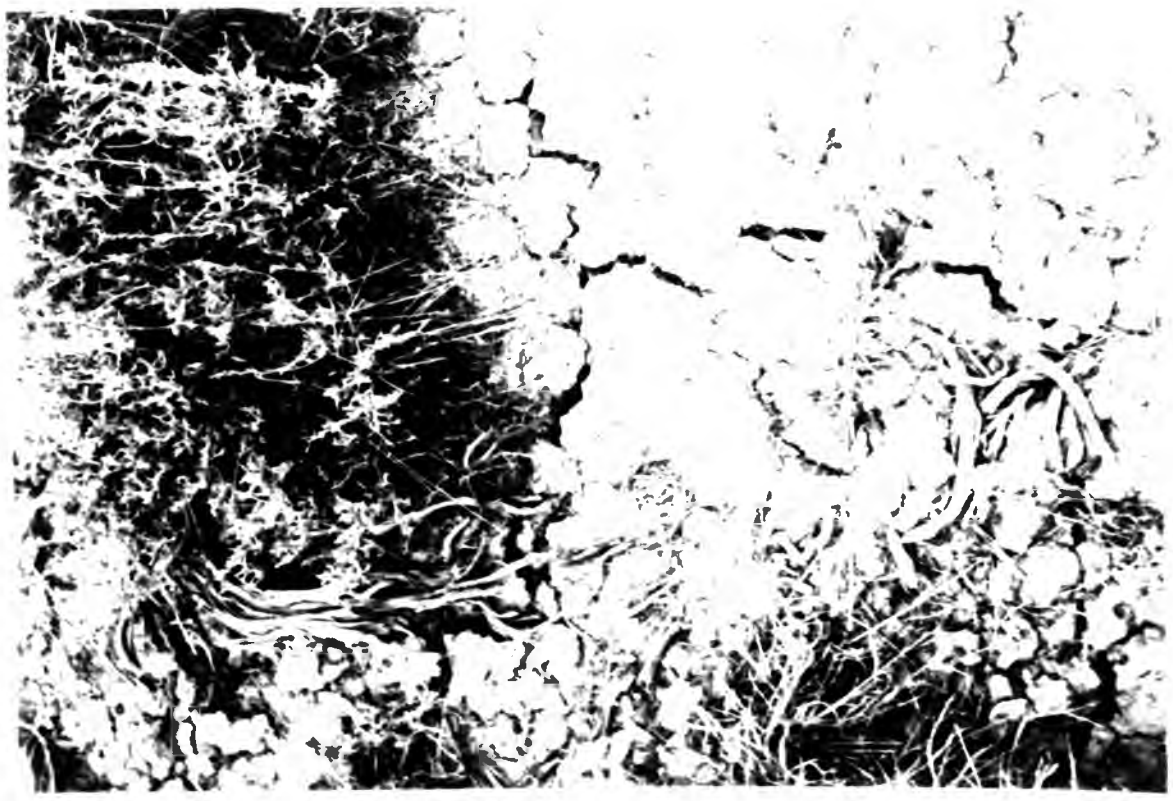

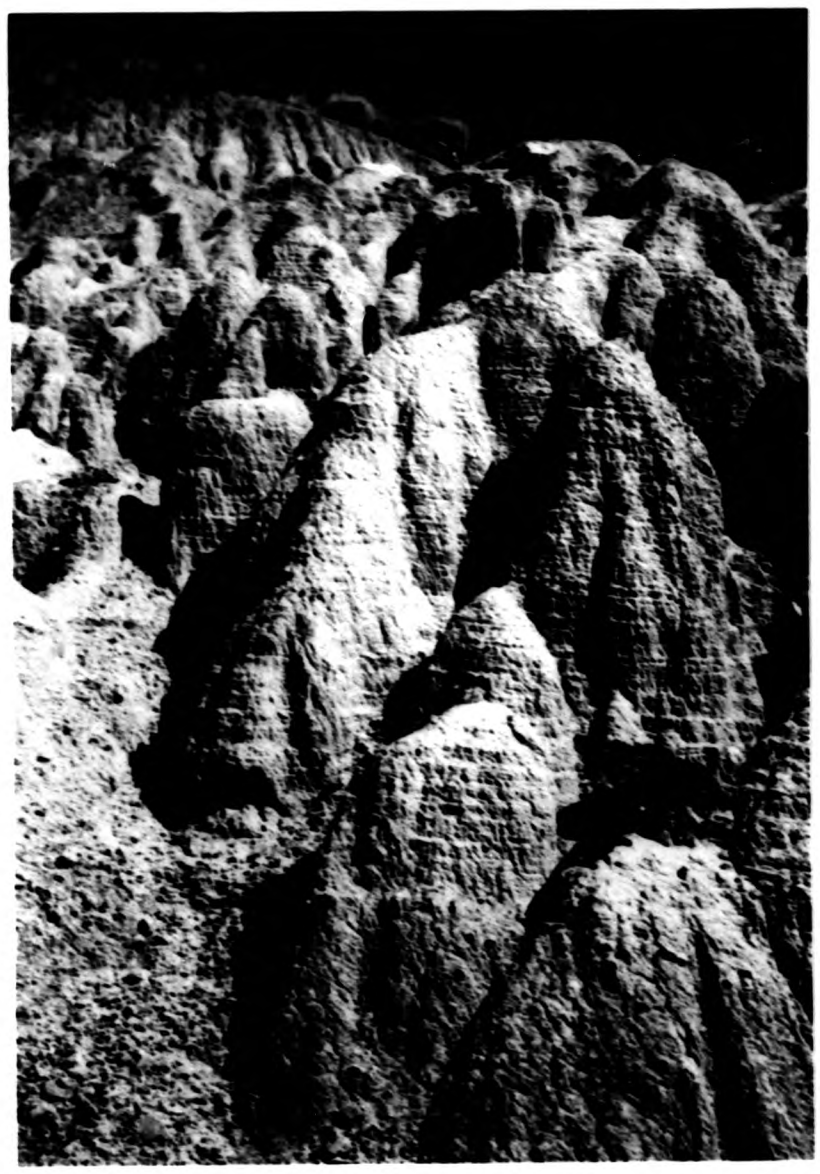

Photo 8 : The 'inverted eggbox' appearance of the degenerate piped sites in the upper part of the Large Discontinuous Tributary, located beneath a thin sandstone lens

Fig 10 - a The 'inverted eggbox' appearance of the dezenegrate piped sites in the upper part of the large Discontinuous tributary, located beneath a thin sandstone lens

Active pipes appear to be particularly associated with convex topographic forms (Figure 5) because of the hydraulic gradients and outfall possibilities which such sites provide. In some locations, pipe collapse has clearly accelerated gully extension, and in some areas actually initiated gullying, but this is felt to be the exception rather than the rule (Baillie, Faulkner et al, 1984). Field observations suggest that pipes form more commonly in the pre-existing convexities produced by the normal surface wash erosion of this area. Trenching of the surface wash gullies produces steep banks which provide the head and outfall necessary for the onset of piping, and in places are quite actively backwearing by this process. Thus, whilst it is recognised that piping does not contribute significantly to gully initiation, it may play a secondary, cosmetic role in channel widening in parts of the watershed headwaters, and may be a source of sediment to the accumulating channel flow. The role played by pipes in sediment production and geomorphic behaviour generally is reviewed in more detail in Chapter 5.

(ii) The shale slopes

Apart from gully bed and banks, most of the watershed outside the headwaters possesses a good vegetation cover. The Solentz soils which are present on these shale slope areas are therefore protected from high intensity rainfall and gully development. The soils show no sign of piping here, rather the soil profile develops a thin but distinctive A horizon which seems to be associated with a reduction in E.S.P. values. The soils described by Fox and Nishimura in this zone were characterised as possessing both magnesium and calcium in the profile. Heede (1971) noted that soils in these areas were 'stable', having E.S.P. values 1.0 (Appendix 2).

The soils on the shale slope area vary with aspect. Whereas on the south-facing areas the soil development remains thin, Fox and Nishimura (1957) point out that on north-facing slopes, denser stands of aspen and oakbrush have protected the soils from erosion. Here the thickness of the dark, organic layer varies from 23 cm to 25 cm, whereas on the south-facing aspects of the shale slopes the eroded soils vary from 0 to 20 cm in total depth, and on sites where vegetation is this thin the soil type may revert to the degenerate

Solonetz associated with zone (i). Clearly, these shale slope areas are liable to be very sensitive to surface wash erosion. These slopes are considered as a source of sediment in more detail in Chapter 5.

(iii) Main channel alluvium

On the lower course of the main channel, fairly deep alluvial deposits can be seen which are derived from the adjacent Wasatch shales. These are layered in places, possessing horizons of fine-grained material which may be alluvial or colluvial. The material is probably fairly recent, Pleistocene or later (Hack, 1942). The soil development is better here, drainage is improved and some soils support western wheat or western bluegrass. Despite the cover and the improved nature of these alluvial materials, they can still pipe, and in these deposits Heede (1971) described an impressive pipe complex which extended back into the main gully banks 5.5 metres which was "...associated with a dense vegetation cover", although "...no pipe inlets were found at a distance greater than 25 ft. (7.6m.) from the present edge of the gully." This would appear to reinforce the observations made earlier relating topographic convexity and pipe extension. Failure and bank collapse, especially in association with slopes weakened by piping, appears an important process on the main channel, contributing considerable material to channel processes. In conjunction with bed scour in these locations it must be imagined that this is an actively eroding channel zone. This possibility is once again considered in more detail in later Chapters.

(C) Aspect and vegetation cover

Along with variations in parent material, aspect (and the vegetation cover which it controls) largely explains the pattern of soils described above. The south-facing badlands area (i) is devoid of tree cover and supports only low-level shrubs, whereas the shale slope areas (ii) all have some sort of tree cover, especially on north and east-facing sites. The valley alluvium (iii) supports mostly grasses.

The control that aspect exerts on vegetation is visible from the aerial photo (Photo 2), and from the contoured vegetation map (Figure 4, back folder). In order to illustrate the highly asymmetrical vegetation response resulting from differences in aspect apparent on these Figures, and to provide a basis for the surface wash estimates which follow in Chapter 4, the vegetation cover within the watershed was mapped on a grid basis in the field in 1975 in conjunction with the U.S. Forest Service.

Using north-south compass bearings and a tape held horizontally, a series of cells were laid out across the watershed which had sides 61 metres long. The position of the tape and compass lines used to construct the percentage vegetation cover map are indicated on Figure 4 by an external grid. The total number of cells mapped was 142.

In each cell, percentage vegetation cover was estimated and type noted. At sites where quaking aspen (Populus tremuloides) and scrub oak (Quercus gambeli) were present, cover was always 100% because of the closed tree canopy. Elsewhere, where tree stands were separated and mixed with low-level shrub, such as silver sagebrush (Artemisa cana), or serviceberry in association, cover ranged from 60% to 100%. Where tree species were absent and brush was predominant, cover was rarely 100%, being mostly sage. Most sites were mapped with a cover of 40% to 60%. On the concavities at the base of the long slopes and in the alluvium in the lower channel, western wheat (Agropyron Smithii) was found, and other hydrophytic plants such as Thurber's fescue, Idaho fescue and bottlebrush squirreltail . These covers were quite dense, associations being mapped in cover ranges of 50% to 70%, depending on local conditions. In the headwater areas, bare sites were extensive and cover rarely reached 30%, being again sagebrush. Thus in general a strong correlation was found between percentage cover and cover type. Only percentage cover is mapped on Figure 4. From Figure 4, all steep south and south-west facing sites above 2470 metres are devoid of cover, whereas all north, north-east and east-facing slopes throughout have a cover of 100% (Photo 9). Below 2470 metres, south-facing and west-facing slopes have generally less cover than sites at the same elevation which face east or south-east. All flat sites on the lower part of the watershed support the grass associations, but these are absent

Photo 9 : A south-east facing view down the basin taken from the headwaters of the continuous network. This shows the steep nature of the watershed as well as the strong aspect-induced variations in vegetation cover

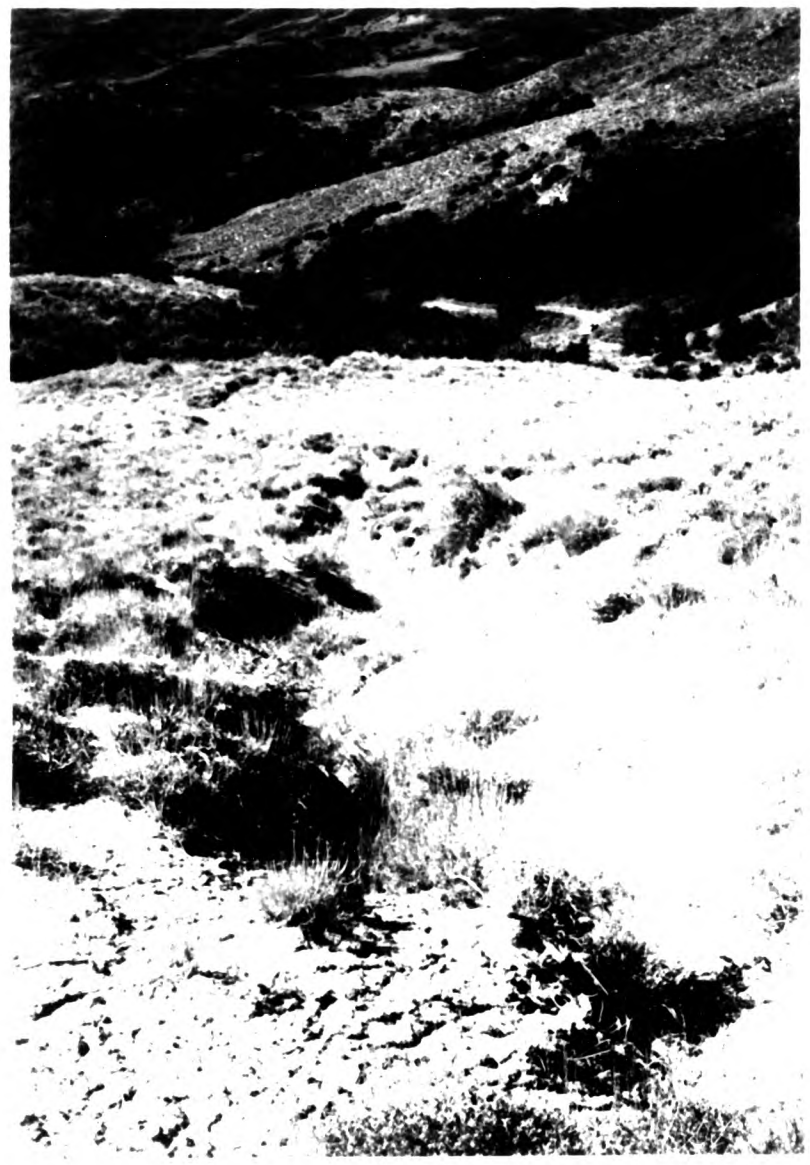

Photo 9 : A south-east facing view down the basin taken from the headwaters of the continuous network. This shows the steep nature of the watershed as well as the strong aspect-induced variations in vegetation cover.

Photo V-1 : A south-east facing view down the basin taken from the headwaters of the continuous network. This shows the steep nature of the watershed as well as the strong aspect-induced variations in vegetation cover.

above 2470 metres, and on flat sites are replaced by sagebrush, or the occasional isolated oak tree.

Rouse (1970) and Toy (1980) linked radiation receipts to evapotranspirative losses. At Alkali, particularly on the moister, north, north-east and east-facing slopes, much lower evapotranspirative losses retain sufficient moisture to support a good tree cover. This cover protects underlying ground from raindrop impact, and there is thus no evidence of surface runoff. South-east facing slopes are also moderately well-protected, and the difference between the upper south and south-west facing part of the watershed shows that the extra westerly aspect strongly influences cover density. In contrast, large radiation receipts on the higher, drier sites in the watershed rapidly reduce soil specific retention to below wilting point. This is more inclined to occur earlier on the Solonetz sites, which rarely produce wide tolerance conditions in any case, being highly alkaline, and higher up in the watershed where a more vertical soil water movement is most likely. Consequently, the south and south-west facing parts of the area have a much thinner cover, and are prone to surface wash erosion.

To draw together some of these observations, the variables influencing cover type and density are:-

(1) Aspect. This is the main control on vegetation cover type and density in the watershed.

(2) Elevation. This appears to be the second most important control, since above 2,470 metres western wheat is always replaced by silver sagebrush on flat sites, and the brush associations found on south and south-west facing slopes below this elevation rarely carry any vegetation above. It is thought that lower elevations have a more favourable soil moisture environment than higher up the watershed.

(3) Slope angle appears to be the third most significant variable, because it affects the extent of erosion on bare sites above 2470 metres and controls whether or not sagebrush or the aspen-oak association predominates in the lower elevation zones. Aspect does not have great variation here and so slope angle seems to be the controlling factor locally.

(D) Spatial process intensity domains as inferred from vegetation response, aspect and topography

The temporal process intensity domains will have specific spatial expressions within this complex terrain. For instance, overland flow intensity following summer storms will clearly be more extensive on the unprotected surfaces. The link between aspect, vegetation and surface wash was noted by Hack and Goodlett (1960), who found "...the drainage network is more developed on the south-west than in the north-east side of the (Appalachian) mountains..." and by Hadley (1966), who noted "...sheet erosion is 50 to 75 per cent greater on slopes that have southerly and south-westerly exposures than slopes that have other exposures...".

It is therefore strongly inferred that overland flow has a spatial intensity domain in the upper north-east part of the watershed which is related to the extent of bare surfaces here. Flows generated on bare sites rapidly exploit the parent material of degenerate Solonetz soils, which along with the sediment from piped sites will provide a large water and sediment input to the channel intensity domain. Depending on antecedent conditions and event size, transmission loss is likely downstream on the main channel below 'X', the main point of tributary junction. Additionally, flow volume is unlikely to increase significantly on this section since deprived of a lateral input, and so deposition may even occur.

Snowmelt flow generation follows a very different pattern to overland flow. It is known that snowpack accumulation favours elevation and north-facing slopes in particular, and that these slopes melt out last. Applied inferentially at the scale of Alkali Creek this would suggest a short early runoff from the headwater areas, and a long, delayed snowmelt flood from the western headwater tributary. Melt flows would increase in volume downstream, gaining considerably from the west bank of the main channel below the main point of the tributary junction. The spatial hillslope snowmelt domain is consequently variable with respect to aspect and elevation is the spatial overland flow domain, but in an <u>inverse</u> manner, such that the main channel could be regarded as possibly a process dominance domain for snowmelt. By contrast with the channel overland flow domain, it may be that during melt sediment is largely supplied by main channel scour, and bank collapse.

These suggestions are illustrated on Figure 6, in which a hypothetical pear-shaped basin with a central channel is shown to have varying radiation receipts, and therefore varying vegetation response. These parameters therefore constrain the spatial hillslope domain intensity for overland flow and for snowmelt runoff, leading to asymmetrical hillslope domains and inferentially, a complex, temporally variable channel intensity domain for each process.

(III) ALKALI CREEK: THE GULLY NETWORK

The gully network which drains this diverse landscape begins within the badlands soil zone (i) which occupies a relatively small proportion of the total area. There appear to be no visible drainage channels on the well-vegetated shale slope area (ii), and such depressions as can be found here show no sign of carrying concentrated flows of any magnitude (see Figure 4).

The gully network has pronounced asymmetry, favouring the upper, north-east corner as compared to the north-west. Gullies initiate here on the degenerate and easily transported Solenetz clayshales, which are prone to swelling and slaking on high intensity raindrop impact. When not extensively cracked, this slaking results in low infiltration capacities on these materials, so that rills are rapidly produced which coalesce by cross-grading and micro-piracy (Horton, 1945) to form permanent gullies. Some gullies terminate upstream in headcuts, and have small-scale headcuts in their beds as well as evidence of pipe outlets in their banks, similar to the situation described by Schumm and Hadley (1957). Most of the gullies terminate upstream, however, in finger-tip rills, which is the form more commonly associated with Hortonian overland flow (Chapter 1). As was suggested in Section II(B), piping appears to have for the most part only a minor role in gully initiation in the study area.

The rills coalesce and take on a regularly-spaced, dendritic pattern, and although the integrated channel systems become almost discontinuous in some places where low gradients are associated with the headwater zone sandstone ledges, nevertheless the whole network

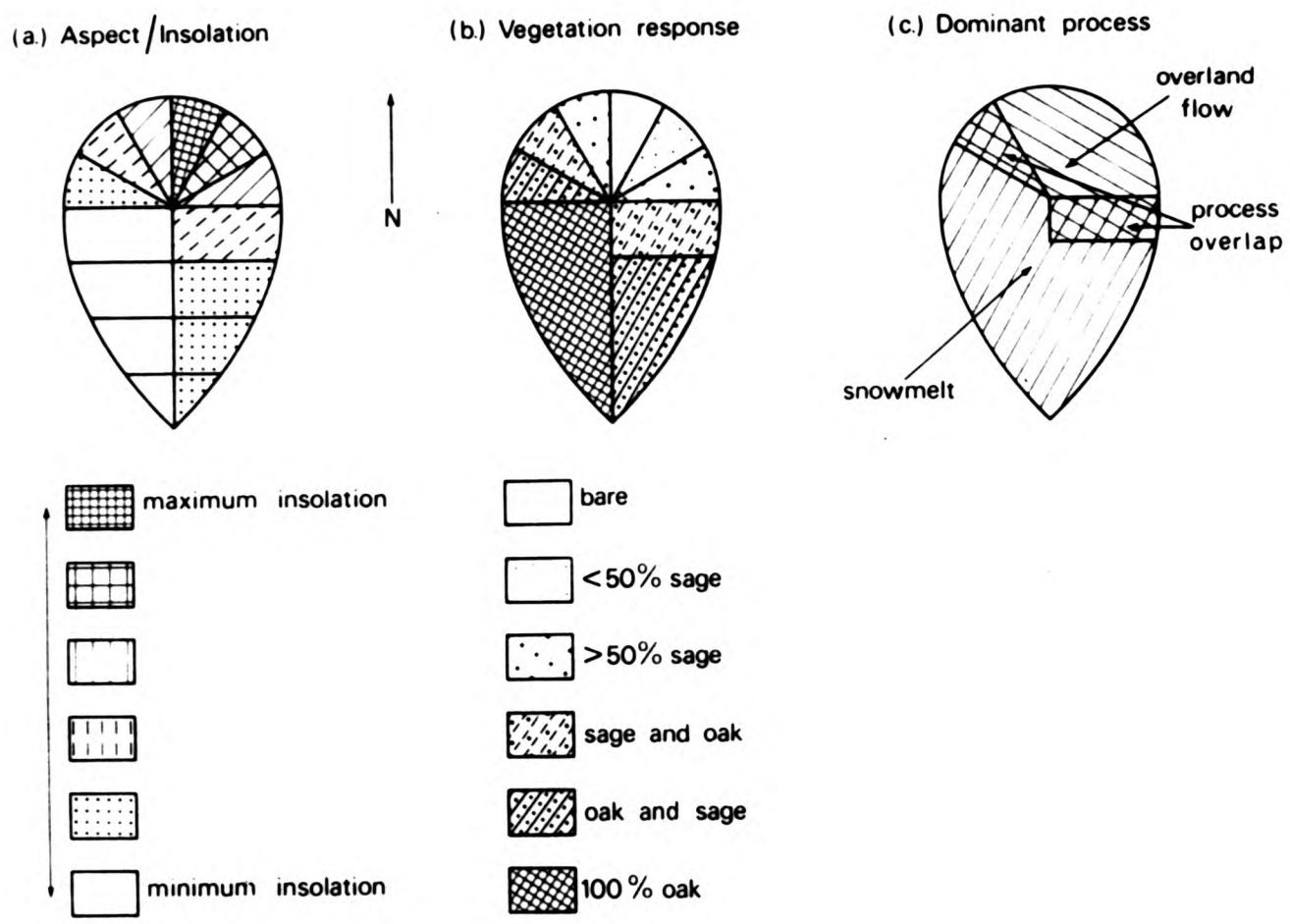

Figure 6: Hypthetical constraints on spatial domain dominance in a south-facing basin

is more or less well-coordinated above 'X'. Below this point, both the discontinuous and continuous gully systems coalesce into a single axial channel which is long and has no tributaries. In the headwater areas of both systems, gradients vary from 0.08 to 0.25m/m, dropping to 0.01 to 0.03 m/m on the main channels. The discontinuous tributary terminates in a small fan. On the main channel of the continuous network, five rock-check dam structures have been put into position as an erosion prevention measure by the U.S. Forest Service in 1963 (Heede, 1966).

Chapter 1 explained that the view taken in this investigation is that "... mesoscale landforms represent a palimpsest of interlocking and superimposed process-response systems ..." (Chorley, 1978a). It is further considered here that because of the sensitivity of the easily eroded material described at Alkali Creek and the speed with which change presumably occurs, this environment is likely to carry the stamp of the dual process domain interaction discussed in Chapter 1 in a clear form, and from this perspective it has been assumed that the overall excavated channel form in the study area will represent a 'palimpsest'of the kind Chorley (1978a) means. It was explained in Chapter 1 that one of the aims of this study is to explore how well flow simulations of the two main processes can be used to explain this form, and in fact such simulations follow in Chapters 3 and 4. Sequential surveys of the complete excavated gully size were undertaken, in 1962, 1975 and 1980, and so a brief consideration of gully morphology follows. A more detailed consideration of these patterns in terms of the flow simulations is reserved for the final Chapter.

(A) Field surveys of gully morphology

Gully morphology data were collected in the three fieldwork periods. For each survey, throughnet variations in the cross-sectional area of the excavated gully form, and in the bed and bank gradients of the sample sites were monitored throughout both the continuous gully network and its discontinuous tributaries. The sampling network is shown in detail on Figure 7 (back folder). The variables measured at each site shown on Figure 7 were as follows; the local bed (Sc) and bank (Sb) gradients through the sample sites at right-angles to the plane of section; total excavated channel

width (W); and mean depth (D). From these last two variables, the whole excavated cross-sectional form (this is not the bankfull cross-section) can be approximated by XA = W x D. All gradients were measured downstream in degrees using a clinometer, and then converted to percentage slope, although in some later calculations data are used in the units metre/metre. No difficulty was experienced in deciding on the excavated gully width measurement site, and width was measured in metres with tapes held horizontally using a spirit bubble. An engineer's levelling staff was held at five equidistant points across the plane of section, and a mean depth thereby calculated, again in metres (Photos 10 and 11). Distance downstream (Lm) of all the sample sites was noted in metres, again using a tape held horizontally. Using the enlarged photogrammetrically contoured air photo (Photo 2) which provides the base for Figure 4 (back folder), values for total channel length above each site (Lt) were calculated for all sites, (Appendix 3).

The original survey, conducted in 1962 by the U.S. Forest Service, went upstream on the continuous network as far as the upper tributary junction,' Y' (Figure 7). Because the objective of this original Forest Service survey was to isolate suitable sites for checkdam location, the sampling interval was irregular depending on the needs of the engineers, and this is true of the survey in the same year of the large discontinuous tributary. Overall, 32 cross-sections were surveyed on the discontinuous gully in 1962, and 53 on the main channel using the design described by Heede in 1966, (Figure 7). Siting was chosen to maximise the sediment holding capacity of the upstream section, and thus occupied locally steep bed sites.

In 1975, assistance was obtained from the Forest Service to resurvey all of these sites. This survey was conducted with the intention of following the sample design and field methods chosen by the Forest Service in 1962. In the event, quite a few sites could not be located accurately, so extra sites were measured where there was rather a large gap between adjacent sites. These points, as before, have been located on Figure 7. Below the main tributary junction, X, 47 sites were surveyed, and 33 on the large discontinuous tributary. The variables measured were the same as those measured in 1962, that is : Sb, Sc, Lm, W and D, together with Lt. (Appendix 3).

Photo 10 : Field team measuring channel gradients with an abney level and tape. In 1975 the check dams on the main channel necessitated readings both above and below emplacement

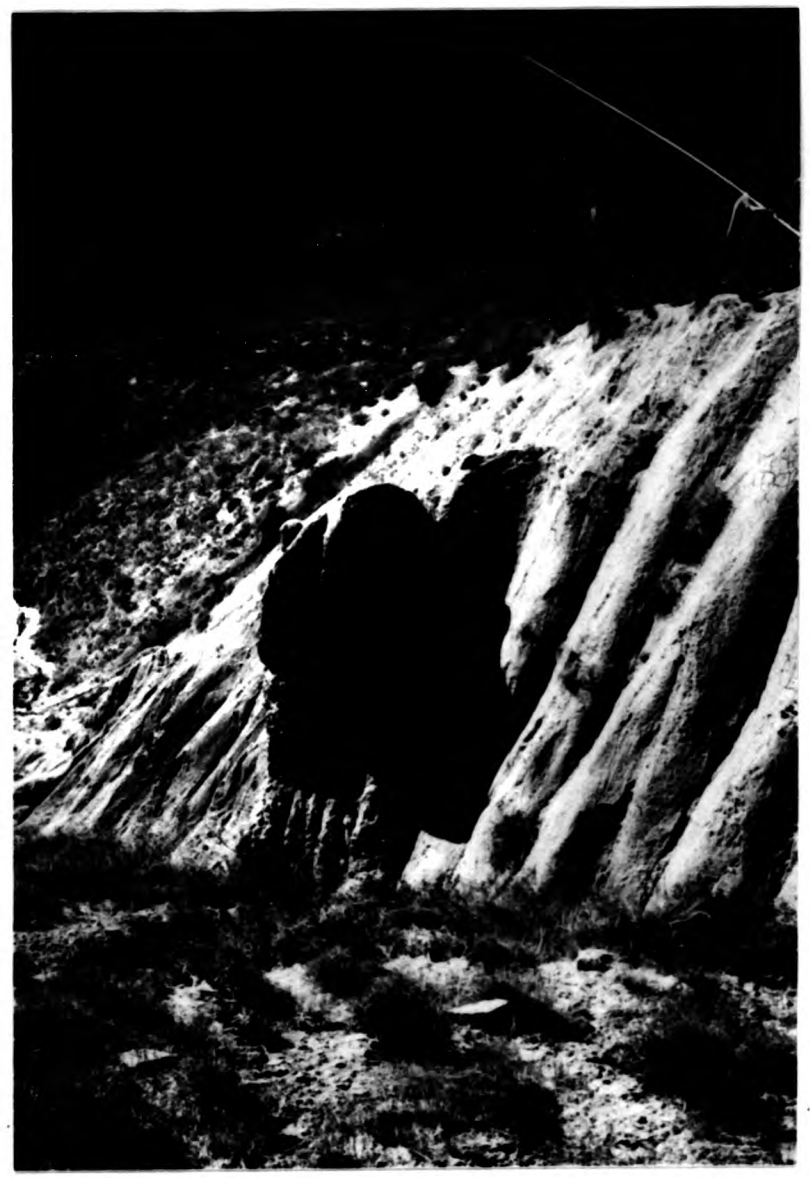

Photo 11 : Balking at the prospect of surveying the cross-sectional area at 'Z'

Photo 10 : Field team measuring channel gradients with an abney level and tape. In 1975 the check dams on the main channel necessitated readings both above and below emplacement

Photo 11 : Balking at the prospect of surveying the cross-sectional area at 'Z'

Because the headwater areas were felt to be important, these channels were included in the 1975 survey. In this area, cross-sections were noted at an interval of 30.5 metres along the channel. In all, 51 extra head-water sites were surveyed, including 5 on the small, discontinuous gully in the upper western part of the watershed.

In 1980, the 1975 survey was repeated on the large discontinuous gully, using the pegs left on site in 1975 as a guide, (Figure 7, and Appendix 3). For all sites in all three years, cross-sectional area and channel gradient, Sc, have been plotted in their downstream positions and contiguous network points have been joined together. As sequential data is available, these have been superimposed to indicate the changes between surveys. These graphical displays are included as Figure 8, which shows the behaviour of these parameters through the continuous network: and as Figure 9, which displays these data for the sequential surveys of the large discontinuous gully. Preliminary observations can be made from these Figures.

(i) Downstream variations in channel gradient, Sc

There is clearly a tendency for downstream sites to be of a lower slope than the headwaters in all mapped years, indicative of a general concavity in the drainage net. However, in both systems (Figures 8a and 9a), this tendency is considerably modified, not only by the check dams on the lower course of the continuous network, but also by the presence of the three lowest sandstone ledges which run across the bottom half of the headwater source areas. On Figure 8a, the three lower sandstone lenses are indicated. (Below Y, sandstone lenses are no longer present in the structural sequence). Entry onto a sandstone outcrop causes a sudden reduction in channel gradient in all cases.

This effect is particularly evident on the discontinuous tributary, whose headwaters are not extensive. Examining Figure 10a, and taking for the moment just the 1975 pattern as an example, the display of downstream data consists of two concave sequences. After the first high gradient sites (between 0 to 75 metres downstream) the gradients fall off as the channel encounters the first two exposed sandstone ledges, between 75 and 100 metres downstream.

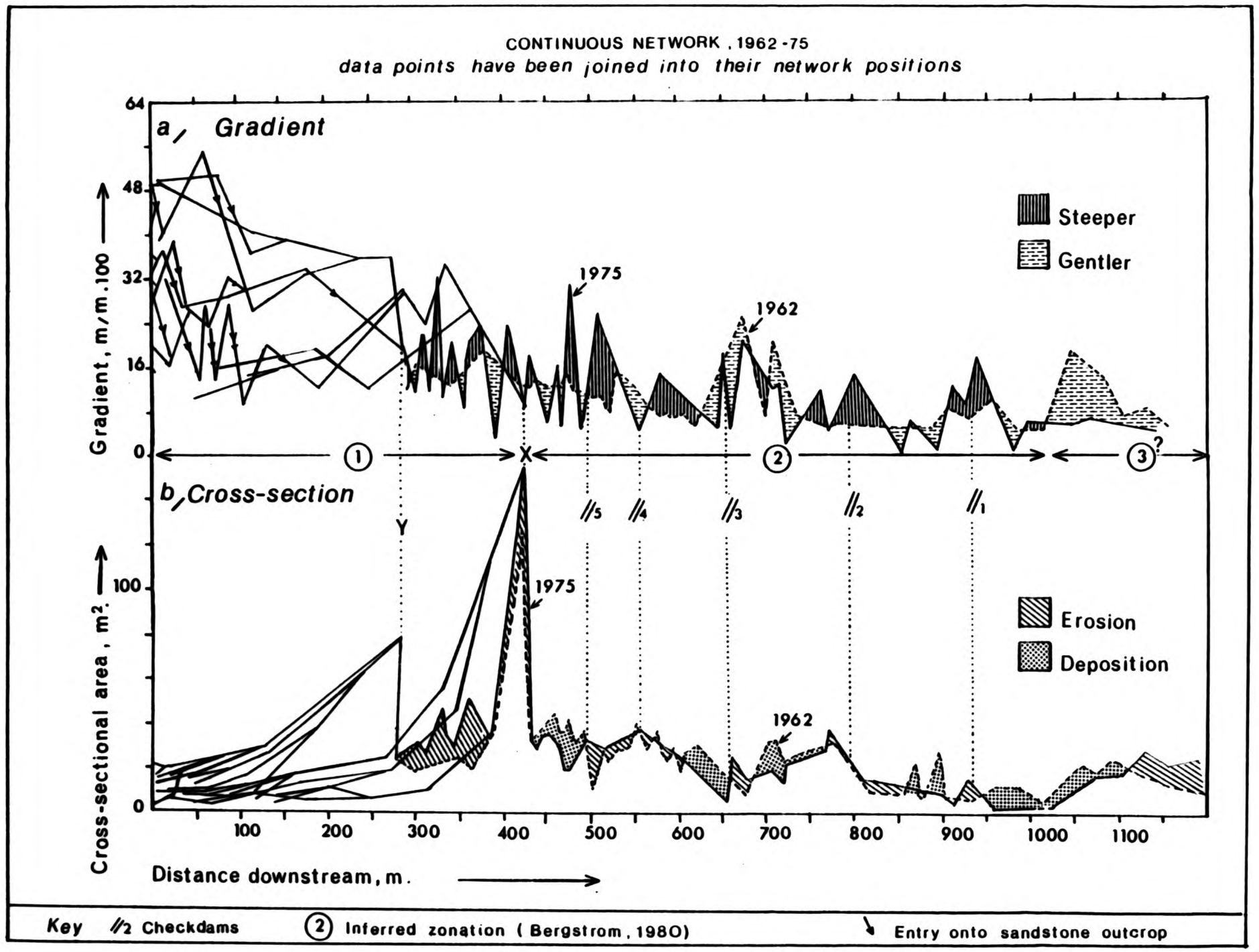

Figure 8: Morphology with distance on the continuous network

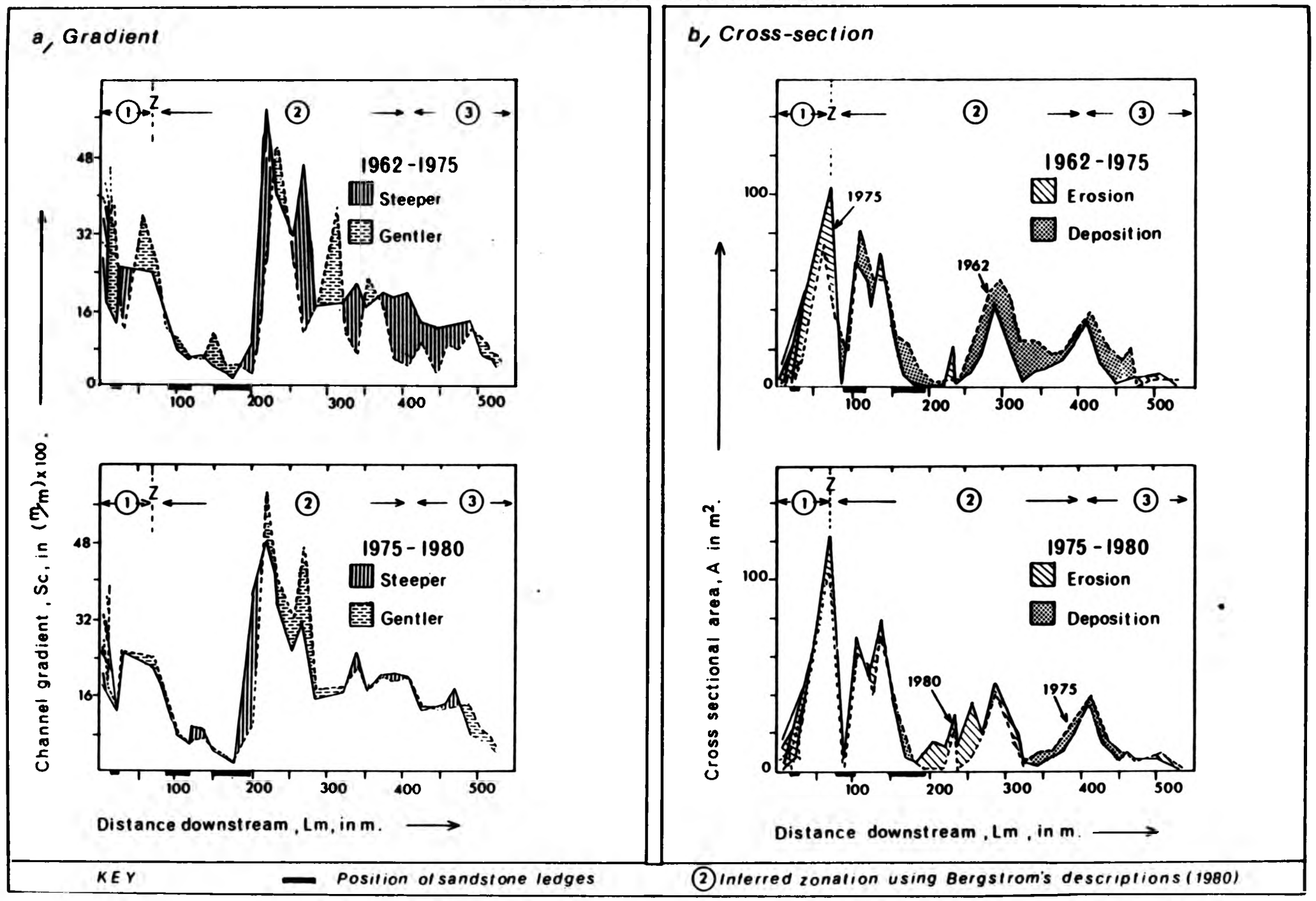

Figure 9: Morphology with distance on the large discontinuous tributary

Below this, gradients increase slightly once more, only to become almost horizontal again between 150 and 180 metres downstream, as the channel enters onto the lowest sandstone ledge in the structural sequence. Immediately downstream, the channel steepens dramatically again (Photo 12) following thereafter a systematic gradient reduction. The channel enters onto the fan at approximately 532 metres downstream.

(ii) Downstream variations in gully size, XA

Cross-sectional size, (XA), has been plotted on Figures 8b and 9b, on downstream axes, joining together contiguous network points as before, allowing comparison with the downstream channel gradient plots.

Although the pattern of excavation for the continuous network (Figure 8b) is influenced in 1975 below X by the presence of the check dams some generalisations can be again made. For instance, whereas gradient generally flattens with distance, cross-sectional area in the headwaters shows an inverse trend, rising to peak values at the two main points of headwater tributary junction, at Y, and more significantly, at X. This is true on all surveys. Thereafter, the excavated extent drops considerably, adopting on its main course a fluctuating pattern in which cross-sectional area declines downstream to a minimum at approximately 1000 metres from source. In contrast to the headwater sites, the decline in excavation extent below X follows the gradual reduction in gradients here. Data for the unmanaged gully, in 1962, indicated that in the last 100 metres of main channel, cross-sectional area again increased with steepening, although this tendency is not visible in 1975.

The observation that tributaries appear to have an inverse relationship between excavation and gradient, whereas the main channel has a positive relationship, is also true of the large, discontinuous tributary (Figure 9b). Headwater values of cross-sectional area rise up to point 'Z', whereas gradient is generally reduced. Since there are, however, only four sites actually on headwater tributaries, and all have downstream distances less than 20 metres, this tendency is hard to pick up on Figure 9. On the main part of this channel, however, steep sites are

Photo 12 : A view up towards the rim of the watershed from inside one of the trenches commonly located beneath the sandstone ledges which traverse the upper part of the watershed

Photo 12 : A view up towards the rim of the watershed from inside one of the trenches commonly located beneath the sandstone ledges which traverse the upper part of the watershed

Photo 12 : A view up towards the rim of the watershed from inside one of the trenches commonly located beneath the sandstone ledges which traverse the upper part of the watershed

positively related to the most excavated sites, and, in addition, the drop in gradients downstream from the last sandstone ledge mirrors a general reduction in excavation, dropping to zero on entry onto the fan at its end.

Thus it is possible to conclude that two distinct zones can be identified on both systems, which have different morphological relationships. The existence of these zones is reinforced by inspection of the erosional and depositional patterns displayed by the sequential data, which is discussed below.

(iii) Downstream variations in erosion and deposition, 1962-75 and 1975-80

By superimposing the gradient and cross-sectional area plots for 1962, 1975 and, in the case of the large discontinuous tributary, for 1980 on Figures 8 and 9, the type of channel change which has occurred between survey sites is inferred. Although the lack of spatial accord between one survey site and that of a subsequent time may lead to a misrepresentation of the absolute change, nevertheless several ovservations are possible.

- Headwater areas -

In both headwater areas, up to and including X and Z respectively, excavation increased for all sites surveyed, both between 1975 and 1980. This parallelled, for all sites, a reduction in channel gradient. This zone is therefore seen as entirely erosional, in which the excavation and lowering of gradients is concomitant with an extension of headwaters and removal of eroded material

- Large discontinuous gully -

Erosion of the headwater areas in the discontinuous gully clearly resulted in silting up, or deposition almost all along the channel below Z between 1962 and 1975, and this appears to parallel a reduction of gradient especially on the sandstone ledges between 150 metres and 200 metres downstream. Further downstream however, towards the fan, the effect of deposition was to steepen the channel. Between 1975 and 1980, sites below the sandstone ledge

have been re-excavated (200/230 metres downstream) causing a steepening again of this section. Below Z, therefore, the gully appears to fluctuate between cut and fill cycles, the overriding tendency between 1962 and 1970 being towards deposition, and in 1975 to 1980 towards erosion. Trenching just below the bottom sandstone ledge occurs in both periods.

- Main channel, continuous network 1962-1975, and management effects -

On Figure 9 the pre-management main channel on the continuous network can be compared with the 1975 channel following 12 years of sediment check-dam emplacement. Although there is no clear pattern of change other than can be accredited to the check dams, towards the basin mouth, there has been considerable erosion. The sedimentation which appears to have occurred in the discontinuous gully in this period does not appear to have occurred on the main channel. This contradiction is addressed in Chapter 6.

The local effect of the dams has clearly been to lessen the gradients and to reduce the cross-sectional area and increase gradient below their position. This effect can be read directly from Figure 8. This might imply that the dams have been a guarded success in this period. The fourth and second have been the least effective, and evidence of erosion was found in these structures, both in 1975 and in 1980.

(iv) Zonation

Morphological zones within erosive, semi-arid and snow-fed networks have been suggested by other workers. It was explained in Chapter 1 that Schumm (1977) sub-divides the fluvial system into three zones; first zone 1, the drainage net, which is the water and sediment producer; secondly, zone 2, the main river channels which are the transfer components; and thirdly zone 3, which consists of alluvial fans, deltas, and so on, which are the depositional areas. Although apparently Schumm (1977) expects these concepts to be applied at a fairly large scale; M. Harvey [7] claims to have seen these three

---

(7) Mike Harvey, Department of Watershed Science, Colorado State University (pers. comm. 1981)

zones develop within the Rainfall Erosion Facility (R.E.F.) at Colorado State University.

Bergstrom (1980) attempted a functional zonation of three very small (0.3 km^2) catchments in the Kraft badlands in Wyoming, using Schumm's sub-divisions as a conceptual framework. These watersheds experienced erosion from both snowmelt and overland flow events, and so are closely comparable to the Alkali Creek area. Bergstrom surveyed channel width and bed elevation on each watershed after snowmelt, and each summer event over a year. He found that in what would be Schumm's zones 2 and 3, snowmelt flows caused a decrease in bed elevation, but left the headwaters relatively untouched. By contrast, the headwater areas experienced a drop in elevation and channel width (current width was used) following two of the four storms on two of the basins. One summer storm event caused an increase in bed elevation in the zone 1/zone 2 boundary, but this dropped again following the next event, indicating first storage and then 'flushing' at this site. Overall, after one year, zone 1 had a negative sediment budget, and zone 2 a positive sediment budget. In zone 3, however, although there was an overall larger storage time for sediment it was inclined to retrench, possible because of oversteepening due to deposition in zone 2. Bergstrom (1980) consequently saw the 3 zones in terms of Production, Deposition and re-Erosion (the P-D-E sequence). The re-erosion in zone 3 is associated with snowmelt flows.

At this stage it is not possible to associate channel changes in the study area to specific events, yet zonation is clearly evident. On the continuous network there also appears to be a headwater area which is predominantly erosive (above X on the continuous network, and above Z on the large discontinuous tributary). Below this, a second zone can be identified which contains a single channel which experiences 'cut and fill' changes. The tendency on the large discontinuous tributary is towards deposition between 1962 and 1975, and erosion between 1975 and 1980. The continuous network, however, appears to have a more erosional second zone between 1962 and 1975, and at the lower end of the main channel, apparently considerable erosion occurred between the two surveys in which the channel size increased by over 50%. Whether a third zone can be identified in this landscape, therefore, is debatable, since the fan at the end of

the discontinuous system points to a different third zone in this latter system. It could be that the fan is liable to retrench at some extreme event, in which case it could be loosely viewed as "... a third zone characterised by re-erosion, in which the residence time for sediment is longer" (Bergstrom, 1980).

Some of the dichotomies introduced here are explored again at the end of the thesis, following the simulations of the main watershed processes.

Chapter 3

SNOWMELT

Any attempt to simulate the pattern of through-net discharges experienced by the network at Alkali Creek during melt requires a consideration of three aspects of snowmelt behaviour. First an assessment must be made of the spatial variation and extent of the snowmelt domain prior to melt (i.e. spatial variations in the depth of an average annual pre-existing snowpack). Secondly, consideration must be given to the environmental controls which will influence the spatial decay of this pack as melt proceeds, especially mappable parameters. Thirdly, a suitable routing procedure must be chosen to convert the melted volume to site values of mean daily discharge.

In this Chapter, literature concerned with snowpack behaviour and the melt process is briefly reviewed, paying particular attention to work which emphasises variables which can be derived from the existing data base in the study area. From this initial review variables are selected which, along with the local snow accumulation estimates presented in the last Chapter, allow an average pre-melt pack to be estimated. Using relationships established elsewhere, this pack is differentially melted in two phases, representing the first and second months of melt on the watershed. This melt volume is routed in a simple additive way through the network and converted to mean daily flow approximations for each of the two months at each sample site.

The three aspects of the snowmelt behaviour outlined above, and the several assumptions involved in the simulations were tested in the field in 1981, and the final sections of the Chapter presents the objectives and results of this field testing. The diurnal and spatial discharge patterns in both early and late melt periods, as measured in the field following melt, are compared with those following the model-based melt of the field-measured pack. The simulation is felt to be validated by these tests.

In the final Chapter, the morphological implications of the simulation and its field validation will be reviewed, and these

patterns compared with those following the summer storms, which are presented in the next Chapter.

(I) FACTORS AFFECTING SNOWMELT

(A) Spatial variations in the depth and water equivalent of an average pack prior to melt

Before snowmelt can be simulated on a watershed, an estimate is required of the pack size and its spatial variation. Although snow water equivalent values, either for a specific month prior to the onset of melt, or a long-term average, can be obtained from local snowcourses, continuous data is rarely available for more than one snowcourse adjacent to specific watersheds. As a result, extrapolation is needed, usually on the basis of environmental controls. The U.S. Corps of Engineers (1956) point out that "... of all the terrain parameters, elevation is the principal one which must be taken into account in determination of basin water equivalent from point snowcourse measurements".

Although snow as a precipitation fraction (Laucher, 1976), the number of snowfall days (Barry, 1981) and the duration of snow (Jackson, 1978) increase linearly with height, the variation of snow depth with altitude is generally more complex, even when local differences due to relief effects and small scale terrain features are ignored. Parallelling work undertaken in the Wasatch Range in Colorado by Peck (1972), Caine (1975) found in the San Juan range in Colorado that although snowdepth increased linearly with elevation the coefficient of variation of snowdepth at each site was inversely related to elevation. This was explained in two ways. First, there is a longer season of snow accumulation at higher elevations so that at 3500 metres the season is twice as long as that at 2600 metres. Secondly, Caine suggests that there is an interaction between topography and atmospheric factors. For example, in snowy winters there is a high frequency of cold lows, which cause widespread precipitation with relatively more falling at low elevations whereas in winters with light accumulation, there is a higher frequency of local storms which nevertheless provide sufficient snowfall to keep the higher pack closer to average depth.

Many orographic precipitation models now include a linear depth/elevation assumption (Barry, 1981), but the low elevation variability remains a problem. Some of the variation noted by Caine (1975) could also be due to the differing exposures of the 24 snowcourse sites. The U.S. Corps of Engineers (1956) define a variable called 'exposure sector', which is the "... sum of the sectors of a circle half-mile radius, centred on the snowcourse, within which there is no land higher than the points on the snowcourse". In this voluminous study of 4 major experimental watersheds experiencing snowfall, the U.S. Corps of Engineers found that 'exposure sector' was the most important variable causing differences in snow depth when elevation range was low (such as on open prairies), but was second in importance to elevation where ranges were great. Using data for pre-melt snow water equivalent (= depth x density) on snowcourses in their Central Sierra Snow Laboratory (C.S.S.L.) as dependent variable in a multiple regression, they found that exposure sector came high up the list on the step-wise model, following elevation. They discovered that for every 10^{o} increase in exposure sector there was a 1.27 cm to 1.90 cm decrease in snow water equivalent. This variable is significant, of course, because of its effect on wind speed and drift direction. In a snow survey at Schefferville, Cowan (1966) found that wind was a strong influence on snowdepth. In the maps produced in this latter study, snowdepth was at a maximum adjacent to forest stands on the upwind side, parallelling the conclusions made by the U.S. Corps of Engineers for prairie sites. Woo and Sauriol (1980) also noted that on flat, exposed watersheds in North West Territories wind drove snow into channel and gully beds, depleting exposed sites and artifically enhancing the pack accumulating over the channels. Meiman (1968) reports similar relationships between snow hydrology in general, and the variables elevation and aspect, particularly emphasising how slope orientation affects both accumulation and melt.

Other variables which significantly affect snow accumulation are vegetation and slope angle. In the C.S.S.L. study, no significant effect of forest was found. However, in other investigations in the Colombia River Basin by Ingebo, cited by the U.S. Corps of Engineers (1956), snow water equivalent was found to be linearly reduced by canopy interception, although the importance of shrubs was little "... the effect of grasses and most low lying shrubs on the

accumulation and melting of the snowpack is minor...Forests, on the other hand, show great influence on snow accumulation, especially between sites that are in clearings and those beneath forest crowns." This effect was also noted by Gary and Troendle (1982). Vegetation effects are more significant in controlling melt rates than accumulation rates, (see below). In the C.S.S.L. work, slope angle was found to cause a 0.4 cm to a 1.26 cm decrease in snow water equivalent for each 1% increase in slope. This variation is less than that caused by exposure and elevation.

There are therefore several parameters to monitor if an accurate pre-melt pack is to be simulated as input to a snowmelt model. In a desire for simplicity, however, the pack is often assumed to consist of a volume calculated by multiplying the area of ground snow-covered on April 1st of the year of interest (as seen on remote sensed imagery), by the snow water equivalent at the nearest snowcourse. This 'lumped input' approach works well in black-box run-off estimations (Male and Gray, 1981). In other work, the snow cover is zoned by elevation, and the snowcourse depth then weighted for elevation using a regional precipitation/elevation curve. However, failure to include the effects of less significant variables such as exposure sector, vegetation cover, and slope angle could lead to erroneous assessments, especially on small catchments with only moderate elevation range.(1)

In 1980, Thomsen and Striffler produced a simulation of snowmelt for the William's Fork watershed, Arapaho National Forest, Colorado. Because of the area's similarity and proximity to Alkali Creek, this work has considerable significance in the present investigation. The William's Fork study used a modification of the Leaf and Brink (1973) model, but included several improvements, one of which was the use of remote sensed imagery to classify the area into what they refer to as Hydological Response Units (H.R.U's). These were groups of pixels calibrated using the variables of elevation, slope angle,

---

(1) This was a suggestion made by B. Shafer in a personal communication in March 1981, S.C.S. Offices, Diamond Hill, Denver, Colorado

vegetation type and density, soil parameters, and aspect. Vegetation and soil were important in the melt routines, but for presimulation of the precipitation input over a 12 day period, elevation and aspect differences were the significant parameters used. Three aspect classes were used; A, which represents southwest-facing; B, which represents south and west-facing; and C, which represents southeast, north, northeast and northwest-facing slopes. Each H.R.U. was assumed to have a differing input snow water equivalent value (S.W.E.), and to respond differently to melt parameters. By classifying by aspect and elevation, the snowpack water equivalent prior to melt could be positively weighted with elevation, and inversely with aspect, but during melt routines could be weighted the other way around, i.e. positively with aspect, and inversely with elevation.

However, convenient as it is, the use of aspect as an input variable needs some justification. At William's Fork watershed, (and this is also true for Alkali Creek) aspect must be assumed to act initially as a surrogate for exposure sector, which is here greatest on the southwest-facing slopes; since the upper northeast and north-facing slopes are protected by the high rim of the watershed. Although somewhat arbitrary, when drawing up the weighted relationships between snow water content and elevation for each aspect (or exposure) class great care was taken to refer to data from four local snowcourses, each having differing elevations near to that of the William's Fork area, and each having differing exposures.(2) The four snowcourses chosen by Thomsen and Striffler (1980) were No 05K145 at Berthoud summit (3444 m), No 05K21 at Jones Pass (3170 m), No 05K04 at Middle Fork (2743 m), and No 06K20 at Glen Mar (2704 m). These data, which represent nearly 50 years of record, were used along with LANDSAT imagery to derive mean April 1st snowwater equivalent values at a range of elevations and exposures, leading to graphical relationships which could be used to calibrate a snowpack on April 1st. These are shown as dashed lines on Figure 10 for the three aspect classes used. On this Figure, the centre of the six elevation zones used at Alkali Creek are shown for information.

---

(2) This comment was made in discussions with W. Striffler, Colorado State University, Watershed Science Department, in May 1981

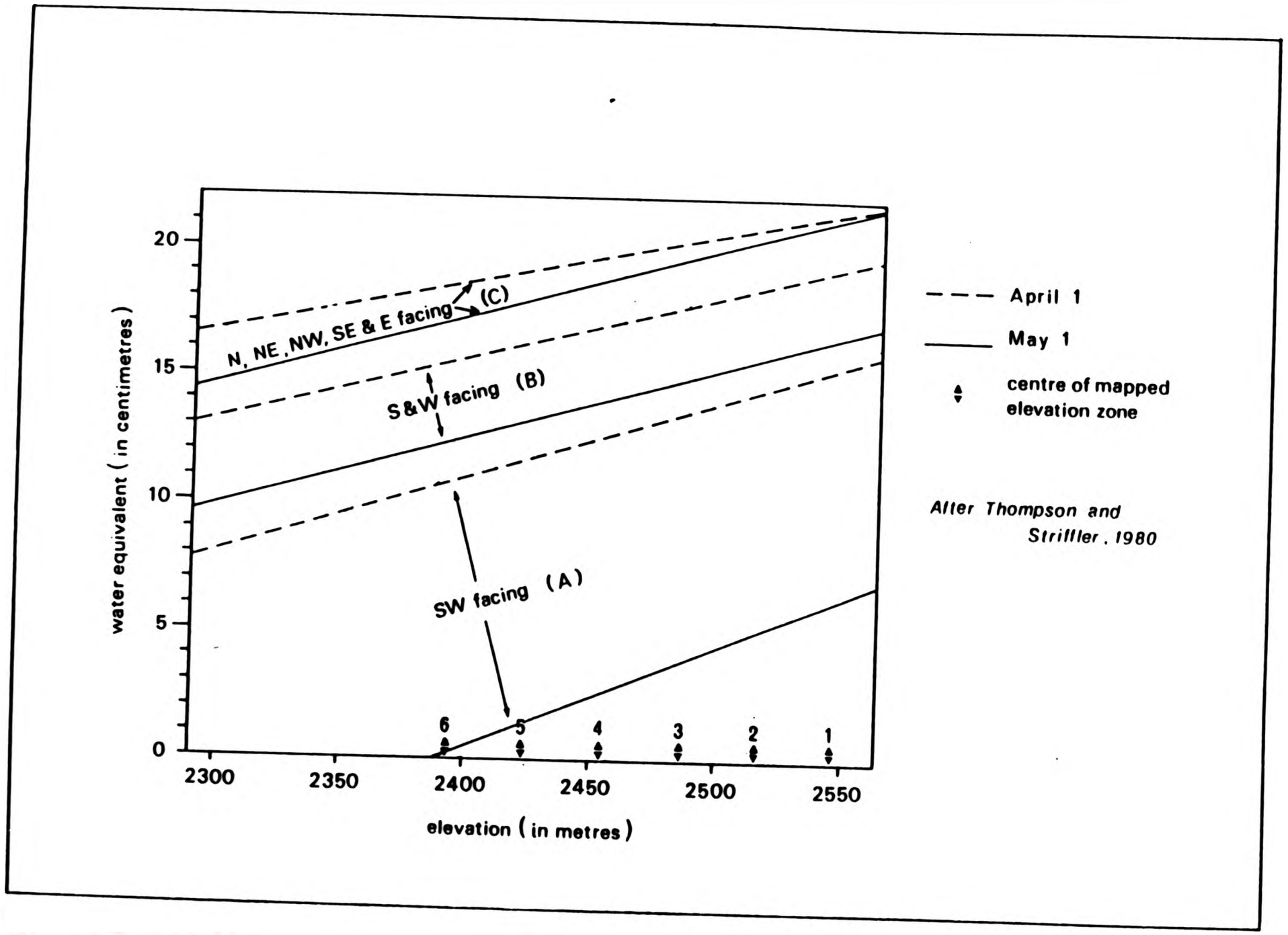

Figure 10: Relationship between snow water equivalent and elevation on April 1 and May 1 at Williams' Fork watershed, Colorado, on slopes of differing aspect.

The melting of this input pack, which will be discussed later, produced by May 1st a depleted snowpack which possessed the graphical properties shown in a heavier line on Figure 10. This is referred to as the 'May 1 update' by Thomsen and Striffler (1980). This in turn provides an input pack for the May melt routines. The watershed was snowfree by June 1st using this procedure.

William's Fork watershed is much larger (476 km^2) than the Alkali Creek watershed (0.4 km^2), but in other ways the areas are very comparable. Both in terms of mouth elevation (2380 m for William's Fork, 2377 m for Alkali Creek and in terms of basin orientation (over 70% of William's Fork faces south or southwest, over 60% for Alkali Creek), the areas are alike. For these reasons, and for simplicity, the relationships illustrated on Figure 10 were utilized to simulate a pre-melt snowpack in the context of the current investigation. No variations in pre-melt snowpack due to vegetation or slope angle were therefore assumed.

(B) Temporal and spatial variations in melt rate ; the energy balance approach

The rate of snowmelt at a site can be related directly to the energy transfer in the melt period onto the deposited snow layer. Melting snow absorbs solar radiation (R_s), and net long-wave radiation (R_l) so that total radiation receipts are $R = R_s + R_l$. Other exchanges involve heat transferred by convection and advection (turbulent heat flux, H_t); the latent heat of vaporisation by condensation from the air (latent heat flux H_l) and the conduction of heat from the ground (Soil heat flux, H_s). The latent heat flux may be positive or negative, a negative value indicating evaporation.

Thus the heat balance of the snowcover, BAL, can be calculated as;

$$BAL = R + H_t + H_l + H_s \qquad 3:1$$

(modified from Rachner 1975).

This formulation seems to be generally accepted as a basis for point melt rates, and is also cited by Male and Grey (1981)

The relative importance of the four terms varies during melt, and a consideration of the complete formulae available from Rachner (1975) and Male and Grey (1981) show melt to be a complex and variable process, dominated by a slow rise of air temperatures, but modified by widespread cloudiness, vapour pressure, vertical temperature gradients, albedo, soil temperature gradients and depth. Changes in these variables gradually combine to increase the liquid content of a pack which, at a critical snowdepth, will produce run off at the soil interface.

The snowpack condition is generally identified in terms of its liquid content, and its water holding capacity (or liquid water deficiency). Basically, energy must raise the pack to $0^{o}C$ and melt enough snow to satisfy the water-holding capacity of the snowpack first, before liquid water can reach the soil surface. This causes a lag, which varies with the snow depth. Once liquid water conditions occur at the soil/snow surface, the snowpack is considered 'ripe', and any additional heat input into the pack causes snowmelt runoff. The decline in the local snow water equivalent is consequently related to BAL (the daily budget in cal. $cm^{-2}day^{-1}$), the snowdepth, and snow density. An ideal melt model applies the changing terms in equation 3:1 iteratively to a prescribed pack whose conditions are being constantly modified, and the melted water may then infiltrate, or, after soil saturation, enter the channel directly.

So far the discussion has related to point rates. However, radiation receipts will vary spatially with aspect, elevation, slope angle, and vegetation cover (U.S. Corps of Engineers, 1956), as well as temporally; and this is true of windspeed (dependent on exposure, slope angle and vegetation cover); and soil temperature gradients, which will vary with soil type and vegetation cover. Consequently, all the variables in the calculations of each of the four terms in BAL are so spatially variable, and the pre-melt depth and density of the snowpack additionally so, that it is almost impossible to imagine how a spatial snowmelt runoff simulation might be undertaken on the basis of this energy balance approach. As Thomson and Striffler (1980) understate "...the simulation of runoff from high mountain watersheds has traditionally suffered from ... (1) a lack of basic data to drive the model and (2) a lack of information on the spatial variation of input data".

(II) SNOWMELT RUNOFF SIMULATIONS

Male and Gray (1981) feel that the use of detailed Rachner-type energy balance equations as a method of estimating snowpack runoff is "... not currently feasible for operational purposes". Procedures to model runoff described in the literature show, in fact, that a wide range of approximations are used to simplify the process, choice depending on the forecast period, the data and financial resources available, and the characteristics of the watershed being modelled. Each method attempts to predict the net effect of surrogate or grouped parameters, often expressing them by a single expression or coefficient, relying on the assumption that in practice the timing and amount of melt release to a channel are sensitive to relatively few key factors.

Male and Gray (1981) suggest that there are three areas of generalisation in all such models. First, in the estimation of the extent and variability of the snowcover; secondly, in the estimation of the energy available to melt the snow over a given area; and thirdly in the estimation of the effects of storage on the movement of the melt quantities during transit from the snow surface to the stream channel (routing assumptions). The methods available for the first of these generalisations, i.e. in the estimation of the areal extent and variability of the snowcover, have already been reviewed above (Section IA).

As far as the second of these areas is concerned, i.e. in the estimation of the energy available for melt, (BAL in equation 3:1), most operational procedures rely on air temperature variations alone as an index to substitute for the calculation of this term. This is partly because air temperature data are generally the most readily available, and partly because, as will be seen, these methods produce melt rate predictions which are comparable to those determined from the use of more detailed energy balance equations (Anderson 1973).

In a review of the literature undertaken by Male and Gray (1981), it emerges that no universally acceptable temperature index of snowmelt exists. Air temperature works better as a surrogate for BAL in areas covered by forests, since in these situations, the long-wave

radiation transfer, R_l, between vegetation canopy and the snow is the most important energy flux and is a direct function of the temperature difference between the two surfaces, measurements showing that canopy and air temperatures are closely related. Temperature as a surrogate for BAL is less reliable in open areas, however, since the heat flux components H_s, H_t, H_l, and the short-wave incoming radiation R_s, are not linearly related to air temperature and rely strongly on other parameters such as albedo and windspeed.

The simplest and most common expression relating snowmelt to a temperature index (usually the maximum or mean daily temperature) is:

$$M = Mf\ (T_i - T_b) \qquad 3:2$$

(Male and Grey, 1981)

Where M is melt produced, (cm. of water per unit time),
Mf is a melt factor in cm per ^{o}C. per unit time,
T_i is the index air temperature,
and T_b is the base temperature (usually $0^{o}C$).

This type of approach was used by Leaf and Brink (1973) and Thomson and Striffler (1980). The melt factor, Mf, has been calibrated at five basins in the Tadami river basin in Japan by Yoshida (1962) who not surprisingly found Mf to be very sensitive to canopy density and the exposure of the site to solar radiation. This conclusion reinforced previous work undertaken by the U.S. Corps of Engineers, (1956), who found that Mf on sites with a southern and south-western aspect had values almost twice those for 'sheltered' locations.

In attempting to identify the major variables affecting the melt factor, Eggleston et al (1971) suggest the following relationship;

$$Mf = K \cdot R_I\ (1-A) \qquad 3:3$$

Where A is albedo, and an inverse exponential function of time,
K is an constant which includes a vegetation transmission co-efficient for radiation and is an inverse exponential function of canopy density,

and R_I is an index related to solar radiation exposure and is a function of the angle between the normal to the surface and the direct beam direction (i.e. slope angle and aspect). R_I is calibrated with respect to slope angle and aspect by Male and Grey (1981).

The best way to approach melt simulation, therefore, is to calibrate an area for R_I and K, and then using a local lapse rate from an established Met. station, to apply equation 3:2 to the input pack iteratively as T_i and A change with time. The pre-melt pack size estimation has already been described. Melt routines that have been employed in the models reviewed here (Leaf and Brink, 1973; Thomson and Striffler, 1980) use this approach. These models do include two other subroutines which have to be satisfied before the melt volume is routed (soil moisture deficit, and evaporation), but in most cases the former store is satisfied early in the melt, and the loss to infiltration is considered small. Evaporation is normally calculated as a function of canopy cover using an empirical constant to link the two; however the estimation is usually a very small percentage of total energy available for melt (Erickson et al., 1978). Where both infiltration and evaporation can be considered small, melt rate found by employing equation 3:2 closely approximates the actual local rate.

Interestingly, these very simple melt simulations which incorporate merely temperature, aspect, canopy density, slope angle and elevation as variables with which to run the input pack and melt routines work well. Thomson and Striffler (1980) initially calibrated each H.R.U. for premelt snowpack size using the procedures already described, and then after allocating to each a value of R_I and K from the Male and Grey calibrations, used a lapse rate temperature extrapolation from nearby met. stations to obtain the temperature index for equation 3:2. Albedo is assumed to drop in time. After soil moisture and evaporation requirements have been satisfied, melt rate, M, is applied to each H.R.U until the pre-melt pack has gone. After one month of "melt", the pack that was initially modelled has diminished to one that has the snow water relationships with aspect and elevation illustrated for May 1st on Figure 10.

At Alkali Creek, the direct use of these equations to simulate melt was not possible because of the lack of local temperature data. However, because of the environmental similarity to William's Fork watershed, it was decided to use the graphical relationships on Figure 10 themselves to 'melt' a simulated snow snowpack in two stages, representing the last two melt months (assumed to be April, and May) at Alkali Creek. Because the original snowcourse data used represent a 50-year average, a calibrated snowpack using the April 1st graphical relationships on Figure 10 is taken here to represent the total volume available for melt on an average year on slopes with those aspects and elevations. Similarly, the Thomson and Striffler 'depleted' snowpack data (May 1st relationship) represent the water left for melt in an average May on slopes with those aspects and elevations. It follows that the difference between the two snowpacks represents the water melted in April. In this way, melt can be simulated indirectly from actual validated melt relationships established elsewhere.

Male and Grey (1981) suggested that the third area of generalisation in modelling streamflow from melt comes in assessing the effects of storage on the routing of melt volumes. The most common method used to transfer local melt to a channel flow value is to assume the 'reservoir model' on slopes, and the normal unsteady flow routing model (Linsley, 1944) within the channel. In the former, the amount of water moving through the pack under the influence of gravity is related to the rate of surface melting, less the rate at which the melt water reaches the ground. Since this latter value itself can be assumed a linear function of storage, then gravitational flow can be modelled from M (equation 3:2). Water entering the channel from each H.R.U. can thus be estimated as this value multiplied by the area of the H.R.U. This volume is then accumulated along the channel by dividing the channel into a number of discrete reaches, and solving the unsteady flow continuity equation for each reach.

However, the use of kinematic routing procedures is complex enough to justify making efforts to simplify this stage of the development of the Alkali Creek model. The more 'steady' nature of melt flows in comparison to summer storms made a simpler, 'average' volume approach easier to justify in the case of melt than would be the case for storms. In any case, variations in discharge downstream

(the channel intensity domain) were of primary interest in the Alkali Creek study, and to this end considerable emphasis was placed on the generation stage by subdividing the watershed into contributing areas which are assumed to melt out in two stages (the hillslope snowmelt intensity domain: Chapter 1). A decision was made to route the spatial intensity domain flows generated on the slopes additively, and to thereby obtain an average site daily discharge. These averages were later adjusted to represent a diurnal hydrograph at each site by field calibration. Although this method has flaws, it was considered simpler to calibrate a spatial model for temporal variations in the field, rather than attempting the reverse procedure given the constraints on time imposed on the study. Field validation will later be shown to justify this decision.

(III) MELT OF A SIMULATED SNOWPACK IN THE FIELD AREA

(A) The simulated snowpacks on April 1st and May 1st.

(i) Recording raingauge estimates of average pack size

In Chapter 2, an estimation procedure was described for the assessment of the snow water equivalent value of the Alkali Creek snowpack on April 1st, and May 1st, for each year indicated on Figure 2, using the recording raingauge records as a basis. In order to further validate this procedure, and from this validation to derive a pack size estimate for the events which occur 50% of the time at the rain gauge, the snow water equivalent estimate for Alkali Creek in each of these two months was plotted against the actual snow water equivalent as monitored at the McClure Pass snowcourse over the same period using log-transformed regression. The results of this test are illustrated on Figure 11. It is clear that the April estimates for Alkali Creek are not significantly related to those for McClure Pass, although most of these data plot within the same range. The May estimates over this same period are, however, related significantly (at the 5% level) to those values monitored on the snowcourse at McClure Pass. The wider spread of the McClure Pass data assist in obtaining this good statistical fit. (All data used to construct Figure 11 are included in Appendix 1, regression statistics are in Appendix 12).

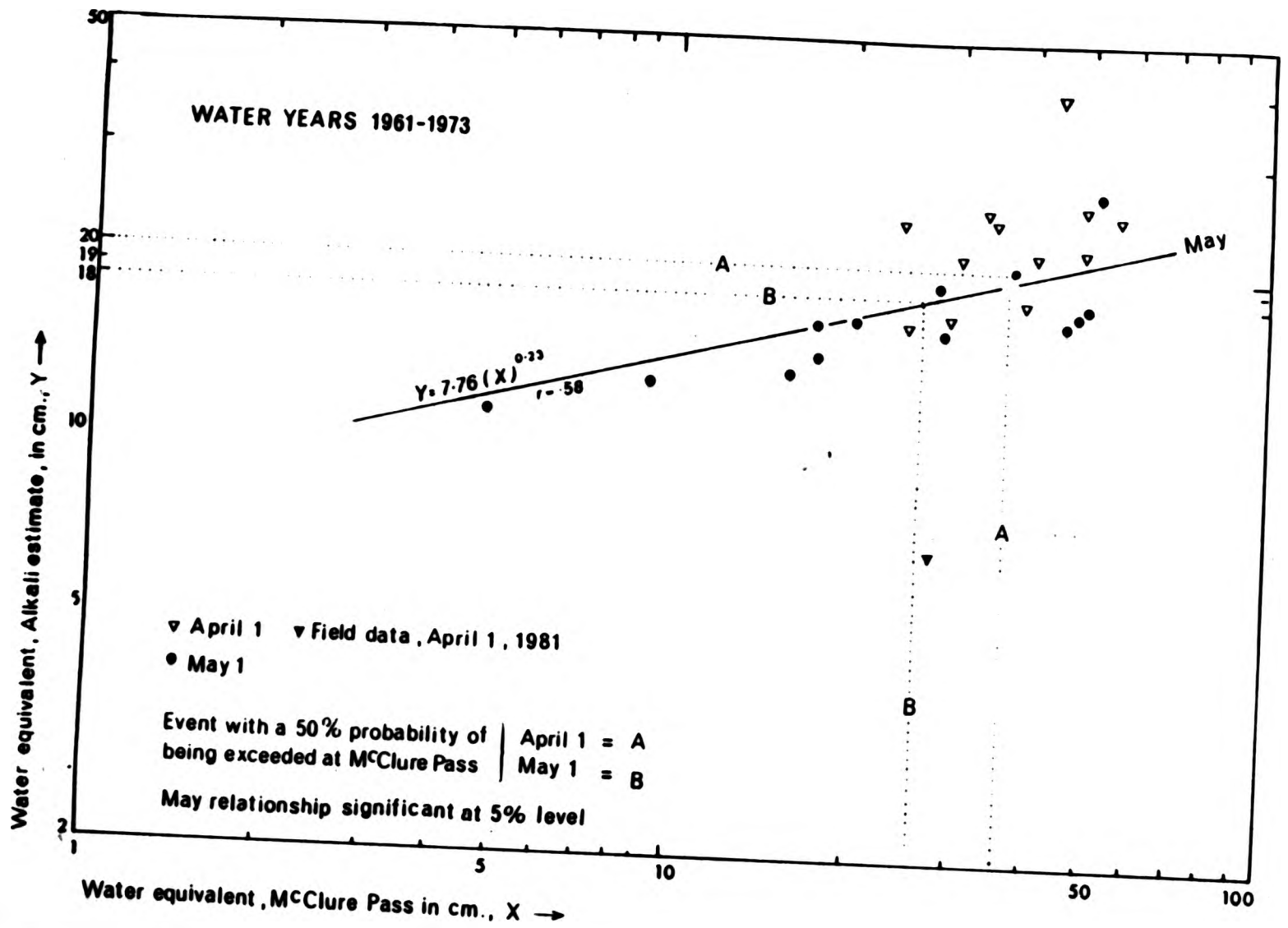

Figure 11: Relationship between the Alkali Creek snow water equivalent estimate, and actual data from the McClure Pass snowcourse, (used to derive an 'average' May 1 and April 1 pack size estimate at the Alkali R.R.G)

Since Alkali data are only available over a 12 year period, it was not appropriate to use these data to assess the event which occurred 50% of the time directly. However, it was possible to find the events which have a 50% chance of being exceeded on April 1st and May 1st at McClure Pass by utilising the 50 years of record available for this site and constructing the Pearson Type III event frequency curve for both months (these plots are available from the S.C.S. in Denver, Colo., the April relationship being discussed later as Figure 16). These 50% probability snowpack water equivalent values at McClure Pass on April 1st (A) and on May 1st (B) are marked on the abscissa of Figure 11. By moving up from the May 1st value to the May best-fit regression, the 'average' May 1st pack size at Alkali Creek can be read. This is not particularly viable for April 1st as the scatter is so great; nevertheless, an estimate from the April best-fit regression (Appendix 12) has been indicated. These Alkali snow water estimates for May 1st and April 1st (hereafter, the 'average' snow water values) represent the best approximations to the snow water equivalent values of the Alkali Creek snowpack on an average year that can be obtained from the recording raingauge records. They are:

Average S.W.E. Alkali Creek R.R.G. on April 1st = 20.65 cm.
Standard Error = 2.21 cm.
Average S.W.E. Alkali Creek R.R.G. on May 1st = 17.74 cm.
Standard Error = 1.08 cm.

(ii) The applicability of the Thomson and Striffler relationships (Figure 10) at Alkali Creek.

Although the aspect and elevational weighting assumptions, and the simple routing procedures to be adopted, could not be validated without fieldwork, there were two aspects of the relationships illustrated on Figure 10 which could be confirmed prior to simulation. These are firstly the timing assumptions, and secondly the general pack size assumptions.

As far as timing of the melt is concerned, a two month melt, from April 1st to June 1st, seems to be entirely applicable to the field area. Heede (1977) noted that the melt at Alkali Creek takes

approximately six to eight weeks for completion in a normal year, and notes found on the raingauge charts confirm this observation. Melt commences in most years sometime in early April, and is complete by June 1st in all years.

The second aspect of the relationships shown on Figure 10 which could be confirmed prior to their application in the simulation is the general volumetric range that they represent. By turning to Figure 4 (back folder) it can be seen that the R.R.G. at Alkali Creek is sited at an elevation of 2410 m, with a northwest aspect. The graphs on Figure 10 suggest that the following average snow water equivalent values represent such a site on the two dates of interest;

Average S.W.E., R.R.G. site, April 1st = 19.03 cm.
Average S.W.E., R.R.G. site, May 1st = 17.79 cm.

Since both these values fall within the standard error of the estimates discussed above on Figure 11, the general volumetric range of a snowpack that would be simulated using Figure 10 as a basis was thus taken to be sufficiently close to real field conditions in an average year as to justify proceeding with the simulation.

(iii) The procedure used to simulate the snowpack

The watershed at Alkali Creek was initially divided into six elevation zones each 30.5 m high, as indicated on Figure 7 (back folder). The choice of six was made on the basis that any more zones would have made the calculations unwieldy, fewer would have reduced the level of accuracy unnecessarily. The heights at the midpoints of each of the six zones are marked on the abscissa of Figure 10. The watershed was then subdivided into contributing areas for each of the cross-sections surveyed for morphology between 1962 and 1980. Contributing area delimitation has also been indicated on Figure 7. Using the three aspect classes (A, B, and C) chosen for operational purposes by Thomson and Striffler (1980), each of these contributing areas was allocated to an aspect class. If one slope fell across several elevation zones, each slope subdivision was separately allocated. This was done as illustrated on Figure 12, which demonstrates the whole procedure for the small subcatchment shaded in stipple on Figure 7 (back folder) as an example. After subdivision, the line of true slope was drawn down the unit at right angles to the contours, and then a protractor was

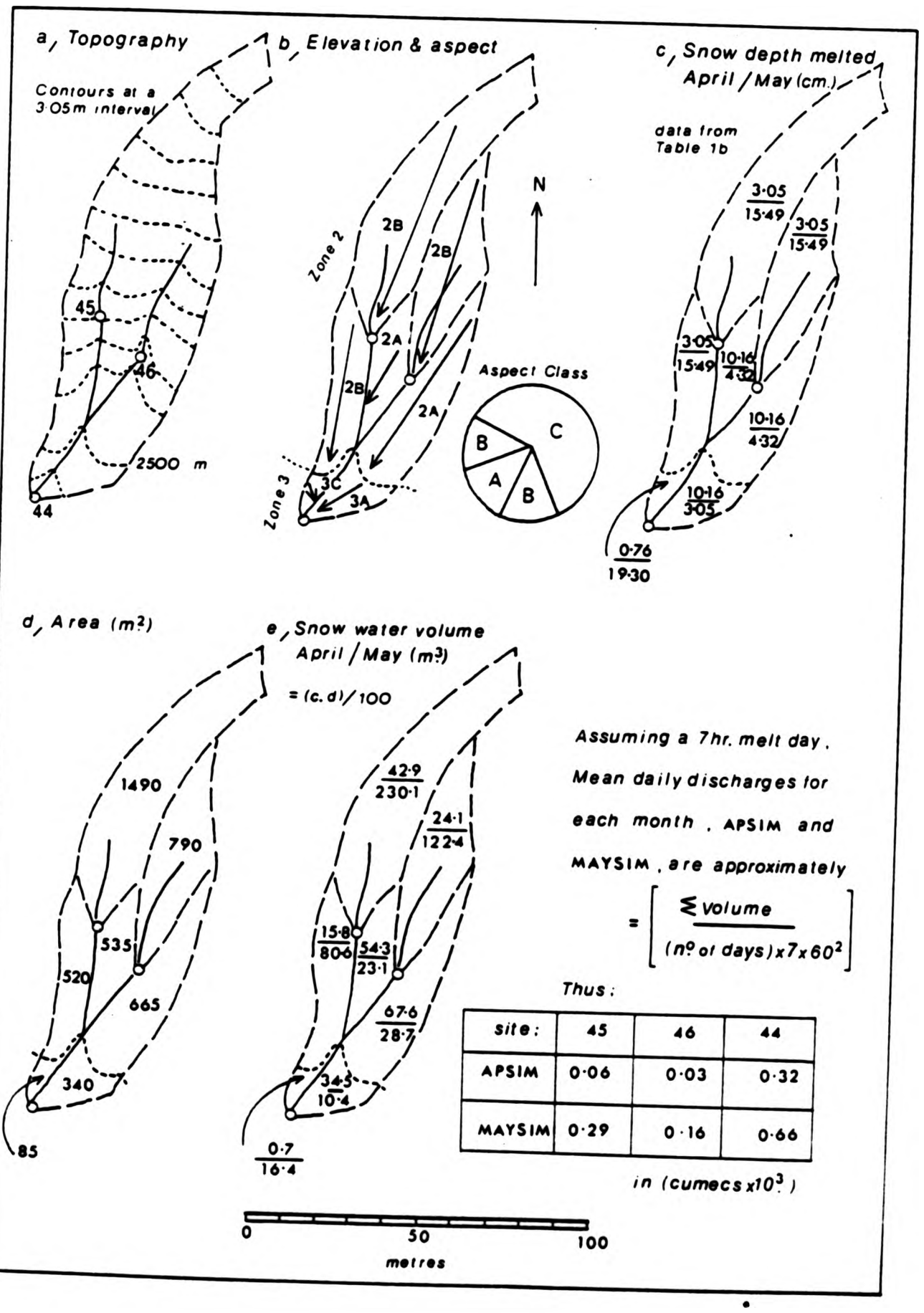

Figure 12: The calculation of APSIM and MAYSIM

held against the line and the aspect class determined, (b). As can be seen, cross-sections 45 and 46 drain slopes entirely within zone 2, but cross-section 44 drains these slopes, and also others which lie partly in zone 2, and partly in zone 3. In the latter situations, separate values were allocated. After this, a table was produced (Table Ia), which lists the snow water equivalent values in each aspect zone and elevation class (in cm.) at the midpoint of the six elevation zones used in the study area, for both April 1st and May 1st. These data were read directly off Figure 10. On Table Ib, the difference between the April 1st values and the May 1st values have been calculated to give the values of water depth melted from the pack in each category during April. Assuming the pack to be completely melted by June 1st, the May 1st value is taken to represent the water depth melted during May.

Using Table Ib, and returning to the watershed map, these values were written onto each contributing area, (Figure 12c), providing a method whereby a map could be produced of the simulated hillslope spatial intensity domains for snowmelt in both April and May.

(iv) Simulated snowmelt domains, April 1st and May 1st.

The simulated April snowmelt domain is illustrated for the whole watershed on Figure 13, and for May on Figure 14. These maps represent the values from Table 1b as applied across the watershed. A comparison of the two patterns illustrates the direction in which the spatial process intensity domain will shift in time. Whereas in April merely the southwest facing slopes produce runoff in the upper northeast part of the watershed, in May the pattern reverses. Rather than concentrating runoff in the gully network above X, in May the bulk of the remaining snowpack collapses, and these flows favour the main channel slopes below X, and in part the west fork of the headwater network above X. The large discontinuous tributary in both months drains decreasingly concentrated flows downstream, debouching in May onto a fan now almost devoid of snow. The May pattern particularly highlights the dramatic asymmetry of the snowmelt domain, which, if the graphical predictions are correct, favours the main channel on one bank only.

Table I

(a) Water equivalent in differing aspect and elevation zones (cm)

April 1 / May 1	Height at centre of elevation zone (m)					
	2545 (Zone 1)	2515 (Zone 2)	2484 (Zone 3)	2454 (Zone 4)	2423 (Zone 5)	2393 (Zone 6)
SW facing (class A)	14.99 / 5.59	14.48 / 4.32	13.21 / 3.05	12.45 / 1.78	11.43 / 1.02	10.41 / 0.0
S & W facing (class B)	19.30 / 16.51	18.34 / 15.49	17.78 / 14.73	17.02 / 14.22	16.26 / 12.95	15.49 / 12.43
N, NE, SE, NW and E facing (class C)	21.06 / 20.83	20.57 / 20.0	20.07 / 19.30	19.56 / 18.80	19.05 / 18.03	18.29 / 16.76

(b) Depth of snowmelt water from respective zones (cm) in the last two melt months

April / May	Height at centre of elevation zone (m)					
	2545 (Zone 1)	2515 (Zone 2)	2484 (Zone 3)	2454 (Zone 4)	2423 (Zone 5)	2393 (Zone 6)
SW facing (class A)	9.40 / 5.59	10.16 / 4.32	10.16 / 3.05	10.67 / 1.78	10.41 / 1.02	10.41 / 0.0
S & W facing (class B)	2.79 / 16.51	3.05 / 15.49	3.05 / 14.73	2.80 / 14.22	3.31 / 12.95	3.04 / 12.45
N, NE, SE, NW and E facing (class C)	0.25 / 20.83	0.51 / 20.01	0.76 / 19.30	0.76 / 18.80	1.02 / 18.03	1.52 / 16.76

Source : Thomson & Striffler, 1980

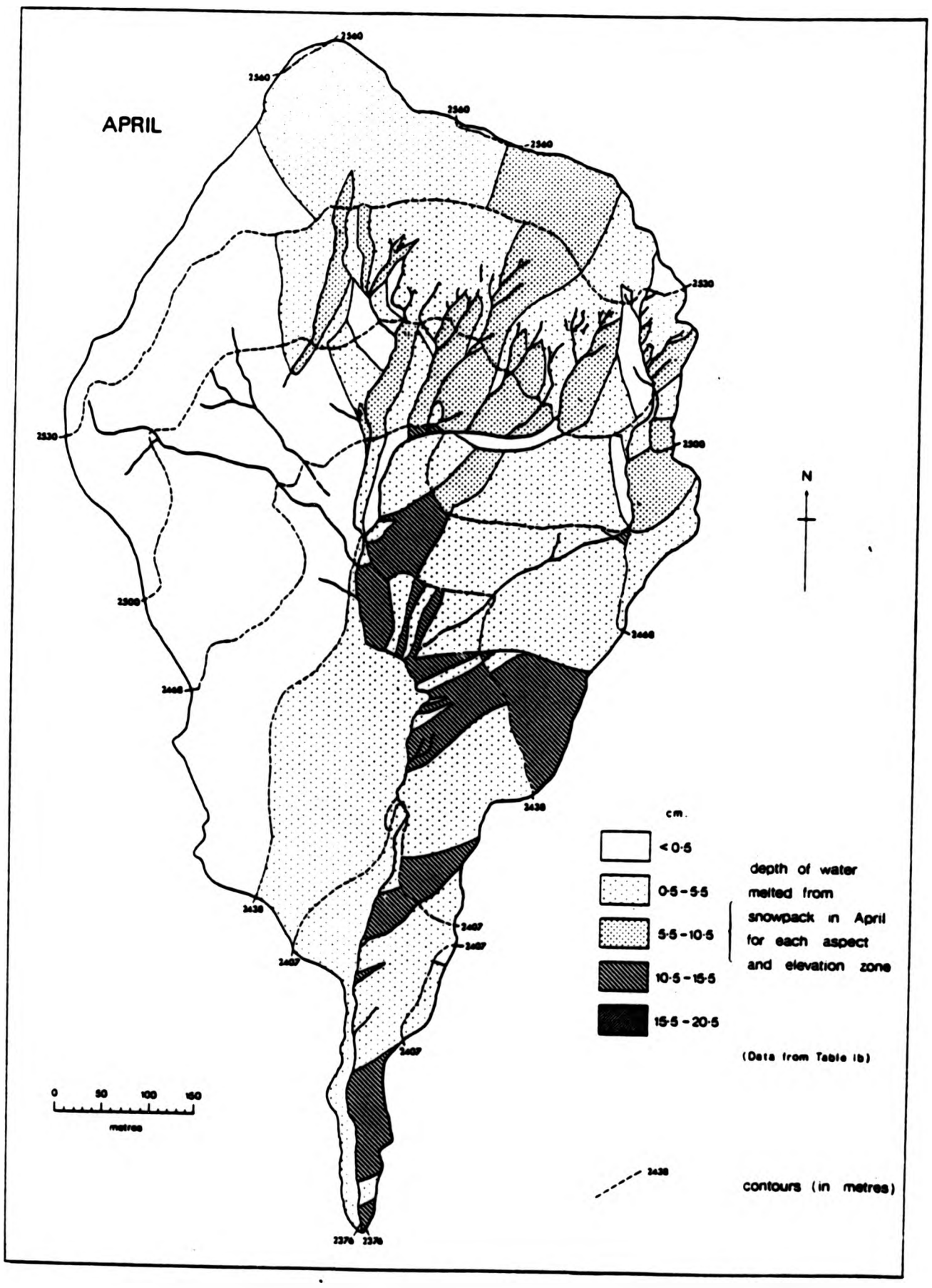

Figure 13: The hillslope spatial intensity domain for snowmelt runoff : April

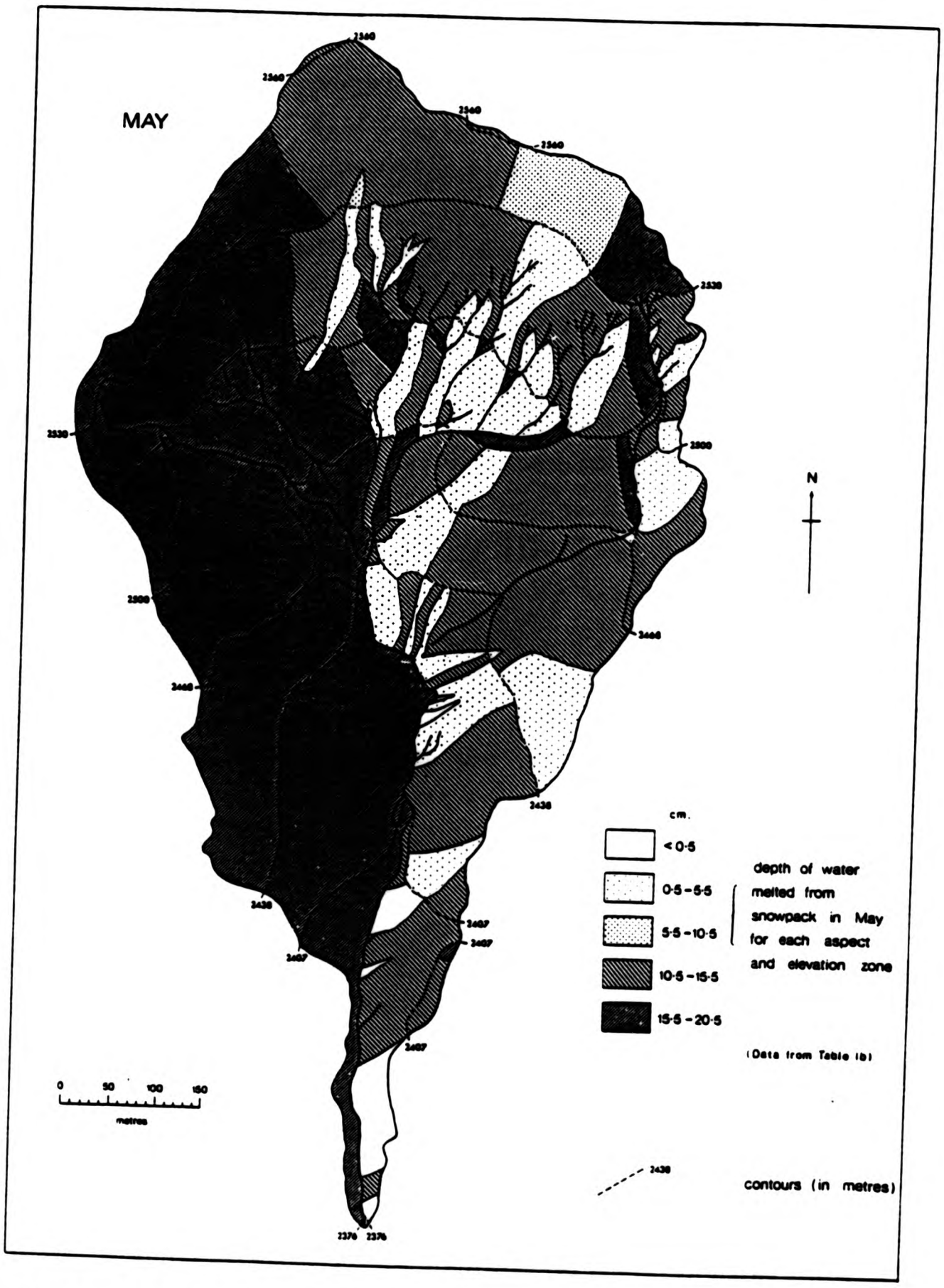

Figure 14: The hillslope spatial intensity domain for snowmelt runoff : May

(B) The simulated flows, APSIM and MAYSIM

Returning to Figure 12, the area of each unit was next calculated, using both polar planimeter (for large areas) and gridsquare calculations (for small areas), shown on Figure 12d. To calculate the melt volume (in m^3) from each unit in each month these areas were multiplied by the appropriate meltwater depth (Figure 12c) having converted this latter value to metres, producing the values indicated on Figure 12e. Assuming a melt day of 7 hour length, mean daily discharges in cumecs for each month, APSIM and MAYSIM, can be calculated by summing monthly melt volumes down the network, and dividing this value by the number of days in the month (30 for April, 31 for May) multiplied by (7×60^2), at each cross-section. The table on Figure 12 shows the resulting values of APSIM and MAYSIM for cross-sections 44 to 46 in cumecs ($\times 10^3$). This procedure was undertaken for all 212 sites, and the resulting data are available in Appendix 4. Using the FORTRAN programme GPHPLT (3), the resulting through-net flow accumulation patterns were plotted for each month and the results are shown on Figure 15.

The following observations can be made from an examination of these simulated mean daily flow accumulation patterns:

(1) In May, the contribution from the headwater west fork is considerably greater than that from the east fork of the network, reversing the situation that occurs in April.

(2) There is little difference in the mean daily pattern of runoff volumes in the east fork of the network in April and May.

(3) Apart from the east fork of the headwater network, the flow volume throughout the network is considerably greater in May than in April, reaching at the basin mouth nearly a fourfold difference.

(4) Using the simple additive routing procedure, the flow accumulates downstream as would be expected in both months, but in May the mean daily discharge increments at tributary junctions are dramatic, particularly at junction Y, and even more so, at X.

---

(3) Kindly supplied and modified for the current purposes by Dr. M. Frost, Department of Geography and Geology, The Polytechnic of North London

Figure 15 : The downstream pattern of APSIM and MAYSIM

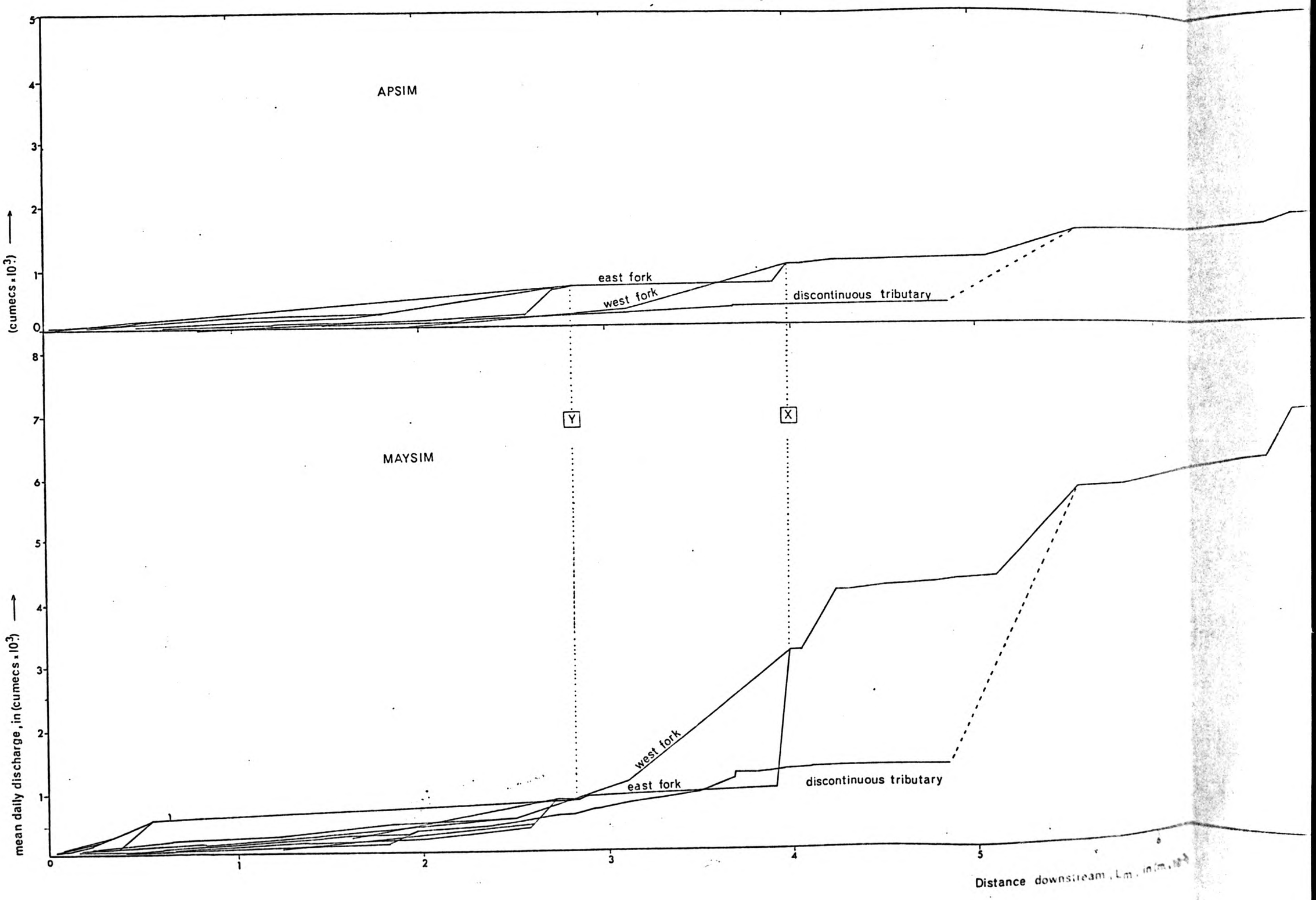
APSIM
MAYSIM
(cumecs × 10³) ⟶
mean daily discharge, in (cumecs × 10³) ⟶
east fork
west fork
discontinuous tributary
Y
X
0
1
2
3
4
5
6
7
8
Distance downstream, L m, in (m × 10³)

discontinuous tributary

X

discontinuous tributary

4

5

7

8

9

10

11

Distance downstream, Km

cross-sections joined together into

contiguous network positions

NETWORK KEY

west fork

east fork

Y

X

discontinuous tributary

N

0 100

m

(5) Despite the existence of the fan, the discontinuous tributary appears to provide a flow contribution into the main channel of some considerable magnitude in May. This seems to conflict with morphological evidence unless the meltwater enters the main channel from this tributary via transmission through the fan.

(6) The unchannelled west bank contribution in May causes an increase of quite considerable magnitude onto the main channel below X, particularly between X and the point where the large discontinuous tributary terminates in a fan.

(IV) FIELD TESTING OF THE SIMULATION

The timing, and average annual pack size assumptions which are implicit in the simulation procedure as described were justified above prior to the presentation of APSIM and MAYSIM. However, the use of aspect and elevation as variables with which to precalibrate these packs around the average recording raingauge snow water equivalent values for April 1st and May 1st could not be validated from existing data, and required field testing. Additionally, the simple additive routing procedure involved was clearly somewhat arbitrary, and so also required some field calibration. A programme of fieldwork was therefore planned in the spring of 1981 which allowed these two aspects of the simulation to be tested.

Clearly, it would have been preferable to arrive in the field to a pack of near to average dimensions. Unfortunately, a visit to the S.C.S. offices in Diamond Hill, Denver, Colorado in late March, 1981 revealed that the snow year 1980-1981 promised to be the snow drought of the decade. By plotting the Pearson Type III event frequency curve for the April 1st snow water equivalent values at McClure Pass over 30 years of record (Figure 16, and Appendix 5), it can be seen that the end of March/early April snow water equivalent at McClure Pass had an 84% chance of being exceeded in subsequent years. Initially, this seemed a serious setback to the fieldwork. However, on reflection it became clear that the objectives of the fieldwork were not totally dependent on a good snow year. Rather, it was felt that since the spatial variations around the recording raingauge value were of interest, these could be monitored on any

Figure 16: SNOW WATER EQUIVALENT, April 1 1950 - 1981
McClure Pass, Colo.

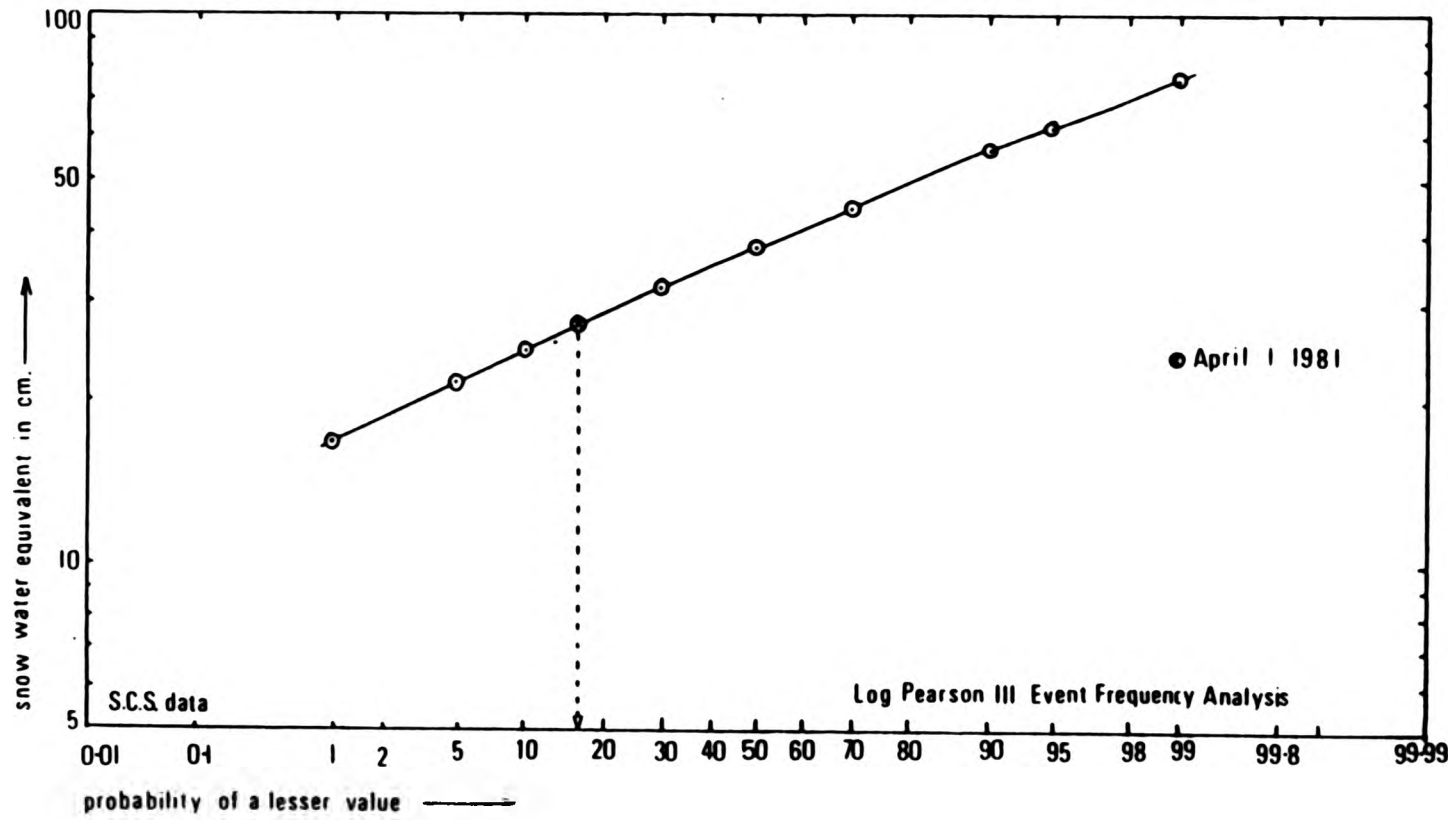

size snowpack, and then correlated with those variations predicted around the raingauge site value for an average year. This procedure could still establish the validity of the aspect and elevation weighting assumptions, since the absolute size of values does not affect the strength of the correlation value derived from the spread of the values. Similarly, rather than comparing field monitored daily discharges with APSIM and MAYSIM to validate the routing method, the field-monitored snowpack, rather than the simulated snowpack, could be routed in order to make this comparison. The assumptions in the routing method would be quite adequately validated in this way.

The following sections describe the snow survey and its calibration against the simulated snowpack, the routing of this snowpack, and the testing of the discharges predicted by this routing against those monitored in the field, including the diurnal calibration.

(A) The snow survey

The first visit to the field area on April 1st, 1981, revealed that the watershed had already lost some snow on the southwest-facing slopes (Photo 13). Figure 17 illustrates the field survey of total extent of snow cover that was undertaken on both April 1st and April 18th of the fieldwork period. In one sense, this lack of snow on southwest-facing slopes was disturbing, since although April is usually the first melt month, this abnormal year's pack had clearly started to melt earlier than anticipated, such that the snow picture presented correlated, at least visually, more with the pattern anticipated for early May (see Figures 13 and 14). In another sense, the clear asymmetry of the melt so far gave initial support to the aspect and elevation-zone dominated spatial melt picture painted by the simulations.

(i) Methods

Because the southwest-facing slopes were mostly snow-free, the original plan to sample all aspect and elevations classes identified on Table 1 for snow water equivalent using a snowcourse survey proved impossible, and the survey had to be restricted to all aspect classes B and C, in all elevation zones, with the aspect class A sited remaining unsampled. The choice of snowcourse locations within each aspect and elevation class was determined in the end by

Photo 13(a) : Alkali Creek on the first day of snowmelt fieldwork, April 1st,1981

Photo 13(b) : The south-west facing slope in the foreground had already melted out completely, in contrast to the facing slope with a north-easterly aspect which still held snow

Photo 13(a) : Alkali Creek on the first day of snowmelt fieldwork, April 1st, 1951

Photo 13(b) : The south-west facing slope in the foreground had already melted out completely, in contrast to the facing slope with a north-easterly aspect which still held snow


816
ALKALI CREEK

Figure 17 : The extent of snow cover at the beginning, and half-way through the fieldwork period in 1981

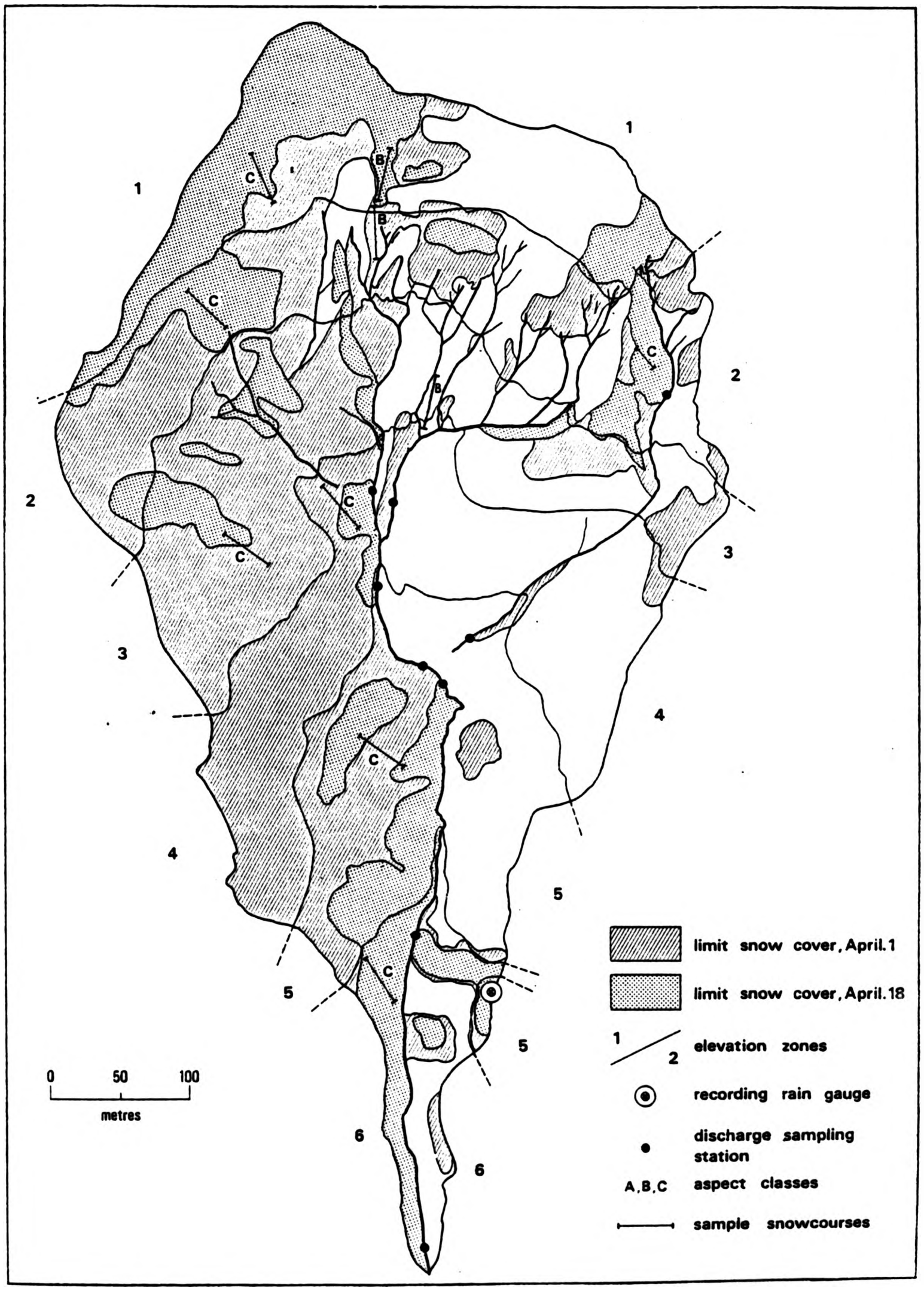

practical considerations, although a more ambitious sampling design had been originally planned to embrace both vegetational effects and a variety of slope angles. In the field, only a few sites in each sample category were both easily accessible and also provided a long enough clear slope length to accommodate the 20 ft (61 m) length necessary for conventional snowcourse procedures. The sample design is illustrated on Figure 7 (back folder). The ten instrument positions are also indicated on each snowcourse on this diagram.

The method used by the Soil Conservation Service to conduct snowcourse surveys is explained in the S.C.S. booklet No. 169 "Snow Survey Sampling Guide", U.S.D.A., (1973). Because of the generosity of the S.C.S. both in Denver and Glenwood Spring offices, no difficulty was found in obtaining the necessary equipment for the completion of the field surveys. The snowshoes, skipole, balance, sampler and booking sheets necessary are illustrated on Photo 14.

The procedure to survey a snowcourse is as follows. Firstly, the sampling tube is assembled ensuring that all three sections are attached. Secondly, the line of section is taped onto the ground, the total length of 61 metres being marked by survey pins every 20ft (6.10 metres). The tape is held as close to horizontal as possible down the line of true slope. At each pin, the clean sampling tube is held vertically with the cutting end down and driven into the snow to the ground surface. The depth of the snow can then be read from the side on the calibrated aluminium sampler to the nearest half inch (centimetre). The tube is then turned one turn to the right to cut the core loose from the earth. By looking through the slots in the sampling tube, the core length can be read. This is done to ensure that the core length is at least 90% of the snow depth. Using a pocket knife, soil and litter is removed from the cutter and tube and core length adjusted if necessary. The sampling tube is then carefully balanced onto the weighing cradle, to which the spring balance is attached. The spring balance is suspended from a ski pole (Photo 15). In this way, the weight of the tube and core can be read from the calibrations on the balance scale. On the scales, the graduations are a linear function of water content in inches (centimetres). Turning the tube so that the cutter is upwards, the tube is tapped against the snowshoes to remove the snow. The process is repeated at each sample site. To ensure that

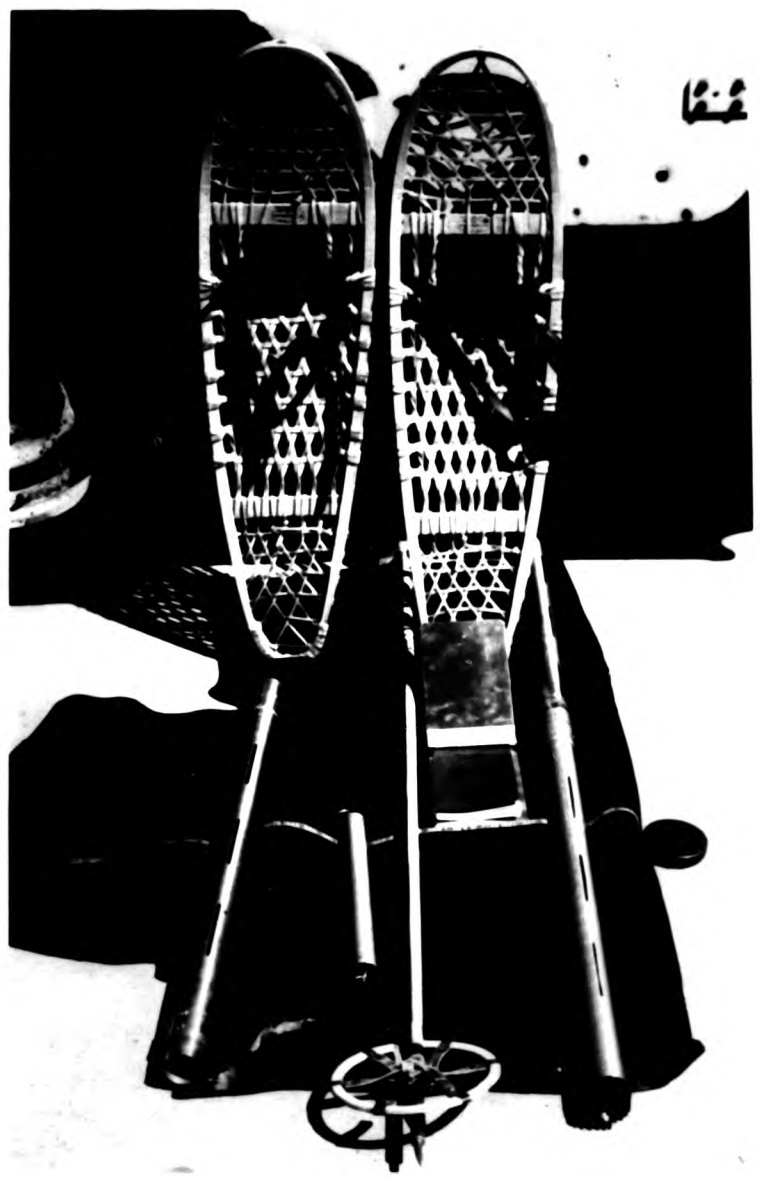

Photo 14 : The snowshoes, skipole,spring balance cradle, tape and aluminium sampler necessary for a full survey

Photo 15 : The equipment in use

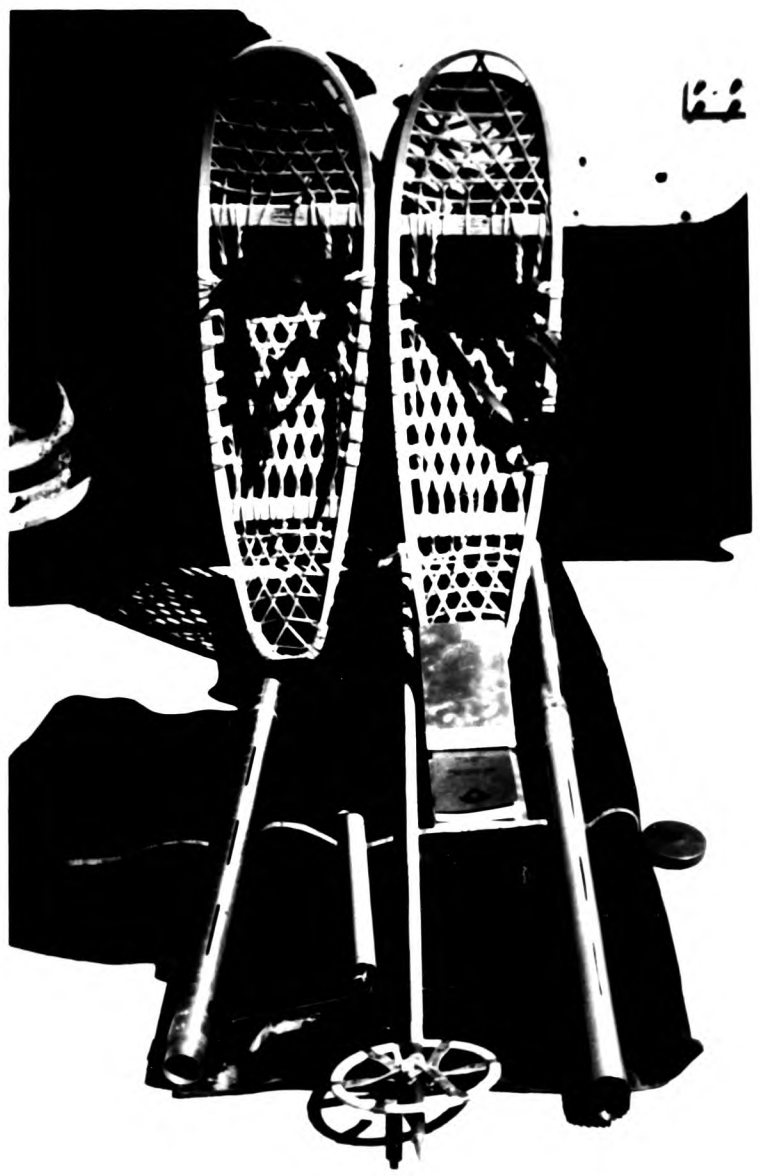

Photo 14 : The snowshoes, skipole,spring balance cradle, tape and aluminium sampler necessary for a full survey

Photo 15 : The equipment in use

Photo 14 : The snowshoes, skipole, spring balance
cradle, tape and aluminium sampler
necessary for a full survey

Photo 15 : The equipment in use

all readings are comparable, density is worked out (water equivalent/snowdepth) since densities on one snowcourse should, on a clear course, be closely similar, usually not varying more than 3%. From the ten readings on one snowcourse, the average snow water equivalent for that site can be calculated.

It took a very long time to get into the field each day, and this considerably restricted each stage of the field programme. It took four days to finish the surveys, leaving only a few remaining days for the discharge surveys, which had to wait until the end of the first week in April for the early April data. Also, it was clear by mid April that by May 1st all the snow would be gone. As a result of this, it was decided that a complete mid-month resurvey of all sites should be conducted to pick up the late melt effects, and to retain the empirical objective of modelling melt in two stages.

(ii) Results

The results of the April 1st to 4th snow survey of all sites still containing snow on April 1st, 1981, at Alkali Creek are included as Appendix 6. In addition to the snowcourses already outlined, two extra small patch surveys were undertaken. These were done on what appeared to be drift sites on the leeward side of two gully beds in elevation·zone 2, aspect class C. These are noted on Figure 7 (back folder) and data included as before in Appendix 6. In the event, the data from these two sites were not significantly different from those for the 2C snowcourse, and the effect of drifting seems to be restricted to the expected effect associated with exposure and already in-built in the model. Table IIa summarises the field snowcourse data for both the early and mid-month surveys. As can be seen from both Figure 17 and this table, by April 16th snow had melted from the three lowest aspect class B sites in addition to the six class A sites that were initially snowfree, leaving only nine snowcourse sites available for the mid-month survey.

To validate the use of aspect and elevation as parameters with which to calibrate the snowpack on an average year at Alkali Creek both prior to, and during melt, actual field data in Table IIa should be compared to the predicted patterns with aspect and elevation presented previously on Figure 10 and Table Ia. However, several

Table II

(a) Water equivalent in differing aspect and elevation zones (cm)
April 1st-4th, 1981, and April 16th-20th, 1981 (field data)

April 1-4 / April 16-20	Height at centre of elevation zone (m)					
	2545 (Zone 1)	2515 (Zone 2)	2484 (Zone 3)	2454 (Zone 4)	2423 (Zone 5)	2393 (Zone 6)
SW facing (class A)	- / -	- / -	- / -	- / -	- / -	- / -
S & W facing (class B)	6.60 / 2.54	5.84 / 1.50	4.47 / 0.51	2.54 / -	1.50 / -	0.5 / -
N, NE, SE, NW and E facing (class C)	8.41 / 5.64	7.75 / 4.85	7.42 / 4.03	5.89 / 3.56	6.48 / 2.51	6.05 / 3.07

(b) Depth of snowmelt water from respective zones (cm) between
April 1st-15th and April 15th-30th, 1981

April 1-15 / April 15-30	Height at centre of elevation zone (m)					
	2545 (Zone 1)	2515 (Zone 2)	2484 (Zone 3)	2454 (Zone 4)	2423 (Zone 5)	2393 (Zone 6)
SW facing (class A)	- / -	- / -	- / -	- / -	- / -	- / -
S & W facing (class B)	4.06 / 2.54	4.34 / 1.50	3.96 / 0.51	2.54 / -	1.50 / -	0.5 / -
N, NE, SE NW and E facing (class C)	2.77 / 5.64	2.90 / 4.85	3.39 / 4.03	2.33 / 3.56	3.97 / 2.51	2.98 / 3.07

Source: Field snow courses - Appendix 6

problems arise in such a comparison. A first area of difficulty arises because of the anomalous nature of the field year snowpack size. Sites without snow must be excluded from the analyses, because absence of snow cannot be really regarded as having a numerical value of zero, and this leaves rather a small sample size, particularly for the mid-month data. Another problem arises with respect to the melt timing. Strictly speaking, the April 1st to 4th snow water equivalent values found in the field should be regressed against the April 1st predicted values from Table Ia, and also May field data against predictions for May 1st. However, since in 1981 the watershed was snowfree by May 1st, and in addition, the snowpack distribution on April 1st bore more resemblance to that expected on May 1st, it was not clear whether April should be regarded as the first or second melt month in the field season of 1981. If the latter were to be assumed true, then the early April field survey data should be regressed against the May 1st predictions. Because of this problem, both regressions were conducted (Figure 18, a and b). Similarly, problems arise with the mid-month field survey. Is the melt to be assumed to be a normal two month melt compressed into April (in which case the April mid-month data should be compared with the May 1st predictions), or, applying strict rules of comparison, should April 16th to 20th field data be compared to mid-month prediction values (calculated as April +$\frac{(\text{April-May})}{2}$)?

Again to circumvent this difficulty, both tests were applied (Figure 18, c and d).

Apart from these logistical problems, further difficulties arise in the interpretation of the linear regressions and their confidence limits. Normally when actual values are regressed against predictions, one is testing how closely a one-to-one relationship applies. A perfect predictive model is therefore one in which actual and predicted values are identical, such that a regression of the former on the latter produces a straight line through the origin which has a regression coefficient (gradient) of one, and perfect correlation (product moment correlation of 1), i.e. actual, (y) = predicted, (x). In the anomalous field year, there would obviously be a negative intercept on the ordinate, but a regression coefficient of 1 was still to be expected. The standard least squares regression procedures that are available fit the line

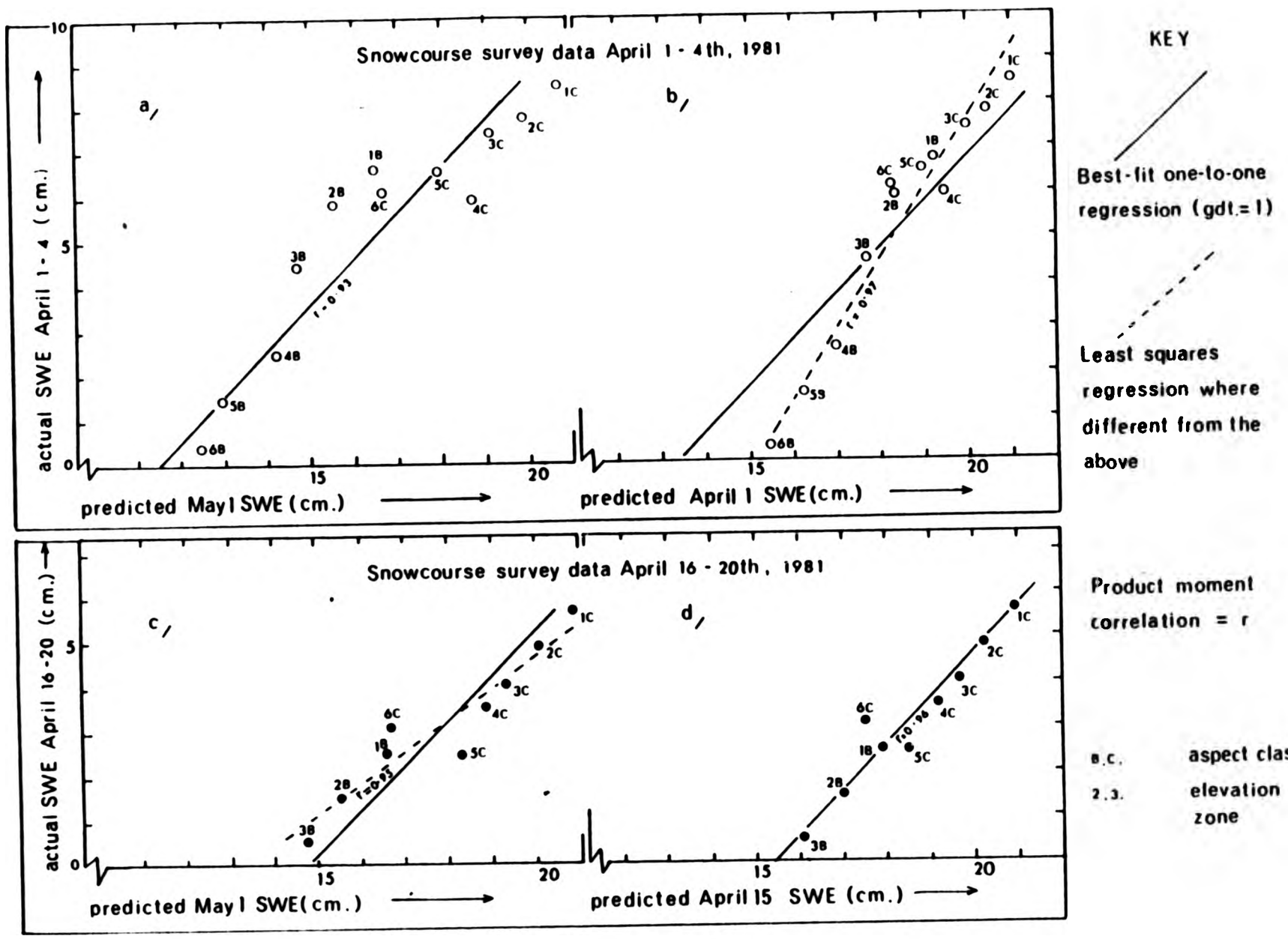

Figure 18: Regressions relating the early fieldwork S.W.E values to (a) April 1 predictions, and (b) May 1 predictions; and also relating the mid-month fieldwork S.W.E values to (c) May 1 predictions, and (d) April 15 predictions

through the spread of data which minimises the squares of the deviations from the line, and this is not necessarily the line with a regression coefficient of 1. There is no method available with which the confidence limits or product moment correlation can be determined for a regression line with a fixed gradient, so that if the least squares regression does not have a gradient of 1, there is no method to ascertain the correlation coefficient of the one-to-one line. In the context of the current investigation, the question arises as to whether a least squares regression with a regression coefficient of 1 that has a product moment correlation of 0.93 (as for Figure 18a) is a 'better' predictive regression than that for Figure 18b, in which the least squares regression has a coefficient of 1.32, and a product moment correlation of 0.97. It was finally decided that the only method available was to test whether the standard error of the regression coefficient in the case with the best correlation coefficient allows sufficient latitude as to embrace the case where the regression coefficient is 1. Applying these criteria, the second test works 'better' than the first in both cases, implying that the field survey data corresponds most closely with April predictions in both cases. This is a significant consideration in the later routing of the pack and in the interpretation of the results of the routing. The complete analyses of the regressions shown on Figure 18 are included in Appendix 12.

Fortunately, despite these problems the scatter around the regressions is small. The most anomalous data point on Figure 18 is that for the 6C snowcourse in the mid-month survey, for which the snowdepth is greater than would be expected from the trend of the other sites. This is the site with the lowest gradient (7°, the other sites having ground gradients of between 9° and 23°). This suggests that slope angle, if included as a variable, might have improved the fit. Vegetation effects may also explain some of the scatter, for example on snowcourses 4C and 5C in both surveys. These sites both have 100% vegetation cover, 5C including oak brush, and both have less snow than would be expected from the trend of the other sites. These variations, although interesting in themselves, do not remove the significance of the two April regressions, which, using the Student's 't' test are both significant at the 1% level. In fact, it is possible from these surveys conducted, to infer strongly that the use of aspect and elevation as variables with

which to calibrate snowpacks prior to, and during melt is supported by these analyses, and there appears to be no reason to modify either the methods or conclusions made from the earlier presented snowpack simulations.

(B) Routing of the field-monitored snowpacks

In an attempt to validate the routing assumption in the simulations, the field-monitored snowpack relationships summarised on Table IIa were extrapolated as before, across the watershed. This was done by constructing Table IIb, on which the depth of water melted from the respective aspect and elevation zones between April 1st and 15th, and April 15th and 30th, 1981, are tabulated. These values were obtained by assuming the snow water depth as monitored by the April 16th to 20th survey data to have melted in the last two weeks of April, and the difference between the two surveyed snow water values to have melted during the first two weeks of April. Using the same method as used for the simulated flows, APSIM and MAYSIM, (Figure 12), these values were used to predict the mean daily discharges in the field at each of the 212 cross-sections sampled for morphology between 1962 and 1980. To do this, accumulated volumes were divided by $(7 \times 60^2 \times 15)$, for each 7 hour melt day in the 15 day periods. These discharges were entered as FW (1) and FW (2) respectively (for the early and late fieldwork periods) into the data file, and using the FORTRAN programme GPHPLT, the accumulated downstream patterns were produced. These patterns are shown on Figure 19. Not surprisingly, they parallelled those anticipated for April on Figure 15 exactly, except that of course the values are considerably less. The pattern also shows the melt discharges early in the field period to be almost a third greater throughout the main channel length than those predicted for the last two week period. (The values of FW (1) and FW (2) as routed through the network are included in Appendix 4, where they can be compared with APSIM and MAYSIM).

(C) The discharge survey

The objectives of the discharge survey were first, to validate the routing assumptions in the simulation by comparing mean daily discharges at a sample of points through the Alkali network with the

Figure 19 : The downstream patterns of the snowpack routings, FW(1) and FW(2)

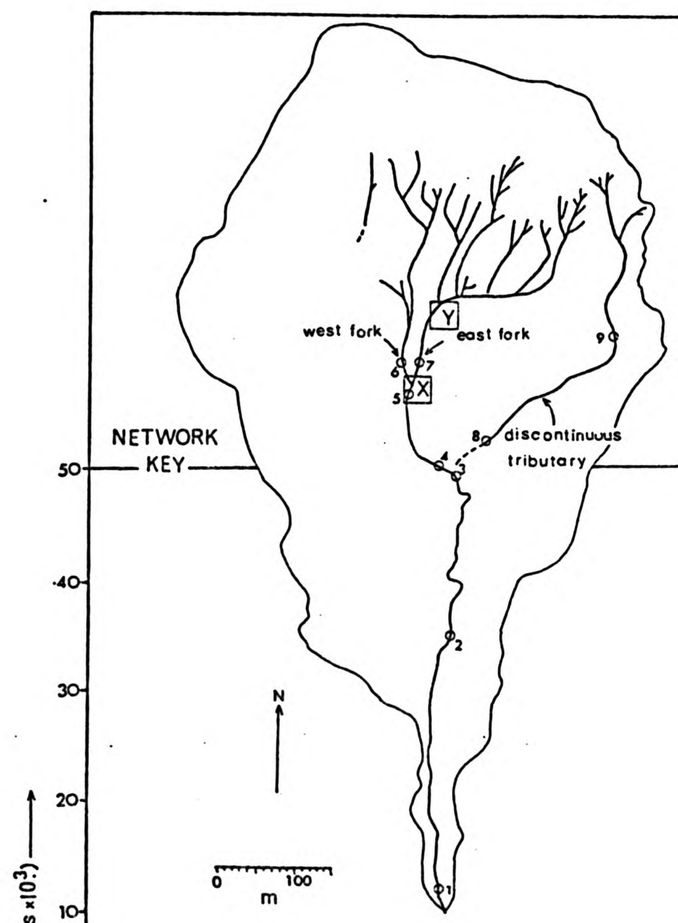

field discharge data ▾ April 7th

⊙ April 19th

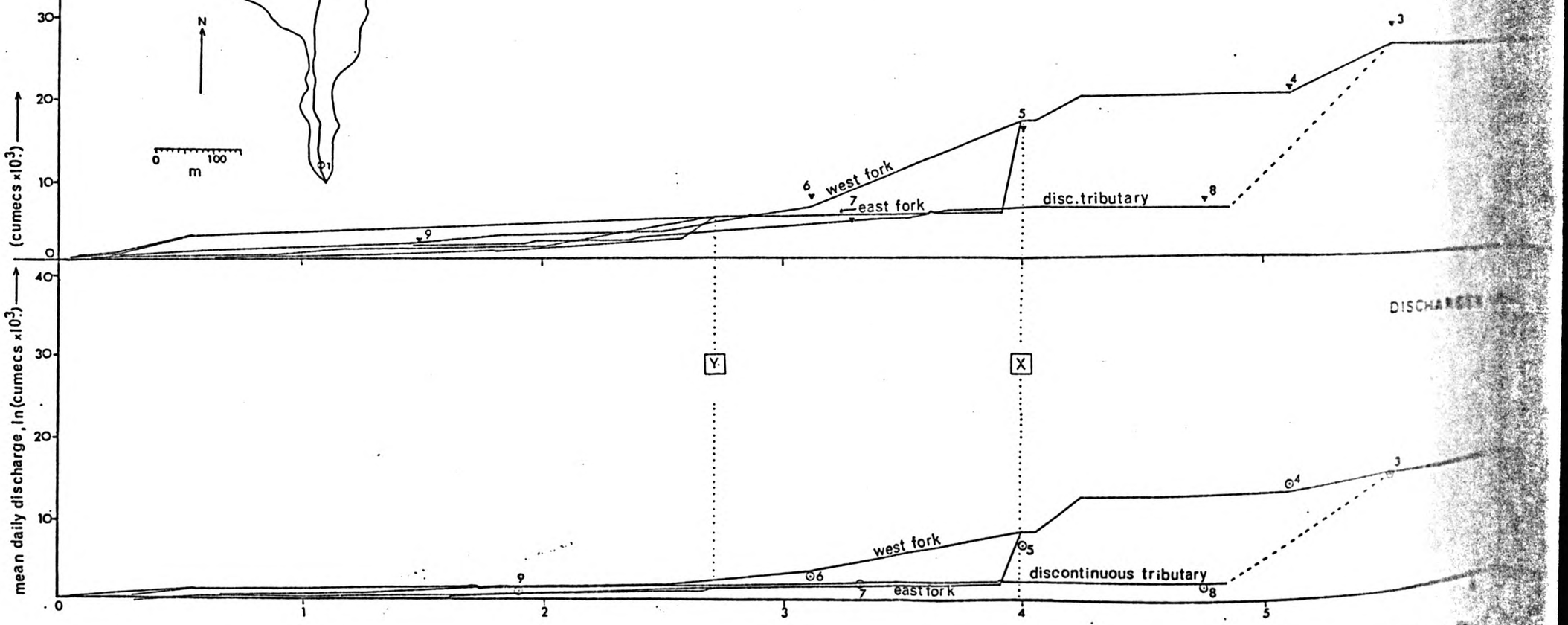

cross-sections joined into
contiguous network positions

DISCHARGES GENERATED BY ROUTING SNOWMELT APRIL 1 - 15th

disc. tributary

DISCHARGES GENERATED BY ROUTING SNOWMELT APRIL 15 - 30th

discontinuous tributary

Distance downstream, Lm , in [illegible]

predicted patterns listed at FW (1) and FW (2) and secondly, to calibrate these mean daily discharges for diurnal variations.

The diurnal discharge variations at the basin output point were sampled twice, in both cases immediately preceding the spatial surveys on April 7th, and 19th respectively. This was because the subsequent spatial surveys of discharge would obviously have to be carried out during the daily peak flow period, when flow remained constant for a time long enough to allow comparable spatial readings to be taken, and without a preceding diurnal sample, it would be difficult to infer at exactly which part of the day this occurred. Also, since the routing predicts mean daily discharges, a relationship would have to be established between daily peak and daily mean discharges, (even though this was something of a generalisation) in order that the two sets of data could be compared.

(i) Diurnal variations

On April 5th, and on April 18th, 1981 the diurnal range of discharges experienced at the Alkali Creek watershed output point were monitored using a standard Ott current meter held at two-thirds maximum depth within the channel cross-section for 100 seconds every half hour, from 11 a.m. to 5 p.m. All field booking sheets and discharge summary data are included in Appendix 7, and the data have additionally been plotted onto a timebase for both diurnal samples on Figure 20.

On April 5th, sampling started at 11 a.m., by which time there was already some flow within the channel. By 5.30 p.m. the channel was starting to freeze over slightly, and since it was clear that flow would soon reduce to a trickle, sampling was abandoned for the day. On April 18th, there was some flow within the channel at 11 a.m. but insufficient depth for the operation of the propellors of the current meter, and it was not until 12.30 p.m. that sampling proper could begin. At 5.30 p.m. discharge had started to fall, and so sampling was once again abandoned at this time.

Throughout the simulations, a 7 hour melt day has been assumed. These diurnal plots would support the use of this length of melt day in deriving a mean daily discharge from routed volumes, and there

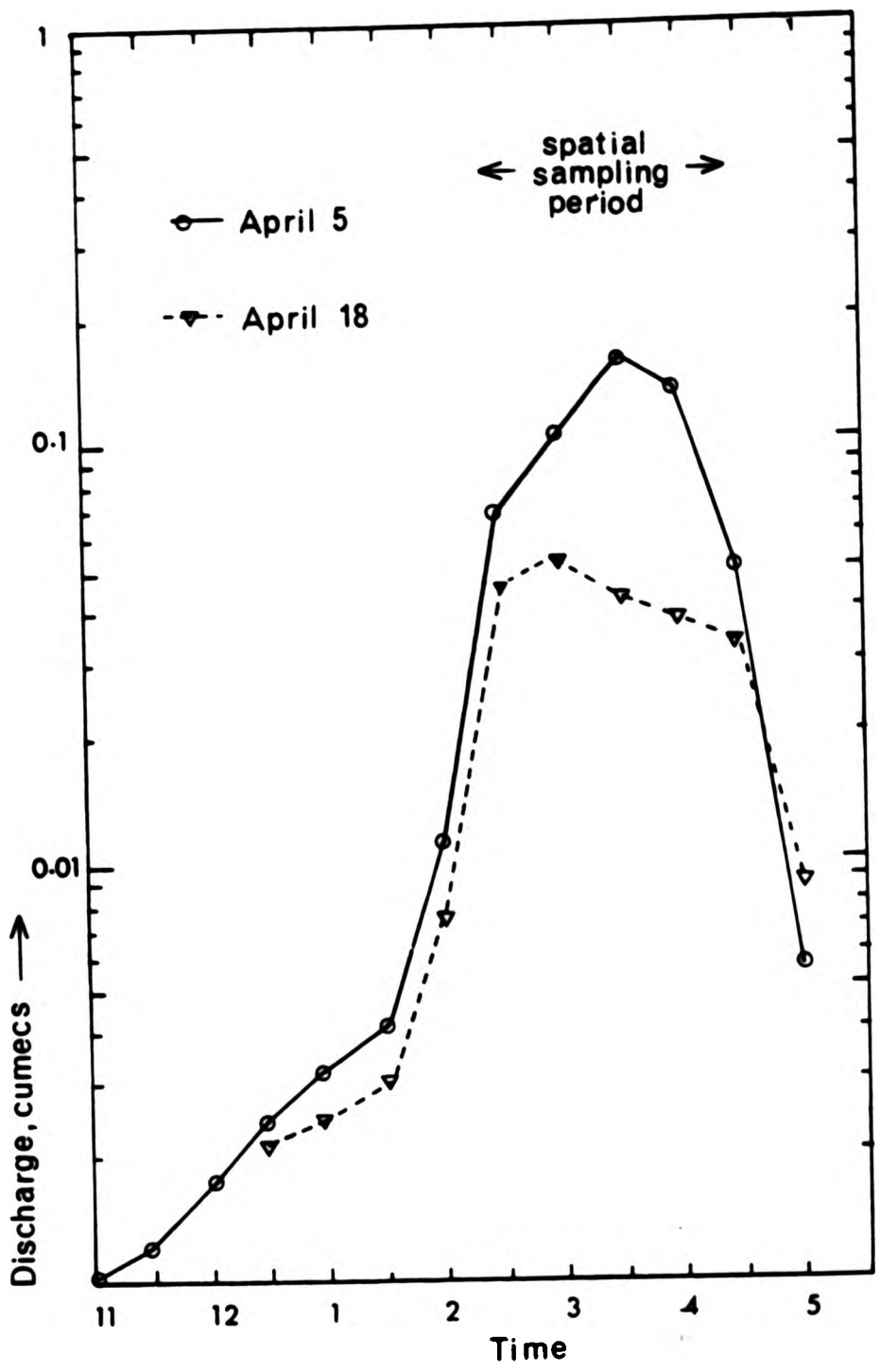

Figure 20: Diurnal discharge variations during the fieldwork snowmelt runoff survey; April 5th and April 18th, 1981

appeared to be no reason to adjust the simulations for a shorter or longer melt day value.

From Figure 20, it is clear that on both occasions, diurnal discharge variations are considerable, ranging from 0.001 cumecs to 0.140 cumecs on April 5th and from a trickle to 0.053 cumecs on April 18th. It is possible, in fact, to derive from these data approximate mean daily discharge over the period sampled on each day, and thus obtain a peak flow to mean flow ratio. The results of the calculation of these ratios is included in Appendix 7, showing that the ratio, k, of peak to mean flow on April 5th was 3.35, and on April 18th was 2.94. These two values of k are taken to represent the link between peak and mean daily discharges throughout the watershed in the first two weeks, and last two weeks of April during the April fieldwork period respectively, and are used below to compare the field (peak) spatial survey with mean daily discharges predicted from the routing of the field monitored pack.

(ii) Spatial variations

On April 7th and April 19th, following the monitoring of diurnal discharge variations, a spatial survey of peak daily discharges was planned. These patterns were to be taken to represent the average spatial patterns of snowmelt flows during the first half, and second half of April 1981, respectively. Figure 20 indicates that the time of day when discharge remains relatively constant around a peak value was between 2 p.m. and 4.30 p.m., and so sampling was limited to this time period. This limitation, plus other fieldwork commitments at this time, necessarily constrained the number of sites that could be sampled, and it was estimated that only nine could be attempted. These discharge sample sites (Figure 7, back folder) were chosen to represent the flow through critical reaches of the network. For instance, both the west and east forks of the headwater network are sampled by sites 6 and 7 (which correspond to cross-sections 7 and 23 on the 1975 morphological survey). The point X (cross-section 6 in the 1975 morphological survey) where these flow contributions join was sampled by site No. 5 (Photo 16). The large discontinuous tributary was sampled at points 8 and 9 (sites 194 and 59, respectively on the 1975 survey) to assess the possibility of transmission loss. Whether or not runoff from the

Photo 16 : Field site No.5 at 2pm on 7th April,1981

Photo 16 : Field site No.5 at 2pm on 7th April,1981

Photo 2 : Field site No.3 at 2pm on 7th April,1977

large discontinuous gully is picked up by the main channel is sampled by sites 4 and 3 (corresponding to sites 172 and 171 on the 1975 survey). These are respectively above and below the point where the fan 'hits' the gully. Sites No. 2 and 1 (respectively 161 and 152 in 1975) pick up the trend of the main channel accumulation, the latter being the basin output point where the diurnal survey was conducted. (The correspondence of these sites has been noted on the discharge simulation listings in Appendix 4). All field techniques were as for the temporal survey. Data are in Appendix 7.

In order to quantify the level of correlation between the actual mean discharge and predicted data, the peak daily discharges at sites 1 to 9 for each survey were plotted on a log-log regression against the peak daily discharges from predictions. These data, (Q_{sim} on Figure 21) were calculated by multiplying the mean daily prediction values for each site FW (1) and FW (2) respectively by the appropriate value of k. These data are listed in Appendix 7, the results of the regression shown on Figure 21, and the details of the regression analyses included in Appendix 12. As can be seen, the exponents in these log-log plots (which would be 1.0 for a perfect fit), are 0.89 and 0.93, and the constants also close to unity. Both regressions have correlation coefficients significant at the 0.1% level using Student's 't' test. This, without doubt, supports the principles on which the original routing was based, and concludes the field validation of the simulations APSIM and MAYSIM.

As an interesting additional validation of the mean daily discharges predicted by MAYSIM, field data was collected at the basin output point in 1964 by Heede (1971). Figure 2 shows that 1964 is a snow year close to the averages noted in this Chapter. Over a three day period in 1964, Heede (1977) recorded peak daily discharges ranging from 0.227 cumecs to 0.543 cumecs. As a comparison, the mean daily discharge predicted by MAYSIM at the output point was 0.084 cumecs. Since the ratio, k, peak to mean is usually around 3 (from fieldwork), then an average peak daily estimate is (3 x 0.084) cumecs = 0.251 cumecs, within the range monitored by Heede.

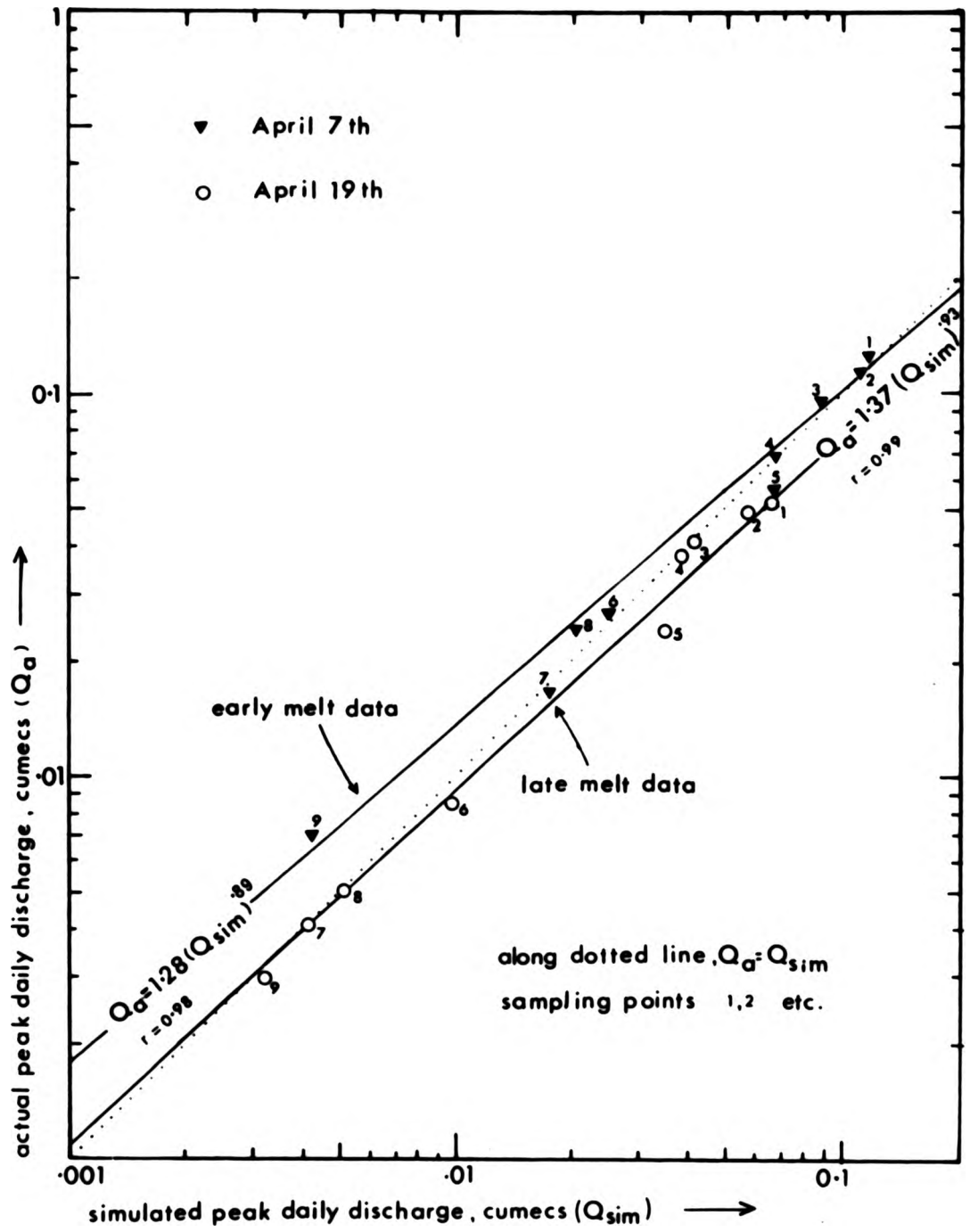

Figure 21 : Actual peak daily discharge at field sites compared with predicted values. Early and late fieldwork period best-fit log regressions shown

(V) CONCLUSIONS

The downstream snowmelt accumulation patterns APSIM and MAYSIM demonstrate the considerable assymetry of melt flows early and late in the melt process. As simulated, snowmelt at Alkali Creek clearly favours the main channel of the network below X, into which the bulk of the north and east-facing May snowpack drains. Additionally, the demonstrated emphasis on the main channel supports the intuitive observations made in Chapter 2 that the main channel below X might carry a disproportionately large snowmelt discharge when compared with the downstream flow volumes found from the melt of the headwater snowpack.

Three other points that are of general relevance can be made from the work presented in this Chapter. First, the methodology chosen to represent the melt process appears to work well. Not only were the predicted aspect and elevation-related differences in hillslope spatial domain intensity found, but also the asymmetrical pattern of the routed flows accorded with the field-monitored values. This not only justifies the approach but also suggests that by concentrating on the variations in the hillslope domain intensity perhaps in other areas, the more important spatial variability of the channel domain intensity (which must occur in basins with differing topographic orientations) would emerge. It could be hypothesised, for instance, that in a north-facing basin at the same elevation, a small early melt flow on the main channel would be followed by a late, considerably more voluminous pattern of flows in the head-waters, with obvious implications for sediment flushing and erosion.

Secondly, it is recognised that APSIM and MAYSIM represent merely monthly averages, so that in reality the mean daily discharges at each site will gradually change as the air temperature rises. For sites on the east fork of the headwater net on a normal year, mean daily discharges will drop during the melt sequence. For other sites in the west fork of the net and on the main channel, Figure 15 shows that the mean daily flows will gradually increase up to the point when the entire pack has collapsed.

Thirdly, the diurnal discharge data presented on Figure 20 show that diurnal variations at most sites are considerable. On a poor snow

year like 1981 such fluctuations may exceed the entire range of spatial variations in the network, and may also have an important role in the erosion and transportation of watershed sediment. A consideration of this effect is consequently included in the treatment given to melt and sediment behaviour in Chapter 5, in which summer storms are also considered in terms of sediment uield. The next Chapter addresses the problem of simulating summer storms on the watershed.

Chapter 4

OVERLAND FLOW

The recording raingauge records at Alkali Creek show the summer months to be characterised by short-duration, high-intensity storms. The suggestion was made in Chapter 2 that these events generate an uneven spatial pattern of overland flow, which originates predominantly within the upper south-west facing parts of the network headwaters, which are largely vegetation-free.

In this Chapter, these suggestions are further substantiated by the field-testing of a simulation model of spatial overland flow accumulation patterns on the Alkali Creek watershed. The choice of a suitable method is initially developed by reference to literature concerning both the generation and routing of overland flow following such rainstorms. Following this, a simulated rainfall event, in which 10mm (0.01m) of rain is assumed to fall over a period of 1 hour is considered, and by applying Hortonian principles this event is assumed to produce runoff on bare surfaces within the watershed. The volumes generated in this way are then routed through the channel network. This is done by first assuming a simple triangular hillslope hydrograph as a lateral input function, using a procedure originally suggested by Ragan (1966), and by then routing these lateral inputs down the channel network using a procedure modified from that presented by Freeze (1978).

The model is tested against its assumptions, which are concerned with channel roughness, a fixed hillslope velocity, and low infiltration. Although the model was found to be relatively stable over a range of assumed channel roughness and hillslope velocity values, a field infiltration survey did not support the assumption of no infiltration on bare sites. Infiltration data suggest instead that the percentage of the event rainfall eventually becoming runoff varies with the event intensity and duration, and additionally that the timebase of the hillslope hydrograph is less than the model assumes, since time to infiltration capacity rate is about 20 minutes on most field sites. As a result, a method of precalibrating the model to incorporate these effects when specific events are involved is finally proposed.

The model is applied to an event monitored in the field in June, 1981, and the results of a suitably precalibrated run of the model compared to monitored field discharges during the same event. These results imply some transmission loss on the main channel, and so a method is proposed and adopted to allow for this effect. Using the model in this form, and referring to the long-term raingauge records for the watershed finally allows a variety of events to be simulated. The geomorphological implications of these conclusions, and those made at the end of the last Chapter, are explored in Chapters 5 and 6, which follow.

(I) FACTORS AFFECTING OVERLAND FLOW GENERATION FOLLOWING SUMMER STORMS

The significant contribution made by Horton (1933, 1939a,b; 1945) to the modelling of overland flow is well-known and extensively reviewed elsewhere (Chorley, 1978b; Emmett, 1978; Dunne, 1978). In the last twenty years, the general applicability of the Hortonian model has been questioned, especially in humid temperate climates in which low intensity rainfall, with a fairly high annual total, results in a good vegetation cover and therefore high infiltration rates. Observations in such environments have led to the development of the partial area model of runoff generation, which, being based on consideration of throughflow, is more appropriate to such climates (Hewlett and Hibbert, 1967; Kirkby and Chorley, 1967; Betson and Marius, 1969; Weyman, 1970; Dunne and Black, 1970). Although these developments might imply that the Horton model is consequently devalued, Dunne (1978) points out that "... the various models of storm runoff are complementary rather than contradictory ..." such that "... differences in emphasis between studies of runoff reflect the physical geography of the regions in which the experiments were carried out". Chorley (1978b) confirms that the Hortonian model still provides "... a satisfactory model for the disposition of water on and within poorly vegetated slopes having thin soil covers", and is therefore the most appropriate model to adopt in arid and semi-arid lands (Dunne, 1978).

Because, as has been demonstrated, this description applies to the climate of the study area, a Hortonian approach to the generation of overland flow is adopted in this Chapter. This decision, and the

modifications made, are justified below by reference to Horton's theory and its assumptions insofar as they relate to the study area. Reference is also made to recent studies in comparable environments. A later section reviews the complications introduced when considering the routing of these generated flows through the channel system itself.

(A) Infiltration

Horton (1933) recognised that with prolonged rain, infiltration capacity would decrease asymptotically as changes in surface moisture, increasing effects of raindrop impact (slaking), closing of the surface suncracks, and swelling and breakdown of the soil structure combined to cause the gradual sealing of the surface. He proposed the following negative exponential decay function to describe the process, which was assumed to start after an initial short period of depression storage ;

$$f = f_c + (f_o - f_c) e^{-kt} \qquad 4:1$$

where f = maximum rate of instantaneous infiltration in in/hr at which the given soil can absorb precipitation as it falls

f_c = the limiting, steady minimum infiltration rate, assumed to be more or less constant for a given soil

f_o = the initial maximum infiltration rate at the start of the storm (at t=0)

k = permeability, a positive constant

and t is time in hours since the storm started.

The value f_c represents the ultimate steady value of f_t. In the original model, a comparison between infiltration capacity rate, f_c with rainfall intensity, i, produces a rainfall excess which is assumed to accumulate downslope as the area drained per unit of contour length, a, increases. After f_c is reached, therefore, Hortonian overland flow can be calculated in $cm^3.sec^{-1}$. per unit of contour length as :

$$q_o = (i - f_c).a \qquad 4:2$$

The value of a is equivalent to distance from the divide on slopes without plan curvature. In these situations, depth of flow can be related to the distance from the divide by a power law (Kirkby, 1969).

Horton assumed q_o to be the only contribution to the storm peak in the channel, and to be generated more or less simultaneously over the watershed. After a relatively short period, stream flow would achieve a steady state. When rainfall ceased, overland flow disappeared, first at the head of the slope, and then progressively downslope, usually within an hour or so.

Since this original formulation, the negative exponential nature of the infiltration curve has been substantiated in field experiments, for example Musgrave (1935), Neal (1938), Colman and Bodman (1943), Hills (1970), Smith (1972) and Knapp (1978). However, other aspects of the model have been criticised. For instance, fundamental to the whole conception of the uniformly generated flow is the assumption that infiltration capacity is exceeded by rainfall intensities early in the storm, and by implication the reduced infiltration capacity rate is areally constant. This is most likely to be true when surface infiltration rates are artificially reduced to a very low value by slaking and surface sealing caused by the sort of high intensity raindrop impact originally described by Ellison (1944), and experimentally reproduced by Wischmeier and Smith (1958). However, if the surface is not sealed, minimum infiltration rates will be dependent on subsoil properties, and therefore spatially variable with soil type. In these situations, the time taken to achieve f_c will vary, being also dependent on antecedent soil moisture conditions. Where these considerations apply, the spatial uniformity of overland flow generation as conceived by Horton is no longer valid. Thus Chorley (1978b) views Horton's model as occupying an end position in a "... more or less continuous spectrum of such models... ", in which the spatially variable partial area model (where overland flow is only generated on saturation) occupies the opposite end to the Horton model.

It is now considered that Horton's model is really only applicable in a narrow range of environments, those with high intensity; short-duration rain as the norm, and where unprotected soils, prone

to swelling when wet, are present. This tends to limit true Hortonian flow to arid and semi-arid regions.

There are some situations, however, where outside these climatic zones the above equations might apply, and overland flow be generated for even fairly low rainfall intensities. These are situations where infiltration rates are low because of low subsoil permeability. Since, according to Rubin (1966) this may be a more common cause of overland flow, there has been a tendency to prefer, for modelling purposes, the Philip (1957) infiltration model. This explains f in terms of soil properties such as capillary potential, and gravity forces. Philip's explanation for the negative exponential decay form of the infiltration curve is ;

$$f = A + Bt^{-\frac{1}{2}} \qquad 4:3$$

where A = the conductivity flow under gravity at a steady state of transmission

and B = the diffusion flow, representing the filling up of pore spaces from zones of high to low porosity by capillary flow, and is inversely time-dependent.

Philip's model has been regarded as preferable to Horton's model on two counts, first because it gives a better prediction for short-term infiltration rates, (Kirkby 1969), and secondly because in this formulation diffusion, which is dependent on antecedent moisture conditions, physically explains the time lag between the onset of rain, and the attainment of overland flow. Field experiments suggest that antecedent moisture is very important in determining both the time to runoff peak, and the amount of runoff in situations where infiltration rates are not diminished by surface sealing. Yair and Lavee (1976), Dunne and Black (1970), Yair and Klein (1973), Yair et al (1978), and Scoging (1982) in particular have criticised the basic Hortonian assumption in their literature. Sometimes the two situations occur side by side. In a study of infiltration rates, antecedent moisture, and runoff rates on differing lithological units in the Steveville badlands, Alberta, Bryan, et al (1978), and Hodges and Bryan (1982) found that the threshold value for rainfall to initiate runoff on bare, dry surfaces at a single site on cracked shale units was almost double

that needed on an initially wet surface for the same value of rainfall intensity, and runoff was not spatially uniform. On shale lithologies, too, slope angle was found to be a significant control on runoff rates. Only the most gentle slopes at basal concavity produced overland flow, which was deduced to be evidence of saturation overland flow, and the partial area model was taken to be appropriate for these units. Runoff occurred whenever rainfall intensities of over 5 mm/10 mins were applied, but on drier sites with low antecedent moisture, intensities of over 3 mm/3 mins were needed to generate runoff, and on all shale units, only rills carried water during overland flow. By contrast, adjacent fine-grained sandstone units slaked easily, and erosion monitored by pins was uniform over all units of this lithology independent of slope angle. Overland flow generation, therefore, conformed to the Hortonian model. Here runoff was generated earlier, too, and runoff was frequent whenever intensities exceeded 0.5 mm/min. This study also emphasised the role of pipes in hydrograph production, with suggestions of surging as pipes flushed into channels when hydrostatic conditions altered within the subsurface system.

The Alberta badlands are drier than the present study area (325 mm/yr) and support little vegetation (Faulkner, 1970), but in lithological terms the sandstone units are very like the sandier units within the Wasatch Formation. However, the variations cited above between differing lithological units in terms of their hydrological response do suggest caution in the wholesale adoption of the Hortonian model within the context of the current investigation. However, there is plenty of evidence for surface slaking in the study area, and observations made during the three main fieldwork periods only confirmed that a Hortonian model would be appropriate, especially on the bare surfaces.

(B) Rainfall intensities

For Hortonian flow, rainfall intensities must exceed infiltration capacities early in the storm. Rainfall simulations (e.g. Emmett, 1978; Scoging, 1982) have largely supported the idea that high rainfall intensities are necessary for Hortonian flow. Most areas cited as producing runoff of this type fall into the semi-arid climatic zone, where sudden intense storms are common. Thornes

(1976) cites events with intensities of up to 50 mm/hr at Almeira, Spain, and Renard and Keppel (1966) explain that "... high intensity, short duration convective thunderstorms .. cause most of the runoff in ephemeral streams of the southwest United States". They suggest that on watersheds the size of Walnut Gulch in Southern Arizona, and the Almagordo watershed in Mexico, 60 to 70 per cent of the 355 mm/yr falls as a result of intense, small diameter storms which "... rarely cover an entire watershed". Storms of this sort are common in the Upper Colorado River basin as well. Laronne (1982) considers the erosional implications of high intensity events with "... small area coverage", and in Chapter 2 the evidence for rainstorms with intensities sufficient to produce overland flow on bare sites at Alkali Creek was strongly inferred from the recording raingauge trace. Although the possibility that storm paths cause variations in intensity across the study area cannot be established from a single raingauge trace, it is considered here that because of the very small size of the study area (0.4 km^2) this is unlikely to be a problem. For simplicity, a spatially uniform event is considered in the flow simulation presented here. This event, thought to be representative of the range of events presented in Chapter 2, is assumed to have a total precipitation of 10mm, falling for an event duration of 1 hr (intensity 10 mm/hr). The representative nature of this choice will be further examined in the final section of the Chapter.

(C) Vegetation

Outside the arid zone vegetation is effective in reducing the impact of high intensity rain when it occurs. As rainfall totals increase, the intensity of individual events lessens, and vegetation density increases (Langbein and Schumm, 1958). As a secondary effect, vegetation litter promotes thicker soils which have a better humic horizon and therefore higher infiltration capacities. Although on this topic speculation has tended to be more widespread than hard field data, research data that are available tend to support this picture (Knapp, 1978, Musgrave and Holtan, 1964, Whipkey, 1969). Kirkby and Chorley (1967) have suggested that where there is appreciable soil and vegetation, especially humus and litter "... little runoff may be expected to occur over much of the drainage basin except in the most intense storms". Thornes (1976) quotes the

use by Zingg (1940) of a weighting factor to be applied to sites with differing vegetation cover when attempting to predict erosion rates. Bare sites were weighted at 1, all other covers less, confirming an early recognition of the protective role of vegetation.

These observations are particularly applicable to watersheds within the semi-arid zone. Chorley (1978b) cites several examples of semi-arid watersheds where overland flow was never observed when vegetation cover was present, suggesting that many storms may be expected to produce overland flow of the Hortonian type from limited bare contributing sites at much lower rainfall intensities than are required to exceed the infiltration capacities over the whole basin, and so to produce universal overland flow. This work supports the earlier observations of Kirkby (1969), Kirkby and Chorley (1967).

The study area has been described previously as semi-arid, having a mean annual precipitation of 480 mm p.a. As has been seen, the winter snow melts during a relatively short period in late March and early April. The ground is therefore still fairly moist in April and May on the slopes that have contained the most snow and which are the last to melt. It was demonstrated in the last Chapter that these slopes face predominantly north, north-east, north-west and south-east, and it was also shown in Chapter 2 that the most dense vegetation cover occurs on these slopes (Figure 4, back folder). This is not surprising, as they are sites where soil moisture regimes are the most suitable in the growing season, and the most protected from radiation during the heat of the summer. It is therefore expected, both from the literature reviewed here and from field observation, that the summer storm pattern described in Chapter 2 will produce runoff primarily on bare sites on the south-west facing slopes, and this implies the assumption that covered sites have infiltration capacities that exceed the normal range of events in the area, but that on bare sites this is not the case. In the first stage of the modelling undertaken in this Chapter, therefore, all the rain which falls on the bare sites is assumed to runoff instantaneously, and all the rain of the simulated event which falls on the covered sites infiltrates. It is clear that these assumptions will need considerable substantiation and so a field infiltration survey was planned which at a later stage serves to recalibrate the model against these assumptions. At this

stage the use of these assumptions makes the nature of the routing procedure simpler to describe, especially the calculation of the generated volumes.

(II) ROUTING

Considerable experience in the field investigation of overland flow generation on hillslopes has led Emmett (1978) to claim that overland flow rarely persists for any length as sheet wash. Concentrations of flow "... weave anastomosing paths downslope and often give the appearance of flow in a wide, braided channel". Whereas laminar flow is assumed as long as the slope profile is fairly smooth, higher Reynold's numbers, indicating increased turbulence, may be produced where flows accumulate or accelerate due to profile irregularities. This situation is highly conducive to the formation of rills and gullies (Emmett, 1978; Scoging, 1982).

Despite the complexity of the flow paths, as suggested by these observations, Emmett's work in particular has tended to support the general Hortonian picture as presented by equation 4:2, in which formulation rainfall which does not infiltrate builds up downslope in a manner which is proportional to the area drained per unit contour length. Thus, for simple volumetric calculations of the total amount of overland flow generated at a particular hillslope base in a defined event, attention need only be directed towards calculation of contributing area and the rainfall excess after f_c. The implication is that slope angle is not a significant variable in the calculations. As Kirkby (1980b) suggests, "... in semi-arid areas, topography has no influence on overland flow production". Since in previous sections, it was suggested that retaining a vegetation cover can be assumed not to generate Hortonian flow to any extent except in the most extreme storms, then assuming this to be true, the effective contributing area for overland flow generation between two adjacent cross-sections on a channel is equivalent to the total bare area on both side slopes, AB. This value can be calculated as the total area on each side slope between cross-sections, divided by the percentage vegetation cover on those slopes. In addition, if on these bare sites the total infiltration can be considered negligible in comparison with

the rainfall intensity of the event, then for an event of intensity i and total during T, in which a total of :

$$r = (i.T) \qquad 4:3$$

the depth of flow at each site during the event is approximated by r, and the generated volume from the contributing unit is :

$$Vol = (AB.r) \qquad 4:4$$

Whereas at the flow generation stage, slope angle may not be a significant variable in the calculations, it is generally accepted that the rate at which this generated flow moves across the hillslope is characterised by an expression such as the Manning formula, in which the velocity of overland flow is seen as dependent on slope gradient and surface roughness, and increasing with length. This flow, when delivered as lateral input to a channel system, controls the rate at which channel flow builds up, but in the channel phase of runoff, the storage of flow may occur both as a local depth change and as an increase in channel width, in a manner determined by both continuity and energy balance considerations. In other words, flood routing is a complex estimation procedure which involves the simultaneous solution of at least one shallow flow equation for several parameters.

(A) Background

At an early stage in the work for this Chapter, a simple lagged-volume model was proposed for the simulation of watershed hydrographs. The great advantage of this simple routing procedure appeared to be that a continuously varying hydrograph is produced without having to utilize, and therefore solve numerically, differential equations; and despite the lack of allowance for transmission losses the results were initially encouraging. But the disadvantage of assuming that each flow contribution behaved as if it were on a constant velocity conveyor belt, not mixing or being delayed by accelerations and decelerations of flow was that the output hydrographs were very unsmoothed, and there was a conspicuous lack of recession flow, especially on the downstream graphs produced. In fact these lower sites seemed to display a slow

build-up of flow not normally associated with hydrographs in semi-arid areas[1], and although it was clear that this happened in this case because small contributions from the main channel were arriving well ahead of the bulk of the headwater contributions, the question arose as to why this does not normally happen in the real world. The answer was initially thought to be that these early flows would normally be absorbed by hillslope infiltration or by transmission loss early in the event.

A more careful examination of the underlying assumptions of the model, and further sensitivity testing revealed more serious flaws in this approach. The first problem emerged when the model was tested for stability against the model assumptions - particularly the assumption of a constant channel velocity in the channel phase of the routing. The tests revealed that the changes resulting from quite small changes in the channel velocity assumption were dramatic, in some cases constituting over 55% of the range of discharge values taken through the original hydrograph. In fact, in a similar sort of model, in which a constant network velocity was also assumed, Rodriguez-Iturbe and Valdes (1979) considered the effect of varying the velocity assumption in this model and found their results to be similarly sensitive (Valdes et al., 1979). Other problems associated with their model were also discussed, in particular the observation that the Instantaneous Unit Hydrograph that they produced could only be really considered as the pattern that an additional unit input would produce on a hydrograph that had already reached equilibrium level. This was because for adjacent sites velocity was bound to vary on the rising and falling limbs, only being close to a constant value at peak flows. This second problem similarly applies to the method described above for the Alkali simulation. Uneven flows associated with the rising stage which occur in reality store water volume at each site on the rising limb, which is then released during the hydrograph recession. This is a major cause of the recession limb found on most hydrographs (Viessmann, Harbaugh and Knapp, 1972; Linsley, Kohler, and

---

(1) Thornes, J.B.T. pers comm., June 1983

Paulhus, 1949). By excluding storage effects, therefore, this model fell prey to one of the major dangers in modelling cited by Freeze (1978) "... failure to represent the actual mechanism at a fundamental level.".

So these problems have been addressed in an alternative attempt to characterise hydrographs that would be likely to result from the simulated rainfall event. In the method that is presented here, all slope discharges from a volume generated in a manner described by equation 4:4 are converted to discharge values by representing this volume as the area under a triangular-shaped lateral inflow function. This method has been utilized by Ragan (1966) and will be discussed in more detail below. In the channel stage of the model, this lateral inflow is added iteratively into a kinematic routing procedure for the channel network, in a manner simplified from a scheme presented by Freeze (1978). The method that was adopted here is developed in the next section, after which the results of a range of tests on the model are presented. Fieldwork aimed towards establishing the validity of the infiltration assumption follows, and the model is then rerun on a basis more in tune with these findings, and tested against field discharge data. Transmission loss is considered at that stage, as is the possible range of events which might result from a varied set of summer events on the watershed. This latter discussion makes use of the long-term recording raingauge records presented initially in Chapter 2.

(B) The theoretical basis of dynamic routing models

For the purpose of dynamic modelling, the aim is usually first to simulate hillslope hydrographs by considering the shallow flow equations as described by Freeze (1978), and then to reroute these as lateral inputs within the channel using another set of flow equations. In these situations both hillslope and channel flow timings depend ultimately on the variations in velocities in both slope and channel, which in turn vary in both phases as site flow depth is affected by spatial changes in slope and roughness.

The shallow flow equations as described by Freeze (1978) derive from field experiments, notably those of Emmett (1978) who combines the equation for overland flow ;

$$q_{(x,t)} = d.v \qquad 4:5$$

where d is flow depth in metres at distance x and time,t

and v is mean slope velocity in m/sec, also at (x,t)

and $q_{(x,t)}$ is the hillslope discharge per unit contour width at distance x and time t.

with the Manning equation for v at (x,t) ;

$$v = \frac{d^{\frac{2}{3}}.s^{\frac{1}{2}}}{n} \qquad 4:6$$

where n is the Manning roughness coefficient derived from field tables provided for example by Barnes (1964)

and s is the slope gradient in m/m and which for kinematic approximations (discussed below) is taken to be equivalent to the frictional slope

to give ;

$$q_{(x,t)} = \frac{s^{\frac{1}{2}}.d^{\frac{5}{3}}}{n} \qquad 4:7$$

These formulations have been extensively tested, notably by Emmett (1978) and Scoging (1982). In Emmett's work, laboratory and field experiments were compared, and higher field roughnesses were found to retard the flow and cause an increase in flow depth, vegetation being the main cause of increased roughness. Average field velocities were variable spatially, but through time at the slope base appear to have remained fairly constant. Over a series of experiments, a mean velocity of 0.0457 m/sec was recorded over a range from 0.015 to 0.100 m/sec (variations occurring with both roughness and slope angle). These values compare favourably with the values cited by Kirkby (1969) as ranging from 200 to 300 m/hr (0.055 to 0.083 m/sec).

Several hydrologists have used equation 4:7, in conjunction with the continuity equation to route inputs which arrive laterally to a linear system - either a slope profile, or a channel - as the basis for a mathematical flow routing model (Wooding, 1965; Woohiser and

Liggett, 1967; Betson and Ardis, 1978; Freeze, 1978). In the hillslope case, the lateral input is the rainfall arriving at intensity i. Assuming a non-infiltrating surface, across which distance is x and where time is t, we have for a unit width a continuity statement in the following form :

$$\frac{\partial(d)}{\partial t} - i + \frac{\partial}{\partial x}\left|\frac{s^{\frac{1}{2}}.d^{\frac{2}{3}}}{n}\right| = 0 \qquad 4:8$$

or: (storage) - (input) + (output) = 0

(C) The kinematic approximation

To solve this equation 4:8 for hillslope flow, an assumption is usually made that at these presumably low discharges, a balance is achieved between gravitational and frictional forces, at which stage the flow is referred to as sub-critical. The Froude number, F, is used, where ;

$$F = v/\sqrt{g.d} \qquad 4:9$$

and g is the acceleration due to gravity, 981 $cm.sec^{-2}$ to assess whether or not this is the case. Woohiser and Liggett (1967) have shown that if F is less than 2.0, flow is presumed to be sub-critical.

The great advantage of this assumption is that in these cases, frictional slope and topographic slope may be taken as equivalent. Outside this possibility, a statement of energy utilization is needed in addition to equation 4:8, in order to solve for the frictional slope. If the approximation holds, the numerical solution is considerably simplified, and equation 4:8 can be solved for $d_{(x,t)}$ using a procedure which will be developed in the next section in detail for the channel case. Once $d_{(x,t)}$ is known, then $q_{(x,t)}$ can be calculated for all (x,t) using substitution in equation 4:7. This is referred to as the kinematic case.

In the channel stage of these models, the output from the hillslope model, $q_{(x,t)}$ becomes the lateral input function. If the flow in the channel remains sub-critical, then equations 4:7 and 4:8 are reapplied. In this case, distance will be described as y, channel

distance, and s and n replaced by S and N, the channel slope and roughness at y. Because width is varying as well as depth to accommodate storage, depth is replaced by cross-sectional area (W.D), where W is channel width, and D is channel depth. Time, t, takes the same values.

The use of the kinematic approximation in the channel phase of flow routing must be undertaken with care. As has been suggested, with supercritical flows a statement of energy utilization is additionally needed. The two full equations are explored by Freeze (1978), and are referred to by him as the shallow flow equations. Duluz-Vieira (1983) refers to them as the St. Venant equations, and the conditions under which the kinematic approximation hold are explored more fully in this latter paper. Because the solution of the full equations is complicated, the tendency has been to make the kinematic approximation wherever possible. For instance, Wooding (1965) states that "... for long, fairly uniform rivers and channels, it is generally assumed that quasi-steady conditions hold at any point, and that to a good approximation, a dynamical balance exists between boundary stresses and the gravity component in the direction of flow". However, following Woohiser and Liggett (1967), Duluz-Vieira (1983) considers that in the channel case, not only must the Froude condition be met, but also that a factor which Woohiser and Liggett (1967) denoted by k should be greater than 10. The dimensionless form of k is given by ;

$$k = S.\ \Delta y/F^2.D \qquad 4:10$$

where Δy is the incremental distance on the y plane.

Duluz-Vieira calls k the 'kinematic wave number', and emphasises the need to check both F and the k wave number at all computational stages in any investigation.

Even if the kinematic approximation holds, the channel phase has the additional computational difficulty of having to allow storage to occur in both the depth and width dimensions in the channel. If for fairly small channels the width is assumed to remain constant downstream (Viessman, Harbaugh and Knapp, 1972 suggest a constant one metre width), then all storage conveniently goes into the depth

dimension. This is probably not as serious a source of error as might be assumed, since in fact there seems to be no reason not to 'drop' storage into a parameter called depth which in reality is a substitution parameter for the variables width, and depth. This assumption will therefore be made in the present study.

By taking width as unity for all y, then for a channel flow model in which sub-critical flows are anticipated, equation 4:9 becomes ;

$$\frac{\partial(D)}{\partial t} - q_{(x,t)} + \frac{\partial}{\partial y}\left|\frac{S^{\frac{1}{2}}.D^{\frac{2}{3}}}{N}\right| = 0 \qquad 4:11$$

where all variables are as previously defined and where in most circumstances $q_{(x,t)}$ is the slope-base discharge per unit contour length at y, resulting from the hillslope convolution model described by equations 4:8 and 4:7.

(D) The numerical scheme.

Several investigations (e.g. Ragan, 1966; Freeze, 1978; Field and Williams, 1983) have produced finite difference approximations for the hyperbolic partial differential equation 4:11. Such schemes can be of three types, explicit, implicit, or employing the use of 'characteristics' (Freeze, 1978). The method described below is an explicit method which is referred to by Freeze (1978) as the 'single-step Lax-Wendroff method'. This utilizes the Taylor expansion of a function in order to derive a numerical scheme to approximate its derivative.

To explain more fully, the Taylor expansion of the functions $f(x+\Delta x)$ and $f(x-\Delta x)$ where Δx is the increment in the x plane is given by two following expressions ;

$$f(x+\Delta x) = f(x) + \Delta x f'(x) + \frac{\Delta x^2}{2!}f''(x) + \frac{\Delta x^3}{3!}f'''(x) + \ldots$$

$$f(x-\Delta x) = f(x) - \Delta x f'(x) + \frac{\Delta x^2}{2!}f''(x) - \frac{\Delta x^3}{3!}f'''(x) + \ldots$$

and subtraction gives ;

$$f(x+\Delta x) - f(x-\Delta x) = 2\Delta x f'(x) + \frac{2\Delta x^3 f'''(x)}{3!} + \ldots$$

so that ;

$$f'(x) = \left\{ \frac{f(x+\Delta x) - f(x-\Delta x)}{2\Delta x} \right\} - \frac{\Delta x^3 f'''(x)}{3} - \ldots . \qquad 4:13$$

In the first-order Taylor expansion of a function, the term $[\Delta x^3 f'''(x)/3]$ and all subsequent terms are assumed in total to converge on zero, and are therefore ignored. This is only true in actual fact if Δx is very small, so the incremental steps, Δx, in any numerical scheme should be kept as small as possible in comparison to the value of the derivative.

We now turn to the expansion of equation 4:11 along these lines. For this purpose, reference is made to the (y,t) plane shown on Figure 22a. On this diagram, D represents the channel depth as in equation 4:11. The problem to be addressed is the calculation of $D_{(y,t+1)}$ from $D_{(y,t)}$, and also from the adjacent values of D at t, i.e. $D_{(y-\Delta y,t)}$ and $D_{(y+\Delta y,t)}$. To do this, the $(\partial/\partial y)$ term in equation 4:11 is expanded around the point y, keeping increments to a minimum. The minimum possible in the current investigation is the distance between sites where channel slope data are available. The expansion is ;

$$\frac{\partial}{\partial y}\left\{ \frac{S^{\frac{1}{2}} . D^{\frac{5}{3}}}{N} \right\} = \left\{ \frac{((S_{(y+\Delta y)})^{\frac{1}{2}} / N_{(y+\Delta y)})(D_{(y+\Delta y,t)})^{\frac{5}{3}} - ((S_{(y-\Delta y)})^{\frac{1}{2}} / N_{(y-\Delta y)})(D_{(y-\Delta y,t)})^{\frac{5}{3}}}{2\Delta y} \right\} \qquad 4:14$$

In the next stage, the $(\partial/\partial t)$ term is expanded, in this case around the point $(t+\frac{1}{2})$, allowing therefore $(2\Delta t)$ to be equal to 1, simplifying the expansion. This gives ;

$$\frac{\partial}{\partial t}(D) = D_{(y,t+1)} - D_{(y,t)} \qquad 4:15$$

Finally we note that the average value of the lateral contributions, $q_{(x,t)}$ through the distance $2\Delta y$ is equal to ;

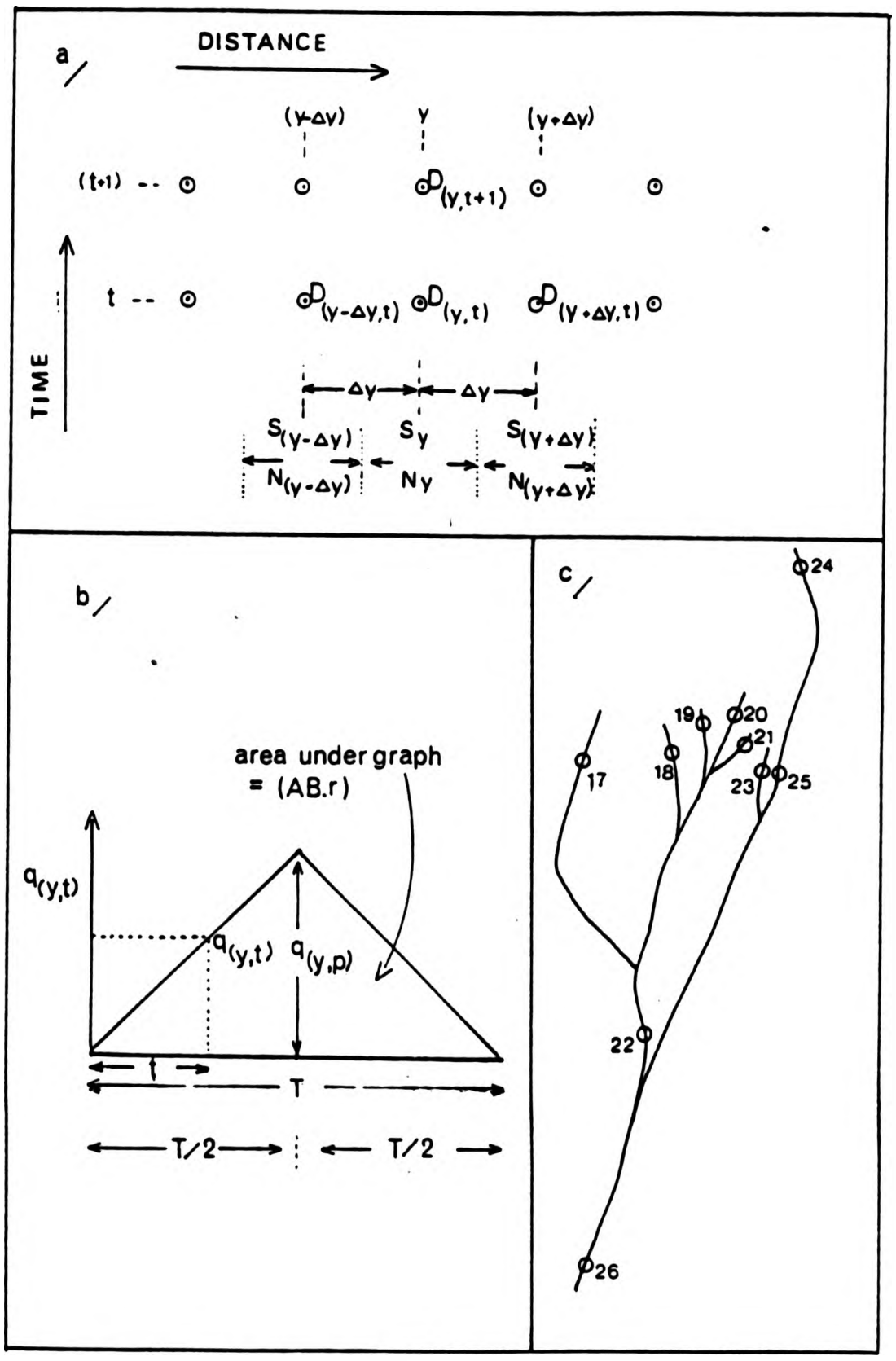

Figure 22: The development of the numerical scheme
(a) The (y,t) plane
(b) The triangular lateral input function
(c) The part of the network used as an example in the text

$$q(x,t) = \left[\frac{q(y,\ t) + q(y+\Delta y,t)}{2\Delta y}\right] \qquad 4:16$$

noting that $q_{(y,t)} = \int_{y=y}^{y=y-\Delta y} q_{(x,t)}.dy$ because $q_{(x,t)}$ was formulated originally for a unit contour length. Similarly $q(y+\Delta y,t) = \int_{y=y+\Delta y}^{y=y} q(x,t).dy$. Putting together equations 4:14 to 4:16 gives finally ;

$$D(y,t+1) = D(y,t) + \left[\frac{q(y,t) + q(y+\Delta y,t)}{2\Delta y}\right] - \left[\frac{((S_{(y+\Delta y)})^{\frac{1}{2}}/N(y+\Delta y))(D(y+\Delta y,t))^{\frac{5}{3}} - ((S_{(y-\Delta y)})^{\frac{1}{2}}/N(y-\Delta y)(D(y-\Delta y,t))^{\frac{5}{3}}}{2\Delta y}\right] \qquad 4:17$$

which is of course in the form ;

$$\text{depth} = \frac{\text{lastdepth} + (\text{lateral flow} + \text{lastsite flow} - \text{nextsite flow})}{\text{distance from last to next site}}$$

From $D_{(y,t+1)}$ it is now quite simple to calculate the discharge at (y,t+1) which is referred to here as $Q_{(y,t+1)}$, using ;

$$Q_{(y,t+1)} = \frac{S_y^{\frac{1}{2}} .D_{(y,t+1)}^{\frac{2}{3}}}{N_y} \qquad 4:18$$

The expansions of the Taylor series simply to the first two terms, as has already been emphasised, require that the incremental steps be kept as small as possible. Woohiser and Liggett (1967) have examined these requirements for the partial differential case in question, and show that the difference approximation becomes unstable if ;

$$(\Delta y/(\ |Q|\ /D\ + \sqrt{g.D})) < \Delta t \qquad 4:19$$

which is called the Courant condition. In general, this requires keeping the timesteps smaller than the incremental distance steps where possible. Thus in the model presented here, Δt has been kept to 1 sec. There must be checks on this condition throughout any numerical scheme (Freeze, 1978).

Provided that all conditions are met, and that the lateral input functions, $q_{(y,t)}$ and $q_{(y+\Delta y,t)}$ are known, as well as S, N, and y for all sites, then equations 4:17 and 4:18 can be solved for all (y,t), by a simple iterative computation scheme, in which there are two nested loops corresponding to the two expansions. It is conventional to run through the sites in the y direction first, then moving on to the calculations for the next time interval for all sites, and so on. This procedure was adopted for the model of overland flow in the channel phase at Alkali Creek, except that instead of separately modelling the lateral input functions $q_{(y,t)}$ and $q_{(y+\Delta y,t)}$ iteratively using a kinematic procedure, the method described below was employed, first suggested by Ragan (1966).

(E) The lateral input functions $q_{(y,t)}$ and $q_{(y+\Delta y,t)}$.

The computational logistics of modelling over 400 contributing slope hydrographs iteratively in kinematic schemes (using equations 4:7 and 4:8) was considered excessive, and a simpler method of routing the volumes of water generated laterally (equation 4:4) into the channel in the form of a hydrograph was considered along the lines adopted by Ragan (1966), and cited by Freeze (1978). In this method, the hillslope hydrograph is approximated by an isosceles triangle, the base of which is the duration of the hydrograph, T. This is approximated as the rainfall time, less time to f_c, plus the time taken to drain the longest length of slope in the contributing unit once rainfall has ceased. This latter term is calculated by assuming a mean hillslope velocity for the slope drain period, v. In the case of the current investigation, runoff is initially assumed to occur instantaneously, so that on the first runs of the model the hillslope hydrograph duration at y, T_y, is calculated as ;

$$T_y = 3600 + (\text{slopelength}/v) \qquad 4:20$$

where 3600 is the number of seconds in a 1 hour rainfall event, and where slopelength is the maximum length of slope in the units contributing on either sideslope to the site y. The mean hillslope velocity is initially selected as the mean of Emmett's cited velocities from field experiments (Emmett, 1978), the conservative value 0.0457 m/sec (see page 80).

For the calculation of $q_{(y,t)}$, the lateral input function for the whole of the incremental distance Δy at time t, consider the diagram included as Figure 22b. From this it is clear that up to $(T_y/2)$, we have ;

$$\frac{q(y,t)}{t} = \frac{2q(p)}{T_y} \qquad 4:21$$

and also it is possible to observe that the volume drained from that unit is (AB.r), as developed in equation 4:4. So;

$$(AB.r) = \frac{T_y}{2} . (q_{(p)}) \qquad 4:22$$

so that substituting for $q_{(p)}$ from 4:21 into 4:22 gives ;

$$q(y,t) = \frac{4.t.(AB.r)}{(T_y)^2} \qquad 4:23$$

Similarly, after $(T_y/2)$, we have ;

$$q(y,t) = \frac{4.(T_y-t).(AB.r)}{(T_y)^2} \qquad 4:24$$

After T_y, the expression is set to zero ;

$$q(y,t) = 0 \qquad 4:25$$

Now attention is directed to the lateral input function for the next downstream length increment, $q_{(y+\Delta y,t)}$. Up to $(T_{(y+\Delta y)}/2$ we have;

$$q(y+\Delta y,t) = \frac{4.t.(AB.r)}{(T_{(y+\Delta y)})^2} \qquad 4:26$$

where in this case AB is the incremental bare area relating to $(y+\Delta y)$. After $(T_{(y,+\Delta y)}/2)$, the relationship becomes ;

$$q_{(y+\Delta y,t)} = \frac{4.(T_{(y+\Delta y)} - t).(AB.r)}{(T_{(y+\Delta y)})^2} \qquad 4:27$$

After $T_{(y+\Delta y)}$, the expression is set to zero as before ;

$$q_{(y+\Delta y),t)} = 0 \qquad 4:28$$

The fact that there are three differing conditions for each of these expressions means that in the modelling of overland flow using equations 4:17 and 4:18, the timestep in the timeloop must be compared with both T_y and $T_{(y+\Delta y)}$ and the appropriate equation preselected, i.e. for $q_{(y,t)}$, one of the three equations 4:23, 4:24 or 4:25, and for $q_{(y+\Delta y,t)}$, one of the three equations 4:26, 4:27, or 4:28. In the computational scheme finally developed, these conditions were set as an array of Boolean functions.

(F) Keying in the network positions

One problem with the application of equations 4:17 and 4:18 to the Alkali Creek watershed is the problem of the dendritic nature of the headwater net. Whereas equation 4:17 was assumed to apply to a linear system, at Alkali Creek a network of tributaries exists, part of which is illustrated on Figure 22c. At some of these sites, discharge at the last, or upstream site ($Q_{(y-\Delta y,t)}$), will be supplemented by additions from up to four additional tributaries. This applies at sites 22 and 26 on the Figure.

To accommodate this problem, the following scheme was devised. For each site, the number of the last site, the numbers of up to four tributaries, and the number of the next site were entered into the data file for that site as variables, called 'last'. 'trib1', 'trib2', trib3', and 'trib4', and 'next'. The data file for the points shown would therefore be in the form shown on Table III.

TABLE III The form of the data files.
(using sites shown on Figure 22c)

Site	Last	Trib1	Trib2	Trib3	Trib4	Next	Slopelength	AB	Δy	S	N
17	0	0	0	0	0	22					e
18	0	0	0	0	0	22					s
19	0	0	0	0	0	22					t
20	0	0	0	0	0	22					i
21	0	0	0	0	0	22	Data collected				m
22	17	18	19	20	21	26	from fieldwork				a
23	0	0	0	0	0	26	and map analysis.				t
24	0	0	0	0	0	25					e
25	24	0	0	0	0	26					s
26	25	22	23	0	0	etc.					

Thus whilst the programme is calculating discharge at say site 22, the information in the first six columns allows the correct last and next site discharges to be utilized in the calculations, and also allows the input, or last site discharge calculation to be supplemented by discharge calculated on the four tributaries named. The way in which this works in the programme is more easily understood by inspection of the programme itself, which will be described in more detail in Section (III)B below.

(G) Areas of sensitivity in the model

In the discussion so far, it has been emphasised that assumptions of various kinds are involved, and this section reiterates these and outlines the various ways in which the effect of varying these assumptions may be checked. These do not include the assumptions about the role of vegetation and lack of bare site infiltration at this stage; these latter assumptions, which were considered at length in Section A, will be examined with the aid of an infiltration survey in Section D, at which stage modifications if necessary can be made. Neither does this include the question of the representative nature of the simulated event size. This will be considered in Section E, and after an examination of the long-term

raingauge records, a variety of events of differing sizes will be modelled. But before these sorts of considerations, relating to field conditions, are pursued, the routing procedure and its areas of assumption must be thoroughly examined.

It was made clear in the description of the theoretical aspects of kinematic modelling that this scheme only applies to sub-critical flow. Thereafore, at all computational stages it is important that the Froude number and the k wave number be calculated, and a warning signal included as output at stages in the programme run where supercritical conditions occur. Similarly, the Courant condition should be similarly calculated as a warning that the incremental step sizes are inappropriate to a stable solution. In the programme presented below, these conditions are all included in the calculations at each site at each time interval.

In addition to these computational restrictions, the results obtained will of course be dependent to some extent on the value of any variable derived by estimation. These are the channel roughness values at each site, N; and the mean hillslope velocity estimate of 0.0457 m/sec., taken from Emmett's (1978) field data. Although field- and map-derived values of slopelength, channel slope, S, channel incremental distances, Δy, and the bare area in each incremental unit, AB, are readily available, channel roughness, N, was obtained for only 9 sites in the field, and then only in the qualitative manner described by Barnes (1964), in which sites are allocated N values more or less on the basis of subjective impressions (see Appendix 11), although assistance is available from a range of photos. Freeze (1978) suggests that "... there is no suitable theoretical foundation for the Manning formula, and this fact identifies the friction factor, N, as the weakest link in the combination of parameters that underlies our conceptual-deterministic approach". Similarly Ragan (1966) explains that his model of channel routing produces results which are "... sensitive to errors in the roughness coefficient". Clearly, a sensitivity test of the model against the range of roughness values finally applied is therefore necessary prior to its further use as an explanation for morphological change.

raingauge records, a variety of events of differing sizes will be modelled. But before these sorts of considerations, relating to field conditions, are pursued, the routing procedure and its areas of assumption must be thoroughly examined.

It was made clear in the description of the theoretical aspects of kinematic modelling that this scheme only applies to sub-critical flow. Thereafore, at all computational stages it is important that the Froude number and the k wave number be calculated, and a warning signal included as output at stages in the programme run where supercritical conditions occur. Similarly, the Courant condition should be similarly calculated as a warning that the incremental step sizes are inappropriate to a stable solution. In the programme presented below, these conditions are all included in the calculations at each site at each time interval.

In addition to these computational restrictions, the results obtained will of course be dependent to some extent on the value of any variable derived by estimation. These are the channel roughness values at each site, N; and the mean hillslope velocity estimate of 0.0457 m/sec., taken from Emmett's (1978) field data. Although field- and map-derived values of slopelength, channel slope, S, channel incremental distances, Δy, and the bare area in each incremental unit, AB, are readily available, channel roughness, N, was obtained for only 9 sites in the field, and then only in the qualitative manner described by Barnes (1964), in which sites are allocated N values more or less on the basis of subjective impressions (see Appendix 11), although assistance is available from a range of photos. Freeze (1978) suggests that "... there is no suitable theoretical foundation for the Manning formula, and this fact identifies the friction factor, N, as the weakest link in the combination of parameters that underlies our conceptual-deterministic approach". Similarly Ragan (1966) explains that his model of channel routing produces results which are "... sensitive to errors in the roughness coefficient". Clearly, a sensitivity test of the model against the range of roughness values finally applied is therefore necessary prior to its further use as an explanation for morphological change.

On page 4:13 the source of the assumed hillslope velocity during slope drainage was cited as being that value representing the mean of those obtained in the field by Emmett (1978). However, it is clear that hillslope gradients and variations in hillslope roughness will affect local values of the mean velocity during drainage. How important this possible source of error is can only be assessed by again varying the value given in the programme and inspecting the stability of the results over the range of tests. In Section C which follows, therefore, the model is first presented, and then subjected to a range of tests on N and on v.

(III) SIMULATION OF OVERLAND FLOW AT ALKALI CREEK

This section describes the methods and results of the simulation, and the sensitivity tests described above. The validation, (as far as this is possible) of the generation assumptions follows in Section D, using field infiltration and discharge data following an event similar to the simulated event. Transmission effects are considered at that stage. In Section E, a wider range of events are simulated in an attempt to characterise an annual pattern.

(A) Delimitation of flow source areas, and the construction of the data files

Since a good percentage vegetation cover map was available from field survey (Figure 4, back folder), this was used as a basis on which to calculate the slope overland flow contributions to the channel at each site. On Figure 7 (back folder), the spatial extent of the overland flow domain is suggested, along with the divisions of the contributing areas for each site as used for the snowmelt simulations. By overlaying Figures 4 and 7, the percentage bare area is easily determined. Since the area of each delimited contribution is already known, the total bare area in each of these can be calculated. The complete procedure is illustrated on Figure 23, using the small shaded area on Figure 7 as an example. On Figure 23a, contributing areas are delimited for cross-sections 44 to 46. On Figure 23b, the percentage bare area is indicated (from Figure 4). On Figure 23c, the total area in each contribution is

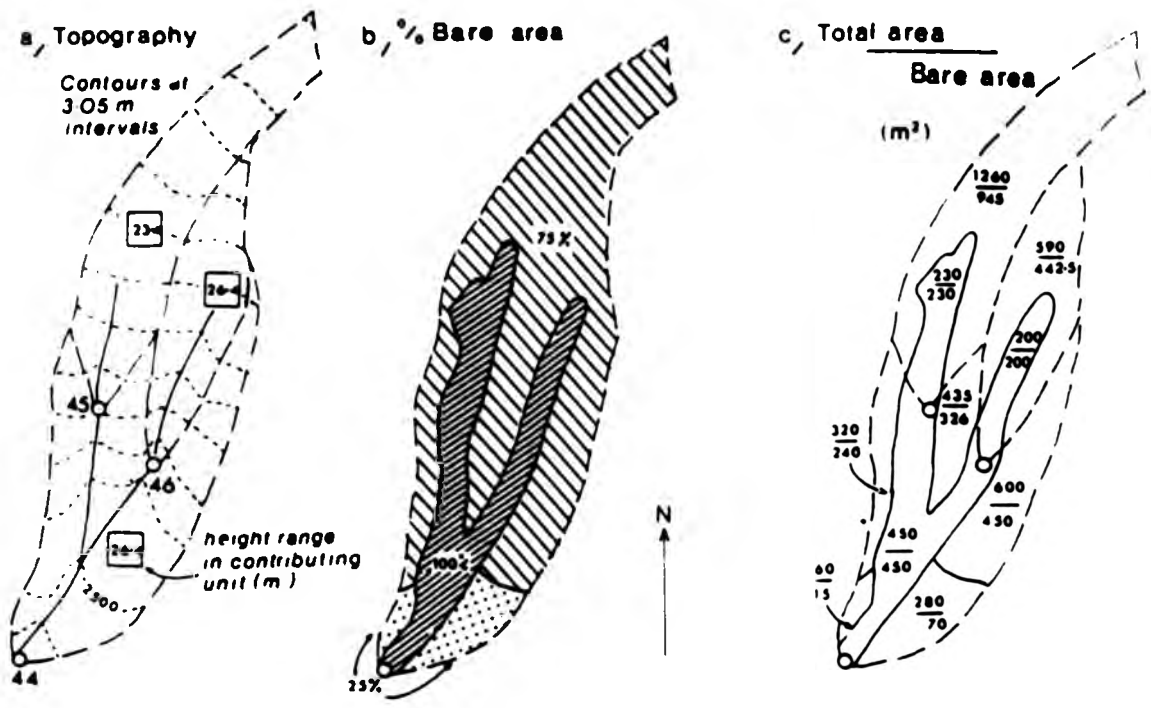

For a simulated event in which 1cm.(·01m.) of rainfall is assumed to runoff in 1hr., runoff volume at each site, Vol , is estimated as;

$$\text{Vol} = \sum \text{Bare area} \times 0{\cdot}01 \quad m^3$$

In Chapter 5:
Sediment yield from surface wash in a year, SED, is a function at each site of ; $\left| \sum \text{Bare area} \times \text{elevation range in contributing unit} \right|$ in m^3

Thus.

site	45	46	44	
Vol	11·88	6·48	34·56	m^3
SED	27·51	16·92	81·75	$m^3 \times 10^{-3}$

Figure 23 : The calculation of overland flow volume totals from each contributing area for a hypothetical event

multiplied by the percentage bare area to give the total bare area for each.

Using this procedure, the intensity of the spatial overland flow domain can be illustrated. Figure 24 shows this pattern, and, as would be expected it is highly asymmmetrical, indicating that the use of bare areas as a surrogate for overland flow intensity will generate flows which originate within the immediate channel zones in the headwaters, which are southwest facing. Below the main tributary junctions, contributions are confined to a narrow 20 to 30 metre wide zone which encompasses the channel banks predominantly. The large discontinuous tributary does not appear to be connected through bare area to the main channel, and this gully terminates instead in a fan which has a cover of over 80%.

In addition to the calculation of AB, each site was keyed in to the network and allocated a roughness value, N. This latter value was found in the field to vary from 0.055 in the headwater areas to 0.040 on the main channel. This suggested a method of allocating N values to all unmonitored sites, using stream order. First order channels were allocated N values of 0.055, second order 0.050, third order 0.045, and fourth order, 0.040. These values were entered into the data file. Values of channel slope, S, through each site were taken from the 1962 main channel survey (Appendix 3) to avoid the channel slope modifications caused by the recent installation of the sediment check dams which affects the 1975 survey data. However, no data except for the 1975 slope values were available for the headwater sites, so channel slope S was taken from these data in those cases. For the channel length increment values, Δy, the length of channel between each site, (or, in the case of there being more than one last site, all the lengths between these and the site in question) were measured from Figure 7 (back folder), as well as the maximum length of each two-sided contributing unit. This allowed a data file in the form of Table III to be constructed for the continuous network, and also for the small and large tributaries which are discontinuous. The former was named ROUTEB.DAT, the small discontinuous gully file was called ROUTEA.DAT and the large discontinuous gully file was called ROUTEC.DAT. These are included as Appendix 8, site numbers having been typed in, although these are not needed in the actual operation of the programme.

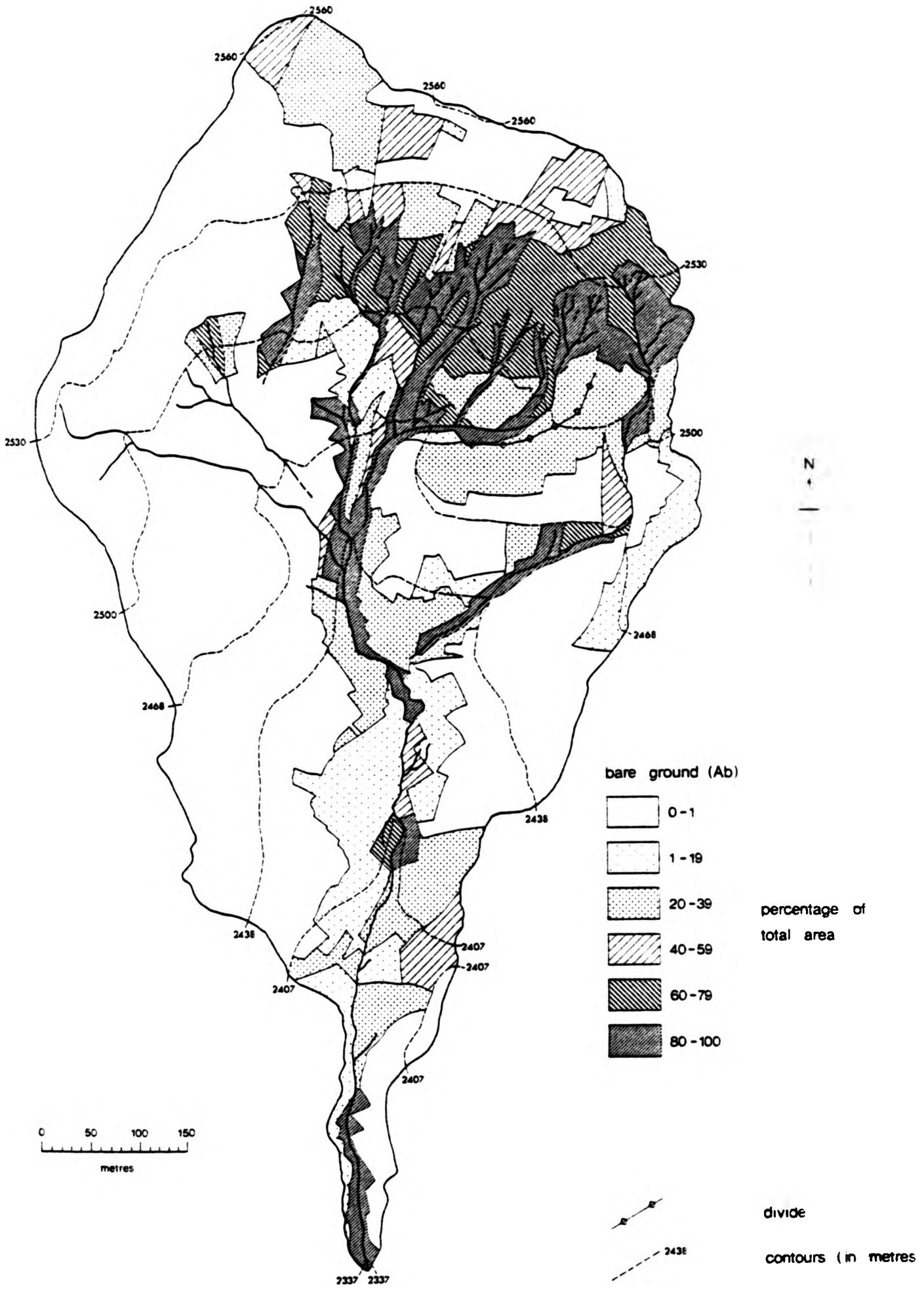

Figure 24 : The hillslope spatial intensity domain for overland flow

(B) The routing programme, ROUTE.PAS

The procedure outlined in Section B was conducted on the data files by means of a PASCAL programme, ROUTE.PAS, which has been included in Appendix II. It has been fairly fully annotated with comments, so no further description of the coding is included in this text.

Every two minutes, the discharge at selected sites is written into an output file. The sites chosen are the 9 sites shown on Figure 7 (back folder) for which field discharge data were obtained, although all or any sites could in fact be selected out of the 103 selected sites on the continuous network, and 43 on the large discontinuous network. It is noted here that these two systems are assumed to operate as two separate systems for the purposes of overland flow modelling, since the evidence of the fan at the terminal point of the large discontinuous gully suggests that summer storm runoff from this system never enters the main channel. ROUTEA.DAT was only used to test the operation of the programme, and no data from this run is presented here.

This is a very large programme, running as it does through 103 data points on the continuous network 7200 times. It takes 8 minutes of computer time on the North London Polytechnic DEC 10 computer, which has meant that the number of sensitivity runs was restricted to the expected extreme values that might be taken by the sensitive parameters. Throughout the first 5 runs, a constant check was made on the output listings to see whether the flow had become critical or whether the Courant condition was not being met. Fortunately, for these runs at least, this was not the case. Once the output file had been reformatted, the site data were entered into the graph plotting programme GPHPLT.FOR, described previously in Chapter 3, and the hydrographs inspected. The results of the first five runs are presented in the next section.

(C) The sensitivity runs

On the first 5 runs of ROUTE.PAS, no infiltration was assumed, and the simulated rainfall event, in which 10mm (0.01 m) of rain fell in 1 hour was assumed to runoff immediately. This allowed the duration of the hillslope hydrograph to be described by equation 4:20. The

assumptions that were tested in these runs were discussed in Section B(vii). For run 1, field N estimates and the value of v as derived from the Emmett (1978) data was used. In the next two runs, channel roughness was varied over a considerable range. In the last two runs, the mean hillslope velocity was varied. The actual values used are tabulated on Table IV.

Table IV The Sensitivity Runs

RUN	REMARKS	ROUGHNESS AT STREAM ORDER				v
		1	2	3	4	
1	Field N estimates Emmett's mean v	0.055	0.050	0.045	0.040	0.0457
2	'Smooth' Emmett's mean v	0.045	0.040	0.035	0.030	0.0457
3	'Rough' Emmett's mean v	0.065	0.060	0.055	0.050	0.0457
4	Field N estimates 'fast drain v'	0.055	0.050	0.045	0.040	0.0650
5	Field N estimates 'slow drain v'	0.055	0.050	0.045	0.040	0.030

The results of these runs for the field sites 1 to 7 for the continuous net, and sites 8 and 9 on the large discontinuous gully are included as Figures 25 to 32. The results from site 4 have not been included because as can be seen from the location of sites 3 and 4 shown on Figure 7 (back folder), these are very close together and there seemed little point in including two sites having similar results.

Figure 25

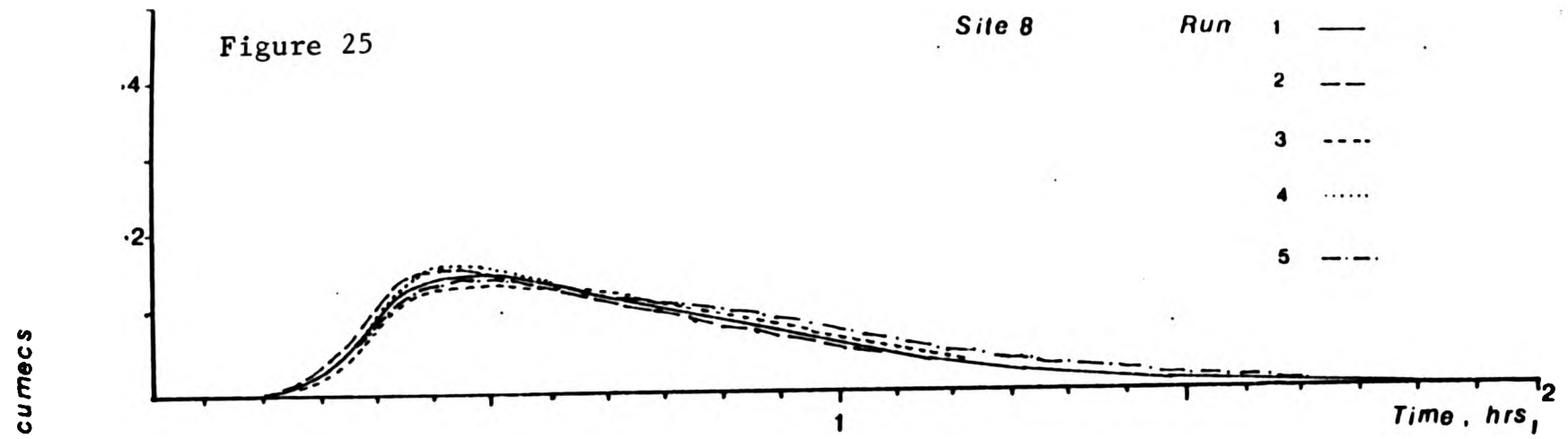

Figure 26

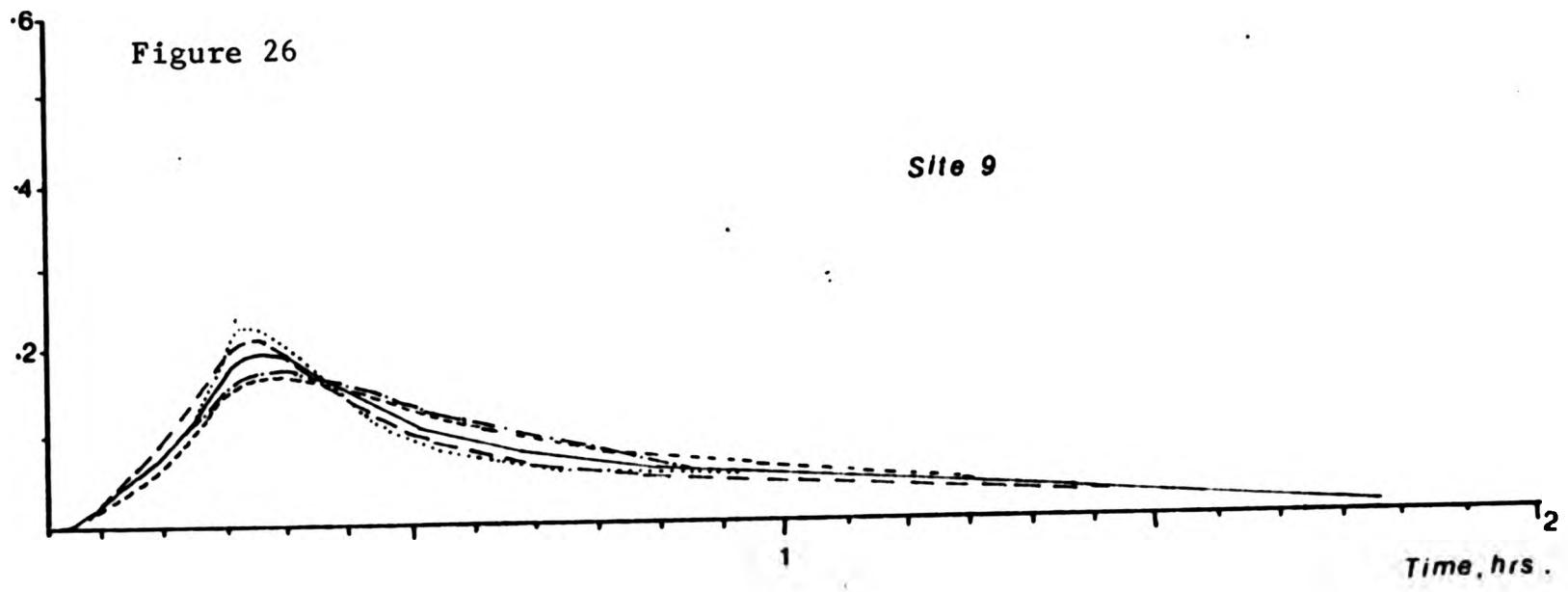

Figure 27

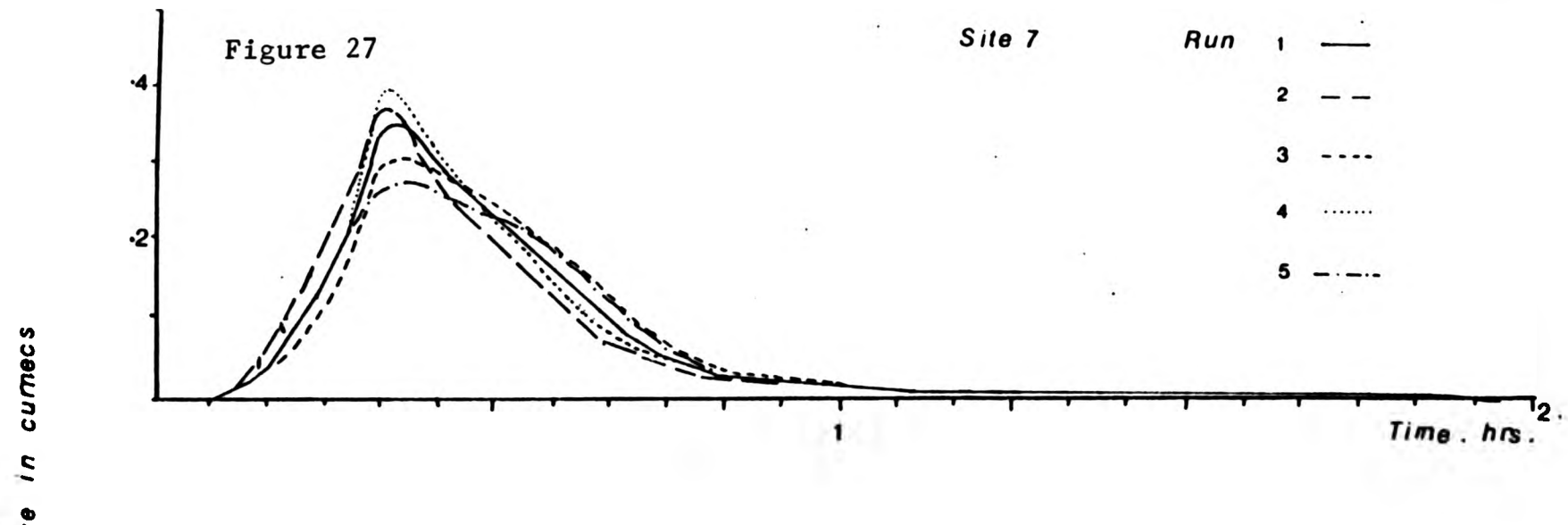

Figure 28

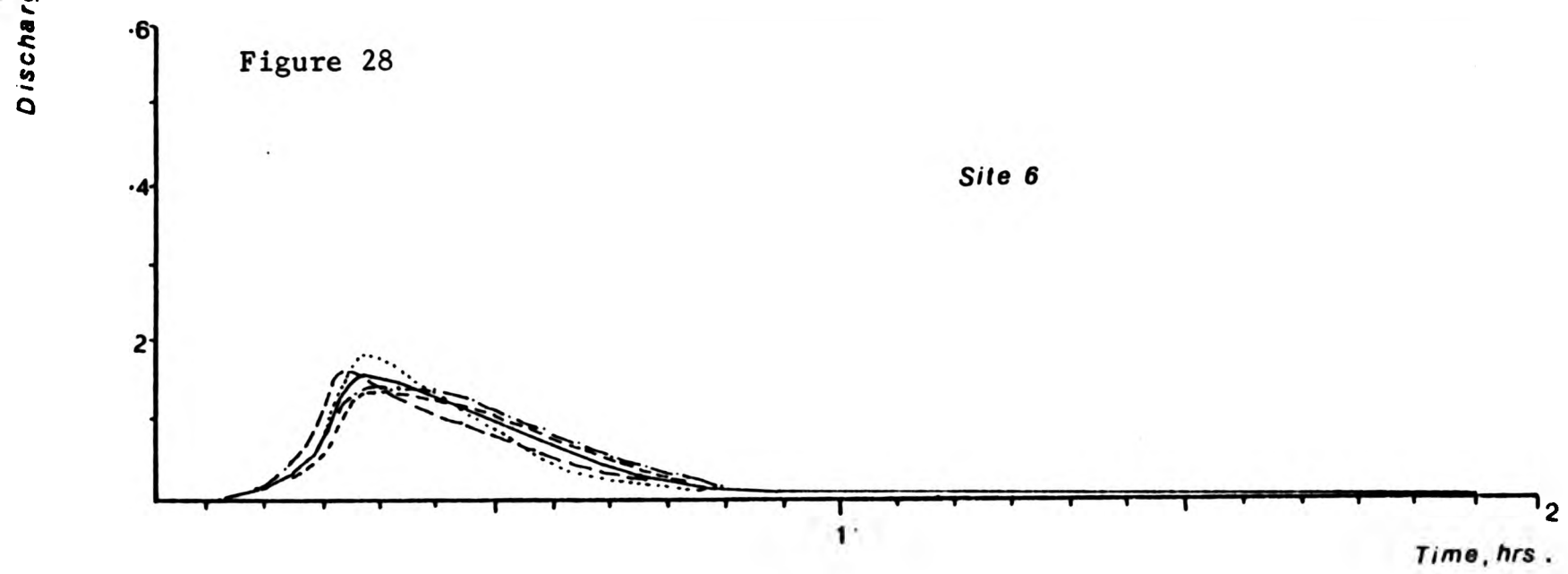

Figure 29

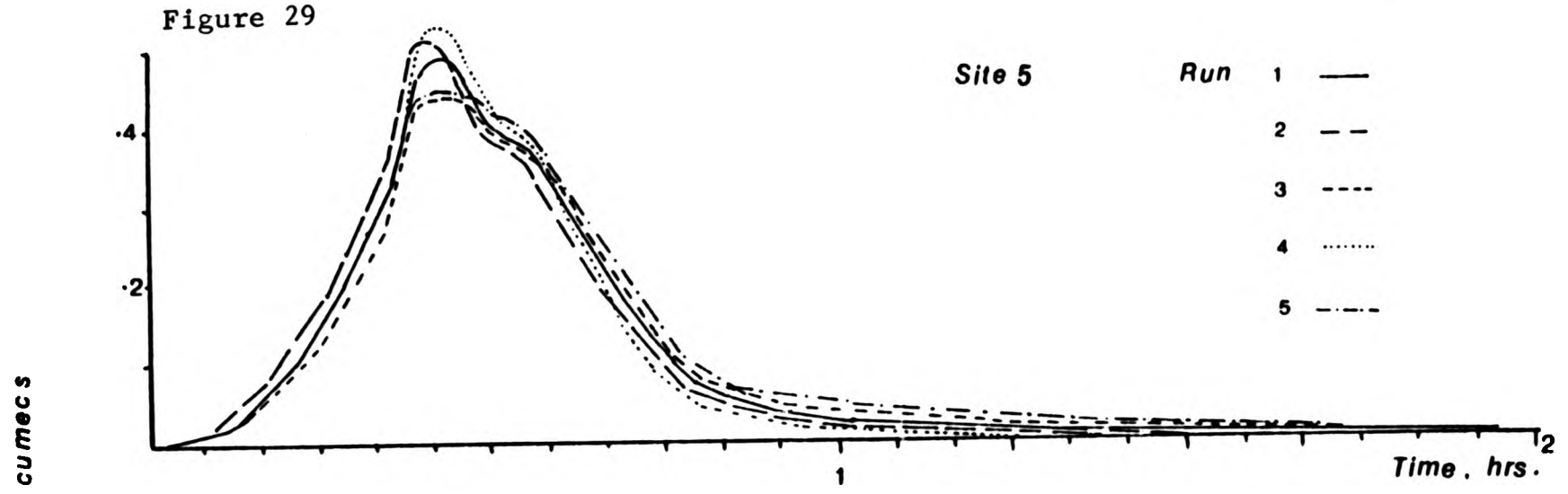

Figure 30

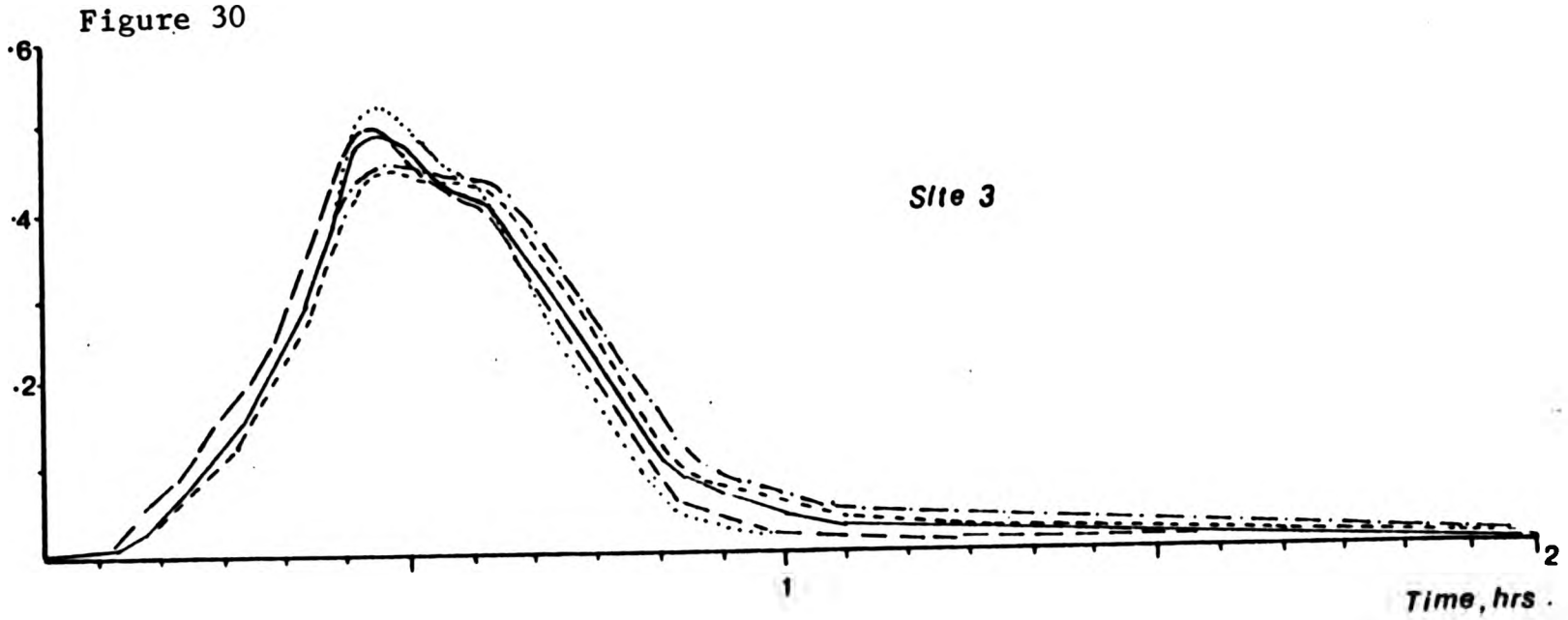

Figure 31

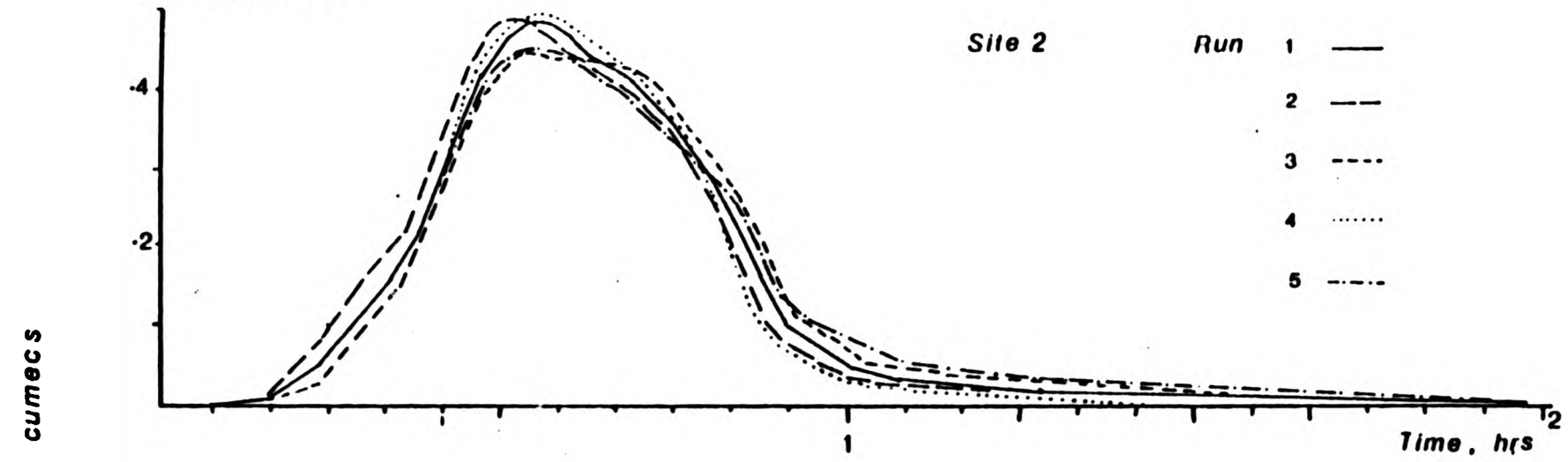

Figure 32

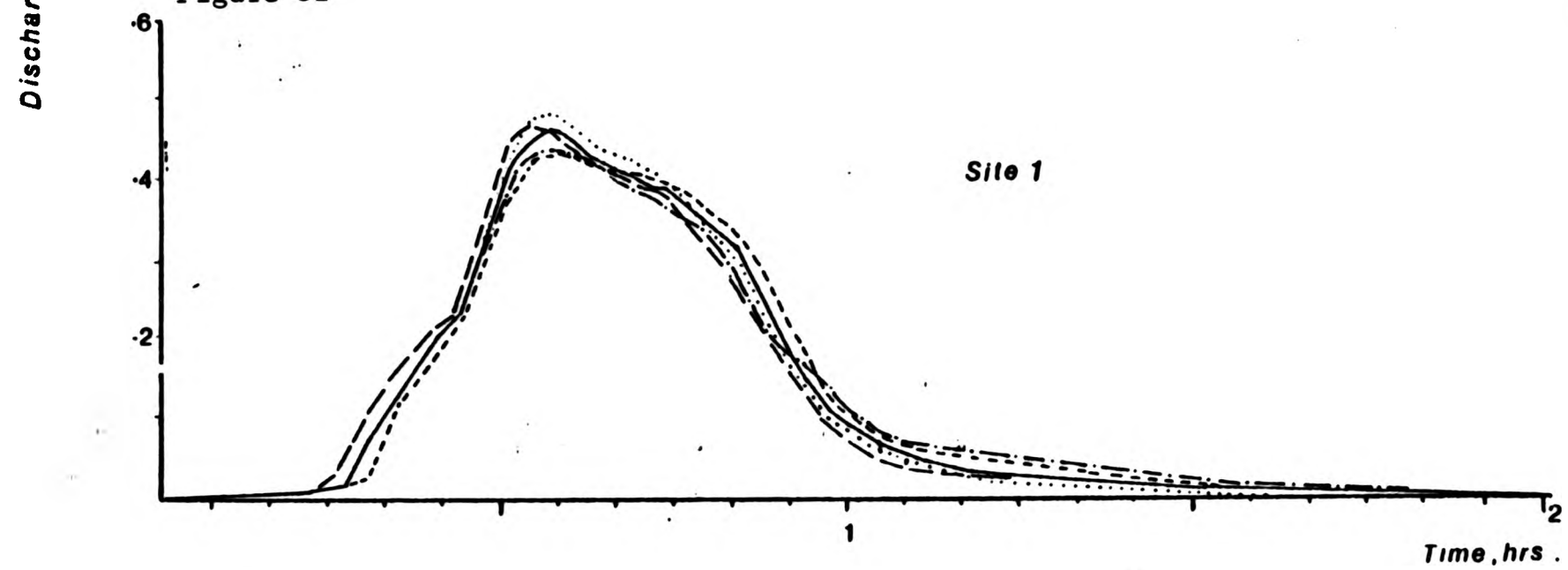

(i) Sensitivity to roughness estimates.

On all sites, the effect of changing the roughness values to a lower range (comparing runs 1 and 2) is to increase the size of the peak by an estimated 5 to 10% for a 20% change in the roughness estimates. The rise time to peak is very slightly increased, and the graphs all decay earlier, although the overall time of the hydrographs seems hardly affected. By constrast, increasing the range of roughness values has almost exactly the opposite effect, in that the size of the peak is reduced, again by an estimated 5 to 10% for a 20% change in the roughness values. It is noted that the 'rough' values are indeed very high for the sort of channel at Alkali Creek which has no really large bedload throughout its course, and the 'smooth' values are again extremely low for natural, steep headwater channels. Although these changes are indeed interesting, they do not seem however to indicate a huge dependence of the model on the roughness values selected. In all the runs that were conducted, the whole set of 8 hydrographs presented in Figures 25 to 32 retained their character and differences with respect to each other, and so it is concluded here that the model can be regarded as relatively insensitive to the choice of the roughness coefficients. As a result of this conclusion, the field-based roughness estimates as used in run 1 will be used from now on without change.

(ii) Sensitivity to the mean hillslope velocity value, v.

An examination of equation 4:20 might suggest that the effect of changing the mean hillslope velocity estimate to a higher value will be to shorten the timebase of the hillslope hydrographs at each site, by reducing the slope drainage time. Inspection of runs 4 and 5 shows that the effect that this has on the hydrographs is to increase the size of the peak in a manner similar to reducing channel roughness, in other words a fast drainage time increases the peak by about 10% for an almost 50% increase in the value of v. In contrast, reducing the value of the mean hillslope velocity during drainage (run 5), reduces the peak size, and the recession is longer and later, although only by a few minutes. In these cases the effect of changing the hillslope velocity across a range which is up to 75% of the original value has the effect of changing hydrograph characteristics by never more than an estimated 15%.

It is difficult to evaluate the strength of these conclusions. It would appear, however, that the procedure described in Section B and undertaken by ROUTE.PAS is fairly robust. It might also be noted that the effects of changing both variables makes sense in physical terms, and lends support to the expectation that the algorithm for ROUTE.PAS comes closer to representing the real world "... at a fundamental level" (Freeze, 1978) than had been achieved in the earlier ill-fated efforts to simulate overland flow at Alkali Creek. As a final test on the model, the area under the curves was estimated with a polar planimeter and converted to volume of runoff using the axes to convert the scale. These values were compared with the values anticipated by summing (ABx0.01) throughout the network. The two figures corresponded in all cases. This is strong evidence that the model is working correctly.

It is, therefore, possible to make some observations about the simulated flood wave generated by ROUTE.PAS by comparing the site hydrographs produced on the first run.

(D) Discussion of the results of run 1

Figure 33 summarises the run 1 hydrographs for sites 1 to 9 (excluding site 4) as located on Figure 7 (back folder). Some observations can be made from the pattern displayed.

(1) The two main headwater forks, represented by sites 6 (west fork) and site 7 (east fork) show the sort of contrast which might be expected for these sites. The volume of total runoff, represented by the area under the curves, is considerably greater on the east fork, and because of the longer length of these channels in this part of the headwater net, the hydrograph peaks slightly later than the hydrograph for the west fork. The size of the peak, as simulated here for site 7, is almost twice as great on the east fork (site 7) in contrast to the west fork (site 6), but recession takes about the same length of time in both cases.

(2) The hydrograph for site 5, which is the point denoted by 'X' in previous Chapters, peaks just after the two headwater tributaries (sites 6 and 7), and as anticipated, the peak size is considerably greater than on either of its two feeder

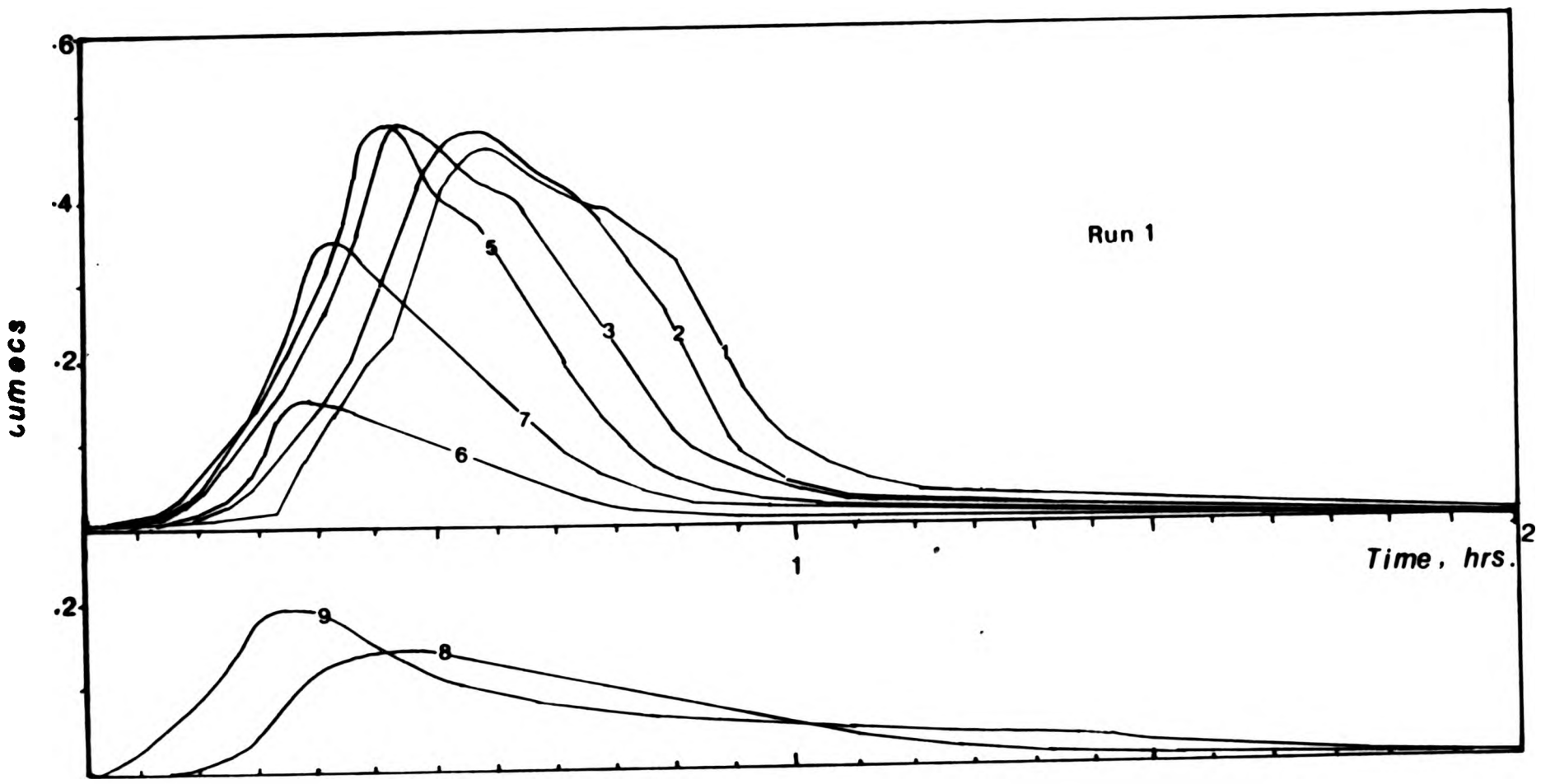

Figure 33 : Run 1 ; a comparison of the ROUTE.PAS output floodwave from sites 6 and 7 in the headwaters to site 1 at the basin mouth. Sites 8 and 9 are on the large discontinuous tributary

channels. The difference in hydrographs between sites 6 and 5 is striking, indicating a rapid change of flow conditions along this section of the channel. The 'bumps' on the recession curves which first appear at site 5 appear to be related to the different timings of the hydrograph peaks at sites 6 and 7.

(3) Below site 5, the hydrograph peak increases slightly up to site 3, and although the volume of runoff increases by the estimated 7.8%, because of lateral increases, lower channel gradients appear to slow the flow down and the volume is stored and appears to be added to the recession limb. This effect is even more noticeable between sites 2 and 1. It must be concluded that an inverse down-net velocity gradient causes attenuation of a flood wave even before transmission losses are considered. This important effect will be discussed in more detail in a later section.

(4) There is not much of a peak at all in the large discontinuous tributary by comparison, and the long, poorly-supplied length of channel between sites 8 and 9 appears again to be the focus of peak attention.

(5) The hydrographs are not, in general, quite as 'flashy' as might be expected from a semi-arid system with such high relief. However, since the model has been shown to be stable over a range of roughness and slope drainage times, the only explanation for this might be the assumption of an isosceles-shaped lateral input hydrograph. In reality, the lateral input function may be negatively skewed, which may have an effect on the overall shape of the results. It is interesting to note that Ragan (1966) who used this lateral triangular function, presents hydrographs as output which are similarly lacking strong negative skew. There was insufficient time at this stage to explore this possibility further.

The next section explores the nature of the assumptions on which the flow is generated in the model by presenting the results of a field infiltration survey conducted in the summer of 1980. The model can be then rerun to approximate the field conditions more closely, and compared with the results of a discharge survey undertaken after a real field event.

(IV) FIELD TESTS OF THE MODEL

(A) The infiltration survey

The main assumptions concerning infiltration were outlined in the context of the literature earlier. To summarise these, it was assumed that infiltration rates are uniformly low and less than rainfall intensity of the simulated event on bare surfaces, independent of lithology and slope angle, and uniformly high and greater than the intensity of the simulated event on slopes where vegetation cover is present. In order to examine these assumptions, an infiltration survey was designed to cover a variety of lithologies and vegetation types.

(i) Logistics of the survey, and site descriptions.

Using the grid which was already on the ground following the production of the vegetation map (Figure 4, back folder), cells in this matrix were sampled randomly across the watershed as a basis for the infiltration survey. The highest point in each grid square was arbitrarily chosen as the point at which to sample each square, and the specific location of each of these points in relation to the cells of the vegetation survey are indicated on Figure 4.

At each of the 24 sample sites, the vegetation density as mapped in the complete cell on Figure 4 was noted, as well as the local site vegetation type, the maximum slope angle through the site in m/m, and the site aspect, employing the same three classes as used in the snow melt survey (A, B, and C). It was felt that there might be a danger that the canopy conditions, as mapped in each cell used in the vegetation survey, might not really represent the conditions at the actual site where the infiltrometer was placed. To establish whether this was the case, the canopy density as viewed directly above the site, and the ground cover conditions (litter or bare ground) were separately noted.

It was implicit in the review of the literature concerning infiltration (section IA) that vegetation cover affects infiltration capacity rates not only by preventing high intensity rainstorms from slaking the soil surface, but also by affecting soil structure.

Vegetation litter and the action of roots not only improve the soil moisture regime and organic matrix of the soil, but have the physical effect of maintaining a more broken soil surface which is conducive to infiltration. A preliminary consideration of these effects at Alkali Creek was presented in Chapter 2. To substantiate these observations at the local level, and therefore to gain more support for the use of bare area as a surrogate for overland flow intensity, an examination of the infiltrometer site soil conditions was also made in the field. Parent materials, already discussed using Figure 5 as a basis in Chapter 2, were also noted.

A summary of these site conditions is included (Table V), and although the data presented is mostly qualitative, various inferences may be drawn from this which largely substantiate the links which have already been suggested between these parameters. These observations can be listed as follows ;

(1) There is support on the table for inferring a link between aspect and percentage vegetation cover. For instance, all sites with a cover density of 60% or less face either south-west (class A), or south, west, or east (class B). Only north, north-west, or north-east facing slopes (class C) support a 100% vegetation cover as mapped in the survey, although there are clearly some local anomalies (e.g. sites 16, 20 and 21).

(2) As suggested in Chapter 2, there is a clear relationship between cover density and cover type. For instance, all 100% cover sites support either the oakbrush, or aspen-oakbrush association, whereas sites with less than 60% cover support predominantly sagebrush where vegetation is present, although the occasional scattered tree is present at sites 2 and 5.

(3) Although it might be anticipated that slope angle exerts an influence on the soil conditions, especially the depth of an organic horizon, this is not supported by the site data. In fact there is apparently no relationship between slope angle and any other parameter on Table V.

(4) Local infiltrometer site conditions do mostly correlate with canopy density as calculated on a cell basis, and rather naturally this is particularly true of the high % covers. Variations mostly occur in the range of cell density values

TABLE V. INFILTRATION SURVEY : SITE CONDITIONS

(SITES LISTED IN ORDER OF DECREASING COVER DENSITY).

Site No.	Aspect Class	% Veg. cover	Cover Type	Local Infiltrometer Site Conditions	Soil Type (P* indicates presence of pipes)	Parent Material	Site Slope m/m	Infilt Capacity (mm/hr).
22	C	100	Aspen and Oakbrush	Closed canopy : ground litter	Solonetz - but with good organic horizon, 10cm.	Sst. Lens	0.44	54
18	B	100	"	"	Solonetz - organic horizon 5 cm.	Clayshales over sst.lens	0.20	48
19	B	100	Oakbrush	"	Solonetz - but with good organic horizon, 10 cm.	sst. lens	0.20	42
13	C	100	Oakbrush	"	Solonetz - " "	"	0.07	23
8	C	100	Aspen and Oakbrush	"	Solonetz - organic horizon 5 cm.	Clayshales	0.26	18
23	C	100	"	"	Solonetz " "	"	0.48	18
4	B	100	Oakbrush	"	Solonetz - poor organic horizon	"	0.28	1
20	A	100	Oakbrush	"	Solonetz - but with good organic horizon, 10 cm.	"	0.32	24
16	A	85	Oakbrush	Partially closed canopy: ground litt.	Solonetz - organic horizon 5 cm.	"	0.25	18
24	B	85	Oakbrush	Fairly open canopy: litter & bare patches	Solonetz	"	0.20	9
9	B	81	Isolated patch of oakbrush	Some open patches: little litter	Degenerate Solonetz: Open cracks, no organic horizon (P*)	"	0.27	12
17	C	80	Oakbrush	Partially closed canopy: litter	Solonetz - Organic horizon 5 cm.	"	0.48	18
21	A	80	Oakbrush & Western wheat	" : bare patches	Solonetz " "	"	0.22	12
11	C	80	Aspen and Oakbrush	" : bare patches	Solonetz - no organic horizon	"	0.34	0
15	B	75	Oakbrush	" : litter	Solonetz - but with organic horizon 5 cm.	sst. lens	0.33	32
3	A	60	Sagebrush	Dense network of roots	Solonetz - no organic horizon	Clayshales	0.35	24
6	B	58	Sagebrush	Local bare site	Degenerate Solonetz : cracks columnar structure	Clayshales	0.28	9
14	B	45	Sagebrush	Bare: Fan of small gully	Laminations over Solonetz	Clayshales	0.17	4
2	B	40	Oakbrush & sagebrush	Scattered trees: locally bare site	Degenerate Solonetz: Cracks	Clayshales	0.27	6
5	C	39	Aspen and Oakbrush	" "	"	Clayshales	0.26	6
1	B	38	Sagebrush	Bare site	"	Clayshales	0.19	1
10	A	25	Sagebrush	"	" (P*)	Clayshales	0.22	5
12	A	0	Sagebrush	"	" (P*)	Clayshales	0.27	0
7	A	0	Sagebrush	" with rills	"	Clayshales	0.30	0

TABLE V. INFILTRATION SURVEY : SITE CONDITIONS

(SITES LISTED IN ORDER OF DECREASING COVER DENSITY).

Site No.	Aspect Class	% Veg. cover	Cover Type	Local Infiltrometer Site Conditions	Soil Type (P* indicates presence of pipes)	Parent Material	Site Slope m/m	Infilt Capacity (mm/hr).
22	C	100	Aspen and Oakbrush	Closed canopy : ground litter	Solonetz - but with good organic horizon, 10cm.	Sst. Lens	0.44	54
18	B	100	"	"	Solonetz - organic horizon 5 cm.	Clayshales over sst.lens	0.20	48
19	B	100	Oakbrush	"	Solonetz - but with good organic horizon, 10 cm.	sst. lens	0.20	42
13	C	100	Oakbrush	"	Solonetz - " "	"	0.07	23
8	C	100	Aspen and Oakbrush	"	Solonetz - organic horizon 5 cm.	Clayshales	0.26	18
23	C	100	"	"	Solonetz " "	"	0.48	18
4	B	100	Oakbrush	"	Solonetz - poor organic horizon	"	0.28	1
20	A	100	Oakbrush	"	Solonetz - but with good organic horizon, 10 cm.	"	0.32	24
16	A	85	Oakbrush	Partially closed canopy: ground litt.	Solonetz - organic horizon 5 cm.	"	0.25	18
24	B	85	Oakbrush	Fairly open canopy: litter & bare patches	Solonetz	"	0.20	9
9	B	81	Isolated patch of oakbrush	Some open patches: little litter	Degenerate Solonetz: Open cracks, no organic horizon (P*)	"	0.27	12
17	C	80	Oakbrush	Partially closed canopy: litter	Solonetz - Organic horizon 5 cm.	"	0.48	18
21	A	80	Oakbrush & Western wheat	" : bare patches	Solonetz " "	"	0.22	12
11	C	80	Aspen and Oakbrush	" : bare patches	Solonetz - no organic horizon	"	0.34	0
15	B	75	Oakbrush	" : litter	Solonetz - but with organic horizon 5 cm.	sst. lens	0.33	32
3	A	60	Sagebrush	Dense network of roots	Solonetz - no organic horizon	Clayshales	0.35	24
6	B	58	Sagebrush	Local bare site	Degenerate Solonetz : cracks columnar structure	Clayshales	0.28	9
14	B	45	Sagebrush	Bare: Fan of small gully	Laminations over Solonetz	Clayshales	0.17	4
2	B	40	Oakbrush & sagebrush	Scattered trees: locally bare site	Degenerate Solonetz: Cracks	Clayshales	0.27	6
5	C	39	Aspen and Oakbrush	" "	"	Clayshales	0.26	6
1	B	38	Sagebrush	Bare site	"	Clayshales	0.19	1
10	A	25	Sagebrush	"	" (P*)	Clayshales	0.22	5
12	A	0	Sagebrush	"	" (P*)	Clayshales	0.27	0
7	A	0	Sagebrush	" with rills	"	Clayshales	0.30	0

which are between 40 to 60%, where occasionally the local site is bare despite a fairly high mapped % cover. This effect is noticeable at sites, 1, 2, 5, 6 and 14. In these situations it may be that the % cover estimated for the cell may not be a sensitive enough variable with which to characterise infiltration conditions. The implications of this will be explored later.

(5) Soil type, although not considered in great detail, appears to be a product of both parent material and vegetation cover. For sites with mapped vegetation densities over 80%, all sites had a ground litter cover which was clearly contributing to an organic horizon. An exception to this rule is site 9, which is really a special case as the local materials were prone to piping, and although there was a good cover in this isolated patch of oakbrush, piping was evident around the site. For sites with a cover density between 60% and 80%, organic horizons were only occasionally noted, and soils in this category demonstrated surface cracking. Litter was sparse, and in some cases piping was suspected from the shape of the resulting infiltration curves. When cover dropped below 50%, none of the soils demonstrated an organic horizon, all were cracked on the surface and were therefore classed as degenerate Solonetz following the terminology developed in Chapter 2. At sites 10 and 12 the presence of pipes was strongly inferred from large, occasionally eroded large surface cracks. An exception in this category is site 14, which was located on the fan at the lower end of the small discontinuous tributary gully. Here the soil displayed some lamination associated with deposition at that location.

The over-riding effect of the lithological variations across the watershed is to modify this pattern, so that lithology is seen here as a secondary rather than a primary influence on soil type variations. The location of the sandstone lenses which are the main cause of these effects was illustrated in Chapter 2 (Figure 4). For sites where sandstone was clearly the main parent material, the lack of the sodium-rich clayshale base has allowed a deeper organic horizon to develop, significantly distinguishing these soils from those of adjacent, otherwise similar sites. For example, it is useful to compare sites 11 and 15; and sites 22 and 23. A glance

at the infiltration curves (Figure 34) for this pair of sites suggests that this difference has had a considerable effect on the final infiltrability rates.

The conclusion to be drawn here is therefore that the percentage cover density on the sites chosen for the infiltration survey correlates well with both ground cover conditions and the description of the soil. However, the sandstone lenses influence the depth of the organic horizons where they occur. The effect of these site descriptions on the infiltration curves is explored next, after a description of the field method employed to produce them.

(ii) Methods

The infiltration survey was conducted on the 24 field sites using a home-made double-ring infiltrometer constructed as described by Evanko (1950) from two commercial food cans. The inner ring had a diameter of 6" (15.02 cm) and an outer ring diameter of 8" (20.32 cm). These sizes were decided upon by considerations of expediency, although luckily the sizes do seem to relate to common usage (Hills, 1970). Water was fed directly into both rings, the inner ring having been previously calibrated using a vernier scale attached to the inner ring. The outer and inner rings were initially filled, and subsequent readings taken against the scale, using the meniscus position. The advantage of the method over the ponded water reservoir method preferred by Hills (1970) is that no disturbance occurs to the water level position, and although the effects of hydraulic head do vary in this method as time proceeds, Bouwer (1963) suggested a method whereby corrections could be made for the remaining head in both rings after 1 hour, allowing such considerations to be taken into account. The water supply for the day's survey was carried into the field in a 2 gallon canteen in a backpack. The complete survey took 6 days to complete, from July 17th to 23rd, 1980. Ground conditions were very dry and no rain fell during the fieldwork period.

At each site the infiltrometer was pushed into the ground to a depth of 2 cm and readings against the scale were taken every 5 minutes and converted to hourly equivalents. The final infiltrability (to use the expression coined by Thornes, 1976, for the final, low

Figure 34 : Field-monitored infiltration curves
classified by site cover density

The numbers on the curves refer to the survey sites shown on Fig 4

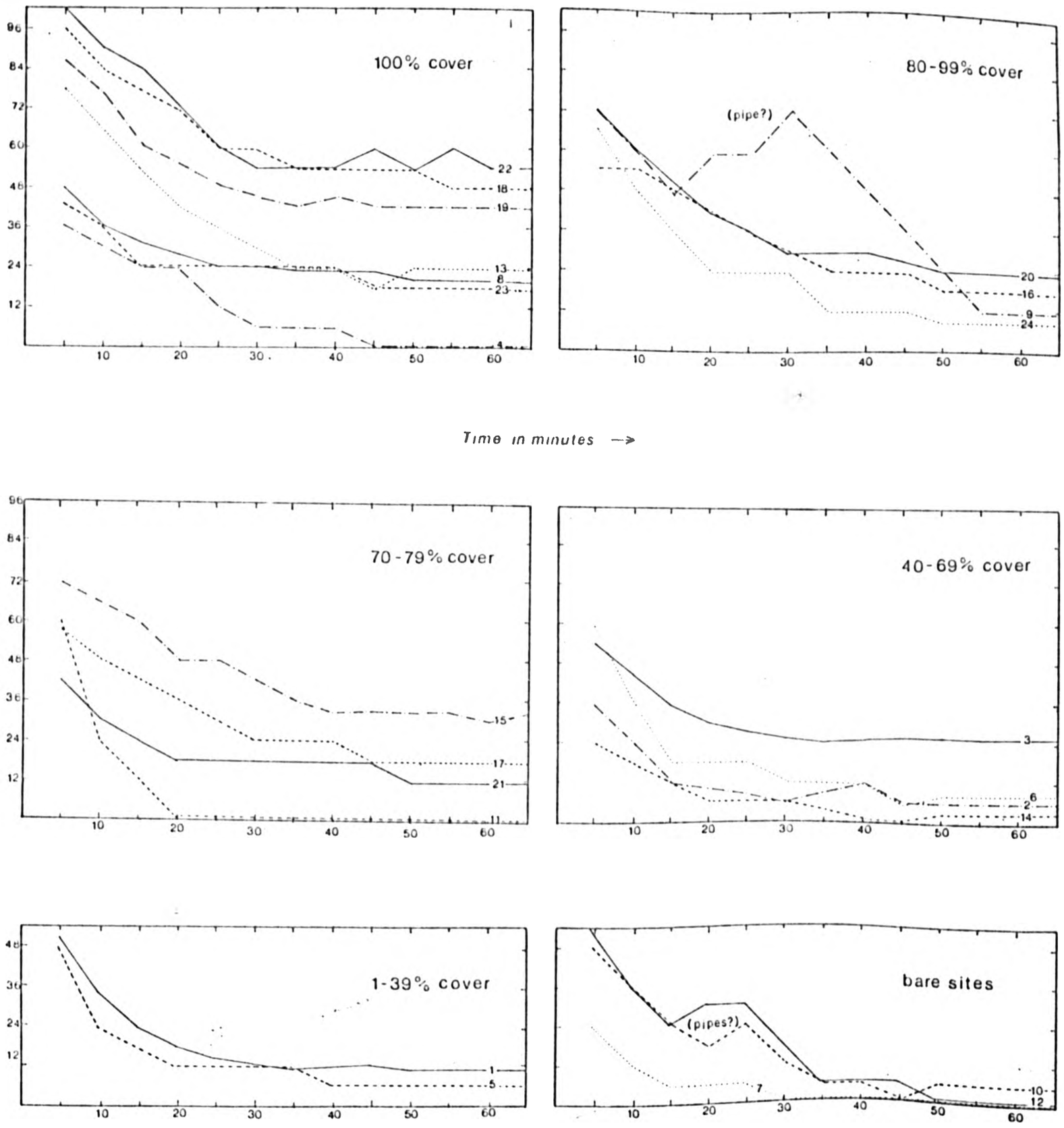

The numbers on the curves refer to the survey sites shown on Fig 4

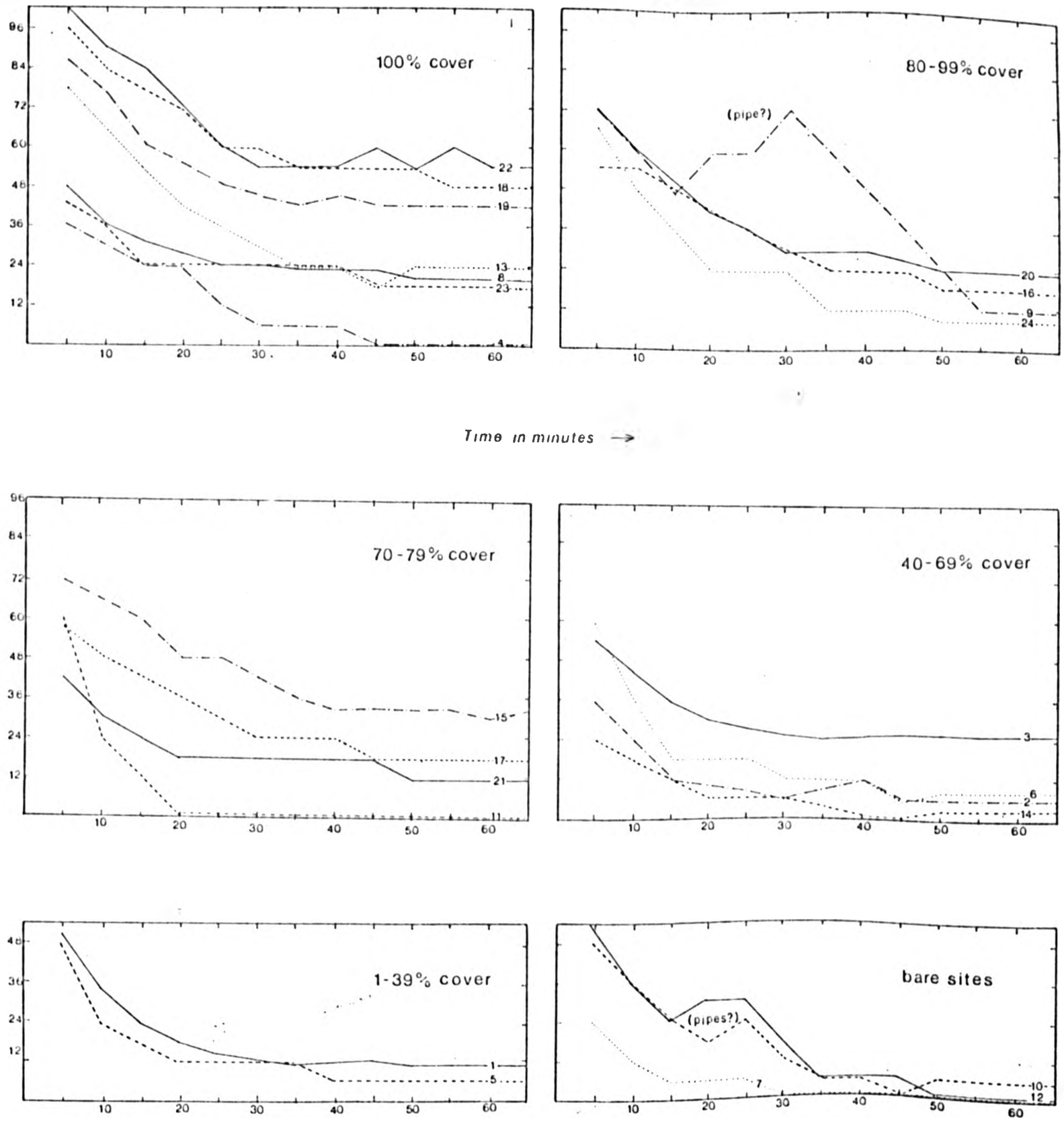

infiltration rate) was adjusted by the Bouwer method where necessary when considerable head remained in both rings after 1 hour. The results of the survey have been plotted on Figure 34, and field data included as Appendix 9. Final infiltrability has been included for comparison purposes in the last column of Table V.

The considerable limitations of the cylinder infiltrometer method have been extensively discussed elsewhere (Hills, 1970). The most significant limitation is generally accepted to be that cylinder infiltrometers do not attempt to simulate the impact of rain on the surface, meaning that the infiltration of rain as it falls to the ground is not considered. The values obtained, it is argued, represent more the effects of subsoil transmissibility variations than the effects of surface sealing, a particularly strong criticism when rates on bare surfaces are under consideration. In such environments, sprinklers of various types are preferable. Despite these reservations, however, the sort of instrumentation necessary for rainfall simulation to be undertaken in the current investigation was not available, so that in the end the homespun method described above had to suffice. The first practical difficulty encountered was that of sloping sites. The requirement that level of penetration of the cylinders should be uniform all the way round the instrument is somewhat in conflict with the requirement to keep the water surface a consistent distance from the top of the instrument. The latter requirement was met rather than the former when the problem arose. Secondly, even a 2 cm penetration was not possible on particularly hard sites, and hammering the tins in ran the risk of excessively breaking the ground surface. If litter was present, this had to be cleared locally to get the cylinders in, and on sagebrush sites roots had to be avoided.

(iii) The curves.

Once again it aids clarity if the main observations to be made from the appearance of the infiltration survey data are itemised. We note from Figure 34 that ;

(1) Whether or not initial infiltration or final infiltration is considered, all the infiltration rates as monitored in the

field are low. Under oak woodland on clay loams, Hills (1970) quotes infiltration capacity rates of between 150 and 3200 mm/hr, whereas at Alkali Creek the maximum rate in any 5 minute interval was the initial rate of 100 mm/hr at site 22 under a cover of 100% oakbrush.

(2) All the infiltration curves, with three significant exceptions, display the inverse decay pattern expected from both the Hortonian equation (equation 4:1) and the Philip model (equation 4:3). The three exceptions relate to the sites already described (Table V) as showing evidence of piping. Sudden increase in velocity at depth as infiltrating water hits a pipe is thought to be responsible for these strange infiltration curves.

(3) Despite the wide range of scatter in each of the vegetation density classes shown on Figure 34, there appears to be a relationship between final infiltrability of the site and the cover density. This effect is more clearly shown on Figure 35, from which it can be inferred that the scatter also increases with increasing cover density, as indicated by the envelope curve. It is concluded here that infiltration capacities, therefore, do increase with vegetation density as mapped on a cell basis, but that variations occur which reflect the two main sources of generalisation considered previously. In particular, Table V shows that the sites with the lower than expected rates, (considering that they had over an 80% cover) were locally bare despite being in high cover density cells (for example, site 11). Secondly, higher than expected infiltration rates on low % cover sites are all on, or close to sandstone outcrops, where a more receptive subsoil situation is likely to exist. There is the inevitable anomaly from these generalisations, however, and there seems to be no reason why site 4 refused to accept any further infiltration after 45 minutes.

These data serve to reinforce observations made earlier concerning influences on infiltration rate variations, and although the patterns described are not strong enough to justify a statistical treatment, a relationship between cover and final infiltration rate seems to have been at least qualitatively established from this investigation.

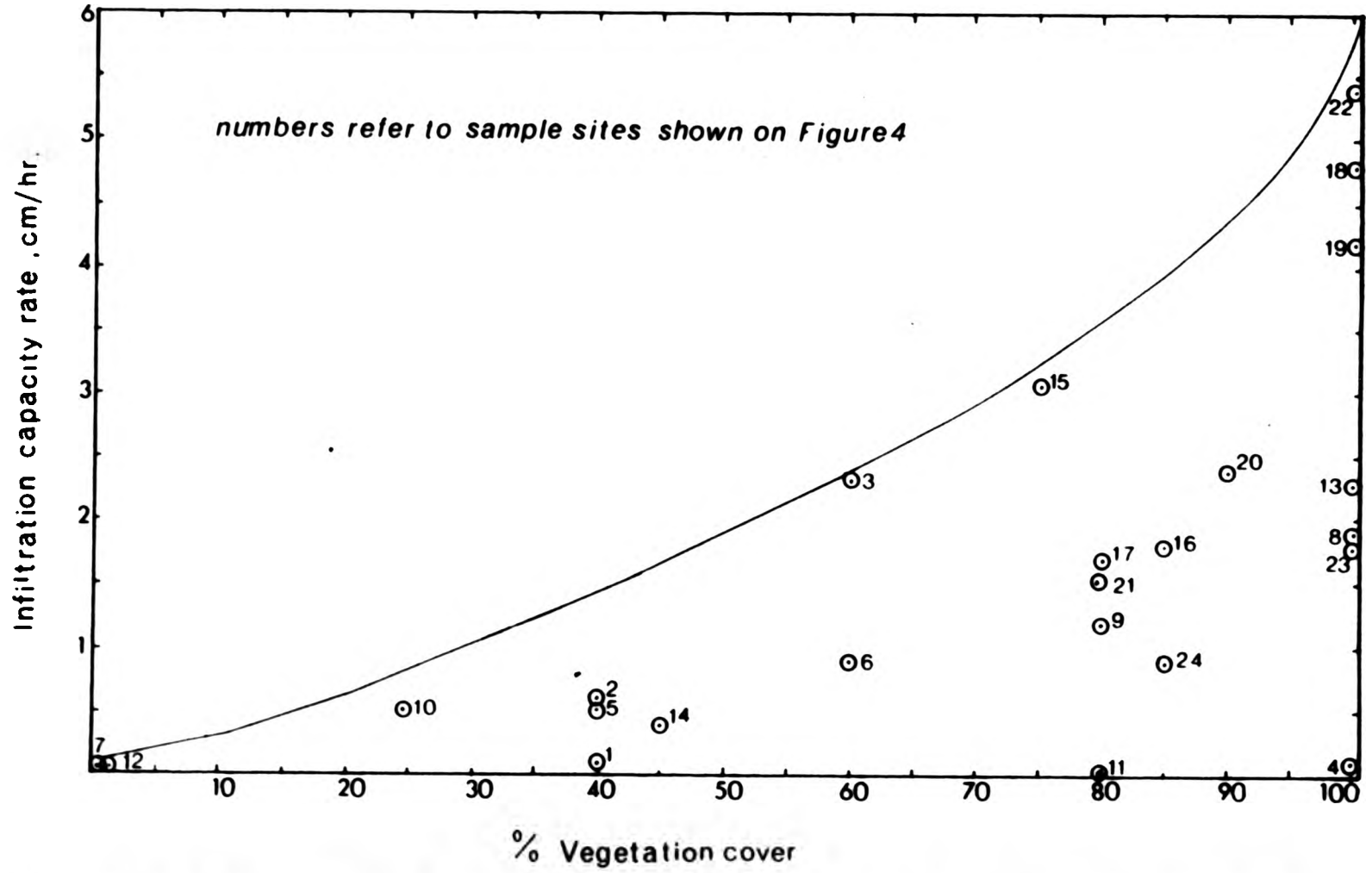

Figure 35 : Relationship between infiltration capacity and cover density on the sites monitored in the infiltration survey in July, 1980

(iv) Comparison between the field infiltration rates and the intensity of the sampled and simulated events: implications for runoff.

In the models presented earlier, generation of overland flow is assumed to be Hortonian, i.e. to follow the pattern described by equation 4:2. To make the model as simple as possible, only bare surfaces were assumed to generate flow, so that in these models contributing area a, becomes AB. Additionally all the rain which falls on these sites is assumed to runoff, so that f_c is assumed insignificant in relation to i and hillslope discharge is therefore described as equation 4:4.

A comparison between the monitored infiltration curves during the 1 hour field test, and the assumed and monitored rainfall events allows these assumptions to be evaluated. If it is understood that the infiltration curves do represent infiltration of rainfall during a rainfall event, and if 10mm of rain falls at an intensity of 10 mm/hr, then the infiltration data would suggest that none of the sites monitored would generate overland flow instantaneously. Figure 34 suggests that after 15 minutes, site 7 would produce runoff at a rate of 5 mm/hr, rising to 10 mm/hr at the end of the event. The sites 2, 4 and 11 would be the next to produce runoff, again first at a fairly low rate, rising after an hour to rates equal to the difference between 10mm and the final infiltrability of the site. Of the locally bare sites (1, 2, 5, 6, 7, 10, 12 and 14), all would generate Hortonian flow at a level which can therefore be assessed by comparing the event duration and intensity with the infiltration curves for these sites.

Of the sites with local cover on Table V, only sites 1, 4 and 24 could be expected to produce any rapid response runoff during the simulated event, the rainfall being lost either as eventual evaporation from an interception store, or by entering the channel as throughflow later in the event, or by being lost to plant use or a low water table. Under a well-developed canopy, ground levels of rainfall intensity must, however, be lower than above the canopy, so that even on sites 1, 2 and 24 there may be no runoff during an event the size of that under consideration. On the well-covered sites some enlargement of the spatial domain of overland flow may

occur especially when events such as that of August 24th, 1971, are considered. The largest event on the raingauge record, this storm produced 27.94 mm of rain in half an hour, falling therefore at an intensity of 55.88 mm/hr, (Figure 42).

These considerations support the use of bare area as a basis for overland flow generation calculations, so that the use of AB in equation 4:4 is considered here to be supported by the data presented on Figures 34 and 35. However, inspection of the infiltration curves and the line of argument developed above indicate two sources of error in the hillslope generation calculations, that is the use of the unmodified rainfall amount as a basis for volume calculations, and the assumption of instantanous runoff on the bare sites.

Taking the first of these problems, and considering only bare, or locally bare sites for reasons considered above, the infiltration curves on Figure 34 show that none of these will generate 100% runoff. The percentage of rain which becomes runoff for any event will depend on both the intensity and the duration of the event in comparison with the infiltration curve. This is demonstrated on Figure 36, on which diagram the infiltration curve for a hypothetical site has been overlain by a diagrammatic representation of the rainfall event. It can be seen that the percentage of the event precipitation which becomes runoff can be calculated as the percentage of the rectangle formed by the superimposed lines which is above the infiltration curve. For the simulated event, this procedure applied to the bare or locally bare sites on the infiltration survey (see Table III) gives for sites 1, 2, 5, 6, 7, 10, 12 and 14 the following percentages; 10, 15, 13, 8, 57, 25, 26 and 48 respectively. The average of these values is 25%, indicating that the precipitation which becomes runoff is not 10mm, but more likely to be 2.5mm on average.

A second source of error in the simulation is the assumption that the runoff duration is equal to rainfall time, plus the time taken to drain the slope. For all the bare or locally bare sites in the infiltration survey, runoff duration is in fact equal to the rainfall time less the time to infiltration capacity, plus the time taken to drain the slope. The average time to infiltration capacity

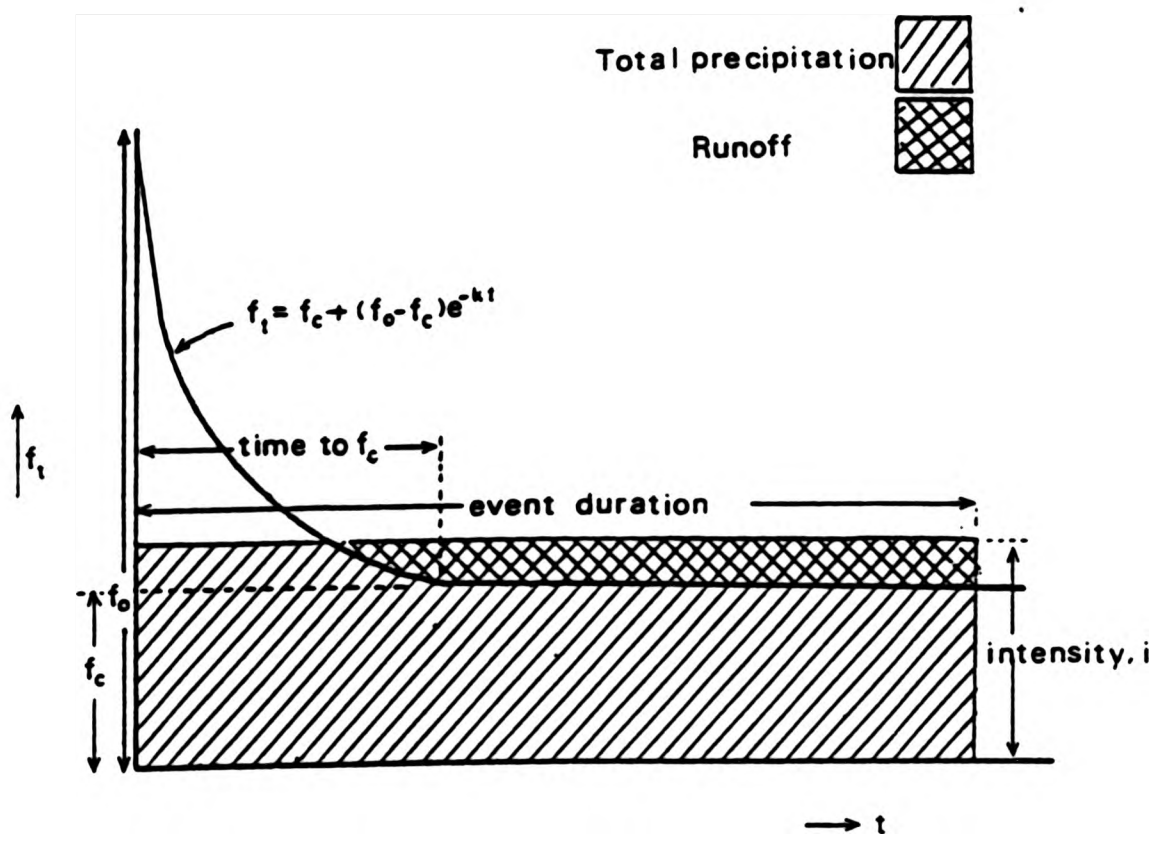

Runoff time = (event duration-time to f_c) + slope length/v

Runoff = (ppn) (% of rectangle above the curve)

Figure 36 : Method whereby the runoff for particular events was calculated

on these curves is 20 minutes. As a result, equation 4:20, presented earlier is more suitably calculated as ;

$$T = (\text{Rainfall duration} - 1200) + (\text{slopelength}/v) \qquad 4:29$$

The simulations undertaken using ROUTE.PAS must therefore be preceded by first, a comparison of the event intensity and duration information with the bare site infiltration curves as illustrated on Figure 34, and then the time to f_c assessed, and used to alter the hillslope hydrograph timebase, as suggested by equation 4:29. On this basis, any sort of event can be simulated.

The simulations do not consider the fate of the infiltrated water. Clearly on much of the watershed with over 100% cover, some of the infiltrating water is likely to reach the channel via pipeflow during the event, or, much later as delayed flow. Neither of these sources of flow has been considered here, and it is only possible to note that such contributions are likely to extend the recession limb of real hydrographs when compared to the simulated ones. It is assumed that these effects are not a significant control on the hydrographs, however, especially during larger events.

(B) Run 6: a simulation of a real field event, with hillslope infiltration and comparison with field discharge measurements.

On June 4th, 1981, an event was monitored at Alkali Creek. In a standard raingauge, 1.31 cm (13.1 mm) of rain was collected over 1.25 hrs. Runoff from this event was monitored in a field discharge survey. This event is used in this section to test the field validity of the routing model, ROUTE.PAS insofar as this is possible with just one sampled event.

Using the pre-model calibration procedure outlined in the last section, the % runoff from the event was calculated to be 38%, which as before was the mean of calculations on sites, 1, 2, 5, 6, 7, 10, 12 and 14. The time to f_c was again taken to be 20 minutes (1200 seconds) as this time is taken here to be independent of event size. With these modifications, ROUTE.PAS was run for a sixth time on the data files. Once again, the flow criteria and the stability

conditions held throughout the run. The results are shown on Figure 37. This pattern can be compared to the field discharge data which are also included on the same axes. The dotted lines are used to join the field data to their supposed equivalents on the simulation. These data are discussed following a description of the field discharge survey.

(i) The field discharge survey.

Using a standard Ott (C2) current meter held at the position of assumed mean velocity (at ⅔ maximum depth) in the channel, discharges were calculated on the network by the usual method of width and mean depth calculations, noting that ;

$$q = w.\bar{d}.\bar{v} \qquad \text{in cumecs} \qquad 4:30$$

The event moved down the channel as a well defined tongue of water (Photos 17 and 18) and since the author was at the base of the large discontinuous gully when the rain started, the survey was started at site 8, and then up to site 9, and then to sites 7, 6, 5, 4, 3, 2 and finally site 1 (site numbers as on the simulations and Figure 7, back folder). Discharges were taken approximately every 5 mins, taking 2 mins to conduct one reading and several more to slither between the sites. At site 1, it was clear that the flood wave had not completely passed, so readings were continued here every 5 mins, until no more flow occurred.

Some subjective observations were made during the course of this event. First, it was apparent that the early flows observed in the large discontinuous gully were losing to transmission loss on the channel bed. This is most clearly seen as the flood wave moves forward, but it is difficult to be sure thereafter how extensive the effect is. Secondly, as can be seen on Photo 19, the depth of infiltration after the event was barely more than 2 cm on bare slope surfaces. This indicates that there had been some infiltration, although after rainfall ceased the ground very rapidly dried out again. Thirdly, on the clayshale sites, the polygonal cracking associated with the pipe inlets did not seal up. Infiltration was presumably therefore still quite high during the event despite the evidence on non-cracked surfaces elsewhere that slaking had occurred. These observations confirm the importance of the nature

Photo 17 : A well-defined tongue of water led the front of the flood monitored on June 4th, 1981. View upstream at site 2

Photo 18 : The leading edge of the flood wave

Photo 17 : A well-defined tongue of water led the front of the flood monitored on June 4th, 1981. View upstream at site 2

Photo 18 : The leading edge of the flood wave

Photo 17 : A well-defined tongue of water led the front of the flood monitored on June 4th, 1984. View of stream at Site 2

Photo 18 : The leading edge of the flood wave

Photo 19 (a): A shallow infiltration depth was the case on most bare sites following the field-monitored storm on June [illegible]

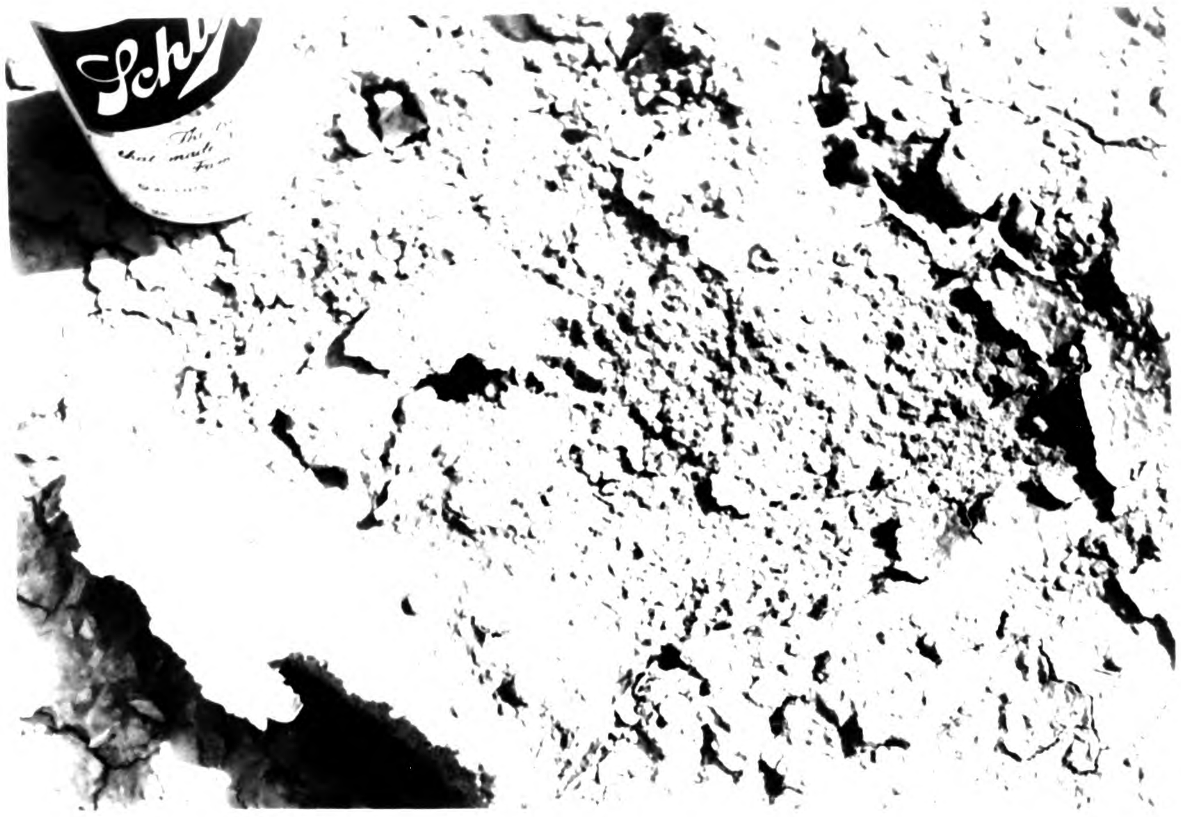

Photo 19 (b) Surface sealing associated with raindrop impact, and the swelling of surface soil [illegible] appear to have contributed to the low infiltration at bare sites.

Photo 19 (a) : A shallow infiltration depth was the case on most bare sites following the field-monitored storm on June 4th,1981

Photo 19 (b) Surface slaking associated with raindrop impact, and the swelling of suface colloids appears to have contributed to the low infiltration at some sites

Photo 19 (a) : A shallow infiltration depth was the case on most bare sites following the field-monitored storm on June 4th,1981

Photo 19 (b) Surface slaking associated with raindrop impact, and the swelling of suface colloids appears to have contributed to the low infiltration at some sites

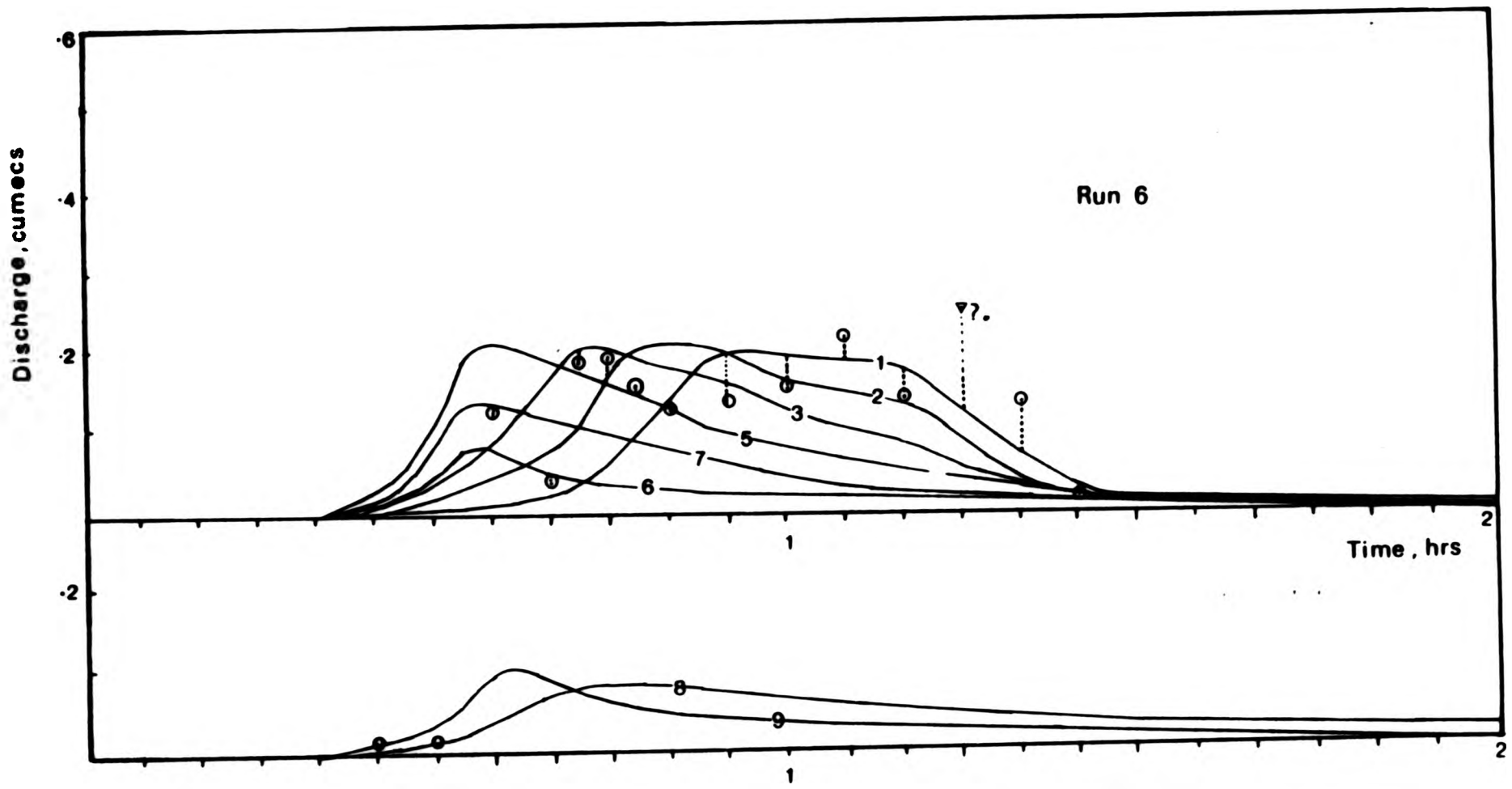

Figure 37 : Run 6; the result of routing the field-monitored event, and comparison with field data at appropriate times and sites (linkages inferred).
The numbers on the graphs relate to field sites 1-9.

of the surface materials in controlling infiltration rates and response to high intensity impact as outlined by Bryan, (1982) and Scoging (1982) but unfortunately also cast doubt on the infiltration curves obtained by using the ponding method. However, the field infiltration curves were all that was available to calibrate the model so this has to remain here merely as a note of caution. The transmission loss effect, however, may be modelled in a tentative way by comparing the downstream site discharges with the model. A discussion of the results of this test and transmission loss calibration is presented below. Finally, and most significantly, no runoff was seen on any of the sites retaining a vegetation cover, and although there was insufficient time to observe all the field infiltration sites during the event, visual evidence would suggest that runoff was restricted to the sort of areas predicted on Figure 24.

(ii) Comparison between the pattern of runoff predicted by Run 6, and field discharge data.

As was suggested above, the field discharge survey data (which is included in Appendix 10), was collected as a spatial survey across the field sites finishing at site 1, where thereafter a temporal sample was taken until runoff ceased. Consequently the data cannot be regarded as a complete test on Run 6 because it was simply impossible to be at all sites at all times during the event. In general, however, Figure 37 indicates that the values obtained from the field survey show some parallel with the range of values obtained from a routing of the runoff excess of the event (as calculated using the method shown in Figure 36) using ROUTE.PAS. If all the discharge values predicted from Run 6 are correlated with the field data at the equivalent site and at the estimated sample times, the product moment correlation r, can be seen from Appendix 12 to be 0.78, which is significant at the 5% level for 15 data points. The coefficient of determination shows us that 61% of the variation in the field data can be explained by the model. This is a good result.

Inspection of the pattern displayed by the field discharges and the simulation may cast some doubt on the validity of the data point to which a question mark has been attached on Figure 37. This is the

highest discharge value monitored, and is well above the range of the other data, yet is only ten minutes before flow ceased entirely at site 1 and would presumably be expected to be a low recession flow data point. Possibly some error has crept into the field calculations here, but there appears no way to substantiate this. Without this data point, the coefficient of determination would improve to 0.82.

Apart from this observation, it is clear that most of the discharges at site 1 in the field were considerably less than the hydrograph prediction from ROUTE.PAS. Subjective observations made in the last section indicated that some transmission losses might be expected for the main channel sites, which would explain the difference here. As a result, an attempt was made to explore the effect of including transmission loss in the simulations, using the Run 6, site 1 hydrograph and the temporal field data as a basis.

(iii) Transmission Loss

Renard and Keppel (1966) suggest that "... Quantitative information on the effects (of transmission) losses on downstream hydrographs is not ... generally available". Most work has been undertaken on watersheds of much greater area than Alkali Creek, and the bed material often appears to be larger. The relationship between transmission loss and runoff volume in the early Walnut Gulch experiments in Arizona suggested transmission loss to be as much as 30% of the peak flow entering the measurement section, occurring on the lower channel beds, although a later publication seems to imply that this was a considerable overestimate (Murphy, Diskin and Lane, 1972). In 1978, Butcher and Thornes used a kinematic routing method to simulate flows in ephemeral streams on watersheds in the Sierra Nevada, Spain. All had large bed material size and width-to-depth ratios over 40:1. Spatial variability of downstream flows was hypothesised as a result of bed infiltration. Field monitored values of up to 30 mm/min were found on flow events lasting up to 5 to 6 hours, site values fitting the negative exponential model of Koskiakow cited by Dixon (1975). Loss volumes calculated in this way were included in the model, being subtracted from runoff generations at the end of each reach. Survival lengths of flows of varying magnitude were considered, and the relationship was found to

be non-linear, with smaller infiltration rates producing disproportionately longer survival lengths.

In a summary of the main effects of transmission loss on the form of the hydrograph, Murphy, Diskin and Lane (1972) suggest that the amount lost to transmission is related to bed porosity and the specific yield of the alluvium, the geomorphology of the channel, and the hydrograph rise time and the size of the peak at the head of the section under study. Because of the time-dependency of the effect as explained by Butcher and Thornes (1978), early flows will clearly suffer far more from this effect than later flows, and the rising limb of the hydrograph far more than the falling limb. This proposition is reinforced by the work of Renard and Keppel (1966), who suggested that the transmission loss effect is more dominant during the rising stage of the hydrograph. Because the channel at Alkali Creek has its highest width-to-depth ratios below the point where the tributary junctions are, and here the lowest gradients are to be found, it is considered here very likely that the early very low flows prior to the main peak on sites 1, 2 and 3 will be absorbed for most events, particularly if antecedent conditions are dry.

It is possible to develop a simple transmission loss model for the lower course sites in the Alkali Creek network (below X) by incorporating some of these observations into an inverse time-dependent model similar to that developed by Ostiachev, and cited by Dixon (1975). This latter worker suggested that transmission loss (mm) is calculated by multiplying a constant by the inverse square root of time since runoff commenced. It is suggested by the work of Renard and Keppel (1966) that the constant should be more suitably replaced by a parameter which is the value of transmission loss when t = 1, but which changes with the value of the discharge. The following expression meets these criteria :

$$Tr = Q_t \,.k.\, t^{-\frac{1}{2}} \qquad 4:31$$

where Tr is transmission loss, in cumecs in this case
and Q_t is discharge at time t in cumecs
and k is the proportion of the flow when t = 1 which is expected to be lost to bed infiltration, probably a function of the channel form ratio.

Values of k can be tried in turn, and the best fit to field data found. For instance, if after 1 second, 15% of the discharge is anticipated as being lost to the bed, then k = 0.15. An initial (t = 1) 30% loss would mean k = 0.3, and so on. The actual value of the product is likely to be greater at the peak than elsewhere, but the whole amount is affected by time, generally dropping as runoff time increases. A PASCAL programme, SEEP.PAS, was written for attachment to ROUTE.PAS. It is separately included in Appendix 11, and simply modifies the output from ROUTE.PAS by subtracting site values of Tr from the site discharge, Q_t. The new data can be compared to the field discharge estimates to assess the improvement in the fit.

Figure 38 shows the results of this procedure as applied to the simulated site hydrograph for Site 1 on Run 6 (first seen on Figure 37). The field data from the temporal survey conducted at this site are also shown. The behaviour of equation 4:31 is indicated here for comparison, for values of k of 0.15 and 0.30. Also included on this Figure are the results of three correlation tests. These represent the relationship between the field sites and the simulation values first without transmission loss, then for the adjusted values when k is 0.15, and then 0.30. The relationship between the temporal survey data is poor but improves with an assumed transmission loss. The optimum value for k is 0.15, which gives the better fit. All these regressions are included in Appendix 12 as before.

The results of the transmission loss simulation having improved for a transmission run where k = 0.15 in equation 4:31, it was decided that in the next section, where the hydrographs for a variety of events on the watershed are simulated, that for all sites on the main channel, (i.e. sites below X, numbers 3, 2 and 1) a transmission procedure be included in ROUTE.PAS to simulate transmission loss in these locations. On all subsequent runs of the model, therefore, this loss must be assumed on these sites.

Overall the field data have not substantiated the 'no infiltration' assumptions, and a procedure was therefore devised to reduce runoff by an amount which takes the infiltration data into account. Simulating the field-monitored event in this way gives a model which

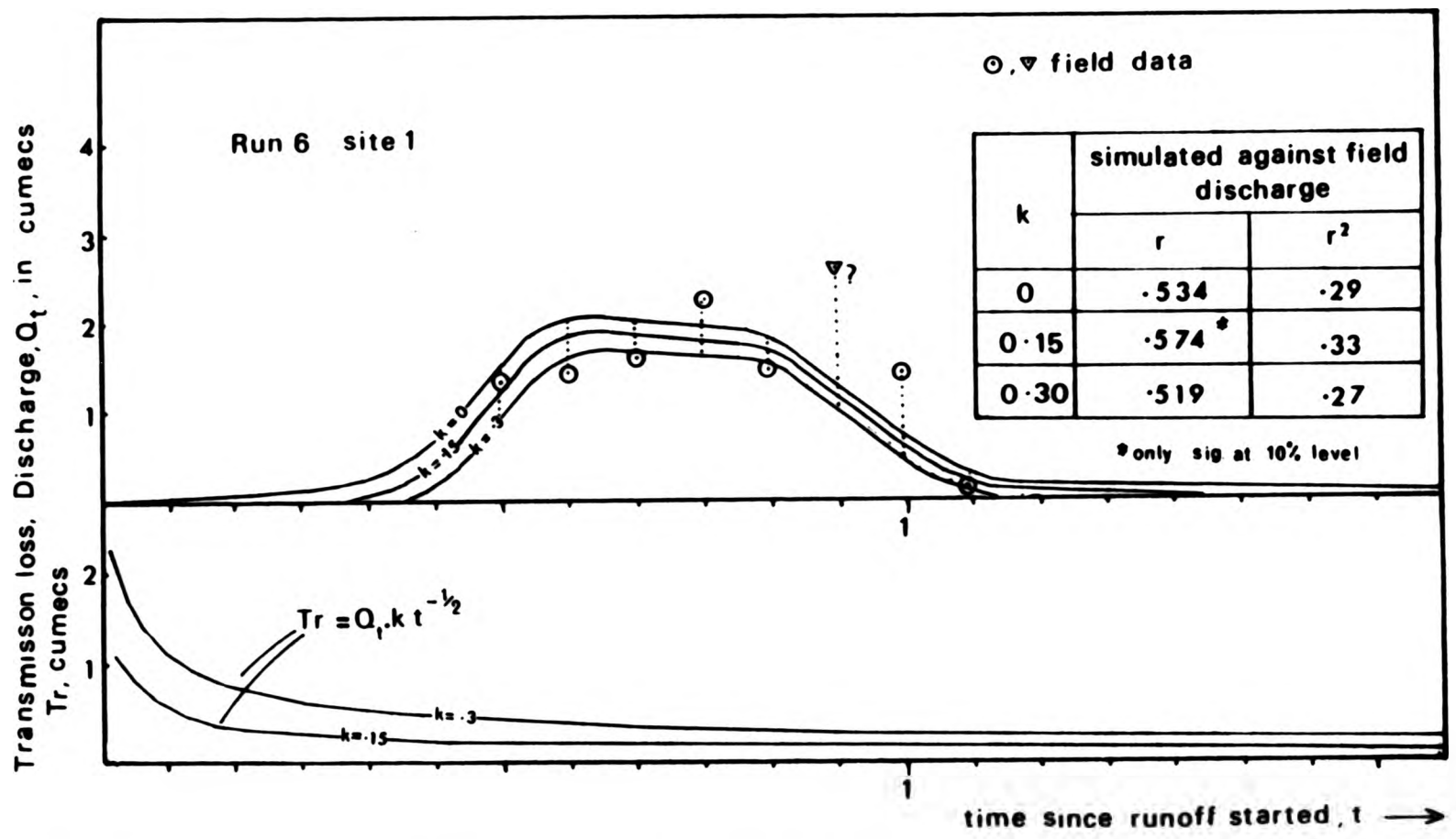

Figure 38 : Adjustment of Run 6 for transmission loss - various values of k

significantly predicts the field data which were collected, sparse though they are in relation to the long-term operation of the watershed. Inclusion of transmission loss on sites below 'X' (site 5) improves the fit here, and is from now on adopted as part of the routing process. The model having proved to be convincing in a variety of situations, attention is now given to the simulation of the longer-term event patterns at Alkali Creek.

(V) SIMULATION OF SUMMER STORMS WITH A RANGE OF RECURRENCE PROBABILITIES

In Chapter 2, six years of recording raingauge data were presented as Figure 2. The summer storms were analysed from the raingauge trace in terms of their intensity, duration, and total event precipitation (this last parameter being the product of the first two), and these data are available in Appendix 1. In this section, use is made of these data to identify events for simulation. The intention is to simulate events which are common occurrences, and to compare these results with the hydrographs likely to result from 'freak' or highly improbable events. Although six years does not perhaps represent a long enough record for this exercise, the results are illuminating, pointing to the conclusion that the most common events on the watershed are likely to have a very different geomorphic role in comparison with the extreme events. This area will be explored in the final two Chapters.

Since the model ROUTE.PAS runs on events of a prescribed total precipitation and duration, this section concentrates first on establishing the recurrence probabilities for the event total record, and then attempts to link event totals to particular durations using regression analysis. From the picture produced in this way, four events are chosen for simulation, after which the results are presented.

(A) Event probabilities

On Figure 39, the probability of the total event precipitation for any event being of a greater value is analysed using the Log Pearson III Event Frequency analysis method that was described for use on

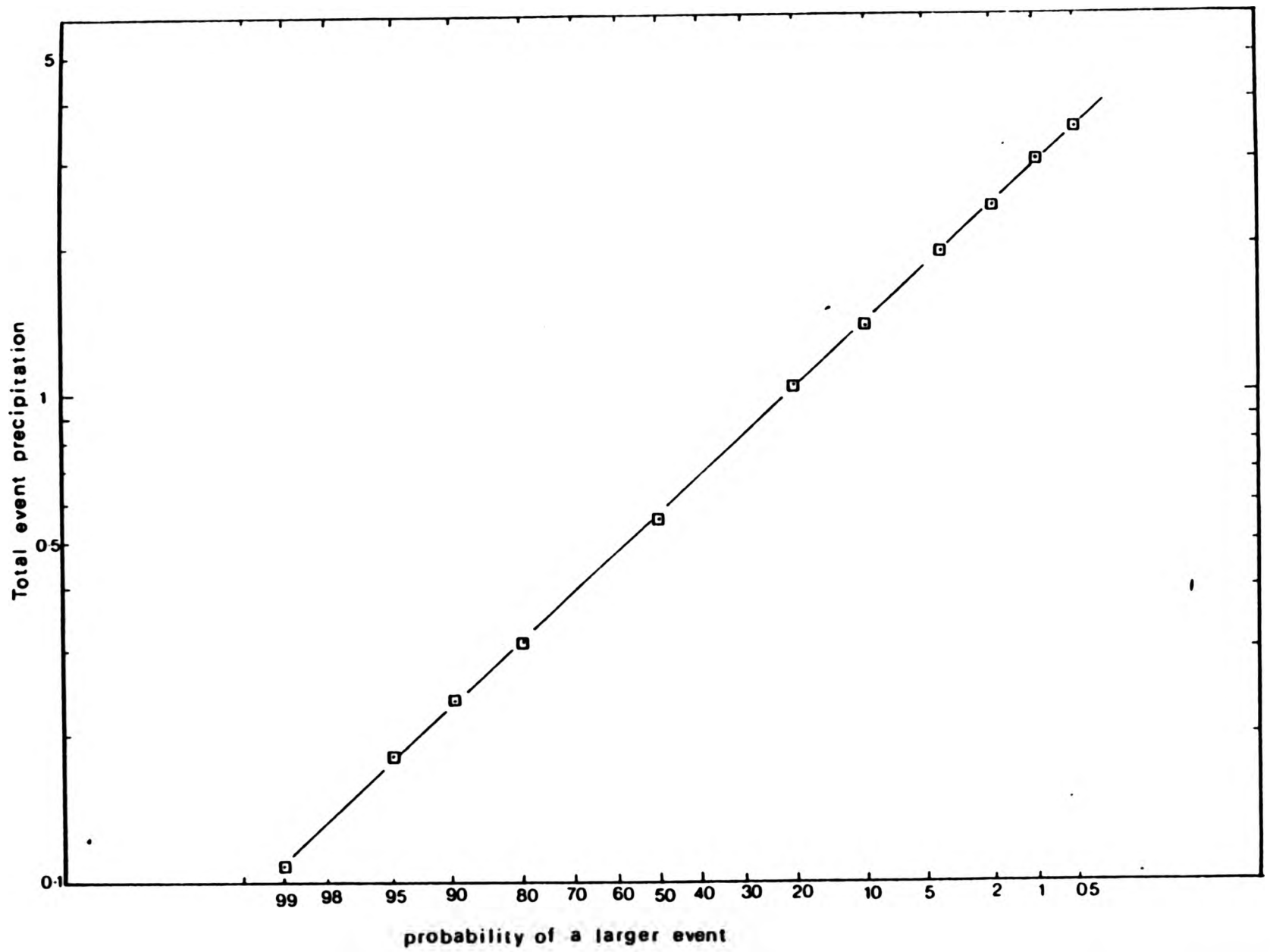

Figure 39 : Log Pearson III Event Frequency analysis conducted on the Alkali Creek summer storm data in Appendix 1. Total precipitation for the event is used

the snowmelt records in the last Chapter. The events with probabilities ranging from 0.5 to 99% are identified and plotted, and details have been included in Appendix 5. There are 11 points plotted across the range of possibilities, and it was decided to use these 11 events in subsequent discussion. For this purpose, it was necessary to consider the sort of duration over which these events took place, and to identify incidentally their intensity characteristics.

(B) Event totals related to intensity and duration.

Figure 40 relates event intensity and duration, and Figure 41 links the total event precipitation (the product of intensity and duration) to the event duration. Although the significance levels of this latter regression are spurious for obvious reasons, it is possible to use this regression to link particular event totals to particular event durations with some level of confidence. The log-log regression equation shown is therefore used to calculate the duration of the 11 events identified on Figure 39. These data are listed as the second and third columns of Table VI.

Plotting the precipitation event intensity against event duration for the 95 events in the six years of record reveals a good relationship between these properties (Figure 40). The inverse log-log plot which results has a best-fit regression line which is signficant at the 5% level. It is perhaps not surprising that the longer events, which as can be seen from Figure 2 occur mainly as prolonged, low intensity showers in October, have the lowest intensities, whereas the high intensity events which occur in July and August but are only of short duration.

Once again the relationship predicts the event intensity from the event duration, and the data can be added to Table VI to form the first column. Knowing the intensity and duration of the 11 events of interest allows the runoff percentage to be calculated for all locally bare sites using the method described on Figure 36. The relevant data are listed in the remaining columns of Table VI, allowing the average percentage runoff on locally bare sites for events with those specific intensities and durations to be calculated. Regression data are in Appendix 12.

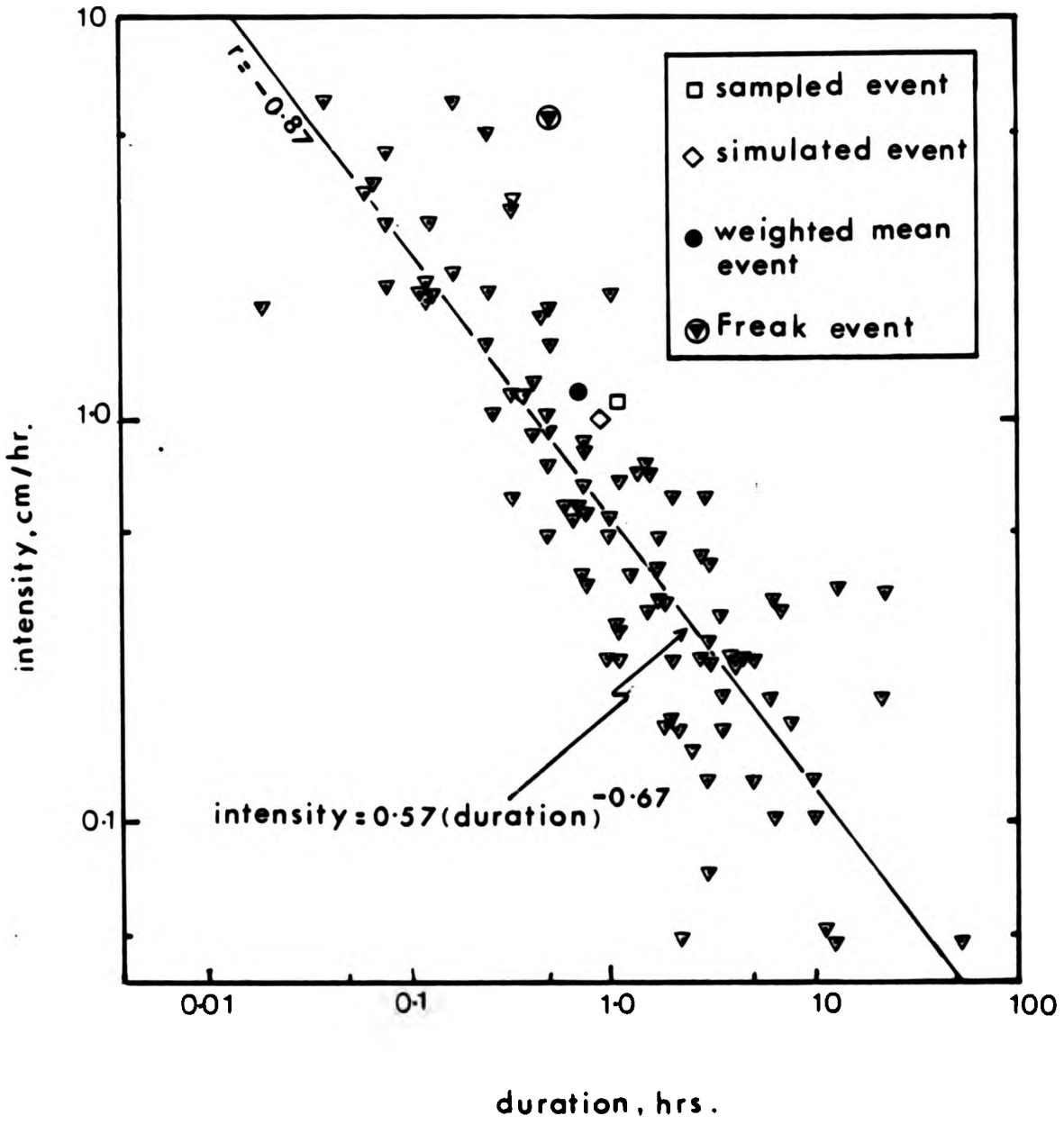

Figure 40 : Relationship between the intensity and the duration of the 95 summer storms which occurred on the watershed between 1967 and 1972

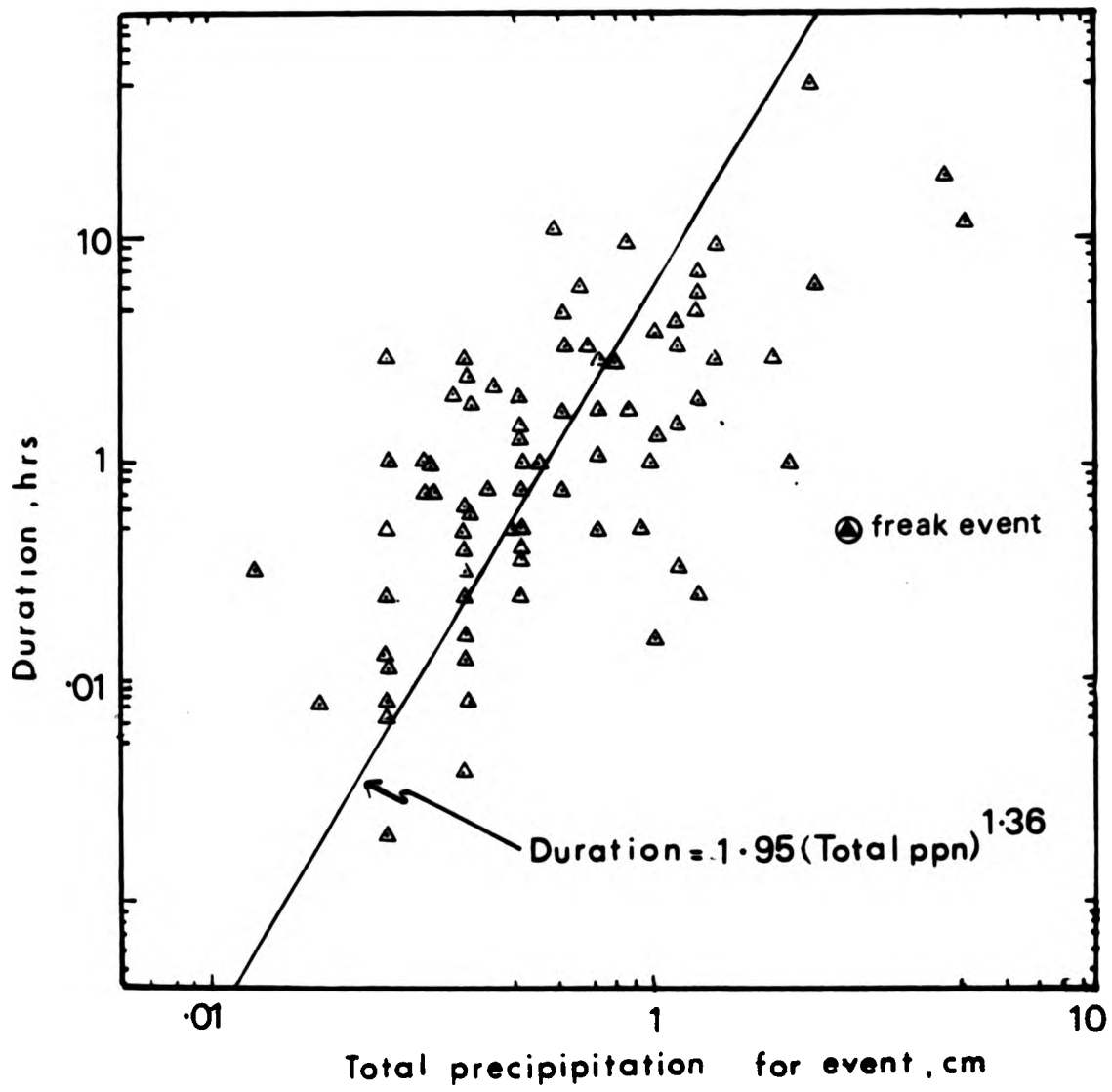

Figure 41 : Relationship between the duration and total precipitation of the 95 summer storms which occurred on the watershed between 1967 and 1972

Table VI

The calculation of % event runoff, using known event intensities and durations, and using the field-monitored infiltration data shown on Figure 34. The method used is illustrated on Figure 36.

Locally bare sites only are used

Intensity (mm/hr)	Duration (hrs)	% probability of larger value of total ppn for event	% of event listed becoming runoff on Sites; 1	2	5	6	7	10	12	14	Average %
26.26	0.100	99	0	0	0	0	2	0	0	2	0.5
17.51	0.187	95	0	15	12	3	31	0	0	20	10.1
13.15	0.287	90	0	15	5	0	35	0	0	22	11.0
10.47	0.394	80	0	24	7	5	55	7	0	33	16.0
5.27	0.888	50	0	18	15	0	80	40	35	37	28.3
3.65	1.945	20	0	0	0	0	90	14	70	52	28.3
2.70	3.044	10	0	0	0	0	95	7	65	60	35.0
2.00	4.758	4	0	0	0	0	95	5	75	65	36.7
1.61	6.619	2	0	0	0	0	98	0	85	61	31.0
1.37	8.358	1	0	0	0	0	99	0	90	40	28.8
1.16	10.735	0.5	0	0	0	0	100	0	95	0	23.5
* 55.88	0.5	-	75	86	93	78	100	77	80	85	81.0

* The Freak event which occurred on August 24th, 1971.

On Table VII, reworking these data allows the number of mm from a particular event total which becomes runoff to be calculated by multiplying the total by the % runoff figure estimated on Table VI. Inspection of the infiltration curves once again gives no reason to alter the time to f_c estimate used in Run 6, and so the value of the rainfall duration less time to f_c can also be identified. Using this method it is theoretically possible to model all 11 of the events on the list using ROUTE.PAS. In the event only three were chosen, for reasons explored in more detail below.

(C) Choice of events for simulation

Each of the 11 events for which the probabilities of a greater value have been identified on Figure 39 and tabulated on Table VII, can be regarded as representing the midpoint of a class of events. For instance, the 95% probability event, in which 1.79 mm of total precipitation occurs, can be regarded as the midpoint of a class running from (1.132+1.79)/2 = 1.461 mm to (1.79+2.35)/2 = 2.12 mm, and so on. Using classes identified in this way, the % frequency of events in each class can be calculated for all the 95 events on record. The % frequencies for the classes whose midpoints are the fifth column on Table VII are listed as the last column. These data reveal that the 90% probability event, the 80% probability event, the 50% probability event and the 20% probability event classes together represent 82% of all events analysed, the others representing very improbable cases.

Taking the three smallest events in terms of precipitation on the list, it is clear from this that little runoff will occur during these events, since despite very high intensities, their short duration ensures little or no runoff when compared to the infiltration curves. All precipitation for these events can therefore be considered to infiltrate on most locally bare sites and so are insignificant, both in terms of frequency and runoff.

Turning to the events with the highest precipitation totals (which have between 10 and 0.5% probabilities of a larger precipitation total), the method used here implies that these events produce large totals because of extraordinarily long durations, falling at low intensities for up to 10 hours. Representing altogether only 13% of

Table VII

Characteristics of Selected Summer Storms, and the selection of events for Simulation Runs.

% probability of larger value of total ppn for event	Intensity (mm/hr)	Duration (hrs)	% event runoff (from Table VI) (B)	Total ppn for event (mm) (A)	mm. of ppn becoming runoff (mm) (A x B)	Duration less f_c time (hrs)	% Frequency at class mid point	
99	26.26	0.100	0.5	1.132	.0057	-	2	
95	17.51	0.187	10.1	1.79	.1808	-	3	
90	13.15	0.287	11.0	2.45	.2640	-	15	
80	10.47	0.394	16.0	3.09	.494	0.0637	30	* Run 7
50	5.27	0.888	28.3	5.62	1.471	0.558	25	* Run 8
20	3.65	1.945	28.3	10.00	2.833	1.615	11	* Run 9
10	2.70	3.044	35.0	13.90	4.860	2.714	7	
4	2.00	4.758	36.7	19.31	7.09	4.4277	2	
2	1.61	6.619	31.0	24.62	7.63	4.289	1	
1	1.37	8.358	28.8	29.21	8.41	8.028	2	
0.5	1.16	10.735	23.5	35.11	8.25	10.405	2	

Run 10 = The 'freak' event which occurred on August 24th, 1971, in which 27.94 mm fell in 0.5 hrs at an intensity of 55.88 mm/hr. The percentage event runoff for this event (Table VI) was calculated as 81%, so that 25.15 mm became runoff, and that the duration less time to f_c will be 0.166 hrs (10 mins).

all events on the watershed, these clearly represent the low intensity, long duration events which are occasionally experienced in the late summer months in the study area. As will be shown in the next section, the very small intensities mean that only on sites where f_c approaches zero will runoff occur for such events. When this does occur, the long duration will produce such a long timebase for the hillslope hydrographs that the simulation results predict a slow trickle of runoff over a long runoff period. Once again, these are not likely to be major runoff events, therefore, but such events may have a role in transporting the very fine fraction and redepositing this on the main channel. Attention is therefore directed towards the three asterisked events on Table VII. Because this sort of event represents common occurrences on the watershed, they have therefore been selected for the simulation runs 7, 8 and 9. The results of these are presented in the next section.

As a contrast to these three events, the records of events for Alkali Creek (Appendix 1) was inspected for the largest event which had both a very high intensity and a high duration. Figure 42 shows a photocopy of the actual raingauge trace for the selected event. This event, which occurred on August 24th, 1971, plots well away from the regression lines on Figures 40 and 41 where it has been indicated as a black triangle, because it has an unusually high intensity (55.88 mm/hr) and a relatively long duration (0.5 hrs). In statistical terms this event represents a 'freak' occurrence. Because of its high intensity and duration, the percentage runoff for this event (as calculated using the method shown on Figure 36) is 81%, so that of the 27.94 mm which fell, 25.15 mm became runoff (Table VI). The duration of the event, less time to f_c, becomes 10 minutes (0.166 hrs). This 'freak' event is modelled as Run 10 in the next section.

(D) Results

The results of the three runs, Run 7, Run 8, and Run 9 are included as Figures 43, 44 and 45. The results of the routing of the 'freak' event are shown on Figure 46. Run 7 could be described as the results of routing a short duration, moderately high intensity event of the sort that occurs 30% of the time at Alkali Creek. Run 8 could be described as the result of routing a moderately long

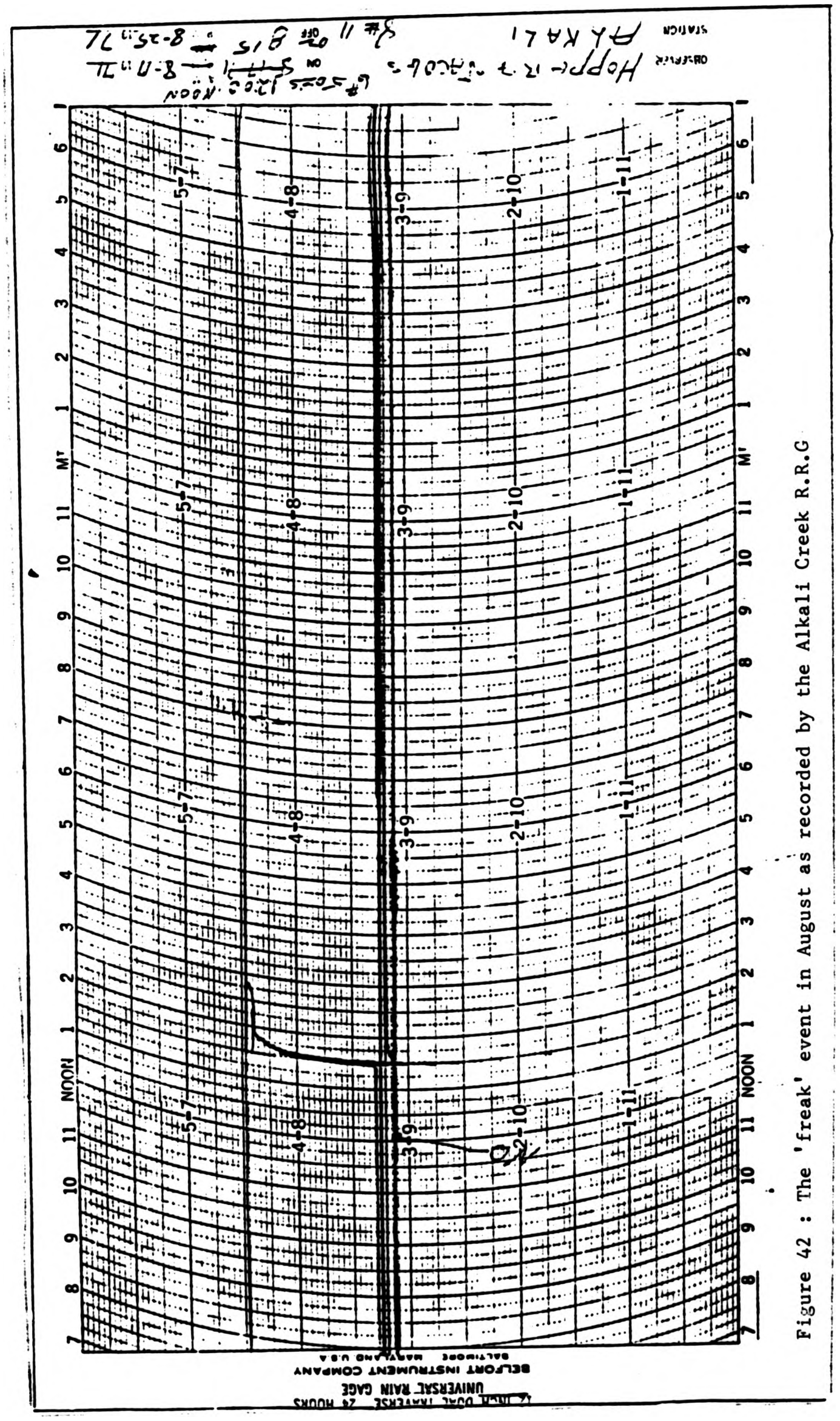

Figure 42 : The 'freak' event in August as recorded by the Alkali Creek R.R.G

Figure 43

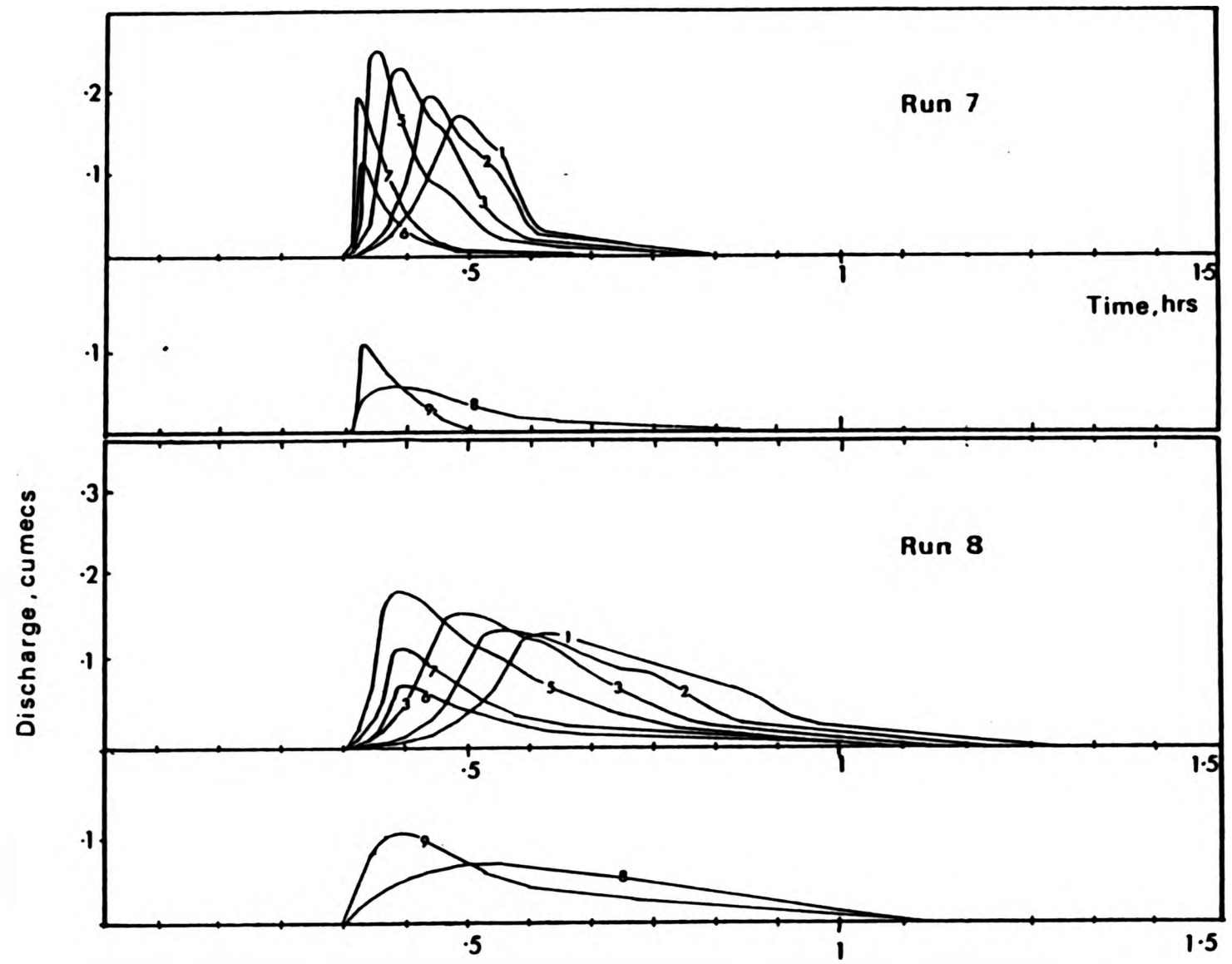

Figure 44

Figure 45

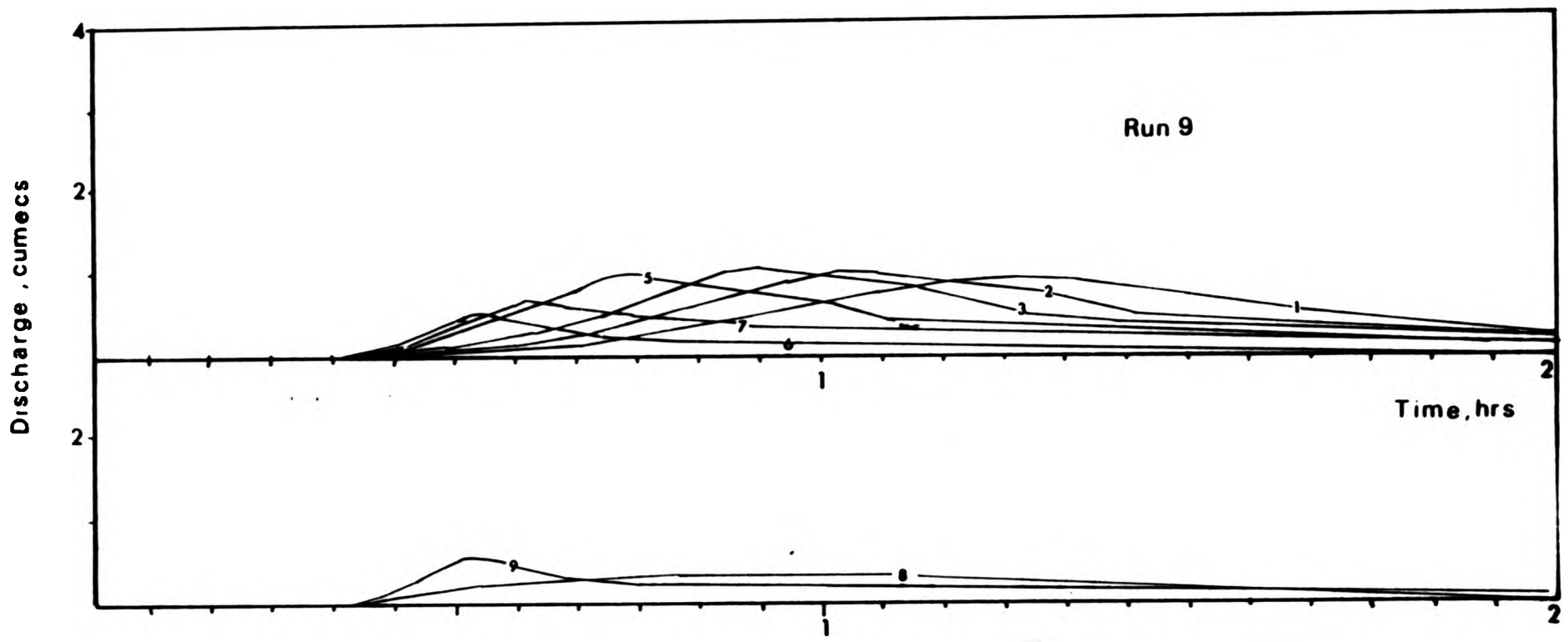

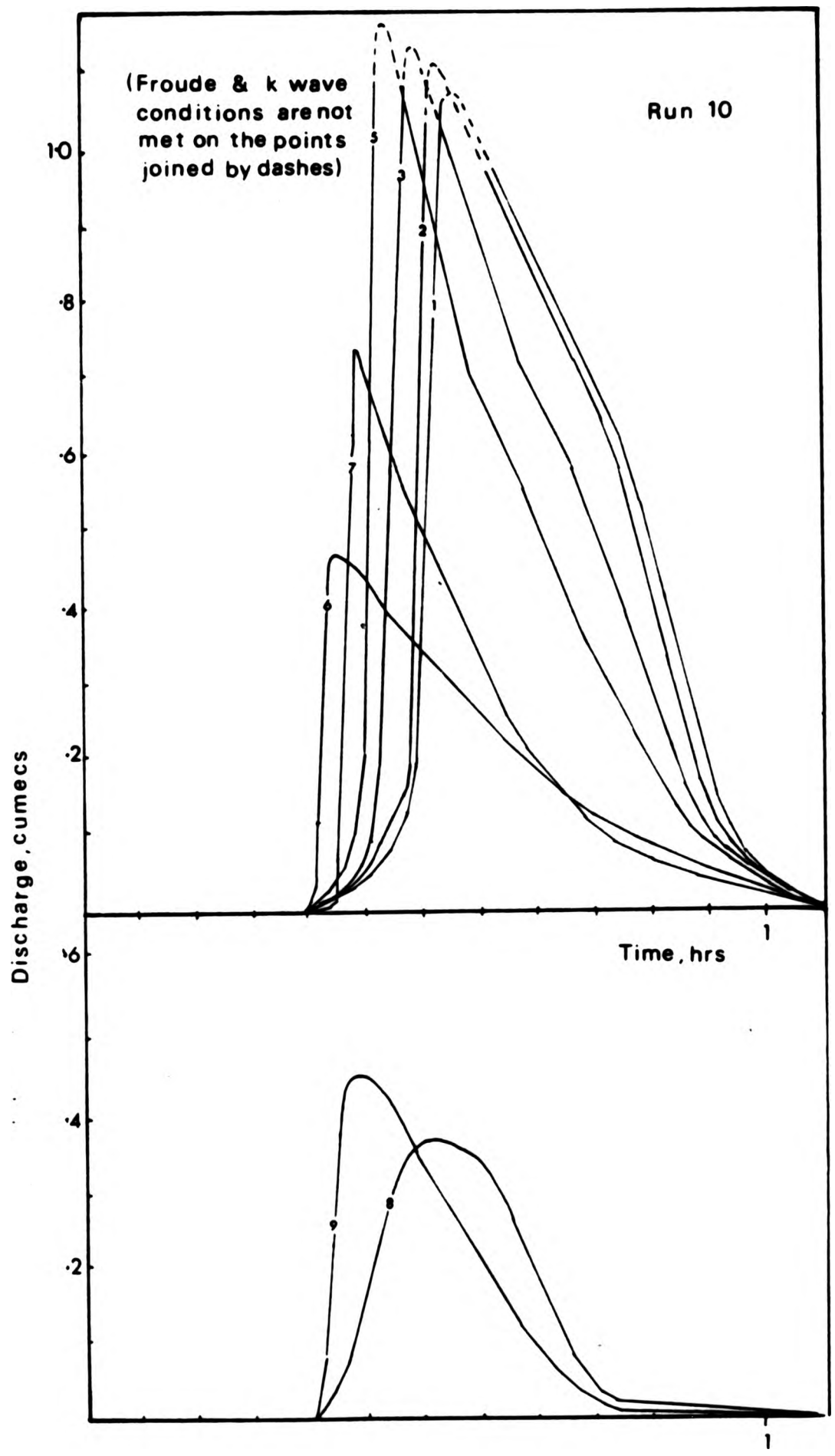

Figure 46 : Run 10, the 'freak' event in August, 1971

duration, low to moderate intensity event, of the sort which occurs 25% of the time at Alkali Creek, and Run 9 could be described as the result of routing a long duration event of fairly low intensity, of the sort that occurs 11% of the time. Run 10 is the result of routing the largest 'freak' event in the six years of record, one having high intensity and moderate duration, which very rarely occurs.

The most significant aspect of the first three runs is how little runoff is produced in these simulations. Run 9, although representing the largest amount of runoff, is spread over such a long timebase (not all of which has been included on the diagram) that the maximum discharge achieved is only 0.057 cumecs at site 3 after 53 minutes. Even without the inclusion of transmission loss, the discharge does not reach 0.1 cumecs anywhere on the Run. Imagination allows the sort of hydrograph that the 10% probability events etc., would produce ; - they would all be even more attenuated than this.

Run 7 shows the sort of flashiness commonly associated with semi-arid hydrographs, although the volume of runoff is considerably less than on Run 9. The peak discharge achieved is 0.221 cumecs at site 5 after 24 minutes, recession having finished at all sites after 50 minutes. This sort of event, common on the watershed, peaks at site 5 and shows attenuation thereafter partly because of a predisposition in the model (see comment on page , point 3) and partly because of the inclusion of transmission losses in the simulations for sites 3, 2 and 1. There are obvious geomorphological implications of this effect, which will be explored in more detail later. The effect is particularly striking on the large discontinuous tributary where during none of the three runs representing 'normal' events on the watershed is any significant runoff peak produced.

Run 8 demonstrates characteristics half way between the two extremes, Run 7 and Run 9, already described. The largest discharge achieved anywhere on this Run is at site 5 after 55 minutes, where a peak value of 0.172 cumecs is obtained on the simulation. The volume of runoff increases in all models downstream but neither the size of the peak nor the peakedness of the hydrograph increases.

We reach the important conclusion that all flows attenuate below site 5 on the watershed, that all common events produce only moderate peaks, and that there are as many events in a year which have 'flat' or non-flashy shapes as those (as in Run 7) which have a flashier appearance. Furthermore, inspection of the results from Run 10 leads to the even more interesting conclusion that very occasionally an event will occur on the watershed which is so dramatic in its impact as to completely override the effect of the more common events.

The simulated Run 10, although not fulfilling the Froude and k wave requirement at the peaks, gives some indication of the relative significance of the more common events as compared to the 'freak' occurrence. The peak discharge obtained was 1.17 cumecs at site 5 after 12 minutes on this simulation, clearly contrasting with the more frequent events. At this stage the study moves naturally to a discussion of the geomorphological implications of the conclusions made in this and the last Chapters, and these implications are considered in the light of the morphological data first presented in Chapter 2.

Such a discussion is contained in the next two Chapters.

Chapter 5

SHORT-TERM GEOMORPHIC IMPLICATIONS : SEDIMENT BEHAVIOUR

This Chapter explores some of the implications of the simulations of the two main runoff processes at Alkali Creek which were described in the two previous Chapters, looking specifically here at sediment transfer.

At the beginning of this thesis, it was argued that at this short-term scale, the drainage basin shape and slope operate as independent controls on the contemporary water and sediment transfer mechanisms. This allowed the flow generation models to be formulated using these morphological properties. Remaining at the same scale, this section brings the two process domains together as annual patterns of sediment movement through the watershed channel systems, and explores these patterns for spatial domain overlap.

After an initial consideration of the theoretical background, a second section of this Chapter explores the sediment sources for both summer storms and snowmelt arguing partly from observations made in the field. The following section considers the sediment transfer mechanisms involved in the two processes, presenting here the sediment concentration and discharge data collected during the snowmelt and the summer storm field work periods. These data allow the spatial sequence of sediment lodgment and entrainment to be inferred during the sampled events.

In a fourth section, extrapolation of these sediment relationships, in conjunction with the simulations which have been presented in the last two Chapters, allows a method to be proposed from which the site sediment yields during snowmelt and during the main types of summer storm runoff may be calculated. Viewed together, these downstream patterns allow annual sediment budget estimations for particular sites within the network to be made (both with and without the 'freak' storm, run 10). Finally, the spatial rate of change of sediment yield for each of the simulated events is used as a surrogate for short-term geomorphic change during the events. Mapping these rates of change down the network allows the mechanisms of the longer-term sediment transfer to be considered as a link to gully morphology which is discussed in Chapter 6.

(I) APPROACHES TO SEDIMENT YIELD ESTIMATION

A vast body of literature exists on this subject, and there are many important texts and literature overviews available on all aspects of sediment behaviour (Allen, 1970; Agricultural Research Service, 1975; Kirkby and Morgan, 1982; and Swanson, et al, 1982). At one end of this vast spectrum of research lies the field of Fluid Mechanics, exploring the links between hydraulics and sediment detachment and entrainment (Raudkivi, 1967; Allen, 1970). This area of the literature, although of value to the geomorphologist working at the plot level, is not reviewed here since these considerations are outside the scale of interest of the current investigation. Good summaries of the principles involved are provided for geomorphologists by Thornes (1979), and Richards (1982). As will be shown, the sediment type in the study area is all fine-grained and no granular or gravelly material was found on the watershed. As a result, the literature concerned with sediment movement in this size category is not considered here either.

Most of the remaining literature which tackles the modelling of sediment yield from the landscape appears to be largely concerned with surface wash erosion. Sediment removal of this type is assumed to be associated with the summer storm hydrographs simulated for a variety of events in the last Chapter. The importance of this process in comparison to other sediment generating processes (for instance piping, and bank scour and collapse) will be reviewed in the following section in reference to empirical field experiments conducted elsewhere. A search of the literature failed to produce any sediment yield model especially designed for the modelling of sediment yield from snowmelt, either at the slope or at the basin scale.

Sediment yield models for surface wash may be subdivided into two categories; physically-based models (or 'White Box' models), in which the detachment and transport capacities of runoff events are linked to rainfall intensity, and hillslope discharge; and secondly empirally-based models (often in a 'Black Box' format) which use field-derived estimates of erosion rates from mapped parameters supposedly linked to sediment yield, or which use sediment rating relationships as predicative tools along with some sort of record of

discharge (individual hydrographs, flow-duration curves, etc.). It is implied by Kirkby (1980b) that at the present level of research, the former are to be preferred over the latter for slope studies.

For modelling at the basin scale, however, empirical models are more commonly used. This is because sediment is often not uniformly detached and transported when viewed at this scale, and also because sediment may be lodged in channels, complicating the use of the sediment detachment and transport equations when applied over a wider area. Both types of models are reviewed in relation to the current investigation in the following section.

(A) Physically-based models

These models attempt to simulate first the shearing detachment of particles which occurs on non-cohesive sediments by estimating the 'detachment capacity' of both rainfall (D_r) and runoff (D_f) in terms of rainfall and flow parameters. By utilising a large body of experimental literature, Meyer and Wischmeier (1969), and later Meyer (1971) formulated D_r and D_f as :

$$D_r = C_1 AI^2 \qquad 5:1$$

where A is the incremental area downslope

C_1 is the rainfall-soil detachment coefficient (derived by Meyer from published literature and research) and I is rainfall intensity

and

$$D_f = C_2 Aq^{\frac{2}{3}} S^{\frac{2}{3}} \qquad 5:2$$

where A is as above

C_2 is a runoff-soil detachment coefficient similarly derived and where q is runoff rate, and S is slope gradient.

Secondly, sediment transport by rainfall (splash, T_r) and by runoff (T_f) are further formulated in similar terms, so that ;

$$T_r = C_3 SI \qquad 5:3$$

where C_3 is a rainfall soil transport coefficient similarly derived, and I and S are as above

..and $$T_f = C_4 q^{\frac{1}{3}} S^{\frac{1}{3}} \qquad 5:4$$

where C_4 is a runoff-soil transport coefficient

and q and S are as above

These relationships may be linked to the overland flow models described in the previous Chapter in a fairly explicit way.

Although this model was later developed more fully (Foster and Meyer, 1972, 1975) it is described here in its 1969 form because of a clearer link with the runoff production model in Chapter 4.

An important aspect of these ideas is the comparison suggested between total detachment capacity, D, ($D = D_r + D_f$) and total transport capacity T,($T = T_r + T_f$) at each time interval during the storm, and at each point downslope. This is important for sediment routing because the actual sediment yield increment downslope must be modelled as the lesser of the two values. If G is the actual rate of sediment transport (averaged across the slope), then Kirkby (1982) suggested this condition can be expressed as :

$$\frac{dG}{dx} = D \quad \text{if either } \frac{dT}{dx} \geqslant D \text{ or } G < T \qquad 5:5$$

where x is distance downslope, and other symbols are as before.

If D and T can be modelled using a kinematic model as in the last Chapter, then a suitable calibrated site (Meyer, 1971) can be modelled for sediment yield using equation 5:5 in conjunction with a continuity equation such as the one proposed by Kirkby (1982). Such approaches have led to a range of larger scale deterministic models (Bennett, 1974).

Although these "... Physically based models have greater potential at the plot scale" .. (Kirkby 1980b), and so, as will be explained below are not really very suitable for the complex environment of Alkali Creek, they have been described here because the conditions imposed on sediment transport by equation 5:5 point to an important aspect of sediment yield in general. That is, if sediment transport is not at total transport capacity but at total detachment capacity, then sediment transport is unlikely to be a close function of discharge, q, but more closely related to the rainfall intensity at any one site. The implications of this situation in which the transport rate is described as 'supply-limited' are that the hillslope sediment rating relationships are likely to show wide variation from one event to the next, and hysteresis is therefore likely to be a characteristic of individual events. In the situation where sediment transport nears total transport capacity, then less hysteresis on the hillslope hydrograph, and a high level of inter-event reliability is to be expected. The corollary to this argument is that rating curves are more likely to be applicable outside the event or events for which the data were obtained only if a supply of sediment in a form which is both easily detached and transported is readily available to all watershed events. As long as no exhaustion of sediment supply can be assumed, rating relationships for one event are likely to be matched during other, subsequent events. The section following the literature review examines the sediment sources at Alkali Creek in these terms.

(i) Physically based models at the basin scale.

The complexities introduced by sediment yield modelling at the basin scale are explored by Thornes (1980). Even on slopes, it is becoming increasingly recognised that well-developed rill systems may be assumed to have higher sediment yield than inter-rill areas, thus complicating the use of those equations described above. Additionally, where vegetation cover is present, a variable area of overland flow between events of differing intensities (as discussed in Chapter 4) may cause the effective wash contributing area to expand and contract. Thornes (1980) also noted that as sediment and water move downslope they encounter a decrease in slope gradient. Examination of equation 5:4 shows that unless there is a compensating increase in local site discharge, site transporting

capacity will fall, and point deposition may result. Other causes of deposition on the slope are widening of the channel or rill, ponding and retardation by vegetation, and transmission loss of the flow down-channel.

These problems are compounded when basin-scale behaviour is of interest, and at this scale there is the additional possibility that even during summer events, sediment is more commonly derived from bank collapse and other in-channel sources. This is probably a problem in gullied landscapes. Thornes (1980) quotes the work of Anderson (1954) to demonstrate that "... Bank erosion may provide up to one-third of the total sediment load, and in rilled and gullied areas this is much larger because of the high level of coupling between the channel and slopes...". These observations have been made in many investigations of sediment yield in active gully systems, and this source of sediment will be considered in more detail in a later section. There is no doubt that in the field season of 1981 channel sources and bank collapses provided the bulk of sediment supplied to the snowmelt flows.

For all these complicating reasons, physically-based models were ruled out for current use, although the theoretical discussion has usefully highlighted the importance of sediment availability in surface wash processes. A more empirical method was consequently sought to link the simulations to erosion, transportation and deposition of watershed sediments. For wash supply, the use of morphological surrogates was explored, and basin sediment rating relationships considered as a method of predicting yield from the unquantifiable sources on the channel bed and banks.

(B) Empirically-based models

Empirically-based models which employ surrogate parameters to predict sediment removal are still commonly found in the literature. At the hillslope scale, these models link simple morphological variables such as slope gradient and distance from the divide to site sediment transport rates (usually giving annual estimates). The Universal Soil Loss Equation (USLE) is often employed at the scale of individual fields, but basin-scale estimates are sometimes undertaken, where comparison with monitored

yield allows 'Sediment delivery ratios' to be calculated (Renfro, 1982). Geomorphologists are not over-enthusiastic about this 'lumped parameter' approach (Kirkby, 1980b), although it is still quite extensively used (Swanson, et al, 1982); Mitchell and Bubenzer, 1980).

The dynamics of landscape evolution require, it would seem, a more delicate tool with which to examine the relative importance of different slope erosion events, and channel events. As Dietrich, et al (1982) have emphasised "... The degree to which one process affects another, and the importance of a transport process to the sediment budget are both dependent on the magnitude and frequency of recurrence of the process at a place". The background of these ideas in geomorphic research was explored in Chapter 1, and it was pointed out there that a long-term record of discharges, in conjunction with sediment concentration data during these events, allows a comparison to be made of the relative role of large, infrequent events in comparison to common, low intensity events at a site (Piest, 1965). Other work has related the concept to specific within-net sediment flushing events (e.g. the work of Harvey, 1977; and the Dietrich paper cites others). Even so, the problems of within-net storage, although often described has not yet its own methodology. This Chapter proposes a method whereby sediment transfer mechanisms might be demonstrated using the event frequency data and the flow simulation models of the last two Chapters.

(i) The surface wash contribution : use of morphological indices

Considerable effort has been expended by geomorphologists in an attempt to couch both rainsplash and surface wash transport rates in terms of easily monitored morphological parameters, rather than in terms of hydraulic process (equations 5:1 to 5:4), and major contributions have been made by Zingg (1940); Horton (1945); Kirkby (1969); Kirkby and Kirkby (1974); and Schumm (1964). Most of this work evolves from or utilises experimental studies of soil or sediment erosion of both splash and wash on plot studies during actual events (Emmett, 1978), or artificial rainfall (Yair and Lavee, 1976; Bryan, 1974, Scoging, 1982) or using stakes and marker stones (Schumm, 1964; Campbell, 1974).

Regressions of field-monitored rates, TR, in Tonnes/metre width of slope/unit time, are usually undertaken against slope gradient (S) and distance from the divide, on the basis that the former influences velocity (equations 4:6 and 5:4) and the latter flow volume (Chapter 4). Carson and Kirkby (1972) and Thornes (1980) have summarised some of these experiments. Rain-splash net flux (volume/unit width/unit time) correlates with the sine (or sine^2) of the slope angle, the former relationships having an exponent varying from 0.75 to 1.0. Zingg (1940), using data from five Soil Conservation Service Experiment stations found that if the total sediment transport rate, TR, (wash + splash) were to be formulated generally as ;

$$TR \propto x^a S^b \qquad 5:7$$

where a and b are exponents

and TR, x and S are as previously defined,

then the data fit satisfactorily around a regression in which 'a' takes the value 1.6, and b = 1.4. Musgrave (1947) used USDA data and derived data for which a = 1.35 and b = 1.35. Kirkby (1969) found for a ploughed field in Maryland that a = 1.73 and b = 1.35. As a result of these investigations, it becomes clear that "... a reasonable uniformity ..." has been demonstrated which "... suggests that power laws of this sort provide suitable empirical models in the variation of surface wash with topography" (Kirkby, 1972). Since, in recent publications Kirkby (1980a) has taken to modelling surface wash processes in the general form ;

$$TR \propto x^{2.0} S^{1.0} \qquad 5:8$$

then this expression was adopted in the recognition of surface wash sources to the gully network at Alkali Creek. It has already been suggested that surface wash is but one possible source of sediment to channel flows, the others being sediment from piped sites, and bed scour and bank collapse. Such an expression will therefore identify merely the <u>relative</u> spatial difference which might exist annually from this one source. This is developed later.

(ii) Site yield calculations

Site yields can be calculated using data continuously collected at river sections. First, concentration data (if available) are plotted against discharge (Richards, 1982; Gregory and Walling, 1973) yielding best-fit regressions in the form ;

$$C = kQ^n \qquad 5:9$$

where K is an empirical constant,
n is the regression exponent,
Q is discharge,
and C is sediment concentration in mg/l.

To obtain a sediment discharge function, discharge is multiplied by its relevant concentration as predicted by the regression to obtain

$$CQ = kQ^{n+1} \qquad 5:10$$

The procedure may be then expanded to calculate sediment yield by using a simple programme to preduct CQ from Q and then integrating the CQ function. This method was utilised in the present investigation to calculate the sediment yield during individual events, although in most other studies a flow duration curve is linked to expression 5.10 (rather than the hydrograph itself).

(a) Applied to events of differing magnitudes and frequencies ; the approach to the present investigation.

Given that event frequency data are available, Wolman and Miller (1960) showed that the event producing the maximum sediment is the peak of the (frequency . CQ) distribution, and that if the distribution is unimodal, the event so identified may be referred to as the 'dominant event'. However, as considered in Chapter 1 and emphasised by Richards (1982) "... particularly in semi-arid environments, it is an over-simplification to assume that a single event can represent the range of morphologically significant discharges..." quite apart from the observation which is supported by the evidence of the last two Chapters that "... the importance of a given event or sequence of events in moulding the landscape will vary with the spatial distribution of the event...". (Wolman and Gerson, 1978). From the simulations presented in the last Chapter it is now clear that neither a flow duration curve approach nor a

frequency distribution obtained merely for a single output site would have allowed the functional aspects of the watershed to emerge; rather such information would have masked the spatial patterns of both events and in particular the way in which the relative importance of each of the two domains varies from the headwaters to basin mouth. In both the east and west forks of the headwater area and on the main channel there is now evidence that a bi-modal temporal pattern is likely to characterise the runoff, the existence of the second 'mode' in the distribution depending on the probability of a freak event (such as Run 10, described in Chapter 4) occurring during the time period under consideration. Additionally, the nature of this distribution is clearly dependent on the position that the site occupies in the network.

Consequently, it was considered preferable here not only to separate the summer events from the snowmelt events for a temporal comparison of the relative importance of site yields, but also to examine the spatial variations in site yield for specific events as well, allowing the complete dynamics of sediment movement to be considered. Sediment movement in the study area is clearly complex, and it may be possible to discover using this method whether, for instance, sediment is deposited on the main channel during the summer events as the peak size drops from point X down the main channel, and whether snowmelt operates as a flushing mechanism, as might be inferred so far.

In an attempt to substantiate these suggestions, it is argued that if simple temporal rating relationships, established for the field-monitored summer storm and snowmelt events, can be shown to be extrapolatable in the spatial domain across the watershed, then these can be then linked to the simulations presented in the last two Chapters to calculate site event yields. By weighting summer and winter events for frequency (Chapter 2), the relative 'importance' of the two process intensity domains can be assessed in a tangible way. This can be done not only on a temporal basis for each site (considering budgets both with and without the inclusion of a 'freak' event in the annual budget), but also in a spatial sense, allowing patterns of annual sediment transfer to be described forming a link to the morphological tests explored in Chapter 6.

(b) Problems of extrapolation of sediment rating relationships to describe sediment behaviour in watersheds.

Unfortunately, the constant and exponent in equation 5:9 are unreliable. Richards (1982) cites the work of Bogardi (1974), who apparently suggests that the regression coefficient increases with higher mean discharges and runoff per unit area, but decreases with increased catchment width and hydrological 'flashiness', the argument being that wider catchments present more opportunity for wash load deposition before runoff reaches the channel, and that in 'flashier' regimes relatively low discharges include higher proportions of sediment. Additionally, in areas with seasonal variations in sediment availability from slope sources, reservations have been expressed about the predicability of an annual curve. Meade (1978) found higher concentrations in the summer than in the cool season for similar discharges on the east coast of the United States. These results paralleled Walling's (1974) observations on Devon catchments, in which summer sediment concentrations for similar events were four times those for winter concentrations in identical storms, and of Gutierrez (1983) who demonstrated this phenomenon on a watershed in New Mexico.

Even within one event, rising and falling stage relationships may differ, most suspended sediment relationships demonstrating some sort of hysteresis (Richards, 1982). It may be that a 'supply-limited' condition either in the hillslope phase of runoff, or in the channel, reduces concentrations on either the rising limb (a lag relationship) or on the falling limb (a lead relationship). Whether the relationship is a lead or lag tends to be related to the nature of the sediment sources and their distance from the monitoring point. Richards (1982) explains "... If sediment supply is predominantly derived from bank erosion or immediate channel margins the rising water table introduces new sources of sediment which are exhausted by the time the flood recedes...", presumably causing a lead relationship.

Brice (1966) presents data for summer storm 'flash floods' in the Medicine Creek Basin in Nebraska. He found 'lead' relationships, and argued that variability in concentration and length of lead occurs because of a variety of supply states which vary from event

to event. However, Schick (1978) found lag relationships on Sinai sites in Israel, and suggested that supply was limited by tractive forces at early, low flows but later when these materials were in transport, they were deflocculated and stayed in suspension long after the flow peak had passed. Lag relationships may also reflect sediment transfer delays from a source a considerable distance from the monitoring point. Complicating the picture further, mass movements make more sediment readily available to the channel processes and such slumped material may take several erosion events to be removed in the river's sediment load, during which period the sediment relationships can be different in comparison to those before the event (Bello, 1978; Piest et al, 1975).

This overview of the literature suggests that in general, an event need not be 'supply-limited' in the hillslope phase to emerge non-saturated at the basin mouth if within net deposition (lodging) is occurring; similarly, an event which is 'supply-limited' in the hillslope phase may derive its load later from these same lodged deposits, or from the main channel banks, resulting in a wide range of 'lead' and 'lag' explanations. In general, since predictability in rating relationships, and other arguments developed later in this thesis, rely on the assumption that watershed materials are easily detached and transported during most normal watershed events, (the 'supply-limited' or 'transport-limited' argument discussed theoretically in Section A(i)), the next section considers potential sediment sources in these terms.

However, the level of generality introduced by extrapolation from temporal sediment rating relationships obtained during field-monitored events into the spatial domain can only eventually be explored from an examination of real data collected spatially as well as temporally. This is undertaken and discussed in Section III.

(II) SOURCES OF SEDIMENT

Sediment supply from surface wash, piping and bank collapse is reviewed here in terms of the erodibility of the source, and the mechanism, seasonality, and availability of these materials to channel processes. The aims are first to substantiate the

assumption in the last section that we are dealing here with a sensitive landscape, in which sediment is readily available for transport, and secondly to separate out the pattern of lateral (wash) sediment supply from those sources available in the channel (bank collapse and piping) for purposes of later discussion.

(A) Surface wash supply to channels during summer storms

Since rainfall intensity controls the detachment and transporting capacities of both storm rainfall and runoff, and overland flow and discharge largely control the transporting capacities of the storm rainfall and runoff (equations 5:1 to 5:4) it is clear that the temporal and spatial factors affecting overland flow generation which were reviewed in Chapter 4 also control the spatial pattern of surface wash sediment supply from slope to channel. Although this would imply that the preferable way to model this supply in the catchment would be to link these latter equations to the slope part of ROUTE.PAS, the overland flow model, the several problems reviewed in the previous sections (not to mention the problems of calibrating the parameters C_1 to C_4 in the detachment and transportation formulate) led to the conclusion that surface wash supply to the channel could not be estimated in any absolute way. As a result the simpler use of surrogate morphological indices to illustrate the relative spatial pattern of this supply would suffice.

(i) Sediment type and surface properties

Foster and Meyer (1975) have argued that detachment can be considered to be limited by sheer stresses on the eroding surface, and Evans (1980) has examined the criteria for erosion in terms of surface sediment properties. These stresses can be framed in terms of the size and the cohesion of the materials involved, so that in environments which possess particularly large-grained or granular materials, supply to channels is likely to be limited by the detachment capacities of rainfall and runoff. However, this type of supply-limited situation seems unlikely on the shale slopes in the study area because the materials are fine and dispersive (Chapter 2).

Although fine dispersive materials may often form slaked surfaces not conducive to further detachment, slope surfaces in the study

area show evidence at some sites of the sort of loosening and crumbing of the surface that Schumm (1964) noted on the Mancos Shales in Western Colorado. These saline shales are similar to those in the study area and were found by Schumm (1964) to be rapidly disaggregated by the growth of granular ice crystals in the late winter period. He argued that the crystals act as growth centres for needle ice and, in conjunction with the simultaneous drying of adjacent soil sites could cause massive loosening of the clay surface. These processes were considered sufficient to destroy small hillside rills on a seasonal basis, usually the late melt period. Seasonal destruction of similar features has been noted by Harvey (1984b) in the Howgill Fells, Cumbria.

Crumbed, loosened surfaces were linked more closely to high ESP values than to frost action by Hodges and Bryan (1982) in the badlands of Alberta, where sodium in the montmorillonite structure was considered a distinguishing factor. Hogg (1978) explained how these surfaces (which are often referred to as 'popcorn') retained high infiltration capacities throughout most of the moderate intensity events (rarely over 300 mm/hr) which characterised the area (Campbell, 1982; Gutierrez, 1983). These observations parallel those made earlier concerning processes on the Chadron units in South Dakota made by Schumm (1956a). Although in both of these latter investigations 'creep' mode of evolution was considered a possibility rather than surface wash on 'popcorn' surfaces, Hogg (1978) and Hodges and Bryan (1982) do not exclude the possibility of surface wash erosion, especially after prolonged rainfall. Hogg (1978) suggested that occasionally debris flows might occur. Despite observing 'popcorn' surfaces in the Mancos shale gully he investigated in 1982, however, Laronne felt that "... surface wash processes dominate the export of matter..." from his study area.

Although these surface types were noted in the study area in the late melt period on certain disaggregated sites on piping pedestals near to channel margins, they were not a regional characteristic of the slope surface. More common were widely-spaced, hexagonal cracks with a well-defined slaked surface, testifying to surface wash processes. Additionally, field observations during the monitored event revealed surface wash to be occurring early in the storm

especially away from the piped areas. Dispersion was almost immediate, and anastomosing overland flow rivulets were brown with sediment even near divides, some of which were left with the rill 'stringers' after the event as described by Hodges and Bryan (1982). These observations confirm the non-piped sites away from the channels to be a major source of surface wash sediment, and do not point to a supply-limited situation in these areas, rather the reverse.

(ii) Spatial variations in sediment removal rates downslope.

Kirkby (1980b) implied that rills are more important sediment sources than the inter-rill areas. However, most of the significant rills were mapped as part of the network in the present study, so that this sort of downslope variability is not considered relevant to wash estimation here. Nevertheless, other sources of spatial variability in the study area do present difficulties if equation 5:8 is to be adopted to estimate lateral wash contribution to watershed channels from slopes. It was observed for instance, that vegetation does affect runoff patterns and sediment behaviour downslope, and the observations made by Thornes (1980) were borne out in the field. Sagebrush and western wheat grass are more commonly located on the top of the sandstone outcrops which act as low-gradient benches running across the headwater slopes (Chapter 2), and the combined effect of the low gradients and the vegetation operate together here to delay the downslope progression of the sediment-rich flows. In some situations tributary rills become discontinuous downslope for this reason. During the smaller summer storm events it is even possible that local mid-slope deposition may occur, so that some sediment does not reach the channel at all. The roots of western wheat on the top of sandstone lenses were occasionally packed around with this locally deposited sediment, which on excavation was up to a few centimetres deep and laminated. This is more common on slopes with long basal concavities.

Although slope shape effects obviously cause localised slope sediment lodging, field investigation led to the conclusion that the headwater network is largely characterised by a slope and channel system with the "... high level of coupling..." (Thornes, 1980) which is usually associated with a fairly rapid and efficient

sediment transfer mechanism, and in subsequent discussions the hillslope lodging of sediment due to local gradient reductions on slopes will be assumed to be but a minor complication in the arguments later developed.

To avoid the overestimation of the proposed sediment transport index using equation 5:8 due to vegetation effects, however, calculations were only conducted for bare sites, and then only for bare sites which were connected continuously to channels. Thus, small patches of bare ground which met over 75% vegetation cover downslope were excluded from the calculations on the basis that the vegetation acts as a trap for these sources except possibly during the most extreme events. There was sufficient evidence in the undergrowth around oakbrush sites to justify this decision.

(iii) Contribution to channel flow

In this section, equation 5:8 is used to assess spatial differences in wash supply to the gully network. As Chapter 4 demonstrated, the percentage and actual value of the bare area in contributing units can be easily established with the aid of Figures 4 and 7. To relate the sediment transport rate, TR, (rate per unit of contour width over a specified time) to the contribution at the base of one side of a channel length increment, y, then TR must be multiplied by y and (assuming a near-rectangular contributing area), the slopelength, x, (equation 5:8) then becomes the mean slope length in the contributing unit over y. If these generalisations are accepted then the total area in the unit, At, is equal to (x.y). The reduction that the unit experiences because bare ground is less than total area is (Ab/At). Finally, therefore, if the overall relief of the contributing unit is h, then slope of the unit is S = (h/x), and equation 5:8 reduces to ;

$$TR_{tot} \propto x^2 . y . \frac{h}{x} \left(\frac{Ab}{At} \right)$$

which is ;

$$TR_{tot} \propto Abh \qquad 5:11$$

This value was calculated for both side slopes and totalled to give an index of the sediment transported annually into the channel increment by the mechanism of surface wash. These data have been included in Appendix 13. The size of the between-site increments calculated on this basis has been mapped across the network of Figure 47.

This Figure shows that the headwater areas experience much larger contributions from wash than is the case below 'X', and when viewed in conjunction with the downstream overland flow hydrographs, suggests that if sediment concentrations prove to increase as discharge increases down the network during the monitored field event, then the bed and banks of the main channel might be providing considerable sediment to the watershed summer storm events on the main channel on the rising limb. The potential offered by the piped sites and the channel bed and banks are explored below.

(B) Piping: sediment production and channel supply to summer and winter events

(i) Piping-prone materials and hydraulic prerequisites.

High ESPs (Lee, 1968; Heede, 1971) are usually a preprequisite for pipe development. In the study area, Heede (1971) found that all ESP values for non-piped gully side slopes were less than 1.0, whereas those with pipes averaged 12.0 (Chapter 2). High ESP value occurred in patches in the headwaters, and on some sites in valley alluvium (Heede, 1971). However, other clay characterisits (for instance the presence of montmorillonite and a steep hydraulic gradient, resulting in a high rate of pore-water movement) are additional locating influences, and "... one of these conditions, if well-developed, may offset the lack of another..." (Thornes, 1980). Harvey (1982) found that the orientation and nature of tension cracks tended to be correlated with pipe orientation and size, and Slaymaker (1982) found that the vertical variations in the hydraulic conductivities of the varves in his study area in Penticton, B.C. encouraged lateral seepage over relatively impermeable layers, focussing the location of gradient pipes. Gutierrez (1983) found piping to be encouraged beneath the more permeable sandstone units.

Figure 47 : Sediment sources for channel flow in the study area

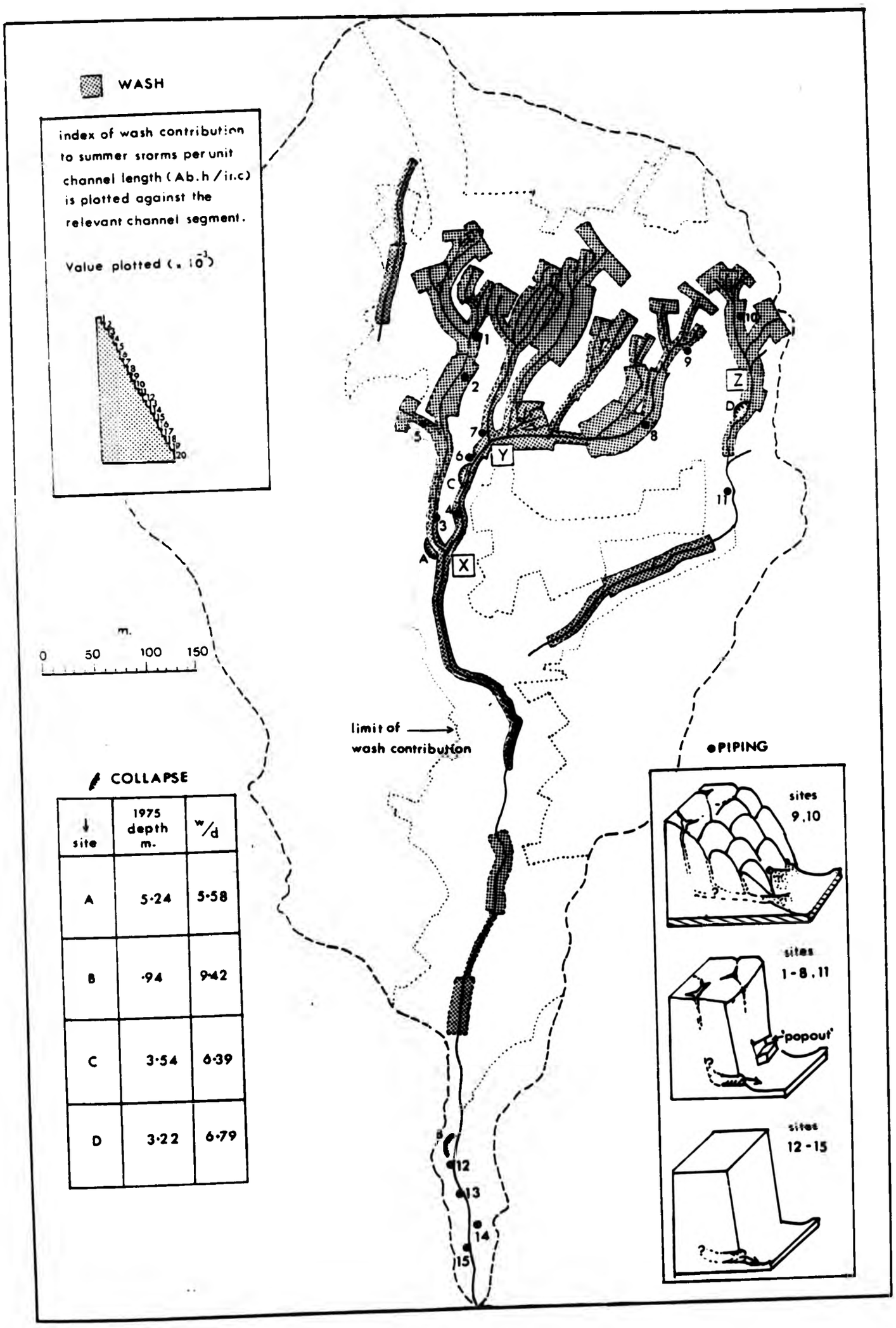

site	1975 depth m.	w/d
A	5·24	5·58
B	·94	9·42
C	3·54	6·39
D	3·22	6·79

(ii) Location and topographic expression

Combinations of these suitable locating factors are likely to be found most commonly on gully banks which are often the wettest sites and provide the necessary hydraulic outfall possibilities. Infiltrating water rapidly deflocculates and entrains clay particles along these focal planes which then rapidly enlarge into circular pipes.

Heede (1971) has documented the pipes in the study area extensively, although some of the main pipes he surveyed are outside the study basin, and others could not be found ten years after his original survey, having been replaced by new features. From Heede's (1971) study and from field observation, the most important locating factor on the study area is the gully bank, although not all gully banks were piped. Heede (1971) found that many pipes had an 'L' shape cross-section, with a vertical section which connected on the surface to a 'sink'. These sinks may originate around tension or desiccation cracks, which may be enlarged by frost action. At a suitable permeable horizon and with a suitable hydraulic gradient, the direction of pore water movement and, therefore, of pipe development changes from vertical to horizontal. Most simple pipes in the study area have this form.

The headwaters of the large discontinuous gully demonstrated by far the largest pipe complex on the watershed (Photos 8 and 20), but bank sites both above and below this location were pipe-free, indicating that local lithological variations are also of prime importance. The site shown on Photo 20 is just below one of the sandstone benches that run across the headwater area, and so the sort of effect noted by Gutierrez and mentioned above may well be operative here. The pipes here are complex, extend back into the gully bank several metres, and appear to have degenerated into an 'eggbox' type of topography. They do not appear to be very active currently, however, and much fresher but smaller features were found elsewhere. Heede (1971) described a process where pipes effectively 'burn themselves out' and this may be the case at this site.

Photo 20 : The extent of the degenerate piping complex located beneath a sandstone lens in the headwaters of the large discontinuous tributary (a close-up of this site is shown on Photo 8)

Photo 20 : The extent of the degenerate piping complex located beneath a sandstone lens in the headwaters of the large discontinuous tributary (a close-up of this site is shown on Photo 8)

Photo 20 : The extent of the degenerate piping complex located beneath a sandstone lens in the headwaters of the large discontinuous tributary (a close-up of this site is shown on Photo 8)

Fifteen separate pipes were mapped in the study area in 1980 (Figure 47). They can be loosely placed into three categories. First, the 'egg-box' gully complex type which are limited to sites below the sandstone benches, and appear degenerate (Photo 20). Second, small active pipes in the headwater areas, often adjacent to moderately fresh-looking channel headcuts and located always in a gully wall. Finally small pipe outlets only, which were found mostly on east-facing banks near to the basin mouth and in the valley alluvium.

(iii) Pipes in sediment production

The necessary hydraulic conditions are encouraged not only by topographic convexity of the channel bank, but by the propensity of the lower slope sites to be wetter during snowmelt than upslope sites. Several investigations have hypothesised that snowmelt is a suitable time for pipe enlargement, rather than the summer months when slope-base saturation is unlikely to be prolonged if it ever does occur. Thornes (1980) suggests that "... the high moisture levels required are probably produced by prolonged infiltration or saturated conditions due to snowmelt rather than a sudden incidence of large amounts of precipitation". Pipeflow was observed during the snowmelt fieldwork period, although the pattern of active pipes shifted during melt. In April, pipes 3, 4, 7 and 11 carried flow during early melt, whereas pipes 12, 13, 14, and 15 carried a considerable flow in the later melt period. This is in contrast to pipe complexes 1, 2, 5, 8, and 9 which are volumetrically smaller than the main complex 10, but which carried no flow at any time during fieldwork. The headwater pipes carried a small amount of flow in late April only.

The pipeflows are sediment rich and appear to be rapidly flushing snowmelt subsurface water. Although piping is clearly a major source of sediment at particular active sites on the watershed, therefore, and at differing times during the melt period, they are localised, and, therefore, not considered here to be a major source of sediment to channel flows. However, pipes may be important secondarily, since piped sites are more vulnerable due to the lowering of shear strength of bank materials, and loss of support. As a mechanical process, however, the collapse of sites weakened by piping is no different from the collapse of other materials.

(C) Bank collapse

Apart from the first order channels in the headwater areas, the data presented in Chapter 2 show that both the discontinuous gully, and the continuous network are currently well-excavated. Although progressive bed scour is certainly likely to entrain fine sediments by normal tractive processes, the banks supply sediment more extensively when collapse occurs and the disintegrating blocks become readily available for entrainment. Bradford and Piest (1980) consider this to be a major gully process, and have described such an event to be an 'erosion threshold'. Certainly, when such events occur, there is a sudden and irreversible change in channel morphology, and sediment regime changes, although sediment effects are transient when viewed at the scale addressed here.

(i) Spatial controls

In a study of the erosional development of valley-bottom gullies cut into loessic materials in Nebraska, Bradford and Piest (1980) found that failures of the gully banks were of three types; deepseated circular failures, slab failures, and basal collapse failures. Only the last type are found in the study area. These include sites where a vertical column of bed material appears to have 'popped out' and this loss of base support caused slumping of the overlying material (Photo 5.). These 'pop outs' appear to be connected to the tension-cracking of columnar-structured valley-bottom alluvium in the study area; Heede (1977) noted that these features provide a suitable outfall site for pipe development. Piping will further reduce shear strength locally; consequently, the collapse of the valley-bottom alluvium is strongly indicated.

Other factors play a more crucial role. Waterlogged sites are far more prone to failure for many obvious reasons (Carson and Kirkby, 1972), and Brice (1966), Mosley (1972), Harvey (1984b), and Patton and Schumm (1981) all support the Bradford and Piest (1980) view that snowmelt is an important cause of bank collapse because slope base saturation is likely to be prolonged at this time of the year. Additionally, the incised depth of the gully is important. High banks are more likely to fail on undercutting because here downslope gravitational stresses are proportionately more destabilising,

although this is rather dependent on the orientation of potential shear surfaces to the bank. It is also useful to note that the failure of a long, high bank will contribute more sediment to the channel than the failure of a low bank with a similarly disposed shear plane.

With efficient removal of collapse material, the larger the gully form, the more collapse will occur; although Andrews (1982) felt the gully width-to-depth (w/d) ratio gradually becomes important in gully stabilisation. He concluded that the lowest w/d ratios were the most likely to fail, and thereby suggested that progressive stabilisation might be indicated by a progressive increase in w/d ratios through time.

In conclusion, high, steep piping-prone gully banks on the valley alluvium are more likely candidates for collapse then shallow wide non-piping gully banks on the Wasatch shales. These observations were borne out by the field survey. On Figure 47, collapse site locations are indicated both prior to and following the snowmelt field season. Their (w/d) ratios and depths are also noted for interest.

(ii) Location and timing of collapse events in the study area

In 1980, bank collapse deposits were noted in two main locations, both on the main channel. Recent, fresh debris was noted at the base of site 'A', but the second failure was apparently older and the debris at the base of the failure surface had been removed (site 'B'). In 1981, following the monitored field period, two fresh but fairly small slumped blocks were noted. One (site 'C') was between sites X and Y (Figure 47, and Photo 21), and the second was on the large discontinuous tributary (site 'D'), immediately below a trenched section on the headwater system. Both demonstrated a shear plane which was almost vertical, indicating that the columnar nature of these materials provides the necessary failure surfaces. In fact all failures were additionally associated with trenched sites on the gully beds, where the excavated form of the gully has a particularly high depth and low (w/d) ratio. (Figure 47). The older of the failure features mapped in 1980 (site 'B') showed signs nearby of other earlier bank collapse, and since these sites were on the west

Photo 21 : Fresh slumped material located between sites 'X' and 'Y' on the continuous network. The survey pin on the slumped material gives an indication of scale.

The photgraph was taken following the melt survey on April 30th, 1981

Photo 21 : Fresh slumped material located between sites 'X' and 'Y' on the continuous network. The survey pin on the slumped material gives an indication of scale.

The photgraph was taken following the melt survey on April 30th, 1981

Photo 21 : Fresh slumped material located between sites 'X' and 'Y' on the continuous network. The survey pin on the slumped material gives an indication of scale.

The photgraph was taken following the melt survey on April 30th, 1981

bank of the main channel in all cases might indicate that long-term wetting during the prolonged melt period on this side of the channel during May might be important here.

The lack of currently visible headwater collapse sites in the piped headwaters is explained by the small gully depths there, although on some sites piping has flared the channel banks back into a less precipitous form in any case. More significantly, it is probable that the main channel alluvium maintains high pore-water pressures more frequently and for longer periods during melt than is the case in these headwater areas. All these factors combine to make the channel below Y, and the discontinuous gully below Z, more likely to supply sediment from bank collapse than the headwater areas. The lack of notable vegetation on the excavated gully banks around X, Y and Z suggests that these sites are affected on a longer-term basis.

(D) Sediment availability from these three sources in relation to sediment entrainment by channel flow.

In environments where sediment availability is limited by the rate at which bedrock is weathered, the length of time for weathering between significant erosive events as well as the weathering rate itself become important criteria in the prediction of removal rates (Kirkby, 1972). It has been suggested that whilst weathering is limited, a series of closely-spaced events may exhaust sediment supply (Harvey, 1977, 1984b) leading to rating relationships with poor inter-event reliability and possibly hysteresis, particularly towards the end of the event sequence. However, the discussion above suggests that exhaustion is unlikely to be a common feature of summer storm sediment behaviour at Alkali Creek, because even the unweathered shale is erodible, and the main channel alluvium has poor cohesion and is generally available for removal from both bed and banks not only because of bank collapse and piping, but as an in-situ source. Easily erodible sediment should therefore be available for all runoff events.

During summer storms, sediment detachment (controlled by rainfall intensity) limits sediment entrainment in the early stages of the event (equations 5:1 and 5:3) but once runoff commences, removal must be eventually limited by the transport capacity of the flow

(equations 5:2 and 5:4). In a situation where supply is unlimited, similar intensity events might therefore be assumed to generate flows with similar sediment concentration/discharge relationships both within and between events. If sediment size is large or cohesion great, Evans (1982) suggests that there may be a threshold intensity below which sediments are not detached, leading to a situation where the C/Q function established above this threshold is inapplicable below it. However, this seems unlikely to be the case with the fine-grained, dispersive clays in the study area; in fact it was shown previously that an event of not exceptionally high intensity detached and entrained sediment readily.

During snowmelt, sediment is likely to be readily available both from piping and from bank collapse. Piest et al (1975) suggest that there are two separate stages in the sediment entrainment of collapse sediment. First, bank collapse material at the slope base from the last failure is removed, and renewed scour occurs. This is associated with the rising limb. Second, fresh collapse occurs at the event peak, supplying sediment to flows on the falling limb. Depending on event size, this material may or may not be completely reworked, so that some material may be left for subsequent events. When discharge peaks diurnally, as during melt, these observations suggest that each day offers potential for scour and flushing. The strong hysteresis that they found on collapse rating curves was clearly because in their case sediment supply was limited outside the collapse event, which is not the case here. Collapse actually occurred during the sampled event in the study area, and so these observations can be tested later.

All these observations suggest we are dealing here with a landscape of high sensitivity, so that prior to the fieldwork season there was little reason to believe that discharge would not set the limit on sediment concentration since sediment appeared readily available to all watershed processes, and no transport threshold exists between the smaller and larger events because of the fine-grained dispersive watershed materials. However, the discussions do not rule out these possibilities, especially bearing in mind the work of others (Section IB(ii)b). Consequently, relationships were established both for summer storms and for diurnal snowmelt variations, partly to test these points, but with the main objective of site sediment yield estimation during the simulated annual runoff pattern.

(III) SUSPENDED SEDIMENT RATING RELATIONSHIPS DURING FIELD-MONITORED EVENTS

Sediment relationships were established for both the field-monitored summer storm event, and during diurnal discharge changes in the early and late melt season. Sampling locations were the same as those for discharge (Chapter 3, Chapter 4, and for locations, Figure 7). Because both temporal and spatial discharge and concentration data were therefore available, sediment rating relationships for both processes in space and in time could be constructed using equation 5:9.

(A) Methods

Since suspended sediment is non-uniformly distributed with width and depth across the channel (Richards, 1982), both vertical and transverse integration were necessary during site sample collection. The usual type of depth integrating sampler was constructed at P.N.L. (Photo 22), the design being based on guidelines supplied by the U.S.D.A. for the construction of their USDH-48 model shown in Richards (1982). All samplers of this type fail to sample close to the bed where concentrations are the highest, and despite being streamlined to minimised turbulence the larger design necessary for the accommodation of the 1000ml. bottle does tend to distort the flow if depth is less than 0.5m. Chien (1952) suggests that the first source of error is minimised for fine sediments or turbulent conditions since in these situations the theoretical suspended sediment distribution with depth is more likely to be uniform and therefore the unsampled proportion is a lower percentage of the total load. This is truer for deep channels than for shallow channels, though, and may be the cause of some errors in the present study. Flow distortion was a real problem on the lower discharges sampled, and so in all cases attempts were made to choose the local site with greatest depth to minimise this error.

The sample bottle was changed at every station and the bottles were carried out of the field the same day. The local SCS office offered the opportunity for the vacuum filtration of the 1000ml samples through a fine-grained, pre-weighed filter, and for the oven drying of the filter plus sediment at 80°C. The suspended sediment

Photo 22 : The P.N.L sediment sampler, designed to U.S.D.H.-48 design specifications

Photo 22 : The P.N.L sediment sampler, designed to U.S.D.H.-48 design specifications

Photo 22 : The P.N.L sediment sampler, designed to U.S.D.H.-48 design specifications

concentration was then calculated as the sediment weight divided by the filtrate volume, giving a value in mg/litre. This is equivalent to p.p.m. for concentrations up to 7000mg/l (Richards, 1982), and most of the samples taken were below this value. The resulting data are included in Appendix 7 next to discharges obtained during melt, and in Appendix 10 next to the summer event discharge data. Figure 48 shows the rating curves for both of the diurnal surveys (April 5th and April 18th, 1981) at site 1. Figure 49 shows the pattern of concentrations collected spatially during snowmelt on April 7th and 19th, 1981, with network linkage inferred. Similarly, Figure 50 shows the rating relationship during the sampled summer storm event on June 4th, 1981, established for temporal changes in discharge at site 1. Collection started 30 minutes after the storm had commenced since the spatial survey was undertaken first. As for discharge measurements, a sample was taken thereafter at 5 minute intervals until runoff had ceased. Figure 51 shows the spatial data collected during this event, and as for the snowmelt spatial data, network linkage has been inferred. This plot represents a variety of different times during the event (Appendix 10). Additionally, all the snowmelt data (both the spatial and the temporal data) have been regressed together, and all the summer event data have been combined in the same way. All regression statistics are in Appendix 12. In a final test, all the concentration and discharge data (all events, spatial and temporal) have been regressed together in a combined regression.

Although all the regressions are significant, the established relationships generalise a scatter which is interesting in itself, and which is therefore examined with several objectives in mind. First, the temporal relationships are explored for hysteresis. Secondly, spatial data for both melt and summer storms are explored from site to site to establish the extent to which within-net variations were occurring, and to contrast summer storm runoff events and snowmelt in this respect. Thirdly, since some doubt was cast on the extent to which temporal relationships might be used for spatial extrapolation, the temporal and spatial relationships and their attendant scatter were compared and then data regressed together as explained above with this consideration in mind. Finally, since the summer event regression might indicate a 'supply-limited' condition on the watershed the influence of varying regression constants and exponents is explored.

(B) Snowmelt relationships

(i) Temporal : Figure 48

The strength of diurnal snowmelt sediment concentration/discharge relationships on both sample dates (taking all points as a single data set) strongly confirms that discharge exerts a major control on suspended sediment concentrations at the basin output point over the two sample melt days. The best-fit line is just more than a linear relationship, as demonstrated by the exponent of 1.17. In a discussion of the values generally taken by the exponent in the concentration/discharge regression, Gregory and Walling (1973) conclude that "... it may be that the concentration exponent generally lies between 1.0 and 2.0...", although elsewhere values nearer to 1.0 than 2.0 appear to be the norm (Leopold and Maddock, 1953). Others have found lower values; for data collected during runoff events in the Iowan gullies described by Piest, et al (1975), the concentration exponent was between 0.4 and 0.5. However, their relationships demonstrate bank collapse hysteresis and show quite a large amount of scatter.

Point suspended sediment concentration data collected by Heede (1977) on three snowmelt days, one in 1964, one in 1975, and one in 1976 have been plotted on Figure 48 on the same axes. These data have not been included in the calculations, since it was unclear whether or nor the sample site was exactly the same as that used in the present study. Heede's 'main gully' is outside the study area, but 'gully No. 3' is in fact the study basin used here (pers. comm 1974). Only this 'gully No. 3' data have been plotted, most of which fall within the general range predicted by the regression equation. However, Heede's concentration value of 35,000 ppm on one day in 1964 is over three times the value predicted by the fieldwork period regression line (10,264 ppm at 0.2 m^3/s) suggesting that his data would fit a regression relationship with a higher exponent. Heede (1977) accredits the proportionately lower concentrations in 1975 and 1976 to the efficacy of the sediment dams located on the lower part of the main channel in the study area between 1964 and 1975 (Chapter 2). This reason for the high 1964 concentration data cannot be ruled out; in fact, some deposition on the main channel might be occurring because of these dams, possibly modifying the regression relationship.

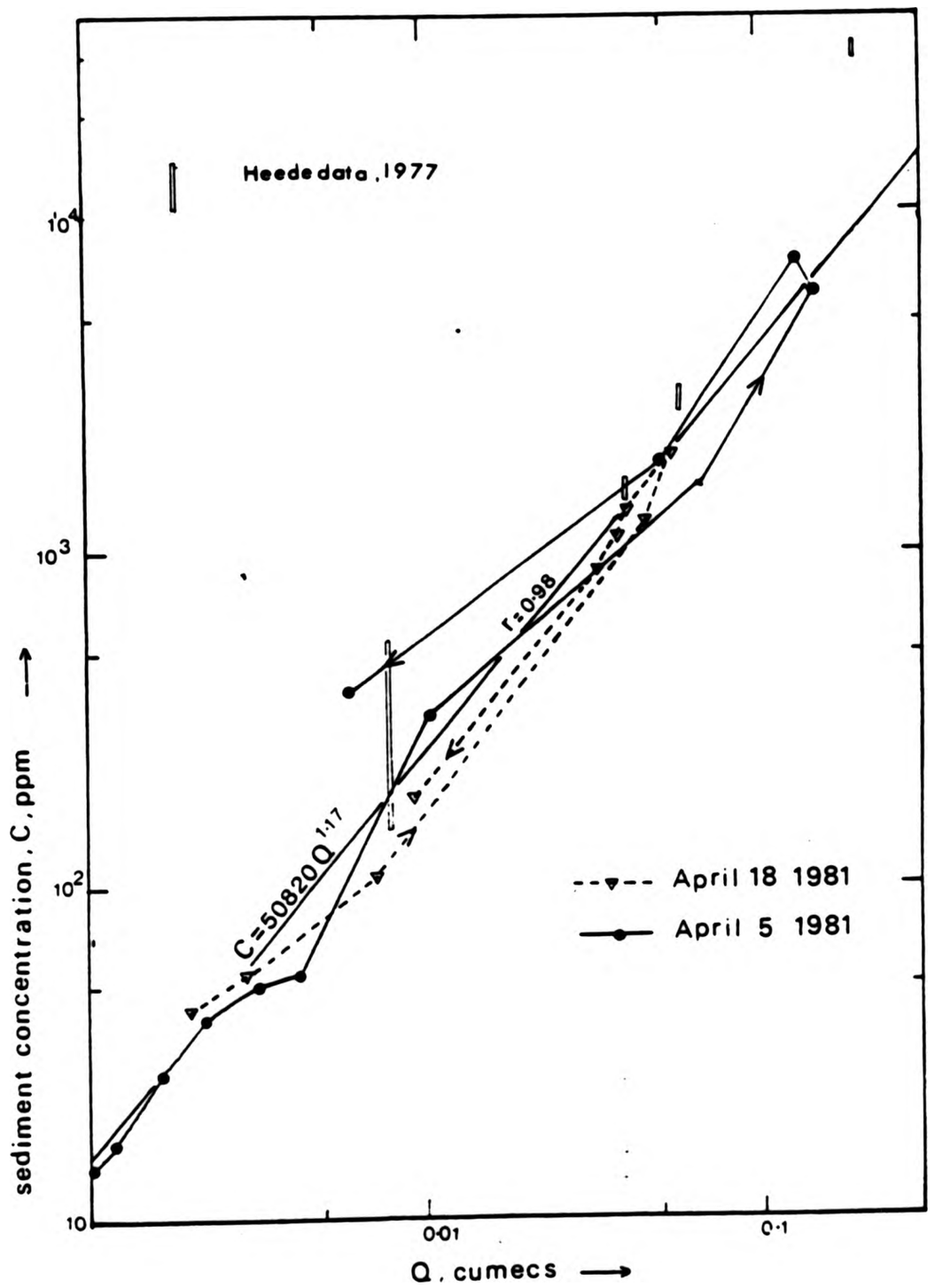

Figure 48 : Diurnal suspended sediment rating relationships during snowmelt; April 5th and April 18th, 1981

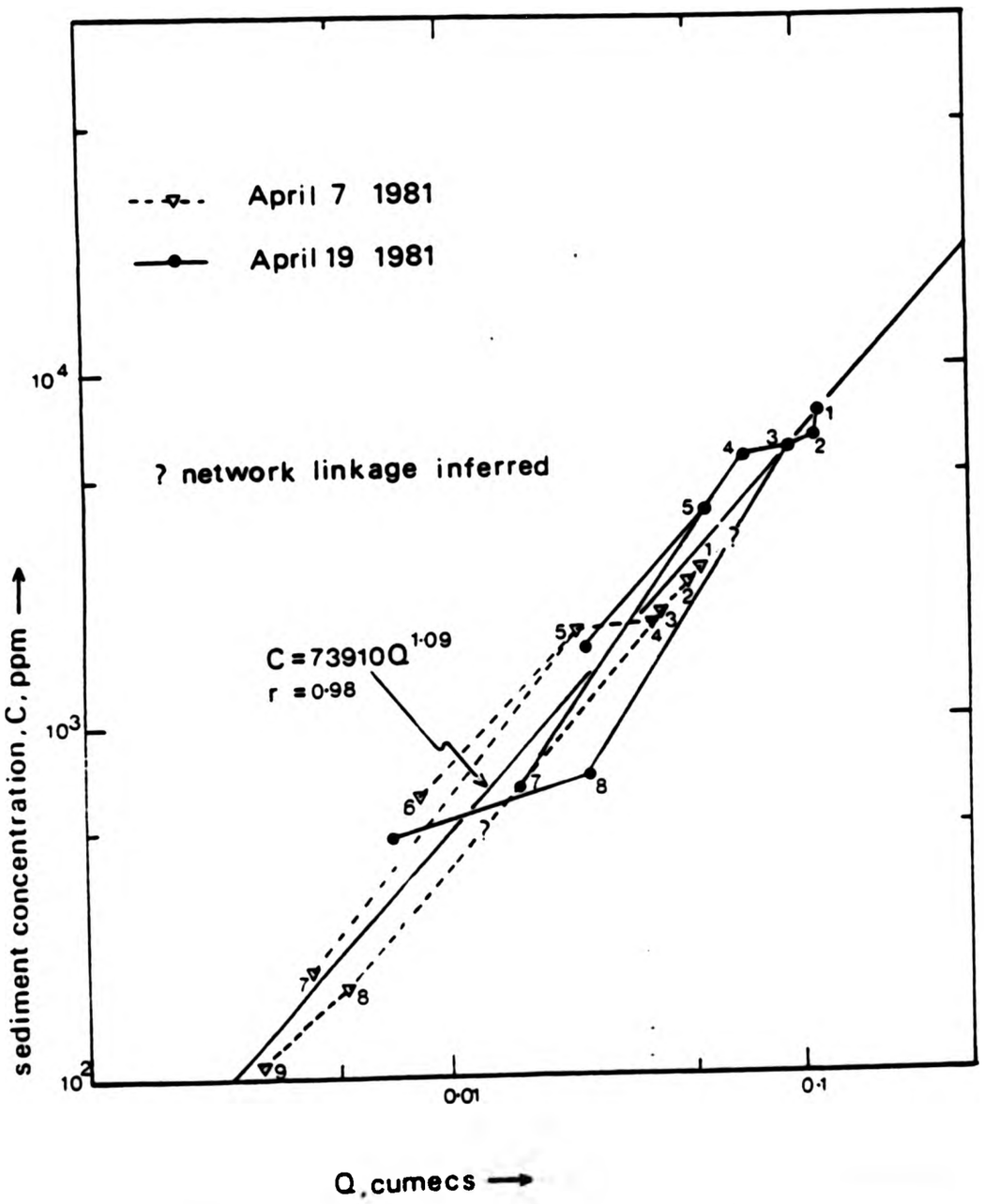

Figure 49 : Spatial suspended sediment relationships during snowmelt, April 7th and April 19th, 1981

The hysteresis demonstrated by both diurnal plots is slight, but on April 18th demonstrates a 'lag' effect, with rising limb concentrations lower than the falling limb. In Section C(ii), two bank collapse episodes were described. These occurred on April 18th, the first between sites X and Y on the main channel, the other on the large discontinuous tributary. The former event may have been the cause of the increased sediment to the channel on the falling limb, resulting in sediment 'pulse' on the event recession in a manner similar to that described by Piest, et al, (1975), but it is also clear that the effect of this process is minor, and that the rating relationships are in general a very good fit (r = 0.98).

(ii) Spatial : Figure 49

Sediment concentrations were sampled spatially across the watershed during melt on two dates; April 7th and April 19th, 1981. Timing the survey to occur between 2 and 3 p.m. (the peak time for diurnal flow) allowed a comparison to be made between the temporal relationship discussed above, and the variations in concentration resulting from an increase in discharge downstream. As in the case of the temporal data, the data fit well around the regression line shown when both data sets are viewed together, confirming that spatially as well as temporally suspended sediment concentration is controlled largely by discharge increases.

The best-fit regression equation differs slightly in exponent (1.09 as compared to 1.17) from that of the temporal relationship. The scatter of points for April 7th reveals that the reason for this difference is the relatively higher concentrations for a given discharge on sites 6, 7 and 5 (which represent the west fork, the east fork, and site 'X') than would be expected given the main channel sites 4, 3, 2 and 1. It is noted here that site 1 on the spatial survey on April 7th might be expected to have the same concentration and discharge values as for the temporal plot at peak, and this assumption is supported by the data. Similarly, on April 19th, sites 6, 7, 5, and 4 have higher concentrations than would be expected bearing in mind the position of the data points for sites 3, 2, and 1, adding to the effect already described. The higher upstream values have the overall effect of lowering the regression exponent.

Two observations can be made from this. First, on the deeply excavated sites near 6, 7, and including site 5, the rate of increase in sediment concentration is higher than apparently is the case on the main channel. On April 7th it could be argued that this represents a relative dilution of flows on the main channel, presumably by meltwater from the channel margins, and a relative lack of readily available sediment from bed scour and bank collapse on this day below site 5. A second possible explanation is that sediment is being deposited on the low angle fill behind Heede's check dams. On April 19th, however, which is the day following the minor collapse episode between site 'Y' and 'X' (site 5), sediment concentration remained relatively high right down to site 4 on the main channel, and on this day the rate of sediment concentration increase only dropped towards sites 3, 2, and 1.

These data represent such a small sample that it is dangerous to draw too many inferences, but it could be argued that availability of sediment from the bank collapse episode just above site 5 on April 18th may explain the different rate of concentration increase between sites 5 and 4 on the two sample days. Speculating further from this, it is interesting to consider whether the temporal regression would parallel the spatial regression more closely if sediment (such as supplied by the April 18th collapse event) were readily available not only between sites 4 and 5 but all the way down the main channel. The data presented would imply that this is the case. Supporting this conjecture is the observation that such conditions would result in a rating curve with a higher exponent, one that might more readily embrace Heede's 1964 values. In 1964, prior to check dam emplacement, Heede (pers. comm. 1974) states that the entire banks of the main gully channel on the gully below 'X' were unstable, further substantiating these conjectures.

(iii) All snowmelt data

Whatever the reason for the relatively minor variations around the regression lines, they are encouragingly similar, and it is possible to conclude that the temporal melt regression could have been used to predict the spatial relationships fairly well. This allows the amalgamation of the two data sets with a view towards producing a general predictive relationship. Using all spatial and temporal data together, they fit well around the expression ;

$$C = 80930Q^{1.21} \qquad 5:12$$

with a correlation coefficient r = 0.97 significant at the 0.5% level (n = 41, Appendix 12). This equation is used to link the melt flow simulation data to CQ (sediment discharge) from here onward, given that ;

$$CQ = 80930Q^{2.21} \qquad 5:13$$

(c) Summer storm relationships

In general the sediment rating relationships during the field-monitored event on June 4th, 1981 were established with considerably less confidence than was the case with snowmelt. This was partly due to the short-lived nature of the storm (Chapter 4), and the necessary difference in sampling time for each spatial data point, simultaneous sampling during the event being an obvious impossibility. Quite a wide scatter of points results, suggesting that the regression equations need cautious examination.

(i) Temporal : Figure 50

From 30 minutes into the monitored event on June 4th, 1981, and every 5 minutes thereafter, both discharge and sediment concentration were sampled at site 1, and the resulting data are plotted on Figure 50. Clearly, the good correlation between the parameters (r = 0.95) is largely dependent on the 60-minute data point, and otherwise the data are rather bunched together. When joined together into a time sequence, they show a fairly rapid increase in sediment concentration with discharge up to the event peak. For reasons outlined in Chapter 4, some doubt might be cast on the discharge value calculated for this point which represents conditions 40 minutes into the event; and without this data point the local values of sediment concentration rise in a simpler sequence. After the peak has passed, however, sediment concentrations remain high as discharge drops, giving a fairly strong lag hysteresis to the relationship.

All these sediment concentrations are fairly low in comparison with those collected during snowmelt; for example a discharge of 0.15

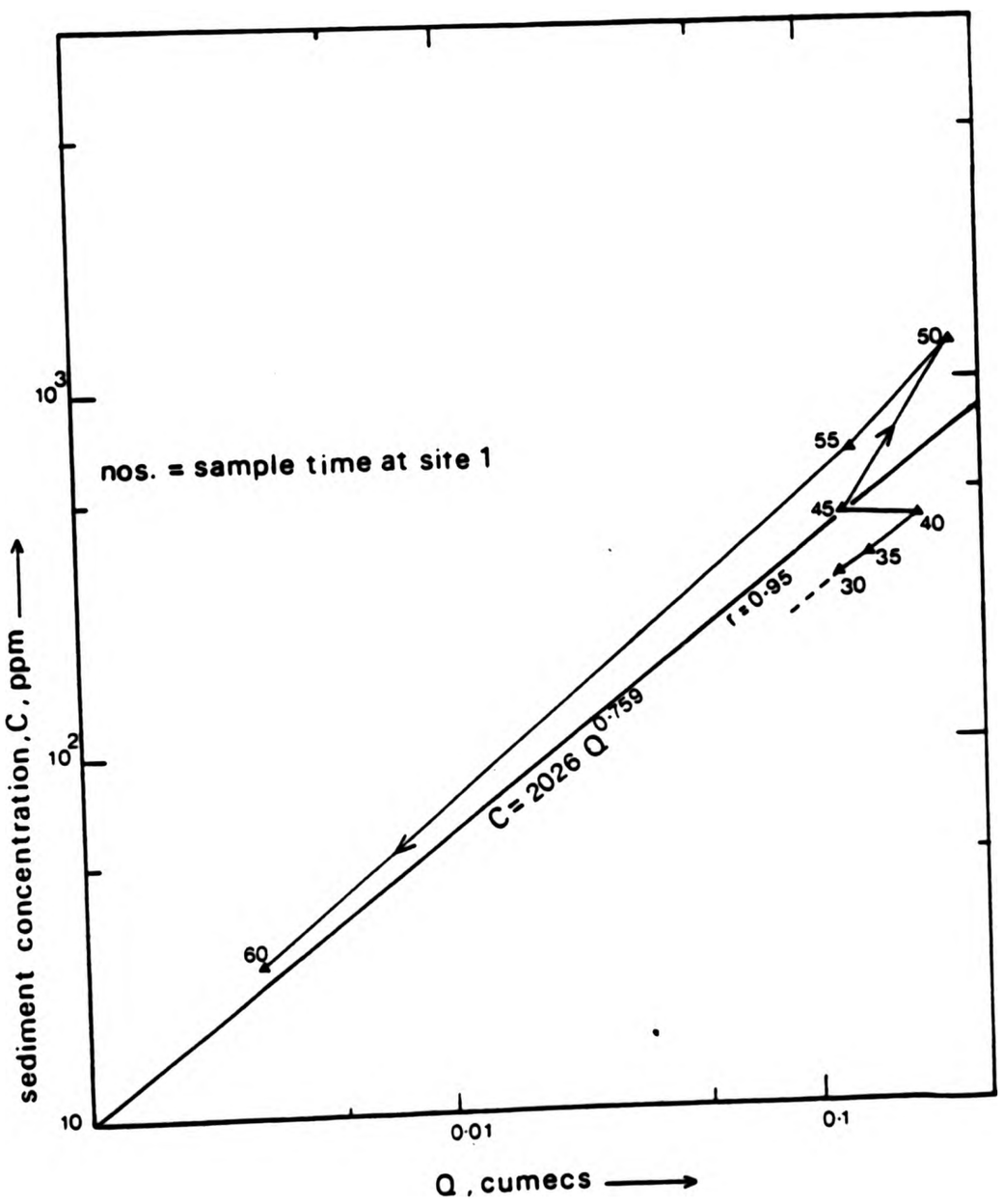

Figure 50 : Temporal summer event suspended sediment rating relationship during field-monitored event on June 4th, 1981

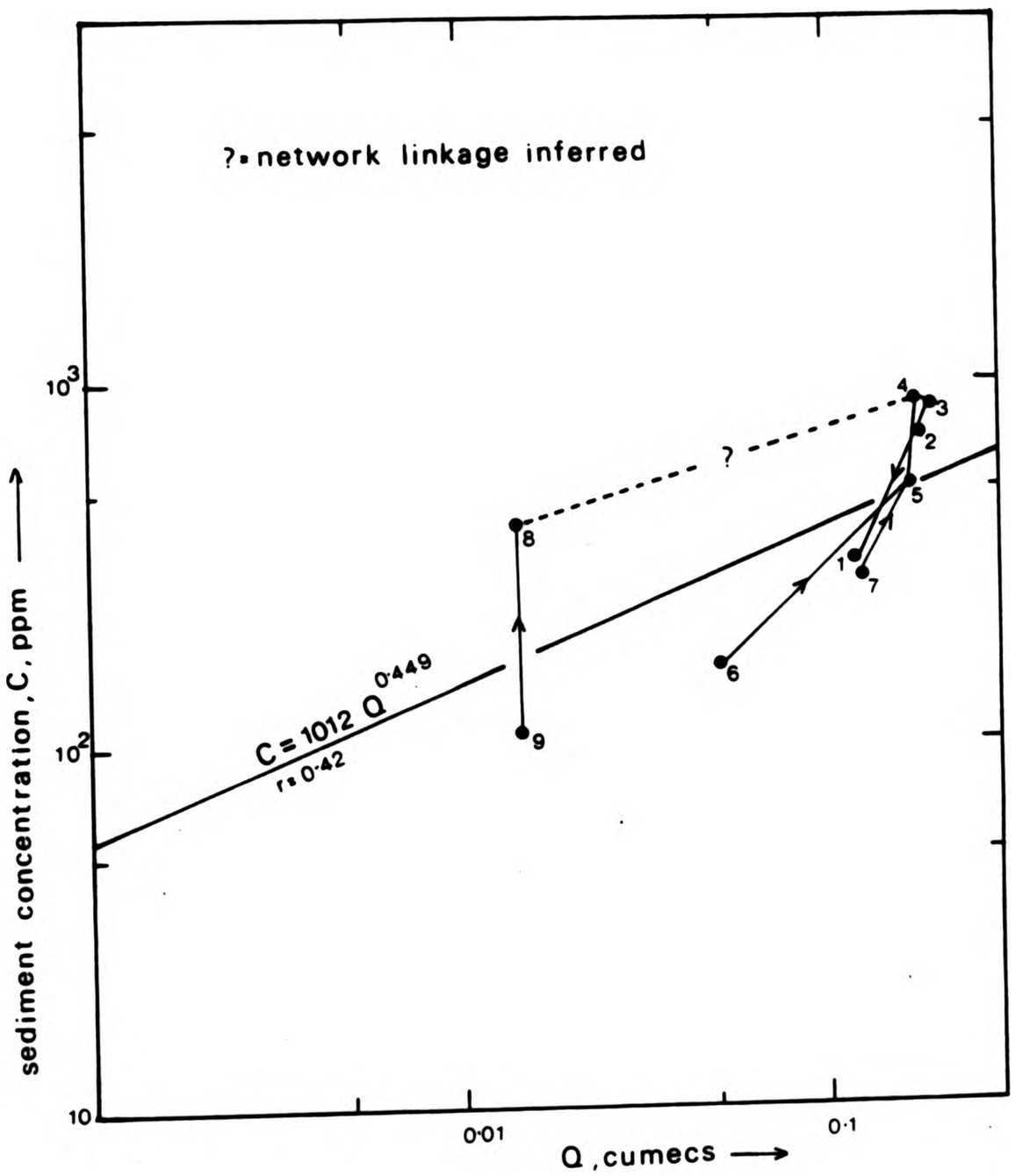

Figure 51 : Spatial summer event suspended sediment rating relationship , data collected during the field-monitored storm on June 4th, 1981

cumecs having a sediment concentration approximately ten times less than for the same discharge during snowmelt. The considerable difference between the summer and winter relationship, in addition to the hysteresis, suggests that there may be some difference in sediment availability between the winter and summer events despite initial suggestions to the contrary. Indeed, the hysteresis may imply that sediment availability on the main channel is restricted so that only during the event recession do the erodible hillslope wash sources register at the basin mouth. Alternatively, the pattern shown on Figure 50 may be the result of sediment deposition on the low gradient main channel above the sample site. In the lower part of the main channel, discharge decreases downstream generally throughout the event, and velocity may be decreasing at a rate which exceeds the rate of discharge reduction. This could arguably cause deposition prior to the event reaching the basin mouth. This process may be encouraged by the low gradient fill behind Heede's checkdams for reasons considered above.

These points might have been clarified had full simultaneous spatial data collection been possible. However, it was possible only to sample at staggered time intervals, so the interpretation of these data is limited.

(ii) Spatial : Figure 51

Taking the anomalous data point first, it can be seen that site 8, on the large discontinuous tributary had a very high concentration when sampled early in the storm. The headwater site 9, on the same tributary had a similar discharge but was carrying sediment at much lower concentrations when sampled 5 minutes later. Site 8 is just above the alluvial fan and field observations revealed that flow was infiltrating into the fan surface and material was being actively deposited whilst sampling was being undertaken. The high value therefore represents a situation immediately prior to deposition, and can be considered anomalous.

The remaining data represent a variety of sample times during the monitored event at sites 1 to 7, and all tend to bunch together in the same manner as was apparent in the temporal rating relationship (Figure 50). The peak passed sites 3 and 4 at the same time as the

survey did, and the spatially 'rising stage' discharge data (sites 6, 7, 5, and 4), although representing sampling intervals of 5 minute separation, do show a tendency for concentration and discharge to increase in harness. As discharge drops spatially (sites 3, 2, and 1), the concentration data again fall in the prescribed manner. As a result, the regression equation on Figure 51, with its weak correlation (0.42) and lower exponent than the temporal data (0.45 compared to 0.76) may be considered of rather limited value, since based on the inclusion of the anomalous point 8, and the dissociated point 9. However, if sites 1-7 are viewed with the temporal data collected at a point on that same network, then the relationship is strengthened.

(iii) All summer storm data

(a) The problem of relating temporal to spatial data

Bearing in mind the few data points, the weak nature of the correlations, and the possibility that the event was supply-limited, extrapolation beyond this event must be undertaken with considerable reservation. If sites 8 and 9 are excluded from the combined regression analyses, the temporal relationship becomes stronger, and the spread is improved. The combined relationship is ;

$$C = 2130\ Q^{0.76} \qquad 5:14$$

for which r = 0.93, and which is significant at the 1% level (n = 13, Appendix 12). Linking to sediment discharge gives ;

$$CQ = 2130\ Q^{1.76} \qquad 5:15$$

which can be linked to the ROUTE.PAS simulations to estimate yield at watershed points. However, it is recognised that this combined regression relationship relates only loosely to the large discontinuous gully, and all future extrapolation from equation 5:14 is undertaken from here onward with the limitations of the data from which the equation is derived implicitly assumed.

(b) The problem of inter-event reliability

A more serious problem, however, is the apparent lack of similarity between the melt and summer event relationships. In fact the differences between equations 5:12 and 5:14 suggest that either main channel deposition is occurring more during storms than melt (as discussed above), or that poor sediment availability has restricted the C - Q relationship when viewed in comparison with the situation during melt.

As a result, inter-event reliability during summer (even for those 25% of events listed on Table VII which are similar to that of June 4th, 1981) is not indicated by the field data; nor, therefore is much confidence gained concerning the continued use of the combined regression 5:14 alone for summer site yield calculations. It is likely that by contrast, the summer events may vary considerably, from 'supply-limited' events characterised by low exponents, to 'transport-limited' events which may occur when rainfall intensities are higher. This is because on these latter occasions, more sediment may be detached earlier by those high intensities, leading to easier transportation nearer to transport capacity downstream. Such a regression could be hypothesised to be closer to the combined regression equation for watershed events, which is ;

$$C = 9132Q^{0.81} \qquad 5:16$$

using previous notation, and for which n = 54, r = 0.77, (sig. at the 0.5% level).

Because of these conjectures, a decision was finally made to calculate the sediment yield of the simulated summer runs in the watershed twice in the following discussions, once using equation 5:14 (loosely described as a 'supply-limited' case), and then again using equation 5:16 (closer to the 'transport-limited' case). This means that all tests, percentage yields, statistics, differencing procedures and comparisons concerned with yield are all undertaken twice, allowing the effects of limited sediment availability to be considered.

(IV) ANNUAL SEDIMENT YIELDS AND SITE BUDGETS

In this section, the snowmelt models, APSIM and MAYSIM which were presented in Chapter 3 are combined with known diurnal fluctuations to simulate the complete two month melt regime experienced by all network sites. When viewed in conjunction with equation 5:13, these data allow the total annual yield throughout the melt period to be estimated by integration, resulting in a value in metric Tonnes for all network sites. Similarly, a range of 'probable' runoff events following summer storms (as simulated in Chapter 4 using ROUTE.PAS) are linked to the two sediment relationships established above (equations 5:14 and 5:16), so that from these simulations the total site yield for the summer period can also be estimated for both the 'supply-limited' and 'transport-limited' case.

Together these calculations allow the relative importance of the annual pattern of watershed events to be identified in terms of sediment yield for sites in the headwaters, on the main channel, and on the large discontinuous tributary. The relative roles of snowmelt and summer storms may be assessed at different points from this perspective. In addition to undertaking comparisons of two rating regressions for summer calculations, the analyses and budgets were conducted both with and without the effect of a 'freak' event (run 10, Chapter 4).

(A) Characterising the runoff pattern at each site.

(i) Snowmelt

In Chapter 3, the mean daily site discharges during April and May (APSIM and MAYSIM, Appendix 4) were established, and the pattern of diurnal variations around these mean values was demonstrated from field data collected on two separate occasions at the basin mouth during the field season (Figure 20, and Appendix 7). Bearing in mind the importance of diurnal fluctuations, a simple method was sought whereby a diurnal hydrograph at each watershed site could be constructed using the simulations and the diurnal field data for the output point of the basin.

Using known peak-to-mean ratios (Appendix 7B) the peak daily discharge at each site in both April and May is calculated. Next, using the diurnal hydrograph presented as Figure 20, a set of ratios are calculated (one for each 10-minute interval on a 7-hr hydrograph, giving 43 separate ratios) which link peak discharge to local time discharge. These are referred to as T-ratios, and take the value 1.0 at the event peak, getting smaller as discharge falls. These T-ratios are listed in Appendix 14(A), and convert the local peak discharge in both melt months at any site into a diurnal hydrograph. This procedure was included in the programme designed to calculate snowmelt yield, which is described later. Each site is assumed to experience 30 such diurnal hydrographs in April, and 31 in May.

(ii) Summer storms

In Chapter 4, the pattern of storm events on the watershed was considered in some detail. The 95 storm events (Table VII) that might potentially produce overland flow over the 6 years of record fall into three categories. First, there are some storms of very high intensity but of such short duration that initially high infiltration rates were never exceeded. These represented about 20% of events. Secondly, events occasionally occur of such low intensity that although a fairly high total amount may fall, they are never likely to exceed local infiltration rates and therefore again produce insignificant runoff (14% of events). Of the remaining 66% of events, 30% are of the type represented as Run 7 in the last Chapter; another 25% are of type Run 8; and 11% are of type Run 9.

On average, the watershed will experience 16 events per year (the 95 events averaged over the 6 years of record). Of these, 30% (i.e. 4.8 events, rounded up to 5) will be of type Run 7; similarly 25% (i.e. 4) will be of type Run 8; and 11% will be of type Run 9 (approximately 2 events). It must be assumed that the remaining 5 events fall into one or other of the two categories outlined in the preceding paragraph. In an attempt to ascertain an annual pattern of sediment production at Alkali Creek, these frequency data were used to weight the ROUTE:PAS simulations by their probability.

Since data files for all these runs were readily available as output from ROUTE.PAS simulations, a complete year of annual watershed runoff could be simulated, weighting the Runs as appropriate.

(B) The yield calculations : YIELD.PAS (1) and (2)

Two PASCAL programmes were written to calculate site sediment yield. These have been included in Appendix 11. The first (YIELD1.PAS) constructs the daily melt hydrographs using the T-ratio method described above, and then utilises equation 5:13 to convert the discharge at each 10-minute interval into a value of sediment discharge. This gives 42 data points for a 7-hr melt day. For each of these time 'slices', sediment yield is calculated for that time interval. In the programme this parameter is called 'int', and is worked out using the trapezoidal method. For example, if sediment discharge in mg/l at a first time interval is designated 'sedqt', and after 10 minutes the sediment discharge in mg/l is 'sedqtnext', then the area under the curve formed by these points is ;

$$int = \frac{(sedqt + sedqtnext)}{2} \cdot \frac{60 \cdot 10}{1000} \quad \text{in Kg.}$$

i.e. $int = 0.3(sedqt + sedqtnext)$ in Kg. 5:17

The whole event yield is the sum of all the 'int' values. For a monthly total, this number is multiplied by 30 (or 31). YIELD1.PAS is annotated with comments so that the coding is not described in this text.

YIELD2.PAS, the summer storm yield calculation programme, is almost identical to that devised for melt calculations of yield, except that the programme reads the exponent and regression constant either from equation 5:14 or 5:16 as appropriate. The event hydrograph at each site is also input directly. The input file to YIELD2.PAS is simply the output from ROUTE.PAS, i.e. an array of arrays. For both the continuous network and for the large discontinuous gully, this 'record' type of input consists of an array called run [site] of hydrographs, q[t]. Since the discharge data are presented every two minutes over a two hour hydrograph (rather than every 10 minutes over a seven hour day as for melt calculations), then the constant

in equation 5:17 can be calculated to be 0.06 rather than 0.3. Site event yields through the network were weighted (see below, last section, and Appendix 14) to give summer site totals.

In Appendix 14, the input files and output data for all the yield calculations for melt and summer events, and for both the continuous network and discontinuous gully are included with considerable annotation. The April and May total melt yields were added together to give a site yield for 'all melt' in Tonnes, and for both uses of the summer regressions, a summer total calculated both with and without the inclusion of run 10. In other words, 'sumless' = (5 x rn7sed + 4 x rn8sed + 2 x rn9sed); and 'sumplus' = ('sumless' + rn10sd); using symbols applied in Appendix 14. The result is generally in Tonnes, although some listings are in Kg for ease of comparison.

(C) Seasonal sediment yield with distance

On Figure 52, the 'all melt' yields, and 'smplus' and 'smless' for both cases of regression use are displayed in their contiguous downstream positions for all sites below the left- and right-hand fork field sampling points, 6 and 7 on the main system. The headwater data were too confused in display and have, therefore, been excluded from the diagram. It should be noted that the diagram shows melt and summer storm data on different vertical scales. Similarly, Figure 53 shows the same relationships for the whole of the large discontinuous tributary, and in this case there has been no necessity for vertical scale differences or exclusion of headwater sites.

On Table VIII(a), the April and May yields, and the weighted storm yields using the 'supply-limited' regression (n = 0.76, k = 2130) have been calculated as percentages of the annual site total for each of the 9 field-monitored sites (Figure 7, back folder). This has been repeated a second time on this Table with the additional inclusion of sediment yield from run 10 so that the effect of a 'freak' event can be assessed in proportional terms. On Table VIII(b), the tabulation is repeated using the 'transport-limited' regression (n = 0.81, k = 9132). Some of the more interesting contrasts which emerge from these tables are summarised on Table VIII(c).

TABLE VII (a) YIELD OF SIMULATED WATERSHED EVENTS

Using (n = 0.76, k = 2130) for summer event calculations

Field Site No. / Sediment Source	1	2	3	4	5	6	7	8 Disc Gully end	9
APRIL MELT									
Total APRIL yield, in tonnes	17.491	13.427	9.161	5.115	3.477	0.198	1.444	0.347	0.007
% of site total, excluding 'freak' event, (run 10)	4.070	4.167	4.928	4.839	6.473	3.765	30.052	4.509	1.632
% of site total, including 'freak' event, (run 10)	4.052	4.144	4.880	4.757	6.268	3.492	26.466	4.360	0.901
MAY MELT									
Total MAY yield, in tonnes	411.735	308.216	176.081	99.940	46.566	4.915	3.060	7.153	0.212
% of site total, excluding 'freak' event (run 10)	95.801	95.656	94.712	94.542	92.273	93.477	63.683	92.956	49.417
% of site total, including 'freak' event (run 10)	95.382	95.118	93.798	92.953	89.356	86.68	56.085	89.873	27.284
SUMMER STORMS									
RUN 7 yield, weighted x 5, in tonne	0.191	0.2055	0.262	0.253	0.256	0.070	0.116	0.122	0.137
% of site total, excluding 'freak' event (run 10)	0.0444	0.0638	0.141	0.2393	0.476	1.331	2.414	1.585	31.935
% of site total, including 'freak' event (run 10)	0.0442	0.0634	0.140	0.2353	0.461	1.234	2.126	1.533	17.632
RUN 8 yield, weighted x 4 in tonnes	0.246	0.244	0.290	0.285	0.283	0.045	0.123	0.032	0.035
% of site total, excluding 'freak' event (run 10)	0.0572	0.076	0.156	0.270	0.527	0.855	2.560	0.416	8.158
% of site total, including 'freak' event (run 10)	0.0570	0.075	0.154	0.265	0.510	0.794	2.254	0.402	4.504
RUN 9 yield, weighted x 2, in tonnes	0.118	0.121	0.117	0.117	0.134	0.030	0.062	0.041	0.038
% of site total, excluding 'freak' event (run 10)	0.0274	0.037	0.063	0.111	0.249	0.571	1.290	0.533	8.858
% of site total,including 'freak' event (run 10)	0.0271	0.037	0.062	0.109	0.241	0.794	1.136	0.515	4.891
RUN 10 yield, (no weighting) in tonnes	1.887	1.821	1.812	1.806	1.759	0.412	0.651	0.264	0.348
% of site total when included in annual calculations	0.437	0.562	0.965	1.680	3.171	7.266	11.932	3.317	44.788
TOTAL SITE YIELD, including 'freak' event (run 10) in tonnes	431.668	324.034	187.723	107.516	55.47	5.670	5.456	7.959	0.777
TOTAL SITE YIELD, excluding 'freak' event (run 10) in tonnes	429.781	322.213	185.911	105.710	53.717	5.258	4.805	7.695	0.429

TABLE VII (b) YIELD OF SIMULATED WATERSHED EVENTS

Using (b = 0.81, k = 9132) for summer event calculations

Field Site No. / Sediment Source	1	2	3	4	5	6	7	8 Disc Gully end	9
APRIL MELT									
Total APRIL yield, in tonnes	17.491	13.427	9.161	5.115	3.477	0.198	1.444	0.347	0.007
% of site total, excluding 'freak' event, (run 10)	4.055	4.146	4.877	4.749	6.248	3.501	25.535	4.2845	0.771
% of site total, including 'freak' event, (run 10)	3.981	4.050	4.686	4.434	5.508	2.701	17.292	3.786	3.006
MAY MELT									
Total MAY yield, in tonnes	411.735	308.216	176.081	99.940	49.566	4.915	3.060	7.153	0.212
% of site total, excluding 'freak' event (run 10)	95.449	95.179	93.750	92.797	89.070	86.914	54.113	88.319	23.348
% of site total, including 'freak' event (run 10)	93.709	92.962	90.064	86.634	78.517	67.062	36.643	78.055	9.106
SUMMER STORMS									
RUN 7 yield, weighted x 5, in tonnes	0.738	0.795	1.022	0.989	1.005	0.266	0.453	0.149	0.167
% of site total, excluding 'freak' event (run 10)	0.171	0.245	0.544	0.918	1.806	4.704	8.011	1.840	18.392
% of site total, including 'freak' event (run 10)	0.168	0.240	0.523	0.857	1.592	3.629	5.425	1.626	7.173
RUN 8 yield, weighted x 4 in tonnes	0.944	0.937	1.121	1.102	1.098	0.167	0.469	0.363	0.413
% of site total, excluding 'freak' event (run 10)	0.219	0.289	0.597	1.023	1.973	2.953	8.294	4.482	45.484
% of site total, including 'freak' event (run 10)	0.215	0.283	0.573	0.955	1.739	2.279	5.616	3.961	17.740
RUN 9 yield, weighted x 2, in tonnes	0.460	0.451	0.435	0.551	0.502	0.109	0.228	0.087	0.109
% of site total, excluding 'freak' event (run 10)	0.107	0.139	0.232	0.512	0.902	1.927	4.032	1.074	12.004
% of site total,including 'freak' event (run 10)	0.105	0.136	0.222	0.478	0.795	1.487	2.730	0.949	4.682
RUN 10 yield, (no weighting) in tonnes	8.009	7.723	7.685	7.662	7.480	1.674	2.696	1.065	1.420
% of site total when included in annual calculations	1.823	2.330	3.931	6.642	11.849	22.841	32.284	11.621	60.996
TOTAL SITE YIELD, including 'freak' event (run 10) in tonnes	439.377	331.549	195.505	115.359	63.128	7.329	8.351	9.164	2.328
TOTAL SITE YIELD, excluding 'freak' event (run 10) in tonnes	431.368	323.826	187.820	107.697	55.648	5.655	5.654	8.099 •	0.908

TABLE VIII (c)

ANNUAL YIELD DATA FOR PARTICULAR NETWORK SITES
ALL DATA IN TONNES/YR

Yield \ Site	1 Network Mouth	5 Main Junction 'x'	6 L.H. Headwater Fork	7 R.H. Headwater Fork
Melt Total	429.226	53.043	5.113	4.504
Summer Total n = 0.81 k = 9 132	2.142	2.605	0.542	1.150
+ Run 10	10.151	10.685	2.216	3.846
Annual	431.368	55.648	5.655	5.654
+ Run 10	438.377	63.128	7.329	8.351
Summer Total n = 0.76 k = 2130	0.555	0.673	0.143	0.301
+ Run 10	2.442	2.432	0.557	0.952
Annual	429.781	53.717	5.258	4.805
+ Run 10	431.668	55.470	5.670	5.456

Figure 52

DOWNSTREAM YIELD : CONTINUOUS NETWORK BELOW FIELD SITES 6 AND 7

(on these plots, the vertical scales of melt and storm data differ by a factor of 25)

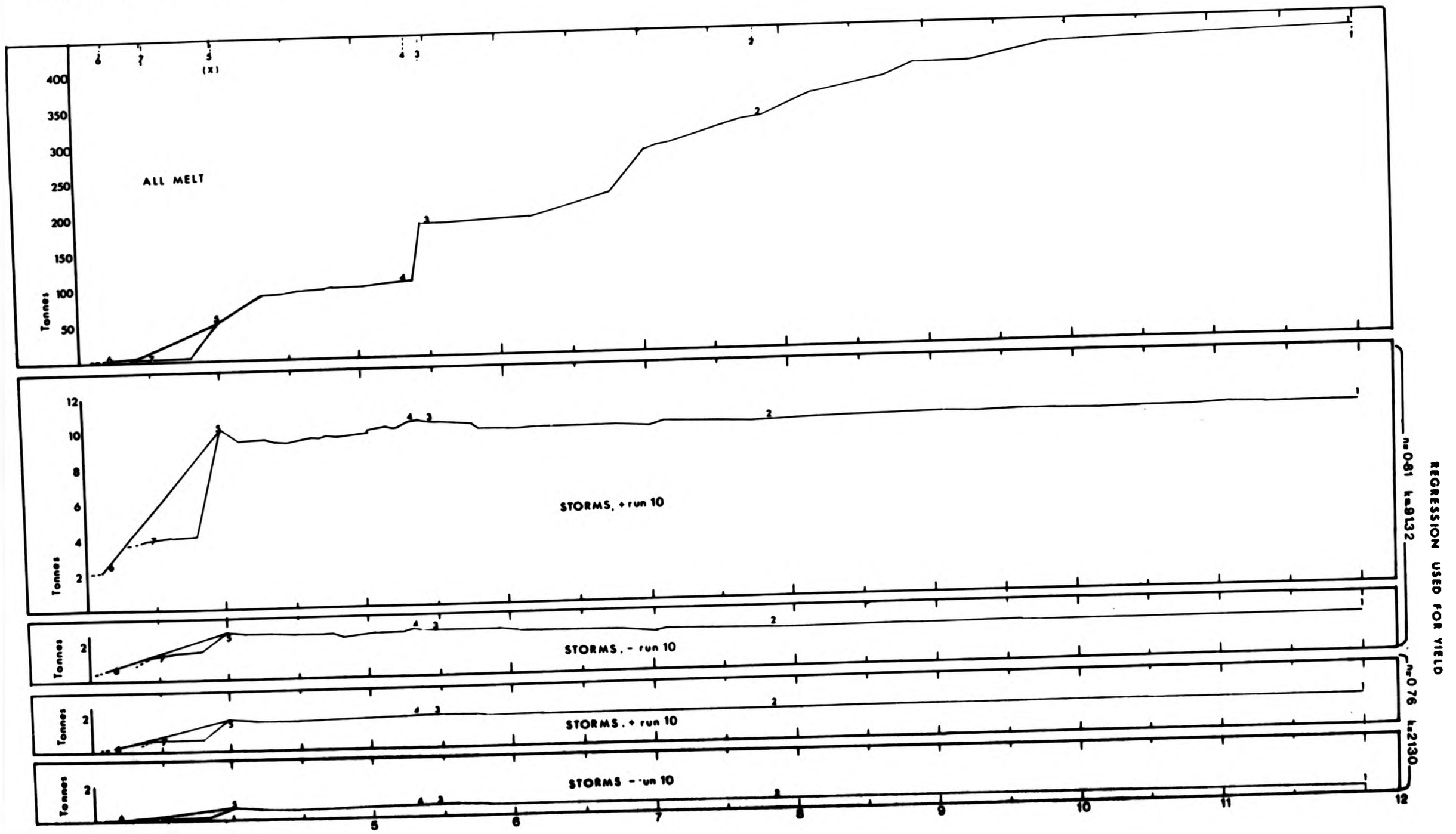

Figure 53

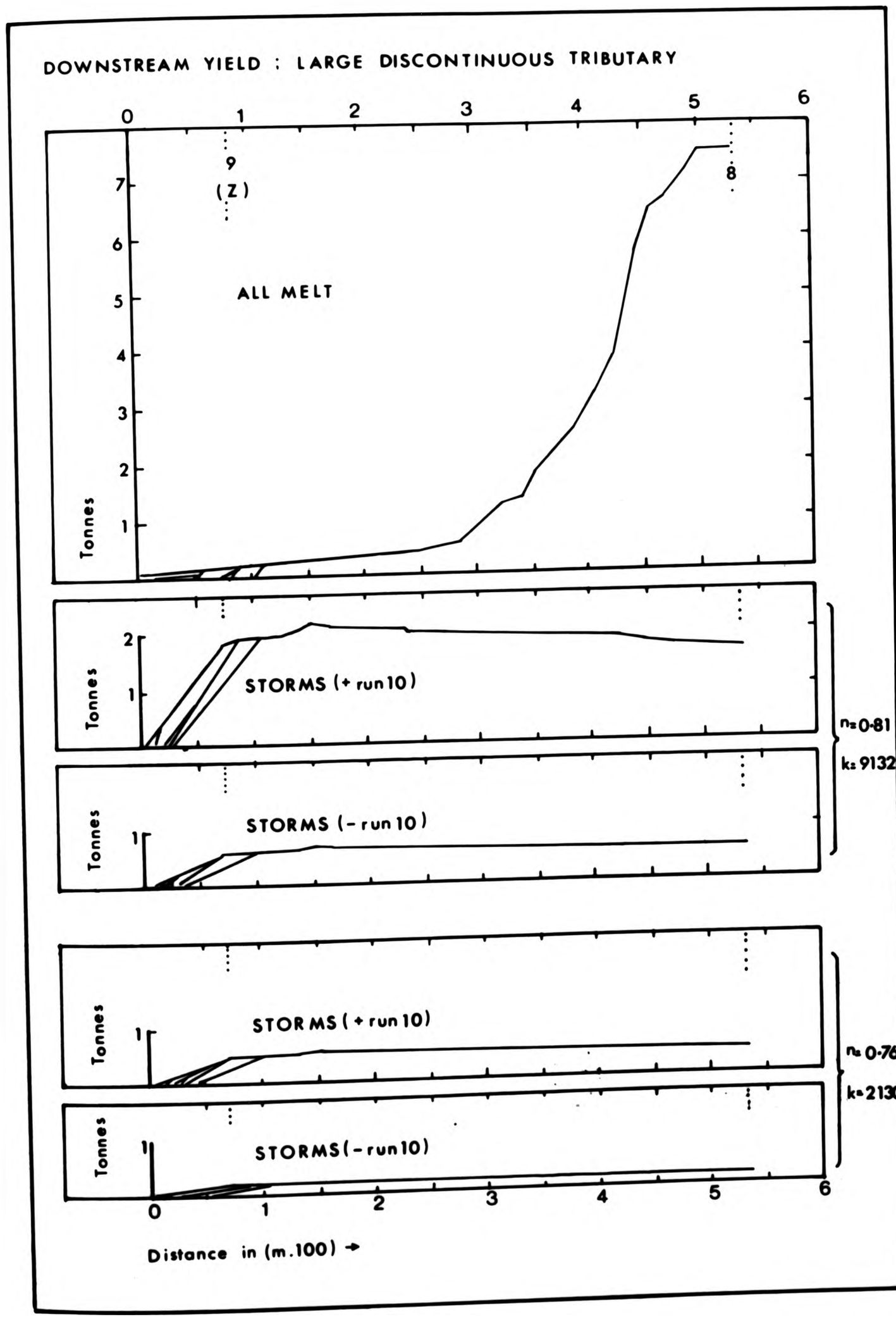
DOWNSTREAM YIELD : LARGE DISCONTINUOUS TRIBUTARY
0
1
2
3
4
5
6
9
(Z)
8
7
6
5
4
3
2
1
Tonnes
ALL MELT
2
1
Tonnes
STORMS (+ run 10)
n= 0·81
k= 9132
1
Tonnes
STORMS (- run 10)
1
Tonnes
STORMS (+ run 10)
n= 0·76
k= 2130
1
Tonnes
STORMS (- run 10)
0
1
2
3
4
5
6
Distance in (m.100) →

Some observations can be made from Figures 52 and 53 and these Tables, concerning the relative impact of melt and summer sediment yield ;

(1) Snowmelt dominates the sediment yield picture at Alkali Creek especially for sites on the main channel of the continuous network (Figure 52).
(2) The dominance of melt is less overwhelming on the lower course of the discontinuous gully than expected.
(3) Snowmelt dominance decreases considerably above 'X' and around 'Z' in the headwater areas, where for some sites melt and 'normal' summer events are almost equal in terms of total sediment yield, depending on which summer regression is employed. Using the 'transport-limited' regression and including the effects of a 'freak' event, summer sediment removal would dominate some headwater sites, for instance the top half of the large discontinuous tributary (Figure 53).
(4) The inclusion of a 'freak' event in the summer yield calculations, whichever regression is used, increases all site totals for summer by a factor of 3 to 4.
(5) A 'normal' summer at Alkali Creek appears from the values presented here to have a merely cosmetic role in the mobilisation of sediment.

Other observations which may be made concern the spatial rates of change evident on the plots ;

(1) During summer events, the rate of sediment yield increase with distance although high in the first order channels, is a maximum around the main tributary junctions, especially 'X' (Figure 52).
(2) This also occurs during melt, but other rapid rates of yield increase occur. One is due to the inclusion of the large amount of unchannelled melt flows just below X from the western bank, and another corresponding to the inclusion of the large discontinuous gully melt flows around field sites 3 and 4.
(3) On the large discontinuous tributary, the pattern is repeated.
(4) The main channel from sites 5 to 1 and the large discontinuous tributary from 9 to 8 experience the greatest contrast in terms of rates of sediment yield increase with distance taking the annual patterns as a whole. Sediment yield increases rapidly

downstream during melt, but decreases with distance downstream during summer storm events, suggesting deposition is the normal pattern of sediment behaviour on this stretch of the main channel in the summer. It is inferred that the main channel sediment regime is therefore the most varied, especially on the large discontinuous tributary (Figure 53, and Table VIII).

(D) The proportional role of differing events

The use of the 'supply-limited' regression shows all sites in these circumstances to be to varying degrees dominated by snowmelt yield, even with the inclusion of a 'freak' storm. To simplify the ensuing discussion, therefore, the relative importance of summer storms versus melt will from now on consider the most optimistic set of yield calculations, i.e. those calculated for the summer yields using the 'transport-limited' regression. By doing this, it is implicity assumed that these calculations may overestimate if sediment is not available for the storm events.

Taking Table VIII(b) data only, therefore, the two most interesting aspects are first, the relative importance of the two main processes and the manner in which domain dominance shifts from headwaters to basin mouth, and second the absolute values of yield in Tonnage terms, both at the basin output point and at other key sites on the watershed. There are considered below in that order.

(i) Site observations (using summer regression n = 0.81, k = 0132)

(1) On the western fork of the headwater net (site 6), 90% of the total sediment yield is produced by snowmelt runoff, 10% by summer storms. When an extreme event is included, however, the snowmelt yields represent 70% of the increased total, and that one single summer runoff episode is estimated as then producing about 23% of the annual yield.
(2) In the east fork of the headwaters, (site 7), summer storm events remove 20% of the sediment in an average year, rising to 46% if the 'freak' event is considered. In this latter situation, this one event would dominate the budget totals, representing 32% of the annual sediment removal.

(3) At X (site 5 on the Table) however, only 5% of the sediment moved in an average year can be accredited to summer storm events. This reflects the sudden increase in melt flows here from the western unchannelled slopes draining into the main gully between sites 6 and 5 in May. This percentages goes up to 17%, however, if the large event is included. Again, in the latter situation 12% of the total can be accredited to this one unusual event.

(4) Between sites 5 and 1, the proportional impact of summer storms drops considerably because the absolute sediment yield from these events drops, whereas that for snowmelt increases fairly rapidly.

(5) At the basin mouth (site 1), the late melt period dominates site sediment removal, representing 97% of yield if the 'freak' event is included, and over 99% if a normal year is considered.

(6) On the large discontinuous tributary, conclusions are more tentative because of the lack of confidence placed in the summer field data in this part of the watershed. Bearing this in mind, however, the data indicate that 93% of the sediment transported past the site approaching the fan (site 8) is done so by melt, although when the 'freak' event is included this falls to 82%.

(7) By contrast, the headwater site carries only 24% of the site total during melt, falling to 9% if a 'freak' event is included. The main cause of this change in the relative dominance of the processes downstream is the large late melt from the slopes adjacent to the lower gully course here.

(ii) Recognition of intensity domains

Since there are clear contrasts of process dominance emerging, Figure VIII(c) was produced to highlight these for key network sites. These figures substantiate the "overlapping process intensity domain" conceptual picture presented in Chapters 1 and 2, at least in terms of sediment yield.

At site 'Y' (field site 7), the two domains are almost balanced in a year including the 'freak' event. Headwater data upstream from this point reveal that these channels are increasingly affected by summer storm behaviour, so that in such a year this area will constitute a zone of summer storm dominance. The west fork of the headwater net

(site 6) is predominantly affected by snowmelt processes in an average year, although less so if an abnormally large summer storm occurs. The site where all the tributaries join, (site 5, or 'X'), is affected much more by melt than summer storms in an average year, although if a major event occurs the summer storm intensity domain shifts down-net resulting in a reduction of the overall melt impact in percentage terms here. The zone of overlap, and its nature, therefore, depends on the occurrence and nature of any abnormal event, its intensity and duration. However, summer storm dominance seems unlikely ever to move downstream as far as to include site 5, at least from the data presented here which are in any case optimistic in terms of summer storm impact. It is, therefore, concluded that the watershed constitutes a snowmelt dominance domain except in the farther tributaries.

Below site 4, Figure 52 shows that the sediment regime is overwhelmingly dominated by melt flow. This effect is exacerbated by the observation that although summer events will be erosive on their rising limbs and depositional on their falling limbs everywhere on the watershed, the net effect of storm behaviour below site X is one of diminishing yield with distance, whereas the snowmelt yield is predicted to increase with distance.

Since snowmelt dominates the main channel yield, and since it is assumed that main channel sediment sources here are the bed and banks of the gully itself, then snowmelt acts to flush out the sediment lodged here from the operation of summer events. The large discontinuous gully echoes these patterns, although melt dominance is less overwhelming. The lower course again is a predominantly snowmelt zone, and the headwaters eroded by surface wash mechanisms. On this tributary, the equality of the two domains in terms of impact is much closer, rather similar in fact to the headwater net above 'Y'. The existence of the fan here remains something of a mystery, although several possible reasons could be proposed which are reviewed at the end of section E.

(iii) Comparison with other areas

Well over 95% of the Alkali Creek sediment is moved in May, which is approximately 7% of the year. By contrast, at site 9, in the

discontinuous tributary headwaters, a normal year sees 76% of the sediment removed by six short erosive summer storms, i.e. less than 2% of the time. These great contrasts result from the dual nature of the landscape processes and the strongly asymmetrical spatial controls on each in the generation phase.

Temporally unequal sediment transfer is being increasingly recognised in many areas. Meade (1982) explains that for the Atlantic drainage of the United States "... because it is the product of stream flow and concentration sediment discharge increases even more strongly than concentration ... consequently most of the sediment is carried by these rivers during only a few months of the year ..." concluding therefore that over 80% of the sediment was carried only 10% of the time even in this fairly humid environment. These sorts of observations are especially true in arid and semi arid areas (Gutierrez, 1983). Schick (1978) emphasised the over-riding influence of "... the all-important and usually very transient event" in sediment movement, and resulting morphological relationships. In his Eastern Sinai study area, he suggests that all transfers of fluvial sediment occur less than 10% of the time. Piest (1965) examined the relative importance of large, medium and small storms in semi arid areas and demonstrated the disproportionate amount of work done by the infrequent, large events.

It is also apparent that snowmelt flows 'flush' out sediment lodged below 'X' by summer storms. Seasonality in sediment production by hillslope processes, and the relative importance of lodged sites has been explored by Harvey (1984b) who calculated the annual sediment yields in his study area in the Howgill Fells. An annual cycle of sediment production and flushing, similar to that described by Schumm (1964), detaches sediment from hillslopes partly by mass movement in the winter months and this is flushed from the system in the spring. Subsequent summer events are likely to be deprived of sediment, depending partly on the efficiency of the spring events. Whether or not the sequence is repeated in the next season depends on the efficiency with which summer events have removed stabilising fan material from the lower parts of the slopes, rendering them once again likely to failure. These effects, and the contrast that they make with the flushing sequences in the study area, are summarised on Table IX.

TABLE IX: SEDIMENT LODGEMENT AND FLUSHING: COMPARISON WITH OTHER AREAS

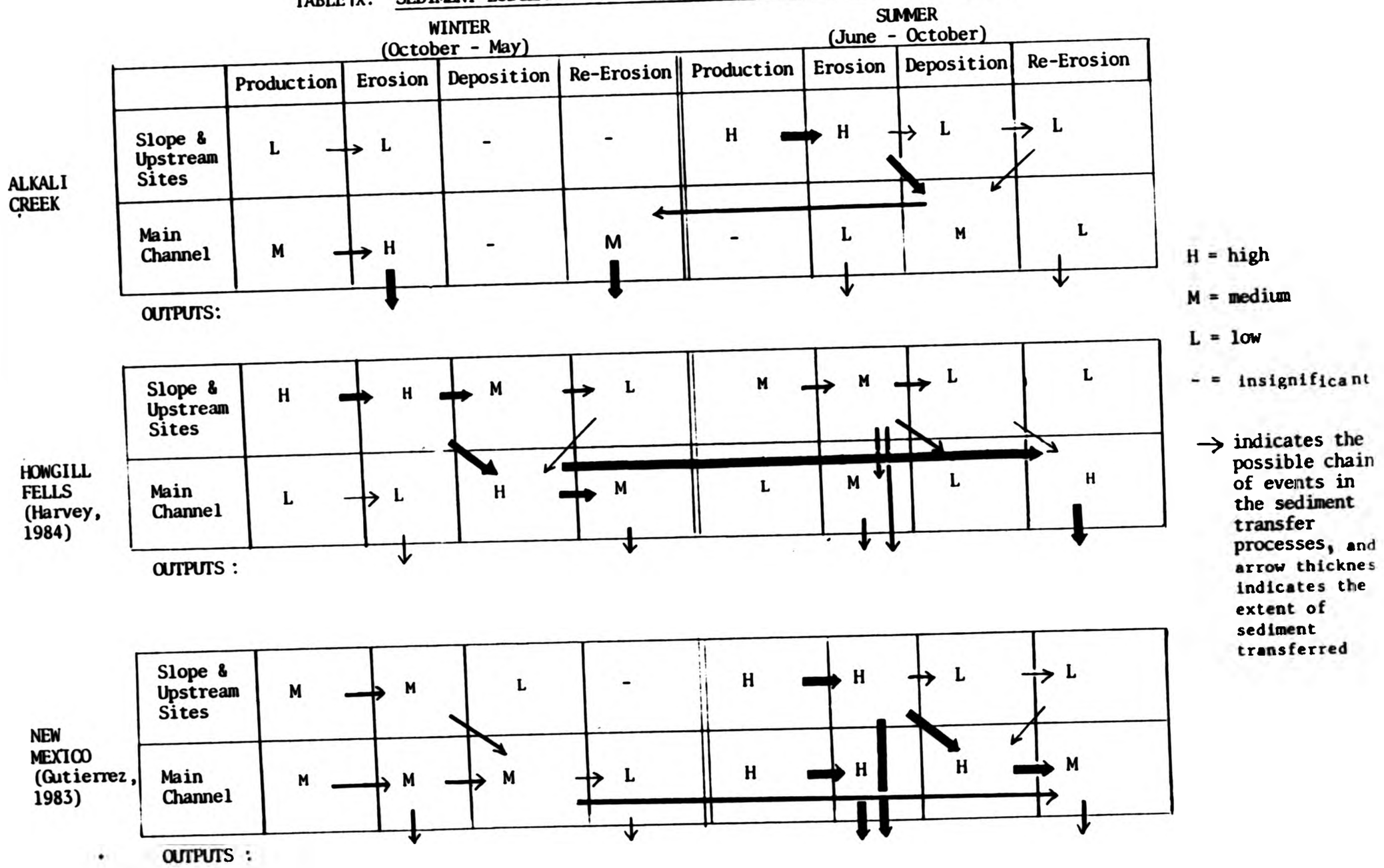

Gutierrez (1983) argued that in the watersheds in his semi arid study areas in New Mexico, Arizona and Utah sediment was removed in "... seasonal pulses rather than at a constant rate". The timing of the flushing events, and the spatial location of sources and of deposition and re-erosion sites can be inferred to be different again from either the Alkali snowmelt environment, and the Howgill Fells humid-temperate climate with its winter runoff maxima, (Table IX). The summer events in both of the latter situations result in a net flushing of winter-lodged (in the case of New Mexico) or winter-produced sediments (in the case of Howgill Fells), whereas at Alkali Creek the melt flows of spring are the main mechanism flushing summer lodged sediments out of the watershed. Although spatial variations in lodging and flushing of sediments are to a certain extent scale and aspect-dependent (cf end of Chapter 3); nevertheless, Table IX illustrates interesting general climatic constrasts.

Spatial zonations of small watersheds on the basis of function (the P-D-E sequences described by Patton and Schumm, 1981; and Bergtrom, 1980) were related to morphological zones in the study area in Chapter 2. At that stage it was suggested that flow simulations of the two main processes in the study area, and considerations of sediment transfer associated with each would allow a more considered explanation of morphology than was possible merely from the sequential data. The previous sections have shown that here sediment transfer resulting from the dual operation of the landscape processes goes some way towards supporting these early inferences. However, the above discussion diverges from the zonations described by Bergstrom (1980) in several key areas. Although, for instance, the headwaters (zone 1) are clearly the only production zone, these areas do not emerge as being as strongly erosive as initially envisaged, and tributary junctions are by far the most heavily exploited sediment source on the watershed. Also, although some deposition occurs below 'X' in zone 2 (paralleling observations made by Butcher and Thornes, 1978; and Schick, 1978), nevertheless 'scour and fill' associated with the second zone must be seen in the context of an overwhelmingly negative sediment budget. In fact it will be shown later that the erosion rate in zone 2 (per unit channel length) exceeds that for channels in zone 1. Chapter 6 will explore the obvious morphological implications of these results.

Few studies have emphasised the link between snowmelt erosion and the preferential exploitation of sediments on the lower channel beds and banks. An outstanding exception is the work of Nodolski, et al, (1981) who found that snowmelt was encouraging bank collapse particularly, and that in the East-central Sierra headwater study areas snowmelt produced over 90% of the local sediment yields, which is the case here.

Because of the emphasis on tributary junction which emerges from these discussions, the bank collapse mechanisms around these locations are rather important. Piest et al (1975) recognised that where gully trenching focussed collapse episodes, these points became the most significant sediment supply sites, a fact recognised by Patton and Schumm (1981) in their South Dakota, Nebraska, and New Mexico arroyos. Lehre (1982) also made similar observations. These observations all lead to the conclusion that a different picture of geomorphic change characterises the area than is conventionally associated with semi-arid landscapes in Colorado; one which emphasises snowmelt erosion, and which focusses attention on channel scour and bank sources for downstream sediment removal rather than surface wash mechanisms.

(E) The absolute yields of different sites, using sites 1 to 9 for comparison

The data presented in Table VIII(b) allow absolute annual yield to be calculated. Observations are again itemised below, and again relate to the ($n = 0.81$, $k = 9132$) regression.

(1) The tonnage produced by all events in an average year on this small watershed (area 0.4 km^2) represents a yield of 1078 Tonnes/km^2/year, increasing to 1098 Tonnes/km^2/year if a 'freak' event is included. Both these values plot fairly well on the graphs presented by Schumm (1965) linking climatic parameters to sediment yield; and Richards (pers. comm. 1984) considers these values to be comparable with data he obtained in similar environments (his values ranged from 1000 to 2000 Tonnes/km^2/year). The yield calculated was also considered a 'reasonable assessment, perhaps a little conservative' by Walling (pers. comm. 1984).

(2) The annual sediment yield increases about 8-fold between sites 5 and 1 in an average year, entirely as a result of sediment entrained during melt, so the bed and banks of the channel here must be providing the bulk of a large total. In budget terms, less than 1 Tonne is deposited here by 'normal' storms, and this does not increase if a 'freak' event is included. During melt, by contrast, 376 Tonnes are removed. Overall, sediment loss on this section averaged 0.5 Tonnes/metre/yr.

(3) Comparing site 5 and the joint yields for sites 6 and 7 shows that 45 Tonnes/yr. is removed on this short 20m section, the erosion rate therefore being about 2.25 Tonnes/metre/yr. This could account for the heavily trenched character of these sites (Chapter 2).

(4) Between sites 8 and 9 on the discontinuous tributary, 0.6 Tonnes of sediment are deposited on a year which includes a 'freak' event, whereas melt removes about 7 Tonnes. These data suggest that this tributary behaves in a manner similar to the continuous net above site 7, and that it is more affected by summer events overall in comparison to the continuous network, particularly in upstream sections.

(5) Below site 8 on the discontinuous tributary there is morphological evidence of persistent deposition in the form of an alluvial fan, and no permanent channel persists through the feature. Although the plot on Figure 53 might suggest that on the lower course of the gully the rate of sediment yield increase with distance is strongly positive in the channel lower sections (which during melt must be associated with an erosive channel), this diagram shows that the spatial rate of yield increase starts to flatten off towards the fan as lateral melt flows are inhibited here, possibly explaining the tendency for deposition. However, there is clearly a problem here with the snowmelt runoff model, which of course was not routed using channel gradient as were the summer events. Attenuation effects are the only way in which deposition can be explained here, since a downstream peak discharge drop leads (as in the ROUTE.PAS simulations) to a decreasing yield with distance when lateral inputs are inhibited.

(V) SCOUR AND FILL

(A) Approach

No attempt is made here to quantify the absolute amount of scour and fill each event causes between all adjacent watershed survey sites; instead the differencing method proposed below is viewed as producing maps which describe merely the propensity for such behaviour. The method is described by reference to Figure 54.

If a channel section L metres long is bounded upstream and downstream by sites A and B as indicated, the sediment budget for a given event or events in that section is described by the normal budget equation utilised in ROUTE.PAS which is ;

$$\text{Input} - \text{Output} = \text{Change in storage} \qquad 5:18$$

In the section shown the change in storage, Δvol, is the cross-sectional area change at each site ΔXA multiplied by L. In all three cases shown, input to the section during the event(s) is the site yield at site A (Y_A) plus the lateral sediment contribution from surface wash during the event(s), (TR), plus sediment contributed to the section from pipes (P). So input = Y_A + (TR+P). Similarly, in all three cases shown, the output is the yield at B, Y_B. The change in cross-sectional area per unit metre of channel in the section, ΔXA, is therefore (Y_B - (Y_A + (TR+P)))/L, a negative value indicating deposition.

Two problems are immediately apparent. First, the approach appears dubious in situations where bank collapse occurs. Referring to Figure 54(C), it might appear that since collapse sediment is more readily entrained than in situ sources, then subsequent availability in the section is modified. Additionally, slumped material may protect local banks from undercutting during later events, not only diminishing the possibility of subsequent failure at that site but potentially destabilising another adjacent downstream section by deflecting the flow path to another bank. From event to event, therefore, bank collapse events are quite likely to exhibit a high level of spatial as well as temporal autocorrelation, involving both negative (basal protection) and positive (adjacent site collapse

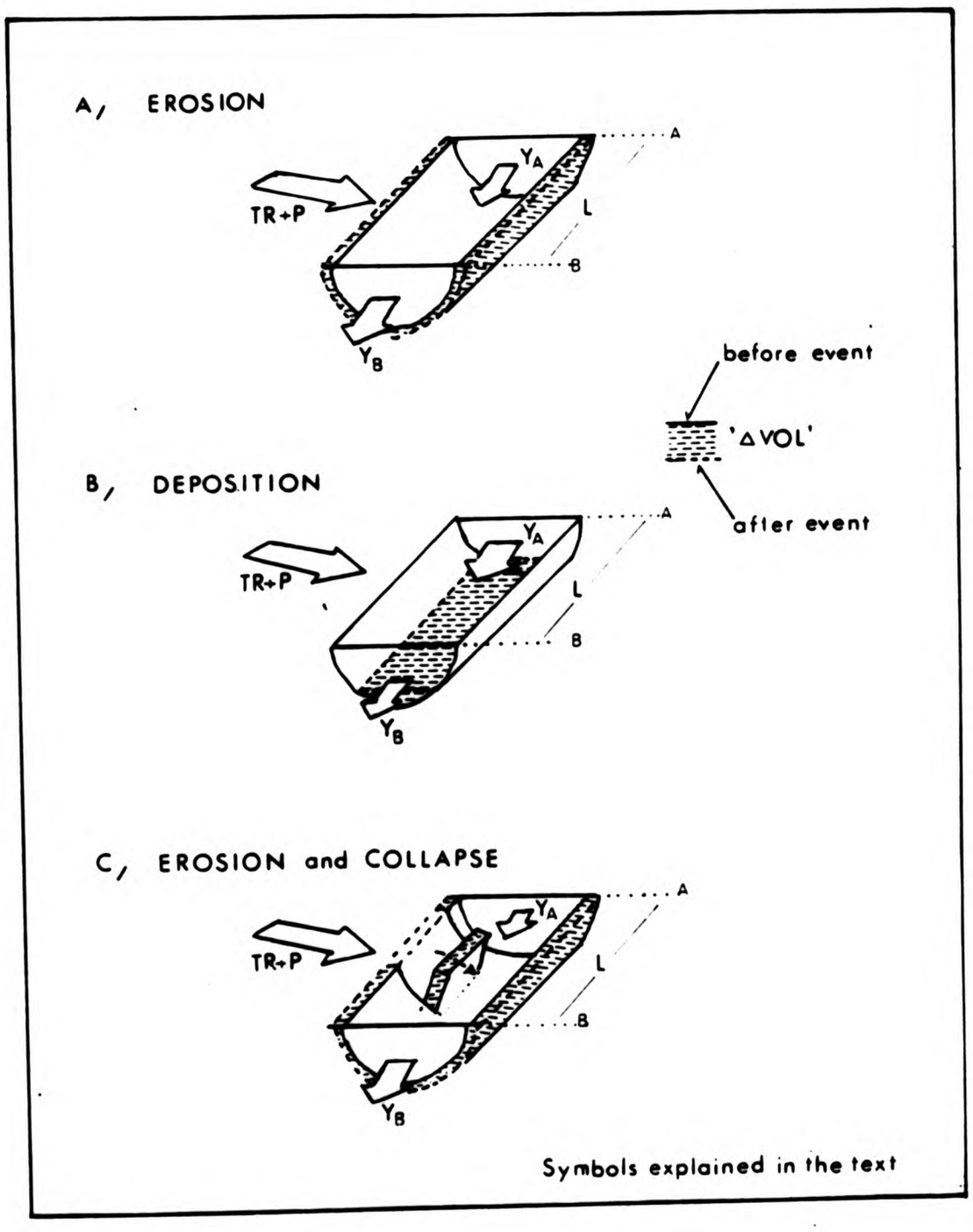

Figure 54 : A conceptualisation of three possible situations involved in the calculation of scour and fill using sediment differencing methods as discussed in the text.

exacerbation) aspects. Feedback effects of this kind were hinted at in Section III, and have been noted by Lehre (1982) in the context of sediment yield modelling, and also by Bello (1982) and Piest (1975) who doubted that inter-event prediction of sediment yield was possible when collapse was strongly indicated.

Although short-term effects like this complicate local erosion and deposition patterns, the rating curves for snowmelt suggest that a collapse event modifies sediment behaviour less than other workers found in their study areas. So as far as the sediment budget calculations for the reach shown in Figure 54(c) are concerned, it is argued for simplicity that the collapse of a volume of sediment from the channel banks 'fills in' the local cross-section with the same volume of sediment as the space which it vacates, and from this perspective the collapse event is irrelevant to the calculations involved in equation 5:18.

However, the possibility that not only collapse, but normal scour and fill alter morphology to such an extent that the overall mechanics of the system in its subsequent operation are affected is a basic problem in discussions like this. In Chapter 1, the suggestion was made that threshold behaviour should be regarded as an aspect of the longer-term operation of the landscape. So although, in the long-term, irreversible channel morphological change due to bank collapse may be a significant consideration, at the scale addressed here the catastrophic nature of the process is effectively ignored. Because of these and other problems of inter-event causality, the differencing method will be used merely to map propensity, and threshold behaviour and the other problems suggested above will be tackled in Chapter 6.

The second problem is that (TR + P) is unquantifiable for individual events. In fact, the plan here is to calculate differences as $(Y_A - Y_B)/L$, which, of course, ignores these lateral contributions. In summer events in the headwaters, where (TR + P) is considerable (Figure 47), the value of ΔXA will be consequently overestimated in the case of erosion (ΔXA positive), and under-estimated in the case of deposition (ΔXA negative). Clearly the spatial differences calculated present a truer picture of in-site erosion and deposition patterns on the main channel where lateral

contributions are relatively small, and for all snowmelt events at all watershed sites. Since the watershed is emerging as a predominantly snowmelt landscape, in which the lateral sediment input is deduced to be minor, this seems less of a problem here. However, lateral wash contributions (TR + P) are important in the headwaters for the summer events, so this will be allowed for in subsequent discussions and tests.

(B) The differencing programmes, SEDIF.PAS (1) and (2)

Two programmes calculate the differenced values for melt (SEDIF1.PAS) and storms (SEDIF2.PAS). They are very similar, and are included in Appendix 11. Since adequately annotated, the coding is not discussed in this text. SEDIF1.PAS, reads the melt yields, SEDIF1.DAT (Appendix 14), and calculates the spatial rate of sediment yield increase with distance during melt between contiguous network sites, using network 'keys' as before. The programme can be simply altered to read the large discontinuous tributary data file, SEDIFC.DAT, which is also in Appendix 14(B). In another form (SEDIF2.PAS) the programme has been modified in a simple fashion to read the summer storm yields (Appendix 14). The programme was run twice, once for the 'supply-limited' yields, which are called SEDIFA.DAT, and once for the 'transport-limited' yields, SEDIFB.DAT. These datafiles are in Appendix 14(B). The output from these runs is in Appendix 14(C), and is also tabulated against gully morphology in Appendix 15.

The rates of sediment yield change are seen as an index of event scour and fill during specific events or groups of events. The data were used to draw difference maps as was done for the TR index (Figure 47), which similarly mapped spatial differences. Maps were considered preferable to plots because of the difficulty of separating tributary influences in graphical form. However, some generality is introduced when data are mapped as 'bands' around channel sites. The rates of change of sediment yield with length have been plotted for 'supply-limited' summer events both with and without the freak event, (Figure 55), and the same again for the 'transport-limited' case, (Figure 56). On Figure 57, the 'allmelt' differences have been plotted, and on Figure 58 the annual differences have been mapped for both uses of the regression,

Figure 55 : Summer sediment yield differences with distance (using n =0.76)

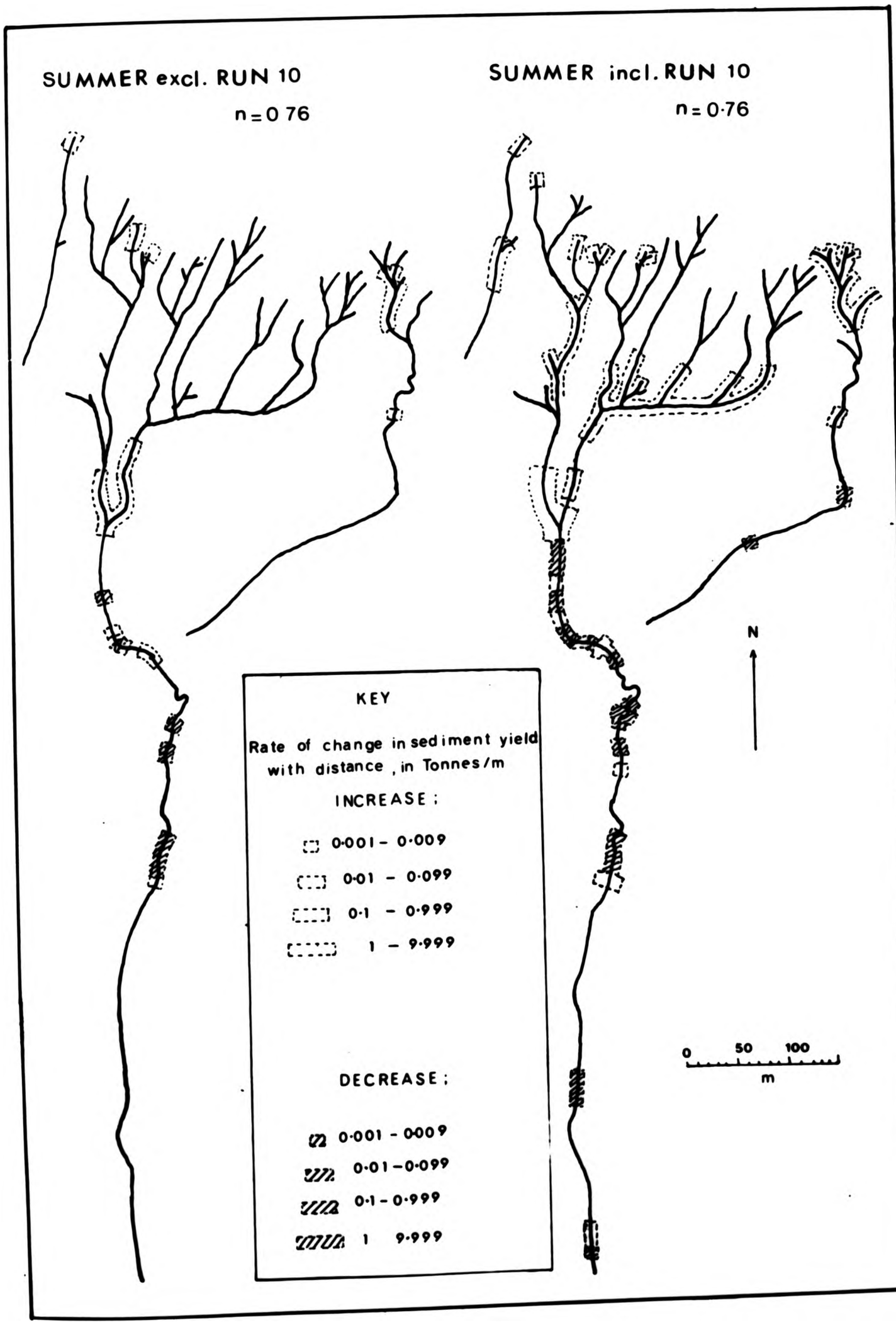

Figure 56 : Summer sediment yield differences with distance (using n=0.81)

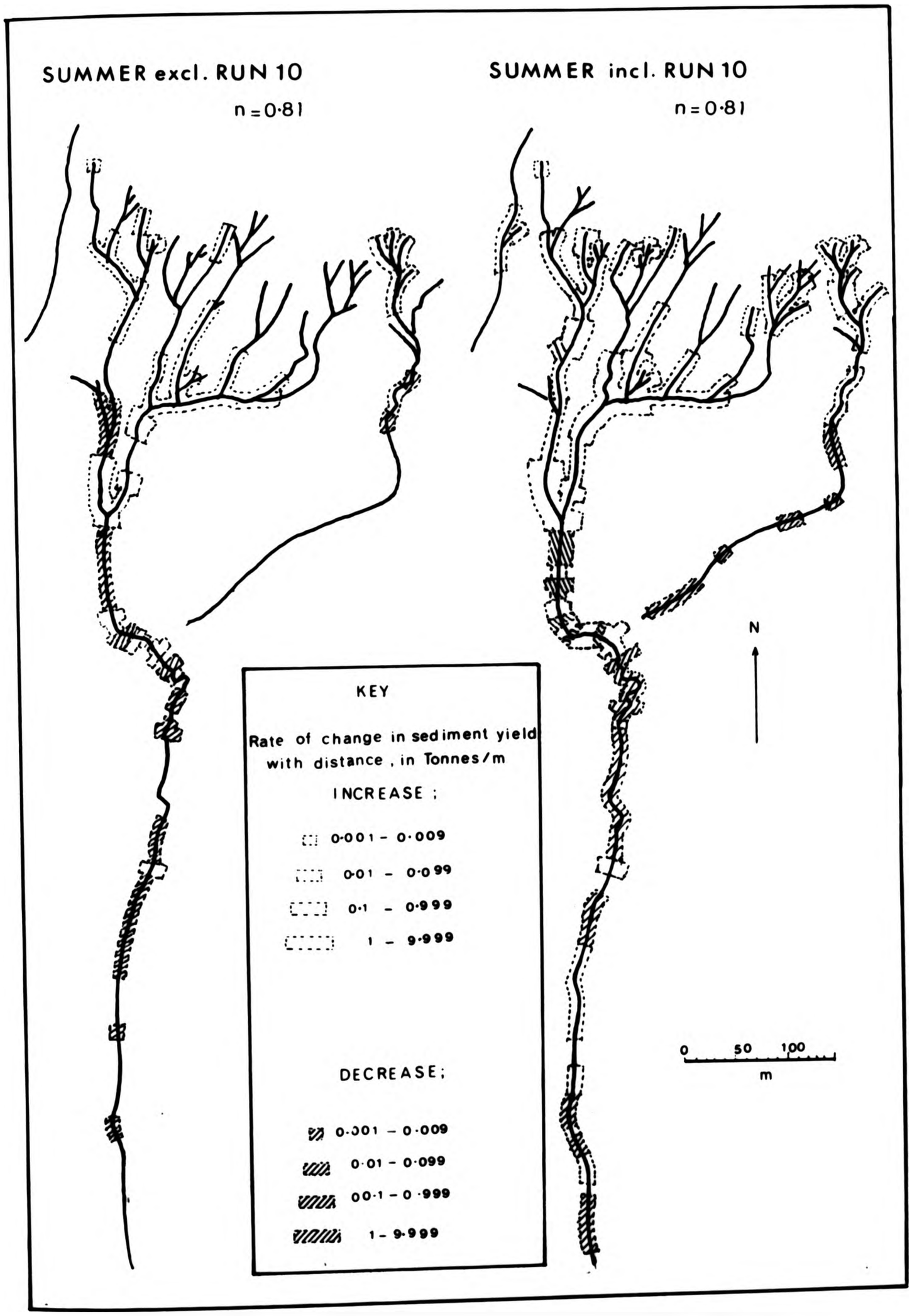

Figure 57 : All melt sediment yield differences with distance

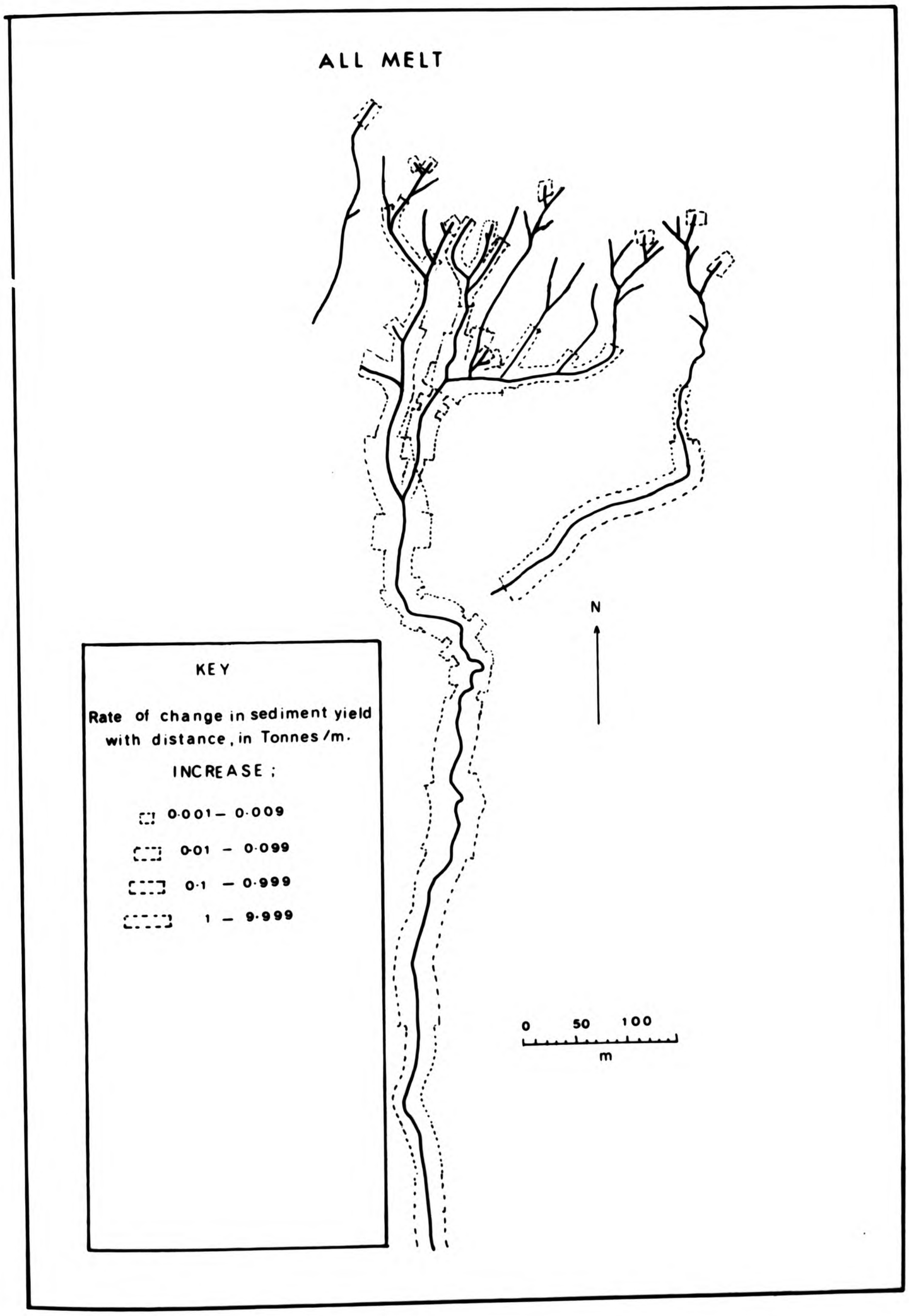

Figure 58 : Annual sediment yield differences with distance (including run 10)

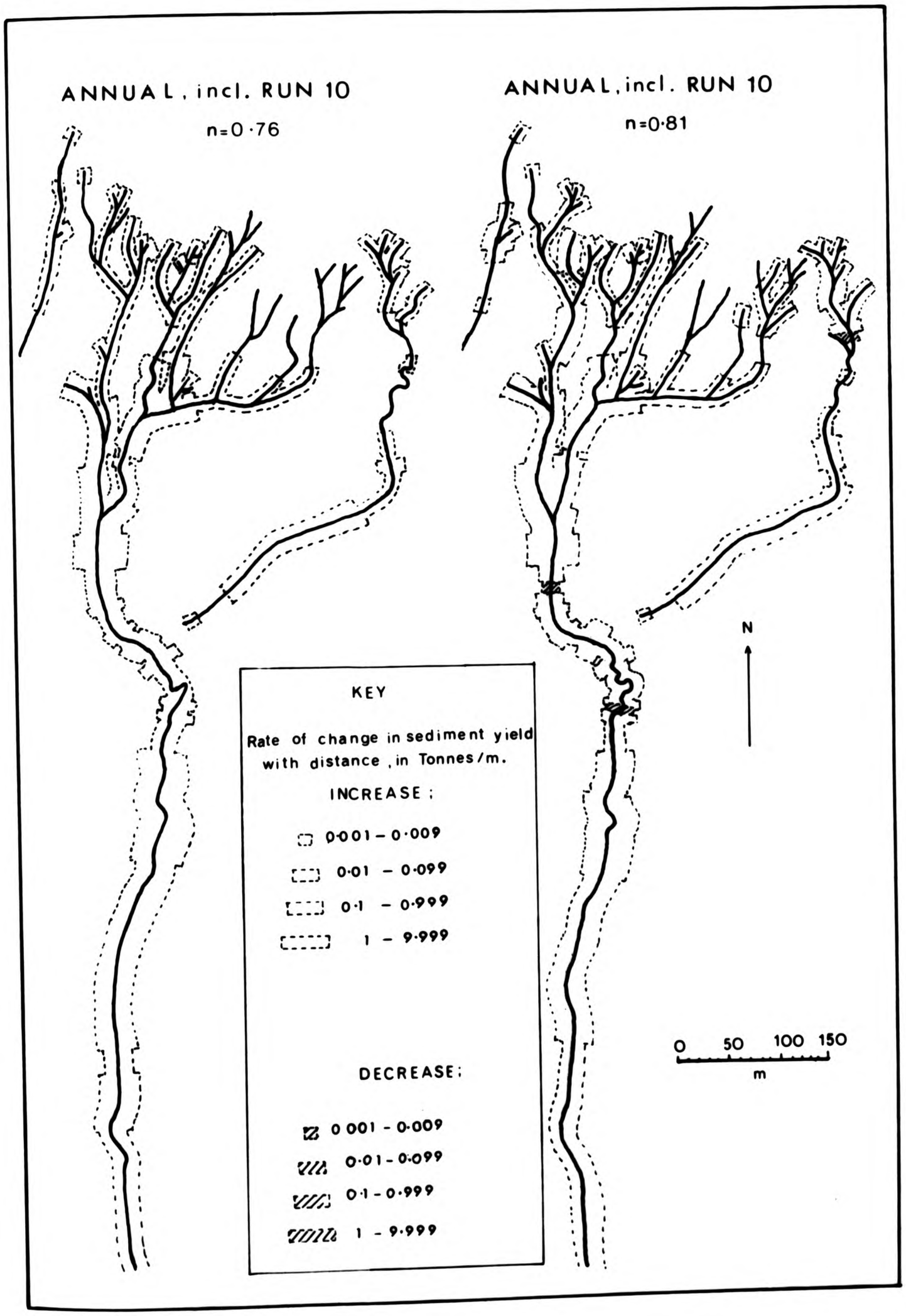

including the effect of a 'freak' event. No map has been constructed to show the annual pattern without the effect of an extreme event because this is not very different from the melt difference map for obvious reasons.

The data are displayed on the plots as either increases (erosion) or decreases (deposition). Because of the wide range in values, the width of the 'bands' increases on a log scale, as indicated on the key.

(C) Patterns in an 'average' year

(i) Summer storms : observations from Figures 55 and 56

(1) All four of the summer patterns indicate deposition on the main channel, alternating with sections on which erosion is predicted. The net change is not great. The same is true of the large discontinuous tributary, although the lower depositional zone has far fewer sections where local rates of yield increase.

(2) All the patterns show an erosional environment in the headwaters which focusses on the tributary junctions Y and X in particular. However, bearing in mind the patterns of surface wash increments in the headwaters laterally (Figure 47) and the discussions in the previous section, the (TR+P) contribution may be a considerable source of error in the headwaters, and the scour pattern suggested is likely to be considerably overestimated because of this, especially at locations near to channel initiation sites - the finger-tip rills. It was pointed out in an earlier section that these often had sediment 'stringers' in their beds. At such locations, the (TR+P) contribution is at a maximum (Figure 47 and discussion).

(3) The combined effect of normal summer events is overridden by the overwhelming impact of a 'freak' event on the watershed.

(4) The effect of selecting the different regressions is one of degree, that is the 'transport-limited' rates of change pattern predicts proportionately greater rates of change but in similar locations to those predicted by the 'supply-limited' regression.

(ii) Snowmelt : observations from Figure 57

(1) In both melt months, all sites experience an erosional environment everywhere on the catchment in the interpretation made here.

(2) Erosion focusses on the section of the main network immediately below sites 6 and 7 on the headwater net, and at a couple of sites on the main channel as lateral contributions build up in terms of runoff; clearly the average value of erosion rate on the main channel (calculated above as 0.5 Tonnes/m) encompasses quite a range of specific site values. Thus although the central part of the watershed emerges as the most erosive environment, some main channel sites are predicted to be locally very erosive indeed.

(3) As was observed above, summer deposition, although normally small, focusses on the main channel below 'X' where the most significant amounts of melt scour occur. Clearly the early snowmelt flows operate as a flushing mechanism for summer deposited material, and the late melt operates to rescour fresh sediment in excess of the deposited material. Renewed scour of in-situ materials is the net effect of a normal year's operation.

(iii) Annual patterns ; Figure 58

Figure 58 shows the effect of totalling both the summer and winter differences shown in Figures 56 and 57, i.e. the 'winter' and 'summer' differences, to show the net result of the annual pattern of scour and fill. Here the calculations have been conducted only with the inclusion of the effects of a 'freak' event, although both the 'supply-limited' and the 'transport-limited' regressions have been tried. The overall effect is one of scour throughout the basin whichever regression is employed, although there are places on the main channel where the rate of deposition is predicted to be locally greater than the annual rate of erosion. On years which experience a 'freak' event, therefore, these sites experience a rapid annual rate of scour and fill.

(D) Conclusions

The watershed at Alkali Creek is differentially scoured by the two main mechanisms of runoff and sediment removal. In the

interpretation made in this Chapter an annual cycle of sediment lodging, re-entrainment, scour, and bank collapse is suggested, which produces an overall negative budget for all sites when viewed on an annual basis, although the pattern and relative dominance of the processes and mechanisms changes from site to site. For the bulk of the watershed, snowmelt runoff is the main erosion process operating during most 'normal' years.

In April the main channel acts as a conduit through which sediments deposited on the main channel by summer events are re-entrained, whilst at this time limited headwater erosion occurs. In May, the continued late melt flows will (unless a major infrequent summer storm event occurred the previous summer) scour and entrain fresh sediment from the bed and banks of the main channel and the western headwaters. The erosion around the point where the headwater tributaries join, (around sites, 5, 6, and 7) in May is predicted to be between 10 and 100 times greater per unit channel length than elsewhere on the catchment (Figure 57). It is hypothesised that bank collapse events are focussed at this network point.

During the summer months a modest amount of erosion occurs which also concentrates on the lower part of the west and east forks of the headwaters, at 'X' and 'Y', where collapse material following winter failures may be rescoured from local slope bases, further rendering these sites unstable. Although these patterns might imply that the fingertip tributaries are also quite erosive during summer events, Figure 47 showed that in-channel scour may be less intensive than the summer predictions suggest because of lateral sediment input here. Below 'X', deposition occurs in summer on the main channel, but represents only a small fraction of the sediment scoured from these sites during melt. Considering events beyond those recurring annually, differenced run 10 sediment yield data suggest that patterns during large events are <u>less</u> depositional on the main channel, indicating a variable point of sedimentation for events of differing intensities and frequencies, and complex behaviour in the zone of domain overlap.

Colorado landscapes are usually viewed as predominantly surface wash landscapes, dominated by processes which emphasise a hillslope sediment source, and in which sediment is removed through a central

channel conduit to some sort of sediment 'sink' such as an alluvial fan (Schumm, 1977). The data presented here point to a somewhat different picture in which snowmelt dominates sediment removal on an annual basis, even in this south-facing topographic position. Spatially, channel erosion is a major source of sediment, and tributary junctions are the most rapidly eroding parts of the landscape by a factor of about 10 on an annual basis. There is perhaps a need to describe a longer-term erosion model for Alkali Creek in which change is led and controlled by conditions around tributary junctions.

Chapter 6

MORPHOLOGICAL RELATIONSHIPS

This Chapter searches for an explanation for the contemporary pattern of gully excavation as outlined in Chapter 2, using the flow models and sediment yield differences considered at some length in Chapters 3 to 5. Section I explores the background to the methods adopted in terms of the conceptual framework developed in Chapter 1. Following this, Section II considers the contemporary form relationships in the gully system, and in Section III the discussion broadens to consider the implications for longer-term change, beyond the period for which the R.R.G. records are available.

(I) METHODOLOGICAL CONSIDERATIONS

(A) Spatial and temporal autodependence

> "Cause and effect, means and ends, seed and fruit, cannot be severed, for the effect already blooms in the cause, the end pre-exists in the means, the fruit in the seed ..."
>
> Essays on Composition, Emerson.

It has been argued that because of the high level of autodependence in channel behaviour (Lehre, 1982), fluvial geomorphologists should ideally attempt to tackle the many levels of feedback between form and process by direct deterministic modelling (the 'realist' or 'white box' approach described by Chorley, 1978). Even in the short-term operation of the gully, local channel gradient is modified after each event by the erosional and depositional pattern shown on Figures 55 to 58, such that the distribution of shear stresses within the channel will be subsequently modified. This will have an enhancing or a damping effect on the spatial pattern of erosion and deposition during the next event, and so on. As well as recognising the 'normal' autodependence which occurs spatially across a channel reach (Thornes, 1982) or a knick-point (Pickup, 1975; Alexander, 1976), Lehre (1982) recognises three ways in which temporal autodependence operates "... first, extreme events undermine or weaken slopes so that they fail in subsequent smaller events. This destroys the independence of events ... Secondly, a

particularly large rainfall event may evacuate a large proportion of sediment stored in swales, thereby reducing the amount available for mobilisation in subsequent large storms. Thirdly, as sediment fill increases, its probability of failure in a storm of a given size increases... ".

Unfortunately, deterministic process-response models which tackle continual adjustment are so far only developed for hypothetical, constrained situations (Kirkby, 1971; Calver, Kirkby and Weyman, 1972; Smith and Bretherton, 1972; Huggett and Thomas, 1982), and very few address threshold behaviour (Thornes, 1981, 1983). There are in any case problems not only in the definition of initial conditions (Huggett, 1980) and instability (Thornes, 1981), but in the choice of a suitable algorithm for the process (Smith and Bretherton, 1972). These problems are particularly acute when real-world application of the scheme is intended. For these several reasons, the application of such an approach to the current investigation was abandoned.

Outside the possibility of direct modelling, it is usual at the meso-scale to establish inferential statistical links between 'process' and 'form', selecting the former from a range of possible independent indices of the flow regime, such as stream power, peak or bankfull discharge. Morphological parameters are then correlated with or regressed against these predictors to assess their validity or the level at which they may be argued to 'explain' form (the 'black box' or 'functionalist' position; Chorley, 1978a). These methods are adopted in this Chapter, and the independent variables chosen are first, the sediment yield differences mapped on Figures 55 to 58 because of their obviously predictive nature, and secondly the stream power of peak watershed events. These choices were made on the basis that "... morphology is essentially a response to the sediment behaviour of the channel", and "... it is assumed that entrainment and transport of sediments can be explained in terms of stream power" (Thornes, 1980).

In selecting regression tests, it is necessary to clarify two aspects of their use. These are first, the independence requirement for the observations in such tests; and secondly, the interpretation of the regression residuals in terms of the causal model. This

latter consideration introduces the idea that the two tests may be illustrating different aspects of watershed behaviour, so the following sections also discuss the level of explanation of geomorphic behaviour which can be attached to the two independent variables.

(B) The 'independent observations' requirement of regression tests.

Despite the clear importance of the spatial and temporal autodependent nature of channel response as outlined above, regression tests not only fail to address this important set of mechanisms, but most significance tests assume that it is not occurring. Despite a long history of the use of such tests in geomorphology (Leopold, Wolman, and Miller, 1964; Schumm, 1956; Dury, 1969; Graf, 1979; and discussed by Richards, 1982) in all these cases the strict independence requirements are not really being met, especially when data are contiguous observations on a single channel reach. One way to minimise the problem is to use data points on the tributary sites alone first (as these suffer less from auto-correlation) and to examine whether or not headwater trends are maintained on the main channel by reconducting tests with these points included. This compromise is made in the tests which follow.

(C) Sensitivity, threshold behaviour, and the interpretation of regression residuals

If the success of the simulations of water and sediment process presented in the last three Chapters is to be explored by inferential tests, interpretation of residuals must be undertaken with care given that the real causal mechanism is left undefined. In the quotation on page 6:1, Lehre (1982) suggests that channel form response to predicted patterns of erosion and deposition (in this case, the differenced yield data mapped on Figures 55 to 58) may not be a progressive adjustment of form, but may by contrast depend on how the spatial patterns of critical stress following a single event relate to the power of subsequent flows. Lehre (1982) showed that the manner in which channel sites are rendered sensitive to change is complicated by temporal autodependence, so that especially in a dual process landscape the timing of periods when

critical stress is exceeded is difficult to predict and may not necessarily be associated with peak runoff events. Additionally, once sites reach critical 'threshold' stress levels, subsequent erosion is focussed at just a few sites, where headcuts, bank collapse failures, or fan-head trenches may form. During the formation of such features, change is more 'explosive' than 'progressive', at least in the short-term. Particularly in the case of fan-head trenching, response may be considered 'catastrophic', in that network topology may be so radically modified by the mid-net integration of previously dissociated, discontinuous systems that the subsequent spatial intensity pattern of the whole network runoff processes themselves is altered. In such cases, a return to the original morphological state is impossible (Chapter 1).

It must therefore be assumed that the varying sensitivity of the landscape will tend to cause scatter around the relationship relating the sediment yield differences to morphology, and that as far as the sediment difference regression tests are concerned, a low coefficient of determination may not necessarily indicate that this chosen independent variable misrepresents channel process, merely that it does not predict threshold response to that process well.

Richards (1982) considers stream power to be a useful 'control' parameter in geomorphological investigations as it is a measure of the rate of doing work at a site. As this parameter incorporates channel gradient, and since Schumm (1980) considers this to be an important criterion in distinguishing gullied from ungullied locations, it might be argued that some index of stream power of peak watershed flows might perform well in the explanation of form response. Graf (1979a) has also shown that measures of flow force in conjunction with considerations of bed resistance works well in morphological explanation of sites of threshold exceedence. Consequently an index of stream power of peak flows might be anticipated, in conjunction with considerations of bed resistance, to show the excavation potential of event extremes, so that residuals may be interpreted in terms of threshold behaviour across materials of differing sensitivity and resistance (such as the sandstone ledges which are high resistance sites). However, partly because peak power indices are not frequency-weighted, high levels of explanation may mislead. This is considered next.

(D) Levels of explanation expected from these tests

The complex response of single process domains was discussed in Chapter 1, in which review several assumptions commonly associated with semi-arid landscapes were listed. One of these was that these regimes are considered to evolve almost entirely by the overcoming of resistance thresholds during intense, infrequent events. Harvey (1984a) considers that "... forms created by extreme events may suffer little modification from intermediate events", such that in the absence of a flushing mechanism associated with melt "... the persistence of extreme forms is high". The assumption here is that not only is the power of such extremes high, but also that smaller events are not capable of exceeding threshold stresses everywhere on the watershed and therefore make little, or only local impact, even if weighted for frequency. In an insensitive watershed, therefore, in a conventional semi-arid area, the power of extreme flows might be expected to be the 'best' explanatory tool.

It has already been suggested, however, that the nature of watershed materials is a crucial consideration in the determination of landscape sensitivity to the persistent versus the extreme events (Chapter 1). If easily eroded materials are present, and the less intense events dominate in terms of sediment removal, then the impact of even a major summer storm will persist less. The landscape will therefore reflect more closely the stream power and sediment removal patterns of the more frequent events. For the study area, it was shown in Chapter 5 that both melt and summer events carry sediment at high concentrations so that it was concluded (since no transport threshold emerges between the persistent and extreme events) that on parts of the watershed overwhelmingly affected by melt flows (the melt dominance domain) that the summer storms, however large, must be incapable of making a morphological impact on the channel which persists beyond the next snowmelt season. This conclusion is reached bearing in mind that even the 'freak' simulated watershed event removed a trivial amount of sediment in comparison to the annual snowmelt flushing. However, the emphasis on the spatial variability of process dominance in the channel system allows the observation that there are parts of the watershed far more sensitive to both the stream power and patterns of sediment removal of extreme summer events (Chapter 5). These

areas are the domains of summer storm dominance in the upper parts of the large discontinuous tributary and the east fork of the continuous headwater net. Because of the 'summer-sensitive' nature of these areas they may be anticipated to be more akin to conventional, non-melt semi-arid areas in their morphological response. By this is meant that these zones may have a more disjointed and interrupted geomorphic history characterised more by threshold behaviour around extreme events. This is not to say that threshold-exceeding behaviour does not occur on the main channel during extreme summer storms, but that the morphological record of such an event is not maintained in the latter location, because of the overwhelming impact of progressive melt scour.

These deliberations suggest that the annual sediment yield difference patterns described in Chapter 5 represent the most powerful independent tool for morphological explanation of the watershed, on the basis that these values are a measure of weighted watershed behaviour. Additionally, the power of peak simulated melt flow (during May) might be anticipated to behave well also, at least on those parts of the watershed in the melt dominance domain. However, any correlation between the power of summer extreme events and main channel morphology must not here be interpreted as a causal relationship for the reasons discussed above. In parts of the watershed where summer events dominate sediment removal, however, it may be that the power of an event such as run 10 could be a powerful tool in the prediction of sites of threshold-exceeding behaviour, since on these sites summer storm impact persists beyond the melt period. Also, since Graf (1979a) uses a measure of stream power in conjunction with considerations of bed resistance, the tool has the additional advantage of allowing the interpretation of plot residuals. The sections which follow, using both tools, consequently allow several questions concerning the sensitivity and nature of the watershed response to its prevailing climatic regime to be addressed more clearly than if either had been undertaken alone.

II REGRESSION TESTS

(A) Morphology and the differenced sediment yield of simulated events

The first independent parameters chosen to explore these links were the spatial sediment yield differenced data. Section B explores the role of the stream power of peak flows. In both cases the independent variables are treated as controls on form and form change. The gully cross-sectional size as mapped in 1975, and recent changes in gully size (1975-1980 on the large discontinuous tributary, and 1962-1975 everywhere except the network headwaters) are consequently treated as dependent or 'response' parameters.

(i) Methods

Watershed data were initially separated into three data sets; the network headwaters above and including site 'X', (56 data points, referred to here as UB.DAT); the main channel of the continuous net excluding site 'X' (47 data points, referred to here as LB.DAT) and the large discontinuous tributary data (33 data points, referred to here as LDT.DAT). For each set of data, two files were constructed, one to include the 'supply-limited' sediment yield differences for summer event calculations, and one to include the 'transport-limited' differenced yield data. For simplicity, these will be referred to as case A and case B, so that the six data files are UBA.DAT; UBB.DAT; LBA.DAT; LBB.DAT; LDTA.DAT; and LDTB.DAT.

Table X lists the variables in these files, which are included in full in Appendix 15. Only the large discontinuous gully was mapped in 1980, and only this and the main channel in 1962, so that differences in cross-sectional form are only available as listed.

The headwater data set were examined first (UBA.DAT, UBB.DAT) for reasons explained above. In all cases linear scatter plots were obtained first. Where these indicated a lack of normality, data were log-transformed. If product-moment correlations revealed significant relationships, regression equations were calculated.

Table X Variable definitions, and contents of datafiles listed as Appendix 15

(a) Headwater file

UBA.DAT, UBB.DAT

Variable Number	Variable Codename	Description	Previously Plotted On
1	ID	Routed ID number (Used in ROUTE.PAS)	n/a
2	XA	Cross-sectional area in 1975 in m^2	Figure 8
3	WINDIF	Winter sediment yield difference with distance, in kg/m.	Figure 57
4	SMLESS	'Average' summer sediment yield difference with distance, kg/m.	Figures 55 & 56
5	ANLESS	'Average' annual sediment yield difference with distance, kg/m	-
6	SMPLUS	Summer sediment yield difference with distance in kg/m. (including run 10)	Figures 55 & 56
7	ANPLUS	Annual sediment yield difference with distance, in kg/m. (including run 10)	Figure 58

(b) Main channel file

LBA.DAT, LBB.DAT

Variable Number	Variable Codename	Description	Previously Plotted On
1	ID	(AS ABOVE)	
2	XA		
3	ΔXA62	Cross-sectional area change between 1975 and 1962, in m^2	Figure 8
4	%ΔXA62	Percentage cross-sectional area change (1975-1962) over the 1962 value.	-
5	WINDIF	(AS ABOVE)	-
6	SMLESS		
7	ANLESS		
8	SMPLUS		
9	ANPLUS		

(c) Large discontinuous tributary file

LDTA.DAT, LDTB.DAT

Variable Number	Variable Codename	Description	Previously Plotted On
1	OLD ID	(AS ABOVE)	Figure 9
2	XA		
3	ΔXA75	Cross-sectional area change between 1980 and 1975 in m^2	Figure 9
4	ΔXA62	(AS ABOVE)	-
5	%ΔXA75	Percentage cross-sectional area change (1980-1975) over 1975 value	-
6	%ΔXA62	(AS ABOVE)	-
7	WINDIF		
8	SMLESS		
9	ANLESS		
10	SMPLUS		
11	ANPLUS		

(ii) Results

Initially, linear regressions were attempted between the relationships which proved to be significantly correlated in their untransformed state. Relationships were sought between the morphological and the differenced sediment yield variables by taking XA (var 2) as the dependent variable against the differenced variables (vars 3 to 7) in turn. As can be seen, from the results listed in Table XI, all plots (except for the XA/SMLESS relationship) are significant when all data points are considered, however, subsequent plots revealed that this was because of the strong skew in the original observations, such that the extreme value at site 'X', (Figure 7), caused the misleadingly good fit. When this extreme value was removed, the Table shows that the headwater data had considerably weaker relationships which only predicted the value of the extreme point in the loosest fashion. These observations relate to the data on both Table XI(a) and XI(b).

From these regression data, two main observations can be made :

(1) The 'all data' relationships are spurious because the extreme value removal reduces r^2 by at least 50% in all cases. However, some of the relationships without 'X' are still significant at the 5% level and additionally have similar regression coefficients and constants to those for the relationship with 'X' included, for instance the XA/ANPLUS relationship.

(2) In both Table XI(a) and (b), the regression constants and coefficients for the ANPLUS and SMPLUS relationships are similar to those for the ANLESS and SMLESS relationships, and fit slightly better.

As a result of these two observations, a decision was made to repeat the regression tests, but with log-transformed values. In these cases the extreme values are not widely separated from other data, so the 'no extreme' tests were not needed. Additionally, the regressions were only conducted with ANPLUS and SMPLUS because of observation (2) above. The results of the log-transformed tests are included in Table XII(a) and (b).

Table XI Sediment yield differences: Headwater regressions

(a)

Linear regressions : UBA.DAT.(using 'supply-limited' regression)						
Dep. var \ Indep.var		WINDIF	SMLESS	ANLESS	SMPLUS	ANPLUS
XA	n	56	56	56	56	56
	b	0.2787	8.0536	0.2757	3.5093	0.2588
	a	7.5185	6.8754	7.4060	6.1276	7.4059
	r	0.8535	0.5259	0.8545	0.8448	0.8540
	r^2	0.73	0.28	0.73	0.71	0.73
	seb	0.02	1.77	0.02	0.30	0.02
XA (less site 'X')	n	55	(no separation of extremes	55	55	55
	b	0.52		0.4882	3.5894	0.5128
	a	6.4825		6.4305	6.0694	6.1571
	r	0.4398		0.4379	0.3207	0.4502
	r^2	0.19		0.19	0.10	0.20
	seb	0.15		0.14	1.46	0.14

n = number of data points used
a = regression intercept
b = regression coefficient
r = product-moment correlation
r^2 = coefficient of determination
seb = standard error of b.

(b)

Linear regressions : UBB.DAT (using 'transport-limited' regression)						
Dep. var \ Indep.var		WINDIF	SMLESS	ANLESS	SMPLUS	ANPLUS
XA	n	56	56	56	56	56
	b	0.2786	0.25056	0.2662	0.7978	0.2078
	a	7.5185	6.0775	7.1285	6.4993	7.2287
	r	0.8535	0.5902	0.8561	0.8457	0.8542
	r^2	0.73	0.35	0.73	0.72	0.73
	seb	0.02	0.47	0.02	0.07	0.02
XA (less site 'X')	n	55	(no separation of extremes	55	55	55
	b	0.5275		0.4036	1.0933	0.4817
	a	6.4825		6.3405	5.6846	5.3114
	r	0.4398		0.4303	0.3406	0.4772
	r^2	0.19		0.19	0.12	0.23
	seb	0.15		0.12	0.41	0.12

Table XII Sediment yield differences: Headwater regressions (logged)

(a)

log/log regression, UBA.DAT (using 'supply-limited' regression)				
Dep. var \ Indep. var		WINDIF	SMPLUS	ANPLUS
XA	n	56	56	56
	b	0.2994	0.2551	0.3906
	a	0.6734	0.6796	0.5177
	r	0.5294	0.2363	0.4700
	r^2	0.28	0.06	0.22
	seb	0.07	0.14	0.10

(b)

log/log regression, UBB.DAT (using 'transport-limited' regression)				
Dep. var \ Indep. var		WINDIF	SMPLUS	ANPLUS
XA	n	56	56	56
	b	0.2994	0.2695	0.3910
	a	0.6734	0.5292	0.3974
	r	0.5294	0.2893	0.4274
	r^2	0.28	0.08	0.18
	seb	0.07	0.12	0.11

(n, a, b, r, r^2, and seb as on Table XI)

Clearly, summer relationships are poor, although those tabulated on Table XII(b) are slightly better than (a). The relationships listed on Table XII(b) have been plotted on Figure 59. Some observations can be made from the tabulated and plotted data.

(1) The fairly good relationship between the predicted annual sediment yield difference pattern, using a 'transport-limited' rating relationship and including the effect of a 'freak' event in the watershed, is largely a result of the pattern of winter differences in the headwater zone, which is a better fit than the annual pattern. The winter pattern dominates the pattern of annual differences, explaining the good relationship here. These observations support the conclusions made at the end of the last Chapter, in which it was argued that the continuous net was strongly influenced by sediment yield patterns during melt.

(2) The weak positive relationship between the summer yield differences (including a 'freak' event and using the 'transport-limited' rating regression) would have been considerably improved if allowance had somehow been made for the effect of lateral sediment supply (TR + P) on the first-order channel sites, as indicated on Figure 59. Figure 54 (and discussion) indicated that sediment differences at some sites might not solely reflect the exploitation of material in the channel cross-section, and Figure 47 suggested that in particular first order, finger-tip sites experience a large lateral sediment contribution (TR) not allowed for in the differencing calculations. In fact, the overall relationship in the headwaters would have been improved had such allowance been possible.

(3) The relationship between the predicted annual rate of sediment yield change with distance and the cross-sectional area of the gully is from Figure 59 ;

$$XA = 2.44(ANPLUS)^{0.39} \qquad 6:1$$

for which n = 56, r = 0.43

Although it might have been anticipated that the differenced yield data would predict gully excavation linearly, these results indicate

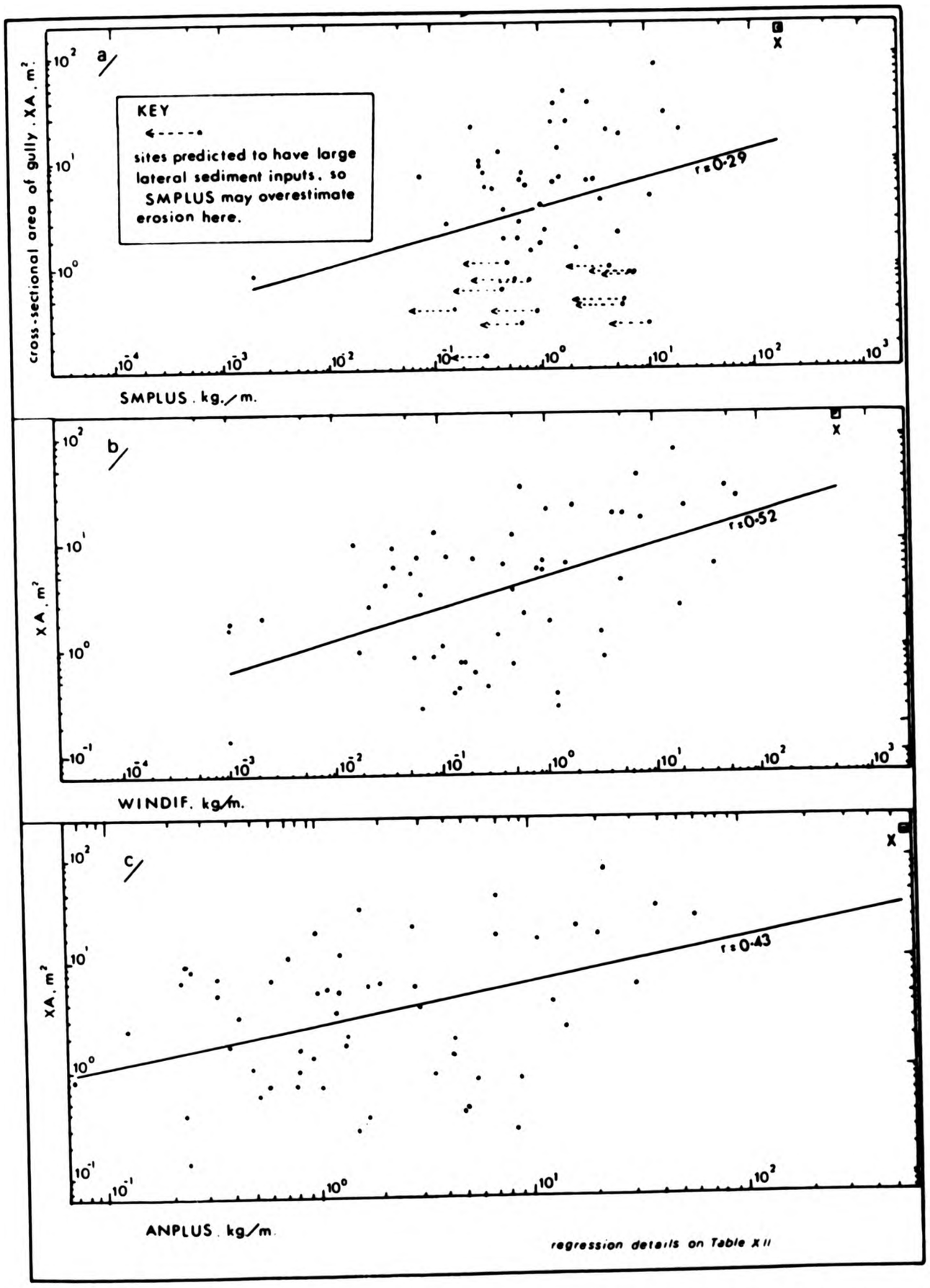

Figure 59 : Headwater log regressions relating cross-sectional gully size, XA, to (a) Spatial sediment yield differences in summer (SMPLUS, using n=0.81 regression); (b) Spatial sediment yield differences during melt (WINDIF); and (c) Annual spatial sediment yield differences (ANPLUS, using n=0.81 regression)

this is not the case, rather the non-linear exponent which characterise the best-fit log-transformed regression suggests a consistent overestimation by the independent variable, close to the cube root of differenced sediment yield values correlating most closely with overall channel size. However, it was explained in Chapter 5 that the differencing procedure was regarded as producing maps which merely describe the propensity for erosional or depositional behaviour, and the method may be consistently overestimating erosion on the heavily excavated sites during melt.

The next stage in the procedure was to conduct the same tests on the main channel data. Additionally, in this part of the watershed the variable ΔXA62 (variable 3) and %ΔA62 (variable 4) can be used as dependent variables and regressed against the seasonal and annual differenced data (variables 5 to 9) to assess the extent to which channel change in this period can be explained by yield change. Because cross-sectional area varied so little in this section, and possibly because the emplacement of check dams on the lower course of the channel tends to focus erosion and deposition locally (Chapter 2), no significant linear relationships were found between XA, ΔXA62, %ΔXA62 and the independent variables, none of the relationships having an r^2 value greater than 0.1. In general, the scatter on the plots overrode any weak trends because the XA values and changes all take similar values. As suggested earlier, the lack of accord between the 1962 and 1975 survey site locations (so that XA change was calculated by interpolation; Figures 8a and 9a), may explain the poor performance of XA-change variables in general.

Although log-transformations are inappropriate to the form change data because of negatives, the log-transformed cross-sectional size data for the continuous network were regressed against the variables WINDIF. ANSPLUS and SMPLUS to establish whether or not the main channel sites confirmed the headwater plot trend shown on Figure 59 or increased the scatter. The result of conducting these tests on the network data are included as Tables XIII(a) and (b), which includes the log-log regression results. Since on four sites deposition was predicted (Appendix 15) it was necessary to exclude those values from the regressions, again on the basis that logs of negative values are undefined. The cases where this applies have been identified (in these cases n = 99 rather than 103).

Table XIII Sediment yield differences : All continuous network regressions

(a)

log/log regressions : all network (using 'supply-limited' regression)				
Indep. var / Dep. var		WINDIF	SMPLUS	ANPLUS
XA	n	99	103	99
	b	0.308	- 0.0881	0.3593
	a	0.698	1.0337	0.5796
	r	0.7211	- 0.0299	0.6728
	r^2	0.52	0.00	0.45
	seb	0.03	0.29	0.04

(b)

log/log regression : all network (using 'transport-limited' regression)				
Indep. var / Dep. var		WINDIF	SMPLUS	ANPLUS
XA	n	99	103	99
	b	0.308	0.0905	0.4127
	a	0.698	0.7768	0.4294
	r	0.7211	0.0181	0.6690
	r^2	0.52	0.00	0.45
	seb	0.03	0.50	0.05

(n, b, a, r, r^2, and seb as defined on Table XI)

The plots of the XA/WINDIF and XA/ANPLUS relationships are shown on Figure 60. This Figure shows rather dramatically that the trend established for the headwater data is maintained on the main channel, and that both of the two plotted relationships are improved by the addition of the main channel data. In fact, the continuous network data shows that the winter regression equation explains 52% of the variation in the network pattern of cross-sectional size. In contrast, the summer yield differences are not related to the cross-sectional size of the gully at all. Figure 60 allows direct comparison with Figure 59 and these plots together supply very convincing evidence that the snowmelt sediment yield increase pattern on the watershed largely explains variations in channel size.

Finally, data for the large discontinuous tributary were considered. In these tests, the gully cross-sectional size, XA, was first considered against the five independent variables in log-transformed state, removing negative values as before, and using both the 0.81 and 0.76 sediment concentration regression exponent for yield difference calculations. No significant relationships were found, none having an r^2 value greater than 0.1. Despite this, XA was regressed against the log-transformed values of WINDIF, and ANPLUS using the 0.81 field regression (the two previously successful independent variables) for interest, and allowing direct comparison with Figure 60. These results are listed as Table XIV(a). Because it is believed that these poor relationships were again due to a lack of spread in the data, these relationships are not plotted, but the XA/ANPLUS data in logged form have been added to the network data to established whether or not they plot within the confidence limits of the Figure 60 regression. As can be seen from the resulting plot (Figure 61, Table XIV c), the spread of the original relationship is not improved. Nevertheless, the regression coefficient of the continuous network data relationship alone (0.417) had a standard error of 0.05. Since the addition of the discontinuous tributary XA/ANPLUS data only changes the regression coefficient to 0.377, and because this falls within the standard error of the continuous network regression coefficient, there is consequently only a 33% chance that the addition of the tributary data alters the continuous network relationship significantly. The same sort of conclusions were obtained from an examination of the XA/WINDIF regression relation regression coefficients.

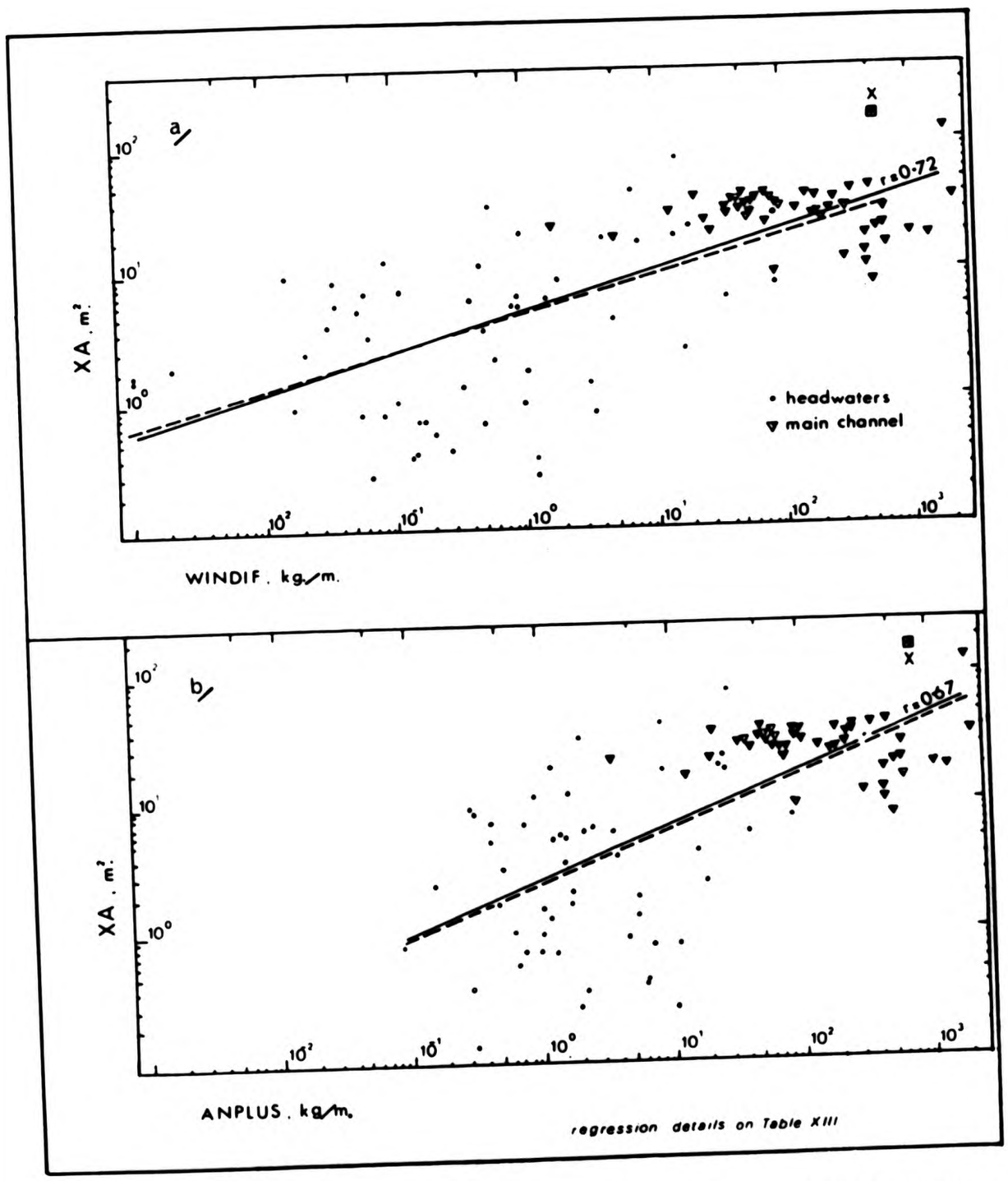

Figure 60 : Continuous network log regression relating cross-sectional gully size, XA, to (a) Spatial sediment yield differences during melt (WINDIF); and (b) Spatial sediment yield differences on an annual basis (ANPLUS, using n=0.81 regression for summer difference calculations)

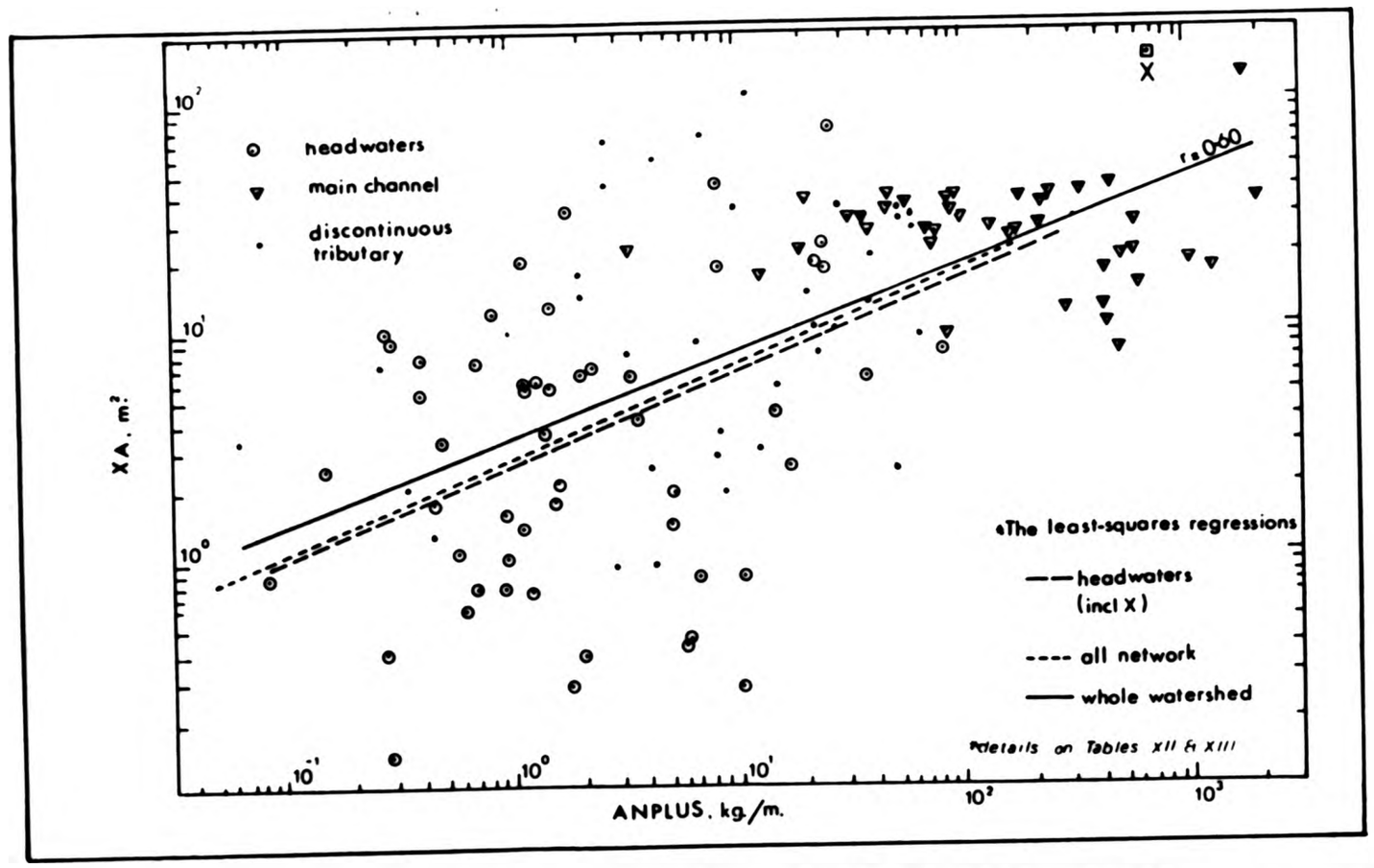

Figure 61 : Whole network log regression relating cross-sectonal gully size, XA in m^2, to the simulated spatial sediment yield differences calculated on an annual basis (ANPLUS, using the 0.81 regression for summer difference calculations)

Table XIV Sediment yield difference: Large discontinuous tributary, and entire watershed regressions.

(a)

log/log regressions, LARGE DISCONTINUOUS TRIB. (using 'transport-limited' regression)				
Indep. var→ / ↓ Dep. var.		WINDIF	SMPLUS	ANPLUS
XA	n	33	33	33
	b	0.1353	0.5248	0.3045
	a	0.8883	0.4506	0.5566
	r	0.2520	0.2492	0.1527
	r^2	0.06	0.06	0.025
	seb	0.09	0.37	0.35

(b)

linear regressions, LARGE DISCONTINUOUS TRIB. (using 'transport-limited' regressions)		
Indep. var→ / ↓ Dep. var		SMPLUS
△XA 62	n	33
	b	1.5137
	a	- 0.5293
	r	0.4694
	r^2	0.22
	seb	0.51
%△XA 62	n	33
	b	6.0459
	a	- 5.0205
	r	0.4665
	r^2	0.22
	seb	2.06

(c)

log/log regression, ENTIRE WATERSHED (using 'transport-limited' regression)		
Indep. var → / ↓ Dep. var		ANPLUS
XA	n	130
	b	0.3733
	a	0.5217
	r	0.5982
	r^2	0.36
	seb	0.04

(n, b, a, r, r^2, and seb as on Table X1)

The strength of the entire watershed relationship between these parameters is consequently established by these tests; 36% of the variation in the gully size can be explained by the predicted annual rate of sediment yield increase with distance (including the effect of a 'freak' event and using a 'transport-limited' regression for summer yield calculations) - Table XIV(c). The best-fit relationship is ;

$$XA = 3.32\ (ANPLUS)^{0.37} \qquad 6:2$$

for which n = 130, and r = 0.60 (negative values of ANPLUS excluded). This is significant at the 0.1% level.

Turning to the channel cross-sectional form change on the large discontinuous tributary, it was apparent that again log-transformations on these data were not desirable, first because the dependent variables ΔXA62, %ΔXA62, ΔXA75, and %ΔXA75 were more or less normally distributed, and second because they contain too many important negative values to make their exclusion viable.

The linear regressions between these four dependent variables produced only two relationships for which r^2 was over 0.1. Once again, the non-significant correlation data have not been listed, but on Table XIV(b) and Figure 62 the regressions for the two most significant relationships are shown. These are first the overall cross-sectional size change between the field surveys in 1962 and 1975 against the summer sediment yield differenced rate including the effect of a 'freak' event; and secondly the same relationship taking change as a percentage value (the ΔXA62/SMPLUS and %Δ XA62/SMPLUS relationships).

Although not highly significant, these results seem to suggest that between 1962 and 1975 the erosional and depositional pattern of summer events overrode the pattern predicted for melt alone. The failure of the ANPLUS or ANLESS parameter to explain form change in this period implies that either the summer events have not been sufficiently weighted here, or melt effects are overcalculated. However, Figure 62 does show that on some of the lower tributary sites erosion occurred, whereas the SMPLUS pattern predicts deposition and this anomaly could be accredited to melt erosion on

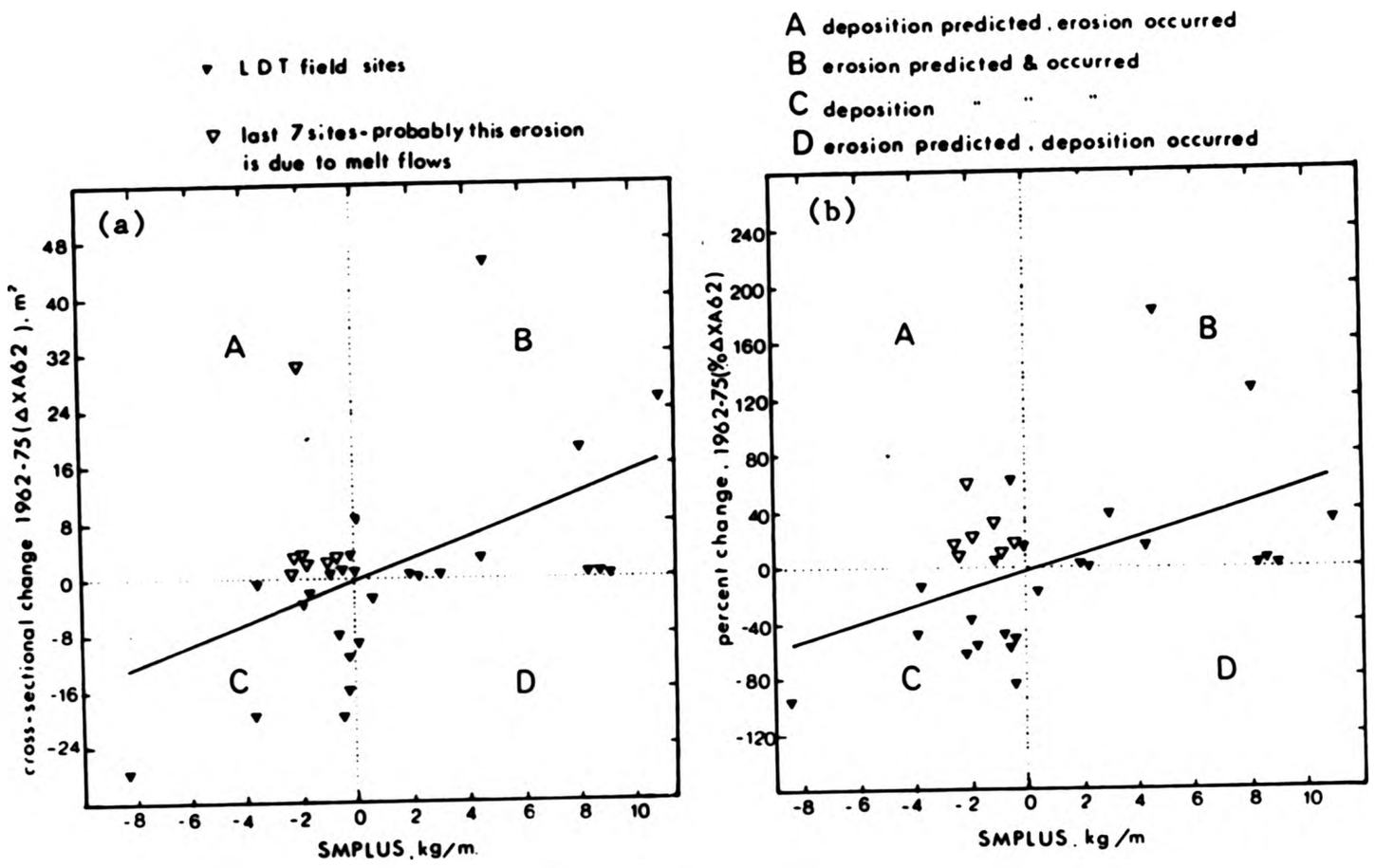

Figure 62 : Large Discontinuous Tributary, linear regressions relating (a) Cross-sectional gully size change 1962-1975 (ΔXA62); and (b) Percentage cross-sectional gully size change 1962-1975 (%ΔXA62) to the simulated summersediment yield differences with distance (SMPLUS, including the effect of run 10 and using the 0.81 regression for summer difference calculations)

the lower course. In any event, previous discussion (Section 1(D), and Chapter 5) suggested that this part of the watershed is more sensitive to summer storm behaviour, and these results certainly lend support to this argument.

(iii) Discussion

A good relationship between the annual pattern predicted for sediment removal rates (especially for the case which includes the effect of a 'freak' event), and overall gully size has been demonstrated for all watershed data. Additionally, since the winter yield pattern makes up most of the combined pattern, the cross-sectional area as mapped in 1975 reflects more the pattern of melt yield differences than summer patterns on most parts of the watershed. These conclusions relate less to the large discontinuous tributary, which is more affected by summer events in any case (Chapter 5), and on which poor relationships generally were found. A weak link between summer behaviour and the 1975-62 form change patterns has been demonstrated.

By and large the choice of 'supply-limited' or 'transport-limited' regression for the calculation of summer yields affects these conclusions in only a minor way. In most of the tests the 'transport-limited' case performs the best. Whether or not a 'freak' event is included in the calculations considerably affects the argument in several places, however. The inclusion of the effects of such an event improves, for instance, the prediction of channel change on the tributary data between 1962 and 1975. The fit of the data which include the effect of a 'freak' event is in all cases an improvement over results from tests where the event is excluded. This introduces the possibility that the events to which at least part of this system have responded over the period which saw the growth of the gully to its present size have not been modelled, events which have recurrence intervals beyond the timespan considered here.

(B) Morphology and the stream power of peak simulated events.

In a discussion of the independent 'control' parameters on channel form, Richards (1982) emphasises the importance of peak discharges

in morphological adjustments. However, he goes on to point out that "... the quantity of water imposed on the channel is less important than its capacity to do work". The energy expended by discharge Q in a unit channel reach in which the elevation drops from h_1 to h_2 is ;

$$\rho_w g Q h_1 - \rho_w g Q h_2 = \rho_w g Q(h_1 - h_2) = \rho_w g Q S \qquad 6:3$$

where ρ_w is water density
and S is channel slope = $(h_1 - h_2)$ on a unit channel length
and g is acceleration due to gravity

which is the rate of potential energy expenditure per unit length of channel (the rate of doing work, or stream power). Other alternative power criteria are available, and are listed by Richards (1982). Here work by Bagnold (1966), Yang (1972), Yang and Song (1979), and Yang, Song and Woldenburg (1981) have been of particular value and stream power has been used convincingly by Smith and Bretherton (1972) to develop a sediment transport model of basin evolution. Thornes (1980) similarly has recognised the value of this parameter as a 'control' parameter in explanatory models of sediment movement and morphological change.

The use of channel gradient, S, in the calculation of this 'control' variable involves a certain amount of circular reasoning, since it is clear that if XA is regarded as an index of the overall growth of the gully throughout its history obviously during this time channel gradient itself was a dependent and changing parameter. This issue raises again the temporal and spatial autodependence mechanisms discussed in Section 1(A). To circumvent the logistical difficulties here, it is assumed that during the time that saw the growth of the gully to its present size, an overall concavity must be assumed to have always characterised downstream channel gradient patterns. Schumm and Lichty (1965) saw the necessity for such artificial divisions of variable causality outside the possibilities of iterative modelling.

Strahler (1952) emphasised over thirty years ago the importance of considerations of force and resistance in geomorphic explanation.

More recently, Graf (1979,a) developed these ideas in a study of arroyo trenching, in which gully excavation was seen as the dependent variable, and stream power and bed resistance both equally important control parameters. He later showed how these data might be considered to occupy positions on a cusp catastrophe (Graf, 1979,b). Obviously materials of varying resistance to erosion will vary in their response to changes in stream power. Lithological variations across the headwaters of the study area do seem to affect channel morphology (Chapter 2), so in the analyses which follow the pattern of residuals from the regressions are considered in terms of these lithological variations in a manner similar to that employed by Graf (1979b).

(i) Methods

An index of power of the largest simulated summer event (the freak event, run 10) and of the stream power of the peak diurnal May flow was obtained in the following way. For QSMELT, the peak discharge value during melt (Appendix 7) was multiplied by the site gradient as mapped in 1975, the only year with a full watershed survey (gradient data in Appendix 3, resulting values in Appendix 16). For QSRN10, this same gradient was multiplied by the peak discharge of the 'freak' event obtained as described in Chapter 4. For plotting and regression purposes, these data were coupled with the morphological data (Appendix 15) and were initially separated into headwater data (QSUB.DAT), main channel (QSLB.DAT) and discontinuous tributary data (QSLDT.DAT). Examination of the raw data once again revealed a lack of normality in the distribution, and extremes were separated as for the differenced sediment yield data, and as a result, log transformations were considered necessary as before on all tests of channel morphology against stream power.

(ii) Results

Regression statistics for the significant regression relationships between the dependent variables XA, ΔXA62 and ΔXA75 (all logged, and also their percentage change values) have been listed on Table XV. As before, the headwaters are examined first.

Table XV : Stream Power regressions

(a)

log/log regression, QSUB.DAT			
Indep. var / Dep. var		QSMELT	QSRN10
XA	n	56	56
	b	0.4946	0.7401
	a	1.1728	0.2728
	r	0.5612	0.5938
	r^2	0.31	0.35
	seb	0.10	0.14

(b)

log/log regression, QSLB.DAT			
Indep. var / Dep. var		QSMELT	QSRN10
XA	n	47	47
	b	0.3480	0.6659
	a	1.1937	0.5321
	r	0.2209	0.5245
	r^2	0.05	0.28
	seb	0.23	0.16

(c)

log/log regression, ALL NETWORK DATA			
Indep. var / Dep. var		QSMELT	QSRN10
XA	n	103	103
	b	0.4738	0.8335
	a	1.1415	0.2778
	r	0.7354	0.7565
	r^2	0.54	0.57
	seb	0.04	0.07

(d)

log/log regression, LARGE DISC. GULLY			
Indep. var / Dep. var		QSMELT	QSRN10
XA	n	33	33
	b	0.0836	0.2255
	a	0.9337	0.7822
	r	0.0987	0.1482
	r^2	0.01	0.02
	seb	0.15	0.27

(e)

log/log regression, WHOLE WATERSHED			
Indep. var / Dep. var		QSMELT	QSRN10
XA	n	136	136
	b	0.4071	0.7713
	a	1.0584	0.3421
	r	0.6285	0.6713
	r^2	0.40	0.45
	seb	0.04	0.07

(n, b, a, r, r^2, and seb as defined on Table XI)

Table XV(a) shows a good relationship between headwater cross-sectional area and the power of both the melt and extreme summer event flows, that for the latter data having a higher regression coefficient because the stream power values increase more rapidly on this simulated flash flood (Figure 46). The main channel data, QSLB.DAT were examined next (Table XV(b)). Here the XA/QSRN10 relationship is significant, but not the melt relationship. Although the regression coefficient in the XA/QSRN10 relationship is lower (0.67) than that of the headwater relationship between these variables (0.74) the difference is within the standard error of the regression coefficients of both values, and despite the poor relationship between XA and QSMELT on the lower gully, the same observation could be made about the regression coefficients for these two data sets, justifying the use of a combined regression for all the network data. The XA/QSNR10 relationship is plotted on Figure 63, the XA/QSMELT relationship on Figure 64. Table XV(c) lists the regression statistics. On the plots the best-fit combined regression line, and that of the headwater data and the main channel data viewed alone have also been drawn in.

On the large discontinuous tributary, neither of the relationships tested on Figures 63 and 64 are significant for the system (Table XV(d), but despite this, these large discontinuous tributary data have also been plotted on the same axes as the data for the continuous network to test the data spread. On Figures 63 and 64, the regression equation for the whole watershed including the QSLDT.DAT data have been drawn in (Table XV(e)). Although in both cases the discontinuous tributary data do not improve the fit around the regression line, the data do plot within the confines of the confidence limits placed on the regression coefficients. The two best-fit relationships for the entire watershed are first, for the stream power of the melt flows ;

$$XA = 11.44(QSMELT)^{0.41} \qquad 6:4$$

for which n = 136, r = 0.63, r^2 = 0.40
and which is significant at the 0.1% level

and, second, for the stream power of the 'freak' event, run 10 ;

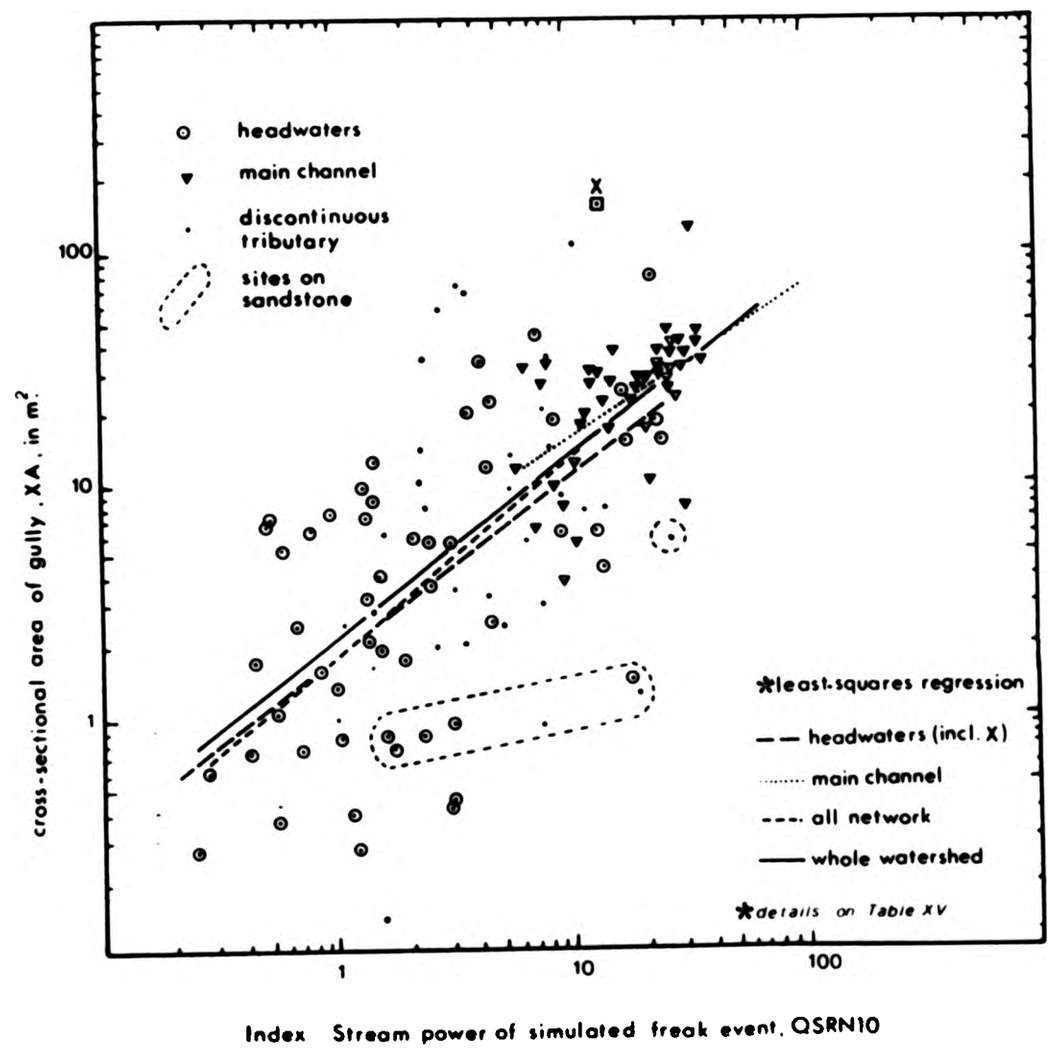

Figure 63 : Whole network log regression relating cross-sectional area of the gully in m^2, to Index stream power of simulated freak event run 10, QSRN10

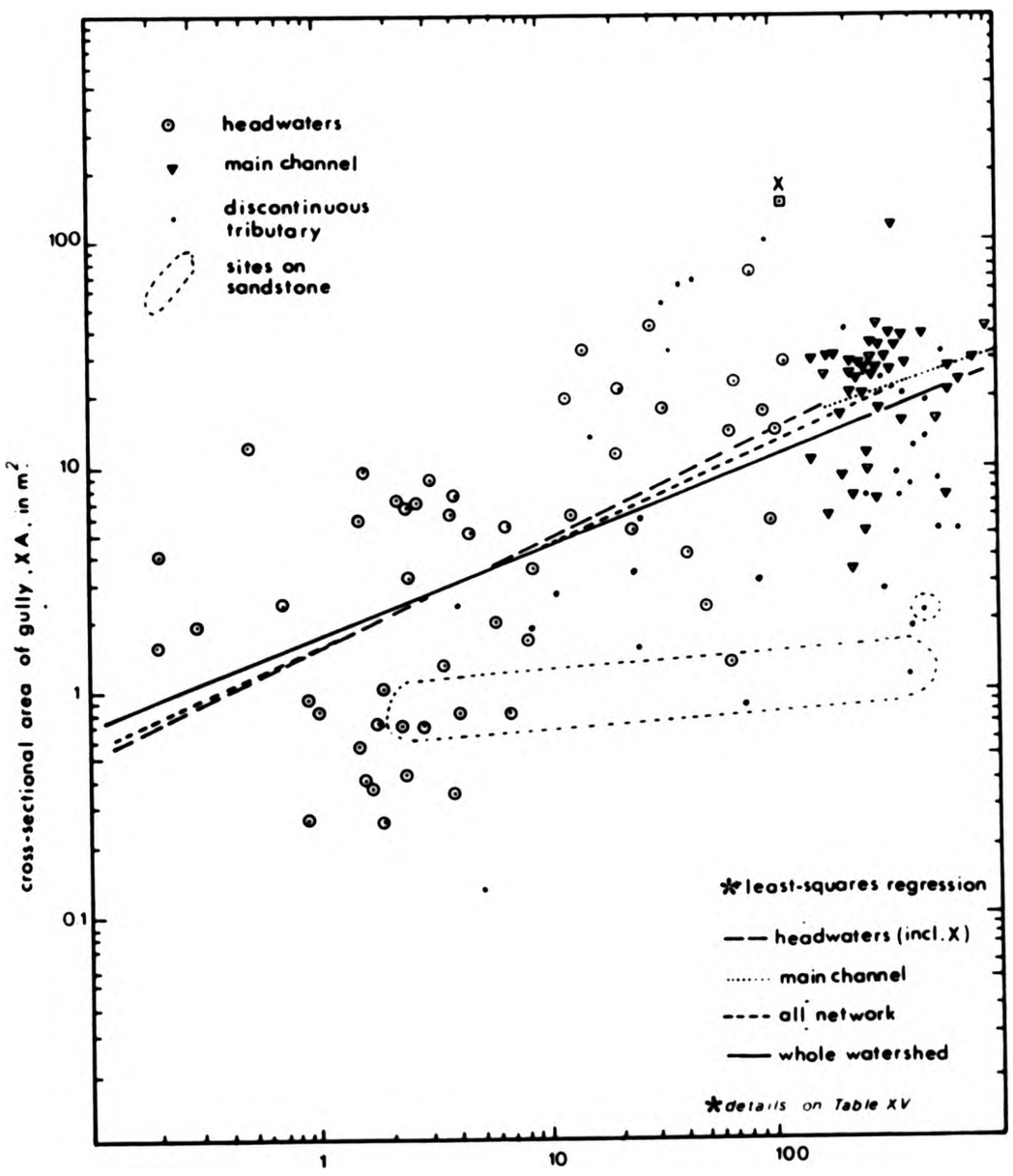

Figure 64 : Whole network log regression relating cross-sectional area of the gully in m^2, to Index stream power of simulated late melt daily peak flow, QSMELT

$$XA = 2.20(QSRN10)^{0.77} \qquad 6:5$$

for which n = 136, r = 0.67, r^2 = 0.45
and which is also significant at the 0.1% level.

(iii) Discussion, and the explanation of some power plot residuals

Graf (1981) observed from his fieldwork in the Henry mountains in Utah that "... when proceeding through a drainage network, the most powerful streams are those in the middle", showing that this can be argued to result from peak attenuation and transmission loss in combination with a decrease in channel gradient downstream. In Chapter 2, it was hypothesised that for summer events in the watershed a power pattern downstream which peaked at headwater junctions was likely for both processes, although for melt flows the power of all events would be much less likely to lose power as rapidly downstream as summer storms. The last section has demonstrated that these effects do occur as anticipated, and that perhaps not surprisingly these power 'peak' sites coincide with the location of the most heavily trenched sites on the watershed and incidentally localise the more common threshold-exceeding events (bank collapse and headcut locations).

Although from Table XV(e), the summer 'freak' event power pattern appears to 'explain' gully morphology 'better' than the melt events, Chapter 5 and sections I(D)a and II(A) above have demonstrated that in terms of sediment removal the melt events are overwhelmingly dominant on most watershed sites. Consequently it is concluded here that the good correlation between summer storm power patterns and patterns of watershed excavation represent the reinforcement of existing patterns presculptured by melt flows rather than a formative or direct causal link.

To summarise these results, the most important morphological control at Alkali Creek is the sediment removed during melt and the power pattern of these flows (Figures 60 and 63). In summer most small events are erosive in the headwaters and reinforce and destabilise further the scour and bank collapse at the main tributary junctions 'X', 'Y' and 'Z', but deposit a small amount of sediment on the main channel (Figures 55 to 58), and on the fan at the end of the large

discontinuous tributary. This sediment is removed the next spring by melt flows on the main channel but not completely on the tributary. On the main channel, melt flows remain erosive all the way down the watershed, and maintain the long axial channel here, which was described as a unique characteristic of melt semi-arid landscapes in Chapter 1. Large 'freak' occurrences in the summer reinforce the erosional tendencies on the main channel (Figure 62) but this is not to be regarded as a causal relationship.

(iv) Discussion of some power plot residuals

Scatter on the power plots can be explained in terms of variations in bed resistance. Using Figures 4, 7(back folder) and 8, sites which fall on mapped sandstone outcrops were identified. Of the headwater sites, only five could be confidently considered in this category, and three on the discontinuous tributary (Figure 9). These locations have been indicated on Figures 63 and 64. Clearly these points have very large residuals, and exclusion of these would improve the regression fit on these plots.

Graf (1979,a,b) examined the relationship between channel excavation and erosion 'force' (he used a tractive force estimate) for a variety of gullies in the Colorado Front ranges. He interpreted data points in these sorts of positions on his graphs in terms of Catastrophe Theory (Zeeman, 1976). In this perception, plots such as Figures 63 and 64 can be viewed as sections through a 3-dimensional cusp of the single-fold type. Graf (1979,b) suggested that in considering the situations in which arroyos were likely to trench, the cross-sectional area of the eroded form of the channel could be considered the dependent variable, and the two independent variables could be tractive force (or stream power), and bed resistance. The fold of the cusp is positioned at those values of power critical for trenching at specific bed resistance values, such that at critical values of power and resistance a knife-edge or threshold exists at which point either an increase in power or a decrease in resistance causes a catastrophic shift in gully form. Schumm (1980) saw this threshold to be triggered at critical valley gradients, but as he himself points out, his data could perhaps be better interpreted in the manner suggested by Graf (1979,b). Others have considered this model for other processes such as braiding

(Schumm, 1980; using the work of Lane, 1957, and Leopold and Wolman, 1957). In the study area, the existence of distinct, high resistance lithological units in the headwaters of the network focus trenching below these outcrops, yet on the ledges, characteristically small cross-sections are common.

The 'path' of a channel from the gully network headwaters to the basin mouth can be hypothetically traced with reference to the sort of 3-axial cusp figure drawn by Graf (1979b) in the following way. High up in the headwaters, the threshold stream power necessary for the initiation and maintenance of a trenched channel is easily exceeded, yet low overall power results in modest cross-sectional areas to the trenches formed, depending on the rate of discharge increase downstream. Entry on to the highly resistant sandstone unit may mean that stream power is now insufficient for trenching, and the water flow itself increases in width and decreases in depth as it traverses a low-angled ledge that it is incompetent to erode (Photo 23). Positive feedback ensues; deposition of material and the increased W/D ratio causes flow reduction by transmission loss, further reducing stream power. At these sites, the lower values of excavated cross-section will be found, positioned on the lower part of the cusp. If flow is sufficient to maintain continuity beyond the sandstone unit, entry onto the Wasatch shales once again may still, despite the lower of power in the previous section, be sufficient to overcome local, lowered resistance and trench once again. If stream power is insufficient to overcome this threshold for trenching, however, then the depositional phase will continue and eventually all flow will be lost and a mid-slope or mid-channel alluvial fan will form.

Much of what happens downstream from these sites depends on the rate of downstream discharge increase, and therefore on the watershed topological relationships, and the fan-formation stage may be forestalled by a sudden stream power increase which will be associated with a tributary junction. Because tributary junctions are likely to be erosive and heavily trenched by the persistent stream power increases which characterise such sites, headcuts form locally which may migrate up the channels, resulting in a morphological integration of the gully through alluvial deposits lying in the channel beds upstream. This is most likely to occur

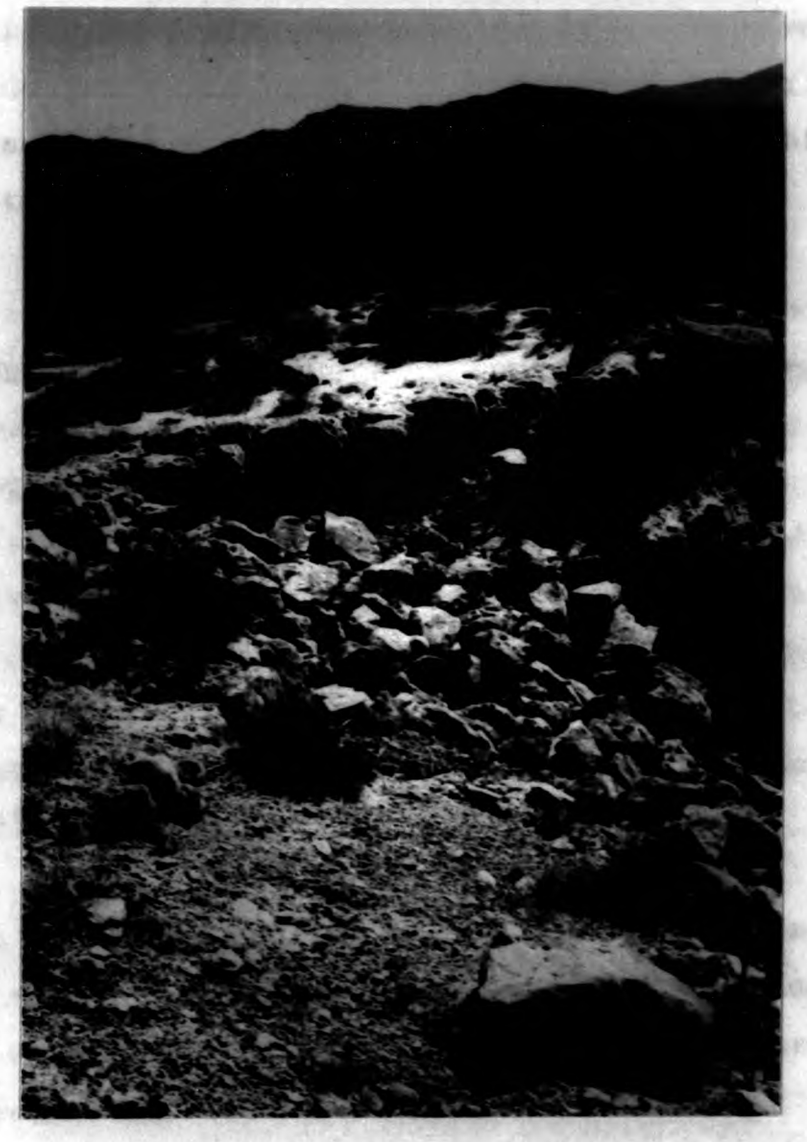

Photo 23 : The sandstone lens as experienced by the large discontinuous tributary. This exposure is in the bed of the channel, and clearly must affect the ability of normal watershed events to maintain a trenched channel form

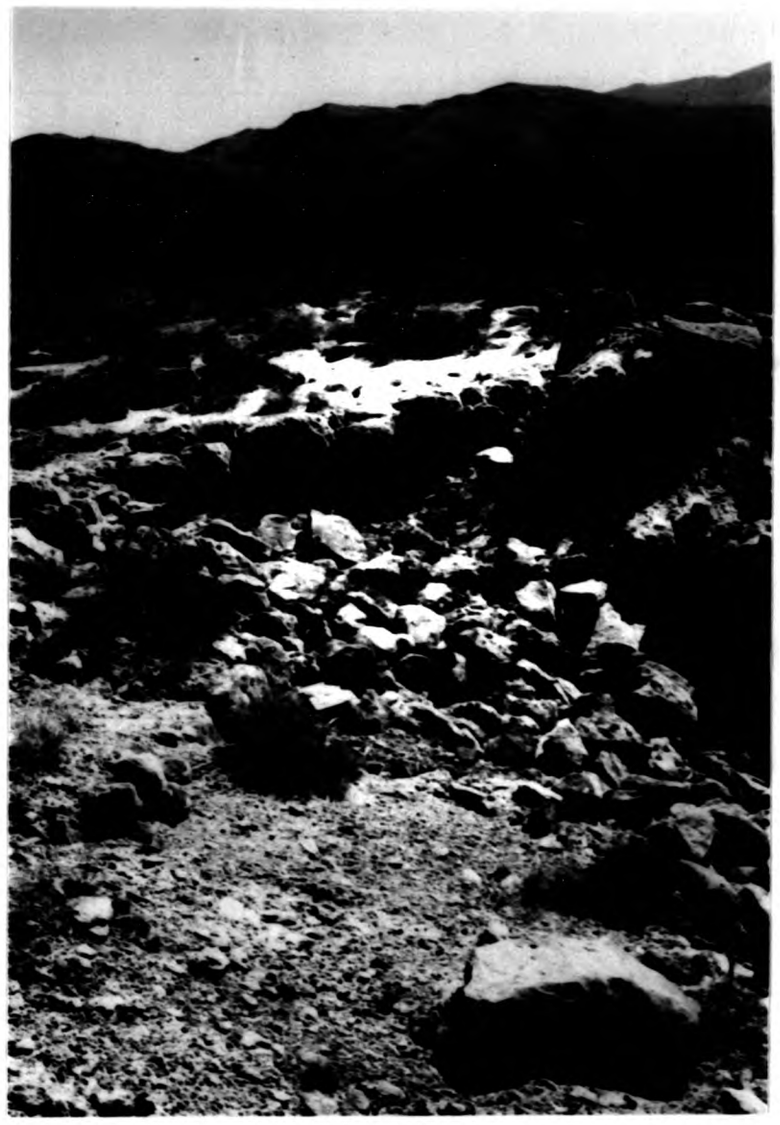

Photo 23 : The sandstone lens as experienced by the large discontinuous tributary. This exposure is in the bed of the channel, and clearly must affect the ability of normal watershed events to maintain a trenched channel form

during extreme events. Since the breaching of fans at the termination of discontinuous tributaries on flanking slopes is also indicated at such infrequent events, then the complete network may integrate internally in this way, and this may be the most significant gully growth mechanism characterising the area in the long-term. Heede (1977) has described the process from field observations elsewhere, and Graf (1983) also considers this sort of network integration.

In the study area, trenching and power increases will characterise the tributary junctions 'X', 'Y', and 'Z', but beyond these sites the contemporary form with low gradients will result in a lower stream power for flows even if discharge peaks increase. In the case of summer events, where attenuation of the peak also occurs, power will be dropping off spatially more rapidly than is the case during melt. During melt, the model presented here suggests that stream power on the continuous net increases once again towards the basin mouth, and this may explain the third re-scoured zone noted here (Chapter 2).

It is therefore not surprising that excavation is maximised at junctions, and that excavation is maintained, but to a lesser extent, on the main channel of the network, nor that a lack of continuity characterises the headwater tributaries. The combined stream power pattern of the two intensity domains viewed together is strongly reflected in the overall pattern of excavation, so that the power and excavation data, when projected from the 'cusp' onto the XA/QS axes, would show a spread not dissimilar to that found on Figures 63 and 64.

(C) Summary

Chapter 5 showed snowmelt to be by far the more important process on the main channel, and Section A in this Chapter has shown that the sediment yield differences of weighted snowmelt flows correlate well with morphology. It is consequently argued that despite a good agreement between the power of summer extreme events on this part of the watershed (Section B of this Chapter), melt flows maintain the morphology here, and all summer events, infrequent or not, rework trivial amounts of sediment and are cosmetic or insignificant.

Given that events with a recurrence interval beyond the 7 years for which records are available have not been considered, the correlation between QSRN10 and XA (Figure 62) does not reflect control of the dependent variable by the independent variable, merely that melt-controlled trends are reinforced during rare summer floods.

On a year that sees a major storm, however, some parts of the landscape will be preferentially eroded, and Section B showed that this is especially true in the summer storm dominance domain in the headwaters of the discontinuous gully. In such years, these parts of the watershed can be considered to be dominated by storms, and that the melt flows here are merely cosmetic. These latter parts of the watershed are therefore 'extreme-event sensitive', whereas the former are not. This has implications for the likelihood and location of threshold-exceeding, catastrophic events such as fan breaching and network integration.

The possibility that irreversible morphological changes may occur on some parts of the landscape, enlarging and integrating the network during threshold-exceeding episodes in a manner outlined in the previous section means that although the contemporary process simulations explain gully morphology quite well it is not possible to conclude that the history of the study area is one of slow, progressive adjustment to this climatic regime, and extrapolation into a longer-term perspective must be undertaken with caution.

III PERSPECTIVES

In a search for generality in this study we are constrained by the knowledge that the spatial controls on the two runoff processes presented here shift with basin shape, slope, and orientation, so that the patterns of sediment lodging and flushing described are specific to the unique topography, shape and orientation of the study area, since these factors determine the intensity of each domain in its generation phase, the spatial accumulation patterns of the generated flows, and consequently the relative dominance of each domain in various parts of the watershed. For example, the north-facing watershed above the study area (A in Photo 24) shows

Photo 24 : A comparison between the extent of vegetational response and erosion in the study area, its' north-facing neighbour (A) and the watershed immediately adjacent, which is quite extensively eroded (B)

Photo 24 : A comparison between the extent of vegetational response and erosion in the study area, its' north-facing neighbour (A) and the watershed immediately adjacent, which is quite extensively eroded (B)

little sign of summer storm erosion because of the protection provided by vegetation in this topographic position. As the proportion of the basin with predominantly north-facing slopes increases, so does the dominance of the snowmelt domain. A study in such a basin would have produced very differing patterns of sediment lodgement and flushing, although it is important to point out that the methodology would have remained entirely appropriate.

Similarly, the last paragraph of the preceding section suggests caution in temporal extrapolation. Since in the long-term network integration is strongly indicated, the conclusions must be seen to relate to the particular stage that the watershed has attained in its evolution. For confirmation of the transience of this watershed, the adjacent catchment (B on Photo 22) reveals greater erosion and a far greater extent of network integration than the study area, despite a similar lithology, orientation and size. The difference between the two basins possibly implies that gullying started earlier in basin A. There is evidence that a local rancher grazed this basin extensively in the 1930s, and it is still outside the boundary of the Alkali Creek Soil and Water Project fenceline; (Heede, 1977). Alternatively, growth rates for the basins are dissimilar. Since once thresholds are exceeded, growth usually accelerates until a new adjustment is made (Schumm, 1980), both explanations might apply. Given the large sediment yield budget for the study area, the state of this adjacent watershed is further evidence that Alkali Creek is in a state outside equilibrium.

These points emphasise the enormous variety necessarily found when two process intensity domains, each differently influenced by environmental controls in the generation phase, operate together on one piece of ground, especially when each process is erosive and when threshold behaviour is strongly inferred as a possible growth mechanism. What does emerge strongly from the research undertaken here is the worth of the dual domain approach, because this is the area in which generality clearly exists. Application of these same techniques in basins of differing orientations, size relationshps, topology, elevation, relief and stage would allow a calibration of some of the ways in which this variety might be expressed on other landscapes of the western slope.

In the two sections which follow, a comparison is made between the nature of dual domain semi-arid landscapes and the conventional picture of semi-arid terrain, and secondly the longer-term future of the watershed is finally considered.

(A) Comparison between the geomorphic nature of alpine and non-alpine semi-arid areas

Several observations may be made which distinguish dual domain landscapes from those without a significant winter snowfall. For instance, it was suggested in Chapter 1 that erosion at headwater sites is usually considered to be quite high in semi-arid areas, but it has emerged here that these sites are not as erosive as originally thought, and headwater sites may well be receiving more sediment laterally than can be removed by the normal flow range within the channel. Since in this orientation melt flushing is less effective in the headwaters than elsewhere, a picture of a network expanding by headward growth is inappropriate (Howard, 1971). By contrast, the overlap between the two domains at tributary junctions suggests that these sites are the most rapidly changing parts of the study area by a factor of at least 10 on an annual basis. Such reinforcement would not occur in the absence of the melt season. The particular emphasis that tributary junctions receive in snow-fed semi-arid areas may lead to an overall network concavity in the longer term.

It is also generally agreed (Chapter 1) that semi-arid landscapes, because of their intermittent climate, the power of the most extreme events, and the 'sediment-lodging' nature of more frequent events (Harvey, 1984a) are particularly suitable environments for the application of a geomorphic model in which internal change is led by the trenching of lodged deposits during extreme events and of episodic, sometimes irreversible change across thresholds (Schumm, 1973, 1977). It is implicit in this that threshold stress levels are exceeded only rarely and at those extremes. However, Chapter 1 showed that this line of argument depends not only on the magnitude and frequency of the more common watershed events, but also on their power in relation to the sensitivity of the watershed materials; in fact emphasis on extreme events assumes that most low power events mobilise sediment merely in trivial amounts. In the study area, all

events mobilise sediment readily, and Chapter 5 showed that when weighted for frequency, the diurnal fluctuations associated with a two month melt make this the dominant process, at least on the main channel. It has been shown that this explains the presence of the long axial channels which are common in the region. Again this stands in contrast to non-melt semi-arid areas.

As far as the assumption concerning the prevalence of sites suitable for trenching is concerned, previous discussions have suggested these are more limited under the alpine regime. Although it is true that the attenuation demonstrated to occur during normal summer events is likely to leave sediment lodged at tributary junctions, on alluvial fans, and on the top of sandstone ledges, two months of diurnal melt flows on the main channel ensure that such deposits are unlikely to persist beyond the next melt season. From the discussion at the end of Chapter 5, and surrounding Figures 55 to 58 it is possible to conclude that only where summer storms dominate or are more evenly balanced is sediment likely to build up by deposition the sort of lodged deposits and gradients which act as candidates for trenching during subsequent events of the 'catastrophic' kind. Such sites are located in the study area on the sandstone ledges of the headwater areas, and at the end of the large discontinuous tributary, a system far more evenly balanced in terms of two domains than elsewhere. The sandstone, being resistant to the power of all but the largest events, is the only part of the watershed where erosion is probably truly limited to such extreme occurrences. The fan at the base of the tributary, however, appears to be a suitable candidate for trenching at lower power events, as it is not constituted out of high resistant materials. It is also the most interesting possibility in terms of catastrophic change to the network.

(B) Thresholds and the long-term future of the watershed

It was pointed out in Chapter 1 that the threshold events which dominate the geomorphic picture, and the events which can be regarded as merely 'noise' around a trend of progressive adjustment to the prevailing climatic regime depend to a certain extent on the spatial and temporal scale at which the question of landform evolution is addressed. Given a uniformly low resistance landscape,

the sudden increase in power at tributary junctions and the consequent bank failure and formation of headcuts which migrate back up feeder channels might be regarded as a normal part of the progressive erosion of the landscape in the meso-scale, although each headcut and bank failure episode has by its very nature been caused by exceeding some local resistance threshold for the materials involved, and in the short-term and on a small spatial scale such events appear sudden, irreversible and morphologically catastrophic. At the meso-scale at which most of the arguments in this thesis have been addressed, such events are 'noise' around contemporary erosional trends.

Nevertheless, the operation of sites prone to persistent threshold-exceeding behaviour of this kind may have a different status in contemporary terms than they would have in landscapes where only overland flow operates. For instance, it was inferred in the previous section that sites 'X', 'Y', and 'Z' would probably be less prone to constant undermining in these latter circumstances since deposition associated with summer storms immediately below tributary junctions would build up in the absence of the spring rescouring of this material, assisting in the stabilisation of local slope-base conditions. In the dual operation of the system outlined here, tributary junctions are sites of domain 'reinforcement', and emerge as the most currently active sites, and because of this, the threshold-controlled process of bank collapse is encouraged here. In the context of an overall negative sediment yield budget at these sites, preferential destabilisation must continually occur, and although short-term stability may be attained immediately after a particular collapse episode by basal protection, the junction sites must be moving up-net in the timespan addressed here. Encouraged by this persistent instability, and given that these sites lose sediment at a rate which is between 10 to 100 times greater than elsewhere on the watershed, the watershed is tending towards overall concavity under its prevailing regime.

In the long-term, trenching of the fan at the end of the 'summer-sensitive' tributary is an increasing possibility. Chapter 5 showed that the fan at the end of the gully is formed and maintained by deposition of sediment which would occur below 'Z' in the absence of snowmelt flow but which is rescoured and then transferred further

down the long axial main channel by lateral flows during melt. However, this is unlikely to be a balanced process each year. A mainly depositional pattern of change between 1962 and 1975 suggests that summer events may have been more active during this period than melt (Section A of this Chapter), yet channel change between 1975 and 1980 shows a reworking of this deposited material, possibly under a period of melt dominance, which may have had the effect of moving material further down onto the front edge of the fan. At some stage it may be that slopes at the far end of the fan can build up in this way such that eventually intrinsic thresholds for trenching are exceeded without the need to invoke an extreme event for the process to occur. In any event, the breaching of this feature would result in network integration and a period of considerable local scour both above and below the point of fusion, and after which the overall mechanics of the dual process system would take on a new direction. It is felt likely that where summer events dominate landform evolution this type of network integration may be a very important aspect of long-term change.

As the whole topology of the network changes by internal integration the relative proportion of slopes of different aspects in tributary headwaters and the effective size of tributary contributing areas become themselves dependent, not independent variables. The details of this process are impossible to predict, but would inevitably lead to a more textured net, not dissimilar to that found in the neighbouring basin (B on Photo 24).

Markgraf and Scott (1981) present a pollen diagram taken from valley-bottom deposits on a site just below the mouth of the study area. From this is is possible to infer a progressive dessication of the local area dating from 5000 B.P. to the present. The mid-Holocene altithermal and the neo-glacial cooling found on other diagrams from the western slope are not apparent, although the sudden influx of sage and other xerophytic grasses and weeds at around 5000 B.P. follows patterns found elsewhere. During this warming period if must be assumed that it was the reduction in the dominance of snowmelt processes on the south-facing sites which partly explains the decline in the arboreal species, so that the sagebrush expanded into an area which was becoming increasingly responsive to summer storm behaviour. Although there are

conflicting views on the effect that such changes have on channel alluviation (Knox, 1984), these slow shifts in the relative dominance of the two process intensity domains described here during this time could explain the pre-existing valley-bottom alluvium into which the gully system is currently excavated as the result of an earlier, untrenched snowmelt regime. Only as parts of the landscape have become more sensitive to summer storms has the possibility of trenching become increasingly likely, leading to the situation seen today. Whatever the original trigger for this catastrophic response to an environmental warming, it is argued here that the extensive gullying found today was inevitable.

(C) Conclusions

Simulation of the prevailing watershed processes has revealed that even in this south-facing topographic position, snowmelt semi-arid landscapes are mostly eroded by snowmelt runoff and consequently stand in contrast to non-melt semi-arid landscapes in several important respects. Not only are headwater areas less erosive than expected but the tributary junctions, fed by melt flows, are chronically unstable, and are more erosive than would be the case without the flushing action of the spring melt. Apart from these sites, whose behaviour dominates the contemporary geomorphology, longer-term possibilities include the catastrophic trenching of fans, but it is argued that this process is restricted to those parts of watershed sensitive to summer storm behaviour; otherwise melt flushing is so effective that the opportunity for sedimentation and the formation of sites conducive to sudden and unpredictable trenching rarely occurs. In terms of the concepts outlined in Chapter 1, the main channel is likely to be 'morphologically overadjusted' to extreme events in a manner not normally found in non-melt semi-arid areas.

Conditions at tributary junctions suggest a meso-scale tendency towards concavity of the network, but in the longer term change is more likely to be controlled by the pattern of fusion of what must be assumed, at least initially, to be disconnected, discontinuous systems forming at points of inflexion on the pre-existing topography. Integration of these systems in time is encouraged by an increase in their effective catchment size as headwaters expand,

so that flows sufficient to trench the fans at their base are increasingly probable. This newly integrated system is annually scoured by snowmelt flows which remove the bulk of the contemporary sediment deficit, leading to a more extensive and more heavily scoured axial main channel than would otherwise be the case.

By initially identifying the general constraints on runoff from both snowmelt, and following summer storms on the watershed, and using these principles to simulate the details of the sediment transfer patterns which are unique to this basin it has been possible to show that these patterns explain contemporary morphology with some confidence. Combining these patterns has allowed the identification of sites of domain damping (of the summer storm efficacy on the main channel due to the dominance of melt flows here), of domain reinforcement (of both processes on headwater tributary junctions) and of longer-term oscillatory response (such as the fan at the termination of the large discontinuous tributary). In the context of a regional tendency towards dessication, the possibility of network integration through the fan seems increasingly likely. Given the current large negative sediment yield budget, the landscape must be viewed in this timespan as chronically transient such that the details of the longer-term picture remain obscure.

The main contribution that the study makes to geomorphology lies in the further application of the methodology which has been quite successfully established here. It has been demonstrated that if sufficient attention is paid to the spatial and temporal controls on runoff generation, then runoff simulation models can be produced which go some considerable way towards explaining a complex contemporary morphology. It is considered that these methods could be usefully applied outside this example with the aim of not only further calibrating the variety necessarily found when two hydrological process intensity domains operate together on one piece of ground, but of focussing more attention on the interesting, distinctive, but largely neglected geomorphology of snow-fed semi-arid erosion systems.

BIBLIOGRAPHY

AGRICULTURAL RESEARCH SERVICE, 1975, Prospective and Present technology for predicting sediment yields and sources, A.R.S., U.S.D.A., Proc. of Sediment yield workshop, Oxford, Missisippi, Vol. No. ARS-S-40.

ALLEN, J.R.L., 1970, Physical Processes of Sedimentation, London, Geo. Allen and Unwin.

ALEXANDER, D.A., 1976, "The role of profile disturbances in channel morphology." University College (Univ. of London) Dept. of Geog. Occ. Paper No. 29.

ANDERSON, E.A., 1973, "National Weather Service river forecast system - snow accumulation and ablation model." N.O.A.A. Tech. Memo. NWS-HYDRO-17, U.S. Dept. Commer., Washington, D.C.

ANDERSON, H.W., 1954, "Suspended sediment discharge as related to streamflow, topography and land-use," Trans. Am. Geophys. Un., v. 35(2), p. 268-281.

ANDREWS, E.D., 1982, "Bank stability and channel width adjustment, East Fork River, Wyoming." Wat. Res. Res.,18(4), p. 1184-1192.

BAGNOLD, R.A., 1966, "An approach to the sediment transport problem from general physics," U.S.G.S. Prof. Paper, 422I, 37p

BAILLE, I., FAULKNER, H. et. al., 1984, "Topography and piping in semi-arid areas, and some implications for soil conservation," Env. Mgmt. (in press)

BARNES, E.A., 1967, "Roughness characteristics of natural channels," U.S.G.S. Wat. Supp. Paper, 1849.

BARRY, R.G., 1981, Mountain Weather and Climate, Methuen, 313pp.

BELLO, A., et. al., 1978, "Field experiments to analyse runoff, sediment and solute production in the New England region of Australia," Zeit. fur Geomorph, Sp. Suppleband 29, p. 180-190.

BENNETT, J.P., 1974, "Concepts of mathematical modelling of sediment yield," Wat. Res. Res., v.10(3), p. 485-492.

BERGSTROM, F.W.,1980, "Episodic behaviour in badlands: efects on channel morphology and sediment routing," M.Sc. Thesis (un-pub.), C.S.U. Watershed Science Dept., Fort Collins, Colo.

BETSON, R.P., and ARDIS, V., 1978, "Implications for modelling in Surface-water Hydrology," Ch. 8 in Kirkby, M.J. (Ed.) Hillslope Hydrology, p. 295-316.

BETSON, R.P., and MARIUS, J.B., 1969, "Source areas of storm runoff", Wat. Res. Res., v. 5, p. 574-582.

BLONG, R.J., GRAHAM, O.P., and VENESS, J.A., 1982, "The role of sidewall processes in gully development, some N.S.W. examples", Earth Surface Processes, v. 7(4), p. 381-385.

BOGARDI, J., 1974, Sediment transport in alluvial streams, Budapest, Akademiai Kiado.

BOUWER, H., 1983, "Theoretical effects of unequal water levels in the infiltration rate determined with buffered cylinder infiltrometers", J. of Hydrology, v. 1, p. 29-34.

BRADFORD, J.M., et. al., 1978, "Failure sequence of gully headwalls in Western Iowa", Soil Sci. Soc. Am. J., v. 42, No. 2, p. 323-328.

BRADFORD, J.M., and PIEST, R.F., 1980, "Erosional development of valley-bottom gullies in the Upper Midwestern United States", in Coates and Vitek (Eds.) Thresholds in Geomorphology, Binghamton Series, p. 75-102

BRICE, J.C., 1966, "Erosion and deposition in the loess-mantled Great Plains, Medicine Creek Drainage basin, Nebraska", U.S.G.S. Prof. Paper No. 352-H.

BRUNSDEN, D., and THORNES, J.B., 1979, "Landscape sensitivity and change", T.I.B.G., v. 4, No. 4, p. 463-484.

BRUSH, L.M., and WOLMAN, M.G., 1960, "Knickpoint behaviour in non-cohesive materials: a laboratory study", Geol. Soc. Am. Bull., v. 71, p. 59-74.

BRYAN, R.B., 1974, "A simulated rainfall test for the prediction of soil erodibility", Zeit. fur Geomorph. Sp. Suppleband No. 21, p. 138-150.

BRYAN, R.B., et. al., 1978, "Factors controlling the initiation of runoff and piping in Dinosaur Provincial Park badlands, Alberta, Canada", Zeit. fur Geomorph. Sp. Suppleband No. 29, p. 151-168.

BULL, W.B., 1977, "The alluvial fan environment", Prog. in Physical Geog., v. 1, p. 222-70.

BUTCHER, G.C., and THORNES, J.B., 1978, "Spatial variability in runoff processes in an ephemeral channel", Zeit. fur Geomorph. Sp. Suppleband 29, p. 83-92.

CAINE, N., 1975, "An elevational control of peak snowpack variability", Wat. Res. Bull., Am. Wat. Res. Ass., v. II, No. 3.

CALVER, A., KIRKBY, M.J.,, and WEYMAN, D.R., 1972, "Modelling hillslope and channel flows", in Chorley (Ed.) Spatial analysis in Geomorphology, p. 197-220.

CAMPBELL, I.A., 1974, "Measurement of erosion on badland surfaces", Zeit. fur Geomorph. Sp. Suppleband No. 21, p. 122-137.

CAMPBELL, I.A., 1982, "Surface morphology and rates of change during a ten-year period in the Alberta badlands", in Bryan and Yair (Eds.) Badland Geomorphology and Piping, p. 221-238

CAMPBELL, I.A., and HONSAKER, J.L., 1982, "Variability in badlands erosion: problems of scale and threshold identification", in Thorn, C., (Ed.), Space and Time in Geomorphology, Geo. Allen and Unwin, p. 59-80.

CARSON, M.A., and KIRKBY, M.J., 1972, Hillslope, form and process, Cambridge.

CHIEN, N., 1952, "The efficiency of depth-integrating suspended sediment sampling", Trans. Am. Geophys. Un., v. 33, p. 693-698.

CHORLEY, R.J., 1978(a), "Bases for theory in Geomorphology", in Embleton, C., Brunsden, D., and Jones, D.K.C., Geomorphology; Present problems and future prospects, p. 1-12.

CHORLEY, R.J., 1978(b), "The hillslope hydrological cycle", Ch. 1 in Kirkby, M.J. (Ed.), Hillslope Hydrology, p. 1-32.

COATES, D.R., and VITEK, J.D., (Eds.), 1980, Thresholds in Geomorphology, Geo. Allen and Unwin, 498p.

COLMAN, C.A., and BODMAN, E.B., 1943, "Moisture and energy conditions during downward entry of water into soils", Proc. Soil. Sci. Soc. Am., v. 8, p. 116-122.

COOKE, R.U. and REEVES, R.W., 1976, Arroyos and Environmental Change, Oxford Res. Studies, 205p.

COWAN, R., 1966, "Snow survey at Schefferville, 1964-1965", McGill Sub-Arctic Res. Pprs., No. 21.

CURTIS, B.F., 1975, Cenozoic History of the Southern Rocky Mountains, Geol. Soc. Am., Boulder, Colo.

DAWDY, D.R., 1969, "Considerations involved in evaluating mathematical modelling of urban hydrologic systems", U.S.G.S. Water Supply Paper, No. 159D.

DIETRICH, W.E., et. al., 1982, "Construction of sediment budgets for drainage basins", in Swanson, F(Ed.) U.S.D.A. For. Serv. Pacific N.W. Rep. No. PNW-141, p. 5-23.

DIXON, R.M., 1975, "Infiltration control through surface management", Proc. of the A.S.C.E. Irrigation and Drainage Symposium on Watershed Management, Logan, Utah, Aug. 13-15, p. 543-567.

DULUZ-VIEIRA, J.H., 1983, "Conditions governing the use of approximation for the Saint-Venant equations for shallow surface water flow", J. of Hydrology, Vol. 60, p. 43-58.

DUNNE, T., 1978, "Field studies of Hillslope Flow Processes", Ch. 7 in Kirkby, (Ed.) Hillslope Hydrology, p. 227-289.

DUNNE, T., and BLACK, R.D., 1970, "Partial area contributions to storm runoff in a small New England watershed", Wat. Res. Res., v. 6, p. 1296-1311.

ELLISON, W.D., 1944, "Studies of raindrop erosion", J. Agric. Eng., v. 25, p. 131-6 and 181-2.

EMMETT, W.W., 1970, "The hydraulics of overland flow", U.S.G.S. Prof. Paper No. 662A, 68p.

EMMETT, W.W., 1978, "Overland Flow", Ch. 5 in Kirkby, M. (Ed.) Hillslope Hydrology, p. 145-170.

ERICKSON, D.E.L., LIN, W., and STEPPHUN, H., 1978, "Indices for estimating prairie runoff from snowmelt", Pap. Pres. to the Wat. Symp. - Wat. Stud. Instit. Appl. Prairie Hydrol., Saskatoon, Sask.

EVANKO, A.B., 1950, "A tin can infiltrometer with improvised baffle", Northern Rocky Mtn. Forest and Range Expt. Stn., Missoula, Mont., Research Note 76.

EVANS, R., 1980, "Mechanics of water erosion and their spatial and temporal controls: an empirical viewpoint", Ch. 4 in Kirkby and Morgan (Eds.) Soil Erosion, Wiley.

FAULKNER, P.H., 1970, "Aspects of channel and basin morphology in the Steveville badlands, Alberta", M.Sc. Thesis (unpub.) Dept. of Geog., Univ. of Alberta, Edmonton, Alta., Canada.

FIELD, W.G., and WILLIAMS, B.J., 1983, "A generalised, one-dimensional kinematic catchment model", J. of Hydrology, v. 50, p. 25-42.

FOSTER, G.R., and MEYER, L.D., 1972, "Transport of particles by shallow flow", Trans. A.S.C.E., v.15, p. 99-102.

FOSTER, G.R., and MEYER, L.D., 1975, "Mathematical simulation of upland erosion by fundamental erosion mechanics", in Agric. Res. Serv. (op. cit.).

FOX, C.J., and NISHIMURA, J.Y., 1957, "Soil Survey Report of the Alkali Creek Watershed", U.S.D.A. Forest Serv. U.S. Printing Office, Pub. M-5123. 43p.

FREEZE, R.A., 1978, "Mathematical models of Hillslope Hydrology" Ch. 6 in Kirkby, M. (Ed.), Hillslope Hydrology, p. 177-222.

GARY, H.L. and TROENDLE, C.A., 1982, "Snow accumulation and melt under various stand densities in Lodgepole pine in Wyoming and Colorado", U.S.D.A. Forest Service Res. Note RM-417.

GASKILL, D.L., and GODWIN, L.H., 1966, "Geological map of the Marcellina Mountain quadrangle, Gunnison County, Colorado", U.S.G.S. Quadrangle map, GQ-511.

GRAF, W.L., 1979(a), "The development of montane arroyos and gullies", Earth Surface Processes, v. 4, p. 1-14.

GRAF, W.L., 1979(b), "Catastrophe theory as a model for change in fluvial systems", in Rhodes, D.D., and Williams, G.P. (Eds.) Adjustments of the fluvial system, p. 13-34.

GRAF, W.L., 1982, "Spatial variation of fluvial processes in semi-arid lands", in Thorn, C. (Ed.) Space and Time in Geomorphology, Geo, Allen and Unwin, London, p. 193-217.

GRAF, W.L., 1983, "The arroyo problem" in Gregory, K.J. (Ed.) Background to Paleohydrology, Wiley, p. 279-297.

GREGORY, K.J., and WALLING, D., 1973, Drainage basin, form and process: a geomorphological approach, London, 456p.

GUTIERREZ, A.A., 1983, "Geomorphic processes and sediment transport in badland watersheds, San Juan County, New Mexico", Am. Geom. Field Gp. 1983 Conference in New Mexico: proceedings.

HACK, J.T., 1942, "The changing environment of the Hopi Indians of Arizona", Harvard Univ. Ethnology papers v. 35 No. 1, 85p. (cited in Wright and Frey, (Ed.) Quaternary Geology of the U.S., 1965, Princeton).

HACK, J.T., 1975, "Dynamic equilibrium and landscape evolution", in Melhorn, W. and Flemal, R. (Eds.) Theories of landform evolution, Binghamton, p. 87-102.

HACK, J.T., and GOODLETT, J.C., 1965, "Geomorphology and Forest Ecology of a mountain region in the Central Appalachians", U.S.G.S. Prof. Paper, No. 343, 31p.

HADLEY, R.F., 1962, "Some effects of microclimate on slope morphology and drainage basin development", in U.S.G.S. Research in 1961, p. 13-22.

HARVEY, A.M., 1974, "Gully erosion and sediment yield in the Howgill Fells, Westmorland", Ch. 5 in Gregory and Walling (Eds.) Fluvial Processes in Instrumented Catchments, I.B.G. Spec. Pub. 6, p. 45-58.

HARVEY, A.M., 1977, "Event frequency in sediment production and channel change", in Gregory (Ed.), River Channel Changes, p. 301-315.

HARVEY, A.M., 1982, "The role of piping in the development of badlands and gully systems in Southeast Spain", in Bryan and Yair (Eds.) Badland Geomorphology and Piping, p. 317-336

HARVEY, A.M., 1984a, "Geomorphological response to an extreme flood: a case from Southeast Spain", Earth Surface Processes and Landforms, v. 9, p. 267-279.

HARVEY, A.M., 1984b, "Seasonality of processes on eroding gullies: a twelve-year record of erosion rates", (in press): paper presented to the I.G.U., Paris, 1984.

HEEDE, B.H., 1966, "Design, construction and cost of Rock Check Dams", U.S. Forest Service Research Paper RM-20, 24p.

HEEDE, B.H., 1967, "The fusion of discontinuous gullies: a case study", Int. Ass. Sci. Hydrol. Bull., v. 12, p. 42-50.

HEEDE, B.H., 1971, "Characteristics and processes of soil piping in gullies", U.S.D.A. Forest Service Res. Paper RM-68, 15p.

HEEDE, B.H., 1974, "Stages of development of gullies in the Western United States of America", Zeit. fur Geomorph.. v. 18(3), p. 260-271.

HEEDE, B.H., 1977, "Case study of a watershed rehabilitation project, Alkali Creek, Colorado", U.S.D.A. For. Serv. Res. Paper RM-189, 18p.

HEWLETT, J.D., and HIBBERT, A.R., 1967, "Factors influencing the response of small watersheds to precipitation in humid areas", in Proc. Int. Symp. For. Hydrol., 1965, Penn. State, Univ., Pergamon, p. 275-290.

HILLS, R.L., 1970, "The determination of the infiltration capacity of field soils using the cylinder infiltrometer", B.G.R.G. Tech. Bull, No. 3, 24p.

HODGES, W.K., and BRYAN, R.B., 1982, "The influence of material behaviour on runoff initiation in the Dinosaur badlands, Canada", in Bryan and Yair (Eds.) Badland Geomorphology and piping, p. 13-47

HOGG, S.E., 1978, "The near-surface hydrology of the Steveville badlands, Alberta", M.Sc. Thesis (Unpub.) Univ. of Alberta, Edmonton, Alberta, Canada.

HORTON, R.E., 1933, "The role of infiltration in the hydrological cycle", Trans. Am. Geophys. Un., v. 14, p. 446-460.

HORTON, R.E., 1939(a), "The interpretation and application of runoff-plot experiments with reference to soil erosion problems", Proc. Soil Sci. Ass., v. 3, p. 340-349.

HORTON, R.E., 1939(b), "Analysis of runoff-plot experiments with varying infiltration capacity", Trans. Am. Geophys. Un., v. 20, p. 693-711.

HORTON, R.E., 1945, "Erosional development of streams and their drainage basins, hydrophysical approach to quantitative morphology", Bull, Geol, Soc. Am., v. 56, p. 275-370

HOWARD, A.D., 1971, "Simulation of stream networks by headward growth and branching", Geol. Anal., v. 3, p. 29-50.

HUGGETT, R., 1980, Systems analysis in Geography, Oxford.

HUGGETT, R., and THOMAS, R.W., 1980, Modelling in Geography: a mathematical approach, Harper and Row, London.

HUNT, C.B., 1956, "Cenozoic geology of the Colorado Plateau", U.S.G.S. Prof. Paper, No. 279, 99p.

JACKSON, M.C., 1978, "Snow cover in Britain", Weather, v. 33, p. 298-309.

JONES, A., 1971, "Soil piping and stream channel initiation", Wat. Res. Res., v. 7, p.602-610.

KELLEY, C., 1951, quoted in Bear, F., Soil Chemistry, 1963, Ch. 3: "Chemistry of saline sodic soils".

KEPPEL, R.V., and RENARD, K.E., 1962, "Transmission Losses in ephemeral stream beds", Proc. Am. Soc. Civil Eng: J. of Hydraulics Div., HY3, p. 59-68.

KIRKBY, M.J., 1969, "Infiltration, throughflow and overland flow" and also, "Erosion by water on hillslopes", parts 5(1) and 5(2) of Ch. 5, in Chorley (Ed.), Water, Earth and Man, Methuen.

KIRKBY, M.J., 1971, "Hillslope process-response models based on the continuity equation", T.I.B.G., Spec. Pub. No. 3, p. 15-30.

KIRKBY, M.J., 1972, "Surface water erosion", Ch. 2:8 in Carson and Kirkby (Eds.), Hillslope, form and Process, Camb. Univ. Press.

KIRKBY, M.J., 1976, "Tests of the random network model and its application to basin hydrology", Earth Surface Processes, v. 1:3, p. 197-213.

KIRKBY, M.J., 1978, Hillslope Hydrology, 389p.

KIRKBY, M.J., 1980a, "The streamhead as a significant geomorphic threshold", in Coates and Vitek (Eds.), Thresholds in Geomorphology, Binghamton Series, p. 53-74.

KIRKBY, M.J., 1980b, "Modelling water erosion processes", Ch. 6 in Kirkby and Morgan (Eds.), Soil Erosion, Wiley.

KIRKBY, M.J., and CHORLEY, R.J., 1967, "Throughflow, overland flow and erosion, "Bull. Int. Ass. Sci. Hydrol., v. 12, p. 5-21.

KIRKBY, A.V.T., and KIRKBY, M.J., 1974, "Surface wash at the semi-arid break in slope", Zeit. fur Geomorph., Sp. Suppleband 21, p. 151-176.

KIRKBY, M.J., and MORGAN, R.P., 1980, Soil Erosion, Wiley.

KNAPP, B.J., 1978, "Infiltration and storage of soil water", Ch. 2 in Kirkby (Ed.), Hillslope Hydrology, p. 43-73.

KNOX, J.C., 1984, "Response of river systems to Holocene Climates", Ch. 3 in Wright (Ed.), Late Quaternary Environments in the United States, v.2, The Holocene.

KOTTOWSKI, F.E., et. al. 1965, "Quaternary geology of the Southwest", in Wright and Frey (Eds.), Quaternary of the U.S., Princeton, p. 287-298.

LANE, E.W., 1957, "A study of the shape of channels formed by natural streams flowing in erodible materials", M.R.D. Sediment Series, No. 9; U.S. Army Div., Missouri Riv. Corps. of Eng., Nebraska.

LANGBEIN, W.B., and SCHUMM, S.A., 1958, "Yield of sediment in relation to mean annual precipitation", Tr. Am. Geophys. Un., v. 39, p. 1076-1084.

LARONNE, J., 1982, "Sediment and solute yield from Mancos Shale hillslopes, Colorado and Utah", in Bryan and Yair (Eds.), Badland Geomorphology and Piping, p.181-194.

LAUSCHER, F., 1976, "Methoden zur Weltclimatologie der Hydrometeore. Der Antel der festen Niederschlags am Gemantriederschlag", Arch. Met. Geophys. Biokl., B.v. 24, p. 129-76.

LEAF, C.F., and BRINK, G.E., 1973, "Computer simulation of snowmelt within a Colorado subalpine watershed", U.S.D.A. For. Serv. Res. Paper, RM-99.

LEE, I.K., 1978, (Eds.), Soil Mechanics-selected topics, Butterworths, London.

LEHRE, A.K., 1982, "Sediment budget of a small coastal range drainage basin in North-Central California", in Swanson, F.J. (Ed.), Sediment budgets in Forested Drainage basins, U.S.D.A. For. Serv. Tech. Rept. PNW-141.

LEOPOLD, L.B., 1978, "El Asunto del Arroyo", in Embleton, C., Brunsden, D., and Jones, D., Geomorphology: present problems and future prospects, Oxford, p. 25-39.

LEOPOLD, L.B., and MADDOCK, T., (Jr.), 1953, "The hydraulic geometry of stream channels and some physiographic implications", U.S.G.S. Prof. Paper. No. 252, p. 1-57.

LEOPOLD, L.B., and WOLMAN, M.G., 1957, "River and channel patterns; braided, meandering and straight", U.S.G.S. Prof. Paper. No. 282-B, p. 39-85.

LEOPOLD, L.B., WOLMAN, M.G., and MILLER, J.P., 1964, Fluvial Processes in Geomorphology, Freeman, 521p.

LINSLEY, R.K., 1944, "Use of nomograms in solving streamflow routing problems", Civ. Eng., v. 14, p. 209-210.

LINSLEY, R.K., KOHLER, M.A., and PAULHUS, J.L.H., 1949, Applied Hydrology, McGraw-Hill, 689 pp.

MALE, D.H., and GRAY, D.M., 1981, Handbook of Snow, Principles, Processes and Use, Pergamon, Toronto, 765p.

MARKGRAF, V., AND SCOTT, L., 1981, "Lower timberlime in Central Colorado during the last 15000 years", Geology, 9, p. 231-234.

MEADE, R.H., 1978, "Sources, sinks and storage of river sediment in the Atlantic drainage of the United States", J. Geol., v. 90, No. 3, p. 235-252.

MEIMAN, J.R., 1968, "Snow Hydrology related to elevation, aspect and forest canopy, in Snow Hydrology, Proceedings of workshop Seminar, Can. Nat. Comm. for I.H.D., p. 34-47.

MEYER, L.D., and WISCHMEIER, W.H., 1969, "Mathematical simulation of the process of erosion by water", Trans. Am. Soc., Agric. Eng., v. 12(6), p. 754-758.

MITCHELL, J.K., and BUBENZER, G.D., 1980, "Soil Loss estimation", Ch. 2 in Kirkby and Morgan (Eds.), Soil Erosion, Wiley.

MOEYERSONS, J., and PLOEY, J. de, 1976, "Quantititative data on splash erosion, simulated on unvegetated slopes", Zeit. fur Geomorph., Sp. Suppleband, v. 25, p. 120-131.

MOSLEY, M.D., 1972, "Evolution of a discontinuous gully system", A.A.A.G., v. 62, p. 655-663.

MURPHY, J.B., DISKIN, M.H., and LANE, L.J., 1972 "Bed material characteristics and transmission losses in an ephemeral stream", Ariz. Acad. of Sci.; Hyd. Section II.

MUSGRAVE, G.W., 1935, "The infiltration capacity of soils in relation to the control of surface runoff and erosion", J. Am. Soc. Agron., v. 27, p. 336-345.

MUSGRAVE, G.W., 1947, "The quantititive evaluation of factors in water erosion", J. Soil and Water Conserv., v. 2(3), p. 133-138.

MUSGRAVE, G.W., and HOLTAN, H.N., 1964; Ch. 12 in Chow, Ven Te (Ed.), Handbook of Applied Hydrology.

NADOLSKI, J.A., BROWN, J.C., and SKAU, C.M., 1980, "Sediment loads from headwaters of the East Sierra watersheds", Nevada Univ. System; Recco, Desert and Research Institute, 29p.

NEAL,. J.H., 1938, "The effect of the degree of slope and rainfall characteristics on runoff and soil erosion", Miss. Agric. Gp. Stn. Res. Bull., No. 280.

PATTON, P.C., and SCHUMM, S.A., 1981, "Ephemeral-stream processes - implications for studies of Quaternary Valley Fills", Quat. Res., v. 15, p. 24-43.

PECK, E.L., 1972, "Relation of orographic precipitation patterns to meteorological parameters", in W.M.O., v. 2, p. 234-242.

PHILIP, J.R., 1957, "The Theory of Infiltration", Soil Sci., v. 83; p. 345-357, 435-448, v. 84; p. 163-177, 257-264, 329-339, v.85; p. 278-286, 333-337.

PICKUP, G., 1975, "Downstream variations in morphology, flow conditions and sediment transport in an eroding channel", Zeit. fur Geomorph., v. 19(4), p. 443-459.

PIEST, R.F., 1965, "The role of the large storm as a sediment contribution", Proc. Fed. Int. agency. Sed. Conf; U.S.D.A. Misc. Pub., No. 970, p. 97-108.

PIEST, R.F., et. al. 1975, "Sediment movement from loessial watersheds", in Agricultural Res. Serv. pub. No. ARS-S-40, Oxford, Mississippi.

PLOEY, J. de, and GABRIELS, D., 1982, "Measuring soil loss and experimental studies", Ch. 3 in Kirkby and Morgan (Eds.), Soil Erosion, Wiley.

RACHNER, M., 1975, "A model of the melting process of the snow cover as part of catchment models", I.A.S.H. Proc. of the Bratislava Symposium, Pub. No. 115, p. 198-202.

RAGAN, R., 1966, "Laboratory evaluation of numerical flood routing techniques for channels subject to lateral inflows", Wat. Res. Res. v. 2(1), p. 111-121.

RAUDKIVI, A.J., 1967, Loose boundary hydraulics, Pergamon, Oxford.

RENARD, K.G., and KEPPEL, R.J., 1966, "Hydrographs of ephemeral streams in the Southwest", Am. Soc. Civ. Eng; J. of Hyd. Div., v. 92, NY2, p. 33-52.

RENFRO, G.W., 1972, "Use of erosion equations and sediment-delivery ratios for predicting sediment yield", in Agr. Res. Serv., ARS-S-40, Oxford Mississippi.

RHODES, D.D., and WILLIAMS, G.P., 1979, Adjustments of the Fluvial System, Geo. Allen & Unwin, London, 371p.

RICHARDS, K., 1982, Rivers: Form and process in alluvial channels, Methuen.

RODRIGUEZ-ITURBE, I., and VALDES, J.V., 1979, "The geomorphic structure of hydrologic response", Wat. Res. Res., v. 15(6), p. 1406-1420.

ROUSE, W.R., 1970, "Relations between radiant energy supply and evapotranspiration from sloping terrain; an example", Canadian Geographer, v. 14, p. 37.

RUBIN, J., 1966, "Theory of rainfall uptake by soils initially drier than their field capacity and its applications", Wat. Res. Res., v. 2(4), p. 739-749.

SCHICK, A.P., 1974, "Formation and obliteration of desert stream terraces - a conceptual analysis", Zeit. fur Geomorph.. Sp. Suppleband No. 21, p. 88-105.

SCHICK, A.P., 1977, "A tentative sediment budget for an extremely arid watershed in the southern Negev", in Doehring (Ed.), Geomorphology in Arid Regions, Proc. 8th, Geom. Symp., Binghampton, p. 139-163.

SCHUMM, S.A., 1956(a), "The role of creep and rainwash on the retreat of badland slopes", Am. J. Sci., v. 254, p. 693-706.

SCHUMM, S.A., 1956(b), "The evolution of drainage systems and slopes in badlands at Perth Amboy, New Jersey", Bull. Geol. Soc. Am., v. 67, p. 597-646.

SCHUMM, S.A., 1961, "Effect of sediment characteristics on erosion and deposition in ephemeral stream channels", U.S.G.S. Prof. Paper, No. 352C, p. 31-70.

SCHUMM, S.A., 1964, "Seasonal variations of erosion rates and processes on hillslopes in western Colorado", Zeit. fur Geomorph., Sp. Suppleband, No. 5, p. 215-237.

SCHUMM, S.A., 1973, "Geomorphic thresholds and complex response of drainage systems", in Morisawa, M. (Ed.), Fluvial Geomorphology, Binghamton, p. 299-309.

SCHUMM, S.A., 1977, The Fluvial System, New York, Wiley.

SCHUMM, S.A., 1980, "Some applications of the concept of geomorphic thresholds", in Coates, D.R., and Vitek, J., (Eds.), Thresholds in Geomorphology, p. 473-486.

SCHUMM, S.A., and HADLEY, R.F., 1957, "Arroyos and the semi-arid cycle of erosion", Am. J. Sci., v. 255, p. 161-74.

SCHUMM, S.A., and LICHTY, R.W., 1965, "Time, Space an Causality in Geomorphology", Am. J. Sci., v. 263, p. 110-119.

SCOGING, H., 1982, "Spatial variations in infiltration, runoff and erosion on hillslopes in semi-arid Spain", in Bryan and Yair (Eds.) Badland Geomorphology and Piping, p. 89-113.

SHREVE, R.L., 1974, "Variations of mainstream length with basin area in river networks", Wat. Res. Res., v. 10, p. 1167-1177.

SLAYMAKER, O., 1982, "The occurrence of piping and gullying in the Penticton glacio-lacustrine silts, Okanagan Valley, B.C.", in Bryan and Yair (Eds.) Badland Geomorphology and Piping, p. 305-317.

SMITH, R.L., 1972, "The infiltration envelope: results from a theoretical infiltrometer", Wat. Res. Res., v. 7, p. 899-913.

SMITH, T.R., and BRETHERTON, F.P., 1972, "Stability and conservation of mass in drainage basin evolution", Wat. Res. Res., v. 8(6), p. 1506-1527

STRAHLER, A.N., 1952, "The dynamic basis of geomorphology", Bull. Geol. Soc. Am., v. 63, p. 923-938

SWANSON, F.J., et. al., 1982, "Sediment budgets and routing in Forested drainage basins", U.S.D.A. For. Serv., Pacific N.W. Rep. No. PNW-141.

THOMSEN, M., and STRIFFLER, W.D., 1980, "A watershed information system", Colo. Wat. Res. Res. Institu., C.S.U., Fort Collins, Colo. Completion Rpt. No. 100, 97p.

THORN, C.E., 1978, "The geomorphic role of snow", A.A.A.G., v. 68, No. 3, p. 414-425.

THORNES, J.B., 1976, "Semi-arid erosional systmes", L.S.E. Geographical papers No. 7.

THORNES, J.B., 1977, "Channel changes in ephemeral streams observations; problems and models", in Gregory K., (Ed.), River Channel Changes, Ch. 21, p. 317-335.

THORNES, J.B., 1979, "Fluvial processes", Ch. 7 in Embleton and Thornes (Eds.) Process in Geomorphology, Edward Arnold.

THORNES, J.B., 1980, "Erosional processes of running water", Ch. 5 in Kirkby and Morgan (Eds.) Soil Erosion, Wiley.

THORNES, J.B., 1981, "Structural instability and ephemeral channel behaviour,", Zeit fur Geomorph. Sp. Suppleband No. 36, p. 233-244.

THORNES, J.B., 1982, "Problems in the identification of stability and structure from temporal data series", in Thorn, C.E. (Ed.) Space and Time in Geomorphology, Binghamton.

THORNES, J.B., 1983, "Discharge empirical observations and statistical models of change", Ch. 3 in Gregory, K (Ed.), Background to Paleohydrology, Wiley, p. 51-68.

TOY, T.J., et al., 1980, "Latitude, topography and Potential Irradiation", A.A.A.G., Dec. 1980.

U.K. FLOOD STUDY REPORT, 1979, "Runoff from snowmelt", Ch. 3 in Part 1. Institute of Hydrology, Wallingford, Oxon.

U.S. CORPS OF ENGINEERS, 1956, Snow hydrology: summary of the snow investigations. N. Pacific Division., Portland Oregon, 417p.

VALDES, J.B., FIALLO, Y., and RODRIGUEZ-ITURBE, I., 1979, "A rainfall-runoff analysis of geomorphic I.U.H.", Wat. Res. Res. v. 15(6) p. 1421-1443.

VIESSMAN, W., HARBAUGH, T.E., and KNAPP, J.W., 1972, Introduction to Hydrology, I.E.P., 415p.

WALLING, D.E., 1974, "Reliability considerations in the evaluation and analysis of river loads", Zeit fur Geomorph., Sp. Suppleband No. 29, p. 29-42.

WEYMAN, D.R., 1970, "Throughflow on hillslopes and its relation to stream hydrographs", Bull, Int, Ass, Sci, Hyd., v. 15(3), p. 25-33.

WHIPKEY, R.Z., 1969, "Storm runoff from forested catchments by subsurface routes", Pub. Int. Ass. Sci. Hyd., v. 85(2), p.773-779

WISCHMEIER, W.H., and SMITH, D.D., 1958, "Rainfall energy and its relationship to soil loss", Tr. Am. Geophys. un., v. 39, p.285-291.

WOLMAN, M.G., and GERSON, R., 1978, "Relative scales of time and effectiveness of climate in watershed geomorphology", Earth Surface Processes, v. 3, p. 189-208.

WOLMAN, M.G., and MILLER, J.P., 1960, "Magnitude and frequency of forces in geomorphic processes", J. of Geol., v. 68, p. 54-74.

WOO, M.F., and SAURIOL, J., 1980, "Channel development in snowfilled valleys, Resolute N.W.T., Canada", Geograf, Ann. Ser. A., v. 62(1-2), p. 37-56.

WOODING, R.A., 1965, "A hydraulic model for the catchment stream problem", J of Hydrology, v.3, p. 254-267.

WOOHISER, D.A., and LIGGETT, J.A., 1967, "Unsteady, one-dimensional flow over a plane - the rising hydrograph", Wat. Res. Res. v.3, No. 3, p. 753-771.

WOOHISER, D.A., and TODOROVIC, P., 1971, "A stochastic model of sediment yield for ephemeral streams", Proc. U.S.D.A. Int. Ass. for Statistics in the Phys. Sci., Symp. on Statistical Hydrology, U.S.D.A. Misc. Pub. 1275.

YAIR, A., and KLEIN, M., 1973, "The influence of surface properties on flow and erosion processes on debris-covered slopes in an acid area", Catena. v.1, p. 1-18.

YAIR, A., and LAVEE, H., 1976, "Runoff generative process and erosion yield from arid talus-mantled slopes", Earth Surface Processes, v.1, p. 235-247.

YAIR, A., SHARON, D., and LAVEE, H., 1978, "An instrumented watershed for the study of partial contribution of runoff in the arid zone", Zeit fur Geomorph. Sp. Suppleband No. 29, p. 71-82.

YAIR, et al., 1980, "Present and past geomorphic evidences in the development of badlands landscapes, Zin Valley, Northern Negev, Israel", in Paleoecology of Africa and Islands, v.12, Blakeman, p.125-135.

YANG, C.T., 1972, "Unit stream power and sediment transport", A.S.C.E., J. Hyd. Div., v.98, p. 1805-1826.

YANG, C.T., and SONG, J.B., 1979, "Dynamic adjustments of alluvial channels", in Rhodes, D.D., and Williams, G.P. (Eds.), Adjustments of the Fluvial System, p. 56-67.

YANG, C., SONG, C.C., and WOLDENBURG M., 1981, "Hydraulic geometry and minimum rate of energy dissipation", Wat. Res. Res, v.17, No. 4, p. 1014-1018.

YANG, C.T., and STALL, J.B., 1973, "Unit stream power in dynamic stream systems", Ch. 12 in Morisawa, (Ed.), Fluvial Geomorphology, Binghamton.

YOSHIDA, S., 1962, "Hydrometeorological study of snowmelt", J. Met. Res., v.14, p. 879-899.

ZEEMAN, E.C., 1976, "Catastrophe Theory", Scientific American, v.234, p. 65-83.

ZINGG, A.W., 1940, "Degree and length of landslope as it affects soil loss in runoff", Agric. Eng., v.21, p. 59-64.

APPENDIX 1

A. MEAN DAILY DISCHARGES IN CUMECS, WEST DIVIDE CREEK

Source : Water Resources data for Colorado, Vol.12. 1967-1972.

B. PRECIPITATION RECORDED AT ALKALI CREEK R.R.G, 1961-1972

Source : U.S. Forest Service records held at Rifle Ranger Station, Rifle, Colorado.

C. END OF MONTH SNOW WATER EQUIVALENTS, ALKALI ESTIMATES AND McCLURE SNOW PILLOW DATA, 1961-1973

Sources : Alkali Creek R.R.G data, and U.S. Soil Conservation Service Office, Diamond Hill, Denver, Colorado.

D. ALKALI CREEK SUMMER RAINSTORM DATA

Source : Alkali Creek R.R.G records, 1967-1972.

A. MEAN DAILY DISCHARGES IN CUMECS, WEST DIVIDE CREEK, 1966-1972

	Day	1966-67	1967-68	1968-69	1969-70	1970-71	1971-72
JANUARY	1	0.011	0.028	0.034	0.042	0.164	0.147
	2	0.011	0.028	0.034	0.034	0.159	0.167
	3	0.023	0.025	0.031	0.071	0.159	0.153
	4	0.023	0.025	0.031	0.099	0.159	0.142
	5	0.020	0.028	0.040	0.108	0.159	0.136
	6	0.020	0.034	0.040	0.099	0.161	0.142
	7	0.025	0.040	0.040	0.108	0.249	0.130
	8	0.020	0.037	0.054	0.142	0.249	0.136
	9	0.017	0.037	0.076	0.170	0.207	0.127
	10	0.017	0.037	0.062	0.204	0.249	0.130
	11	0.020	0.037	0.062	0.178	0.249	0.113
	12	0.028	0.034	0.062	0.156	0.266	0.119
	13	0.028	0.034	0.059	0.147	0.340	0.119
	14	0.037	0.031	0.057	0.136	0.340	0.119
	15	0.031	0.031	0.059	0.156	0.258	0.119
	16	0.034	0.034	0.088	0.142	0.224	0.122
	17	0.034	0.037	0.085	0.170	0.207	0.170
	18	0.028	0.034	0.068	0.368	0.178	0.156
	19	0.025	0.037	0.068	0.280	0.187	0.170
	20	0.031	0.037	0.074	0.178	0.178	0.167
	21	0.031	0.034	0.071	0.178	0.224	0.173
	22	0.034	0.037	0.065	0.178	0.258	0.167
	23	0.037	0.045	0.062	0.195	0.283	0.161
	24	0.031	0.045	0.062	0.178	0.249	0.156
	25	0.025	0.034	0.062	0.178	0.232	0.161
	26	0.025	0.031	0.065	0.178	0.232	0.170
	27	0.023	0.034	0.059	0.195	0.207	0.184
	28	0.025	0.034	0.054	0.221	0.258	0.184
	29	0.023	0.034	0.065	0.238	0.283	0.170
	30	0.020	0.031	0.062	0.195	0.275	0.142
	31	0.017	0.025	0.068	0.184	0.224	0.142
FEBRUARY	32	0.011	0.025	0.076	0.187	0.178	0.159
	33	0.014	0.031	0.074	0.184	0.156	0.170
	34	0.017	0.028	0.071	0.170	0.198	0.170
	34	0.017	0.028	0.076	0.176	0.227	0.170
	36	0.017	0.028	0.082	0.170	0.198	0.156
	37	0.020	0.025	0.076	0.164	0.161	0.142
	38	0.023	0.028	0.071	0.153	0.178	0.136
	39	0.025	0.025	0.071	0.142	0.193	0.136
	40	0.028	0.025	0.071	0.142	0.210	0.156
	41	0.028	0.023	0.071	0.142	0.204	0.161
	42	0.025	0.023	0.074	0.136	0.187	0.156
	43	0.023	0.023	0.076	0.127	0.176	0.142
	44	0.023	0.023	0.079	0.127	0.167	0.127
	45	0.025	0.025	0.079	0.113	0.173	0.147
	46	0.034	0.031	0.076	0.108	0.181	0.136
	47	0.034	0.031	0.071	0.102	0.187	0.130
	48	0.034	0.025	0.068	0.091	0.187	0.130
	49	0.031	0.025	0.068	0.091	0.178	0.127
	50	0.025	0.025	0.071	0.096	0.167	0.127
	51	0.025	0.028	0.076	0.102	0.150	0.136
	52	0.028	0.031	0.076	0.108	0.147	0.127
	53	0.031	0.028	0.079	0.113	0.147	0.130
	54	0.025	0.031	0.079	0.113	0.147	0.122

MEAN DAILY DISCHARGES IN CUMECS , cont.

	Day	1966-67	1967-68	1968-69	1969-70	1970-71	1971-72
FEB. (cont.)	55	0.020	0.031	0.076	0.108	0.161	0.113
	56	0.020	0.031	0.076	0.102	0.193	0.113
	57	0.025	0.028	0.074	0.102	0.232	0.113
	58	0.025	0.023	0.074	0.102	0.215	0.119
	59	0.028	0.023	0.076	0.096	0.207	0.122
	60	0.028	0.025	0.082	0.096	0.198	0.119
	61	0.031	0.025	0.082	0.102	0.198	0.119
	62	0.031	0.025	0.082	0.102	0.198	0.116
	63	0.028	0.025	0.088	0.108	0.198	0.113
	64	0.028	0.025	0.091	0.113	0.198	0.113
	65	0.028	0.028	0.088	0.113	0.193	0.119
	66	0.034	0.028	0.091	0.113	0.181	0.122
	67	0.034	0.028	0.091	0.108	0.178	0.122
	68	0.037	0.025	0.096	0.102	0.178	0.119
	69	0.057	0.025	0.096	0.096	0.193	0.122
	70	0.048	0.025	0.096	0.096	0.198	0.122
	71	0.028	0.025	0.096	0.096	0.187	0.122
	72	0.023	0.028	0.096	0.099	0.193	0.122
	73	0.020	0.034	0.096	0 108	0.176	0.122
	74	0.020	0.034	0.099	0.108	0.156	0.122
MARCH	75	0.020	0.034	0.096	0.102	0.122	0.122
	76	0.020	0.031	0.088	0.096	0.142	0.122
	77	0.020	0.028	0.091	0.091	0.164	0.122
	78	0.023	0.028	0.091	0.091	0.176	0.119
	79	0.025	0.028	0.096	0.091	0.187	0.119
	80	0.025	0.031	0.091	0.091	0.198	0.113
	81	0.025	0.034	0.088	0.096	0.187	0.119
	82	0.025	0.034	0.091	0.102	0.187	0.119
	83	0.023	0.028	0.091	0.108	0.178	0.119
	84	0.020	0.023	0.091	0.113	0.178	0.119
	85	0.017	0.023	0.088	0.113	0.167	0.122
	86	0.020	0.023	0.088	0.108	0.161	0.136
	87	0.020	0.028	0.091	0.102	0.156	0.198
	88	0.023	0.034	0.091	0.096	0.156	0.198
	89	0.020	0.034	0.091	0.091	0.161	0.173
	90	0.020	0.034	0.088	0.085	0.156	0.196
	91	0.017	0.034	0.085	0.079	0.147	0.184
	92	0.014	0.028	0.085	0.074	0.142	0.178
	93	0.011	0.023	0.082	0.068	0.136	0.161
	94	0.011	0.020	0.076	0.062	0.136	0.156
	95	0.011	0.020	0.079	0.062	0.136	0.147
	96	0.014	0.017	0.082	0.062	0.136	0.147
	97	0.017	0.017	0.076	0.068	0.130	0.136
APRIL	98	0.023	0.020	0.079	0.074	0.119	0.130
	99	0.023	0.020	0.079	0.074	0.108	0.130
	100	0.020	0.017	0.076	0.068	0.108	0.130
	101	0.014	0.020	0.076	0.068	0.116	0.130
	102	0.011	0.020	0.074	0.074	0.125	0.127
	103	0.011	0.023	0.074	0.085	0.127	0.122
	104	0.014	0.023	0.076	0.085	0.133	0.122
	105	0.017	0.017	0.079	0.085	0.127	0.127
	106	0.017	0.011	0.085	0.079	0.122	0.127
	107	0.017	0.014	0.088	0.074	0.122	0.119
	108	0.014	0.017	0.088	0.074	0.122	0.125
	109	0.011	0.017	0.079	0.074	0.122	0.133

MEAN DAILY DISCHARGE IN CUMECS, cont.

	Day	1966-67	1967-68	1968-69	1969-70	1970-71	1971-72
APRIL (cont.)	110	0.008	0.020	0.076	0.085	0.125	0.139
	111	0.006	0.023	0.071	0.085	0.127	0.142
	112	0.008	0.025	0.071	0.079	0.127	0.142
	113	0.011	0.025	0.079	0.074	0.127	0.147
	114	0.011	0.025	0.082	0.074	0.127	0.136
	115	0.011	0.028	0.082	0.074	0.116	0.142
	116	0.008	0.028	0.074	0.085	0.105	0.147
	117	0.008	0.025	0.074	0.091	0.110	0.136
	118	0.008	0.023	0.079	0.091	0.113	0.136
	11	0.011	0.025	0.088	0.091	0.113	0.142
	120	0.011	0.028	0.088	0.085	0.113	0.142
	121	0.011	0.025	0.088	0.074	0.113	0.133
MAY	122	0.011	0.025	0.082	0.068	0.113	0.125
	123	0.015	0.025	0.079	0.057	0.113	0.119
	124	0.017	0.028	0.079	0.079	0.113	0.127
	125	0.020	0.031	0.079	0.074	0.116	0.136
	126	0.020	0.031	0.079	0.074	0.108	0.125
	127	0.017	0.028	0.085	0.074	0.099	0.136
	128	0.017	0.028	0.091	0.068	0.093	0.136
	129	0.020	0.034	0.102	0.068	0.091	0.142
	130	0.023	0.031	0.113	0.074	0.091	0.142
	131	0.023	0.031	0.108	0.074	0.091	0.139
	132	0.023	0.034	0.102	0.068	0.091	0.136
	133	0.023	0.040	0.096	0.068	0.093	0.133
	134	0.023	0.040	0.096	0.068	0.099	0.127
	135	0.020	0.040	0.096	0.074	0.102	0.130
	136	0.020	0.040	0.102	0.074	0.108	0.130
	137	0.017	0.042	0.105	0.074	0.108	0.133
	138	0.017	0.040	0.108	0.068	0.108	0.139
	139	0.023	0.037	0.108	0.068	0.108	0.139
	140	0.023	0.037	0.105	0.068	0.105	0.147
	141	0.020	0.037	0.102	0.068	0.102	0.153
	142	0.017	0.037	0.105	0.062	0.096	0.159
	143	0.014	0.040	0.113	0.057	0.096	0.164
	144	0.014	0.042	0.119	0.057	0.093	0.170
	145	0.011	0.045	0.119	0.057	0.091	0.164
	146	0.011	0.040	0.113	0.062	0.088	0.159
	147	0.017	0.040	0.113	0.068	0.096	0.153
	148	0.023	0.040	0.116	0.068	0.091	0.142
	149	0.023	0.045	0.119	0.062	0.091	0.139
	150	0.025	0.051	0.122	0.062	0.091	0.147
	151	0.025	0.051	0.122	0.062	0.091	0.142
JUNE	152	0.025	0.048	0.119	0.068	0.099	0.159
	153	0.025	0.045	0.119	0.068	0.102	0.105
	154	0.025	0.045	0.119	0.068	0.105	0.147
	155	0.025	0.045	0.119	0.071	0.108	0.144
	156	0.028	0.045	0.119	0.074	0.113	0.142
	157	0.025	0.045	0.127	0.074	0.113	0.153
	158	0.025	0.045	0.125	0.074	0.119	0.147
	159	0.025	0.045	0.12	0.068	0.119	0.142
	160	0.028	0.051	0.127	0.068	0.108	0.153
	161	0.031	0.057	0.130	0.068	0.099	0.164
	162	0.034	0.062	0.133	0.074	0.091	0.159
	163	0.034	0.068	0.133	0.079	0.091	0.153

MEAN DAILY DISCHARGES IN CUMECS, cont.

	Day	1966-67	1967-68	1968-69	1969-70	1970-71	1971-72
JUNE (cont.)	164	0.034	0.071	0.127	0.057	0.091	0.167
	165	0.037	0.071	0.122	0.085	0.088	0.212
	166	0.045	0.071	0.127	0.085	0.085	0.244
	167	0.057	0.068	0.127	0.085	0.085	0.204
	168	0.057	0.062	0.125	0.085	0.088	0.340
	169	0.054	0.059	0.122	0.091	0.085	0.481
	170	0.048	0.076	0.122	0.102	0.085	0.368
	171	0.076	0.071	0.125	0.113	0.079	0.312
	172	0.102	0.059	0.130	0.108	0.076	0.340
	173	0.142	0.068	0.136	0.108	0.082	0.453
	174	0.170	0.074	0.142	0.108	0.099	0.566
	175	0.170	0.079	0.142	0.113	0.099	0.510
	176	0.156	0.079	0.142	0.119	0.122	0.425
	177	0.156	0.074	0.156	0.125	0.127	0.510
	178	0.184	0.085	0.156	0.130	0.142	0.680
	179	0.198	0.096	0.147	0.136	0.187	0.595
	180	0.198	0.085	0.136	0.142	0.178	0.595
	181	0.170	0.082	0.122	0.136	0.312	0.708
	182	0.147	0.099	0.142	0.130	0.651	0.566
	183	0.142	0.136	0.147	0.125	0.821	0.481
	184	0.170	0.136	0.167	0.125	0.963	0.453
	185	0.156	0.161	0.255	0.136	1.161	0.566
	186	0.142	0.170	0.340	0.142	1.133	0.481
	187	0.164	0.198	0.368	0.147	1.020	0.368
	188	0.229	0.255	0.396	0.147	0.793	0.396
	189	0.340	0.184	0.396	0.136	0.793	0.368
	190	0.425	0.142	0.566	0.130	0.850	0.396
	191	0.396	0.142	0.963	0.136	0.935	0.566
	192	0.481	0.142	1.331	0.156	1.133	0.906
	193	0.538	0.130	1.303	0.170	1.274	1.020
	194	0.481	0.142	0.935	0.170	0.906	1.274
	195	0.396	0.130	1.274	0.198	0.821	1.586
	196	0.538	0.127	1.982	0.227	1.161	1.756
JULY	197	0.651	0.170	2.351	0.198	1.529	1.671
	198	0.396	0.198	2.407	0.184	1.869	2.266
	199	0.396	0.269	2.605	0.198	2.719	1.954
	200	0.396	0.269	2.407	0.184	4.701	1.671
	201	0.396	0.255	1.841	0.198	4.701	1.473
	202	0.340	0.312	1.869	9.184	4.928	1.274
	203	0.481	0.340	2.067	0.178	5.211	1.416
	204	0.680	0.368	2.436	0.195	4.305	1.473
	205	0.850	0.340	3.682	0.178	3.625	1.473
	206	0.510	0.312	5.636	0.187	3.172	1.643
	207	0.481	0.312	6.117	0.195	3.059	1.643
	208	0.538	0.258	7.222	0.178	3.228	1.756
	209	0.425	0.258	7.561	0.178	3.030	2.181
	210	0.425	0.241	6.684	0.204	3.285	2.719
	211	0.396	0.269	4.503	0.283	3.625	3.455
	212	0.510	0.283	3.625	0.651	3.936	3.115
	213	1.048	0.283	3.455	1.274	3.455	2.379
	214	1.416	0.266	4.106	1.444	3.228	2.181
AUG.	215	1.359	0.396	4.984	0.935	3.285	2.209
	216	1.359	0.935	5.381	0.680	3.115	2.492
	217	0.765	0.935	5.806	0.623	3.257	2.549

MEAN DISCHARGES IN CUMECS, cont.

	Day	1966-67	1967-68	1968-69	1969-70	1970-71	1971-72
AUGUST (cont.)	218	0.595	1.643	6.825	0.595	3.568	2.634
	219	0.481	2.152	7.080	0.708	4.701	2.832
	220	0.425	2.832	6.429	1.161	6.684	3.059
	221	0.425	3.682	5.806	2.124	7.561	3.568
	222	0.481	4.531	5.891	3.144	6.599	3.512
	223	0.453	4.248	5.891	4.191	6.202	3.738
	224	0.793	3.682	5.437	5.324	5.891	3.795
	225	1.189	3.115	5.494	5.154	6.684	3.568
	226	2.209	3.965	5.636	4.106	6.117	3.880
	227	2.209	5.098	5.437	4.390	5.352	4.050
	228	2.266	5.664	4.984	7.363	5.211	3.682
	229	2.124	5.947	4.786	8.439	5.579	3.115
	230	1.359	5.664	4.984	8.723	6.684	2.889
	231	1.048	4.531	4.446	8.354	7.476	2.690
	232	1.076	3.682	4.248	7.363	8.383	2.974
	233	2.407	3.682	3.795	11.670	11.300	4.050
	235	2.577	4.531	3.512	12.320	7.986	4.503
	236	2.719	5.664	3.512	12.630	6.344	4.503
	237	2.917	7.080	3.512	12.180	5.211	4.305
	238	3.285	9.912	3.285	12.400	5.069	3.993
	239	3.228	11.380	3.115	12.890	6.117	3.398
	240	3.030	9.685	3.512	11.610	5.891	2.974
	241	3.087	7.137	3.455	10.420	5.126	2.832
	242	3.965	6.684	3.568	10.050	5.211	3.115
	243	3.342	7.307	4.050	10.340	6.514	3.285
SEPTEMBER	244	2.832	8.666	3.682	9.629	8.666	3.285
	245	2.322	10.590	3.568	8.836	9.402	3.228
	246	1.897	12.430	3.512	8.269	8.411	3.172
	247	1.671	12.430	3.285	7.646	7.222	3.059
	248	1.671	12.320	2.832	7.080	5.806	3.342
	249	1.926	11.980	2.719	5.664	5.437	3.568
	250	2.096	11.580	2.690	5.098	5.891	3.512
	251	2.407	10.870	2.690	5.041	5.947	3.738
	252	2.464	9.799	2.889	4.871	6.032	4.305
	253	2.464	9.912	3.172	4.191	4.984	3.993
	254	2.266	9.289	2.775	4.021	4.786	3.682
	255	2.039	7.816	2.520	4.475	4.984	3.568
	256	1.897	6.684	2.379	5.041	5.437	4.361
	257	1.812	5.636	2.407	4.531	5.268	4.106
	258	1.756	4.701	2.294	5.239	4.843	3.512
	259	1.812	4.050	2.096	5.607	4.248	3.115
	260	1.699	3.625	2.067	5.041	4.248	3.059
	261	1.756	3.795	2.605	4.673	3.936	2.832
	262	1.614	3.880	2.294	4.475	3.880	2.464
	263	1.614	4.050	2.266	4.106	3.682	2.351
	264	1.586	3.993	2.379	3.767	3.795	2.379
	265	1.643	3.682	2.039	3.455	4.050	2.464
	266	1.756	3.512	1.841	3.144	4.361	2.266
	267	2.096	3.342	1.671	2.974	4.106	2.067
	268	2.181	3.059	1.529	2.974	3.880	1.869
	269	2.039	2.832	1.416	3.342	3.682	1.728
	270	1.897	3.398	3.172	3.342	3.682	1.671
	271	1.699	3.115	3.030	3.228	4.050	1.643
	272	1.529	3.257	2.605	2.832	3.738	1.614

MEAN DAILY DISCHARGES IN CUMECS, cont.

	Day	1966-67	1967-68	1968-69	1969-70	1970-71	1971-72
SEPT. (cont)	273	1.416	3.115	2.407	2.832	3.455	1.303
	274	1.303	2.832	2.719	2.520	3.228	1.133
	275	1.246	2.832	2.379	2.322	2.974	0.991
	276	1.104	2.690	2.039	2.266	2.634	0.878
	277	0.935	2.549	1.954	2.039	2.464	0.821
	278	0.935	2.407	1.841	1.756	2.294	0.736
	279	0.821	2.322	1.671	1.756	2.266	0.736
	280	0.680	2.266	1.501	1.501	2.152	0.708
	281	0.538	1.982	1.388	1.416	2.152	0.680
	282	0.198	1.841	1.274	1.416	1.982	0.595
	283	0.425	1.699	1.104	1.331	1.869	0.566
	284	0.368	1.699	0.991	1.501	1.643	0.510
	285	0.368	1.699	0.878	1.473	1.473	0.510
	286	0.566	1.558	0.793	1.643	1.388	0.595
	287	0.368	1.416	0.708	1.303	1.274	0.510
OCTOBER	288	0.280	1.359	0.680	1.189	1.161	0.453
	289	0.312	1.246	0.595	1.133	1.048	0.453
	290	0.340	1.133	0.566	0.935	0.878	0.396
	291	0.204	0.991	0.510	0.935	0.793	0.283
	292	0.195	0.991	0.510	0.878	0.680	0.241
	293	0.266	0.793	0.425	0.595	0.595	0.215
	294	0.283	0.566	0.396	0.538	0.566	0.173
	295	0.680	0.510	0.340	0.481	0.481	0.147
	296	0.566	0.453	0.453	0.425	0.396	0.122
	297	0.312	0.368	0.793	0.396	0.340	0.099
	298	0.229	0.312	0.595	0.340	0.312	0.088
	299	0.195	0.275	0.481	0.312	0.312	0.099
	300	0.187	0.241	0.340	0.283	0.340	0.082
	301	0.178	0.215	0.249	0.396	0.396	0.074
	302	0.187	0.396	0.232	0.425	0.425	0.059
	303	0.156	0.340	0.207	0.280	0.425	0.057
	304	0.127	0.340	0.173	0.255	0.312	0.054
	305	0.119	0.283	0.142	0.340	0.266	0.054
	306	0.108	0.283	0.136	0.340	0.258	0.045
	307	0.093	0.368	0.178	0.368	0.215	0.037
	308	0.088	0.275	0.167	0.340	0.207	0.025
	309	0.082	0.340	0.127	0.266	0.198	0.023
	310	0.082	0.340	0.108	0.212	0.167	0.020
	311	0.054	0.283	0.088	0.178	0.142	0.017
	312	0.037	0.368	0.088	0.164	0.136	0.020
	313	0.034	0.595	0.079	0.147	0.122	0.020
	314	0.031	0.340	0.068	0.147	0.122	0.020
	315	0.037	0.249	0.057	0.312	0.136	0.020
	316	0.082	0.249	0.051	0.178	0.130	0.017
	317	0.280	0.266	0.045	0.453	0.113	0.011
NOVEMBER	318	0.113	0.224	0.042	0.396	0.105	0.008
	319	0.099	0.266	0.051	0.221	0.105	0.006
	320	0.082	0.850	0.059	0.178	0.096	0.006
	321	0.054	0.340	0.074	0.142	0.096	0.003
	322	0.042	0.275	0.057	0.119	0.096	0.003
	323	0.034	0.215	0.045	0.108	0.105	0.003
	324	0.025	0.283	0.037	0.099	0.096	0.003
	325	0.028	0.396	0.037	0.108	0.091	0.003
	326	0.025	0.283	0.085	0.113	0.079	0.003

MEAN DAILY DISCHARGES IN CUMECS, cont.

	Day	1966-67	1967-68	1968-69	1969-70	1970-71	1971-72
NOVEMBER (cont)	327	0.020	0.173	0.074	0.108	0.076	0.003
	328	0.017	0.142	0.074	0.099	0.076	0.003
	329	0.020	0.127	0.051	0.082	0.076	0.006
	330	0.017	0.113	0.045	0.082	0.071	0.017
	331	0.017	0.119	0.040	0.136	0.074	0.011
	332	0.017	0.113	0.040	0.212	0.068	0.008
	333	0.014	0.156	0.031	0.187	0.076	0.085
	334	0.011	0.147	0.028	0.113	0.108	0.076
	335	0.011	0.108	0.025	0.099	0.105	0.068
DECEMBER	336	0.011	0.088	0.025	0.071	0.088	0.068
	337	0.011	0.085	0.051	0.065	0.076	0.068
	338	0.014	0.091	0.079	0.076	0.071	0.074
	339	0.017	0.082	0.051	0.091	0.076	0.082
	340	0.037	0.071	0.037	0.119	0.082	0.082
	341	0.093	0.068	0.028	0.082	0.113	0.110
	342	0.037	0.059	0.025	0.076	0.088	0.102
	343	0.017	0.054	0.025	0.096	0.071	0.085
	344	0.017	0.059	0.025	0.212	0.105	0.093
	345	0.014	0.065	0.025	0.156	0.241	0.076
	346	0.011	0.059	0.023	0.093	0.147	0.099
	347	0.008	0.051	0.040	0.176	0.130	0.110
	348	0.014	0.045	0.062	1.558	0.122	0.091
	349	0.040	0.040	0.057	0.312	0.266	0.091
	350	0.031	0.037	0.034	0.195	0.119	0.102
	351	0.040	0.037	0.028	0.156	0.082	0.110
	352	0.136	0.034	0.025	0.127	0.068	0.122
	353	0.034	0.034	0.028	0.108	0.059	0.011
	354	0.020	0.034	0.037	0.108	0.057	0.011
	355	0.017	0.042	0.040	0.481	0.054	0.011
	356	0.014	0.045	0.037	0.340	0.054	0.008
	357	0.014	0.045	0.028	0.212	0.057	0.008
	358	0.014	0.040	0.025	0.156	0.071	0.008
	359	0.037	0.040	0.034	0.127	0.096	0.006
	360	0.028	0.037	0.074	0.113	0.096	0.017
	361	0.017	0.034	0.059	0.099	0.091	0.076
	362	0.011	0.034	0.045	0.088	0.099	0.025
	363	0.008	0.034	0.040	0.088	0.105	0.017
	364	0.008	0.037	0.034	0.147	0.096	0.014
	365	0.020	0.034	0.028	0.156	0.096	0.014

B. PRECIPITATION RECORDED AT ALKALI CREEK R R G

ALL DATA IN CM.

	1962	1963	1964	1965	1966	1967	1968	1969	1970	1971	1972
January	2.97	4.16	2.26	2.67	1.88	2.77	freeze	5.99	2.72	2.87	2.72
February	5.84	4.06	2.79	3.43	1.98	2.84	4.80	2.49	2.44	3.22	0.81
March	3.48	6.32	5.59	7.24	0.91	1.45	1.75	4.01	4.49	4.27	1.85
April	6.50	2.51	7.64	2.41	3.83	2.59	7.82	1.93	6.73	5.23	3.40
May	3.76	1.14	2.77	5.10	3.40	4.19	4.44	0.66	0.53	3.49	0.08
June	1.37	3.40	4.27	3.50	1.62	3.78	0.13	10.87	4.89	0.35	1.65
July	0.66	4.47	2.23	4.49	2.97	5.31	5.51	1.47	4.67	2.36	0.61
August	0.86	6.12	7.06	2.31	7.03	2.82	5.23	9.55	3.02	2.54	3.40
September	3.88	3.40	2.73	12.11	2.49	2.44	1.37	7.06	8.56	4.88	6.37
October	2.54	5.66	0.28	2.59	3.50	1.70	0.61	4.99	4.27	7.06	13.53
November	2.08	3.83	6.20	6.32	5.76	3.05	5.64	2.62	6.20	6.37	13.48
December	2.36	1.93	5.76	2.54	7.85	6.43	2.49	4.01	2.72	6.91	3.48
Total	36.32	46.48	49.61	54.73	41.48	41.07	39.80	55.68	52.24	47.14	54.38

Mean = 47.18 CM. PER ANNUM

1:B:1

C. END OF MONTH SHOW WATER EQUIVALENTS:ALKALI ESTIMATE AND McCLURE SNOW PILLOW DATA.

1961-1973

ALL DATA IN CM.

1961-1962	October	November	December	January	February	March	April
Alkali	4.70	9.55	12.55	15.52	21.36	24.84	18.92
McClure	n.d	n.d	n.d	n.d	52.83	54.86	27.43
1962-1963							
Alkali	2.54	4.62	6.98	11.15	15.21	21.53	13.28
McClure	n.d	n.d	n.d	22.10	24.64	29.72	0.00
1963-1964							
Alkali	0.00	3.84	5.77	8.03	10.82	16.41	15.85
McClure	n.d	n.d	n.d	17.01	23.62	28.45	28.45
1964-1965							
Alkali	0.28	6.48	12.24	14.91	18.34	25.58	15.19
McClure	n.d	n.d	n.d	40.13	43.43	49.28	46.99
1965-1966							
Alkali	2.59	8.91	11.46	13.33	15.31	16.23	11.94
McClure	n.d	n.d	n.d	31.50	42.16	14.64	4.83
1966-1967							
Alkali	3.50	9.27	17.12	19.89	22.73	24.18	14.68
McClure	n.d	n.d	n.d	13.21	27.94	33.02	17.27
1967-1968							
Alkali	1.70	4.75	11.17	(11.17)	(15.98)	(17.72)	(16.68)
McClure	n.d	n.d	n.d	24.89	40.13	38.61	37.85
1968-1969							
Alkali	0.61	6.24	8.74	14.73	17.22	21.23	12.55
McClure	n.d	n.d	n.d	27.94	39.37	49.28	15.75
1969-1970							
Alkali	4.98	7.59	11.63	14.35	16.79	21.28	17.37
McClure	n.d	n.d	n.d	24.13	26.92	40.13	40.39
1970-1971							
Alkali	4.27	10.46	13.18	16.05	19.28	23.54	16.99
McClure	n.d	n.d	n.d	22.35	30.48	33.27	19.05
1971-1972							
Alkali	7.06	13.43	20.34	23.06	23.87	25.73	16.28
McClure	n.d	n.d	n.d	33.27	35.31	23.37	0.00
1972-1973							
Alkali	13.47	27.62	30.50	34.34	36.70	40.98	27.69
McClure	n.d	n.d	n.d	33.27	40.13	46.48	49.78

Data in brackets indicates accumulated values following a freeze of the R R G
n.d = no data available

D. ALKALI CREEK SUMMER RAINSTORM DATA FROM R.R.G. RECORDS

July 1967 - October 1972

			Intensity (cm/hr)	Duration (hrs)	Total Amount (cm)
1967					
July	Day	7	0.864	0.750	0.648
		9	1.880	0.500	0.940
		9	0.102	6.500	0.693
		16	0.965	0.500	0.483
		20	0.305	1.000	0.315
		29	1.524	0.500	0.762
August	Day	8	0.406	0.750	0.312
September	Day	1	0.838	0.750	0.635
		14	2.134	0.080	0.178
1968					
July	Day	3	0.762	0.500	0.381
		12	0.254	3.000	0.762
		23	0.559	1.000	0.559
		25	0.508	1.000	0.508
		25	0.178	2.000	0.356
		25	2.032	1.000	2.032
		29	1.524	0.500	0.762
August	Day	7	3.048	0.080	0.254
		9	0.203	3.500	0.711
		10	0.762	0.500	0.381
		16	0.051	12.000	0.610
		17	0.051	12.000	0.610
September	Day	9	0.762	0.500	0.381
		14	0.330	1.500	0.508
October	Day	3	0.127	10.000	1.397
1969					
June	Day	6	4.547	0.080	0.381
		7	0.178	2.000	0.381
		12	1.524	0.250	0.381
		13	0.254	4.500	1.143
		14	0.076	3.000	0.254
		17	0.127	5.000	0.635
		23	0.356	6.500	2.286
July	Day	1	1.143	0.330	0.381
		17	0.051	2.250	0.442
August	Day	1	1.219	0.420	0.508
		12	0.508	0.500	0.254
		17	1.524	0.250	0.381
		18	1.905	0.020	0.254
		19	3.429	0.330	1.143
		20	3.810	0.070	0.254
September	Day	1	0.406	1.250	0.508
		7	0.584	0.750	0.432
		8	0.254	1.000	0.254
		8	0.127	3.000	0.381
		10	1.016	0.250	0.254
		17	0.254	1.000	0.254
		19	0.610	0.620	0.381
		21	0.711	1.120	0.762
October	Day	3	2.032	0.130	0.254
		3	0.178	7.500	1.270

/contd.

			Intensity (cm/hr)	Duration (hrs)	Total Amount (cm)
October	Day	4	0.178	3.500	0.635
		6	0.051	54.000	2.286
1970					
June	Day	7	0.305	1.000	0.305
		9	0.432	1.750	0.726
		10	0.254	4.000	1.016
		11	0.203	6.000	1.270
		20	5.080	0.250	1.270
July	Day	3	0.635	2.000	1.270
		9	2.286	0.170	0.381
		9	3.048	0.130	0.381
		19	2.032	0.130	0.254
		19	1.143	0.380	0.508
		19	2.032	0.250	0.508
		22	1.016	0.250	0.254
		22	0.610	0.650	0.381
August	Day	19	0.152	2.500	0.381
		21	0.330	3.500	1.143
September	Day	4	0.381	13.000	5.080
		12	0.279	3.000	0.825
		12	0.508	1.750	0.889
		22	0.102	10.000	0.889
October	Day	9	0.203	21.000	4.572
1971					
July	Day	22	0.762	1.500	1.143
		22	0.406	0.750	0.317
		22	3.048	0.080	0.254
August	Day	24	5.588	0.500	2.794
		28	2.286	0.170	0.381
September	Day	2	0.635	3.000	1.905
		9	0.254	5.000	1.270
1972					
June	Day	1	2.032	0.120	0.254
		3	2.286	0.170	0.381
		3	0.686	0.750	0.508
		3	0.914	0.420	0.381
		7	1.016	0.500	0.508
		8	1.524	0.250	0.381
		16	6.096	0.040	0.381
July	Day	20	2.032	0.130	0.254
August	Day	6	6.096	0.170	1.016
		13	0.559	0.660	0.381
		19	0.254	2.000	0.508
		20	0.762	0.500	0.381
September	Day	1	0.635	0.330	0.127
		3	0.762	0.500	0.381
		20	0.356	1.750	0.635
		21	0.457	3.000	1.387
		21	0.737	1.370	1.016

APPENDIX 2

A. COMPARISON OF SOILS WITH AND WITHOUT PIPES, ALKALI CREEK

B. SUPPLEMENTARY SOIL ANALYSES, ALKALI CREEK

Source : Heede, B.H., 1971, "Characteristics and processes of Soil Piping in gullies", U.S.D.A. Forest Service, Research Monograph RM-68.

A. COMPARISON OF SOILS WITH AND WITHOUT PIPES

Soils	Exchangeable sodium percentage	Sodium adsorption ratio	pH (1:5)	Gypsum	Conductivity at 25°C.	Moisture at saturation	Sand	Silt	Clay	Textural class	Number of samples
				meq./ 100 g.	mmhos/ cm.		- - - - Percent - - - -				
Without pipes (Stable)											
Average	[2] 1.0		0.4	7.6	0.7	0.5	45.1	25.4	26.8	47.8	Clay	19
Standard error of the mean	[2] --		.07	.14	.06	.05	1.35	2.53	1.33	2.13		
With pipes (Unstable)[1]											
Average	12.0**		10.7**	8.9**	1.6**	1.7*	38.7	30.7	23.5	45.8	Clay	13
Standard error of the mean	2.27		2.0	.17	.19	.37	3.16	4.05	2.39	2.87		

[1]Statistically significant differences between soils with and without pipes;

**highly significant;

*significant.

[2]For ease of statistical calculations, a mean of 1.0 instead of <1.0 and a standard error of 0.0 were used

B. SUPPLEMENTARY SOIL ANALYSIS, WITH MEANS AND STANDARD ERROR (S.E)

Source of soil	Exchangeable sodium percentage		Sodium adsorption ratio		Conductivity at 25°C.		Gypsum		pH		Number of samples
	Mean	S.E	Mean	S.E.	Mean	S.E.	Mean	S.E.	Mean	S.E.	
					mmhos/cm.		meg./100 g.				
Shale parent material	17.9	1.5	15.7	1.5	0.8	0.1	0.9	0.49	9.7	0.09	4
Gully side slopes:											
Brink	11.2	9.5	11.2	9.3	1.1	.8	.1	.04	--	--	6
Midway	26.7	1.9	25.6	2.4	1.7	.3	.2	.06	--	--	6
Pipe outlet	16.0	3.4	14.2	3.3	.8	.2	.1	.03	--	--	6
Bottom	11.4	3.8	10.0	3.2	.5	.2	.1	.03	--	--	6
Alluvial layers inside pipe	10.1	1.2	8.7	1.0	2.6	.5	.2	.03	9.5	0.03	13
Pipe inlet	13.1	2.8	11.1	2.5	1.9	.6	1.8	1.0	8.6	.4	2
Pipe outlet	14.8	7.5	13.3	7.0	2.2	.8	1.4	.2	8.9	.2	2
Sediment from pipe flow	7.2	1.6	6.2	1.3	--	--	--	--	8.6	.0	2
Deposited below pipes[1]	10.3	.4	8.7	.4	.9	.07	.1	.01	9.4	.04	10

"--" indicates not applicable

[1]From snowmelt flow during springs of 1964 and 1965 from soil pipe 1.

APPENDIX 3

MORPHOLOGICAL DATA

A. CONTINUOUS GULLY NETWORK : headwaters 1975

B. CONTINUOUS GULLY NETWORK : main channel 1962

C. CONTINUOUS GULLY NETWORK : main channel 1975

D. LARGE DISCONTINUOUS GULLY : 1962
1975
1980

Source : Field data

A CONTINUOUS NETWORK: HEADWATERS, 1975

Cross-sections listed in their downstream positions

I.D	W Channel Width in metres	D Channel Mean Depth in metres	XA Section Area in m^2	Sb Bank Gradient %	Sc Channel Gradient %	Lm Mainstream Length in metres	Lt Total Length in metres
17.	2.44	0.15	0.37	32.60	25.20	3.05	3.05
34.	9.14	0.73	6.67	20.40	23.00	3.05	3.05
10.	1.52	0.27	0.41	28.60	27.40	4.57	4.57
16.	1.52	0.18	0.27	18.20	12.00	4.57	4.57
31.	3.35	0.52	1.74	22.00	21.40	4.57	4.57
41.	4.88	0.82	4.00	31.40	22.50	4.57	4.57
18.	3.96	0.18	0.71	36.10	22.50	5.49	5.49
14.	3.05	0.27	0.82	27.20	26.10	6.10	6.10
28.	2.44	0.30	0.73	34.90	33.10	6.10	6.10
38.	2.44	0.24	0.59	30.30	28.00	6.10	6.10
32.	4.27	0.37	1.58	41.00	27.40	7.62	7.62
22.	3.05	0.27	0.82	33.10	28.00	7.92	7.92
21.	4.27	0.46	1.96	36.10	29.70	8.53	8.53
29.	2.44	0.18	0.44	45.60	34.90	10.67	10.67
30.	2.74	0.34	0.93	46.90	34.90	12.19	12.19
49.	9.14	0.64	5.85	50.40	29.70	12.19	12.19
53.	2.44	0.43	1.05	33.70	27.40	13.72	13.72
54.	2.74	0.49	1.34	28.60	30.30	13.72	13.72
42.	6.10	2.04	12.44	50.30	24.70	15.24	15.24
56.	6.71	1.31	8.79	21.40	44.90	16.76	19.81
39	4.27	0.58	2.48	37.30	32.00	21.34	30.48
20.	1.83	0.15	0.27	21.40	19.30	22.86	22.86
27.	3.66	0.58	2.12	23.60	33.70	24.38	24.38
55.	6.10	1.22	7.44	29.10	30.80	27.43	45.72
45.	4.88	0.67	3:27	37.30	26.90	33.53	33.53
46.	8.53	1.13	9.64	39.20	31.40	33.53	33.53
40.	6.71	1.04	6.98	20.40	27.40	39.62	57.91
33.	4.88	1.07	5.22	28.00	33.10	48.77	48.77
8.	2.44	1.04	2.54	19.30	30.80	54.86	70.10
13.	7.32	0.98	7.17	13.10	19.30	64.01	64.01
15.	4.27	1.28	5.47	55.40	39.20	65.53	103.60
48.	1.83	0.21	0.38	7.50	10.00	67.06	67.06
52.	4.27	0.85	3.63	18.20	18.20	80.77	298.70
19.	5.49	1.13	6.20	51.40	29.70	83.82	159.70
44.	2.44	0.30	0.73	15.10	14.10	88.39	155.50
37.	5.49	1.01	5.55	29.70	20.40	97.54	262.10
26.	3.05	0.58	1.77	8.50	13.10	115.80	335.30
12.	10.97	2.04	22.38	37.30	25.30	123.40	234.70
47.	2.44	0.34	0.83	25.80	20.40	125.00	125.00
36.	10.97	1.83	20.08	32.20	29.10	125.30	320.00
51.	1.52	0.09	0.14	12.50	11.00	138.70	356.60
25.	6.10	1.92	11.71	39.20	28.00	161.50	381.00
35.	13.41	2.47	33.12	34.00	32.80	180.10	374.90
11.	5.49	0.79	4.34	12.00	30.30	184.40	471.80
50.	6.71	0.94	6.31	11.50	6.00	199.60	435.90
9.	2.44	0.58	1.42	36.10	41.00	249.90	552.60
43.	8.53	2.19	18.68	21.40	28.40	257.60	823.00
24.	21.34	3.54	75.54	36.10	31.40	281.90	1774.00
7.	6.25	0.98	6.13	26.30	28.60	310.90	705.00
23.	15.24	2.83	43.13	9.50	10.00	339.80	1832.00
6.	29.26	5.24	153.30	9.40	10.80	399.30	2656.00

8 CONTINUOUS NETWORK : MAIN CHANNEL, 1962 (Heede data)

Cross-sections listed in their downstream positions.

I.D	W Channel Width in metres	D Channel Mean Depth in metres	XA Section Area in m^2	Sb Bank Gradient %	Sc Channel Gradient %	Lm Mainstream Length in metres	Lt Total Length in metres
99	14.08	2.29	32.24	13.00	22.70	281.90	1777.00
100	8.14	1.83	14.90	12.50	24.10	294.70	1790.00
101	8.69	2.10	18.25	16.50	32.50	303.00	1798.00
102	11.83	2.07	24.49	12.50	23.30	342.90	1838.00
103	8.90	1.71	15.22	16.00	34.10	360.90	1856.00
104	11.28	2.71	30.57	19.00	36.50	380.10	1875.00
105	26.67	3.85	102.70	13.00	26.10	420.30	2683.00
106	11.34	2.80	31.75	12.50	24.10	431.30	3057.00
107	7.77	3.51	27.27	13.50	20.90	437.70	3064.00
108	11.98	3.35	40.13	12.50	28.40	446.50	3072.00
109	12.34	2.88	35.55	12.50	21.30	457.80	3084.00
110	11.49	3.14	36.08	12.50	22.10	464.20	3090.00
111	11.58	3.11	36.01	13.00	25.30	469.10	3095.00
112	13.05	3.11	40.59	14.50	24.10	474.60	3100.00
113	10.61	2.96	31.41	11.50	20.00	481.60	3107.00
114	13.11	2.83	37.10	11.50	21.10	491.30	3117.00
115	7.04	1.43	10.07	10.50	19.70	503.20	3129.00
116	10.15	2.80	28.42	10.50	19.00	515.70	3142.00
117	9.85	2.26	22.26	8.50	15.90	520.60	3146.00
118	10.55	2.41	25.43	8.00	16.60	525.20	3151.00
119	11.64	2.41	28.05	14.50	18.30	531.00	3157.00
120	10.73	2.62	28.11	14.50	20.70	537.70	3164.00
121	9.91	3.05	30.23	13.50	21.50	544.70	3171.00
122	13.44	2.99	40.19	12.50	25.00	551.70	3178.00
123	9.60	2.93	28.13	9.50	18.30	564.20	3190.00
124	13.50	2.74	36.99	7.50	14.90	576.40	3202.00
125	10.18	2.65	26.98	7.00	14.50	581.60	3207.00
126	9.05	2.44	22.08	7.50	13.70	588.00	3214.00
127	11.92	2.50	29.80	6.50	13.00	594.40	3220.00
128.	10.36	1.71	17.72	7.00	11.00	602.00	3228.00
129	9.33	2.90	27.06	7.00	12.10	606.90	3233.00
130	12.37	2.47	30.55	5.00	12.00	621.50	3247.00
131	6.22	1.28	7.96	24.50	30.00	676.30	3302.00
132	16.22	1.98	32.12	6.50	7.90	701.90	3384.00
133	17.74	1.86	33.00	20.00	35.10	711.10	3393.00
134	10.82	2.13	23.05	15.00	27.30	720.20	3402.00
135	9.69	2.74	26.55	7.00	7.50	736.70	3419.00
136	15.03	2.07	31.11	5.00	6.30	770.80	3453.00
137	14.39	2.26	32.52	5.50	7.90	782.40	3465.00
138	16.13	1.31	21.13	5.00	8.30	819.90	3502.00
139	9.91	0.79	7.83	4.70	9.20	871.40	3554.00
140	5.64	5.8	32.77	5.00	9.00	890.90	3573.00
141	7.13	3.00	21.39	8.50	11.20	908.60	3591.00
142	6.25	3.52	22.00	6.50	10.10	932.40	3615.00
143	9.14	1.31	11.97	10.00	10.00	959.50	3672.00
144	7.89	1.43	11.28	4.50	5.70	986.60	3699.00
145	7.01	1.35	9.46	4.50	6.80	1017.00	3787.00
146	10.76	2.38	25.61	18.50	25.10	1048.00	3818.00
147	16.22	2.74	44.44	14.00	32.80	1084.00	3855.00
148	14.14	2.07	29.27	7.00	22.90	1107.00	3878.00

•

8 CONTINUOUS NETWORK : MAIN CHANNEL, 1962 (Heede data)

Cross-sections listed in their downstream positions.

I.D	W Channel Width in metres	D Channel Mean Depth in metres	XA Section Area in m^2	Sb Bank Gradient %	Sc Channel Gradient %	Lm Mainstream Length in metres	Lt Total Length in metres
149	10.33	1.65	17.04	8.50	20.00	1132.00	3903.00
150	10.06	1.89	19.01	3.00	11.00	1174.00	3944.00
151	12.71	1.31	16.65	3.50	13.90	1199.00	3969.00

C CONTINUOUS NETWORK: MAIN CHANNEL , 1975

Cross-sections listed in their downstream positions.

I.D	W Channel Width in metres	D Channel Mean Depth in metres	XA Section Area in m^2	Sb Bank Gradient %	Sc Channel Gradient %	Lm Mainstream Length in metres	Lt Total Length in metres
193	12.59	1.68	21.15	16.00	29.10	272.80	1768.00
192	14.36	1.55	22.26	20.00	22.90	286.50	1782.00
191	14.60	1.98	28.91	11.00	21.40	299.60	1795.00
190	14.72	1.58	23.26	22.00	20.80	310.00	1805.00
189	15.15	2.10	31.81	12.00	20.70	315.80	1811.00
188	20.48	2.53	51.81	32.00	30.10	326.10	1821.00
187	12.53	2.62	32.83	10.00	27.40	331.60	1827.00
186	10.88	2.47	26.87	20.00	23.10	343.50	1839.00
185	20.79	2.41	50.10	8.00	35.90	355.70	1851.00
183	7.32	0.76	5.56	16.00	34.00	357.80	1853.00
184	13.20	1.28	16.90	20.00	35.70	363.30	1869.00
182	14.02	2.38	33.37	24.00	35.40	374.00	1869.00
181	12.53	2.62	32.83	2.00	35.10	391.10	1886.00
180	27.80	4.51	125.40	24.00	26.10	405.40	2669.00
179	14.54	2.96	43.04	8.00	25.00	424.30	2687.00
178	16.40	1.83	30.01	18.00	24.10	429.20	3055.00
177	14.66	2.41	35.33	5.00	26.00	450.20	3076.00
176	14.87	2.04	30.33	17.00	21.50	462.40	3088.00
175	10.79	1.77	19.10	4.00	23.10	465.40	3089.00
174	11.37	1.68	19.10	32.00	23.00	476.70	3098.00
173	12.59	2.47	31.10	3.80	21.10	491.30	3324.00
172	14.05	1.98	27.82	25.00	19.10	511.20	3137.00
171	14.20	2.59	36.78	4.00	20.00	556.60	3182.00
170	14.23	2.10	29.88	14.80	11.00	582.20	3207.00
169	12.37	0.64	7.92	5.00	15.40	648.90	3275.00
168	11.09	0.52	5.77	19.00	17.10	656.80	3283.00
167	16.67	1.58	26.34	4.00	15.30	661.40	3287.00
166	12.62	1.10	13.88	21.00	28.10	676.70	3303.00
165	10.33	1.77	18.28	12.00	30.00	708.10	3390.00
164	10.94	1.16	12.69	13.00	27.00	719.30	3405.00
163	12.65	1.65	20.87	1.70	27.30	720.60	3610.00
162	18.29	1.58	28.90	12.00	6.00	765.70	3448.00
161	15.09	2.47	37.27	4.00	6.50	773.30	3456.00
160	14.17	1.07	15.16	15.00	8.00	803.20	3485.00
159	11.67	1.04	12.14	0.10	8.50	855.90	3538.00
158	12.04	0.79	9.51	6.00	9.00	867.80	3550.00
157	8.84	0.94	8.31	0.70	10.00	897.30	3567.00
156	8.17	0.46	3.76	13.00	10.00	914.40	3585.00
155	11.89	1.19	14.15	9.50	11.10	928.40	3611.00
154	14.17	1.31	18.56	18.00	10.10	942.80	3636.00
153	6.13	0.46	2.82	1.00	6.60	987.60	3698.00
152	8.60	0.52	4.47	6.00	6.00	997.60	3768.00
221	13.34	1.97	26.37	7.1	6.3	1108.4	3855.00
222	11.49	3.33	38.19	6.3	6.2	1110.7	3878.00
223	12.81	2.132	27.32	7.8	6.0	1113.2	3903.00
224	9.83	3.44	33.83	6.7	5.2	1117.4	3944.00
225	10.10	2.26	22.88	7.1	5.19	1119.9	3969.00
226	11.14	2.14	23.89	7.3	6.1	1119.9	3979.00

D LARGE DISCONTINUOUS TRIBUTARY, 1962

Cross-sections listed in their downstream positions

I.D.	W Channel Width in metres	D Channel Mean Depth in metres	XA Section Area in m^2	Sb Bank Gradient %	Sc Channel Gradient %	Lm Mainstream Length in metres	Lt Total Length in metres
67	13.72	0.49	6.72	37.00	60.00	1.32	71.32
68	14.33	0.52	7.45	30.00	41.00	1.74	91.74
69	11.58	1.19	13.78	12.00	25.80	10.00	122.20
70	22.25	3.59	79.88	36.00	58.30	27.10	139.30
71	13.26	2.59	34.34	26.00	38.40	47.30	248.40
72	10.21	1.86	18.99	13.00	28.30	60.00	275.80
73	25.82	3.17	81.85	10.00	26.70	77.60	293.50
74	26.67	2.16	57.61	6.50	17.70	93.20	309.10
75	25.21	2.19	55.21	6.00	18.10	110.30	423.70
76.	16.95	1.58	26.78	11.50	21.80	124.90	471.80
77	16.58	1.40	23.21	4.50	9.80	142.40	488.30
78	13.56	0.94	12.75	5.00	11.70	154.50	501.40
79	8.69	0.27	2.35	3.00	6.50	177.00	523.90
80	9.91	0.40	3.96	11.00	20.70	193.80	540.70
81	10.21	0.40	4.08	32.00	26.00	210.50	557.50
82	16.61	1.77	29.40	50.00	71.00	230.70	577.60
83	18.59	2.56	47.59	11.50	21.50	243.50	590.40
84	20.27	2.83	57.36	18.00	22.10	261.40	608.40
85	16.46	2.44	40.16	38.00	58.70	286.40	633.40
86	15.45	2.35	35.31	12.00	24.80	298.60	645.60
87	21.34	1.25	26.67	7.00	20.30	316.30	663.20
88	16.00	0.98	15.68	23.00	35.90	379.10	676.10
89	10.04	2.03	20.38	17.00	30.70	350.80	697.70
90	12.65	2.35	29.73	6.50	12.70	363.90	710.80
91	13.56	3.02	40.95	5.00	12.60	383.70	791.60
92	12.50	2.10	26.25	10.00	26.30	401.00	808.90
93	11.13	1.46	16.25	3.00	9.00	421.50	829.40
94	11.83	1.89	22.36	9.50	16.50	434.60	842.50
95	2.80	0.79	2.21	8.50	17.70	442.10	855.30
96	4.66	1.40	6.52	13.00	25.90	467.80	875.70
97	4.48	1.55	6.94	7.00	18.30	479.40	887.30
98	4.60	1.31	6.03	5.00	5.70	491.30	899.20

LARGE DISCONTINUOUS TRIBUTARY, 1975

Cross-sections listed in their downstream positions.

I.D.	W Channel Width in metres	D Channel Mean Depth in metres	XA Section Area in m^2	Sb Bank Gradient %	Sc Channel Gradient %	Lm Mainstream Length in metres	Lt Total Length in metres
62	7.32	0.27	1.98	27.40	22.00	4.57	4.57
64	4.88	0.58	2.83	17.70	9.00	9.14	9.14
63	6.10	0.58	3.54	38.50	30.30	10.67	10.67
65	7.32	0.34	2.49	13.10	25.80	22.86	22.86
66	7.62	1.83	13.94	25.20	43.60	27.43	39.62
61	22.86	4.57	104.50	24.00	28.20	70.10	201.20
218	5.09	0.18	0.92	17.00	17.70	85.65	204.50
217	21.12	3.11	65.68	8.00	18.10	103.30	222.20
216	28.25	1.95	55.09	6.00	21.70	118.90	237.70
60	21.34	1.95	41.61	6.60	8.80	123.40	403.90
215	24.11	2.90	69.92	7.00	9.80	135.90	352.30
214	16.15	2.10	33.91	4.80	11.70	150.60	400.50
213	5.85	1.04	6.08	3.30	6.50	167.00	417.00
59	6.71	0.40	2.68	2.00	6.50	176.80	457.20
212	6.07	0.27	1.64	3.00	20.70	180.10	430.10
211	5.15	0.06	0.31	9.80	26.00	202.70	452.60
210	3.23	0.21	0.68	58.50	70.00	219.50	469.40
58	12.19	1.83	22.31	40.40	25.80	233.20	513.60
209	4.63	0.27	1.25	40.00	21.50	236.20	486.20
208	8.56	0.91	7.79	32.00	22.10	256.30	506.30
207	10.42	1.65	17.19	47.00	58.70	269.10	519.10
57	16.76	2.56	42.91	17.20	22.00	286.50	566.90
206	4.54	0.67	3.04	18.00	24.80	324.30	574.20
205	7.04	1.25	8.80	22.00	20.30	342.00	591.90
204	7.07	1.40	9.90	17.00	35.90	354.80	604.70
203	8.35	1.71	14.28	20.00	30.70	376.40	626.40
202	12.01	1.74	20.90	19.00	33.70	389.50	639.50
201	13.29	2.56	34.02	20.00	12.60	409.30	720.20
200	8.38	1.55	12.99	14.00	26.30	426.70	737.60
199	4.72	0.52	2.45	13.00	9.00	447.10	758.00
198	8.05	1.16	9.34	14.00	16.50	460.30	771.10
197	9.27	0.61	5.65	17.00	17.70	472.70	783.60
196	6.64	1.19	7.90	6.50	25.90	493.50	804.40
195	9.45	1.07	10.11	6.30	18.30	505.00	815.90
194	6.10	0.34	2.07	10.00	5.70	534.00	844.90

LARGE DISCONTINUOUS TRIBUTARY, 1980

Cross-sections listed in their downstream positions.

I.D.	W Channel width in metres	D Channel Mean Depth in metres	XA Section Area in m^2	Sb Bank Gradient %	Sc Channel Gradient %	Lm Mainstream Length in metres	Lt Total Length in metres
224	7.47	1.80	13.45	20.80	22.00	4.57	4.57
226	5.21	0.70	3.65	18.30	9.00	9.14	9.14
225	6.55	0.73	4.78	30.50	30.30	10.67	10.67
227	7.65	0.88	6.73	12.50	25.80	22.86	22.86
228	8.02	1.92	15.40	25.10	43.60	27.43	39.62
223	23.44	5.21	122.10	22.00	28.00	70.10	201.20
252	5.33	1.10	5.86	17.50	17.70	85.65	204.50
252	22.95	3.05	70.00	8.30	18.10	103.30	222.20
251	28.96	1.68	48.65	5.50	21.70	118.90	237.70
222	22.95	2.47	56.69	9.40	8.80	123.40	403.90
250	26.00	2.99	77.74	8.80	9.80	135.90	352.30
249	16.76	2.32	38.88	4.80	11.70	150.60	400.50
248	6.10	1.16	7.08	3.30	6.50	167.00	417.00
221	7.65	0.73	5.58	2.10	6.50	176.80	457.20
247	7.04	0.55	3.87	3.00	20.70	180.10	430.10
246	5.27	2.87	15.12	35.10	26.60	202.70	452.60
245	3.29	3.75	12.34	47.30	70.00	219.50	469.40
220	13.75	2.13	29.29	40.90	25.80	233.20	513.60
244	4.63	2.65	12.27	35.10	21.50	236.20	486.20
243	8.63	4.08	35.21	25.00	22.10	256.30	506.30
242	10.42	1.71	17.82	30.80	58.70	269.10	519.10
219	12.01	4.91	58.97	15.10	22.00	286.50	566.90
241	4.66	0.61	2.84	16.50	24.80	324.30	574.20
240	7.16	0.40	2.86	25.00	20.30	342.00	591.90
239	7.65	0.85	6.50	17.40	35.90	354.80	604.70
238	8.63	1.25	10.79	20.30	30.70	376.40	626.40
237	12.19	1.52	18.53	20.50	33.70	389.50	639.50
236	14.63	2.41	35.26	20.10	12.60	409.30	720.20
235	8.63	1.92	16.57	12.80	26.30	426.70	737.60
234	4.79	0.88	4.21	13.50	9.00	447.10	758.00
233	8.63	1.22	10.53	14.30	16.50	460.30	771.10
232	10.79	0.61	6.58	17.50	17.70	472.70	783.60
231	6.55	1.13	7.40	7.80	25.90	493.50	804.40
230	9.54	0.70	6.68	5.30	18.30	505.00	815.90
229	5.21	0.24	1.25	9.30	5.70	534.00	844.90

APPENDIX 4

SNOWMELT DISCHARGES : SIMULATED SNOWPACK ROUTED AND CONVERTED TO MEAN DAILY FLOWS FOR APRIL AND MAY, AND ACTUAL SNOWPACK DATA, ALSO ROUTED AND CONVERTED TO MEAN DAILY FLOWS FOR EARLY AND LATE FIELDWORK PERIOD IN APRIL, 1981

A. CONTINUOUS GULLY NETWORK : headwaters(1975 sites).

B. CONTINUOUS GULLY NETWORK : main channel(1962 sites).

C. CONTINUOUS GULLY NETWORK : main channel(1975 sites).

D. LARGE DISCONTINUOUS TRIBUTARY :(1962 sites).
(1975 sites).

Source : Simulated snowpack S.W.E data from local snowcourse estimates, routed as explained in text.
Actual snowpack S.W.E values are included in Appendix 6.

A CONTINUOUS NETWORK ABOVE X; HEADWATERS; 1975

Data listed in their downstream positions.

I.D.	APSIM	MAYSIM	FW(1)	FW(2)	
17	0.090	0.490	0.250	0.150	
34	0.300	0.330	0.190	0.040	
10	0.010	0.190	0.070	0.090	
16	0.090	0.490	0.270	0.160	
31	0.000	0.020	0.010	0.000	
41	0.090	0.030	0.010	0.000	
18	0.060	0.320	0.170	0.090	
14	0.020	0.120	0.100	0.000	
28	0.100	0.170	0.090	0.020	
38	0.150	0.170	0.100	0.020	
32	0.000	0.020	0.010	0.000	
22	0.150	0.790	0.420	0.210	
21	0.010	0.030	0.020	0.010	
29	0.130	0.220	0.120	0.030	
30	0.020	0.080	0.050	0.020	
49	0.030	0.160	0.090	0.030	
53	0.040	0.220	0.120	0.070	
54	0.110	0.370	0.190	0.110	
42	0.200	0.060	0.030	0.000	
56	0.040	0.220	0.150	0.020	
39	0.140	0.070	0.040	0.000	
20	0.120	0.140	0.600	0.200	
27	0.330	0.570	0.330	0.090	
55	0.070	0.410	0.210	0.130	
45	0.060	0.290	0.170	0.060 ▼	
46	0.030	0.160	0.090	0.030 ▼	
40	0.580	0.310	0.180	0.000	
33	0.320	0.450	0.260	0.060	
8	1.250	5.290	2.750	1.460	
13	0.210	0.360	0.220	0.030	
15	0.430	1.950	1.040	0.560	
48	0.110	0.530	0.380	0.030	
52	0.580	1.540	1.010	0.440	
19	0.350	1.400	1.210	0.560	
44	0.320	0.660	0.380	0.120 ▼	
37	1.650	1.040	0.620	0.040	
26	1.200	2.040	1.140	0.320	
12	0.460	2.620	1.420	0.680	
47	0.220	0.650	0.460	0.030	
36	1.960	1.340	0.760	0.060	
51	0.580	1.540	1.140	0.440	
25	1.490	2.320	1.310	0.330	
35	2.150	1.400	0.780	0.060	
11	0.940	4.450	2.780	1.410	
50	1.000	2.010	1.240	0.530	
9	1.200	5.010	3.060	1.520	
43	1.940	3.660	2.230	0.770	
24	6.180	8.010	4.800	1.190	
(6*) 7	2.510	10.860	5.980	3.110	
(7*)23	6.360	9.040	5.210	1.360	
(5*) 6	9.400	31.500	16.700	7.890	

APSIM = Computed mean Daily discharges for April at each site, (cumecs x 10^3)

MAYSIM = Computed mean Daily discharges for May at each site,(cumecs x 10^3)

FW(1) = Mean Daily Discharges during the first half of the fieldwork period based on snowpack routing, (cumecs x 10^3)

FW(2) = Mean Daily Discharges during the second half of the fieldwork period based on snowpack routing, (cumecs x 10^3)

I.D. = site number

* = Sites where discharge monitored by velocity meter (see Figure 7)

▼ = Sites used in text to demonstrate routing procedures

B CONTINUOUS NETWORK BELOW X, 1962

Data listed in their downstream positions

	I.D	APSIM	MAYSIM	FW(1)	FW(2)
	99	6.200	8.180	4.870	1.230
	100	6.250	8.540	5.000	1.270
	101	6.270	8.730	5.080	1.310
(7*)	102	6.410	9.200	5.260	1.380
	103	6.450	9.450	5.340	1.400
	104	6.480	9.640	5.390	1.420
(5*)	105	9.880	40.710	19.640	12.140
	106	9.980	40.820	19.670	12.170
	107	10.040	40.840	19.680	12.180
	108	10.060	40.840	19.690	12.190
	109	10.150	41.720	19.940	12.530
	110	10.160	41.780	19.970	12.540
	111	10.160	41.780	19.970	12.540
	112	10.250	41.960	20.020	12.610
	113	10.280	42.350	20.020	12.670
	114	10.310	42.470	20.080	12.670
	115	10.360	42.510	20.070	12.720
	116	11.060	42.920	20.160	12.720
	117	11.150	43.070	20.170	12.720
	118	11.170	43.440	20.220	12.750
(4*)	119	11.230	43.520	20.320	12.780
	120	11.410	43.560	20.390	12.810
(3*)	121	14.690	56.500	26.410	14.460
	122	14.700	56.520	26.410	14.470
	123	14.890	56.570	26.430	14.480
	124	14.960	56.780	26.490	14.500
	125	14.960	56.790	26.500	14.500
	126	14.980	56.890	26.520	14.530
	127	15.080	57.000	26.560	14.560
	128	15.090	57.030	26.570	14.570
	129	15.290	57.050	26.560	14.570
	130	15.310	57.240	26.640	14.620
	131	16.360	61.090	27.920	16.010
	132	17.050	68.440	30.420	18.370
	133	17.140	69.160	30.980	18.540
	134	17.180	69.570	31.120	18.640
	135	17.260	70.720	31.530	18.970
	136	17.450	72.740	32.120	19.340
(2*)	137	17.520	73.130	32.250	19.400
	138	17.910	76.320	33.310	20.480
	139	18.410	78.500	34.080	21.240
	140	18.680	80.130	34.520	21.520
	141	18.730	80.290	34.570	21.560
	142	18.740	80.290	34.570	21.560
	143	18.910	81.430	34.910	21.800
	144	19.090	82.530	35.250	22.030
	145	19.120	82.790	35.340	22.100
	146	19.220	82.890	35.390	22.140
	147	19.410	83.040	35.450	22.200
	148	19.580	83.130	35.490	22.230
	149	19.710	83.250	35.540	22.280
	150	19.750	83.530	35.620	22.340
	151	19.790	83.570	35.640	22.350

APSIM = Computed mean Daily Discharges for April at each site, (cumecs x 10^3)

MAYSIM = Computed mean Daily Discharges for May at each site, (cumecs x 10^3)

FW(1) = Mean Daily Discharges during the first half of the fieldwork period based on snowpack routing, (cumecs x 10^3)

FW(2) = Mean Daily Discharges during the second half of the fieldwork period based on snowpack routing, (cumecs x 10^3)

I.D = site number

* Sites where discharge monitored by velocity meter (see Figure 7)

C CONTINUOUS NETWORK BELOW X, 1975

Data listed in their downstream positions

	I.D	APSIM	MAYSIM	FW(1)	FW(2)
	193	6.200	8.180	4.870	1.230
	192	6.250	8.540	5.000	1.270
	191	6.270	8.730	5.080	1.310
	190	6.310	8.920	5.190	1.330
	189	6.310	8.920	5.190	1.330
	188	6.360	9.040	5.210	1.360
(7*)	187	6.360	9.070	5.210	1.370
	186	6.410	9.200	5.260	1.370
	185	6.440	9.350	5.310	1.380
	183	6.460	9.520	5.360	1.400
	184	6.440	9.350	5.310	1.390
	182	6.470	9.600	5.380	1.410
	181	6.480	9.700	5.410	1.420
(5*)	180	9.400	31.520	16.710	7.890
	179	9.950	40.750	19.640	12.150
	178	9.960	40.780	19.650	12.160
	177	10.090	41.580	19.900	12.480
	176	10.160	41.750	19.960	12.530
	175	10.160	41.760	19.970	12.540
	174	10.250	41.960	20.020	12.610
	173	10.310	42.470	20.050	12.700
(4*)	172	10.680	42.710	20.120	12.720
(3*)	171	14.760	56.530	26.420	14.470
	170	14.980	56.790	26.500	14.500
	169	15.510	60.460	27.680	15.850
	168	15.590	60.760	27.810	15.940
	167	15.600	60.890	27.870	15.980
	166	17.100	68.600	30.630	18.540
	165	17.140	69.160	30.980	18.540
	164	17.180	69.570	31.120	18.640
	163	17.180	69.610	31.130	18.640
	162	17.410	72.420	32.010	19.280
(2*)	161	17.480	72.950	32.210	19.390
	160	17.670	73.540	32.420	19.510
	159	18.190	77.850	33.850	21.020
	158	18.410	78.500	34.080	21.240
	157	18.700	80.200	34.510	21.530
	156	18.730	80.290	34.570	21.560
	155	18.830	80.730	34.650	21.590
	154	18.870	80.960	34.710	21.650
	153	19.090	82.530	35.250	22.030
(1*)	152	19.110	82.690	35.310	22.080

APSIM = Computed mean Daily Discharges for April at each site, (cumecs x 10^3)

MAYSIM = Computed mean Daily Discharges for May at each site, (cumecs x 10^3)

FW(1) = Mean Daily Discharges during the first half of the fieldwork period based on snowpack routing, (cumecs x 10^3)

FW(2) = Mean Daily Discharges during the second half of the fieldwork period based on snowpack routing, (cumecs x 10^3)

I.D = site number

* Sites where discharge monitored by velocity meter (see Figure[7])

D. LARGE DISCONTINUOUS TRIBUTARY, 1962

Data listed in their downstream positions

I.D.	APSIM	MAYSIM	FW (1)	FW (2)
67	0.150	1.240	0.510	0.460
68	0.160	1.370	0.580	0.530
69	0.380	1.690	0.850	0.630
70	0.490	2.000	1.060	0.830
71	0.520	2.450	1.230	1.030
72	0.550	2.550	1.260	1.060
(9*)73	0.620	2.690	1.350	1.090
74	0.670	2.780	1.410	1.100
75	0.750	2.890	1.420	1.110
76	0.770	2.890	1.410	1.180
77	0.900	3.440	1.710	1.250
78	0.940	3.550	1.760	1.300
79	1.350	3.820	1.890	1.310
80	1.440	4.250	2.160	1.340
81	1.550	4.750	2.440	1.370
82	1.710	5.550	2.900	1.450
83	1.760	5.790	3.010	1.460
84	1.930	6.590	3.450	1.510
85	2.170	7.790	4.050	1.560
86	2.250	8.170	4.190	1.580
87	2.450	9.100	4.630	1.610
88	2.600	9.840	4.850	1.620
89	3.080	12.170	5.710	1.650
90	3.050	12.000	5.770	1.650
91	3.180	12.590	5.900	1.650
92	3.230	12.830	5.970	1.650
93	3.240	12.840	5.970	1.650
94	3.240	12.850	5.980	1.650
95	3.250	12.890	5.990	1.650
96	3.250	12.890	5.990	1.650
97	3.250	12.900	5.990	1.650
(8*)98	3.250	12.910	6.010	1.650

APSIM = Computed mean Daily Discharges for April at each site (cumecs, x 10^3)

MAYSIM = Computed mean Daily Discharges for May at each site (cumecs x 10^3)

FW (1) = Mean Daily Discharges during the first half of the fieldwork period based on snowpack routing (cumecs x 10^3)

FW (2) = Mean Daily Discharges during the second half of the field-work period based on snowpack routing (cumecs x 10^3)

I.D. = site number

* Sites where discharge monitored in the field by velocity meter (see Figure 7)

LARGE DISCONTINUOUS TRIBUTARY, 1975

Data listed in their downstream positions

	I.D.	APSIM	MAYSIM	FW (1)	FW (2)
	62	0.000	0.140	0.100	0.060
	64	0.030	0.190	0.050	0.100
	63	0.010	0.180	0.040	0.080
	65	0.020	0.110	0.060	0.020
(9*)	66	0.040	0.220	0.150	0.020
	61	0.130	1.190	0.490	0.440
	218	0.150	1.360	0.570	0.520
	217	0.380	1.460	0.850	0.630
	216	0.460	1.720	0.940	0.740
	60	0.460	1.720	0.940	0.740
	215	0.490	2.000	1.060	0.830
	214	0.510	2.270	1.160	0.950
	213	0.550	2.550	1.260	1.060
	59	0.550	2.590	1.280	1.080
	212	0.590	2.650	1.330	1.090
	211	0.670	2.780	1.410	1.100
	210	0.750	2.890	1.470	1.110
	58	0.770	2.890	1.410	1.180
	209	0.830	3.160	1.580	1.180
	208	0.940	3.550	1.760	1.300
	207	1.150	3.690	1.830	1.310
	57	1.350	3.820	1.890	1.310
	206	1.710	5.550	2.900	1.450
	205	1.760	5.790	3.010	1.460
	204	1.930	6.590	3.450	1.510
	203	2.090	7.390	3.870	1.550
	202	2.170	7.790	4.050	1.560
	201	2.360	8.670	4.440	1.600
	200	2.520	9.440	4.690	1.620
	199	2.920	11.380	5.480	1.640
	198	3.050	12.000	5.710	1.650
	197	3.080	12.170	5.770	1.650
	196	3.180	12.590	5.900	1.650
	195	3.250	12.890	5.970	1.650
(8*)	194	3.250	12.910	6.010	1.650

APSIM = Computed mean Daily Discharges for April at each site (cumecs x 10^3)

MAYSIM = Computed mean Daily Discharges for May at each site (cumecs x 10^3)

FW (1) = Mean Daily Discharges during the first half of the fieldwork period based on snowpack routing (cumecs x 10^3)

FW (2) = Mean Daily Discharges during the second half of the field-work period based on snowpack routing (cumecs x 10^3)

I.D. = site number

Since the 1980 survey was undertaken on these same sites, discharges have not been listed as they correspond to the above.

* Site where discharge monitored by velocity meter (see Figure 7)

APPENDIX 5

EVENT FREQUENCY ANALYSES

A. SNOWWATER EQUIVALENT AT McCLURE PASS ON APRIL 1st, 1950-1980

Appendix contains the method and data used to construct an Event Frequency Curve using the Log Pearson III system*

Source : Data were kindly supplied by the S.C.S. Office Diamond Hill, Denver, Colorado, with assistance from B. Shafer, Hydrologist.

* U.S. Water Resource Council, 1977, Guidelines for determining Flood Flow Frequency , Washington, D.C.

B. SUMMER STORMS AT ALKALI CREEK , 1967-1972

Appendix contains the methods and data used to construct an Event Frequency Curve using the Log Pearson III system*

Source : Data from the R.R.G records at Alkali Creek

* U.S Water Resource Council, 1977, Guidelines for determining Flood Flow Frequency, Washington, D.C.

A SNOW WATER EQUIVALENT AT McCLURE PASS ON APRIL 1st 1950-1980

Log Pearson III Analysis

The log of the S.W.E values for given recurrence probabllities is calculated from the mean of the logs and standard deviation of the logs, and a value called K. This latter is a function of the distribution skewness and the probability level of interest. Values of K for a given skewness is tabulated in most Hydrology texts.

Thus;

log(S.W.E) = (mean of S.W.E's) + K.(STD DEV of S.W.E's)

for each level of probability.

For the SNOW WATER EQUVALENT DATA : log (MEAN S.W.E) = 1.570
log (STD DEV. of the logged S.W.E's) = 0.1418
log Skewness = -0.1557

Hence;

% probability of a greater value	S.W.E, cm.
99	16.76
95	21.34
90	24.38
70	32.00
50	37.34
30	44.45
10	56.13
5	62.74
1	76.71

(DATA - over page)

YEAR	S.W.E, April 1st , cm.
1950	44.19
1951	35.56
1952	68.58
1953	24.38
1954	21.33
1955	35.56
1956	35.81
1957	56.64
1958	38.35
1959	31.75
1960	36.57
1961	22.60
1962	54.86
1963	29.72
1964	28.45
1965	49.29
1966	24.64
1967	33.02
1968	38.61
1969	49.28
1970	40.13
1971	33.27
1972	23.37
1973	46.48
1974	36.58
1975	54.86
1976	37.08
1977	20.07
1978	46.23
1979	55.37
1980	58.93

B. SUMMER STORM EVENT FREQUENCY ANALYSIS, individual storms 1967-1972
Log Pearson III Analysis

As before, the log. of the event precipitation total for given recurrence probabilities is calculated from the mean of the logs and standard deviation of the logs, and a value called K. This latter is a function of the distibution skewness and the probability level of interest.Values of K are readily available from most Hydrology Texts.

Thus;

log(PPN) = (Mean of PPN's) + K.(STD. DEV. of PPN's)

for each level of probability.

For the Summer Storm data log (MEAN PPN) = -0.252
log (STD. DEV) = 0.3039
log (SKEWNESS) = 0.0464

% probability of greater value	K	log(EVENT PPN)	non-log value
99	-2.289	-0.9476	0.113
95	-1.630	-0.7473	0.179
90	-1.276	-0.640	0.245
80	-0.844	-0.5084	0.309
50	0.008	-0.2496	0.562
20	0.839	0.0030	1.005
10	1.297	0.142	1.390
4	1.768	0.2853	1.930
2	2.080	0.380	2.46
1	2.363	0.466	2.92
0.5	2.623	0.545	3.51

Raw data for individual events included as Appendix 1

APPENDIX 6

A. SNOWCOURSE SURVEY, APRIL 1-4, 1981

B. SNOWCOURSE SURVEY, APRIL 16-20, 1981

Source : Field data

A. SNOWCOURSE SURVEY, April 1-4, 1981 (Sample locations noted on Figure 7)

Site: 6C		
Vegetation: Bare/sagebrush		
Slope angle: 7.5°		
Dist, m	Snow depth, cm	Water equiv, cm
0.00	17.78	5.84
6.10	18.54	6.09
12.20	18.54	6.09
18.29	18.54	6.09
24.38	18.54	6.09
30.48	18.80	6.35
36.58	18.54	6.09
42.67	18.29	5.84
48.77	18.54	6.09
54.86	18.29	5.84
	$\Sigma \frac{\text{Depth}}{n}$ = 18.45	$\Sigma \frac{\text{SWE}}{n}$ = 6.05
Density = 0.33		

Site: 5C		
Vegetation: Oak/sage		
Slope angle: 10.25°		
Dist, m	Snow depth, cm	Water equiv, cm
0.00	31.24	6.10
6.10	31.50	6.10
12.20	31.24	6.35
18.29	32.00	6.10
24.38	31.75	6.10
30.48	32.51	6.35
36.58	32.51	6.86
42.67	32.26	7.11
48.77	32.51	6.86
54.86	32.26	6.86
	$\Sigma \frac{\text{Depth}}{n}$ = 31.98	$\Sigma \frac{\text{SWE}}{n}$ = 6.48
Density = 0.20		

Site: 4C		
Vegetation: Mixed shrub/W wheat		
Slope angle: 14.5°		
Dist, m	Snow depth, cm	Water equiv, cm
0.00	9.40	2.29
6.10	18.29	4.83
12.20	20.57	5.08
18.29	21.59	5.33
24.38	27.94	6.35
30.48	33.53	8.38
36.58	33.02	8.13
42.67	33.02	8.13
48.77	33.02	7.62
54.86	34.04	7.62
	$\Sigma \frac{\text{Depth}}{n}$ = 26.44	$\Sigma \frac{\text{SWE}}{n}$ = 5.89
Density = 0.22		

Site: 3C		
Vegetation: Oak/sagebrush		
Slope angle: 17.25°		
Dist, m	Snow depth, cm	Water equiv, cm
0.00	29.97	7.11
6.10	34.29	7.11
12.20	35.05	6.86
18.29	34.80	6.60
24.38	38.10	7.37
30.48	39.88	7.37
36.58	39.88	7.87
42.67	39.88	8.13
48.77	40.13	7.87
54.86	40.13	7.87
	$\Sigma \frac{\text{Depth}}{n}$ = 37.21	$\Sigma \frac{\text{SWE}}{n}$ = 7.42
Density = 0.20		

continued ...

continued ...

Site: 2C		
Vegetation: Oak/sagebrush		
Slope angle: 19.00°		
Dist, m	Snow depth, cm	Water equiv, cm
0.00	35.05	7.11
6.10	35.05	7.11
12.20	34.80	6.86
18.29	34.80	6.60
24.38	36.32	8.64
30.48	37.34	8.89
36.58	36.58	8.64
42.67	36.32	8.38
48.77	35.56	7.62
54.36	35.56	7.62
	$\Sigma\frac{\text{Depth}}{n}$ = 35.74	$\Sigma\frac{\text{SWE}}{n}$ = 7.75
Density = 0.22		

Site: 1C		
Vegetation: Oak/sagebrush		
Slope angle: 9.00°		
Dist, m	Snow depth, cm	Water equiv, cm
0.00	40.64	8.89
6.10	40.64	8.89
12.20	40.64	8.89
18.29	40.64	8.89
24.38	40.64	8.89
30.48	39.12	8.64
36.58	39.10	8.38
42.67	34.54	7.62
48.77	34.54	7.62
54.86	33.53	7.37
	$\Sigma\frac{\text{Depth}}{n}$ = 38.40	$\Sigma\frac{\text{SWE}}{n}$ = 8.41
Density = 0.22		

Site: 6B		
Vegetation: Patch sites: various		
Slope angle: 5° to 10°		
Dist, m	Snow depth, cm	Water equiv, cm
	2.0	0.45
	1.25	0.50
	1.55	0.56
	1.40	0.51
	$\Sigma\frac{\text{Depth}}{n}$ = 1.55	$\Sigma\frac{\text{SWE}}{n}$ = 0.50
Density = 0.32		

Site: 5B		
Vegetation: Patch sites: various		
Slope angle 5° - 10°		
Dist, m	Snow depth, cm	Water equiv, cm
	3.62	1.53
	3.76	1.54
	3.55	1.29
	3.48	1.42
	4.00	1.69
	$\Sigma\frac{\text{Depth}}{n}$ = 3.68	$\Sigma\frac{\text{SWE}}{n}$ = 1.50
Density = 0.41		

continued ...

continued ...

Site: 4B		
Vegetation: Patch sites: various		
Slope angle: 7.5° to 14.50°		
Dist, m	Snow depth, cm	Water equiv, cm
	6.68	2.50
	6.60	2.55
	6.90	2.52
	7.11	2.65
	6.69	2.50
	$\Sigma \frac{\text{Depth}}{n}$ = 6.79	$\Sigma \frac{\text{SWE}}{n}$ = 2.54
Density = 0.37		

Site: 3B		
Vegetation: Patch sites: various		
Slope angle: 17.0°		
Dist, m	Snow depth, cm	Water equiv, cm
0.00	26.67	5.84
6.10	26.67	5.84
12.20	27.94	6.10
18.29	12.70	2.79
24.38	10.16	1.78
	$\Sigma \frac{\text{Depth}}{n}$ = 20.83	$\Sigma \frac{\text{SWE}}{n}$ = 4.47
Density = 0.21		

Site: 2B		
Vegetation: Sagebrush		
Slope angle: 16.0°		
Dist, m	Snow depth, cm	Water equiv, cm
0.00	30.99	6.86
6.10	26.67	5.84
12.20	26.67	5.84
18.29	23.62	5.08
24.38	23.67	5.08
30.48	22.86	4.83
36.58	28.96	6.35
42.67	28.96	6.35
48.77	28.70	6.35
54.86	26.67	5.84
	$\Sigma \frac{\text{Depth}}{n}$ = 26.78	$\Sigma \frac{\text{SWE}}{n}$ = 5.84
Density = 0.22		

Site: 1B		
Vegetation: Mixed brush inc. sage		
Slope angle: 15.0°		
Dist, m	Snow depth, cm	Water equiv, cm
0.00	34.54	7.62
6.10	34.54	7.62
12.20	34.54	7.62
18.29	34.54	7.62
24.38	29.97	6.60
30.48	28.96	6.35
36.58	28.96	6.35
42.67	27.94	6.10
48.77	22.86	5.08
54.86	22.86	5.08
	$\Sigma \frac{\text{Depth}}{n}$ = 29.97	$\Sigma \frac{\text{SWE}}{n}$ = 6.60
Density = 0.22		

continued ...

continued ... **Extra patch survey in zone 2C**

Site: 2C patch No 1		
Vegetation: oak/bare		
Slope angle: 23.00°		
Dist, m	Snow depth, cm	Water equiv, cm
0.00	46.48	10.16
6.10	43.18	8.89
12.20	30.48	7.62
18.29	29.21	7.37
24.38	22.86	6.35
	$\Sigma \frac{\text{Depth}}{n}$ = 34.44	$\Sigma \frac{\text{SWE}}{n}$ = 8.08
Density = 0.23		

Site: 2C patch No 2		
Vegetation: oak/sage		
Slope angle: 10.0°		
Dist, m	Snow depth, cm	Water equiv, cm
0.00	29.21	7.11
6.10	29.21	8.38
12.20	32.26	8.89
18.29	41.40	11.18
24.38	9.14	2.54
	$\Sigma \frac{\text{Depth}}{n}$ = 28.24	$\Sigma \frac{\text{SWE}}{n}$ = 7.62
Density = 0.27		

B. SNOWCOURSE SURVEY, APRIL 16-20, 1981 (Sample locations noted on Figure 7)

Site: 6C		
Vegetation: Bare/sagebrush		
Slope angle: 7.5°		
Dist, m	Snow depth, cm	Water equiv, cm
0.00	8.79	2.94
6.10	9.50	3.00
12.20	9.50	3.10
18.29	9.50	3.10
24.38	9.58	3.10
30.48	9.59	3.10
36.58	9.80	3.35
42.67	9.54	3.10
48.77	9.30	2.84
54.86	9.53	3.10
	$\Sigma \frac{\text{Depth}}{n}$ = 9.46	$\Sigma \frac{\text{SWE}}{n}$ = 3.07
Density = 0.32		

Site: 5C		
Vegetation: Oak/sagebrush		
Slope angle: 10.25°		
Dist, m	Snow depth, cm	Water equiv, cm
0.00	14.48	5.08
6.10	13.46	4.57
12.20	14.73	5.08
18.29	1.24	0.08
24.38	1.24	0.10
30.48	1.25	0.08
36.58	7.11	2.28
42.67	7.62	2.54
48.77	6.10	2.03
54.86	10.16	3.30
	$\Sigma \frac{\text{Depth}}{n}$ = 7.74	$\Sigma \frac{\text{SWE}}{n}$ = 2.51
Density = 0.32		

Site: 4C		
Vegetation: Mixed shrub/W wheat		
Slope angle: 14.5°		
Dist, m	Snow depth, cm	Water equiv, cm
0.00	0.40	0.10
6.10	0.70	0.09
12.20	0.70	0.10
18.29	0.08	0.10
24.38	16.26	5.84
30.48	21.08	7.62
36.58	17.27	6.35
42.67	17.78	6.35
48.77	16.26	5.84
54.86	9.40	3.30
	$\Sigma \frac{\text{Depth}}{n}$ = 9.99	$\Sigma \frac{\text{SWE}}{n}$ = 3.56
Density = 0.36		

Site: 3C		
Vegetation: Oak/sagebrush		
Slope angle 17.25°		
Dist, m	Snow depth, cm	Water equiv, cm
0.00	10.41	3.56
6.10	10.92	3.81
12.20	10.67	3.55
18.29	11.09	4.10
24.38	12.00	4.08
30.48	14.00	4.10
36.58	12.70	4.57
42.67	12.70	4.57
48.77	12.70	4.57
54.86	10.67	3.36
	$\Sigma \frac{\text{Depth}}{n}$ = 11.79	$\Sigma \frac{\text{SWE}}{n}$ = 4.03
Density = 0.34		

continued ...

continued ...

Site: 2C		
Vegetation: Oak/sagebrush		
Slope angle: 19.0°		
Dist, m	Snow depth, cm	Water equiv, cm
0.00	13.72	4.83
6.10	11.68	4.06
12.20	12.45	4.32
18.29	12.45	4.43
24.38	17.27	6.10
30.48	17.78	6.60
36.58	17.53	6.60
42.67	17.53	6.35
48.77	7.37	2.54
54.86	7.37	2.54
	$\Sigma \frac{\text{Depth}}{n} = 13.51$	$\Sigma \frac{\text{SWE}}{n} = 4.84$
Density = 0.36		

Site: 1C		
Vegetation: Oak/sagebrush		
Slope angle: 9.0°		
Dist, m	Snow depth, cm	Water equiv, cm
0.00	20.83	7.37
6.10	19.05	6.86
12.20	17.78	6.35
18.29	17.78	6.35
24.38	17.78	6.35
30.48	17.53	6.10
36.58	16.26	5.84
42.67	5.59	4.32
48.77	5.59	4.32
54.86	5.08	2.58
	$\Sigma \frac{\text{Depth}}{n} = 14.32$	$\Sigma \frac{\text{SWE}}{n} = 5.64$
Density = 0.39		

Site: 3B		
Vegetation: Patch sites: various		
Slope angle: 10° to 17°		
Dist, m	Snow depth, cm	Water equiv, cm
	2.00	0.70
	3.07	1.25
	2.00	0.80
	1.00	0.05
	2.01	0.05
	$\Sigma \frac{\text{Depth}}{n} = 2.01$	$\Sigma \frac{\text{SWE}}{n} = 0.51$
Density = 0.25		

Site: 2B		
Vegetation: Patch sites: various		
Slope angle: 10° to 17°		
Dist, m	Snow depth, cm	Water equiv, cm
	3.31	1.50
	4.07	1.45
	4.00	1.54
	4.00	1.50
	4.00	1.50
	$\Sigma \frac{\text{Depth}}{n} = 3.84$	$\Sigma \frac{\text{SWE}}{n} = 1.50$
Density = 0.39		

continued ...

continued ...

Site: 1B		
Vegetation: Mixed brush, incl. sage		
Slope angle: 15.000°		
Dist, m	Snow depth, cm	Water equiv, cm
0.00	5.84	2.29
6.10	5.84	2.29
12.20	6.35	2.54
18.29	6.35	2.54
24.38	6.35	2.54
30.48	5.84	2.29
36.58	6.60	3.05
42.67	6.86	3.30
48.77	6.35	2.29
54.86	5.84	1.78
	$\Sigma \frac{\text{Depth}}{n} = 6.22$	$\Sigma \frac{\text{SWE}}{n} = 2.54$
Density = 0.38		

APPENDIX 7

A. FIELD DISCHARGE CALCULATIONS : SNOWMELT

(i) SPATIAL DATA April 7th, 1981
April 19th, 1981

(ii) TEMPORAL DATA
April 5th, 1981
April 18th, 1981

B. DERIVATION OF INDECES TO RELATE PEAK TO MEAN DAILY FLOWS

C. PEAK DAILY DISCHARGES FROM FIELD DATA. SIMULATED MEAN AND PEAK DAILY DISCHARGES AT THE SAME SITES, including SUSPENDED SEDIMENT CONCENTRATIONS: SUMMARY TABLE.

(i) SPATIAL DATA April 7th, 1981
April 19th, 1981

(ii) TEMPORAL DATA
April 5th, 1981
April 18th, 1981

Source : Field data, and simulations from snowpack routing

A. FIELD DISCHARGE CALCULATIONS; SNOWMELT

(i) SPATIAL DATA (sample locations noted on Figure 7)

APRIL 7th.1981

Site	Width,w, (m)	Mean Depth,d, (m)	Revs/sec,n, at dmax	Velocity,v, (m/sec)	Discharge,Q = w.d.v (cumecs)
1	0.82	0.28	2.19	0.562	0.1290
2	0.73	0.41	1.48	0.380	0.1132
3	0.81	0.33	1.40	0.360	0.0960
4	0.88	0.28	1.12	0.280	0.0699
5	0.47	0.22	2.11	0.538	0.0549
6	0.42	0.11	2.28	0.581	0.0253
7	0.39	0.08	2.27	0.580	0.0166
8	0.97	0.07	1.40	0.360	0.0249
9	0.33	0.07	1.25	0.322	0.0070

APRIL 19th,1981

1	0.50	0.25	1.60	0.420	0.0520
2	0.50	0.26	1.51	0.385	0.0491
3	0.52	0.25	1.22	0.311	0.0401
4	0.53	0.26	1.18	0.285	0.0393
5	0.31	0.21	1.48	0.380	0.0238
6	0.27	0.10	1.26	0.314	0.0084
7	0.14	0.11	1.15	0.283	0.0042
8	0.82	0.07	0.32	0.089	0.0051
9	0.48	0.07	0.35	0.092	0.0030

(ii) TEMPORAL DATA:(Diurnal variations at bottom of watershed , Station 1)

APRIL 5th.1981

Time					
11.00	0.41	0.13	0.052	0.019	0.0010
11.30	0.42	0.14	0.060	0.021	0.0012
12.00	0.43	0.14	0.082	0.027	0.0016
12.30	0.43	0.15	0.115	0.034	0.0022
13.00	0.44	0.15	0.170	0.047	0.0031
13.30	0.45	0.16	0.220	0.059	0.0042
14.00	0.47	0.16	0.600	0.154	0.0116
14.30	0.58	0.27	1.180	0.428	0.0671
15.00	0.60	0.30	2.330	0.592	0.1065

/cont.

/cont.

Time	w	d	n	v	Q
15.30	0.83	0.33	2.010	0.511	0.1399
16.00	0.82	0.28	2.180	0.555	0.1276
16.30	0.43	0.22	2.020	0.513	0.0485
17.00	0.40	0.15	0.350	0.092	0.0055
17.30	Freezing				

APRIL 18th.1981

12.00	No flow				
12.30	0.44	0.13	0.100	0.035	0.0020
13.00	0.44	0.14	0.100	0.039	0.0024
13.30	0.45	0.14	0.135	0.046	0.0029
14.00	0.47	0.17	0.315	0.089	0.0071
14.30	0.48	0.20	1.83	0.469	0.0450
15.00	0.50	0.25	1.66	0.424	0.0530
15.30	0.51	0.24	1.30	0.335	0.0410
16.00	0.50	0.24	1.26	0.325	0.0390
16.30	0.48	0.22	1.25	0.322	0.0340
17.00	0.48	0.19	0.36	0.100	0.0092
17.30	Freezing				

B. DERIVATION OF INDECES TO RELATE PEAK TO MEAN DAILY FLOW

April 5 Using the Diurnal data collected on April 5th,1981,

Maximum discharge = 0.140 cumecs

Minimum discharge = 0.001 cumecs

Mean Discharge = 0.0402 cumecs

Therefore k = Ratio of Max to Mean = 3.35

April 18th

Using the data collected on April 18th,1981

Maximum discharge = 0.053 cumecs

Minimum discharge = 0.000 cumecs

Mean discharge = 0.018 cumecs

Therefore k = Ratio of Max to Mean = 2.944

The average ratio over the melt period monitored is 3.147

C. PEAK DAILY DISCHARGES FROM FIELD DATA, SIMULATED MEAN AND PEAK DAILY DISCHARGES AND SUSPENDED SEDIMENT CONCENTRATIONS OF MEASURED FLOWS: SUMMARY TABLES

(i) SPATIAL DATA (Sample locations noted on Figure 7)

APRIL 7, 1981

Site	Field discharge data Peak daily flows	Simulated discharge data using routed snowpack		Sediment data
	(cumecs)	Mean (cumecs)	Peak = Mean x k* (cumecs)	(ppm)
1	0.1290	0.0353	0.1183	7,692
2	0.1132	0.0322	0.1080	6,650
3	0.0960	0.0264	0.0884	6,080
4	0.0699	0.0204	0.0682	5,570
5	0.0549	0.0196	0.0657	3,970
6	0.0253	0.0060	0.0250	1,585
7	0.0166	0.0052	0.0174	635
8	0.0249	0.0060	0.0201	6,150
9	0.0070	0.0013	0.0042	4,745

APRIL 19, 1981

1	0.0520	0.0221	0.0651	2,763
2	0.0491	0.0194	0.0570	2,491
3	0.0401	0.0145	0.0427	2,012
4	0.0393	0.0128	0.0377	1,891
5	0.0238	0.0121	0.0356	1,807
6	0.0084	0.0031	0.0091	617
7	0.0042	0.0014	0.0041	202
8	0.0051	0.0016	0.0051	182
9	0.0030	0.0011	0.0032	108

k* refers to the constant which was derived in the previous section relating mean to peak daily discharges as determined from diurnal discharge data.

continued ...

(ii) TEMPORAL DATA (Diurnal variations at the bottom of the watershed, Section 1)

APRIL 5. 1981

Time	Field discharge data (cumecs)	Sediment concentration (ppm)
11.00	0.0010	14
11.30	0.0012	17
12.00	0.0016	27
12.30	0.0022	40
13.00	0.0031	50
13.30	0.0042	55
14.00	0.0116	313
14.30	0.0671	1,635
15.00	0.1065	1,654
15.30	0.1399	6,130
16.00	0.1276	7,597
16.30	0.0485	1,814
17.00	0.0055	338

APRIL 18. 1981

12.00 no flow		
12.30	0.0020	43
13.00	0.0024	47
13.30	0.0029	54
14.00	0.0071	106
14.30	0.0450	1,216
15.00	0.0530	1,951
15.30	0.0410	1,316
16.00	0.0390	1,107
16.30	0.0340	891
17.00	0.0092	181

APPENDIX 8

DATAFILES FOR THE OPERATION OF ROUTE.PAS

A. SMALL DISCONTINUOUS GULLY (test file).
   CONTINUOUS NETWORK

B. LARGE DISCONTINUOUS TRIBUTARY

Notes :

On these tables the following symbol definitions apply;

Site = local site I.D for routing purposes (Since all sites are still in the same contiguous listing positions, the old site I.D can be read from Appendix 3 if required)

Next, last, etc.. = network keys, as explained in the text

t1...4 = trib1, trib2, trib3, trib4, (all network keys)

SL = slopelength, m

AB = Bare area, m^2

S = Channel slope, m/m

N = Manning roughness

$\triangle$ y = incremental distance in the y plane, m.

Source : Except for N values, which are estimates, all data derived from Figures 4 and 7 (back folder).

ROUTEA.DAT - datafile for the small discontinuous gully.

Site	last	t1	t2	t3	t4	next	SL	AB	Δy	S	N
1	0	0	0	0	0	2	170	5804.0	5.0	0.331	0.055
2	1	0	0	0	0	4	110	1082.0	100.0	0.220	0.055
3	0	0	0	0	0	4	25	45.0	5.0	0.204	0.055
4	2	3	0	0	0	5	44	968.0	100.0	0.314	0.050
5	4	0	0	0	0	5	60	698.0	60.0	0.047	0.050

ROUTEB.DAT - datafile for the continuous network.

Site	last	t1	t2	t3	t4	next	SL	AB	Δy	S	N
1	0	0	0	0	0	2	100.0	204.0	5.0	0.272	0.055
2	1	0	0	0	0	7	55.0	885.0	60.0	0.131	0.055
3	0	0	0	0	0	6	110.0	673.0	5.0	0.182	0.055
4	0	0	0	0	0	6	110.0	970.0	5.0	0.326	0.055
5	0	0	0	0	0	6	120.0	387.0	5.0	0.361	0.055
6	3	4	5	0	0	7	120.0	2149.0	120.0	0.554	0.050
7	6	2	0	0	0	12	40.0	819.0	60.0	0.373	0.050
8	0	0	0	0	0	11	85.0	1064.0	10.0	0.214	0.055
9	0	0	0	0	0	11	30.0	178.0	5.0	0.361	0.055
10	0	0	0	0	0	11	90.0	812.0	5.0	0.331	0.055
11	8	9	10	0	0	12	60.0	1918.0	112.0	0.514	0.050
12	7	11	0	0	0	14	75.0	898.0	90.0	0.120	0.045
13	0	0	0	0	0	14	55.0	337.0	5.0	0.286	0.055
14	12	13	0	0	0	16	80.0	916.0	70.0	0.361	0.045
15	0	0	0	0	0	16	200.0	1430.0	62.0	0.193	0.055
16	14	15	0	0	0	56	80.0	930.0	85.0	0.263	0.045
17	0	0	0	0	0	22	87.0	964.0	18.0	0.236	0.055
18	0	0	0	0	0	22	80.0	288.0	5.0	0.349	0.055
19	0	0	0	0	0	22	53.0	378.0	5.0	0.456	0.055
20	0	0	0	0	0	22	53.0	224.0	7.0	0.469	0.055
21	0	0	0	0	0	22	15.0	90.0	5.0	0.220	0.055
22	17	18	19	20	21	22	75.0	3549.0	150.0	0.085	0.050
23	0	0	0	0	0	26	20.0	90.0	7.0	0.410	0.055
24	0	0	0	0	0	25	45.0	344.0	5.0	0.204	0.055
25	24	0	0	0	0	26	25.0	392.0	50.0	0.280	0.055
26	25	22	23	0	0	49	83.0	378.0	125.0	0.392	0.050
27	0	0	0	0	0	30	63.0	390.0	5.0	0.303	0.055
28	0	0	0	0	0	30	60.0	431.0	22.0	0.373	0.055
29	0	0	0	0	0	30	145.0	2047.0	52.0	0.204	0.055
30	29	27	28	0	0	31	124.0	4247.0	120.0	0.297	0.050
31	30	0	0	0	0	32	100.0	2146.0	60.0	0.322	0.050
32	31	0	0	0	0	49	70.0	867.0	55.0	0.340	0.050
33	0	0	0	0	0	49	85.0	397.0	5.0	0.314	0.055
34	0	0	0	0	0	49	110.0	788.0	10.0	0.503	0.055
35	0	0	0	0	0	37	94.0	1172.0	30.0	0.373	0.055
36	0	0	0	0	0	37	70.0	694.0	35.0	0.392	0.055
37	35	36	0	0	0	48	60.0	1611.0	67.0	0.151	0.050
38	0	0	0	0	0	39	55.0	610.0	15.0	0.504	0.055
39	38	0	0	0	0	40	40.0	1205.0	50.0	0.075	0.055
40	39	0	0	0	0	48	20.0	535.0	56.0	0.258	0.055
41	0	0	0	0	0	45	75.0	582.0	10.0	0.337	0.055
42	0	0	0	0	0	45	85.0	837.0	10.0	0.286	0.055
43	0	0	0	0	0	45	80.0	1483.0	36.0	0.291	0.055
44	0	0	0	0	0	45	80.0	702.0	30.0	0.214	0.055
45	41	42	43	44	0	46	130.0	3800.0	145.0	0.182	0.045

/cont..

/ ROUTEB.DAT, cont.,

Site	last	t1	t2	t3	t4	next	SL	AB	Δγ	S	N
46	45	0	0	0	0	47	70.0	1100.0	60.0	0.125	0.045
47	46	0	0	0	0	48	100.0	949.0	50.0	0.115	0.045
48	47	37	40	0	0	49	136.0	1811.0	95.0	0.214	0.045
49	26	32	33	34	48	50	70.0	2547.0	190.0	0.361	0.040
50	49	0	0	0	0	51	60.0	187.0	10.0	0.160	0.040
51	50	0	0	0	0	52	85.0	272.0	10.0	0.200	0.040
52	51	0	0	0	0	53	90.0	489.0	15.0	0.165	0.040
53	52	0	0	0	0	54	36.0	374.0	22.0	0.095	0.040
54	53	0	0	0	0	55	38.0	586.0	30.0	0.160	0.040
55	54	0	0	0	0	56	20.0	459.0	20.0	0.190	0.040
56	55	16	0	0	0	57	50.0	10147.0	20.0	0.094	0.040
57	56	0	0	0	0	58	55.0	1069.0	40.0	0.130	0.040
58	57	0	0	0	0	59	60.0	325.0	12.0	0.125	0.040
59	58	0	0	0	0	60	27.0	290.0	10.0	0.135	0.040
60	59	0	0	0	0	61	12.0	112.0	10.0	0.125	0.040
61	60	0	0	0	0	62	85.0	835.0	15.0	0.125	0.040
62	61	0	0	0	0	63	32.0	262.0	7.0	0.125	0.040
63	62	0	0	0	0	64	23.0	10.0	3.0	0.130	0.040
64	63	0	0	0	0	65	50.0	378.0	12.0	0.145	0.040
65	64	0	0	0	0	66	50.0	281.0	10.0	0.115	0.040
66	65	0	0	0	0	67	34.0	244.0	10.0	0.115	0.040
67	66	0	0	0	0	68	40.0	279.0	15.0	0.105	0.040
68	67	0	0	0	0	69	85.0	1171.0	15.0	0.105	0.040
69	68	0	0	0	0	70	130.0	543.0	4.0	0.085	0.040
70	69	0	0	0	0	71	63.0	244.0	6.0	0.080	0.040
71	70	0	0	0	0	72	135.0	816.0	3.0	0.145	0.040
72	71	0	0	0	0	73	124.0	628.0	5.0	0.145	0.040
73	72	0	0	0	0	74	25.0	263.0	10.0	0.135	0.040
74	73	0	0	0	0	75	34.0	147.0	7.0	0.125	0.040
75	74	0	0	0	0	76	41.0	415.0	16.0	0.095	0.040
76	75	0	0	0	0	77	60.0	357.0	20.0	0.075	0.040
77	76	0	0	0	0	78	20.0	30.0	5.0	0.070	0.040
78	77	0	0	0	0	79	35.0	114.0	3.0	0.075	0.040
79	78	0	0	0	0	80	40.0	298.0	10.0	0.065	0.040
80	79	0	0	0	0	81	50.0	379.0	10.0	0.070	0.040
81	80	0	0	0	0	82	55.0	66.0	5.0	0.070	0.040
82	81	0	0	0	0	83	65.0	239.0	14.0	0.040	0.040
83	82	0	0	0	0	84	75.0	1351.0	57.0	0.245	0.040
84	83	0	0	0	0	85	90.0	941.0	27.0	0.065	0.040
85	84	0	0	0	0	86	90.0	433.0	4.0	0.200	0.040
86	85	0	0	0	0	87	100.0	446.0	12.0	0.150	0.040
87	86	0	0	0	0	88	130.0	977.0	17.0	0.070	0.040
88	87	0	0	0	0	89	100.0	2538.0	30.0	0.040	0.040
89	88	0	0	0	0	90	95.0	587.0	15.0	0.055	0.040
90	89	0	0	0	0	91	115.0	1210.0	37.0	0.040	0.040
91	90	0	0	0	0	92	140.0	1522.0	50.0	0.047	0.040
92	91	0	0	0	0	93	150.0	2420.0	20.0	0.040	0.040
93	92	0	0	0	0	94	60.0	254.0	20.0	0.085	0.040
94	93	0	0	0	0	95	22.0	20.0	10.0	0.065	0.040
95	94	0	0	0	0	96	105.0	1095.0	40.0	0.100	0.040
96	95	0	0	0	0	97	116.0	673.0	27.0	0.040	0.040
97	96	0	0	0	0	98	32.0	367.0	33.0	0.045	0.040
98	97	0	0	0	0	99	33.0	371.0	33.0	0.185	0.040
99	98	0	0	0	0	100	35.0	515.0	40.0	0.140	0.040
100	99	0	0	0	0	101	40.0	495.0	22.0	0.070	0.040
101	100	0	0	0	0	102	30.0	535.0	26.0	0.085	0.040
102	101	0	0	0	0	103	35.0	740.0	40.0	0.040	0.040
103	102	0	0	0	0	103	20.0	457.0	20.0	0.045	0.040

8:A:2

ROUTEC.DAT - datafile for the large discontinuous gully.

Site	last	t1	t2	t3	t4	next	SL	AB	Y	S	N
1	0	0	0	0	0	5	65.0	605.0	5.0	0.274	0.055
2	0	0	0	0	0	5	62.0	375.0	5.0	0.385	0.055
3	0	0	0	0	0	5	44.0	500.0	5.0	0.177	0.055
4	0	0	0	0	0	5	33.0	448.0	10.0	0.131	0.055
5	4	1	2	3	0	6	45.0	1966.0	150.0	0.240	0.055
6	5	0	0	0	0	8	37.0	790.0	20.0	0.170	0.045
7	0	0	0	0	0	8	62.0	1040.0	30.0	0.252	0.045
8	6	7	0	0	0	9	55.0	2077.0	85.0	0.080	0.045
9	8	0	0	0	0	10	65.0	1330.0	10.0	0.060	0.045
10	9	0	0	0	0	11	72.0	1001.0	15.0	0.070	0.045
11	10	0	0	0	0	12	83.0	740.0	15.0	0.048	0.045
12	11	0	0	0	0	13	43.0	785.0	20.0	0.033	0.045
13	12	0	0	0	0	14	50.0	492.0	12.0	0.030	0.045
14	13	0	0	0	0	15	60.0	602.0	25.0	0.098	0.045
15	14	0	0	0	0	16	80.0	193.0	20.0	0.585	0.045
16	15	0	0	0	0	17	115.0	275.0	15.0	0.404	0.045
17	16	0	0	0	0	18	22.0	276.0	7.0	0.400	0.045
18	17	0	0	0	0	19	50.0	653.0	30.0	0.320	0.045
19	18	0	0	0	0	20	62.0	331.0	12.0	0.470	0.045
20	19	0	0	0	0	21	75.0	261.0	10.0	0.172	0.045
21	20	0	0	0	0	22	107.0	1430.0	50.0	0.180	0.045
22	21	0	0	0	0	23	40.0	142.0	15.0	0.220	0.045
23	22	0	0	0	0	24	164.0	47.0	15.0	0.170	0.045
24	23	0	0	0	0	25	161.0	2087.0	22.0	0.200	0.045
25	24	0	0	0	0	26	100.0	266.0	12.0	0.190	0.045
26	25	0	0	0	0	27	161.0	632.0	21.0	0.200	0.045
27	26	0	0	0	0	28	169.0	507.0	16.0	0.140	0.045
28	27	0	0	0	0	29	177.0	901.0	34.0	0.130	0.045
29	28	0	0	0	0	30	138.0	339.0	10.0	0.140	0.045
30	29	0	0	0	0	31	90.0	218.0	10.0	0.170	0.045
31	30	0	0	0	0	32	87.0	675.0	20.0	0.065	0.045
32	31	0	0	0	0	33	48.0	266.0	15.0	0.065	0.045
33	32	0	0	0	0	33	30.0	124.0	28.0	0.100	0.045

APPENDIX 9

A. INFILTRATION SURVEY

Source : Field data

INFILTRATION SURVEY - August, 1980. **Sites located on Figure 5 (back folder)**

(NB Numbers on face of table refer to no of mm lowered in infiltrometer in 5 mins. To convert to cm/hr, value x 1.2)

Site no	1	2	3	4	5	6	7	8	9	10	11	12	13
(time/mins)									*	*		*	
5	4.3	3.0	4.5	3.0	4.0	5.0	2.0	4.0	6.0	4.0	5.0	5.0	6.5
10	2.8	2.0	2.5	2.5	2.0	3.0	1.0	3.0	5.0	3.0	2.0	3.0	5.5
15	2.0	1.0	3.0	2.0	1.5	1.5	0.5	2.7	4.0	2.0	1.0	2.0	4.5
20	1.5	0.8	2.5	2.0	1.0	1.5	0.5	2.3	5.0	1.5	0.0	2.5	3.5
25	1.2	0.7	2.5	1.0	1.0	1.5	0.5	2.0	5.0	2.0	0.0	2.5	3.0
30	1.1	0.5	2.0	0.5	1.0	1.0	0.0	2.0	6.0	1.0	0.0	1.5	2.5
35	0.9	0.7	2.0	0.5	1.0	1.0	0.0	2.0	5.0	0.5		0.5	2.0
40	0.5	1.0	2.0	0.5	0.5	1.0	0.0	2.0	4.0	0.5		0.5	2.0
45	0.01	0.5	2.0	0.01	0.5	0.5		1.5	3.0	0.0		0.5	1.5
50	0.01	0.5	2.0	0.01	0.5	0.7		1.5	2.0	0.5		0.0	2.0
55	0.01	0.5	2.0	0.01	0.5	0.7		1.5	1.0	0.5		0.0	2.0
60	0.01	0.5	2.0	0.01	0.5	0.7		1.5	1.0	0.0			2.0
capacity rate in cm/hr	0.1	0.6	2.4	0.1	0.6	0.9	0.0	1.8	1.2	0.5	0.0	0.0	2.3
% veg cover	38	40	60	100	39	58	0	100	81	25	80	0	100

***staggered infiltration curve: possible indication of piping.**

continued ...

INFILTRATION SURVEY - August 1980 Sites located on Figure 5 (back folder) continued ...

(NB Numbers on face of table refer to no of mm lowered in infiltrometer in 5 mins. To convert to cm/hr, value x 1.2)

Site no	14	15	16	17	18	19	20	21	22	23	24
(time/mins)											
5	2.0	6.0	4.5	4.5	8.0	7.0	6.0	3.5	8.5	3.5	5.5
10	1.5	5.5	4.5	4.0	7.0	6.0	5.0	2.5	7.5	3.0	4.0
15	1.0	5.0	4.0	3.5	6.5	5.0	4.0	2.0	7.0	2.0	3.0
20	0.5	4.0	3.5	3.0	6.0	4.0	3.5	1.5	6.0	2.0	2.0
25	0.5	4.0	3.0	2.5	5.0	3.5	3.0	1.5	5.0	2.0	2.0
30	0.5	3.5	2.5	2.0	5.0	4.0	2.5	1.5	4.5	2.0	2.0
35	0.2	3.0	2.0	2.0	4.5	3.5	2.5	1.5	4.5	2.0	2.0
40	0.1	2.7	2.0	2.0	4.5	3.5	2.5	1.5	5.0	2.0	1.0
45	0.2	2.7	2.0	1.5	4.5	3.5	2.0	1.5	5.0	2.0	1.0
50	0.2	2.7	2.0	1.5	4.5	3.5	2.0	1.5	5.0	2.0	1.0
55	0.3	2.7	1.5	1.5	4.0	3.5	2.0	1.0	4.5	1.5	0.8
60											
capacity rate in cm/hr	0.4	3.2	1.8	1.8	4.8	4.2	2.4	1.2	5.4	1.8	0.9
% veg cover	45	75	85	80	100	100	90	80	100	100	85

APPENDIX 10

A. OVERLAND FLOW FIELD DATA SUMMARY TABLE, including a comparison with run 6 predictions for equivalent sites.

Suspended sediment data also included

Source : Field data, and the output from run 6 of ROUTE.PAS.

OVERLAND FLOW SUMMARY TABLE. FIELD DATA COLLECTED DURING THE SAMPLED OVERLAND FLOW EVENT, INCLUDING A COMPARISON WITH RUN 6 FOR EQUIVALENT NETWORK SITES. SUSPENDED SEDIMENT CONCENTRATION DATA ARE ALSO INCLUDED.

(i) SPATIAL DATA (sample locations noted on Figure 7)

Site No	Approximate Sample Time	Width (m)	Depth (m)	Velocity m/sec	Q cumecs	ppm	Run 6 Q (cumecs)
1*	30	2.43	0.26	0.193	0.121	295	0.128
2	25	1.36	0.22	0.582	0.175	714	0.157
3	22	1.27	0.28	0.537	0.187	848	0.205
5	20	0.72	0.37	0.623	0.167	507	0.171
6	17	0.72	0.26	0.280	0.052	161	0.063
7	15	0.88	0.39	0.359	0.124	288	0.133
8	5	2.34	0.09	0.064	0.014	403	0.011
9	10	0.82	0.06	0.284	0.014	111	0.011

(ii) TEMPORAL DATA

* Additional data collected at site 1 during field event (every 5 mins)

30 mins ..

Width (m)	Depth (m)	Velocity m/sec	Q cumecs	ppm	Run 6 Q cumecs
2.43	0.253	0.200	0.123	292.3	0.157
2.47	0.236	0.216	0.140	361.9	0.199
3.10	0.230	0.273	0.195	417.1	0.180
2.40	0.187	0.270	0.121	440.3	0.167
3.17	0.154	0.511	0.249	1271.3	0.113
2.66	0.120	0.410	0.130	646.3	0.061
0.24	0.006	0.210	0.003	26.3	0.009

APPENDIX 11

A. PROGRAMS WRITTEN FOR SPECIFIC PURPOSES

(All programs are in PASCAL)

ROUTE.PAS

SEEP.PAS

YIELD.PAS (1) and (2).

SEDIF.PAS (1) and (2)

B. THE BARNES ROUGHNESS TABLE

Source : TE CHOW, Ven, 1964, Handbook of Applied Hydrology

```
PROGRAM

 route(input,output);                (* draft 26th July 1983 *)

CONST
 maxpoints = 103;                    (* no. of data points *)
 v = 0.0457;                         (* Emmett's mean hillslope velocity *)


TYPE
 range= 0..maxpoints;
 info = record
          last,trib1,trib2,trib3,trib4,next:range;
                                     (* all keys to network positions *)
          slopelength,               (* max hillslope length *)
          ab,                        (* bare area *)
          diff,                      (* incremental channel length *)
          s,                         (* channel slope *)
          n,                         (* manning roughness *)
          T,                         (* slope hydrograph duration *)
          last_depth:REAL;
        END; (* info *)
  data_input = array[0..maxpoints] of info;
  conditions = array[1..6] of BOOLEAN;

VAR
  ary : data_input;
  condition : conditions;

(*-------------------------------------------------------------------*)

  PROCEDURE initialise

  (* this sets all variables to 0, and all conditions to false *)

                                  ( VAR ary : data_input;
                                    VAR condition : conditions);

  VAR
    i,k : INTEGER;
   BEGIN
    for i:=0 to maxpoints do
    with ary[i] do
     BEGIN
      last:=0;trib1:=0;trib2:=0;trib3:=0;trib4:=0;next:=0;
      slopelength:=0;ab:=0;diff:=0;s:=0;n:=0;T:=0;
      last_depth:=0;
      for k:=1 to 6 do
        BEGIN
        condition[k]:=false;
        END; (* for *)
     END; (* with *)
   END;(* initialise *)
                                                                  /cont..
(*-------------------------------------------------------------------*)
```

```
/cont..

PROCEDURE  read_in_data

(* this reads the data into the prescribed record *)

                                  (VAR ary:data_input);
VAR
  i : INTEGER;

 BEGIN
  for i:=1 to maxpoints do
  with ary[i] do
   BEGIN
    read (last,trib1,trib2,trib3,trib4,next,
          slopelength,ab,diff,s,n);
    readln;
   END; (* with *)
 END; (* read_in_data *)

(*-------------------------------------------------------------------*)

  PROCEDURE  calculate_T

 (* this calculates the duration of the hillslope hydrograph and then
    stores it as a constant in the record for each network site *)

                                     (VAR ary:data_input);

  VAR
    i : INTEGER;

   BEGIN
    for i:=1 to maxpoints do
    with ary[i] do

    T:= 2700 + slopelength/v;

    (* in which t is equivalent to the rainfall time, plus time to
       infiltration capacity, less time taken to drain the slope *)

   END; (* calculate_T *)

(*-------------------------------------------------------------------*)

  PROCEDURE  discharge_calculation


  (* this utilises the Manning formula to calculate site discharge
  at each time increment from the previous time's depth. This is
  done by storing the last and next site differences as a depth
  increment, but also allows the side slope flow at that time to
  be added in as well. The program runs through the net at each
  second for a 2 hr. period and writes out selected site q's every
  2 minutes. Lateral tributary flows are set to 0 as appropriate.
  Froude and k wave numbers assess the validity of the kinematic
  approximation on the St.Venant equations and print when invalid. The
  Courant condition is also examined, again printed if exceeded *)

                                                          /cont..
```

/cont..

```
                                (VAR ary:data_input;
                                 VAR condition:conditions);

CONST
 time_limit = 7200;             (* TWO hours *)
 g=9.81;                         (* acceleration due to gravity *)

VAR
  q,                            (*channel discharge at site*)
  qt,                           (*hillslope discharge at site*)
  qtnext,                       (*hillslope discharge at next site*)
  qtrib1,qtrib2,qtrib3,qtrib4,qnext,qlast,
                                (* channel discharges in tributaries
                                   and in the next and last sites *)
  length_difference,            (* between last and next sites*)
  LATQ,                         (* qt + qtnext *)
  INQ,                          (* qlast + qtrib[1..4]*)
  OUTQ,                         (* qnext *)
  depth,                        (* local site depth *)
  froude,                       (* Froude number *)
  kwave,                        (* kinematic wave number *)
  Courant:REAL;                 (* the stability condition *)
  time:1..time_limit;
  i,k,link: INTEGER;

FUNCTION FQ(link:integer):REAL;
    BEGIN
      IF (time=1) or (link=0) or ((ary[link].last_depth)<=0)
      THEN FQ:=0
      ELSE FQ:=(exp((5/3)*ln(ary[link].last_depth))
              *(sqrt(ary[link].s))/(ary[link].n))
      END;(*function Q*)

  PROCEDURE  check_conditions

  (* this examines time in relation to the hydrograph duration, since
     the relation of time to T/2 affects which equation is used to
     calculate qt and qtnext,the slope hydrograph discharges.For this
     a triangular hillslope hydrograph is assumed, base T, with an
     area under the plot equal to runoff=[(ab).(event ppn after fc)].
     In this way the discharge at any time,qt,is simply calculated *)

                                (VAR condition:conditions;
                                 VAR ary:data_input;
                                 i:INTEGER;
                                 time:INTEGER);

  BEGIN
    with  ary[i]  do
    BEGIN
    condition[1]:=((time>0) and (time<=T/2));
    condition[2]:=((time>(T/2)) and (time<T));
    condition[3]:=(time>=T);
    condition[4]:=((time>0) and (time<=(ary[next].T)/2));
    condition[5]:=((time>((ary[next].T)/2)) and (time<(ary[next].T)));
    condition[6]:=(time>=(ary[next].T));
    END;(*with*)
  END;(*check  conditions*)
```

/cont..

/cont..

```
 BEGIN

  for time:= 1 to time_limit do
   BEGIN
    for i:= 1 to maxpoints do
    with ary[i] do
      BEGIN
      last_depth:=deptn;
     END;
  for i:=1 to maxpoints do
    with ary[i] do
     BEGIN
      check_conditions (condition,ary,i,time);

      (* in the following expressions, the number 0.0075 represents
         the total event precipitation.By changing this,and also the
         number of flow duration seconds in the expression for T,
         - in this example set to 3/4hr.- different events on sites
         with a variety of ppn.totals and differing times to fc
         can be modelled with this program *)

     IF condition[1] THEN
     qt:=((0.0075*ab)*4*time)/(T*T);
     IF condition[2] THEN
     qt:=((0.0075*ab)*4*(T-time))/(T*T);
     IF condition[3] THEN
     qt:=0;
     IF condition[4] THEN
     qtnext:=(((0.0075*ary[next].ab)*4*time)/
     ((ary[next].T)*(ary[next].T)));
     IF condition[5] THEN
     qtnext:=(((0.0075*ary[next].ab)*4*((ary[next].T)-
     time))/((ary[next].T)*(ary[next].T)));
     IF condition[6] THEN
     qtnext:=0;

      (* in the following instructions, the discharges on all
         laterals,and the last and next site are calculated from the
         previous depths at those sites. The IF conditions set the
         discharges to 0 in appropriate cases *)

      qtrib1:=FQ(trib1);
      qtrib2:=FQ(trib2);
      qtrib3:=FQ(trib3);
      qtrib4:=FQ(trib4);
      qnext:= FQ(next);
      qlast:= FQ(last);

 (* now the site discharge at the present time interval is
    calculated, along with the Froude # and kinematic wave # *)

    length_difference:=diff+ary[next].diff;
    LATQ:=(qt+qtnext);
    INQ:=( qlast+qtrib1+qtrib2+qtrib3+qtrib4);
    OUTQ:=(qnext);
```

/cont..

/cont..

```
        IF ((last_depth +((LATQ+INQ)/length_difference))
                          <=(OUTQ/length_difference)) THEN
        depth:=(LATQ/length_difference)
         ELSE
        depth:=last_depth+((LATQ+INQ - OUTQ)/length_difference);

        IF (depth<=0) THEN q:=0
        ELSE
        BEGIN
        q:=((sqrt(s)*exp((5/3)*ln(depth)))/n);
        froude:=((q/depth)/sqrt(g*depth));
        kwave:=((s*diff)/(depth*froude*froude));
        Courant:=(diff/((q/depth)+sqrt(g*depth)));
        END;


   (* writing instructions *)

IF (i in [16,50,57]) or ( i=73) or ( i=89) or ( i=maxpoints) THEN
(* IF (i=16) or (i=32) THEN*)
(* this expression used for large trib.data, & change maxpoints*)
        BEGIN
        IF (time mod 120=0)
        THEN
         BEGIN
         IF (froude<=2.0) or (kwave>=10.0) or (Courant>=1.0)  THEN
          write (q:6:4)
         ELSE
          write (q:6:4,'courant=',courant:4:2,'   Fr#= ',froude:4:2,
                                  'k wave# = ',kwave:4:1)
         ;writeln;
         END;
        END;
       END;(*with*)
     END;(* for time *)
   END;(* discharge_calculation *)

(*-------------------------------------------------------------------*)

 BEGIN (* main set of instructions to run the procedures *)

  initialise (ary,condition);
  read_in_data (ary);
  calculate_T (ary);
  discharge_calculation (ary,condition);

 END.
(* main *)
```

SEEP.PAS

```
PROGRAM          transmission_loss (input,output);

(* this program calculates transmission loss using the Ostiachev
   method,i.e loss prop.to a constant-(taken here as 0.15 )
   multiplied by the site discharge at that time
   and also by the inverse square root of that time. After
   loss has been calculated as ary[i,3] then the adjusted q is put into
   ary[i,4]. The input file has time in 2 minute intervals (ary[i,1])
   and the discharge at that time as calculated by Route.Pas is in
   ary[i,2]. The constant 0.015 can be varied each time the program is
   run to examine the effect of the assumption that loss after 1hr. is
   15% of the flow at that time*)

CONST
k=0.15;          (*selected 15% loss*)

TYPE
arys=array[1..60,1..4] of REAL;          (*[i,1]is time,[[i,2]is q *)

VAR
ary:arys;
i,j:integer;

BEGIN

for i:=1 to 60 DO
BEGIN
for j:=1 to 2 do
BEGIN
read (ary[i,j]);
END;
readln;
END;
for i:= 1 to 60 DO
BEGIN
ary[i,3]:=(k*(ary[i,2])*(exp((-0.5)*ln(ary[i,1]/60))));
ary[i,4]:=ary[i,2]-ary[i,3];
END;
For i:=1 to 60 DO
BEGIN
   write(ary[i,1]:4:1,ary[i,2]:10:5,ary[i,4]:10:5,ary[i,3]:10:5);
writeln;
END;
END.
```

```
PROGRAM yield1(input,output);

CONST
        timelimit=43;
        maxpoints=103; (*change for large disc. daily data*)

TYPE
        discharges=array[1..maxpoints] of REAL;
        Tratios=array[1..timelimit] of REAL;

VAR
        qm:discharges;(*mean values of diurnal flow*)
        Tr:Tratios;(*which links mean daily flow to
        actual t0 min. q values on a 7 hr hydrograph*)

PROCEDURE initialise (*sets array space to zero*)
                        (VAR qm:discharges;
                             Tr:Tratios);
VAR     t,site:INTEGER;

BEGIN
        for site:=1 to maxpoints do
        qm[site]:=0;
        for t:= 1 to timelimit do
        Tr[t]:=0;
END;(*initialise*)

PROCEDURE read_in_data (*to prescribed arrays*)
                        (VAR qm:discharges;
                             VAR Tr: Tratios);
VAR     t,site:INTEGER;

BEGIN
        for site:=1 to maxpoints do
        BEGIN
        readln (qm[site]);
        END;(*for site*)

        t:=1;
        WHILE NOT eof(input) DO
        BEGIN
        readln (Tr[t]);
        t:=t+1;
        END;(*for t*)
END;(*read_in_data*)
```

/cont..

```
/cont..
PROCEDURE yield_calculation
(* this calculates the integral of the relationship
   yield=kQ^n+1, where yield is CQ, and is known for
   all Q. The only input needed is therefore the
   hydrograph, which is reconstructed from mean
   q(qm), a peak-to-mean ratio, and a series of
   ratios(Tr) linking 10 minute Tr values from field
   data to this value. The trapezoidal method is used
   for the integral'slices'(int) which are summed to
   calculate yield. This procedure runs through the
   network once only *)
                        (VAR qm:discharges;
                             Tr:Tratios);

CONST
        p=3.147;      (*peak-to-mean ratio*)
        n=1.21;       (*exponent of sediment rating relationship*)
        k=80930;      (*multiplying constant in the above*)

VAR
        qt,      (*local q at t*)
        qtnext, (*local q at t+1*)
        sedqt,  (*local sediment q at t*)
        sedqtnext:REAL;
                 (*local sediment q at t+1*)
        int:REAL;
        yield:REAL;(* the summed values of int in Kg.*)
        t,site:INTEGER;

BEGIN
        for site:= 1 to maxpoints do
        BEGIN
        qt:=0;qtnext:=0;sedqt:=0;sedqtnext:=0;
        int:=0;yield:=0;
        for t:= 1 to (timelimit-1) do
          BEGIN
          qt:=(p*qm[site]*Tr[t]);
          qtnext:=(p*qm[site]*Tr[t+1]);
          sedqt:=k*(exp((n+1)*ln(qt)));
          sedqtnext:=k*(exp((n+1)*ln(qtnext)));
          int:=0.3(sedqt + sedqtnext);
          yield:=yield+int;
          END;(*for t*)
        BEGIN (*writing instructions*)
        write(site:4,yield:10:4,qm[site]:7:4);
        writeln;
        END;(*writing instructions*)
        END;(*for site*)
END;(*yield_calculation*)

BEGIN (*main set of instructions to run the procedures*)
        initialise (qm,Tr);
        read_in_data(qm,Tr);
        yield_calculation(qm,Tr);
END.(*main instructions*)
```

```
PROGRAM yield2 (input,output);

(* This version of Yield.Pas reads discharges every 2 minutes from the
   site hydrographs which are output from Runs 7 to 10 of Route.Pas*)

CONST
        timelimit=60; (*number of 2 min intervals in 2 hrs*)
        maxpoints=103; (*change for large disc. gully data*)

TYPE
       sites=RECORD
        q:array[1..timelimit] of REAL;
        END;(* sites *)
        run=array[1..maxpoints] of SITES;

VAR
        ary:run;


PROCEDURE initialise (*sets array space to zero*)
                        (VAR ary:run);
VAR     t,site:INTEGER;

BEGIN
for site:=1 to maxpoints do
   with ary[site] do
        for t:= 1 to timelimit do
          q[t]:=0;
END;(*initialise*)

PROCEDURE read_in_data (*to prescribed arrays*)
                        (VAR ary:run);
VAR     t,site:INTEGER;

BEGIN
        for site:=1 to maxpoints do
         with ary[site] do
           for t:=1 to timelimit do
            read (q[t]);
           readln;
END;(*read_in_data*)

PROCEDURE write_data (*to prescribed arrays*)
                        (VAR ary:run);
VAR     t,site:INTEGER;

BEGIN
        for site:=1 to maxpoints do
         with ary[site] do
         BEGIN
           for t:=1 to timelimit do
            write (q[t]);
           writeln
         END
END;(*write_data*)
```

/cont..

/cont..

```
PROCEDURE yield_calculation
(* this calculates the integral of the relationship
   yield=KQ^n+1, where yield is CQ, and is known for
   all Q. The only input needed is therefore the
   hydrograph, which is read in from the output file
   from Route.Pas (Ch.4). The trapezoidal method is used
   for the integral'slices'(int) which are summed to
   calculate yield. This procedure runs through the
   network *)
                        (VAR ary:run);

CONST
        n=0.76;       (*exponent of sediment rating relationship*)
        k=2130;      (*multiplying constant in the above*)

VAR
        sedqt,  (*local sediment q at t*)
        sedqtnext:REAL;
              (*local sediment q at next time interval*)
        int:REAL;
        yield:REAL;(* the summed values of int in Kg.*)
        t,site:INTEGER;

BEGIN
        for site:= 1 to maxpoints do
        with ary[site] do
        BEGIN
        int:=0;yield:=0;
        for t:= 1 to (timelimit-1) do
          BEGIN
        sedqt:=0;sedqtnext:=0;int:=0;
          sedqt:=k*(exp((n+1)*ln(q[t])));
          sedqtnext:=k*(exp((n+1)*ln(q[t+1])));
          int:=0.06(sedqt + sedqtnext);
          yield:=yield+int;
          END;(*for t*)
         BEGIN (*writing instructions*)
         write(site:4,yield:10:4);
         writeln;
         END;(*writing instructions*)
         END;(*for site*)
END;(*yield_calculation*)

BEGIN (*main set of instructions to run the procedures*)
        initialise (ary);
        read_in_data(ary);
        yield_calculation(ary);
END.(*main instructions*)
```

```
program sedif1(input,output);

CONST   maxpoints=103;

TYPE
        range=0..151;
        info=record
          where,last,trib1,trib2,trib3,
          trib4:range;  (*keys to network positions*)
          apsed,maysed, (*daily April and May sediment
                          yields at point i from Yield.Pas*)
          dist,         (*main channel length*)
          inc,          (*incremental distance between sites*)
          apdif,maydif, (*April & May sed.yld differences
                          between sites*)
          result:REAL;  (*combined effect of two months yield
                          calculation, in tonnes*)
        END;(*info*)
        data_input=array[0..maxpoints] of info;

VAR     ary:data_input;

PROCEDURE initialise
(*this sets all variables in the array to 0*)
                        (VAR ary:data_input);

VAR     i:INTEGER;

BEGIN
For i:=0 to maxpoints do
        with ary[i] do
          BEGIN
          where:=0;last:=0;trib1:=0;trib2:=0;trib4:=0;
          apsed:=0;maysed:=0;dist:=0;inc:=0;apdif:=0;
          maydif:=0;result:=0;
          END;(*for i*)
END;(*initialise*)

PROCEDURE read_in_data
(*this reads all variables into the array*)
                        (VAR ary:data_input);

VAR     i:INTEGER;

BEGIN
For i:=1 to maxpoints do
        with ary[i] do
          BEGIN
           read(where,last,trib1,trib2,trib3,trib4,
                apsed,maysed,dist,inc);
           readln;
          END;(*for i*)
END;(*read_in_data*)
```

/cont..

/cont..

```
PROCEDURE construct_plot_files
(*this produces 5 chained files for plotting by GPHPLT*)
                                        (VAR ary:data_input);
VAR     i:INTEGER;

BEGIN
for i:= 1 to maxpoints do
with ary[i] do
BEGIN
        apsed:=30*apsed;
        maysed:=31*maysed;
        IF(last=0) THEN
          BEGIN
          apdif:=apsed/inc;
          maydif:=maysed/inc;
          END
          ELSE
        IF((last>0) and(trib1=0)) THEN
          BEGIN
            apdif:=(apsed-(ary[last].apsed)/inc);
            maydif:=(maysed-(ary[last].maysed)/inc);
          END
          ELSE
        IF ((last>0) and (trib1>0) and (trib2=0)) THEN
         BEGIN
         apdif:=(apsed-((ary[last].apsed)+(ary[trib1].apsed)))/inc;
         maydif:=(maysed-((ary[last].maysed)+(ary[trib1].maysed)))/inc;
         END
         ELSE
        IF((last>0) and (trib1>0) and (trib2>0) and (trib3=0)) THEN
        BEGIN
         apdif:=(apsed-((ary[last].apsed)+
         (ary[trib1].apsed)+(ary[trib2].apsed)))/inc;
         maydif:=(maysed-((ary[last].maysed)+
         (ary[trib1].maysed)+(ary[trib2].maysed)))/inc;
         END
         ELSE
        IF ((last>0) and (trib3>0) and (trib4=0)) THEN
        BEGIN
         apdif:=(apsed-((ary[last].apsed)+(ary[trib1].apsed)+
         (ary[trib2].apsed)+(ary[trib3].apsed)))/inc;
         maydif:=(maysed-((ary[last].maysed)+(ary[trib1].maysed)+
         (ary[trib2].maysed)+(ary[trib3].maysed)))/inc;
        END
        ELSE
        apdif:=(apsed-((ary[last].apsed)+(ary[trib1].apsed)+
        (ary[trib2].apsed)+(ary[trib3].apsed)+(ary[trib4].apsed)))/inc;
        maydif:=(maysed-((ary[last].maysed)+(ary[trib1].maysed)+(ary
        [trib2].maysed)+(ary[trib3].maysed)+(ary[trib4].maysed)))/inc;
        result:=apdif - maydif;
        write(dist:13:3,apsed:18:5);
        writeln;
END;(*for i writing apsed *)
```

/cont..

/cont..

```
 writeln;
 writeln;

 For i:=1 to maxpoints do
 with ary[i] do
 BEGIN
         write(dist:13:3,maysed:18:5);
         writeln;
      END;(*for writing maysed*)

 writeln;
 writeln;

 For i:=1 to maxpoints do
 with ary[i] do
 BEGIN
         write(dist:13:3,apdif:18:5);
         writeln;
      END;(*for writing apdif*)

 writeln;
 writeln;

 For i:=1 to maxpoints do
 with ary[i] do
 BEGIN
         write(dist:13:3,maydif:18:5);
         writeln;
      END;(*for writing maydif*)
 writeln;
 writeln;

 For i:=1 to maxpoints do
 with ary[i] do
 BEGIN
         write(dist:13:3,result:18:5);
         writeln;
      END;(*for writing result*)
 END;(*construct_plot_files*)


 BEGIN (*main instructions for running the procedures*)
 initialise(ary);
 read_in_data(ary);
 construct_plot_files(ary);
 END.(*main*)
```

```
program sedif2(input,output);
        (* this program calculates the spatial rate of sediment
           yield increase for all the simulated summer storms,
           which are first weighted. A summer total (both with
           and without the 'freak' event) is finally calculated*)

CONST   maxpoints=103;

TYPE
        range=0..151;
        info=record
          where,last,trib1,trib2,trib3,
          trib4:range;  (*keys to network positions*)
          rn7sed,rn8sed,
          rn9sed,rn10sd,(*sediment yields from runs 7-10, -
                          all at point i from Yield.Pas*)
          dist,         (*main channel length*)
          inc,          (*incremental distance between sites*)
          rn7dif,rn8dif,
          rn9dif,rn10df,(* sed.yld differences for all weighted runs*)
          smless,smplus:REAL;
                        (*summer sums,+ or - rn10df*)
        END;(*info*)
        data_input=array[0..maxpoints] of info;

VAR     ary:data_input;

PROCEDURE initialise
(*this sets all variables in the array to 0*)
                        (VAR ary:data_input);

VAR     i:INTEGER;

BEGIN
For i:=0 to maxpoints do
        with ary[i] do
          BEGIN
          where:=0;last:=0;trib1:=0;trib2:=0;trib4:=0;
          rn7sed:=0;rn8sed:=0;rn9sed:=0;rn10sd:=0;
          dist:=0;inc:=0;rn7dif:=0;rn8dif:=0;rn10df:=0;
          smless:=0;smplus:=0;
          END;(*for i*)
END;(*initialise*)

PROCEDURE read_in_data
(*this reads all variables into the array*)
                        (VAR ary:data_input);

VAR     i:INTEGER;

BEGIN
For i:=1 to maxpoints do
        with ary[i] do
          BEGIN
           read(where,last,trib1,trib2,trib3,trib4,
                rn7sed,rn8sed,rn9sed,rn10sd,dist,inc);
           readln;
          END;(*for i*)
END;(*read_in_data*)
```

/cont...

/cont..

```
PROCEDURE construct_output_file
(*this produces an output file which can later be used for  GPHPLT*)
                                        (VAR ary:data_input);
VAR     i:INTEGER;

BEGIN
for i:= 1 to maxpoints do
with ary[i] do
BEGIN
        rn7sed:=5*rn7sed;rn8sed:=4*rn8sed;
        rn9sed:=2*rn9sed;
        IF(last=0) THEN
          BEGIN
          rn7dif:=rn7sed/inc;rn8dif:=rn8sed/inc;
          rn9dif:=rn9sed/inc;rn10df:=rn10sd/inc;
          END
          ELSE
       IF((last>0) and (trib1=0)) THEN
          BEGIN
            rn7dif:=(rn7sed-(ary[last].rn7sed))/inc;
            rn8dif:=(rn8sed-(ary[last].rn8sed))/inc;
            rn9dif:=(rn9sed-(ary[last].rn9sed))/inc;
            rn10df:=(rn10sd-(ary[last].rn10sd))/inc;
          END
          ELSE
       IF ((last>0) and (trib1>0) and (trib2=0)) THEN
        BEGIN
        rn7dif:=(rn7sed-((ary[last].rn7sed)+(ary[trib1].rn7sed)))/inc;
        rn8dif:=(rn8sed-((ary[last].rn8sed)+(ary[trib1].rn8sed)))/inc;
        rn9dif:=(rn9sed-((ary[last].rn9sed)+(ary[trib1].rn9sed)))/inc;
        rn10df:=(rn10sd-((ary[last].rn10sd)+(ary[trib1].rn10sd)))/inc;
        END
        ELSE
       IF((last>0) and (trib1>0) and (trib2>0) and (trib3=0)) THEN
       BEGIN
        rn7dif:=(rn7sed-((ary[last].rn7sed)+
        (ary[trib1].rn7sed)+(ary[trib2].rn7sed)))/inc;
        rn8dif:=(rn8sed-((ary[last].rn8sed)+
        (ary[trib1].rn8sed)+(ary[trib2].rn8sed)))/inc;
        rn9dif:=(rn9sed-((ary[last].rn9sed)+
        (ary[trib1].rn9sed)+(ary[trib2].rn9sed)))/inc;
        rn10df:=(rn10sd-((ary[last].rn10sd)+
        (ary[trib1].rn10sd)+(ary[trib2].rn10sd)))/inc;
        END
        ELSE
       IF ((last>0) and (trib3>0) and (trib4=0)) THEN
       BEGIN
        rn7dif:=(rn7sed-((ary[last].rn7sed)+(ary[trib1].rn7sed)+
        (ary[trib2].rn7sed)+(ary[trib3].rn7sed)))/inc;
        rn8dif:=(rn8sed-((ary[last].rn8sed)+(ary[trib1].rn8sed)+
        (ary[trib2].rn8sed)+(ary[trib3].rn8sed)))/inc;
        rn9dif:=(rn9sed-((ary[last].rn9sed)+(ary[trib1].rn9sed)+
        (ary[trib2].rn9sed)+(ary[trib3].rn9sed)))/inc;
        rn10df:=(rn10sd-((ary[last].rn10sd)+(ary[trib1].rn10sd)+
        (ary[trib2].rn10sd)+(ary[trib3].rn10sd)))/inc;
END
```

/cont..

/cont..

```
    ELSE
rn7dif:=(rn7sed-((ary[last].rn7sed)+(ary[trib1].rn7sed)+
(ary[trib2].rn7sed)+(ary[trib3].rn7sed)+(ary[trib4].rn7sed)))/inc;
rn8dif:=(rn8sed-((ary[last].rn8sed)+(ary[trib1].rn8sed)+(ary
[trib2].rn8sed)+(ary[trib3].rn8sed)+(ary[trib4].rn8sed)))/inc;
rn9dif:=(rn9sed-((ary[last].rn9sed)+(ary[trib1].rn9sed)+
(ary[trib2].rn9sed)+(ary[trib3].rn9sed)+(ary[trib4].rn9sed)))/inc;
rn10df:=(rn10sd-((ary[last].rn10sd)+(ary[trib1].rn10sd)+
(ary[trib2].rn10sd)+(ary[trib3].rn10sd)+(ary[trib4].rn10sd)))/inc;
END;(*calculation of differences*)

For i:=1 to maxpoints do
with ary[i] do
BEGIN
    smless:=rn7dif+rn8dif+rn9dif;
    smplus:=smless+rn10df;
    write(i:7,rn7dif:11:3,rn8dif:11:3,rn9dif:11:3,rn10df:11:3,
          smless:11:3,smplus:11:3);
    writeln;
 END;(*for writing  instructions*)
END;(*construct_output_file*)


BEGIN (*main instructions for running the procedures*)
initialise(ary);
read_in_data(ary);
construct_output_file(ary);
END.(*main*)
```

(B) THE BARNES ROUGHNESS TABLE

Values for the Computation of the Roughness Coefficient

$$n = (n_o + n_1 + n_2 + n_3 + n_4)m_5$$

After Te Chow, (1964)

Channel Conditions			Values
Material involved	Earth	n_o	0.020
	Rock cut		0.025
	Fine gravel		0.024
	Coarse gravel		0.028
Degree of irregularity	Smooth	n_1	0.000
	Minor		0.005
	Moderate		0.010
	Severe		0.020
Variations of channel cross-section	Gradual	n_2	0.000
	Alternating occasionally		0.005
	Alternating frequently		0.010-0.015
Relative effect of obstructions	Negligible	n_3	0.000
	Minor		0.010-0.015
	Appreciable		0.020-0.030
	Severe		0.040-0.060
Vegetation	Low	n_4	0.005-0.010
	Medium		0.010-0.025
	High		0.025-0.050
	Very high		0.050-0.100
Degree of meandering	Minor	m_5	1.000
	Appreciable		1.150
	Severe		1.300

APPENDIX 12

REGRESSION STATISTICS

In this Appendix, the details of statistical tests conducted on various sections of data are included as a supplement to information shown on the face of various Figures in the text. All methods used are as described by YAMANE, T., 1973, Statistics ,Harper and Row.

Notes :

On these lists the following symbol definitions apply;

n = number of data items

r = product moment correlation

r^2 = coefficient of determination

s.e.e = standard error of the estimate

s.e.b = standard error of the regression coefficient

b = regression line slope

a = the intercept of this line with the ordinate, or in the case of log regression the antilog of the value of the dependent variable when antilog of the independent variable is 1.0

(i) Regression analyses shown on Figure 11 (All data included in Appendix 4)

Log transformed data used

(1) April 1st relationship (field data point excluded)

(2) May 1st relationship (excluding all zeros)

	1	2
n	12	10
r	0.49	0.68
r^2	0.24	0.48
s.e.e	2.21	1.08
b	0.33	0.23
a	0.80	0.93

For (1), Log (Alk S.W.E. Apr.1st) = [(0.33log McClure S.W.E Apr.1st)+ 0.80]
The event which occurs 50% of the time at McClure Pass has a S.W.E. value of 36.32 cm., predicting for Alkali Creek 20.65 cm., s.e.e. of 2.21 cm.

For (2), Log (Alk S.W.E. May 1st)= [(0.23 log McClure S.W.E May 1st)+ 0.93]
The event which occurs 50% of the time at McClure Pass has a S.W.E value of 24.38 cm., predicting for Alkali Creek 17.74 cm., s.e.e. of 1.08 cm.

(ii) Regression Analyses shown on Figure 18 (All data included in Tables I and II)

Linear regressions used.

Summary table of regression statistics of actual versus predicted site S.W.E

	Figure 18a	Figure 18b	Figure 18c	Figure 18d
n	12	12	9	9
r	0.93	0.97	0.95	0.96
r^2	0.86	0.95	0.91	0.93
s.e.b	0.11	0.11	0.09	0.11
a	-8.76	-21.39	-9.86	-15.20
b	0.84	1.11	0.73	0.99

Using the criteria discussed in the text, Figures b and d are better fit the than a and c.

(iii) Regression Analyses shown on Figure 21 (All data included in Appendix 7)

Log transformed data used

Table of regression statistics of Q_a against Q_{sim}

	Early melt relationships	Late melt relationships
n	9	9
r	0.993	0.998
r^2	0.991	0.997
s.e.e	0.003	0.001
a	-0.107	-0.135
b	0.887	0.927

(Combined regression shown on Figure 21 is discussed in the text.)

(iv) Regression analysis of data displayed on Figure 38. (Field data are in Appendix 10, simulation data results from Run 6 of ROUTE.PAS)

Linear regressions used

.... all sites included :

n=15

r=0.7804

r^2=0.61

a=0.0270

b=0.7491

.... against field data (excluding value at 0.249) :

n=14

r=0.9081

r^2= 0.82

.... against temporal data, site 1 (correlation data only necessary,:

k=0	k=0.15	k=0.30
r=0.534	r=0.574	r=0.519
r^2= 0.29	r^2= 0.33	r^2= 0.27

(v) Regression Analyses shown on Figures 40 and 41 (All data included in Appendix 1)

Log transformed data used

Summary Table of regression statistics of

(1) Event Duration against precipitation Total (Figure 40)

(2) Event intensity against event duration (Figure 41)

(1)	(2)
n = 95	n = 95
r = 0.6339	r = -0.87
r^2= 0.441	r^2= 0.75
s.e.e=0.04	s.e.e.=0.04
a = 0.26	a = -0.25
b = 0.352	b = -0.67

(vi) Regression analysees shown on Figure 48 (All snowmelt data is in Appx.7)

(all data logged)

n=23
r=0.97
r^2=0.9835
a = 4.706 (antilog=50820)
b = 1.1704

(vii) Regression analyses shown on Figure 49

(all data logged)

n=18
r=0.9769
r^2=0.95
a = 4.8801 (antilog = 79310)
b = 1.0929

All snowmelt data together

n = 41
r = 0.9682
r^2= 0.94
a = 4.9081 (antilog = 80930)
b = 1.212

/cont..

(viii) Regression analyses shown on Figure 50 (All summer data ARE in Appx 10)

(all data logged)

n = 7

r = 0.9524

r^2 = 0.91

a = 3.306 (antilog = 2026)

b = 0.7586

(ix) Regression analyses shown on Figure 51

(all data logged)

n=8

r=0.6505

r^2 = 0.42

a = 3.0050 (antilog = 1012)

b = 0.4149

All data regressed together (excluding sites 8 & 9)

n=13

r = 0.9358

r^2 = 0.88

a = 3.3248 (antilog = 2130)

b = 0.7882

(x) All data regressed together (i.e all melt and summer data, latter excluding sites 8 and 9)

n = 54

r = 0.7708

r^2 = 0.59

b = 0.81

a= 3.9845 (antilog = 9132)

N.B. REGRESSION TESTS CONDUCTED IN CHAPTER 6 ARE INCLUDED IN DETAIL IN THE BODY OF THE TEXT.

APPENDIX 13

CALCULATIONS INVOLVED IN THE CONSTRUCTION OF AN ANNUAL SURFACE WASH INDEX

Headwater data

Continuous network data (1975 sites)

Large discontinuous tributary

Source : Map- derived calculations, using Figures 4 and 7.

CONTINUOUS NETWORK : headwaters

old I.D	Distance, m	(Ab x h) x 10^{-3}
17.00000	3.05000	2.24000
34.00000	3.05000	4.19000
10.00000	4.57000	8.22000
16.00000	4.57000	32.82000
31.00000	4.57000	0.41000
41.00000	4.57000	10.16000
18.00000	5.49000	4.37000
14.00000	6.10000	0.99000
28.00000	6.10000	6.14000
38.00000	6.10000	7.25000
32.00000	7.62000	0.41000
22.00000	7.92000	15.19000
21.00000	8.53000	1.63000
29.00000	10.67000	5.76000
30.00000	12.19000	3.41000
49.00000	12.19000	10.04000
53.00000	13.72000	9.40000
54.00000	13.72000	15.82000
42.00000	15.24000	27.62000
56.00000	16.76000	13.48000
39.00000	21.34000	7.49000
20.00000	22.86000	9.54000
27.00000	24.38000	21.16000
55.00000	27.43000	27.12000
45.00000	33.53000	27.51000
46.00000	33.53000	16.92000
40.00000	39.62000	87.35000
33.00000	48.77000	5.97000
8.00000	54.86000	7.56000
13.00000	64.01000	19.69000
15.00000	65.53000	75.96000
48.00000	67.06000	33.06000
52.00000	80.77000	96.73000
19.00000	83.82000	48.89000
44.00000	88.39000	54.24000
37.00000	97.54000	150.40000
26.00000	115.80000	80.24000
12.00000	123.40000	35.66000
47.00000	125.00000	7.34000
36.00000	125.30000	71.95000
51.00000	138.70000	21.12000
25.00000	161.50000	34.86000
35.00000	180.10000	17.73000
11.00000	184.40000	87.35000
50.00000	199.60000	14.69000
9.00000	249.90000	19.49000
43.00000	257.60000	201.20000
24.00000	281.90000	577.50000
7.00000	310.90000	31.94000
23.00000	339.80000	1.16000
6.00000	399.30000	294.50000

CONTINUOUS NETWORK : main channel

old I.D	Distance, m.	(Ab x h) x 10^{-3}
193.00000	272.80000	2.18000
192.00000	286.50000	1.49000
191.00000	299.60000	1.97000
190.00000	310.00000	1.26000
189.00000	315.80000	0.10000
188.00000	326.10000	0.46000
187.00000	331.60000	0.10000
186.00000	343.50000	1.24000
185.00000	355.70000	3.50000
183.00000	357.80000	12.92000
184.00000	363.30000	0.10000
182.00000	374.00000	1.43000
181.00000	391.10000	1.84000
180.00000	405.40000	294.50000
179.00000	424.30000	18.10000
178.00000	429.20000	1.43000
177.00000	450.20000	2.96000
176.00000	462.40000	13.08000
175.00000	465.40000	0.63000
174.00000	476.70000	5.36000
173.00000	491.30000	4.84000
172.00000	511.20000	7.44000
171.00000	556.60000	400.20000
170.00000	582.20000	10.40000
169.00000	648.90000	20.81000
168.00000	656.80000	2.50000
167.00000	661.40000	0.72000
166.00000	676.70000	20.04000
165.00000	708.10000	1.11000
164.00000	719.30000	5.72000
163.00000	720.60000	0.70000
162.00000	765.70000	72.52000
161.00000	773.30000	15.00000
160.00000	803.20000	20.21000
159.00000	855.90000	28.37000
158.00000	867.80000	12.86000
157.00000	897.30000	52.61000
156.00000	914.40000	1.17000
155.00000	928.40000	6.32000
154.00000	942.80000	2.85000
153.00000	987.60000	15.87000
152.00000	997.60000	1.77000

LARGE DISCONTINUOUS GULLY : all data

old I.D	Distance,m.	(Ab x h) x 10^{-3}
62.00000	4.57000	9.77000
64.00000	9.14000	1.52000
63.00000	10.67000	4.57000
65.00000	22.86000	4.10000
66.00000	27.43000	11.09000
61.00000	70.10000	66.79000
218.00000	85.65000	9.88000
217.00000	103.30000	56.23000
216.00000	118.50000	34.04000
60.00000	123.40000	34.04000
215.00000	135.90000	14.57000
214.00000	150.60000	10.61000
213.00000	167.00000	8.40000
59.00000	176.80000	1.59000
212.00000	180.10000	1.59000
211.00000	202.70000	3.62000
210.00000	219.50000	2.12000
58.00000	233.20000	6.47000
209.00000	236.20000	0.20000
208.00000	256.30000	21.04000
207.00000	269.10000	2.47000
57.00000	286.50000	2.69000
206.00000	324.30000	10.20000
205.00000	342.00000	1.06000
204.00000	354.80000	1.21000
203.00000	376.40000	6.92000
202.00000	389.50000	4.88000
201.00000	409.30000	5.02000
200.00000	426.70000	2.88000
199.00000	447.10000	5.39000
198.00000	460.30000	4.12000
197.00000	472.70000	3.97000
196.00000	493.50000	16.70000
195.00000	505.00000	1.42000
194.00000	534.00000	1.19000

APPENDIX 14

A. T-RATIS USED TO CONVERT PEAK Q TO A LOCAL SITE HYDROGRAPH

Source : Diurnal hydrograph data in Appendix 7.

B. INPUT FILES FOR SEDIF1.PAS : SEDIF1.DAT
SEDIFC.DAT

INPUT FILES FOR SEDIF2.PAS : SEDIFA.DAT
SEDIFB.DAT
CDIFA.DAT
CDIFB.DAT

C. WEIGHTED AND TOTALLED YIELDS FROM THE OPERATION OF YIELD.PAS (1) and (2).

In order as for (B), above.

D. OUTPUT FILES FROM SEDIF.PAS (1) and (2)
SEDIFA.OUT
SEDIFB.OUT
CDIFA.OUT
CDIFB.OUT

Note :
For melt, SEDIF output data is listed as 'WINDIF' against all network sites in Appendix 15

A. T-RATIOS relate to every 10 minute period on the April 5 hydrograph. Calculation method shown in the text.

T RATIO
0.0121
0.0128
0.0136
0.0150
0.0179
0.0207
0.0214
0.0229
0.0250
0.0286
0.0300
0.0436
0.0615
0.0808
0.2051
0.3431
0.4789
0.5597
0.6769
0.7598
0.8506
0.9721
1.000
0.9936
0.9800
0.9078
0.7148
0.5225
0.3574
0.2545
0.1401
0.0372
0.0264
0.0157
0.0129
0.0070
0.0007
0.0001

APPENDIX 14 (B) - SEDIF DATA FILES

Notes:

As a result of running YIELD1.PAS, site yields for a melt day in each of the melt months are obtained in kg. for all the continuous network and the large discontinuous tributary.These data may be read as Apsed and Maysed in the files contained here called SEDIF1.DAT and SEDIF2.DAT. The files are named in this way because they act as the input files to the sediment yield differencing programs.

Similarly, event site yields during runs 7 to 10 are obtained from the operation of YIELD2.PAS. These data were obtained twice, first using the 'supply-limited' regression equation in which n = 0.76, k = 2130, and secondly using the n = 0.81, k = 9132 regression equation. These data are also listed here, as SEDIFA.DAT and SEDIFB.DAT, their equivalent tabulations for the large discontinuous tributary being CDIFA.DAT and CDIFB.DAT. The event yields are all listed without their frequency weightings, and in Kg.

SEDIF1.DAT

Input file for Sediment Difference
Program; Sedif1.Pas. Network data

I.D	last	t1	t2	t3	t4	Apsed.	Maysed	Distance	inc.
1	0	0	0	0	0	0.0048	0.1906	3.05	5
2	0	0	0	0	0	0.0657	0.0808	3.05	5
3	0	0	0	0	0	0.0000	0.0233	4.57	5
4	0	0	0	0	0	0.0048	0.1906	4.57	5
5	0	0	0	0	0	0.0000	0.0002	4.57	5
6	0	0	0	0	0	0.0048	0.0004	4.57	5
7	0	0	0	0	0	0.0020	0.0756	5.49	5
8	0	0	0	0	0	0.0002	0.0090	6.10	5
9	0	0	0	0	0	0.0061	0.0192	6.10	5
10	0	0	0	0	0	0.0146	0.0192	6.10	5
11	0	0	0	0	0	0.0000	0.0002	7.62	7
12	0	0	0	0	0	0.0146	0.5373	7.92	5
13	0	0	0	0	0	0.0000	0.0004	8.53	5
14	0	0	0	0	0	0.0107	0.0335	10.67	5
15	0	0	0	0	0	0.0002	0.0037	12.19	7
16	0	0	0	0	0	0.0004	0.0168	12.19	15
17	0	0	0	0	0	0.0008	0.0335	13.72	10
18	0	0	0	0	0	0.0075	0.1036	13.72	10
19	0	0	0	0	0	0.0273	0.0020	15.24	10
20	0	0	0	0	0	0.0008	0.0335	16.76	30
21	0	0	0	0	0	0.0126	0.0028	21.34	22
22	0	0	0	0	0	0.0090	0.0126	22.86	10
23	0	0	0	0	0	0.0808	0.2646	24.38	18
24	0	0	0	0	0	0.0028	0.1295	27.43	36
25	0	0	0	0	0	0.0020	0.0611	33.53	30
26	0	0	0	0	0	0.0004	0.0168	33.53	35
27	0	0	0	0	0	0.2748	0.0706	39.62	52
28	2	0	0	0	0	0.0756	0.1584	48.77	50
29	0	0	0	0	0	1.4545	33.2893	54.86	62
30	8	0	0	0	0	0.0303	0.0976	64.01	60
31	4	1	7	0	0	0.1436	3.8175	65.53	120
32	16	0	0	0	0	0.0075	0.2260	67.06	50
33	17	18	24	20	0	0.2748	2.2873	80.77	145
34	22	13	12	0	0	0.0918	1.8600	83.82	112
35	25	26	0	0	0	0.0756	0.3638	88.82	67
36	27	10	21	0	0	2.6567	0.9758	97.54	120
37	23	9	14	15	5	1.3312	4.2102	115.82	150
38	31	30	0	0	0	0.1662	7.2464	123.44	60
39	32	0	0	0	0	0.0335	0.3519	124.97	56
40	36	0	0	0	0	3.8601	1.6913	125.27	60
41	33	0	0	0	0	0.2748	2.2873	138.68	60
42	28	37	11	0	0	2.1292	5.5656	161.54	125
43	40	0	0	0	0	4.7184	1.8600	180.14	55
44	38	34	0	0	0	0.7836	22.8743	184.40	90
45	41	0	0	0	0	0.8962	4.0770	199.64	50
46	44	3	0	0	0	1.3312	29.5838	249.94	70
47	45	35	39	0	0	3.7752	14.9679	257.56	95
48	42	43	6	19	47	46.6500	81.9000	281.94	190
49	48	0	0	0	0	46.9782	85.7198	302.97	25
50	49	0	0	0	0	47.2042	94.1174	310.90	15
51	46	29	0	0	0	0.6023	158.5436	339.85	85
52	50	0	0	0	0	48.1368	98.7205	342.90	22
53	52	0	0	0	0	19.6487	106.4858	360.86	5
54	53	0	0	0	0	50.4926	110.6180	380.09	20

/cont.

/ cont.

55	54	0	0	0	0	51.1860	117.2447	399.29	5
56	55	51	0	0	0	115.9028	1598.6015	420.32	80
57	56	0	0	0	0	123.1305	2789.0591	431.29	20
58	57	0	0	0	0	131.9835	2805.4383	431.29	12
59	58	0	0	0	0	133.7114	2808.4219	437.69	10
60	59	0	0	0	0	134.2901	2828.4220	446.53	10
61	60	0	0	0	0	136.9108	2941.3957	457.81	15
62	61	0	0	0	0	137.2036	2950.5829	464.21	7
63	62	0	0	0	0	137.2036	2950.5829	469.09	3
64	63	0	0	0	0	139.8547	2978.2374	474.57	12
65	64	0	0	0	0	140.7445	3038.6326	481.58	10
66	65	0	0	0	0	141.6373	3057.3476	491.34	12
67	66	0	0	0	0	143.1321	3063.5997	503.22	15
68	67	0	0	0	0	164.9510	3128.0802	515.72	15
69	68	0	0	0	0	167.6776	3151.8519	520.60	4
70	69	0	0	0	0	168.5317	3210.9033	525.17	6
71	70	0	0	0	0	170.5024	3223.7488	530.96	3
72	71	0	0	0	0	176.4884	3230.1821	537.67	5
73	72	0	0	0	0	305.3821	5680.0408	544.68	10
74	73	0	0	0	0	305.8334	5684.4047	551.69	7
75	74	0	0	0	0	314.4762	5695.3225	564.18	16
76	75	0	0	0	0	317.6932	5741.3010	576.38	20
77	76	0	0	0	0	317.6932	5743.4953	581.56	5
78	77	0	0	0	0	318.6155	5765.4644	587.96	3
79	78	0	0	0	0	323.2490	5789.6827	594.36	10
80	81	0	0	0	0	323.7144	5796.2970	601.98	10
81	80	0	0	0	0	333.0969	5800.7091	606.86	5
82	81	0	0	0	0	334.0431	5842.7122	621.49	14
83	82	0	0	0	0	385.7590	6729.1700	676.35	57
84	83	0	0	0	0	421.9376	8610.5131	701.95	27
85	84	0	0	0	0	426.7856	8808.2911	711.19	4
87	86	0	0	0	0	428.9499	8921.9970	720.24	12
88	87	0	0	0	0	433.2962	9245.1299	736.78	17
89	88	0	0	0	0	443.7132	9827.7564	770.84	30
90	89	0	0	0	0	447.5848	9942.4573	784.42	15
91	90	0	0	0	0	469.4872	10907.6600	819.91	37
92	91	0	0	0	0	498.3943	11595.0730	871.42	50
93	92	0	0	0	0	514.3919	12123.0840	890.93	20
94	93	0	0	0	0	517.3843	12176.4780	908.61	20
95	94	0	0	0	0	517.9843	12176.4790	932.38	10
96	95	0	0	0	0	528.2347	12554.7640	959.51	40
97	96	0	0	0	0	539.2066	12925.6990	986.64	27
98	97	0	0	0	0	541.0471	13014.2260	1016.51	33
99	98	0	0	0	0	547.2664	13048.3610	1047.60	33
100	99	0	0	0	0	559.0126	13099.6550	1084.17	40
101	100	0	0	0	0	569.6916	13130.4830	1107.34	22
102	101	0	0	0	0	577.9311	13171.6490	1132.33	26
103	102	0	0	0	0	583.4795	13267.9710	1173.76	40
		0	0	0	0	583.0338	13281.7620	1198.78	20

SEDIFC.DAT

Input file for the Sediment Difference
Program, Sediff.Pas; Discontinuous gully.

I.D	last	t1	t2	t3	t4	Absed kg/day	Maysed kg/day	inc	Distance
1	0	0	0	0	0	0.0001	0.0126	5.0	4.57
2	0	0	0	0	0	0.0001	0.0217	5.0	10.57
3	0	0	0	0	0	0.0004	0.0244	5.0	9.14
4	0	0	0	0	0	0.0002	0.0075	10.0	22.86
5	4	1	2	3	0	0.0107	1.3072	150.0	70.10
6	5	0	0	0	0	0.0146	1.7466	20.0	85.65
7	0	0	0	0	0	0.0008	0.0335	30.0	27.43
8	6	7	0	0	0	0.1098	2.0373	85.0	103.30
9	8	0	0	0	0	0.1662	2.9074	10.0	118.90
10	9	0	0	0	0	0.1906	4.0331	15.0	135.90
11	10	0	0	0	0	0.2079	5.3086	15.0	150.60
12	11	0	0	0	0	0.2449	6.8328	20.0	167.00
13	12	0	0	0	0	0.2852	7.4276	12.0	180.10
14	13	0	0	0	0	0.3758	8.2411	25.0	202.70
15	14	0	0	0	0	0.4801	8.9651	20.0	219.50
16	15	0	0	0	0	0.5083	8.9651	15.0	233.20
17	16	0	0	0	0	0.5981	10.8825	7.0	236.20
18	17	0	0	0	0	0.7836	14.0088	30.0	256.30
19	18	0	0	0	0	1.2137	15.2354	12.0	269.10
20	19	0	0	0	0	1.7183	16.4242	10.0	286.50
21	20	0	0	0	0	2.3708	36.9421	50.0	324.30
22	21	0	0	0	0	3.0561	40.4966	15.0	342.00
23	22	0	0	0	0	3.7331	53.6275	15.0	354.80
24	23	0	0	0	0	4.4374	68.7646	22.0	376.40
25	24	0	0	0	0	4.8142	77.0979	6.0	389.50
26	25	0	0	0	0	5.7760	97.2541	21.0	404.30
27	26	0	0	0	0	6.6596	116.9757	16.0	426.70
28	27	0	0	0	0	9.1683	175.4830	34.0	447.10
29	28	0	0	0	0	10.0771	196.3927	10.0	466.30
30	29	0	0	0	0	10.2935	202.9957	10.0	472.70
31	30	0	0	0	0	11.0325	218.5354	20.0	493.50
32	31	0	0	0	0	11.5663	229.9615	15.0	505.00
33	32	0	0	0	0	11.5668	230.7365	28.0	534.00

Input file for sediment difference program
Sedif2.Pas. (Called SedifA.Dat).In this
file the site yields were calculated using
rating relationship for sediment data in which
n=0.76, k=2130.

wre	1st	t1	t2	t3	t4	rn7sed	rn8sed	rn9sed	rn10sed	dist	inc
1	0	0	0	0	0	0.0550	0.0643	0.0525	0.0734	3.05	5
2	0	0	0	0	0	0.1640	0.1758	0.0101	0.7744	3.05	5
3	0	0	0	0	0	0.1287	0.1923	0.0141	6.5539	4.57	5
4	0	0	0	0	0	0.0452	0.0260	0.0146	0.6403	4.57	5
5	0	0	0	0	0	0.0079	0.0060	0.0114	0.5981	4.57	5
6	0	0	0	0	0	0.0278	0.0629	0.0289	4.6450	4.57	5
7	0	0	0	0	0	0.0393	0.0715	0.0566	0.5841	5.49	5
8	0	0	0	0	0	0.3886	0.1438	0.0807	6.8900	6.10	5
9	0	0	0	0	0	0.0204	0.0257	0.0114	0.6055	6.10	5
10	0	0	0	0	0	0.0358	0.0570	0.0114	0.2384	6.10	5
11	0	0	0	0	0	0.0079	0.0090	0.0087	1.9006	7.62	7
12	0	0	0	0	0	0.4094	0.8778	0.6965	2.2453	7.92	5
13	0	0	0	0	0	0.0149	0.5234	0.0381	3.7833	8.53	5
14	0	0	0	0	0	0.0129	0.0443	0.0087	7.7768	10.67	5
15	0	0	0	0	0	0.0079	0.0133	0.0087	8.1037	12.19	7
16	0	0	0	0	0	0.0204	0.2452	0.0565	4.2911	12.19	15
17	0	0	0	0	0	0.0204	0.0165	0.0173	1.2390	13.72	10
18	0	0	0	0	0	0.0092	0.0257	0.0173	2.1370	13.72	10
19	0	0	0	0	0	0.0278	0.0643	0.0257	3.6295	15.24	10
20	0	0	0	0	0	0.0158	0.0106	0.0141	2.1963	16.76	30
21	0	0	0	0	0	0.0358	0.0276	0.0223	0.5483	21.34	22
22	0	0	0	0	0	3.9694	0.4221	0.8787	4.9381	22.86	10
23	0	0	0	0	0	0.7094	0.0210	0.0087	1.9505	24.38	18
24	0	0	0	0	0	0.1211	0.0244	0.0146	2.3684	27.43	36
25	0	0	0	0	0	0.0095	0.0231	0.1225	3.3771	33.53	30
26	0	0	0	0	0	0.0158	0.0231	0.1161	2.3338	33.53	35
27	0	0	0	0	0	0.1152	0.0119	0.0119	0.5568	39.62	52
28	2	0	0	0	0	0.5818	0.2910	0.0244	0.4713	48.77	50
29	0	0	0	0	0	0.1094	0.0457	0.0141	9.6044	54.86	62
30	8	0	0	0	0	1.9744	0.2926	0.1170	9.3311	64.01	60
31	4	1	7	0	0	0.6257	0.4293	0.2139	8.5199	65.53	120
32	16	0	0	0	0	0.0671	0.2398	0.0901	5.9677	67.06	50
33	17	18	24	20	0	0.9924	1.5045	0.2667	36.1190	80.77	145
34	22	13	12	0	0	1.8679	2.2742	4.3850	117.0408	83.82	122
35	25	26	0	0	0	0.1436	0.2539	0.6373	17.4659	88.39	67
36	27	10	21	0	0	1.0023	0.6541	0.0700	18.4536	97.54	120
37	23	9	14	15	5	1.0346	2.0050	0.0934	33.1113	115.82	150
38	31	30	0	0	0	8.7643	1.2509	1.1465	10.8808	123.44	60
39	32	0	0	0	0	0.0769	0.1805	0.1330	6.0887	124.97	56
40	36	0	0	0	0	0.9805	1.4813	0.1544	18.9931	125.27	60
41	33	0	0	0	0	1.0618	2.2888	0.3728	37.2358	138.68	60
42	28	37	11	0	0	1.1710	6.1729	0.3651	37.4109	161.54	125
43	40	0	0	0	0	1.2690	1.8880	0.9303	19.9205	180.14	55
44	38	34	0	0	0	18.1341	6.9430	18.0178	291.6918	184.40	90
45	41	0	0	0	0	1.1063	2.9119	1.1221	41.8655	199.64	50
46	44	3	0	0	0	19.8253	7.4821	20.1855	322.0437	249.94	70
47	45	35	39	0	0	2.6593	8.0278	5.3917	138.9735	257.56	95
48	42	43	6	19	47	20.9292	26.5128	23.4193	625.0923	281.94	190
49	48	0	0	0	0	27.6533	28.2287	26.2580	632.5653	294.74	10
50	49	0	0	0	0	22.8893	29.8111	32.9988	644.5823	302.97	25
51	46	29	0	0	0	13.9629	11.3847	15.1089	412.2640	310.90	95
52	50	0	0	0	0	23.2550	30.8673	31.2246	650.9004	339.85	22

/cont..

/cont..

53	52	0	0	0	0	29.0618	32.4616	35.2705	636.0841	342.90	5
54	53	0	0	0	0	36.1997	33.8307	36.4811	631.7150	360.88	30
55	54	0	0	0	0	36.7543	36.5307	39.2422	626.4522	380.09	20
56	55	51	0	0	0	51.1961	70.8240	67.1020	1758.8562	399.29	20
57	56	0	0	0	0	50.1045	71.3200	56.5804	1629.7732	420.32	40
58	57	0	0	0	0	49.6484	70.7957	58.0051	1646.8978	431.29	12
59	58	0	0	0	0	47.4307	70.2949	58.7061	1616.7706	437.69	10
60	59	0	0	0	0	47.0865	68.4277	59.6691	1613.5084	446.53	10
61	60	0	0	0	0	47.9725	66.5366	60.7255	1651.1447	457.81	15
62	61	0	0	0	0	47.2185	66.4214	60.6549	1682.8441	464.21	7
63	62	0	0	0	0	47.1838	68.4195	60.7548	1666.6206	469.09	3
64	63	0	0	0	0	47.1661	69.2719	60.2691	1692.9130	474.57	12
65	64	0	0	0	0	37.6587	70.3587	59.5526	1714.0891	481.58	10
66	65	0	0	0	0	46.8014	70.1331	59.1999	1759.1531	503.22	15
67	66	0	0	0	0	47.2630	70.8024	58.6780	1759.1531	503.22	15
68	67	0	0	0	0	47.8237	70.3655	58.8996	1793.0846	515.72	15
69	68	0	0	0	0	48.9613	70.3143	58.8333	1752.9178	520.60	4
70	69	0	0	0	0	50.0481	70.8826	58.7400	1767.0377	525.17	6
71	70	0	0	0	0	50.6844	71.2489	58.4188	1806.4694	530.96	3
72	71	0	0	0	0	51.9907	71.8826	58.7065	1845.6397	537.67	5
73	72	0	0	0	0	52.3545	72.5063	58.4234	1812.0011	544.68	10
74	73	0	0	0	0	52.6147	73.0876	57.5442	1810.5653	551.69	7
75	74	0	0	0	0	52.4960	73.5383	57.1306	1794.8396	564.18	16
76	75	0	0	0	0	50.9625	73.8567	57.2263	1776.3560	576.38	20
77	76	0	0	0	0	49.4331	74.0084	57.2908	1723.8902	581.56	5
78	77	0	0	0	0	49.5030	73.3318	57.0658	1722.4552	587.96	3
79	78	0	0	0	0	49.1739	72.7196	58.2267	1732.4589	594.36	10
80	79	0	0	0	0	47.1131	72.3216	57.1599	1733.8854	601.98	10
81	80	0	0	0	0	44.6379	71.5587	57.0357	1744.8297	606.86	5
82	81	0	0	0	0	45.5495	70.8736	57.0351	1764.7308	621.49	14
83	82	0	0	0	0	44.1694	69.2303	57.1640	1782.5485	676.35	57
84	83	0	0	0	0	43.3543	59.7149	58.1591	1791.2181	701.95	27
85	84	0	0	0	0	43.4463	66.5923	58.5975	1817.9517	711.10	4
86	85	0	0	0	0	43.5789	65.3203	59.1364	1821.2200	720.24	12
87	86	0	0	0	0	43.1447	63.7693	59.6184	1815.9480	736.70	17
88	87	0	0	0	0	42.3428	62.4773	60.1346	1800.7930	770.84	30
89	88	0	0	0	0	41.1034	60.9396	60.6173	1820.8274	784.42	15
90	89	0	0	0	0	42.5651	60.5890	60.1878	1839.1557	819.91	37
91	90	0	0	0	0	43.8807	61.1573	58.4553	1848.0420	871.42	50
92	91	0	0	0	0	41.2099	61.7375	58.2993	1859.9242	890.93	20
93	92	0	0	0	0	42.9415	62.7650	58.4189	1862.6484	908.61	20
94	93	0	0	0	0	42.0953	63.6217	58.1309	1848.2262	932.38	10
95	94	0	0	0	0	41.7195	64.7958	58.3230	1864.6320	959.51	40
96	95	0	0	0	0	40.6373	63.5579	59.3246	1866.3570	986.64	27
97	96	0	0	0	0	41.2548	62.7920	59.3158	1849.7474	1016.51	33
98	97	0	0	0	0	40.1772	62.0575	59.6561	1875.5216	1047.60	33
99	98	0	0	0	0	40.0155	61.6692	60.3064	1880.2028	1084.17	40
100	99	0	0	0	0	39.3417	61.7446	60.5089	1906.8591	1107.34	22
101	100	0	0	0	0	39.7303	62.1251	60.8203	1883.3977	1132.33	26
102	101	0	0	0	0	38.5013	61.8701	61.2854	1886.1319	1173.78	40
103	102	0	0	0	0	38.2292	61.5837	59.0397	1887.4042	1198.78	20

Input file for sediment difference program
Sedif2.Pas. (Called SedifB.Dat).In this
file the site yields were calculated using
rating relationship for sediment data in which
n=0.81, k=0132.

wre	1st	t1	t2	t3	t4	rn7sed	rn8sed	rn9sed	rn10sed	dist	inc
1	0	0	0	0	0	0.1806	0.2104	0.1078	2.5313	3.05	5
2	0	0	0	0	0	0.5488	0.5803	0.0305	2.6794	3.05	5
3	0	0	0	0	0	0.4283	0.6418	0.0428	24.7832	4.57	5
4	0	0	0	0	0	0.1471	0.0817	0.0448	2.1979	4.57	5
5	0	0	0	0	0	0.0245	0.0183	0.0346	2.0640	4.57	5
6	0	0	0	0	0	0.0888	0.2063	0.0909	17.2121	4.57	5
7	0	0	0	0	0	0.1259	0.2328	0.1807	1.9980	5.49	5
8	0	0	0	0	0	1.3586	0.4757	0.2619	25.2093	6.10	5
9	0	0	0	0	0	0.0644	0.0807	0.0346	2.1018	6.10	5
10	0	0	0	0	0	0.1145	0.1834	0.0346	0.7948	6.10	5
11	0	0	0	0	0	0.0245	0.0285	0.0265	6.7314	7.62	7
12	0	0	0	0	0	1.4150	3.1312	5.4063	7.9904	7.92	5
13	0	0	0	0	0	0.0474	1.7849	3.0803	13.7440	8.53	5
14	0	0	0	0	0	0.0409	0.1409	0.0265	29.2161	10.67	5
15	0	0	0	0	0	0.0245	0.0407	0.0265	30.4535	12.19	7
16	0	0	0	0	0	0.0644	0.8445	0.1808	15.9215	12.19	15
17	0	0	0	0	0	0.0644	0.0509	0.0530	4.3130	13.72	10
18	0	0	0	0	0	0.0285	0.0807	0.0530	7.5892	13.72	10
19	0	0	0	0	0	0.0888	0.2104	0.0807	13.3470	15.24	10
20	0	0	0	0	0	0.0501	0.0326	0.0428	7.8012	16.76	30
21	0	0	0	0	0	0.1145	0.0868	0.0693	1.8877	21.34	22
22	0	0	0	0	0	15.0472	1.4333	2.9631	17.9964	22.86	10
23	0	0	0	0	0	2.5028	0.0652	0.0265	6.9676	24.38	16
24	0	0	0	0	0	0.4030	0.0766	0.0448	8.4289	27.43	36
25	0	0	0	0	0	0.0296	0.0725	0.3976	12.3453	33.53	30
26	0	0	0	0	0	0.0501	0.0725	0.3772	8.4296	33.53	35
27	0	0	0	0	0	0.3803	0.0367	0.0367	1.9141	39.62	52
28	2	0	0	0	0	2.0118	0.973	0.0766	11.6070	48.77	50
29	0	0	0	0	0	0.3011	0.1463	0.0428	37.2379	54.86	62
30	8	0	0	0	0	7.2334	0.9781	0.3821	34.3549	64.01	60
31	4	1	7	0	0	2.1970	1.4678	0.7149	31.2371	65.53	120
32	16	0	0	0	0	0.2202	0.8060	0.2921	22.8647	64.06	50
33	17	18	24	20	0	3.5496	5.2761	0.8792	138.8341	80.77	145
34	22	13	12	0	0	6.8325	8.3488	15.3289	461.4651	83.82	122
35	25	26	0	0	0	0.4849	0.8514	2.1538	67.0503	88.39	67
36	27	10	21	0	0	3.6129	2.2380	0.2252	70.7381	97.54	120
37	23	9	14	15	5	3.6886	7.1097	0.3008	127.9447	115.82	150
38	31	30	0	0	0	33.2643	4.3840	3.9510	41.0759	123.44	60
39	32	0	0	0	0	0.2538	0.6031	0.4381	23.3229	124.97	56
40	36	0	0	0	0	3.5312	5.2049	0.4986	72.8559	125.27	60
41	33	0	0	0	0	3.7087	8.1620	1.2345	143.1924	138.68	60
42	28	37	11	0	0	4.1950	22.3702	2.6541	144.9527	161.54	125
43	40	0	0	0	0	4.5797	6.6880	31.6130	76.4736	180.14	55
44	38	34	0	0	0	70.1946	25.1720	65.7484	1175.0305	184.40	90

/cont..

/cont..

45	41	0	0	0	0	3.9554	10.4133	3.8134	161.2435	199.64	50
46	44	3	0	0	0	76.8143	27.1494	73.6203	1300.9527	249.94	70
47	45	35	39	0	0	9.7568	29.3499	19.0131	550.9036	257.56	95
48	42	43	6	19	47	81.7242	100.8722	85.3016	2587.3226	281.94	190
49	48	0	0	0	0	107.3972	107.4660	95.8041	2618.6254	294.74	10
50	49	0	0	0	0	89.1465	113.4958	120.8179	2668.0185	302.97	25
51	46	29	0	0	0	53.3096	41.8361	54.5360	1674.4338	310.90	85
52	50	0	0	0	0	90.5577	117.3519	114.2389	2696.2409	339.85	22
53	52	0	0	0	0	107.3972	123.6157	129.2424	2631.9484	342.90	5
54	53	0	0	0	0	141.2805	128.9079	129.2424	2612.1477	360.88	30
55	54	0	0	0	0	143.4328	139.3365	144.2516	2587.6775	380.09	20
56	55	51	0	0	0	200.9931	274.4631	251.2322	7480.0892	399.29	20
57	56	0	0	0	0	196.5523	275.8595	210.6165	6919.0197	412.32	40
58	57	0	0	0	0	194.5431	273.5965	216.0625	6991.4852	431.29	12
59	58	0	0	0	0	185.5437	271.4679	218.7070	6855.8952	437.69	10
60	59	0	0	0	0	184.0158	263.9774	222.4005	6838.6785	446.53	10
61	60	0	0	0	0	187.2963	256.5256	226.4519	6999.6731	457.81	15
62	61	0	0	0	0	183.9540	256.0432	226.1317	7133.4325	464.21	7
63	62	0	0	0	0	183.6023	264.0152	226.5117	7061.4419	469.09	3
64	63	0	0	0	0	183.5756	271.3735	224.6426	7176.5364	474.57	12
65	64	0	0	0	0	145.3065	271.7199	221.9455	7266.6476	481.58	10
66	65	0	0	0	0	182.1553	270.8230	220.5636	7274.3168	503.22	15
67	66	0	0	0	0	184.0885	273.5017	218.5721	7459.5590	503.22	15
68	67	0	0	0	0	186.4210	271.8452	219.4481	7607.4416	515.72	15
69	68	0	0	0	0	190.9400	271.6403	219.1935	7430.6630	520.60	4
70	69	0	0	0	0	195.3294	273.9580	218.8494	7490.6859	525.17	6
71	70	0	0	0	0	197.9066	275.4199	275.6292	7662.4599	530.96	3
72	71	0	0	0	0	203.1907	277.9336	218.7999	7833.9437	537.67	5
73	72	0	0	0	0	204.4706	280.3452	217.6386	7685.4076	544.68	10
74	73	0	0	0	0	205.3513	282.5621	214.1915	7677.6098	551.69	7
75	74	0	0	0	0	204.7537	284.3197	212.579	7608.9510	564.18	16
76	75	0	0	0	0	198.3848	285.5416	212.8635	7526.0410	576.38	20
77	76	0	0	0	0	192.0746	286.0580	213.0675	7293.8141	581.56	5
78	77	0	0	0	0	192.3079	283.3036	212.1766	7286.2773	587.96	3
79	78	0	0	0	0	190.8190	280.8106	216.5729	7328.7666	594.36	10
80	79	0	0	0	0	182.5021	279.1717	212.4556	7333.5395	601.98	10
81	80	0	0	0	0	172.6010	276.0965	211.9652	7380.4652	606.86	5
82	81	0	0	0	0	176.2799	273.3462	211.9296	7466.3259	621.49	14
83	82	0	0	0	0	170.8698	266.8298	212.3674	7542.4885	676.35	57
84	83	0	0	0	0	167.6908	229.0973	216.0926	7582.5234	701.95	27
85	84	0	0	0	0	168.0408	256.3147	217.8935	7700.6948	711.10	4
86	85	0	0	0	0	168.6107	251.2883	220.1030	7712.3924	720.24	12
87	86	0	0	0	0	166.9386	245.1948	221.8083	7695.0796	736.70	17
88	87	0	0	0	0	163.7978	240.1518	223.7923	7633.8767	770.84	30
89	88	0	0	0	0	158.9466	234.1882	225.6730	7722.6931	784.42	15
90	89	0	0	0	0	164.7053	232.7948	223.8451	7801.7665	819.91	37
91	90	0	0	0	0	170.0089	234.9575	217.3002	7839.1515	871.42	50
92	91	0	0	0	0	159.1060	237.1562	216.6162	7891.0269	890.93	20
93	92	0	0	0	0	165.6094	241.0569	217.0988	7902.1475	908.61	20
94	93	0	0	0	0	162.5759	244.3674	215.9234	7840.1478	932.38	10
95	94	0	0	0	0	161.0681	248.9044	216.7378	7909.9141	959.51	40
96	95	0	0	0	0	156.8136	243.8656	220.5839	7916.2487	986.64	27
97	96	0	0	0	0	159.2562	240.7276	220.5877	7847.0607	1016.51	33
98	97	0	0	0	0	155.0312	237.8101	221.9379	7956.8789	1047.68	33
99	98	0	0	0	0	154.4052	236.2991	224.2709	7975.9329	1084.17	40
100	99	0	0	0	0	151.8395	236.5977	226.3230	8094.2232	1107.34	22
101	100	0	0	0	0	153.3466	238.0752	228.0512	7991.1209	1132.33	26
102	101	0	0	0	0	148.5255	236.9656	227.6672	8003.5025	1173.78	40
103	102	0	0	0	0	147.5207	235.6995	229.9417	8009.1702	1198.78	25

CDIFA.DAT, the datafile for the differencing program.
(IN this file, the site yields were calculated using
the field-derived rating relationship in which,n=0.76,k=2130)

Large Discontinuous Gully

wr	lt	t1	t2	t3	t4	rn7sed	rn8sed	rn9sed	rn10sd	dist	inc
1	0	0	0	0	0	0.5966	0.0694	0.1008	9.3971	4.57	5.0
2	0	0	0	0	0	0.6732	0.0970	0.1091	8.5465	10.57	5.0
3	0	0	0	0	0	0.6675	0.1106	0.1272	8.0910	9.14	5.0
4	0	0	0	0	0	0.6338	0.0659	0.1902	8.7252	22.86	10.0
5	4	1	2	3	0	24.5935	8.1464	14.6713	298.3428	70.10	150.0
6	5	0	0	0	0	25.4247	8.1630	15.4369	308.3640	85.65	20.0
7	0	0	0	0	0	1.5741	0.0700	0.2940	9.5438	27.43	30.0
8	6	7	0	0	0	25.9800	8.5820	16.3991	316.4255	103.30	85.0
9	8	0	0	0	0	27.2051	6.5164	17.2935	325.5361	118.90	10.0
10	9	0	0	0	0	28.1250	6.7591	17.9764	337.1449	135.90	15.0
11	10	0	0	0	0	28.7245	9.4336	18.8832	350.4768	150.60	15.0
12	11	0	0	0	0	27.5058	8.8865	19.2222	348.1729	167.00	20.0
13	12	0	0	0	0	27.0226	8.9341	19.6646	344.6125	180.10	12.0
14	13	0	0	0	0	26.4384	8.9096	20.2156	340.3372	202.70	25.0
15	14	0	0	0	0	25.7444	8.9393	20.6192	342.3086	219.50	20.0
16	15	0	0	0	0	25.1507	8.9738	20.8801	344.5845	233.20	15.0
17	16	0	0	0	0	24.9215	9.0106	20.9309	330.5060	236.20	7.0
18	17	0	0	0	0	24.7839	8.9336	21.1223	331.8164	256.30	30.0
19	18	0	0	0	0	24.9381	8.6774	21.2192	326.8991	269.10	12.0
20	19	0	0	0	0	24.7569	8.6144	20.8868	323.5716	286.50	10.0
21	20	0	0	0	0	24.5236	8.5204	20.5007	321.7136	324.30	50.0
22	21	0	0	0	0	24.4783	8.4740	20.7821	319.6990	342.00	15.0
23	22	0	0	0	0	24.6170	8.2779	20.9673	319.2723	354.80	15.0
24	23	0	0	0	0	24.6306	8.1476	21.1925	317.1676	376.40	22.0
25	24	0	0	0	0	24.5266	8.1657	20.6648	312.4557	389.50	6.0
26	25	0	0	0	0	24.5519	8.2053	21.3485	308.5233	409.30	21.0
27	26	0	0	0	0	24.6414	8.1648	21.4452	303.2988	426.70	16.0
28	27	0	0	0	0	24.7753	8.1477	21.2044	290.3066	447.10	34.0
29	28	0	0	0	0	24.6277	8.1713	21.1885	286.0490	460.30	10.0
30	29	0	0	0	0	24.3855	8.2150	20.8926	278.3184	472.70	10.0
31	30	0	0	0	0	24.3818	8.2433	20.7526	273.6523	493.50	20.0
32	31	0	0	0	0	24.4397	8.2501	20.5872	266.7370	505.00	15.0
33	32	0	0	0	0	24.4672	8.1052	20.5279	264.0144	534.00	28.0

CDIFB.DAT, the datafile for the differencing program.
(IN this file, the summer site yields were calculated using the
rating relationship for all sediment data, in which n=0.81,k=9132)

Large Discontinuous Gully

wr	lt	t1	t2	t3	t4	rn7sed	rn8sed	rn9sed	rn10sd	dist	inc
1	0	0	0	0	0	0.2278	2.0494	0.2707	35.2167	4.57	5.0
2	0	0	0	0	0	0.3211	2.3224	0.3162	31.7856	10.57	5.0
3	0	0	0	0	0	0.3691	2.2970	0.3592	30.0792	9.14	5.0
4	0	0	0	0	0	0.2194	2.1740	0.6122	32.5441	22.86	10.0
5	4	1	2	3	0	30.7105	92.2791	42.5337	1212.6299	70.10	150.0
6	5	0	0	0	0	30.7539	95.4208	44.7554	1254.2631	85.65	20.0
7	0	0	0	0	0	0.2317	5.5274	0.8571	35.7547	27.43	30.0
8	6	7	0	0	0	32.3280	97.5550	47.4812	1287.7171	103.30	85.0
9	8	0	0	0	0	24.3874	102.2626	49.9992	1325.6555	118.90	10.0
10	9	0	0	0	0	25.3071	105.7909	51.6434	1374.2374	135.90	15.0
11	10	0	0	0	0	35.5623	108.0724	54.1619	1430.1871	150.60	15.0
12	11	0	0	0	0	33.3910	103.2585	54.4762	1419.8075	167.00	20.0
13	12	0	0	0	0	33.5459	101.3324	55.1952	1404.0479	180.10	12.0
14	13	0	0	0	0	33.4171	98.9648	56.2407	1385.7828	202.70	25.0
15	14	0	0	0	0	33.5121	96.1901	56.7201	1393.4971	219.50	20.0
16	15	0	0	0	0	32.8091	93.8395	56.6540	1402.8187	233.20	15.0
17	16	0	0	0	0	33.7333	92.9030	55.7729	1344.8456	236.20	7.0
18	17	0	0	0	0	33.3963	92.3172	55.3987	1350.1937	256.30	30.0
19	18	0	0	0	0	32.3731	92.8691	54.6361	1329.2440	269.10	12.0
20	19	0	0	0	0	32.0947	92.1173	52.2460	1315.0626	286.50	10.0
21	20	0	0	0	0	31.6965	91.1730	49.6346	1307.1315	324.30	50.0
22	21	0	0	0	0	31.4825	90.9580	49.5026	1298.5488	342.00	15.0
23	22	0	0	0	0	30.6863	91.4774	49.0027	1296.1126	354.80	15.0
24	23	0	0	0	0	30.1439	91.4945	48.6256	1287.8490	376.40	22.0
25	24	0	0	0	0	30.1799	91.0634	47.8951	1267.8693	389.50	6.0
26	25	0	0	0	0	30.2974	91.1321	47.2865	1251.2133	409.30	21.0
27	26	0	0	0	0	30.1044	91.4543	47.1039	1259.2253	426.70	16.0
28	27	0	0	0	0	30.0157	91.9367	45.8356	1174.6527	447.10	34.0
29	28	0	0	0	0	30.0838	91.3488	45.5607	1156.7633	460.30	10.0
30	29	0	0	0	0	30.2366	90.3913	44.8769	1124.6249	472.70	10.0
31	30	0	0	0	0	30.3129	90.3694	44.2484	1104.8116	493.50	20.0
32	31	0	0	0	0	30.3200	90.5765	43.9028	1076.3228	505.00	15.0
33	32	0	0	0	0	29.7620	90.6836	43.7905	1065.0227	534.00	28.0

APPENDIX 14 (C) - YIELDS

Notes :

Taking the data in the previous Appendix, 14(B), total event yields can be calculated. For an 'allmelt' yield, Apsed and Maysed are multiplied by 0.30 and 0.31 respectively (the number of days in April and May respectively multiplied by 10^{-3} for Tonnes) gives an allmelt value in Tonnes/year across the watershed. Here they are listed in Kg for ease of interpretation.

Similarly, the weighted values of rn7sed,etc. for runs 7 to 10 can be summed to give an annual yield for the summer, both with an without the inclusion of the effect of a 'freak' event like run 10 in the annual total. In the tables which follow, therefore

sumless = (5.rn7sed + 4.rn8sed + 2.rn9sed) ; and

sumplus = (sumless + rn10sd).

Data are once again listed in Kg. for ease of interpretation.

LISTING FOR WINTER YIELDS
(VALUE IN KG)

DISTANCE	TOTAL MELT YLD.
339.800	5113.000
342.900	4504.000
360.900	4791.000
380.100	4944.000
399.300	5170.000
420.300	53030.000
431.300	90330.000
431.300	90930.000
437.700	91070.000
446.500	91710.000
457.800	95290.000
464.200	95580.000
469.100	95580.000
474.600	96520.000
481.600	98420.000
491.300	99030.000
503.200	99270.000
515.700	101900.000
520.600	102700.000
525.200	104600.000
531.000	105100.000
537.700	105400.000
544.700	185200.000
551.700	185400.000
564.200	186000.000
576.400	187500.000
581.600	187600.000
588.000	188300.000
594.400	189200.000
602.000	189400.000
606.900	189800.000
621.500	191100.000
676.300	220200.000
701.900	279600.000
711.100	285900.000
720.200	289500.000
736.700	299600.000
770.800	318000.000
784.400	321600.000
819.900	352200.000
871.400	374400.000
890.900	391300.000
908.600	393000.000
932.400	393000.000
959.500	405000.000
986.600	416900.000
1017.000	419700.000
1048.000	420900.000
1084.000	422900.000
1107.000	424100.000
1132.000	425700.000
1174.000	428700.000
1199.000	429200.000

LISTING FOR L.D.G YIELD,
WINTER(VALUE IN KG)

DISTANCE	WINTER YLD
4.570	0.394
9.140	0.768
10.570	0.676
22.860	0.239
27.430	1.063
70.100	40.840
85.650	54.580
103.300	66.450
118.900	95.120
135.900	130.700
150.600	170.800
167.000	219.200
180.100	238.800
202.700	266.700
219.500	292.300
233.200	293.200
236.200	355.300
256.300	457.800
269.100	508.700
286.500	560.700
324.300	1231.000
342.000	1347.000
354.800	1774.000
376.400	2265.000
389.500	2534.000
409.300	3188.000
426.700	3826.000
447.100	5715.000
460.300	6406.000
472.700	6602.000
493.500	7105.000
505.000	7476.000
534.000	7500.000

LISTING OF EVENT YIELDS FOR RUNS OF YIELD2.PAS WITH N=0.76,K=2130
(IN KG):NETWORK

RN7YLD.5	RN8YLD.4	RN9YLD.2	RN10YLD	DISTANCE	SUMMER TOTAL
69.8100	45.5400	30.2200	412.3000	310.9000	557.8000
116.3000	123.5000	62.4500	650.9000	339.8000	753.1000
145.3000	129.8000	70.5400	636.1000	342.9000	981.8000
181.0000	135.3000	72.9600	631.7000	360.9000	1021.0000
183.8000	146.1000	78.4800	626.5000	380.1000	1035.0000
256.0000	283.3000	134.2000	1759.0000	399.3000	2432.0000
250.5000	285.3000	113.2000	1630.0000	420.3000	2279.0000
248.2000	283.2000	116.0000	1647.0000	431.3000	2294.0000
237.2000	281.2000	117.4000	1617.0000	437.7000	2253.0000
235.4000	273.7000	119.3000	1614.0000	446.5000	2242.0000
239.9000	266.1000	121.5000	1651.0000	457.8000	2279.0000
236.1000	265.7000	121.3000	1683.0000	464.2000	2306.0000
235.9000	273.7000	121.5000	1667.0000	469.1000	2298.0000
235.9000	277.1000	120.5000	1693.0000	474.6000	2326.0000
188.3000	281.4000	119.1000	1714.0000	481.6000	2303.0000
234.0000	280.5000	118.4000	1759.0000	503.2000	2392.0000
236.3000	283.2000	117.4000	1759.0000	503.2000	2396.0000
239.1000	281.5000	117.8000	1793.0000	515.7000	2431.0000
244.8000	281.3000	117.7000	1753.0000	520.6000	2397.0000
250.2000	283.5000	117.5000	1767.0000	525.2000	2418.0000
253.4000	285.0000	116.8000	1806.0000	531.0000	2462.0000
260.0000	287.5000	117.4000	1846.0000	537.7000	2511.0000
261.8000	290.0000	116.8000	1812.0000	544.7000	2481.0000
263.1000	292.4000	115.1000	1811.0000	551.7000	2481.0000
262.5000	294.2000	114.3000	1795.0000	564.2000	2466.0000
254.8000	295.4000	114.5000	1776.0000	576.4000	2441.0000
247.2000	296.0000	114.6000	1724.0000	581.6000	2382.0000
247.5000	293.3000	114.1000	1722.0000	588.0000	2377.0000
245.9000	290.9000	116.5000	1732.0000	594.4000	2386.0000
235.6000	289.3000	114.3000	1734.0000	602.0000	2373.0000
223.2000	286.2000	114.1000	1745.0000	606.9000	2368.0000
227.7000	283.5000	114.1000	1765.0000	621.5000	2390.0000
220.8000	276.9000	114.3000	1783.0000	676.3000	2395.0000
216.8000	238.9000	116.3000	1791.0000	701.9000	2363.0000
217.2000	266.4000	117.2000	1818.0000	711.1000	2419.0000
217.9000	261.3000	118.3000	1821.0000	720.2000	2419.0000
215.7000	255.1000	119.2000	1816.0000	736.7000	2406.0000
211.7000	249.9000	120.3000	1801.0000	770.8000	2383.0000
205.5000	243.8000	121.2000	1821.0000	784.4000	2391.0000
212.8000	242.4000	120.4000	1839.0000	819.9000	2415.0000
219.4000	244.6000	116.9000	1848.0000	871.4000	2429.0000
206.0000	247.0000	116.6000	1860.0000	890.9000	2430.0000
214.2000	251.1000	116.8000	1863.0000	908.6000	2445.0000
210.5000	254.5000	116.3000	1848.0000	932.4000	2429.0000
208.6000	259.2000	116.6000	1865.0000	959.5000	2449.0000
203.2000	254.2000	118.6000	1866.0000	986.6000	2442.0000
206.3000	251.2000	118.6000	1850.0000	1017.0000	2426.0000
200.9000	248.2000	119.3000	1876.0000	1048.0000	2444.0000
200.1000	246.7000	120.6000	1880.0000	1084.0000	2448.0000
196.7000	247.0000	121.0000	1907.0000	1107.0000	2472.0000
198.7000	248.5000	121.6000	1883.0000	1132.0000	2452.0000
192.5000	247.5000	122.6000	1886.0000	1174.0000	2449.0000
191.1000	246.3000	118.1000	1887.0000	1199.0000	2443.0000

LISTING OF EVENT YIELDS FOR RUNS OF YIELD2.PAS WITH N=0.81 K = 9132
(IN KG.)NETWORK

DISTANCE	RN7YLD.5	RN8YLD.4	RN9YLD.2	RN10YLD	SUMMER TOTAL
310.9000	266.5000	167.3000	109.1000	2217.0000	543.0000
339.8000	452.8000	469.4000	228.5000	3847.0000	1151.0000
342.9000	537.0000	494.5000	258.5000	3922.0000	1290.0000
360.9000	706.4000	515.6000	258.5000	4093.0000	1481.0000
380.1000	717.2000	557.3000	288.5000	4151.0000	1563.0000
399.3000	1005.0000	1098.0000	502.5000	10090.0000	2605.0000
412.3000	982.8000	1103.0000	421.2000	9426.0000	2507.0000
431.3000	972.7000	1094.0000	432.1000	9491.0000	2499.0000
437.7000	927.7000	1086.0000	437.4000	9307.0000	2451.0000
446.5000	920.1000	1056.0000	444.8000	9259.0000	2421.0000
457.8000	936.5000	1026.0000	452.9000	9415.0000	2415.0000
464.2000	919.8000	1024.0000	452.3000	9530.0000	2396.0000
469.1000	918.0000	1056.0000	453.0000	9489.0000	2427.0000
474.6000	917.9000	1085.0000	449.3000	9629.0000	2453.0000
481.6000	726.5000	1087.0000	443.9000	9524.0000	2257.0000
503.2000	910.8000	1083.0000	441.1000	9710.0000	2435.0000
503.2000	920.4000	1094.0000	437.1000	9911.0000	2452.0000
515.7000	932.1000	1087.0000	438.9000	10070.0000	2458.0000
520.6000	954.7000	1087.0000	438.4000	9910.0000	2480.0000
525.2000	976.6000	1096.0000	437.7000	10000.0000	2510.0000
531.0000	989.5000	1102.0000	551.3000	10300.0000	2642.0000
537.7000	1016.0000	1112.0000	437.6000	10400.0000	2565.0000
544.7000	1022.0000	1121.0000	435.3000	10260.0000	2579.0000
551.7000	1027.0000	1130.0000	428.4000	10260.0000	2585.0000
564.2000	1024.0000	1137.0000	425.2000	10200.0000	2586.0000
576.4000	991.9000	1142.0000	425.7000	10090.0000	2560.0000
581.6000	960.4000	1144.0000	426.1000	9825.0000	2531.0000
588.0000	961.5000	1133.0000	424.4000	9805.0000	2519.0000
594.4000	954.1000	1123.0000	433.1000	9839.0000	2510.0000
602.0000	912.5000	1117.0000	424.9000	9788.0000	2454.0000
606.9000	863.0000	1104.0000	423.9000	9772.0000	2391.0000
621.5000	881.4000	1093.0000	423.9000	9865.0000	2399.0000
676.3000	854.3000	1067.0000	424.7000	9889.0000	2346.0000
701.9000	838.5000	916.4000	432.2000	9770.0000	2187.0000
711.1000	840.2000	1025.0000	435.8000	10000.0000	2301.0000
720.2000	843.1000	1005.0000	440.2000	10000.0000	2288.0000
736.7000	834.7000	980.8000	443.6000	9954.0000	2259.0000
770.8000	819.0000	960.6000	447.6000	9861.0000	2227.0000
784.4000	794.7000	936.8000	451.3000	9906.0000	2183.0000
819.9000	823.5000	931.2000	447.7000	10000.0000	2202.0000
871.4000	850.0000	939.8000	434.6000	10060.0000	2224.0000
890.9000	795.5000	948.6000	433.2000	10070.0000	2177.0000
908.6000	828.0000	964.2000	434.2000	10130.0000	2226.0000
932.4000	812.9000	977.5000	431.8000	10060.0000	2222.0000
959.5000	805.3000	995.6000	433.5000	10140.0000	2234.0000
986.6000	784.1000	975.5000	441.2000	10120.0000	2201.0000
1017.0000	796.3000	962.9000	441.2000	10050.0000	2200.0000
1048.0000	775.2000	951.2000	443.9000	10130.0000	2170.0000
1084.0000	772.0000	945.2000	448.5000	10140.0000	2166.0000
1107.0000	759.2000	946.4000	452.6000	10250.0000	2158.0000
1132.0000	766.7000	952.3000	456.1000	10170.0000	2175.0000
1174.0000	742.6000	947.9000	455.7000	10150.0000	2146.0000
1199.0000	737.6000	943.6000	459.9000	10151.0000	2141.0000

LISTING FOR SITE YIELDS (WEIGHTED), L.DISC.TRIB. HERE YIELDS CALULATED
WITH THE REGRESSION N=0.76,K=2130

(VALUES IN KG)

DISTANCE	SUM-10	RN8SED.4	RN9SED.2	SUMM+10	RN7SED.5
4.570	3.462	0.278	0.202	12.860	2.983
10.570	3.972	0.388	0.218	12.520	3.366
9.140	4.034	0.442	0.254	12.130	3.337
22.860	3.813	0.264	0.380	12.540	3.169
70.100	184.900	32.590	29.340	483.200	123.000
85.650	190.600	32.650	30.870	499.000	127.100
27.430	8.739	0.280	0.588	18.280	7.871
103.300	197.000	34.330	32.800	513.500	129.900
118.900	196.700	26.070	34.590	522.200	136.000
135.900	203.600	27.040	35.950	540.800	140.600
150.600	219.100	37.730	37.770	569.600	143.600
167.000	211.500	35.550	38.440	559.700	137.500
180.100	210.200	35.740	39.330	554.800	135.100
202.700	208.300	35.640	40.430	548.600	132.200
219.500	205.700	35.760	41.240	548.000	128.700
233.200	203.400	35.900	41.760	548.000	125.800
236.200	202.500	36.040	41.860	533.000	124.600
256.300	201.900	35.730	42.240	533.700	123.900
269.100	201.800	34.710	42.440	528.700	124.700
286.500	200.000	34.460	41.770	523.600	123.800
324.300	197.700	34.080	41.000	519.400	122.600
342.000	197.900	33.900	41.560	517.600	122.400
354.800	198.100	33.110	41.930	517.400	123.100
376.400	198.100	32.590	42.390	515.300	123.200
389.500	196.600	32.660	41.330	509.100	122.600
409.300	198.300	32.820	42.700	506.800	122.800
426.700	198.800	32.660	42.890	502.100	123.200
447.100	198.900	32.590	42.410	489.200	123.900
460.300	198.200	32.690	42.380	484.200	123.100
472.700	196.600	32.860	41.790	474.900	121.900
493.500	196.400	32.970	41.510	470.000	121.900
505.000	196.400	33.000	41.170	463.100	122.200
534.000	195.800	32.420	41.060	459.800	122.300

LISTING OF WEIGHTED YIELD FOR SUMMER EVENTS, USING THE YIELD REGRESSION
IN WHICH N=0.81.K=9132. (VALUES ARE IN KG) DISCONTINUOUS TRIB.

DISTANCE	RN7SED.5	RN8SED.4	RN9SED.2	RN10SED	TOTAL -10	TOTAL+10
4.570	1.140	8.196	0.542	35.220	9.878	45.100
10.570	1.605	9.288	0.632	31.790	11.520	43.310
9.140	1.845	9.188	0.718	30.080	11.750	41.830
22.860	1.095	8.696	1.224	32.540	11.010	43.550
70.100	153.600	369.100	85.070	1213.000	607.800	1821.000
85.650	153.800	381.700	89.510	1254.000	625.000	1879.000
27.430	1.160	22.110	1.714	35.760	24.980	60.740
103.300	161.600	390.200	94.960	1288.000	646.900	1935.000
118.900	121.900	409.100	100.000	1326.000	631.000	1957.000
135.900	126.500	423.200	103.300	1374.000	653.000	2027.000
150.600	177.800	432.300	108.300	1430.000	718.400	2148.000
167.000	167.000	413.000	109.000	1420.000	689.000	2109.000
180.100	167.700	405.300	110.400	1404.000	683.500	2088.000
202.700	167.100	395.900	112.500	1386.000	675.400	2061.000
219.500	167.600	384.800	113.400	1393.000	665.700	2059.000
233.200	164.000	375.400	113.300	1403.000	652.700	2056.000
236.200	168.700	371.600	111.500	1345.000	651.800	1997.000
256.300	167.000	369.300	110.800	1350.000	647.000	1997.000
269.100	161.900	371.500	109.300	1329.000	642.600	1972.000
286.500	160.500	368.500	104.500	1315.000	633.400	1948.000
324.300	158.500	364.700	99.270	1307.000	622.500	1929.000
342.000	157.400	363.800	99.010	1299.000	620.200	1919.000
354.800	153.400	365.900	98.010	1296.000	617.300	1913.000
376.400	150.700	366.000	97.250	1286.000	613.900	1902.000
389.500	150.900	364.300	95.790	1268.000	611.000	1879.000
409.300	151.500	364.500	94.570	1251.000	610.600	1862.000
426.700	150.500	365.800	94.210	1259.000	610.500	1870.000
447.100	150.100	367.700	91.670	1175.000	609.500	1784.000
460.300	150.400	365.400	91.120	1157.000	606.900	1764.000
472.700	151.200	361.600	89.750	1125.000	602.400	1727.000
493.500	151.600	361.500	88.500	1105.000	601.500	1707.000
505.000	151.600	362.300	87.810	1076.000	601.700	1678.000
534.000	148.800	362.700	87.580	1065.000	599.100	1664.000

14:C:6

APPENDIX 14 (D)

SEDIF OUTPUT FILES

Note : As noted previously, the total melt differences are listed in Appendix 15 as "WINDIF".

SEDIFA.OUT ; Output file from the operation of Sedif2.pas on SedifA.dat

New ID	rn7dif	rn8dif	rn9dif	rn10df	smless	smplus
1	0.055	0.051	0.021	0.015	0.127	0.142
2	0.164	0.141	0.004	0.155	0.309	0.464
3	0.129	0.154	0.006	1.311	0.288	1.599
4	0.045	0.021	0.006	0.128	0.072	0.200
5	0.008	0.005	0.005	0.120	0.017	0.137
6	0.028	0.050	0.012	0.929	0.090	1.019
7	0.039	0.057	0.023	0.117	0.119	0.236
8	0.389	0.115	0.032	1.378	0.536	1.914
9	0.020	0.021	0.005	0.121	0.046	0.167
10	0.036	0.046	0.005	0.048	0.086	0.134
11	0.006	0.005	0.002	0.272	0.013	0.285
12	0.409	0.702	0.279	0.449	1.390	1.839
13	0.015	0.419	0.015	0.757	0.449	1.206
14	0.013	0.035	0.003	1.555	0.052	1.607
15	0.006	0.008	0.002	1.158	0.016	1.173
16	0.007	0.065	0.008	0.286	0.080	0.366
17	0.010	0.007	0.003	0.124	0.020	0.144
18	0.005	0.010	0.003	0.214	0.018	0.232
19	0.014	0.026	0.005	0.363	0.045	0.408
20	0.003	0.001	0.001	0.073	0.005	0.078
21	0.008	0.005	0.002	0.025	0.015	0.040
22	1.985	0.169	0.176	0.494	2.329	2.823
23	0.197	0.005	0.001	0.108	0.203	0.311
24	0.017	0.003	0.001	0.066	0.020	0.086
25	0.002	0.003	0.008	0.113	0.013	0.125
26	0.002	0.003	0.007	0.067	0.012	0.078
27	0.011	0.001	0.000	0.011	0.012	0.023
28	0.042	0.009	0.001	-0.006	0.052	0.046
29	0.009	0.003	0.000	0.155	0.012	0.167
30	0.132	0.010	0.001	0.041	0.143	0.184
31	0.020	0.009	0.002	0.060	0.031	0.091
32	0.005	-0.000	0.001	0.034	0.006	0.039
33	0.028	0.039	0.003	0.194	0.071	0.265
34	-0.104	0.015	0.045	0.869	-0.043	0.826
35	0.009	0.012	0.012	0.175	0.033	0.209
36	0.034	0.019	0.000	0.143	0.053	0.196
37	0.009	0.051	0.001	0.094	0.060	0.154
38	0.514	0.035	0.027	-0.116	0.576	0.460
39	0.001	-0.004	0.002	0.002	-0.002	0.000
40	-0.002	0.055	0.003	0.009	0.056	0.065
41	0.006	0.052	0.004	0.019	0.062	0.080
42	-0.018	0.124	0.004	0.015	0.109	0.125
43	0.026	0.030	0.028	0.017	0.084	0.101
44	0.417	0.152	0.277	1.820	0.846	2.666
45	0.004	0.050	0.030	0.093	0.084	0.177
46	0.112	0.020	0.062	0.340	0.193	0.533
47	0.070	0.197	0.074	0.774	0.341	1.115
48	0.415	0.217	0.176	2.213	0.807	3.021
49	3.362	0.686	0.568	0.747	4.616	5.363
50	-0.953	0.253	0.539	0.481	-0.160	0.320
51	-0.351	0.182	-0.120	0.948	-0.290	0.659

52	0.083	0.192	-0.161	0.287	0.114	0.401
53	5.807	1.275	1.618	-2.963	8.701	5.737
54	1.189	0.183	0.081	-0.146	1.453	1.307
55	0.139	0.540	0.276	-0.263	0.955	0.692
56	0.120	4.582	1.275	36.007	5.977	41.984
57	-0.136	0.050	-0.526	-3.227	-0.613	-3.840
58	-0.190	-0.175	0.237	1.427	-0.127	1.300
59	-1.106	-0.200	0.140	-3.013	-1.166	-4.179
60	-0.175	-0.747	0.193	-0.326	-0.729	-1.056
61	0.295	-0.504	0.141	2.509	-0.068	2.441
62	-0.539	-0.066	-0.020	4.528	-0.625	3.904
63	-0.058	2.664	0.067	-5.408	2.673	-2.735
64	0.001	0.284	-0.081	2.191	0.204	2.395
65	-4.764	0.435	-0.143	2.118	-4.472	-2.355
66	3.048	-0.060	-0.047	3.004	2.940	5.945
67	0.154	0.178	-0.070	0.000	0.263	0.263
68	0.187	-0.117	0.030	2.262	0.100	2.362
69	1.422	-0.051	-0.033	-10.042	1.338	-8.704
70	0.906	0.379	-0.031	2.353	1.253	3.607
71	1.061	0.488	-0.214	13.144	1.335	14.479
72	1.306	0.507	0.115	7.834	1.928	9.762
73	0.182	0.249	-0.057	-3.364	0.375	-2.989
74	0.186	0.332	-0.251	-0.205	0.267	0.062
75	-0.037	0.113	-0.052	-0.983	0.024	-0.959
76	-0.383	0.064	0.010	-0.924	-0.310	-1.234
77	-1.529	0.121	0.026	-10.493	-1.382	-11.875
78	0.116	-0.902	-0.150	-0.478	-0.936	-1.414
79	-0.165	-0.245	0.232	1.000	-0.177	0.823
80	-1.030	-0.159	-0.213	0.143	-1.403	-1.260
81	-2.475	-0.610	-0.050	2.189	-3.135	-0.946
82	0.326	-0.196	-0.000	1.422	0.130	1.551
83	-0.121	-0.115	0.005	0.313	-0.232	0.081
84	-0.151	-1.410	0.074	0.321	-1.487	-1.166
85	0.115	6.877	0.219	6.683	7.212	13.895
86	0.055	-0.424	0.090	0.272	-0.279	-0.007
87	-0.128	-0.365	0.057	-0.310	-0.436	-0.746
88	-0.134	-0.172	0.034	-0.505	-0.272	-0.777
89	-0.413	-0.410	0.064	1.336	-0.759	0.577
90	0.198	-0.038	-0.023	0.495	0.136	0.632
91	0.132	0.045	-0.069	0.178	0.108	0.285
92	-0.668	0.116	-0.016	0.594	-0.567	0.027
93	0.408	0.205	0.012	0.136	0.625	0.762
94	-0.373	0.343	-0.058	-1.442	-0.088	-1.530
95	-0.047	0.117	0.010	0.410	0.080	0.490
96	-0.200	-0.183	0.074	0.064	-0.310	-0.246
97	0.094	-0.093	-0.001	-0.503	0.000	-0.503
98	-0.163	-0.089	0.021	0.781	-0.232	0.549
99	-0.020	-0.039	0.033	0.117	-0.027	0.091
100	-0.153	0.014	0.018	1.212	-0.121	1.091
101	0.075	0.059	0.024	-0.902	0.157	-0.745
102	-0.154	-0.026	0.023	0.068	-0.156	-0.088
103	-0.068	-0.057	-0.225	0.064	-0.350	-0.286

SedifB.out ; Output file from the operation of Sedif2.Pas on SedifB.Dat.

new ID	rn7dif	rn8dif	rn9dif	rn10df	smless	smplus
1	0.181	0.168	0.067	0.506	0.416	0.922
2	0.549	0.464	0.012	0.536	1.025	1.561
3	0.428	0.513	0.017	4.957	0.959	5.916
4	0.147	0.065	0.018	0.440	0.230	0.670
5	0.025	0.015	0.014	0.413	0.053	0.466
6	0.089	0.165	0.036	3.442	0.290	3.733
7	0.126	0.186	0.072	0.400	0.384	0.784
8	1.359	0.381	0.105	5.042	1.844	6.886
9	0.064	0.065	0.014	0.420	0.143	0.563
10	0.114	0.147	0.014	0.159	0.275	0.434
11	0.018	0.016	0.008	0.962	0.041	1.003
12	1.415	2.505	2.163	1.598	6.082	7.681
13	0.047	1.428	1.232	2.749	2.707	5.456
14	0.041	0.113	0.011	5.843	0.164	6.007
15	0.018	0.023	0.008	4.350	0.048	4.399
16	0.021	0.225	0.024	1.061	0.271	1.332
17	0.032	0.020	0.011	0.431	0.063	0.494
18	0.014	0.032	0.011	0.759	0.057	0.816
19	0.044	0.084	0.016	1.335	0.145	1.479
20	0.008	0.004	0.003	0.260	0.016	0.276
21	0.026	0.016	0.006	0.086	0.048	0.134
22	7.524	0.573	0.593	1.800	8.690	10.489
23	0.695	0.014	0.003	0.387	0.713	1.100
24	0.056	0.009	0.002	0.234	0.067	0.301
25	0.005	0.010	0.027	0.412	0.041	0.453
26	0.007	0.008	0.022	0.241	0.037	0.278
27	0.037	0.003	0.001	0.037	0.041	0.078
28	0.146	0.031	0.002	0.179	0.180	0.358
29	0.029	0.009	0.001	0.601	0.040	0.641
30	0.490	0.033	0.004	0.152	0.527	0.679
31	0.073	0.031	0.005	0.204	0.109	0.314
32	0.016	-0.003	0.004	0.139	0.017	0.156
33	0.104	0.139	0.009	0.763	0.252	1.015
34	-0.397	0.066	0.064	3.457	-0.267	3.189
35	0.030	0.042	0.041	0.691	0.114	0.804
36	0.125	0.064	0.001	0.551	0.191	0.742
37	0.034	0.180	0.002	0.381	0.217	0.598
38	1.986	0.129	0.095	-0.409	2.210	1.802
39	0.003	-0.014	0.005	0.008	-0.006	0.002
40	-0.007	0.198	0.009	0.035	0.200	0.235
41	0.021	0.192	0.012	0.073	0.225	0.298
42	-0.061	0.456	0.036	-0.011	0.431	0.420
43	0.095	0.108	1.131	0.066	1.335	1.400
44	1.672	0.553	1.033	7.472	3.258	10.730
45	0.010	0.180	0.103	0.361	0.299	0.660
46	0.442	0.076	0.224	1.445	0.742	2.187
47	0.266	0.736	0.265	3.150	1.268	4.418
48	1.658	0.885	0.335	9.392	2.879	12.271
49	12.830	2.638	2.100	3.130	17.575	20.705
50	-3.650	0.965	2.001	1.976	-0.684	1.291
51	-1.404	0.684	-0.450	3.956	-1.170	2.786

/cont..

52	0.321	0.701	-0.598	1.283	0.424	1.707
53	16.839	5.011	6.001	-12.859	27.852	14.993
54	5.647	0.706	0.000	-0.660	6.353	5.693
55	0.538	2.086	1.501	-1.224	4.125	2.901
56	1.063	18.658	5.244	160.899	24.965	185.864
57	-0.555	0.140	-2.031	-14.027	-2.446	-16.473
58	-0.837	-0.754	0.908	6.039	-0.684	5.355
59	-4.500	-0.851	0.529	-13.559	-4.822	-18.381
60	-0.764	-2.996	0.739	-1.722	-3.021	-4.743
61	1.094	-1.987	0.540	10.733	-0.353	10.380
62	-2.387	-0.276	-0.091	19.108	-2.754	16.354
63	-0.586	10.629	0.253	-23.997	10.296	-13.700
64	-0.011	2.453	-0.312	9.591	2.130	11.721
65	-19.135	0.139	-0.539	9.011	-19.535	-10.524
66	12.283	-0.239	-0.184	0.511	11.860	12.371
67	0.644	0.714	-0.266	12.349	1.093	13.443
68	0.777	-0.442	0.117	9.859	0.453	10.311
69	5.649	-0.205	-0.127	-44.195	5.317	-38.878
70	3.658	1.545	-0.115	10.004	5.088	15.092
71	4.295	1.949	37.853	57.258	44.098	101.356
72	5.284	2.011	-22.732	34.297	-15.437	18.860
73	0.640	0.965	-0.232	-14.854	1.372	-13.481
74	0.629	1.267	-0.985	-1.114	0.911	-0.203
75	-0.187	0.439	-0.202	-4.291	0.051	-4.240
76	-1.592	0.244	0.028	-4.145	-1.319	-5.465
77	-6.310	0.413	0.082	-46.445	-5.815	-52.261
78	0.389	-3.673	-0.594	-2.512	-3.878	-6.390
79	-0.744	-0.997	0.879	4.249	-0.862	3.387
80	-4.158	-0.656	-0.823	0.477	-5.637	-5.160
81	-9.901	-2.460	-0.196	9.385	-12.557	-3.172
82	1.314	-0.786	-0.005	6.133	0.523	6.656
83	-0.475	-0.457	0.015	1.336	-0.916	0.420
84	-0.589	-5.590	0.276	1.483	-5.903	-4.420
85	0.438	27.217	0.900	29.544	28.555	58.099
86	0.237	-1.675	0.368	0.975	-1.070	-0.095
87	-0.492	-1.434	0.201	-1.018	-1.725	-2.743
88	-0.523	-0.672	0.132	-2.040	-1.064	-3.104
89	-1.617	-1.590	0.251	5.921	-2.957	2.964
90	0.778	-0.151	-0.099	2.137	0.529	2.666
91	0.530	0.173	-0.262	0.748	0.442	1.189
92	-2.726	0.440	-0.068	2.594	-2.354	0.239
93	1.626	0.780	0.048	0.556	2.454	3.010
94	-1.517	1.324	-0.235	-6.200	-0.428	-6.628
95	-0.188	0.454	0.041	1.744	0.306	2.050
96	-0.788	-0.746	0.285	0.235	-1.249	-1.015
97	0.370	-0.380	0.000	-2.097	-0.010	-2.107
98	-0.640	-0.354	0.082	3.328	-0.912	2.416
99	-0.078	-0.151	0.117	0.476	-0.113	0.364
100	-0.583	0.054	0.187	5.377	-0.342	5.035
101	0.290	0.227	0.133	-3.965	0.650	-3.315
102	-0.603	-0.111	-0.009	0.310	-0.723	-0.413
103	-0.251	-0.213	0.207	0.283	-0.257	0.026

CDIFA.OUT: Output file from the operation of Sedif2.Pas on CDIFA.Dat

I.D	rn7dif	rn8dif	rn9dif	rn10df	smless	smplus
1	0.597	0.056	0.040	1.879	0.692	2.572
2	0.673	0.078	0.044	1.709	0.794	2.504
3	0.667	0.088	0.051	1.618	0.807	2.425
4	0.317	0.026	0.038	0.873	0.381	1.254
5	0.734	0.208	0.189	1.757	1.131	2.888
6	0.208	0.003	0.077	0.501	0.288	0.789
7	0.262	0.009	0.020	0.318	0.291	0.609
8	-0.060	0.016	0.016	-0.017	-0.028	-0.045
9	0.613	-0.826	0.179	0.911	-0.035	0.876
10	0.307	0.065	0.091	0.774	0.462	1.236
11	0.200	0.713	0.121	0.889	1.034	1.923
12	-0.305	-0.109	0.034	-0.115	-0.380	-0.495
13	-0.201	0.016	0.074	-0.297	-0.112	-0.408
14	-0.117	-0.004	0.044	-0.171	-0.077	-0.248
15	-0.173	0.006	0.040	0.099	-0.127	-0.029
16	-0.198	0.009	0.035	0.152	-0.154	-0.002
17	-0.164	0.021	0.015	-2.011	-0.128	-2.139
18	-0.023	-0.010	0.013	0.044	-0.020	0.023
19	0.064	-0.085	0.016	-0.410	-0.005	-0.415
20	-0.091	-0.025	-0.066	-0.333	-0.182	-0.515
21	-0.023	-0.008	-0.015	-0.037	-0.046	-0.083
22	-0.015	-0.012	0.038	-0.134	0.010	-0.124
23	0.046	-0.052	0.025	-0.028	0.019	-0.010
24	0.003	-0.024	0.020	-0.096	-0.000	-0.096
25	-0.087	0.012	-0.176	-0.785	-0.251	-1.036
26	0.006	0.008	0.065	-0.187	0.079	-0.109
27	0.028	-0.010	0.012	-0.327	0.030	-0.297
28	0.020	-0.002	-0.014	-0.382	0.004	-0.379
29	-0.074	0.009	-0.003	-0.426	-0.068	-0.493
30	-0.121	0.017	-0.059	-0.773	-0.163	-0.936
31	-0.001	0.006	-0.014	-0.233	-0.009	-0.243
32	0.019	0.002	-0.022	-0.461	-0.001	-0.462
33	0.005	-0.021	-0.004	-0.097	-0.020	-0.117

14:D:5

CDIFB.OUT: Output file from the operation of Sedif2.Pas on CdifB.Dat

I.D	rn7dif	rn8dif	rn9dif	rn10df	smless	smplus
1	0.228	1.640	0.108	7.043	1.976	9.019
2	0.321	1.858	0.126	6.357	2.306	8.663
3	0.369	1.838	0.144	6.016	2.350	8.366
4	0.110	0.870	0.122	3.254	1.102	4.356
5	0.986	2.225	0.546	7.220	3.757	10.977
6	0.011	0.628	0.222	2.082	0.861	2.943
7	0.039	0.737	0.057	1.192	0.833	2.025
8	0.079	-0.160	0.044	-0.027	-0.037	-0.064
9	-3.970	1.883	0.504	3.794	-1.584	2.210
10	0.307	0.941	0.219	3.239	1.467	4.705
11	3.418	0.608	0.336	3.730	4.363	8.093
12	-0.543	-0.963	0.031	-0.519	-1.474	-1.993
13	0.065	-0.642	0.120	-1.313	-0.458	-1.771
14	-0.026	-0.379	0.084	-0.731	-0.321	-1.052
15	0.024	-0.555	0.048	0.386	-0.483	-0.098
16	-0.234	-0.627	-0.009	0.621	-0.870	-0.249
17	0.660	-0.535	-0.252	-8.282	-0.127	-8.409
18	-0.056	-0.078	-0.025	0.178	-0.159	0.019
19	-0.426	0.184	-0.127	-1.746	-0.369	-2.115
20	-0.139	-0.301	-0.478	-1.418	-0.918	-2.336
21	-0.040	-0.076	-0.104	-0.159	-0.220	-0.378
22	-0.071	-0.057	-0.018	-0.572	-0.146	-0.718
23	-0.265	0.139	-0.067	-0.162	-0.194	-0.356
24	-0.123	0.003	-0.034	-0.376	-0.154	-0.530
25	0.030	-0.287	-0.243	-3.330	-0.501	-3.831
26	0.028	0.013	-0.058	-0.793	-0.017	-0.810
27	-0.060	0.081	-0.023	0.501	-0.003	0.498
28	-0.013	0.057	-0.075	-2.487	-0.031	-2.518
29	0.034	-0.235	-0.055	-1.789	-0.256	-2.045
30	0.076	-0.383	-0.137	-3.214	-0.443	-3.657
31	0.019	-0.004	-0.063	-0.991	-0.048	-1.039
32	0.002	0.055	-0.046	-1.899	0.012	-1.888
33	-0.100	0.015	-0.008	-0.404	-0.092	-0.496

APPENDIX 15

DIFFERENCED SEDIMENT YIELD RATES FOR SIMULATED EVENTS AGAINST GULLY MORPHOLOGY DATA AND CHANGE DATA

A. A LISTING OF THESE DATA FOR : the headwaters, 1975
: the main channel*, 1975
: the large discontinuous tributary, 1975*

in which in this case the regression exponent used in the summer yield calculations is 0.76, the constant 2130

B. THE SAME AS ABOVE, only using the regression exponent in the summer yield calculations of 0.81, the constant of 9132.

*The cross-sectional area change data were difficult to assess in cases where survey positions on subsequent years differed. An interpolated value of the cross-sectional area in 1962 was used for sites where this applied to give a comparison with the 1975 positions. A large version of the plots shown on Figures 8 and 9 were used for this purpose.

Differenced sediment yield rates
for the annual pattern of simulated events
against gully morphology (x-area),
main network above X.
(N.B. last site is 'X')

On this table, n=0.76,k=2130 for summer events.

I.D	x-area in sq m	Winter sedif. in kg/m	Summer sedif. in kg/m	Annual sedif. in kg/m	Summer sedif. in kg/m (+rn10)	Annual sedif. in kg/m (+rn10)
1.0	0.366	1.211	0.127	1.338	0.142	1.353
2.0	6.672	0.895	0.309	1.204	0.464	1.359
3.0	0.410	0.145	0.288	0.433	1.599	1.744
4.0	0.274	1.211	0.072	1.283	0.200	1.411
5.0	1.742	0.001	0.017	0.018	0.137	0.138
6.0	4.002	0.031	0.090	0.121	1.019	1.050
7.0	0.712	0.481	0.119	0.600	0.236	0.717
8.0	0.823	0.057	0.536	0.593	1.914	1.971
9.0	0.732	0.156	0.046	0.202	0.167	0.323
10.0	0.586	0.207	0.086	0.293	0.134	0.341
11.0	1.580	0.001	0.013	0.014	0.285	0.286
12.0	0.823	3.419	1.390	4.809	1.839	5.258
13.0	1.964	0.002	0.449	0.451	1.206	1.208
14.0	0.439	0.272	0.052	0.324	1.607	1.879
15.0	0.932	0.017	0.016	0.033	1.173	1.190
16.0	5.850	0.036	0.080	0.116	0.366	0.402
17.0	1.049	0.106	0.020	0.126	0.144	0.250
18.0	1.343	0.344	0.018	0.362	0.232	0.576
19.0	12.440	0.088	0.045	0.133	0.408	0.496
20.0	8.790	0.035	0.005	0.040	0.078	0.113
21.0	2.477	0.021	0.015	0.036	0.040	0.061
22.0	0.274	0.066	2.329	2.395	2.823	2.889
23.0	2.123	0.590	0.203	0.793	0.311	0.901
24.0	7.442	0.114	0.020	0.134	0.086	0.200
25.0	3.270	0.065	0.013	0.078	0.125	0.190
26.0	9.639	0.015	0.012	0.027	0.078	0.093
27.0	6.978	0.201	0.012	0.213	0.023	0.224
28.0	5.222	0.054	0.052	0.106	0.046	0.100
29.0	2.538	17.350	0.012	17.360	0.167	17.520
30.0	7.174	0.061	0.143	0.204	0.184	0.245
31.0	5.466	0.901	0.031	0.932	0.091	0.992
32.0	0.384	0.134	0.006	0.140	0.039	0.173
33.0	3.630	0.479	0.071	0.550	0.265	0.744
34.0	6.204	0.381	-0.043	0.338	0.826	1.207
35.0	0.732	0.165	0.033	0.198	0.209	0.374
36.0	5.545	0.817	0.053	0.870	0.196	1.013
37.0	1.769	1.050	0.060	1.110	0.154	1.204
38.0	22.380	1.717	0.576	2.293	0.460	2.177
39.0	0.830	0.084	-0.002	0.082	0.000	0.084
40.0	20.080	0.971	0.056	1.027	0.065	1.036
41.0	0.137	0.001	0.062	0.063	0.080	0.081
42.0	11.710	0.470	0.109	0.579	0.125	0.595
43.0	33.120	0.563	0.084	0.647	0.101	0.664
44.0	4.337	4.917	0.846	5.763	2.666	7.583
45.0	6.307	1.482	0.084	1.566	0.177	1.659
46.0	1.415	3.196	0.193	3.389	0.533	3.729
47.0	18.680	4.195	0.341	4.536	1.115	5.310
48.0	75.540	15.390	0.807	16.200	3.021	18.410
49.0	18.390	5.130	4.616	9.746	5.363	10.490
50.0	22.260	19.010	-0.160	18.850	0.320	19.330
51.0	6.125	36.240	-0.290	35.950	0.659	36.900
52.0	43.130	6.940	0.114	7.054	0.401	7.341
53.0	26.870	57.220	8.701	65.920	5.737	62.960
54.0	16.900	7.680	1.453	9.133	1.307	8.987
55.0	33.370	45.200	0.955	46.150	0.692	45.890
56.0	153.300	534.400	5.977	540.400	41.980	576.400

Differenced Sediment yield rates for simulated
events, against gully morphology data & changes,
For main network below X.

On this table, n=0.76, k=2130 for summer events

I.D	x-area in sq.m	x-area change 75-62 in sq.m.	% change on 62	Winter sedif. in kg/m	Summer sedif. in kg/m	Annual sedif. in kg/m	Summer sedif. in kg/m (+rn10)	nnual sedif. in kg/m (+rn10)
57.0	125.400	22.700	22.100	1865.000	-0.613	1864.000	-3.840	1861.000
58.0	30.010	-1.740	-5.480	49.450	-0.127	49.320	1.300	50.750
59.0	19.100	-8.170	-29.960	14.430	-1.166	13.260	-4.179	10.250
60.0	35.330	-4.800	-11.960	63.740	-0.729	63.010	-1.056	62.680
61.0	40.170	4.620	12.990	338.700	-0.068	338.600	2.441	341.100
62.0	35.330	-0.750	-2.080	41.940	-0.625	41.320	3.904	45.840
63.0	30.350	-5.680	-15.770	50.830	2.673	53.500	-2.735	48.090
64.0	35.700	-4.890	-12.040	78.070	0.204	78.270	2.395	80.470
65.0	26.210	-5.200	-16.550	189.900	-4.472	185.400	-2.355	187.500
66.0	31.100	-6.000	-16.170	50.580	2.940	53.520	5.945	56.530
67.0	27.820	17.750	176.300	125.200	0.263	125.500	0.263	125.500
68.0	36.780	8.360	29.410	176.900	0.100	177.000	2.362	179.300
69.0	25.620	3.360	15.090	206.200	1.338	207.500	-8.704	197.500
70.0	29.880	4.450	17.500	308.400	1.253	309.700	3.607	312.000
71.0	37.810	9.760	34.790	152.400	1.335	153.700	14.480	166.900
72.0	37.010	8.900	31.660	75.800	1.928	77.730	9.762	85.560
73.0	35.230	5.000	16.530	2111.000	0.375	2111.000	-2.989	2108.000
74.0	36.760	-3.430	-8.530	21.260	0.267	21.530	0.062	21.320
75.0	29.880	1.750	6.220	37.360	0.024	37.380	-0.959	36.400
76.0	43.040	6.050	16.360	476.100	-0.310	475.800	-1.234	474.900
77.0	28.880	1.900	7.040	13.600	-1.382	12.220	-11.880	1.725
78.0	28.310	6.230	28.210	236.200	-0.936	235.300	-1.414	234.800
79.0	33.190	3.390	11.370	88.980	-0.177	88.800	0.823	89.800
80.0	19.730	2.010	11.340	28.280	-1.403	26.880	-1.260	27.020
81.0	26.310	-0.750	-2.770	83.650	-3.135	80.510	-0.946	82.700

/cont..

Differenced Sediment yield rates for simulated events, against gully morphology data & changes, For main network below X.

On this table, n=0.76, k=2130 for summer events

I.D	x-area in sq.m	x-area change 75-62 in sq.m.	% change on 62	Winter sedif. in kg/m	Summer sedif. in kg/m	Annual sedif. in kg/m	Summer sedif. in kg/m (+rn10)	nnual sedif. in kg/m (+rn10)
57.0	125.400	22.700	22.100	1865.000	-0.613	1864.000	-3.840	1861.000
58.0	30.010	-1.740	-5.480	49.450	-0.127	49.320	1.300	50.750
59.0	19.100	-8.170	-29.960	14.430	-1.166	13.260	-4.179	10.250
60.0	35.330	-4.800	-11.960	63.740	-0.729	63.010	-1.056	62.680
61.0	40.170	4.620	12.990	338.700	-0.068	338.600	2.441	341.100
62.0	35.330	-0.750	-2.080	41.940	-0.625	41.320	3.904	45.840
63.0	30.350	-5.680	-15.770	50.830	2.673	53.500	-2.735	48.090
64.0	35.700	-4.890	-12.040	78.070	0.204	78.270	2.395	80.470
65.0	26.210	-5.200	-16.550	189.900	-4.472	185.400	-2.355	187.500
66.0	31.100	-6.000	-16.170	50.580	2.940	53.520	5.945	56.530
67.0	27.820	17.750	176.300	125.200	0.263	125.500	0.263	125.500
68.0	36.780	8.360	29.410	176.900	0.100	177.000	2.362	179.300
69.0	25.620	3.360	15.090	206.200	1.338	207.500	-8.704	197.500
70.0	29.880	4.450	17.500	308.400	1.253	309.700	3.607	312.000
71.0	37.810	9.760	34.790	152.400	1.335	153.700	14.480	166.900
72.0	37.010	8.900	31.660	75.800	1.928	77.730	9.762	85.560
73.0	35.230	5.000	16.530	2111.000	0.375	2111.000	-2.989	2108.000
74.0	36.760	-3.430	-8.530	21.260	0.267	21.530	0.062	21.320
75.0	29.880	1.750	6.220	37.360	0.024	37.380	-0.959	36.400
76.0	43.040	6.050	16.360	476.100	-0.310	475.800	-1.234	474.900
77.0	28.880	1.900	7.040	13.600	-1.382	12.220	-11.880	1.725
78.0	28.310	6.230	28.210	236.200	-0.936	235.300	-1.414	234.800
79.0	33.190	3.390	11.370	88.980	-0.177	88.800	0.823	89.800
80.0	19.730	2.010	11.340	28.280	-1.403	26.880	-1.260	27.020
81.0	26.310	-0.750	-2.770	83.650	-3.135	80.510	-0.946	82.700

/cont..

82.0	30.810	0.260	0.850	95.030	0.130	95.160	1.551	96.580
83.0	7.910	-0.050	-0.630	509.300	-0.232	509.100	0.081	509.400
84.0	18.280	-13.840	-43.090	1352.000	-1.487	1351.000	-1.166	1351.000
85.0	19.270	-13.730	-41.600	1002.000	7.212	1009.000	13.890	1016.000
86.0	20.870	-2.800	-9.450	542.200	-0.279	541.900	-0.007	542.200
87.0	21.640	-4.910	-18.490	596.900	-0.436	596.500	-0.746	596.200
88.0	28.900	-2.210	-7.100	612.500	-0.272	612.200	-0.777	611.700
89.0	35.890	3.370	10.360	244.800	-0.759	244.000	3.577	245.400
90.0	15.360	-5.770	-27.310	626.400	0.136	626.500	0.632	627.000
91.0	10.620	2.800	35.800	443.500	0.108	443.600	2.285	443.800
92.0	17.970	-14.800	-45.160	443.700	-0.567	443.100	2.027	443.700
93.0	9.510	-11.880	-55.570	86.010	0.625	86.640	0.762	86.770
94.0	8.750	-13.250	-60.220	1.800	-0.088	1.712	-1.530	0.270
95.0	12.140	0.170	1.420	303.900	3.080	301.000	0.490	301.400
96.0	12.520	1.240	10.990	438.100	-0.310	437.800	-0.246	437.900
97.0	7.920	-1.540	-16.270	86.510	0.000	86.510	-0.503	86.010
98.0	26.370	0.760	2.960	37.670	-0.232	37.440	0.549	38.220
99.0	38.190	-6.250	-14.060	48.610	-0.027	48.580	0.091	48.700
100.0	27.320	-1.950	-6.660	58.000	-0.121	57.880	1.091	59.090
101.0	33.830	16.790	98.530	58.590	0.157	58.750	-0.745	57.850
102.0	22.880	3.870	20.350	76.560	-0.156	76.400	-0.088	76.470
103.0	23.890	7.240	43.480	25.210	-0.350	24.860	-0.286	24.920

/cont..

Differenced sediment yield rates for simulated events, against gully morphology data and changes, large discontinuous tributary.

(On this table n=0.76, k=2130 for summer event calculations)

old I.D	x-area in sq m	x-area change 80-75 in sq.m	x-area change 75-62 in sq.m	%change over75 value	%change over62 value	winter sedif in kg/m	summer sedif in kg/m (+rn10)	annual sedif in kg/m (+rn10)	summer sedit in kg/m	annual sedit in kg/m
62.0	1.98	11.47	0.00	580.70	0.00	0.079	2.572	2.651	0.692	0.771
63.0	3.54	1.25	0.09	35.44	2.49	0.135	2.504	2.639	0.794	0.929
64.0	2.83	0.82	0.00	28.87	0.00	0.154	2.425	2.579	0.807	0.961
65.0	2.49	4.24	2.31	170.50	13.14	0.024	1.254	1.278	0.381	0.405
61.0	104.50	17.60	24.62	16.84	30.82	0.607	2.888	3.575	1.131	1.818
218.0	0.92	4.95	0.24	540.10	36.14	0.035	0.789	0.824	0.288	0.323
66.0	13.94	1.46	0.16	10.47	1.16	0.127	0.609	0.736	0.291	0.418
217.0	65.68	4.32	8.07	6.58	14.00	2.867	-0.045	2.822	-0.028	2.839
216.0	55.09	-6.44	-0.12	-11.69	-0.22	2.375	0.876	3.251	-0.035	2.340
215.0	69.92	7.82	44.73	11.18	177.60	2.671	1.236	3.907	0.462	3.133
214.0	33.91	4.97	17.96	14.66	122.70	2.418	1.923	4.341	1.034	3.452
213.0	6.08	0.99	-4.05	16.30	-39.94	0.258	-0.495	-0.237	-0.380	-0.122
212.0	1.64	2.23	-2.33	136.20	-58.65	1.637	-0.408	1.229	-0.112	1.525
211.0	3.31	11.81	0.15	356.90	4.68	1.117	-0.248	0.869	-0.077	1.040
210.0	5.68	6.66	0.67	117.30	13.31	1.279	-0.029	1.250	-0.127	1.152
58.0	22.31	0.98	2.91	31.29	15.00	0.056	-0.002	0.054	-0.154	-0.098
209.0	1.25	14.02	-27.88	881.60	-95.71	8.876	-2.139	6.737	-0.126	8.746
208.0	7.79	27.42	-9.60	352.00	-55.20	3.416	0.023	3.439	-0.020	3.396
207.0	17.19	0.63	29.94	3.66	-63.52	4.244	-0.415	3.829	-0.005	4.239
57.0	42.91	10.06	2.75	37.43	6.85	5.199	-0.515	4.684	-0.182	5.017
206.0	3.04	-0.20	-16.13	-6.54	-84.13	13.410	-0.083	13.330	-0.046	13.370
205.0	8.80	-5.94	-8.58	-67.45	-49.36	7.717	-0.124	7.593	0.010	7.727
204.0	9.90	-3.40	-11.49	-34.31	-53.73	28.490	-0.010	28.480	0.019	28.510
203.0	14.28	-3.49	-19.88	-24.44	-58.20	22.290	-0.096	22.190	0.000	22.290
202.0	20.90	-2.37	-20.05	-11.34	-48.96	44.940	-1.036	43.900	-0.251	44.690
201.0	34.02	1.24	2.77	3.64	8.86	31.130	-0.109	31.020	0.079	31.210
200.0	12.99	3.58	-3.24	27.56	-19.98	39.870	-0.297	39.570	0.030	39.900
199.0	2.45	1.76	0.33	71.56	15.75	55.560	-0.379	55.180	0.004	55.560
198.0	9.34	1.19	3.45	12.76	58.51	69.100	-0.493	68.600	-0.068	69.030
197.0	5.65	0.93	-1.07	16.49	-15.88	19.570	-0.936	18.630	-0.163	19.410
196.0	7.90	-0.50	1.88	-6.34	31.13	25.150	-0.243	24.910	-0.009	25.140
195.0	10.11	6.57	1.80	64.96	21.66	24.740	-0.462	24.280	-0.001	24.710
194.0	2.07	0.16	0.76	8.69	58.32	0.858	-0.117	0.741	-0.020	0.838

Differenced sediment yield rates
for the annual pattern of simulated events
against gully morphology (x-area),
main network above X.
(N.B. last site is 'X')

On this table, n=0.81,k=9132 for summer events.

I.D	x-area in sq m	Winter sedif. in kg/m	Summer sedif. in kg/m	Annual sedif. in kg/m	Summer sedif. in kg/m (+rn10)	Annual sedif. in kg/m (+rn10)
1.0	0.3660	1.2110	0.4160	1.6270	0.9220	2.1330
2.0	6.6720	0.9950	1.0250	1.9200	1.5610	2.4560
3.0	0.4100	0.1450	0.9590	1.1040	5.9160	6.0610
4.0	0.2740	1.2110	0.2300	1.4410	0.6700	1.8810
5.0	1.7420	0.0010	0.0530	0.0540	0.4660	0.4670
6.0	4.0020	0.0310	0.2900	0.3210	3.7330	3.7640
7.0	0.7120	0.4810	0.3840	0.8650	0.7840	1.2650
8.0	0.8230	0.0570	1.8440	1.9010	6.8860	6.9430
9.0	0.7320	0.1560	0.1430	0.2990	0.5630	0.7190
10.0	0.5860	0.2070	0.2750	0.4820	0.4340	0.6410
11.0	1.5800	0.0010	0.0410	0.0420	1.0030	1.0040
12.0	0.8230	3.4190	6.0820	9.5010	7.6810	11.1000
13.0	1.9640	0.0020	2.7070	2.7090	5.4560	5.4580
14.0	0.4390	0.2720	0.1640	0.4360	6.0070	6.2790
15.0	0.9320	0.0170	0.0480	0.0650	4.3990	4.4160
16.0	5.8500	0.0360	0.2710	0.3070	1.3320	1.3680
17.0	1.0490	0.1060	0.0630	0.1690	0.4940	0.6000
18.0	1.3430	0.3440	0.0570	0.4010	0.8160	1.1600
19.0	12.4400	0.0880	0.1450	0.2330	1.4790	1.5670
20.0	8.7900	0.0350	0.0160	0.0510	0.2760	0.3110
21.0	2.4770	0.0210	0.0480	0.0690	0.1340	0.1550
22.0	0.2740	0.0660	8.6900	8.7560	10.4900	10.5500
23.0	2.1230	0.5900	0.7130	1.3030	1.1000	1.6900
24.0	7.4420	0.1140	0.0670	0.1810	0.3010	0.4150
25.0	3.2700	0.0650	0.0410	0.1060	0.4530	0.5180
26.0	9.6390	0.0150	0.0370	0.0520	0.2780	0.2930
27.0	6.9780	0.2010	0.0410	0.2420	0.0780	0.2790
28.0	5.2220	0.0540	0.1800	0.2340	0.3580	0.4120
29.0	2.5380	17.3500	0.0400	17.3900	0.6410	17.9900
30.0	7.1740	0.0610	0.5270	0.5880	0.6790	0.7400
31.0	5.4660	0.9010	0.1090	1.0100	0.3140	1.2150
32.0	0.3840	0.1340	0.0170	0.1510	0.1560	0.2900
33.0	3.6300	0.4790	0.2520	0.7310	1.0150	1.4940
34.0	6.2040	0.3810	-0.2670	0.1140	3.1890	3.5700
35.0	0.7320	0.1650	0.1140	0.2790	0.8040	0.9690
36.0	5.5450	0.8170	0.1910	1.0080	0.7420	1.5590
37.0	1.7690	1.0500	0.2170	1.2670	0.5980	1.6480
38.0	22.3800	1.7170	2.2100	3.9270	1.8020	3.5190
39.0	0.8300	0.0840	-0.0060	0.0780	0.0020	0.0860
40.0	20.0800	0.9710	0.2000	1.1710	0.2350	1.2060
41.0	0.1370	0.0010	0.2250	0.2260	0.2980	0.2990
42.0	11.7100	0.4700	0.4310	0.9010	0.4200	0.8900
43.0	33.1200	0.5630	1.3350	1.8980	1.4000	1.9630
44.0	4.3370	4.9170	3.2580	8.1750	10.7300	15.6500
45.0	6.3070	1.4820	0.2990	1.7810	0.6600	2.1420
46.0	1.4150	3.1960	0.7420	3.9380	2.1870	5.3830
47.0	18.6800	4.1950	1.2680	5.4630	4.4180	8.6130
48.0	75.5400	15.3900	2.8790	18.2700	12.2700	27.6600
49.0	18.3900	5.1300	17.5800	22.7100	20.7000	25.8400
50.0	22.2600	19.0100	-0.6840	18.3300	1.2910	20.3000
51.0	6.1250	36.2400	-1.1700	35.0700	2.7860	39.0300
52.0	43.1300	6.9400	0.4240	7.3640	1.7070	8.6470
53.0	26.8700	57.2200	27.8500	85.0700	14.9900	72.2100
54.0	16.9000	7.6800	6.3530	14.0300	5.6930	13.3700
55.0	33.3700	45.2000	4.1250	49.3200	2.9010	48.1000
56.0	153.3000	534.4000	24.9600	559.4000	185.9000	720.3000

Differenced Sediment yield rates for simulated events, against gully morphology data & changes, For main network below X.

On this table, n=0.81, k=9132 for summer events

newID	x-area in m2	x-area change (75-62)	% change on 62	Winter sedif in kg/m	Summer sedif in kg/m	Annual sedif in kg/m	Summer sedif in kg/m (+rn10)	Annual sedif in kg/m (+rn10)
57.0	125.4000	22.7000	22.1000	1865.0000	-2.4460	1863.0000	-16.4700	1849.0000
58.0	30.0100	-1.7400	-5.4800	49.4500	-0.6840	48.7700	5.3550	54.8000
59.0	19.1000	-8.1700	-29.9600	14.4300	-4.8220	9.6080	-18.3800	-3.9510
60.0	35.3300	-4.8000	-11.9600	63.7400	-3.0210	60.7200	-4.7430	59.0000
61.0	40.1700	4.6200	12.9900	338.7000	-0.3530	338.3000	10.3800	349.1000
62.0	35.3300	-0.7500	-2.0800	41.9400	-2.7540	39.1900	16.3500	58.2900
63.0	30.3500	-5.6800	-15.7700	50.8300	10.3000	61.1300	-13.7000	37.1300
64.0	35.7000	-4.8900	-12.0400	78.0700	2.1300	80.2000	11.7200	89.7900
65.0	26.2100	-5.2000	-16.5500	189.9000	-19.5400	170.4000	-10.5200	179.4000
66.0	31.1000	-6.0000	-16.1700	50.5800	11.8600	62.4400	12.3700	62.9500
67.0	27.8200	17.7500	176.3000	125.2000	1.0930	126.3000	13.4400	138.6000
68.0	36.7800	8.3600	29.4100	176.9000	0.4530	177.4000	10.3100	187.2000
69.0	25.6200	3.3600	15.0900	206.2000	5.3170	211.5000	-38.8800	167.3000
70.0	29.8800	4.4500	17.5000	308.4000	5.0880	313.5000	15.0900	323.5000
71.0	37.8100	9.7600	34.7900	152.4000	44.1000	196.5000	101.4000	253.8000
72.0	37.0100	8.9000	31.6600	75.8000	-15.4400	60.3600	18.8600	94.6600
73.0	35.2300	5.0000	16.5300	2111.0000	1.3720	2112.0000	-13.4800	2098.0000
74.0	36.7600	-3.4300	-8.5300	21.2600	0.9110	22.1700	-0.2070	21.0600
75.0	29.8800	1.7500	6.2200	37.3600	0.0510	37.4100	-4.2400	33.1200
76.0	43.0400	6.0500	16.3600	476.1000	-1.3190	474.8000	-5.4650	470.6000
77.0	28.8800	1.9000	7.0400	13.6000	-5.8150	7.7850	-52.2600	-38.6600
78.0	28.3100	6.2300	28.2100	236.2000	-3.8780	232.3000	-6.3900	229.8000

/cont..

81.0	26.3100	-0.7500	-2.7700	83.6500	-12.5600	71.0900	-3.1720	80.4800	
82.0	30.8100	0.2600	0.8500	95.0300	0.5230	95.5500	6.6560	101.7000	
83.0	7.9100	-0.0500	-0.6300	509.3000	-0.9160	508.4000	0.4200	509.7000	
84.0	18.2800	-13.8400	-43.0900	1352.0000	-5.9030	1346.0000	-4.4200	1348.0000	
85.0	19.2700	-13.7300	-41.6000	1002.0000	28.5600	1031.0000	58.1000	1060.0000	
86.0	20.8700	-2.8000	-9.4500	542.2000	-1.0700	541.1000	-0.0950	542.1000	
87.0	21.6400	-4.9100	-18.4900	596.9000	-1.7250	595.2000	-2.7430	594.2000	
88.0	28.9000	-2.2100	-7.1000	612.5000	-1.0640	611.4000	-3.1040	609.4300	
89.0	35.8900	3.3700	10.3600	244.8000	-2.9570	241.8000	2.9640	247.8000	
90.0	15.3600	-5.1700	-27.3100	626.4000	0.5290	626.9000	2.6660	629.1000	
91.0	10.6200	2.8000	35.8000	443.5000	0.4420	443.9000	1.1890	444.7000	
92.0	17.9700	-14.8000	-45.1600	443.7000	-2.3540	441.3000	0.2390	443.9000	
93.0	9.5100	-11.8800	-55.5700	86.0100	2.4540	88.4600	3.0100	89.0200	
94.0	8.7500	-13.2500	-60.2200	1.8000	-0.4280	1.3720	-6.6280	-4.8280	
95.0	12.1400	0.1700	1.4200	300.9000	0.3060	301.2000	2.0500	303.0000	
96.0	12.5200	1.2400	10.9900	438.1000	-1.2490	436.9000	-1.0150	437.1000	
97.0	7.9200	-1.5400	-16.2700	86.5100	-0.0100	86.5000	-2.1070	84.4000	
98.0	26.3700	0.7600	2.9600	37.6700	-0.9120	36.7600	2.4160	40.0900	
99.0	38.1900	-6.2500	-14.0600	48.6100	-0.1130	48.5000	0.3640	48.9700	
100.0	27.3200	-1.9500	-6.6600	58.0000	-0.3420	57.6600	5.0350	63.0300	
101.0	33.8300	16.7900	98.5300	58.5900	0.6500	59.2400	-3.3150	55.2800	
102.0	22.8800	3.8700	20.3500	76.5600	-0.7230	75.8400	-0.4130	76.1500	
103.0	23.3900	7.2400	43.4800	25.2100	-0.2570	24.9500	0.0260	25.2400	

/cont..

79.0	33.1900	3.3900	11.3700	88.9800	-0.8620	88.1200	3.3870	92.3700	
80.0	19.7320	2.0100	11.3400	28.2800	-5.6370	22.6400	-5.1600	23.1200	
81.0	26.3100	-0.7500	-2.7700	83.6500	-12.5600	71.0900	-3.1720	80.4800	
82.0	30.8100	0.2600	0.8500	95.0300	0.5230	95.5500	6.6560	101.7000	
83.0	7.9100	-0.0500	-0.6300	509.3000	-0.9160	508.4000	0.4200	509.7000	
84.0	18.2800	-13.8400	-43.0900	1352.0000	-5.9030	1346.0000	-4.4200	1348.0000	
85.0	19.2700	-13.7300	-41.6000	1002.0000	28.5600	1031.0000	58.1000	1060.0000	
86.0	20.8700	-2.8000	-9.4500	542.2000	-1.0700	541.1000	-0.0950	542.1000	
87.0	21.6400	-4.9100	-18.4900	596.9000	-1.7250	595.2000	-2.7430	594.2000	
88.0	28.9000	-2.2100	-7.1000	612.5000	-1.0640	611.4000	-3.1040	609.4300	
89.0	35.8900	3.3700	10.3600	244.8000	-2.9570	241.8000	2.9640	247.8000	
90.0	15.3600	-5.1700	-27.3100	626.4000	0.5290	626.9000	2.6660	629.1000	
91.0	10.6200	2.8000	35.8000	443.5000	0.4420	443.9000	1.1890	444.7000	
92.0	17.9700	-14.8000	-45.1600	443.7000	-2.3540	441.3000	0.2390	443.9000	
93.0	9.5100	-11.8800	-55.5700	86.0100	2.4540	88.4600	3.0100	89.0200	
94.0	8.7500	-13.2500	-60.2200	1.8000	-0.4280	1.3720	-6.6280	-4.8280	
95.0	12.1400	0.1700	1.4200	300.9000	0.3060	301.2000	2.0500	303.0000	
96.0	12.5200	1.2400	10.9900	438.1000	-1.2490	436.9000	-1.0150	437.1000	
97.0	7.9200	-1.5400	-16.2700	86.5100	-0.0100	86.5000	-2.1070	84.4000	
98.0	26.3700	0.7600	2.9600	37.6700	-0.9120	36.7600	2.4160	40.0900	
99.0	38.1900	-6.2500	-14.0600	48.6100	-0.1130	48.5000	0.3640	48.9700	
100.0	27.3200	-1.9500	-6.6600	58.0000	-0.3420	57.6600	5.0350	63.0300	
101.0	33.8300	16.7900	98.5300	58.5900	0.6500	59.2400	-3.3150	55.2800	
102.0	22.8800	3.8700	20.3500	76.5600	-0.7230	75.8400	-0.4130	76.1500	
103.0	23.3900	7.2400	43.4800	25.2100	-0.2570	24.9500	0.0260	25.2400	

Differenced sediment yield rates for simulated
events, against gully morphology data and changes,
large discontinuous tributary.

(On this table, n=0.81, k=9132 for summer event calculations)

old I.D	x-area in sq m	x-area change 80-75 in sq.m	x-area change 75-62 in sq.m	%change over75 value	%change over62 value	winter sedif in kg/m	summer sedif in kg/m (+rn10)	annual sedif in kg/m (+rn10)	summer sedif in kg/m	annual sedif in kg/m
62.0	1.98	11.47	0.00	580.70	0.00	0.079	9.019	9.098	1.976	2.055
63.0	3.54	1.25	0.09	35.44	2.49	0.135	8.663	8.798	2.306	2.441
64.0	2.83	0.82	0.00	28.87	0.00	0.154	8.366	8.520	2.350	2.504
65.0	2.49	4.24	2.31	170.50	13.14	0.024	4.356	4.380	1.102	1.126
61.0	104.50	17.00	24.62	16.84	30.82	0.687	10.980	11.670	3.757	4.444
218.0	0.92	4.95	0.24	540.10	36.14	0.035	2.943	2.978	0.861	0.896
66.0	13.94	1.46	0.16	10.47	1.16	0.127	2.025	2.152	0.833	0.960
217.0	65.68	4.32	8.07	6.58	14.00	2.867	-0.064	2.803	-0.037	2.830
216.0	55.09	-6.44	-0.12	-11.69	-0.22	2.375	2.210	4.585	-1.584	0.791
215.0	69.92	7.82	44.73	11.18	177.60	2.671	4.705	7.376	1.467	4.138
214.0	33.91	4.97	17.96	14.66	122.70	2.418	8.093	10.510	4.363	6.781
213.0	6.08	0.99	-4.05	16.30	-39.94	0.258	-1.993	-1.735	-1.474	-1.216
212.0	1.64	2.23	-2.33	136.20	-58.65	1.637	-1.771	-0.134	-0.458	1.179
211.0	3.31	11.81	0.15	356.90	4.68	1.117	-1.052	0.065	-0.321	0.796
210.0	5.68	6.66	0.67	117.30	13.31	1.279	-0.098	1.181	-0.483	0.796
58.0	22.31	6.98	2.91	31.29	15.00	0.056	-0.249	-0.193	-0.870	-0.814
209.0	1.25	11.02	-27.88	881.60	-95.71	8.876	-8.409	0.467	-0.127	8.749
208.0	7.79	27.42	-9.60	352.00	-55.20	3.416	0.019	3.435	-0.159	3.257
207.0	17.19	0.63	29.94	3.66	-63.52	4.244	-2.115	2.129	-0.369	3.875
57.0	42.91	16.06	2.75	37.43	6.85	5.199	-2.336	2.863	-0.918	4.281
206.0	3.04	-0.20	-16.13	-6.54	-84.13	13.410	-0.378	13.030	-0.220	13.190
205.0	8.80	-5.94	-8.58	-67.45	-49.36	7.717	-0.718	6.999	-0.146	7.571
204.0	9.90	-3.40	-11.49	-34.31	-53.73	28.490	-0.356	28.130	-0.194	28.300
203.0	14.28	-3.49	-19.88	-24.44	-58.20	22.290	-0.530	21.760	-0.154	22.140
202.0	20.90	-2.37	-20.05	-11.34	-48.96	44.940	-3.831	41.110	-0.501	44.440
201.0	34.02	1.24	2.77	3.64	8.86	31.130	-0.810	30.320	-0.017	31.110
200.0	12.99	3.58	-3.24	27.56	-19.98	39.870	0.498	40.370	-0.003	39.860
199.0	2.45	1.76	0.33	71.56	15.75	55.560	-2.518	53.040	-0.031	55.530
198.0	9.34	1.19	3.45	12.76	58.51	69.100	-2.045	67.050	-0.256	68.840
197.0	5.65	0.93	-1.07	16.49	-15.88	19.570	-3.657	15.910	-0.443	19.130
196.0	7.90	-0.50	1.88	-6.34	31.13	25.150	-1.039	24.110	-0.048	25.100
195.0	10.11	6.57	1.80	64.96	21.66	24.740	-1.888	22.860	0.012	24.760
194.0	2.07	0.18	0.76	8.69	58.32	0.858	-0.496	0.362	-0.092	0.766

15:B:4

Differenced sediment yield rates for simulated
events, against gully morphology data and changes,
large discontinuous tributary.

(On this table, n=0.81, k=9132 for summer event calculations)

old I.D	x-area in sq m	x-area change 80-75 in sq.m	x-area change 75-62 in sq.m	%change over75 value	%change over62 value	winter sedif in kg/m	summer sedif in kg/m (+rn10)	annual sedif in kg/m (+rn10)	summer sedif in kg/m	annual sedif in kg/m
62.0	1.98	11.47	0.00	580.70	0.00	0.079	9.019	9.098	1.976	2.055
63.0	3.54	1.25	0.09	35.44	2.49	0.135	8.663	8.798	2.306	2.441
64.0	2.83	0.82	0.00	28.87	0.00	0.154	8.366	8.520	2.350	2.504
65.0	2.49	4.24	2.31	170.50	13.14	0.024	4.356	4.380	1.102	1.126
61.0	104.50	17.00	24.62	16.84	30.82	0.687	10.980	11.670	3.757	4.444
218.0	0.92	4.95	0.24	540.10	36.14	0.035	2.943	2.978	0.861	0.896
66.0	13.94	1.46	0.16	10.47	1.16	0.127	2.025	2.152	0.833	0.960
217.0	65.68	4.32	8.07	6.58	14.00	2.867	-0.064	2.803	-0.037	2.830
216.0	55.09	-6.44	-0.12	-11.69	-0.22	2.375	2.210	4.585	-1.584	0.791
215.0	69.92	7.82	44.73	11.18	177.60	2.671	4.705	7.376	1.467	4.138
214.0	33.91	4.97	17.96	14.66	122.70	2.418	8.093	10.510	4.363	6.781
213.0	6.08	0.99	-4.05	16.30	-39.94	0.258	-1.993	-1.735	-1.474	-1.216
212.0	1.64	2.23	-2.33	136.20	-58.65	1.637	-1.771	-0.134	-0.458	1.179
211.0	3.31	11.81	0.15	356.90	4.68	1.117	-1.052	0.065	-0.321	0.796
210.0	5.68	6.66	0.67	117.30	13.31	1.279	-0.098	1.181	-0.483	0.796
58.0	22.31	6.98	2.91	31.29	15.00	0.056	-0.249	-0.193	-0.870	-0.814
209.0	1.25	11.02	-27.88	881.60	-95.71	8.876	-8.409	0.467	-0.127	0.749
208.0	7.79	27.42	-9.60	352.00	-55.20	3.416	0.019	3.435	-0.159	3.257
207.0	17.19	0.63	29.94	3.66	-63.52	4.244	-2.115	2.129	-0.369	3.875
57.0	42.91	16.06	2.75	37.43	6.85	5.199	-2.336	2.863	-0.918	4.281
206.0	3.04	-0.20	-16.13	-6.54	-84.13	13.410	-0.378	13.030	-0.220	13.190
205.0	8.80	-5.94	-8.58	-67.45	-49.36	7.717	-0.718	6.999	-0.146	7.571
204.0	9.90	-3.40	-11.49	-34.31	-53.73	28.490	-0.356	28.130	-0.194	28.300
203.0	14.28	-3.49	-19.88	-24.44	-58.20	22.290	-0.530	21.760	-0.154	22.140
202.0	20.90	-2.37	-20.05	-11.34	-48.96	44.940	-3.831	41.110	-0.501	44.440
201.0	34.02	1.24	2.77	3.64	8.86	31.130	-0.810	30.320	-0.017	31.110
200.0	12.99	3.58	-3.24	27.56	-19.98	39.870	0.498	40.370	-0.003	39.867
199.0	2.45	1.76	0.33	71.56	15.75	55.560	-2.518	53.040	-0.031	55.530
198.0	9.34	1.19	3.45	12.76	58.51	69.100	-2.045	67.050	-0.256	68.840
197.0	5.65	0.93	-1.07	16.49	-15.88	19.570	-3.657	15.910	-0.443	19.130
196.0	7.90	-0.50	1.88	-6.34	31.13	25.150	-1.039	24.110	-0.048	25.100
195.0	10.11	6.57	1.80	64.96	21.66	24.740	-1.888	22.860	0.012	24.760
194.0	2.07	0.18	0.76	8.69	58.32	0.858	-0.496	0.362	-0.092	0.766

15:B:4

APPENDIX 16

STREAM POWER INDECES AGAINST GULLY MORPHOLOGY

Data used toconduct the analyses discussed in Chapter 6

A. DATA LISTED FOR

: Network sites

: Large discontinuous tributary sites

INDEX of STREAM POWER of PEAK FLOWS, QS.

As an index of stream power(ρgQS), since ρg is a constant then the percentage slope multplied by the peak discharge Q can be used. The values here of QS are calculated on that basis but should actually be multiplied by 9.81 (981 x 0.01) for units of Joules / sec.

Old ID	x-area	% slope,S	QS,melt	QS, rnu
17.0000	0.3660	25.2000	0.0389	0.5544
34.0000	6.6720	23.0000	0.0239	0.5060
1[illegible].0000	0.4104	27.4000	0.0164	3.0960
16.0000	0.2736	12.0000	0.0185	0.2520
31.0000	1.7420	21.4000	0.0013	0.4494
41.0000	4.0020	22.5000	0.0021	1.5530
18.0000	0.7128	22.5000	0.0227	0.4275
14.0000	0.8235	26.1000	0.0099	1.6440
28.0000	0.7320	33.1000	0.0177	0.6951
38.0000	0.5856	28.0000	0.0150	0.2800
32.0000	1.5800	27.4000	0.0017	0.8494
22.0000	0.8235	28.0000	0.0696	1.0360
21.0000	1.9640	29.7000	0.0028	1.5440
29.0000	0.4392	34.9000	0.0242	3.1760
30.0000	0.9316	34.9000	0.0088	3.1760
49.0000	5.8500	29.7000	0.0149	2.1680
53.0000	1.0490	27.4000	0.0190	0.5480
54.0000	1.3430	30.3000	0.0353	0.9999
42.0000	12.4400	24.7000	0.0047	1.4820
56.0000	8.7900	44.9000	0.0311	1.4820
39.0000	2.4770	32.0000	0.0070	0.6720
20.0000	0.2745	19.3000	0.0085	1.2160
27.0000	2.1230	33.7000	0.0605	1.3820
55.0000	7.4420	30.8000	0.0397	0.9548
45.0000	3.2700	26.9000	0.0245	1.3720
46.0000	9.6390	31.4000	0.0158	1.3190
40.0000	6.9780	27.4000	0.0267	0.5206
33.0000	5.2220	33.1000	0.0469	0.5958
8.0000	2.5380	30.8000	0.5127	4.6510
13.0000	7.1740	19.3000	0.0219	1.3700
15.0000	5.4660	39.2000	0.2406	3.1750
48.0000	0.3843	10.0000	0.0167	1.1600
52.0000	3.6300	18.2000	0.0882	2.5300
19.0000	0.2040	29.7000	0.1309	9.2660
44.0000	0.7320	14.1000	0.0293	1.7630
37.0000	5.5450	20.4000	0.0668	2.5500
26.0000	1.7690	13.1000	0.0841	1.9780
12.0000	22.3800	25.3000	0.2086	4.6300
47.0000	0.8296	20.4000	0.0417	2.3870
36.0000	20.6800	29.1000	0.1227	3.6960
51.0000	0.1368	11.0000	0.0533	1.5730
25.0000	11.7100	28.0000	0.2044	4.5080
35.0000	33.1200	32.8000	0.1445	4.2640
11.0000	4.3370	30.3000	0.4243	13.7000
50.0000	6.3070	6.0000	0.0379	0.7800
9.0000	1.4150	41.0000	0.6464	18.0800
43.0000	18.0800	28.4000	0.3271	8.7190

/cont..

/cont..

24.0000	75.5400	31.4000	0.7915	22.6100
7.0000	0.1250	28.6000	0.9774	13.1600
23.0000	43.1300	10.0000	0.2845	7.2900
6.0000	153.3000	10.8000	1.0710	13.6900
100.0000	14.9000	24.1000	0.6447	17.4000
101.0000	18.2500	32.5000	0.8898	23.5300
102.0000	24.4900	23.3000	0.6746	17.0100
103.0000	15.2200	34.1000	1.0190	24.9600
104.0000	30.5700	36.5000	1.1030	26.7500
105.0000	122.7000	26.1000	3.3430	32.7000
106.0000	31.7500	24.1000	3.0940	30.0500
107.0000	27.2700	20.9000	2.6840	25.9400
108.0000	40.1300	28.4000	3.6460	34.9600
109.0000	44.7900	21.3000	2.7950	26.1600
110.0000	36.0800	22.1000	2.9070	26.9600
111.0000	36.0100	25.3000	3.3280	30.8400
112.0000	40.5900	24.1000	3.1850	29.2300
113.0000	31.4100	20.0000	2.6620	24.0200
114.0000	37.1000	21.1000	2.8220	23.5700
115.0000	10.0700	19.7000	2.6350	22.2000
116.0000	28.4200	19.0000	2.5650	21.7700
117.0000	22.2600	15.9000	2.1570	18.3200
118.0000	25.4300	16.6000	2.2670	19.2400
119.0000	28.0500	18.3000	2.5050	21.2800
120.0000	28.1100	20.7000	2.8400	24.2800
121.0000	30.2300	21.5000	3.8230	24.2300
122.0000	40.1900	25.0000	4.4450	27.7800
123.0000	28.1300	18.3000	3.2600	19.7800
124.0000	36.9900	14.9000	2.6630	15.4700
125.0000	26.9800	14.5000	2.5920	15.0100
126.0000	22.0800	13.7000	2.4530	14.1700
127.0000	29.8000	13.0000	2.3320	13.4400
128.0000	17.7200	11.0000	1.9730	11.3700
129.0000	27.0600	12.1000	2.1700	12.5100
130.0000	30.5500	12.0000	2.1600	12.4100
131.0000	7.9620	30.0000	5.7680	30.9900
132.0000	32.1200	7.9000	1.7010	8.1530
133.0000	33.0000	35.1000	7.6440	36.2200
134.0000	23.0500	27.3000	5.9800	28.1700
135.0000	26.5500	7.5000	1.6690	7.7330
136.0000	31.1100	6.3000	1.4410	6.4950
137.0000	32.5200	7.9000	1.8170	8.1530
138.0000	9.5890	8.3000	1.9930	8.6240
139.0000	7.8290	9.2000	2.2730	9.5770
140.0000	3.7790	9.0000	2.2690	9.4230
141.0000	7.6290	11.2000	2.8300	11.7800
142.0000	5.5000	10.1000	2.5520	10.6700
143.0000	11.9700	10.0000	2.5620	10.5700
144.0000	11.2800	5.7000	1.4800	6.0360
145.0000	6.3790	6.8000	1.7720	7.2150
146.0000	25.6100	25.1000	6.5480	26.6300
147.0000	44.4400	32.8000	8.5670	34.8000
148.0000	29.2700	22.9000	5.9890	24.3200
149.0000	17.0400	20.0000	5.2430	21.2400
150.0000	10.0100	11.0000	2.8910	11.6800
151.0000	16.6500	13.9000	3.6570	14.7800

POWERC.DAT : Listing of data used in the Charter G regressions. In the table slope is as a percentage.

Large Discontinuous Tributary Data.

oldID	x-area m2	x-area change 80-75 m2	x-area change 75-62 m2	%x-area change 80-75	%x-area change 75-62	%slope G	Q peak (melt)	Q peak (rnlo)	QB (melt)	QB (rnlo)
62.0	1.98	11.47	0.00	580.70	0.00	27.400	0.003	0.000	0.000	2.713
63.0	3.54	1.25	0.09	35.44	2.48	30.500	0.006	0.005	0.242	3.273
64.0	2.03	0.02	0.00	20.07	0.00	17.700	0.000	0.002	0.041	1.434
65.0	2.49	4.24	2.31	170.50	13.14	13.100	0.003	0.002	0.041	1.374
61.0	104.50	17.60	24.62	16.84	30.82	24.000	0.038	0.446	0.908	10.700
218.0	0.02	4.95	0.24	540.10	36.14	17.000	0.044	0.451	0.749	7.667
66.0	13.04	1.46	0.16	10.47	1.16	25.200	0.006	0.093	0.158	2.344
217.0	65.68	4.32	8.07	6.58	14.00	8.000	0.047	0.463	0.378	3.704
216.0	55.09	-6.44	-0.12	-11.69	-0.22	8.000	0.053	0.477	0.321	2.882
215.0	68.92	7.82	44.73	11.18	177.80	7.000	0.063	0.488	0.441	3.416
214.0	33.91	4.87	17.96	14.66	122.70	4.800	0.072	0.501	0.347	2.405
213.0	8.08	0.99	-4.05	16.30	-39.94	3.300	0.078	0.485	0.280	1.801
212.0	1.64	2.23	-2.33	136.20	-58.65	3.000	0.085	0.473	0.255	1.418
211.0	3.31	11.81	0.15	358.80	4.68	9.800	0.088	0.458	0.883	4.488
210.0	5.60	8.66	0.67	117.30	13.31	58.500	0.091	0.455	5.339	28.820
58.0	22.31	8.98	2.81	31.28	15.00	40.400	0.091	0.453	3.887	18.300
209.0	1.25	11.02	-27.88	881.60	-95.71	40.000	0.101	0.477	4.028	19.080
208.0	7.78	27.42	-9.60	352.00	-55.20	32.000	0.113	0.443	3.825	14.180
207.0	17.18	0.63	29.84	3.66	-63.52	47.000	0.118	0.424	5.473	19.930
57.0	42.91	16.06	2.75	37.43	6.85	17.200	0.120	0.433	2.057	7.448
206.0	3.04	-0.20	-16.13	-6.54	-84.13	18.000	0.173	0.429	3.116	7.722
205.0	8.80	-5.84	-8.58	-67.45	-49.38	22.000	0.182	0.425	4.018	9.350
204.0	9.90	-3.40	-11.48	-34.31	-53.73	17.000	0.208	0.421	3.531	7.157
203.0	14.28	-3.48	-19.88	-24.44	-58.20	20.000	0.233	0.417	4.658	8.340
202.0	20.80	-2.37	-20.05	-11.34	-48.86	18.000	0.248	0.414	4.664	7.866
201.0	34.02	1.24	2.77	3.64	8.86	20.000	0.274	0.410	5.476	8.200
200.0	12.98	3.58	-3.24	27.56	-19.88	14.000	0.296	0.408	4.141	5.684
199.0	2.45	1.78	0.33	71.58	15.75	13.000	0.359	0.402	4.664	5.228
198.0	2.34	1.19	1.45	12.76	58.51	14.000	0.378	0.398	5.287	5.572
197.0	5.65	0.93	1.07	16.49	15.88	17.000	0.384	0.389	6.527	6.613
196.0	7.20	0.50	1.88	6.34	11.13	6.500	0.396	0.376	2.577	2.444
195.0	10.11	6.57	1.80	64.96	21.66	6.300	0.406	0.376	2.558	2.331
194.0	[illegible]	0.18	[illegible]	8.69	[illegible]	10.000	[illegible]	[illegible]	[illegible]	[illegible]

POWERC.DAT : Listing of data used in the Chapter 6 regressions. In the table slope is as a percentage.

Large Discontinuous Tributary Data.

oldID	x-area m2	x-area change 80-75 m2	x-area change 75-62 m2	%x-area change 80-75	%x-area change 75-62	%slope S	Q peak (melt)	Q peak (rn10)	QS (melt)	QS (rn10)
62.0	1.98	11.47	0.00	580.70	0.00	27.400	0.003	0.099	0.086	2.713
63.0	3.54	1.25	0.09	35.44	2.49	38.500	0.006	0.085	0.242	3.273
64.0	2.83	0.82	0.00	28.87	0.00	17.700	0.006	0.082	0.111	1.451
65.0	2.49	4.24	2.31	170.50	13.14	13.100	0.003	0.082	0.041	1.074
61.0	104.50	17.60	24.62	16.84	30.82	24.000	0.038	0.446	0.906	10.700
218.0	0.92	4.95	0.24	540.10	36.14	17.000	0.044	0.451	0.749	7.667
66.0	13.94	1.46	0.16	10.47	1.16	25.200	0.006	0.093	0.159	2.344
217.0	65.68	4.32	8.07	6.58	14.00	8.000	0.047	0.463	0.378	3.704
216.0	55.09	-6.44	-0.12	-11.69	-0.22	6.000	0.053	0.477	0.321	2.862
215.0	69.92	7.82	44.73	11.18	177.60	7.000	0.063	0.488	0.441	3.416
214.0	33.91	4.97	17.96	14.66	122.70	4.800	0.072	0.501	0.347	2.405
213.0	6.08	0.99	-4.05	16.30	-39.94	3.300	0.079	0.485	0.260	1.601
212.0	1.64	2.23	-2.33	136.20	-58.65	3.000	0.085	0.473	0.255	1.419
211.0	3.31	11.81	0.15	356.90	4.68	9.800	0.088	0.458	0.863	4.488
210.0	5.68	6.66	0.67	117.30	13.31	58.500	0.091	0.455	5.339	26.620
58.0	22.31	6.98	2.91	31.29	15.00	40.400	0.091	0.453	3.687	18.300
209.0	1.25	11.02	-27.88	881.60	-95.71	40.000	0.101	0.477	4.028	19.080
208.0	7.79	27.42	-9.60	352.00	-55.20	32.000	0.113	0.443	3.625	14.180
207.0	17.19	0.63	29.94	3.66	-63.52	47.000	0.116	0.424	5.473	19.930
57.0	42.91	16.06	2.75	37.43	6.85	17.200	0.120	0.433	2.057	7.448
206.0	3.04	-0.20	-16.13	-6.54	-84.13	18.000	0.173	0.429	3.116	7.722
205.0	8.80	-5.94	-8.58	-67.45	-49.36	22.000	0.182	0.425	4.016	9.350
204.0	9.90	-3.40	-11.49	-34.31	-53.73	17.000	0.208	0.421	3.531	7.157
203.0	14.28	-3.49	-19.88	-24.44	-58.20	20.000	0.233	0.417	4.658	8.340
202.0	20.90	-2.37	-20.05	-11.34	-48.96	19.000	0.246	0.414	4.664	7.866
201.0	34.02	1.24	2.77	3.64	8.86	20.000	0.274	0.410	5.476	8.200
200.0	12.99	3.58	-3.24	27.56	-19.98	14.000	0.296	0.406	4.141	5.684
199.0	2.45	1.76	0.33	71.56	15.75	13.000	0.359	0.402	4.664	5.226
198.0	9.34	1.19	3.45	12.76	58.51	14.000	0.378	0.398	5.287	5.572
197.0	5.65	0.93	-1.07	16.49	-15.88	17.000	0.384	0.389	6.527	6.613
196.0	7.90	-0.50	1.88	-6.34	31.13	6.500	0.396	0.376	2.577	2.444
195.0	10.11	6.57	1.80	64.96	21.66	6.300	0.406	0.370	2.558	2.331
194.0	9.07	0.18	0.76	8.69	38.32	10.000	0.406	0.364	4.060	3.640

Figure 4 : Vegetation cover and infiltration survey sample locations


2560
2530
2499
2469

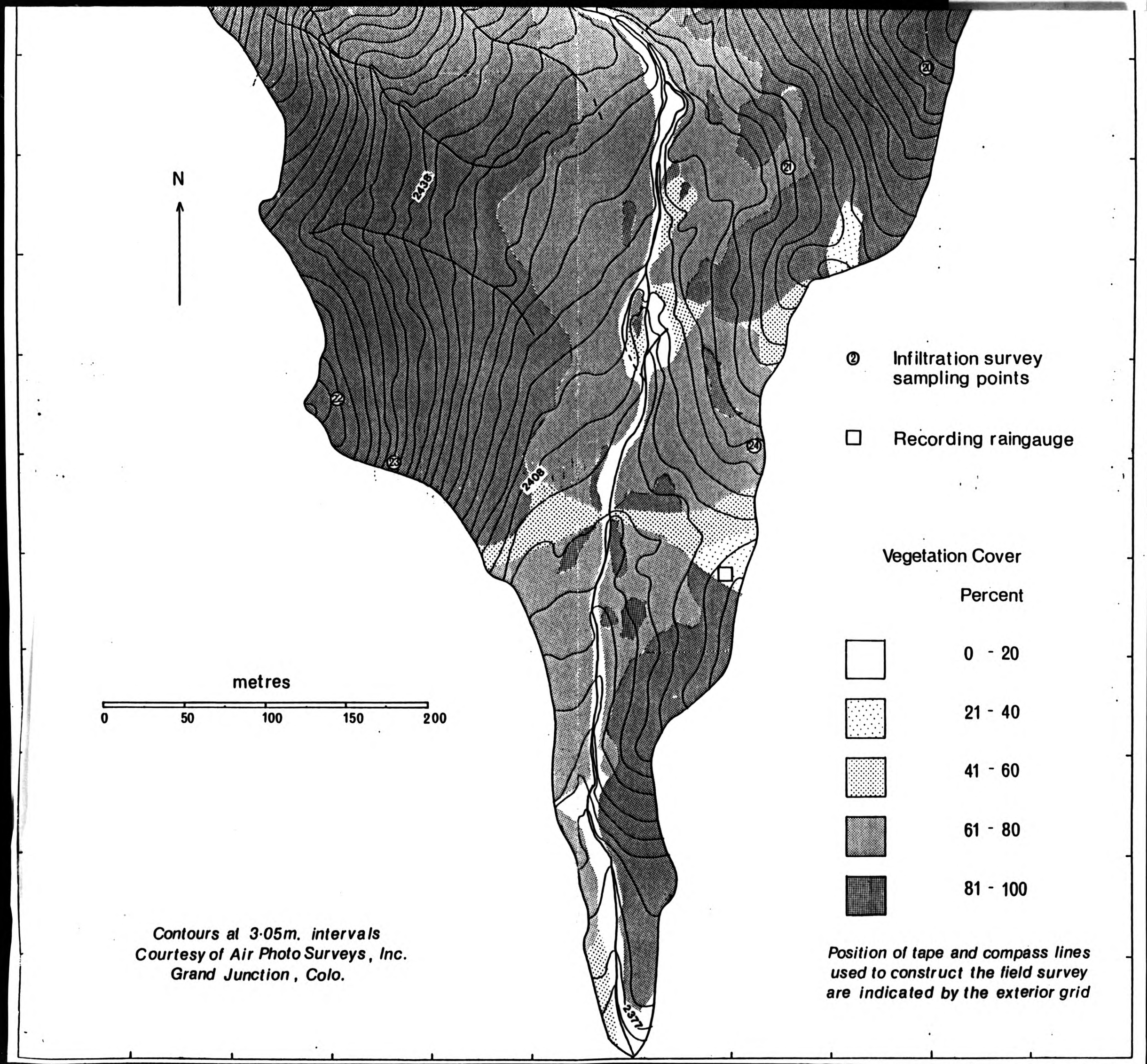

Contours at 3·05m. intervals
Courtesy of Air Photo Surveys, Inc.
Grand Junction, Colo.

Position of tape and compass lines used to construct the field survey are indicated by the exterior grid

Figure 7 : Field survey site locations, and division of watershed into contributing units between survey sites

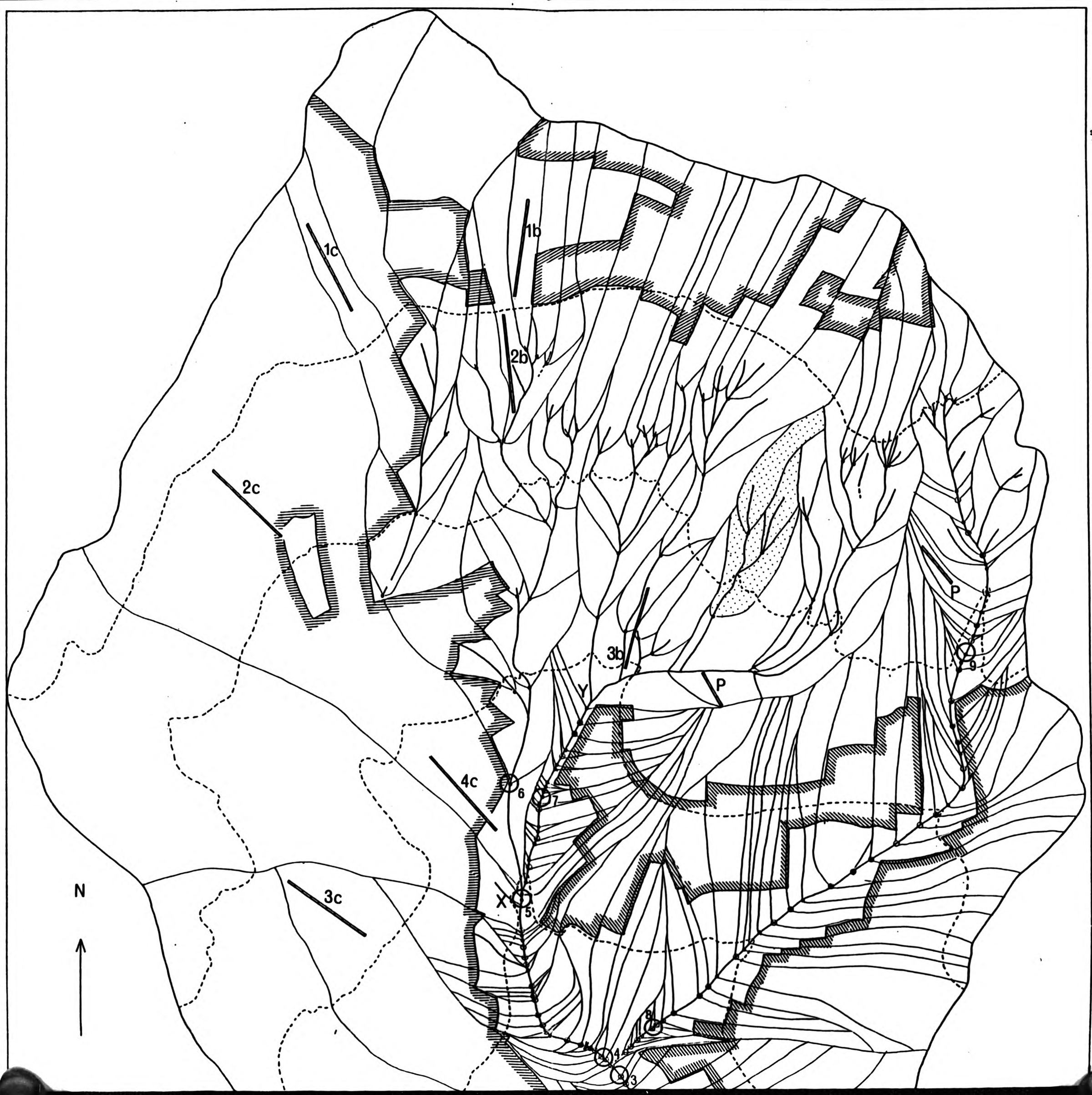
1c
1b
2b
2c
3b
P
Y
P
9
4c
6
7
X
5
3c
N
8
4
3

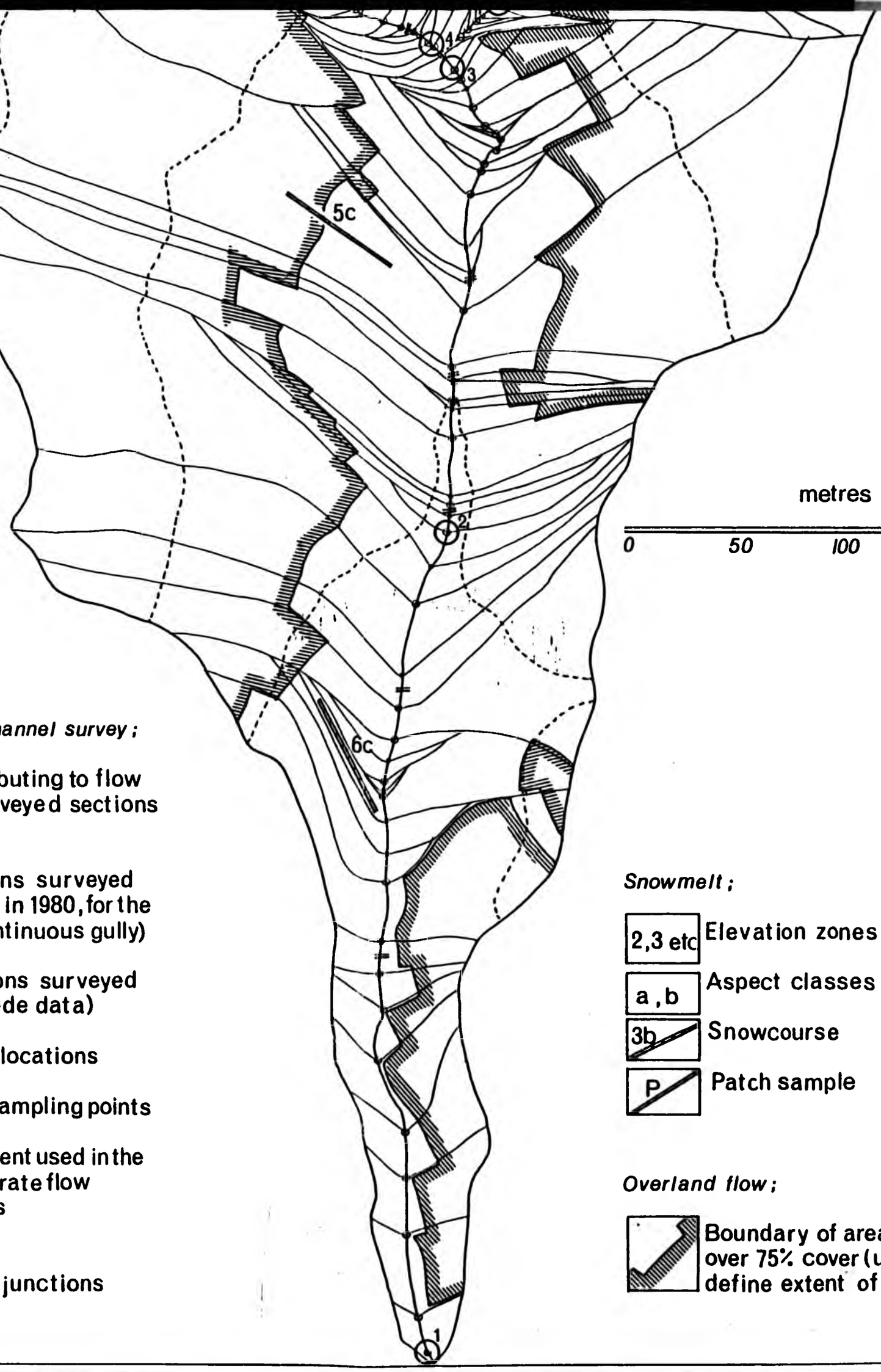

metres

0 50 100 150 200

Flow calculations and channel survey ;

Areas contributing to flow between surveyed sections

Cross-sections surveyed in 1975 (and in 1980, for the large discontinuous gully)

Cross-sections surveyed in 1962 (Heede data)

Check dam locations

Discharge sampling points

Sub-catchment used in the text to illustrate flow calculations

X , Y — Significant junctions

Snowmelt ;

2,3 etc — Elevation zones

a , b — Aspect classes

3b — Snowcourse

P — Patch sample

Overland flow ;

Boundary of areas with over 75% cover (used to define extent of O.F)

IV

D54353'85

END